

# Agronomy Research

Established in 2003 by the Faculty of Agronomy, Estonian Agricultural University

## **Aims and Scope:**

*Agronomy Research* is a peer-reviewed international Journal intended for publication of broad-spectrum original articles, reviews and short communications on actual problems of modern biosystems engineering incl. crop and animal science, genetics, economics, farm- and production engineering, environmental aspects, agro-ecology, renewable energy and bioenergy etc. in the temperate regions of the world.

## **Copyright & Licensing:**

This is an open access journal distributed under the Creative Commons Attribution-NonCommercial-NoDerivatives 4.0 International (CC BY-NC-ND 4.0).  
Authors keep copyright and publishing rights without restrictions.

## ***Agronomy Research* online:**

*Agronomy Research* is available online at: <https://agronomy.emu.ee/>

## **Acknowledgement to Referees:**

The Editors of *Agronomy Research* would like to thank the many scientists who gave so generously of their time and expertise to referee papers submitted to the Journal.

## **Abstracted and indexed:**

SCOPUS, EBSCO, DOAJ, CABI Full Paper and Clarivate Analytics database: (Zoological Records, Biological Abstracts and Biosis Previews, AGRIS, ISPI, CAB Abstracts, AGRICOLA (NAL; USA), VINITI, INIST-PASCAL.)

## **Subscription information:**

Institute of Technology, EMU  
Fr.R. Kreutzwaldi 56,  
51006 Tartu,  
ESTONIA  
e-mail: [timo.kikas@emu.ee](mailto:timo.kikas@emu.ee)

## **Journal Policies:**

Estonian University of Life Sciences, Latvia University of Life Sciences and Technologies, Vytautas Magnus University Agriculture Academy, Lithuanian Research Centre for Agriculture and Forestry, and Editors of *Agronomy Research* assume no responsibility for views, statements and opinions expressed by contributors. Any reference to a pesticide, fertiliser, cultivar or other commercial or proprietary product does not constitute a recommendation or an endorsement of its use by the author(s), their institution or any person connected with preparation, publication or distribution of this Journal.

**ISSN 1406-894X**

# CONTENTS

**M. Arak, O. Liivapuu, V.V. Maksarov and J. Olt**

A justification of the choice of parameters for the picking reel tooth on a lowbush blueberry harvester ..... 1329

**V.P. Aravani, K. Tsigkou, M. Kornaros and V.G. Papadakis**

Laboratory analyses for assessing the potential for biogas production of various agricultural residues in Greece ..... 1339

**V. Bulgakov, J. Olt, V. Nadykto, V. Volskiy, S. Polishchuk, A. Aboltins and H. Beloev**

Theoretical research into directional stability of trailed tandem- type disk harrow ..... 1351

**L. Buša, M. Bertiņš, A. Viksna, L. Legzdīņa and D. Kobzarevs**

Evaluation of carbon, nitrogen, and oxygen isotope ratio measurement data for characterization of organically and conventionally cultivated spring barley (*Hordeum vulgare* L.) grain ..... 1364

**V.Yu. Chernova and B.A. Kheyfets**

China food security assessment ..... 1373

**A.R.G. de Azevedo, H.A. Rocha, M.T. Marvila, D. Cecchin, G.C. Xavier, R.C. da Silva, P.F.P. Ferraz, L. Conti and G. Rossi**

Application of pineapple fiber in the development of sustainable mortars ..... 1387

**C. Di Vaio, A. Testa, A. Cirillo and S. Conti**

Slow-release fertilization and *Trichoderma harzianum*-based biostimulant for the nursery production of young olive trees (*Olea Europaea* L.) ..... 1396

**I. Diordiieva, V. Kochmarskyi, Ia. Riabovol, L. Riabovol and O. Serzhyk**

Enrichment of the winter triticale gene pool under intergeneric hybridization .... 1406

**L.M. dos Santos, G.A.S. Ferraz, H.J.P. Alves, J.D.P. Rodrigues, S. Camiciottoli, L. Conti and G. Rossi**

Comparison of spatial-temporal analysis modelling with purely spatial analysis modelling using temperature data obtained by remote sensing ..... 1423

<b>N. Durnova, M. Simakova, D. Isaev, I. Simakova and A. Simakov</b>	
Morphology of <i>Camellia Sinensis</i> L. leaves as marker of white tea authenticity.	1436
<b>P.F.P. Ferraz, D.H.S. Abreu, B.N. Huallpa, L.S. Santana, D. Cecchin, G.F. Rabelo, G. Rossi and M. Barbari</b>	
Acoustic analysis of cement composites with lignocellulosic residues .....	1446
<b>G.M.G. Ferreira, D. Cecchin, A.R.G. de Azevedo, I.C.R.P. Valadão, K.A. Costa, T.R. Silva, F. Ferreira, P.I.S. Amaral, C.M. Huther, F.A. Sousa, J.O. Castro, P.F.P. Ferraz and M.A. Teixeira</b>	
Bibliometric analysis on the use of natural fibers in construction materials .....	1455
<b>R. Goher and M. Akmal</b>	
Wheat cultivars exposed to high temperature at onset of anthesis for yield and yield traits analysis.....	1467
<b>A.M. Golubev, N.A. Alyoshina, V.E. Anfalov, A.A. Kulikov and V.S. Vdovenko</b>	
Some mechanisms of winter resistance in apricot flower buds in the period of ecodormancy .....	1487
<b>L.A. Grechushkina-Sukhorukova and E.V. Peshchanskaya</b>	
Evaluation of artificial agricultural landscapes biodiversity in Stavropol Botanical Garden .....	1504
<b>I. Karandušovská, P. Hlinka, D. Pálež and T. Szabóová</b>	
Concentrations of CO <sub>2</sub> from composting under different treatments.....	1518
<b>L.E. Kolesnikov, A.A. Belimov, E.Y. Kudryavtseva, B.A. Hassan and Yu.R. Kolesnikova</b>	
Identification of the effectiveness of associative rhizobacteria in spring wheat cultivation.....	1530
<b>L.E. Kolesnikov, M.V. Uspenskaya, M.I. Kremenevskaya, A.G. Orlova, I.E. Razumova and Yu.R. Kolesnikova</b>	
The biological basis for the use of acrylic hydrogel and protein growth stimulant in the soft wheat and triticale cultivation .....	1545
<b>B. Kulishov, D. Minkin, A. Fedorov and A. Novoselov</b>	
Development of the mathematical model of the electric resistance baking process .....	1562

**A. Lenerts, K. Naglis-Liepa, D. Popluga, Dz. Kreišmane, E. Aplociņa, L. Bērziņa and O. Frolova**

Marginal abatement cost curve for an ammonia reduction measure in agriculture: the case of Latvia ..... 1575

**P.H.N. Martins, D. Cecchin, A.R.G. de Azevedo, D.F. do Carmo, R.A. Donagemma, R.M.M. Waite, N.F. Rodrigues, F.A. Sousa, P.I.S. Amaral, C.M. Hüther, C.R. Pereira and V.M.F da Cruz**

Technical and economic pre-feasibility study for the construction of septic tank-filter-sinkhole with alternative material ..... 1586

**N. Nik Bakhsh and I. Riivits-Arkonsuo**

Joint Business-to-Business recovery management: the moderating role of locus of failure..... 1602

**I.I. Novikova, V.B. Minin, J.A. Titova, I.L. Krasnobaeva, A.M. Zaharov and A.N. Perekopsky**

Biological effectiveness of a new multifunctional biopesticide in the protection of organic potatoes from diseases ..... 1617

**Y. Olifir, A. Habryel, T. Partyka, O. Havryshko and H. Konyk**

Diagnosis of the functional state of transformed acid soils agroecosystems depending on long-term anthropogenic loads..... 1627

**J. Olt, V. Bulgakov, V. Bonchik, Z. Ruzhylo, V. Volskiy, V. Melnik, Ye. Ihnatiev and H. Kaletnik**

Theoretical research into operation of rotary potato harvester ..... 1640

**S. Vitolina, G. Shulga, B. Neiberte and S. Reihmane**

Woodworking wastewater biomass effective separation and its recovery ..... 1659

**O. Zavadzka, I. Bobos, I. Fedosiy, H. Podpriatov, O. Komar, B. Mazur and J. Olt**

Suitability of various onion (*allium cepa*) varieties for drying and long-term storage ..... 1675

## **A justification of the choice of parameters for the picking reel tooth on a lowbush blueberry harvester**

M. Arak<sup>1,\*</sup>, O. Liivapuu<sup>1</sup>, V.V. Maksarov<sup>2</sup> and J. Olt<sup>1</sup>

<sup>1</sup>Estonian University of Life Sciences, Institute of Technology, 56 Kreutzwaldi Str., EE51006 Tartu, Estonia

<sup>2</sup>Saint-Petersburg Mining University, Department of Mechanical Engineering, 21 Line, 2, RU199106 Saint-Petersburg, Russia

\*Correspondence: [margus.arak@emu.ee](mailto:margus.arak@emu.ee)

Received: July 18<sup>th</sup>, 2021; Accepted: September 3<sup>rd</sup>, 2021; Published: September 6<sup>th</sup>, 2021

**Abstract.** The functional working tool on the blueberry harvester is its rotating picking reel. Its working element is the picking rake which is attached to the picking reel. A total of four rakes are attached to the picking reel. A picking rake includes an axis which is attached in an articulated manner between the reel's end discs, and pin-shaped teeth which are rigidly attached to it. The picking rake's tooth must be made of a fully flexible material to prevent damage to the blueberry plant. The aim of this research was to determine the flexure of test specimens (plastic rods) which have been constructed from a fully flexible material of different conditions, along with the suitability for use of such flexible material as the teeth on the picking rake. As a result of this study, it became clear that, based on the results from flexure, durability, and residual deformation tests, it is more expedient to choose Ertacetal C (POM-C) as the material for the picking reel's tooth, with a diameter of 4.3 mm.

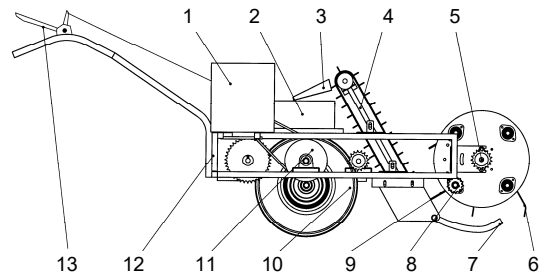
**Key words:** blueberry harvester, elastic modulus, flexible tooth, picking reel.

### **INTRODUCTION**

Blueberry plantations have been established on mineral lands, but also on exhausted milled peat fields (Peatland Ecology Research Group, 2009). Machinery has been created to take care of all technologically-involved operations, including harvesting, where medium and tall blueberry varieties are concerned which have been planted on mineral lands.

According to the available literature (Starast et al., 2007; Olt et al., 2013; Ali, 2016; Retamales & Hancock, 2018), blueberry cultivation consists of a series of technologically-involved operations, of which harvesting is one of the most labour-intensive-, and logistically-demanding operation. Harvesting can be done by machine or hand harvest, with machine harvesting optimizing harvest efficiency (Käis & Olt, 2010; Olt et al., 2013; Takeda et al., 2017).

With lowbush blueberries (*Vaccinium angustifolium* Ait.), which have a plant height of 10–20 cm and whose berries ripen more or less simultaneously (Noormets et al., 2003), it is common practise on mineral lands to harvest them commercially using automated equipment (Fig. 1) and a horizontally-located rotating picking reel (Fig. 2, a, b), with its working element being a picking rake (Heinloo, 2007; Arak & Olt, 2014). The picking rake is of the parallelogram type, which means that a picking rake remains parallel to its initial position at any angle of rotation. The picking rake contains an axis which is attached in an articulated manner between the end discs, to which teeth are rigidly attached in parallel with each other. The teeth are attached to the axis of the picking rake with spacing that allows them to move between blueberry plants without damaging them, while separating the berries from the stalks. This format is also known as a coarse harvester, which means that any impurities (such as leaves, twigs, peat particles, etc) and crushed berries are not separated by the harvester. Therefore the harvester's technologically-involved operations involve separating the berries from the stalks without any damage and to direct them to the exchangeable berry boxes or containers during the operation by means of a chute.



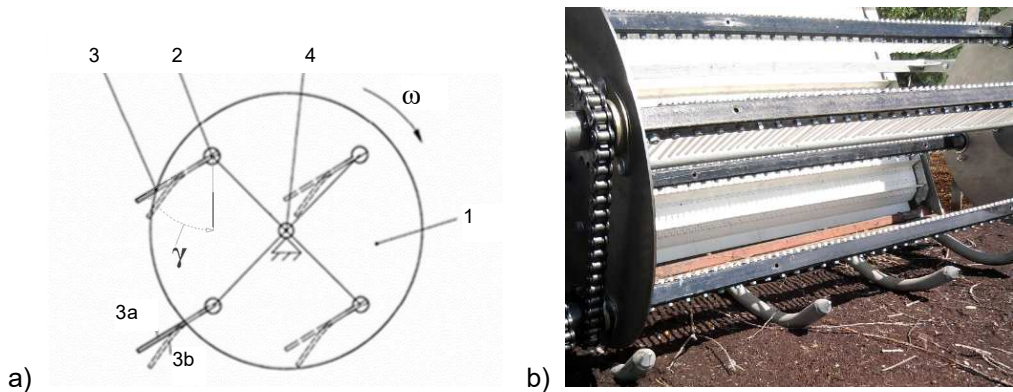
**Figure 1.** The main assemblies and parts of a motoblock-type harvester: 1 – engine; 2 – berry box; 3 – chute; 4 – conveyor; 5 – picking reel; 6 – hook spring-tine; 7 – copying unit; 8 – picking rake; 9 – rake tooth; 10 – wheels; 11 – transmission; 12 – frame; and 13 – steering levers.

The main disadvantage of the motoblock harvester for use with lowbush blueberries is the risk of damaging the plants, such as pulling them out of the ground. The process of damaging and tearing the plants occurs as follows: on a plant with long stems, where the stems are low to the ground in all directions around the centre of the plant due to the weight of the berries, those stems which mainly face in the same direction as the picking rake often get stuck between the picking rake's teeth as the picking rake moves downwards. The stems of a blueberry plant which are caught between three or more teeth are torn to shreds or are pulled out of the ground by the rotating picking reel when the wheel is equipped with rigid teeth (usually made from stainless steel). There is no problem with plants which have low stems of up to 15 cm long, as they mainly remain upright, but it is a serious problem for plants with stems which are longer than 20 cm. The problem comes from poor compatibility between variations in plant growth and the picking reel teeth in currently-available blueberry harvesters.

The simplest technical solution to the problem would be to replace the rigid picking rate teeth with flexible teeth. To accomplish this, a material with suitable properties must be selected for the production of the teeth.

According to Fig. 2, a, the operating elements of the picking reel 1 are horizontal picking rakes, which comprise picking rake teeth, 3, which are rigidly affixed to the axes, 2, which in turn are attached in an articulated manner between the side discs. The picking rake teeth, 3, are designed to be produced from a flexible material in order to prevent damage being inflicted on the blueberry plants. The picking rake teeth, 3, can be located

positions 3a and 3b. The berries are separated from the stalks by means of the teeth, 3, which are moved through the blueberry stalks. In the initial position, 3a, with this being the unloaded position, the picking rake is straight; in the loaded position, 3b, the picking rake is bent (Fig. 2, a). If a picking rake's elastic tooth, 3, gets stuck behind a plant stem or if a plant stem located on the picking rake's path gets stuck between the ends of the teeth, the rotation of the picking reel, 1, places an additional load on the teeth, 3, with the tooth bending and assuming position 3b. When the teeth, 3, bend this means the plant stems are released from between the ends of the teeth and tooth moves past the plant without damaging the stem. After being released from the plant stems, the teeth, 3, reassume their initial shape, as in position 3a. The picking rakes are connected according to the parallelogram principle and the angle  $\gamma$  of the tooth, 3, is adjustable.



**Figure 2.** The blueberry harvester's picking reel: a) the principal schematic; b) prototype, with 1 – picking reel, 2 – picking rake, 3 – rake tooth, 3a – straight tooth, 3b – bent tooth, and 4 – spindle.

The aim of this work was to determine the flexure and durability of test specimens (plastic rods) which have been produced from elastic material which have differing general parameters, ie. observing and testing their suitability for use as picking rake teeth. The modified harvester with the flexible picking teeth may improve harvest efficiency and reduce plant damage, but requires testing to determine the feasibility of using this new harvester technology. Additionally, picking teeth conditions need to be studied to optimize harvest.

## MATERIALS AND METHODS

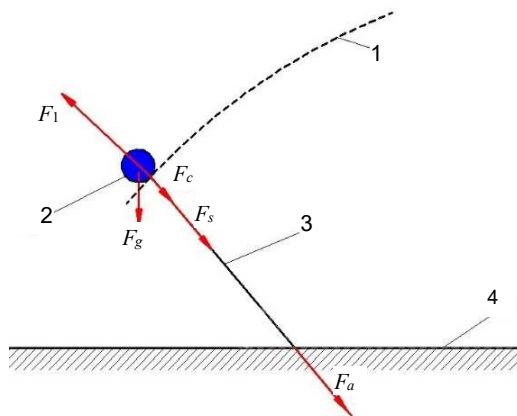
In the case of lowbush blueberry harvesting, the system's elements are the blueberry plant, namely its berries, ie. the crop, along with the plant stalk which supports the berries, and the plantation and working harvester, which together form the blueberry cultivation system and subsystems. When the values of the relationships between the elements are known, it is possible to design harvesting technology in such a way that the requirement of preventing plant and berry damage during harvesting is ultimately fulfilled.

The Fig. 3 describes the forces exerted by the tooth on the berry and the plant during berry picking, where  $F_c$  is the connection force between the berry and the stem,  $F_s$  is the tensile strength of the plant's stem, and the connection force  $F_a$  between the stem and the soil,  $F_l$  is the lifting force,  $F_g$  is the gravitational force,  $E_m$  is elastic modulus of rake's tooth material and  $E_s$  is tensile strength of plant's stem. It is evident from Fig. 3 that, in order to avoid damaging the crop or blueberry plants during harvesting, the harvesting machine must be designed in such a way that the following condition are fulfilled:

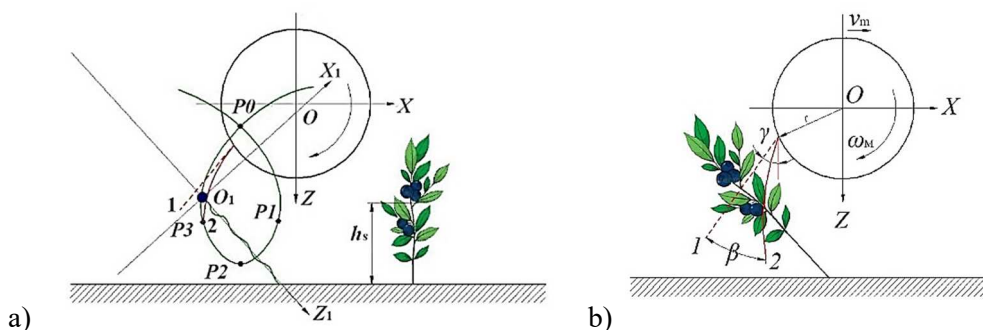
$$\left. \begin{aligned} F_{a,min} &> F_{s,min} > F_l > F_{c,max} \\ E_m &> E_s \end{aligned} \right\} \quad (1)$$

When taking these variables (Arak & Olt, 2017; Arak et al., 2018) into account, the material to be selected for the picking elements or the picking rake's teeth should be able to separate the berries, but should do no damage to the plant, or crush it, or tear it from the ground, and neither should it bruise the berries. Test work was carried out to select suitable material for rake tooth.

Any description of those forces which are applied in the blueberry harvester's picking reel should be based on the coordinate system  $O_1X_1Z_1$  (Fig. 4, a), as related to the berry that is to be removed, where the origin  $O_1$  is located at the connection point between the berry and the stem, axis  $Z_1$  is parallel to the blueberry plant, and the positive direction of the axis is directed towards the berry's surface and mainly forms a right angle with the non-deformed tooth.



**Figure 3.** Those forces which are applied to a blueberry plant by the harvesting machinery flexible picking teeth: 1 – the picking reel's teeth; 2 – the berry on the blueberry plant; 3 – the blueberry stem; 4 – the field surface.



**Figure 4.** A diagram which characterises the work of a picking tooth: a) stages ( $P1$ - $P4$ ) of work of picking tooth; b) angles characterizing the work process for an elastic tooth.

The following forces are applied to the connection point between the berry and the tooth (Fig. 4, a).



In order to separate the berry from the stem, the force  $F_x$  which is applied to the connecting stem must be greater than the connection force  $F_{c, max}$  between the berry and the stem.

The tooth of a picking reel is straight in the unstressed position (Fig. 4, position 1). Due to force  $F_c$ , the stressed tooth attains position 2, which forms a flexure in comparison to the straight tooth, as expressed by the angle of inclination  $\beta$ . The angle of inclination  $\gamma$  of the blueberry harvester's prototype can be changed within the range of  $40^\circ$ – $70^\circ$ .

The extent of any bending is determined by the value of connection force  $F_c$ .

The berry is removed from the stem when the inequality (1) and following condition (2) is fulfilled:

$$\beta < \gamma, \quad (2)$$

where  $\gamma$  is the angle between the non-deformed tooth and the vertical direction.

The calculation of the force being applied to the tooth is based on the following assumptions:

1. The maximum yield of the blueberry plantation: 17,000 kg ha<sup>-1</sup>, or 1.7 kg m<sup>-2</sup> (Siliņa & Liepniece, 2020);
2. The mass of an individual berry: 0.14–3.40 g (Soots et al., 2017);
3. Therefore, about a thousand berries grow over one square metre;
4. The blueberry harvester's prototype (Arak et al., 2018) has teeth that are placed 21.5 mm apart, with a length of 125.0 mm. The maximum working area for one pair of teeth is  $0.27 \times 10^{-3}$  m<sup>2</sup>.

As arising from assumptions 1-4, there are three berries for one pair of teeth during a working cycle (Fig. 4, a, *PI-P3*). When we apply a reserve factor of three, a pair of teeth will pick about ten berries during one working cycle.

According to Arak & Olt (2017), the connection force of berries that are ripe for harvesting was 0.17–0.83 N and 0.89–1.93 N for unripe berries. The numerical ratio between ripe and unripe berries during harvesting season is 80% and 20% respectively. Therefore, the maximum force to be applied to one pair of teeth is 12 N.

The gravitational force which results from the tooth's mass itself is small (0.025 N for a tooth diameter of 4.3 mm and 0.038 N for a tooth diameter of 5.3 mm), and may be dismissed. Likewise, the gravitational force which results from the berry's mass may be dismissed as its maximum value is 0.034 N.

Selecting the materials for the teeth: an engineering plastic Ertacetal C (Acetal Copolymer, POM-C) was chosen as the material for the flexible teeth as it is characterised by its great mechanical strength, its impact strength, and its ability to be treated by cutting in manufacturing process of tooth (Olt & Arak, 2012).

Selecting the diameter of the teeth: two choices of material were selected so that the test could be carried out, with a round cross-section of the diameters of 4.3 mm and 5.3 mm.

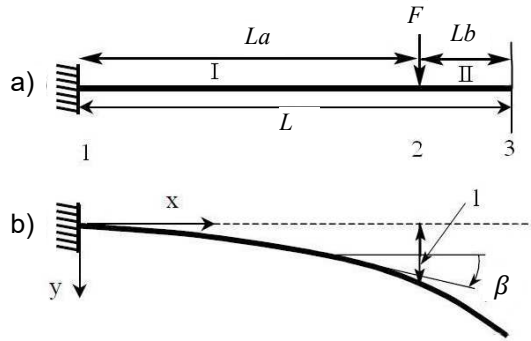
The following tests were carried out when it came to selecting the diameter of the materials being used on the picking reel teeth, *D*:

- 1) Determining the plastic deformation of the teeth by systematically bending the material at various diameters (4.3 mm and 5.3 mm);
- 2) The resistance of the teeth to breaking-in so-called semi-aggressive and aggressive bending modes.
- 3) Measuring the flexure of teeth at various loads.

### Describing teeth flexure theoretically

To investigate the flexure of the picking reel, we consider the tooth as being a cantilevered homogeneous beam (Fig. 5). This beam is characterised by the modulus of elasticity  $E_m$  and the moment of inertia  $I$ .

The finite element method, FEM, has been used to study tooth flexure (Logan, 2007). The picking reel's tooth (Fig. 5) is rigidly attached at point 1 (Fig. 5), and is loaded at point 2 by force  $F$ . The beam is now modelled using two elements, I and II, with nodes 1, 2, and 3.



**Figure 5.** Cantilever beam being subjected a concentrated load: a) unloaded beam; b) loaded beam.

The local stiffness matrices for the elements I and II are  $K_1$  and  $K_2$  respectively.

$$K_1 = \frac{E_m I}{La^3} \begin{bmatrix} 12 & 6La & -12 & 6La \\ 6La & 4La^2 & -6La & 2La^2 \\ -12 & -6La & 12 & -6La \\ 6La & 2La^2 & -6La & 4La^2 \end{bmatrix}, \quad (3)$$

$$K_2 = \frac{E_m I}{Lb^3} \begin{bmatrix} 12 & 6Lb & -12 & 6Lb \\ 6Lb & 4Lb^2 & -6Lb & 2Lb^2 \\ -12 & -6Lb & 12 & -6Lb \\ 6Lb & 2Lb^2 & -6Lb & 4Lb^2 \end{bmatrix}. \quad (4)$$

The total stiffness matrix  $K$  is the result of assembling  $K_1$  and  $K_2$ .

$$K = K_1 + K_2 \quad (5)$$

Through direct superposition and considering (3) and (4), the governing equation for this cantilever beam is:

$$\begin{Bmatrix} F_{1y} \\ M_1 \\ F_{2y} \\ M_2 \\ F_{3y} \\ M_3 \end{Bmatrix} = K \begin{Bmatrix} d_{1y} \\ \beta_{t1} \\ l_t \\ \beta_{t2} \\ d_{3y} \\ \beta_{t3} \end{Bmatrix}. \quad (6)$$

Considering the boundary conditions at node 1, we have:

$$\beta_{t1} = 0 \quad (7)$$

and:

$$d_{1y} = 0. \quad (8)$$

The momentum of inertia  $I$  for the beam with a circular cross-section can be described (Mäkelä et al., 2011):

$$I = \frac{\pi D^4}{64}. \quad (9)$$

Due to the initial task (Fig. 5), we get:

$$F_{2y} = F. \quad (10)$$

Solving the equation (6) by conditions (7), (8), and (10), the displacement at node 2 is:

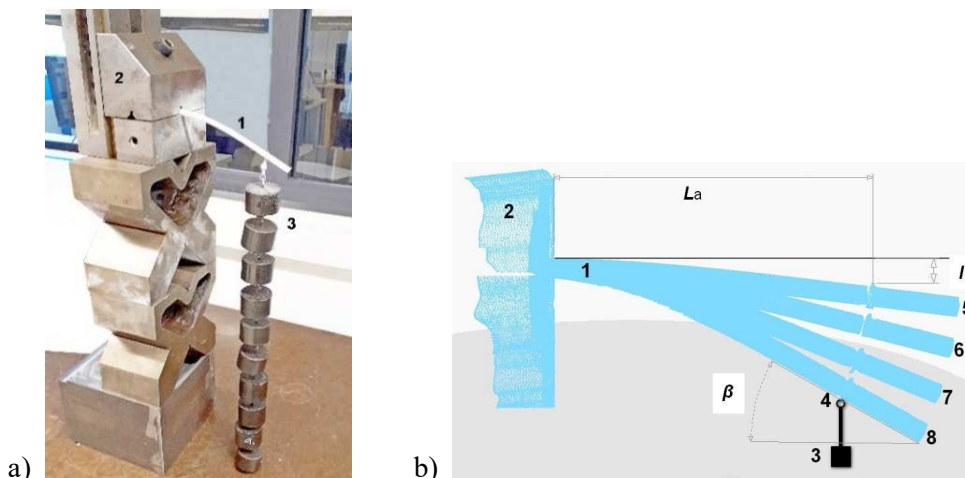
$$l_t = \frac{L_a^3 F}{3E_m I} \quad (11)$$

where  $L_a$  – distance of the attachment point from the point at which the force  $F$  was applied and the slope (in radians) at node 2 can be calculated as:

$$\beta_{t2} = \frac{2L_a^2 F}{E_m I}. \quad (12)$$

### Experiments for studying the flexure of the teeth

Tests were carried out with tooth materials of two different diameters:  $D_1 = 4.3$  mm and  $D_2 = 5.3$  mm (these values have been chosen based on theoretical calculations and material availability). Tooth (1) was connected to the stand (2) as a cantilever (Fig. 6, a). The tooth was stressed with plastic weights (3) which were connected to a point that was 20 mm from the free end. The loads were connected to the tooth (1) using a hinge (4) which ensured that the applied force was vertical. The room temperature was 22 °C and relative humidity was at 26% during the tests (the value of the material's modulus of elasticity  $E_m$  was determined under the temperature and humidity conditions of 23 °C and 50%).



**Figure 6.** Test stand for measuring the tooth's flexure, a): and a digital model of the tooth's flexure b): with three weights (position 5), six weights (position 6), nine weights (position 7), and twelve weights (position 8), where  $l$  is the flexure of the cantilever beam and  $L$  is the distance between the cantilever attachment point and the weight attachment.

The flexures of the tooth (1) under various loads were scanned using a Nikon MCAX20/MMD50 portative laser scanner. After scanning, the resultant data was processed, a digital model was prepared, and flexure measurements were carried out using the software package, ANSYS SpaceClaim 2017.

A universal lathe was used to carry out the durability test on the tooth test specimens. The test equipment contained a fragment of a picking rake to which two tooth specimens were rigidly attached, one with a diameter of 4.3 mm and the other with a

diameter of 5.3 mm. The fragment of the picking rake was installed on the lathe's jaws. A roller acting as an artificial obstacle was attached to the lathe's blade holder to simulate the passage of teeth between blueberry plants and their effect on the teeth in the test. Its distance from the axis of rotation of the picking rake fragment was less than the length of the tooth, while the tooth flexed upon its passing the artificial obstacle. The rotation of the lathe mimicked the work of the teeth upon blueberries being harvested, creating repeated bending cycles. The total number of revolutions for the test piece and therefore also the number of flexings in the teeth was 23,300.

During a field test, a blueberry crop (a mix of several varieties) was harvested from a 0.1 hectare test plot. The test was carried out on Marjasoo Farm in Tartu County, South Estonia. The aim of the test was to check the durability of the flexing teeth in a commercial setting. The picking reel of used harvester has four rakes (Fig. 2, a), every rake has 66 tooth. The length and diameter of the tooth was controlled with the digital caliper ((Mitutoyo 200 mm) during of the installation of them, rotational speed of picking reel was controlled with rotational speed measuring device (ТЧ 10-Р). The flexure of teeth (5 randomly selected teeth on each rake) was measured before and after harvest of test plot with digital angle meter (ADA 20).

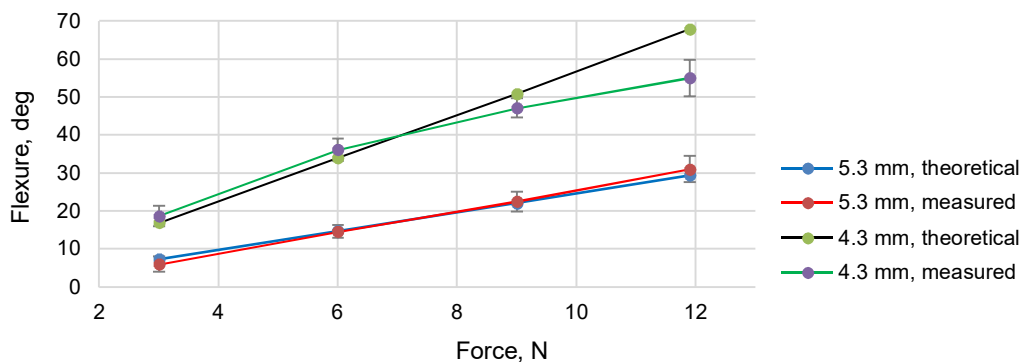
## RESULTS AND DISCUSSION

The theoretical flexures  $l_t$  and  $\beta_t$  and the measured flexures  $l_m$  and  $\beta_m$  for materials of various diameters are given in Table 1 and Fig. 7, where  $l_m$  and  $\beta_m$  are the arithmetic means of the three series of measurements. The calculations were carried out in the Mathcad 15.0 environment. For the theoretical calculations, the value of  $E_m$  was selected to be 3,000 MPa (Mitsubishi, 2020).

The teeth's work in passing through a blueberry plant and in removing the berries from the stem was simulated by loading the teeth with weights.

**Table 1.** Calculated and measured flexures of a tooth with diameters of 5.3 mm and 4.3 mm

$F, N$	$D = 5.3 \text{ mm}$		$D = 4.3 \text{ mm}$	
	$l_t, \text{ mm}$	$l_m, \text{ mm}$	$l_t, \text{ mm}$	$l_m, \text{ mm}$
3.0	8.5	8.8	19.7	23.1
6.0	17.2	17.8	39.6	44.5
9.0	25.7	27.7	59.3	59.3
11.9	34.3	36.7	79.1	69.0



**Figure 7.** Calculated and measured (with standard deviation) flexures (in degrees) of a tooth with diameters of 4.3 mm and 5.3 mm.

Theoretical calculations (Eq. 11 and 12) and test results (Table 1 and Fig. 7) showed that the following results:

1) at maximum load (12 N), the flexure of the 4.3 mm diameter tooth test piece was at 70°;

2) at maximum load (12 N), the flexure of the 5.3 mm diameter tooth test piece was at 35°;

3) the differences between the theoretical and test results for materials with diameters of 4.3 mm and 5.3 mm are 10.1% and 5.1% respectively.

The results show that selected material with both diameters are suitable as materials for a picking reel's teeth as they both fulfil the condition under maximum load which was stipulated by Eq. (2).

The durability tests for the teeth revealed that, upon the long-term loading (23,300 flexings cycles) of the teeth, the residual deformation of a tooth with a diameter of 5.3 mm is up to three times higher than is the residual deformation of a tooth with a diameter of 4.3 mm (Olt & Arak, 2012).

No teeth were broken during the field test, but a flexing effect was observed in the tooth material (in the form of spring-back). The number of revolutions of the teeth during this test was 2,300. The average deviation of the free ends of the teeth from the longitudinal axis was 1.2 mm. After being left at a standstill for three days at a temperature of  $T = 20\text{--}22$  °C, a new set of measurements were carried out with the following results: the permanent deformation in the 4.3 mm diameter teeth had disappeared and they had resumed their original position.

## CONCLUSIONS

As a result of the flexure as the material for the picking reel's teeth, both 4.3 mm and 5.3 mm diameter test specimens were found to be suitable for the production of teeth, with the difference between theoretical and test results for 4.3 mm and 5.3 mm diameter materials being 10.1% and 5.1% respectively.

The flexing teeth do not tear the stem apart and neither do they pull the plants out of the ground, instead bending when an obstacle is encountered and regaining their original shape after clearing the obstacle.

Based on the results of all three tests - the flexure, durability, and residual deformation tests - the Ertacetal C with a diameter of 4.3 mm was shown to be a suitable replacement for standard teeth made from (stainless) steel, that led to reduced plant damage. This diameter was preferred over the 5.3 mm diameter because it has less residual deformation and the initial position recovers faster.

Further research should be done, such as larger field testing that evaluates long-term durability, harvest efficiency, economics of the proposed system, and impacts on berry quality. Also the length of tooth of picking rake and kinematic parameters (rotation speed of picking reel and working speed of the blueberry harvester) are also affect blueberry harvesting and should be additionally studied.

## REFERENCES

- Ali, S. 2016. *Effect of Harvesting Time on Berry Losses During Mechanical Harvesting of Wild Blueberries*. Dalhousie University, Halifax, Nova Scotia, 146 pp.
- Arak, M. & Olt, J. 2014. Constructive and kinematics parameters of the picking device of blueberry harvester. *Agronomy Research* **12**(1), 25–32.
- Arak, M. & Olt, J. 2017. Determination of the connection force between berries and stem in blueberry plants. *Proceedings of the 45th International Symposium on Agricultural Engineering: Actual Tasks on Agricultural Engineering, Opatija, Croatia, 21-24.02.2017*. Ed. Igor Kovacev. University of Zagreb, 589–595.
- Arak, M., Soots, K., Starast, M. & Olt, J. 2018. Mechanical properties of blueberry stems. *Research in Agricultural Engineering (RAE)* **64**(4), 202–208, doi: 10.17221/90/2017-RAE
- Heinloo, M. 2007. A Virtual Reality Technology Based Method for Study the Working Process of a Blueberry Harvester's Picking Reel. *Agricultural Engineering International: the CIGR Ejournal*. Manuscript IT 07 001. Vol. **IX**, 12 p.
- Käis, L. & Olt, J. 2010. Low-bush blueberry machine cultivation technology in plantations established on milled peat fields. Kosutic S. (ed.). *Actual tasks on agricultural engineering*. HINUS, **38**, 271–279.
- Logan, D.L. 2007. *A First Course in the Finite Element Method*. 5<sup>th</sup> Edition. Thomson, 753 pp. ISBN.13: 9780534552985
- Mitsubishi Chemical Advanced Materials. 2020. Web page. [https://media.mcam.com/fileadmin/quadrant/documents/QEPP/EU/Product\\_Data\\_Sheets\\_PDF/GEP/Ertacetal\\_C\\_PDS\\_E\\_01042019.pdf](https://media.mcam.com/fileadmin/quadrant/documents/QEPP/EU/Product_Data_Sheets_PDF/GEP/Ertacetal_C_PDS_E_01042019.pdf).
- Mäkelä, M., Soininen, L., Tuomola, S. & Öistämö, J. 2011. *Technical Formulas - Basic Formulas of Mathematics, Physics, Chemistry and Strength of Materials, and SI Systems of Units*. 3rd Revised Edition. Tammertekniikka, 203 pp.
- Noormets, M., Karp, K. & Paal, T. 2003. Recultivation of opencast peat pits with *Vaccinium* culture in Estonia. Iezzi E. et al. (eds). *Ecosystems and sustainable development*. Southampton, Boston, vol. **IV**(2), 1005–1014.
- Olt, J. & Arak, M. 2012. Design and development of the picking reel of motoblock-type harvester. *Agraarteadus/Journal of Agricultural Science* **23**(2), 21–26.
- Olt, J., Arak, M. & Jasinskas, A. 2013. Development of mechanical technology for low-bush blueberry cultivating in the plantation established on milled peat fields. *Agricultural Engineering* **45**(2), 120–131.
- Peatland Ecology Research Group. 2009. Production of berries in peatlands. Guide produced under the supervision of Line Rochefort and Line Lapointe. Université Laval, Quebec, Canada, 134 pp.
- Retamales, J.B. & Hancock, J.F. 2018. *Blueberries* (2<sup>nd</sup> ed.). Crop Production Science in Horticulture Agriculture, book 29. CABI, 424 pp.
- Siliņa, D. & Liepniece, M. 2020. Variability in yield of the lowbush blueberry clones growing in modified soil. *Agronomy Research* **18**(S4), 2770–2775.
- Soots, K., Krikmann, O., Starast, M. & Olt, J. 2017. Determining the dimensional characteristics of blueberries. *Agronomy Research* **15**(3), 886–896.
- Starast, M., Karp, K., Paal, T., Värnik, R. & Vool, E. 2005. *Blueberry and its cultivation in Estonia*. Estonian University of Life Sciences, 65 pp. (in Estonian).
- Takeda, F., Yang, W.O., Li, C., Freivalds, A., Sung, K., Xu, R., Hu, B., Williamson, J. & Sargent, S. 2017. Applying New Technologies to Transform Blueberry Harvesting. *Agronomy* **7**(33). doi:10.3390/agronomy7020033

## Laboratory analyses for assessing the potential for biogas production of various agricultural residues in Greece

V.P. Aravani<sup>1</sup>, K. Tsigkou<sup>2</sup>, M. Kornaros<sup>2,\*</sup> and V.G. Papadakis<sup>1,\*</sup>

<sup>1</sup>Department of Environmental Engineering, University of Patras, 2 Seferi Str., GR30100 Agrinio, Greece

<sup>2</sup>Department of Chemical Engineering, University of Patras, 1 Karatheodori Str., University Campus- Rio, GR26504 Patras, Greece

\*Correspondence: [kornaros@chemeng.upatras.gr](mailto:kornaros@chemeng.upatras.gr); [vgpapadakis@upatras.gr](mailto:vgpapadakis@upatras.gr)

Received: February 23<sup>rd</sup>, 2021; Accepted: May 27<sup>th</sup>, 2021; Published: June 8<sup>th</sup>, 2021

**Abstract.** Greece produces significant amounts of agricultural and livestock waste. For the needs of this study, Greece was divided into a Northern and a Southern part and relevant proposals were made for residues that can be used for energy production, through anaerobic digestion. For Northern Greece, this study concluded that the most abundant residues and potential substrates for anaerobic digestion valorisation are those of maize, inedible vegetables (including greenhouse vegetables), cattle manure, as well as the residues of beer and wine industry. For Southern Greece, the corresponding substrates are those of maize, inedible vegetables, sheep/goat manure and residues of wine, tomato, orange and olive processing, respectively. Based on the physicochemical characterization of individual feedstocks, corn silage, tomato husks, watermelon, malt, cattle manure, orange, and olive processing residues (olive pomace) were considered as the most suitable feedstocks for anaerobic digestion. Biochemical Methane Potential (BMP) assays for Northern Greece were also performed, testing the most abundant and appropriate residues for anaerobic digestion (of this area), namely corn silage, cattle manure and malt, in order to define their BMP yield as well as their prospective optimum mixtures. It was concluded that the BMP of the mono-substrates is in accordance with literature, while there were no statistically significant differences in the methane yield of all tested mixtures. The residual biomass originating from the three main categories of the agricultural sector (crop residues, agro-industrial residues, and animal manure) in Northern Greece can be efficiently valorised via anaerobic co-digestion, without observing, though, any synergistic effects on methane production.

**Key words:** agricultural residues, anaerobic digestion, biogas, BMP assays, Greece, residue characterization.

### INTRODUCTION

Greece is an agricultural country and considerable proportion of its residual biomass consists of crop residues and livestock manure (Lais et al., 2017). Almost 70% of the total area of Greece is used for agricultural activities. This is the reason why the country exhibits a high biomass potential for renewable energy production (Sagani et al.,

2019). Most European countries use residual biomass as a significant resource for electricity and thermal energy production. However, in Greece, only a small percentage of it is used to meet the electrical energy needs, as the country still largely depends on fossil fuels. In general, 61% of national energy needs are met by fuel imports and the rest (39%) through national energy sources such as lignite (77%) and renewable energy systems (22%) (Moustakas et al., 2020). Despite their vast availability, huge amounts of agricultural residues and animal manures are disposed of uncontrollably in the environment or in landfills, while farmers usually proceed to open burning of residual biomass in their fields, even though these solutions lead to deterioration of the Greek environment (Alatzas et al., 2019).

Residual biomass from the agricultural sector usually appears in the form of crop residues, agro-industrial residues, and animal manure. Vlyssides et al. (2015) have recently estimated the total annual residues production in Greece. According to their study, the production amounts to 45,957,990 t year<sup>-1</sup>, taking into consideration the estimations for the annual production of agro-industrial residues and livestock manure. The theoretical annual potential of agro-industrial residues (such as wheat products, potatoes, olives, fruits, dairy products etc.) was found to be 19,005,490 t year<sup>-1</sup>, while the corresponding amount of livestock manure (cattle, chicken, pigs, sheep etc.) was 26,952,500 t year<sup>-1</sup>. As the estimated residual biomass could be an energy source with essential contribution to the Greek energy balance, studying the energy generation potential of these waste streams is of great importance (Vlyssides et al., 2015). The choice of the energy conversion process depends on the physicochemical properties of biomass, such as its moisture content and the stoichiometric ratio C:N. According to the literature, the described residues are characterized by high moisture content (above 50–55%) and low C:N ratio (below 30), (Skoulou & Zabaniotou, 2007; Vlyssides et al., 2015).

Anaerobic digestion (AD) is a biological process through which different organic wastes can be converted to biogas (methane and carbon dioxide), under anaerobic conditions (Vlyssides et al., 2015; Zhao et al., 2016). AD process can be considered as one of the best environmental and low-cost solutions for the treatment of different biodegradable wastes, which are generated due to anthropogenic activities (Moustakas et al., 2020). The application of AD on single waste streams sometimes implies undesirable inhibitory effects due to toxic compounds or metals' presence. A solution to this problem could be the anaerobic co-digestion of two or more waste streams. This perspective is considered promising enough for overcoming the inhibition effects and thus enhancing the efficiency of the AD process (Dareioti & Kornaros, 2015; Kashi et al., 2017). Even if AD has been extensively studied for several years, in Greece there is still lack of experience concerning biomass residues' valorisation from the three main categories that are produced in Greece, i.e. crop residues, agro-industrial residues and animal manure.

A reliable and simple method to obtain the extent and the rate of organic wastes conversion into methane is the Biochemical Methane Potential (BMP) assays, by which information can be derived about the methane potential of each substrate, the operation conditions and the anaerobic inoculum efficiency. As BMP assays are characterized as a tool for the design optimization and operation of anaerobic digesters, their application is mandatory before any large-scale reactor performance (Tsigkou et al., 2019).



Concerning the aim of this study, Greece was divided into a Northern and a Southern part and relevant proposals were made for residues that can be exploited for energy production through AD. Following our estimations and detailed survey, samples were collected from all promising feedstocks (Northern and Southern Greece) for AD to conduct physicochemical characterization. BMP assays of Northern Greece feedstocks followed, in order to assess the wastes' BMP values and define thus the most promising mixtures as well as their potential synergistic effects, based on detailed design of experiment (DOE).

## MATERIALS AND METHODS

### Materials

As Greece was divided into the Northern and the Southern part, relevant proposals were made for residues that can be used for energy production through the AD process. Briefly, for Northern Greece the most abundant and suitable residues for AD are those of maize, inedible vegetables (vegetables characterized by low quality, including greenhouse vegetables, as well as their crop residues such as stalks), cattle manure, beer and wine industry residues, while for Southern Greece are those of maize, inedible vegetables, sheep/goat manure and residues of wine, tomato, orange and olive processing (two-phase decanter residues). This information is extracted from the data of the Hellenic Statistical Authority (<https://www.statistics.gr/en/statistics/agr>). The areas where the main crops are produced and the main categories of livestock are bred, were determined according to the abovementioned statistical data. The areas with the highest crop production and breeding activity lead respectively to the highest amount of biomass residues.

Samples were collected from all promising feedstocks for physicochemical characterization, followed by BMP assays. Nevertheless, sheep and goat manure presents serious difficulties for its collection due to inaccessibility to the livestock farms and thus it was not considered as potential feedstock, in this study. The raw residues that were evaluated in the current work included (a) crop residues (corn silage, tomato stalks, and watermelon), (b) agro-industrial residues (tomato husks, wine marcs, malt, olive pomace, and orange processing residues), and (c) animal manure (cattle manure). Regarding the crop residues, the corn silage which was used in the current study was spoiled animal feed, while the tomato stalks and the unsuitable for human consumption watermelons were collected directly from the field. The agro-industrial residues, namely tomato husks, wine marcs and malt were collected from the corresponding processing plants. Finally, the cattle manure (liquid part) was collected after the separation of the solid residue.

All samples were collected from small local plants in the area of Patras, Western Greece. Because of their seasonal availability and high tendency to fermentation, all samples were collected fresh and stored in the freezer at -18 °C, before further treatment.

### Anaerobic inoculum

The anaerobic sludge, which was used as inoculum for the BMP assays, was obtained from a pilot-scale mesophilic anaerobic digester with working volume of 15 L operating at the Laboratory of Biochemical Engineering and Environmental Technology, Department of Chemical Engineering, University of Patras (Greece). The digester was

fed with a mixture of bread, meat and fruits/vegetables (which does not meet the quality and safety standards for human consumption) at an Organic Loading Rate of  $0.2 \text{ g VS} \cdot \text{L}_{\text{Reactor}}^{-1} \cdot \text{d}^{-1}$ . Concerning the characteristics of the anaerobic inoculum, TS were measured at  $44.02 \pm 0.31 \text{ g L}^{-1}$ , 53.4% of which were VS.

### **Analytical Methods**

Physicochemical parameters such as pH, humidity, total solids (TS), volatile solids (VS), total suspended solids (TSS), and volatile suspended solids (VSS), total and soluble chemical oxygen demand (t-COD and d-COD), total and soluble carbohydrates (t-CHO and d-CHO), soluble phenolic compounds (d-phenols), total Kjeldahl nitrogen (TKN), proteins, ammonia/ammonium nitrogen ( $\text{NH}_3\text{-N}$ ), fats/oils, total and soluble phosphorus (t-P and d-P) were measured according to the Standard Methods for the Examination of Water and Wastewater (APHA AWWA WEF, 2012). The lignin, cellulose, and hemicellulose content was determined using freeze-dried material from each feedstock according to the protocol of NREL (Sluiter et al., 2011). The biogas composition analysis was conducted using a gas chromatograph (Agilent Technologies 7890A) with a thermal conductivity detector (TCD), as described in detail by Dareioti et al. (2014).

### **Biochemical Methane Potential Assay**

BMP refers to the experimental procedure developed to determine the maximum methane potential of a given organic substrate during its anaerobic decomposition (Owen et al., 1979; Chynoweth et al., 1993). In this study, the BMP assays were carried out concerning Northern Greece residual biomass and more specifically the most abundant residues that are produced during winter and summer, in this area. Both seasons, share the same feedstocks, such as corn silage, malt (main by-product of brewery), and cattle manure.

The experimental design of BMP assays was realized according to DOE (Design of Experiments) for mixtures with a design degree 3 in Minitab, 2019. In DOE for mixtures, the proportions of the constituents are variable, while their total amount remains unchanged. Such DOEs, try to model the blending surface with mathematical equation forms based on data that are procured for the set of mixture compositions. Afterwards the system's response can be estimated for any other desired mixture composition by the developed model (Kashi et al., 2017).

The biogas volume produced is usually expressed in standard pressure (1 atm) and temperature ( $0^\circ\text{C}$ ) conditions (STP conditions) (Dareioti, 2015). The BMP protocol followed in this study was based on the principles described by Angelidaki et al. (2009). Each test was conducted in duplicate. Known amounts of substrate ( $2 \text{ g VS L}^{-1}$ ) and active anaerobic inoculum ( $20\% \text{ v v}^{-1}$ ) were added to 160-mL closed serum vials. Nutrient medium containing macro-micronutrients, vitamins etc., as described in detail by Angelidaki et al. (2009), was also added to the vessels in order to ensure the optimal function of the anaerobic inoculum. Two serum vials with the abovementioned composition (without substrate addition) were used as blank (control) in order to subtract the endogenous methane production of the inoculum. The assay vessels were flushed continuously with  $\text{N}_2/\text{CO}_2$  (80/20% as volume) for about 5 min, after transferring the substrate, the medium, and the inoculum followed by the sealing of the vessels with a thick butyl-rubber stopper and an aluminum crimp (Angelidaki et al., 2009). Once

sealed, the bottles were placed in an orbital shaking water bath at approximately 90 rpm and maintained at a constant mesophilic temperature at 37 °C. The produced biogas was measured daily for the first 6 days of the experiment, while for the remaining experimentation period (34 days) measurements were taken every 2–7 days, depending on the produced biogas volume. A precision gas syringe (50 mL volume) was used for the collection and quantification of the produced biogas. Concerning the final biogas composition, corrections were occurred for the conversion to dry biogas (STP conditions) as well as for water loss during biogas quantification, according to Tsigkou et al. (2019). The final BMP of each sample represents the sum of the total methane produced and released via the gas syringe, as well as the methane contained in the headspace volume. Concerning the evaluation of possible synergistic effects during co-digestion of tested feedstocks, the equation (1) was used, as described in detail by Tsigkou et al. (2021).

$$\text{Expected BMP (ml CH}_4\text{ g VS}_{\text{added}}^{-1}\text{)} = \frac{(V_{S1} \cdot VS_{S1} \cdot BMP_{S1}) + (V_{S2} \cdot VS_{S2} \cdot BMP_{S2}) + (V_{S3} \cdot VS_{S3} \cdot BMP_{S3})}{V_{S1} \cdot VS_{S1} + V_{S2} \cdot VS_{S2} + V_{S3} \cdot VS_{S3}} \quad (1)$$

where  $V$ ,  $VS$  and  $BMP$  are the volume, volatile solids and experimental BMP, respectively for each tested mono-substrate.

## RESULTS AND DISCUSSION

### Physicochemical characterization

The results obtained from the physicochemical characterization of raw feedstocks are presented in Table 1. The characterization of samples showed that almost all raw residues have high moisture content, which is above 50%, except from wine marc residues (30%). In addition, the fats/oils content (especially for the case of olive pomace, wine marcs and tomato husks) are quite high, while the protein content is of the same order of magnitude for all tested substrates. The aforementioned characteristics indicate the potential suitability of these substrates for treatment via anaerobic digestion (Zhao et al., 2016). However, taking into account both the physicochemical analysis as well as visual observation of tomato stalks, it was realized that these crop residues are very fibrous, which could cause serious operating problems (blocking of pumps, valves etc.) in the subsequent anaerobic digestion experiments.

Even though wine marcs are characterized by sufficient amounts of carbohydrates, proteins and lipids, low anaerobic biodegradability is reported in literature (compared to other agro-industrial materials) (Nikolaidou et al., 2016), probably due to the extremely high percentage of lignin (42.64% in our study), which is a limiting factor for the anaerobic digestion process (Zhao et al., 2016). Therefore, corn silage, tomato husks, watermelon, malt, cattle manure, orange and olive pomace were chosen for the anaerobic digestion process due to various limitations of the non-selected substrates (such as high fiber content, low biodegradability etc.).

**Table 1.** Physicochemical characteristics of raw feedstocks

Parameters	Animal manure Crop residues				Agro-industrial residues				
	Cattle manure	Corn silage	Tomato stalks	Watermelon	Tomato husks	Wine marcs	Malt	Olive pomace	Orange peels
	(g L <sup>-1</sup> )	(g kg <sup>-1</sup> )	(g kg <sup>-1</sup> )	(g kg <sup>-1</sup> )	(g kg <sup>-1</sup> )	(g kg <sup>-1</sup> )	(g kg <sup>-1</sup> )	(g kg <sup>-1</sup> ) <sup>5</sup>	(g kg <sup>-1</sup> d.b.) <sup>6</sup>
	Average ± SD								min-max
pH	7.02 ± 0.01	4.95 ± 0.01	6.37 ± 0.03	4.55 ± 0.01	4.44 ± 0.01	4.09 ± 0.03	6.50 ± 0.03	4.86–6.45	3.42–4.47
Alkalinity <sup>1</sup>	11.18 ± 0.01	n.d. ±	n.d.	0.18 ± 0.01	n.d.	n.d.	n.d.	n.d.	1,950–2,062
t-COD	60.80 ± 2.25	332.96 ± 30.93	125.04 ± 36.31	75.64 ± 0.21	90.63 ± 25.58	184.21 ± 17.44	60.74 ± 0.99	n.d.	1,030–1,140
d-COD	20.97 ± 0.74	n.d.	n.d.	67.93 ± 0.94	n.d.	n.d. ±	n.d.	n.d.	n.d.
TS	45.83 ± 3.87	413.95 ± 7.78	274.56 ± 15.65	50.12 ± 5.49	320.82 ± 2.00	693.48 ± 3.43	250.11 ± 2.01	n.d.	151–281.60
VS	33.20 ± 2.92	394.29 ± 7.40	216.31 ± 16.37	44.17 ± 3.21	309.65 ± 1.77	619.06 ± 11.73	240.22 ± 1.65	n.d.	146–203.90
TSS	17.18 ± 1.09	n.d.	n.d.	7.56 ± 0.50	n.d.	n.d.	n.d.	n.d.	n.d.
VSS	14.09 ± 0.75	n.d.	n.d.	7.27 ± 0.37	n.d.	n.d.	n.d.	n.d.	n.d.
Humidity <sup>2</sup>	95.42 ± 0.39	58.60 ± 0.78	72.54 ± 1.57	94.99 ± 0.55	67.92 ± 0.20	30.65 ± 0.34	74.99 ± 0.20	48.20–64.50	71.84–84.90
t-CHO <sup>3</sup>	9.23 ± 1.41	221.96 ± 36.75	25.99 ± 2.40	58.05 ± 5.52	39.62 ± 1.16	55.04 ± 5.65	18.77 ± 2.97	46–146	n.d.
d-CHO <sup>3</sup>	0.55 ± 0.01	n.d.	n.d.	54.83 ± 2.56	n.d.	n.d.	n.d.	n.d.	n.d.
d-phenols <sup>4</sup>	1.01 ± 0.00	n.d.	n.d.	0.31 ± 0.02	n.d.	n.d.	n.d.	0.5–12.20	n.d.
TKN	3.21 ± 0.23	3.80 ± 0.06	3.85 ± 0.20	1.11 ± 0.18	10.45 ± 0.74	8.19 ± 0.85	6.53 ± 0.03	n.d.	11.67–13
Proteins	20.07 ± 1.46	23.76 ± 0.35	24.06 ± 1.23	6.91 ± 1.11	65.31 ± 4.62	51.20 ± 5.30	40.79 ± 0.17	n.d.	65.40–69.40
NH <sub>3</sub> -N	1.97 ± 0.02	0.58 ± 0.10	0.49 ± 0.03	0.07 ± 0.00	0.65 ± 0.02	1.04 ± 0.15	0.71 ± 0.03	n.d.	1.49–1.87
Fats and oils	1.67 ± 0.01	6.60 ± 0.49	5.47 ± 0.12	0.51 ± 0.11	13.98 ± 0.44	32.63 ± 0.29	5.96 ± 2.36	142–262	n.d.
t-P	4.05 ± 0.09	6.01 ± 0.09	6.85 ± 0.22	1.12 ± 0.07	6.79 ± 0.02	12.92 ± 0.18	6.57 ± 0.15	0.50–2.75	1.15–1.21
d-P	0.22 ± 0.01	n.d.	n.d.	1.12 ± 0.05	n.d.	n.d.	n.d.	n.d.	n.d.
Cellulose <sup>2</sup>	n.d.	19.48 ± 1.73	11.11 ± 0.31	n.d.	7.45 ± 0.80	16.51 ± 0.01	7.34 ± 0.68	16.50–22.80	20.03–22.43
Hemicellulose <sup>2</sup>	n.d.	5.16 ± 0.94	8.93 ± 0.49	n.d.	4.67 ± 2.02	16.72 ± 0.01	5.76 ± 0.29	19.10–38.70	11.65–12.50
Lignin <sup>2</sup>	n.d.	4.97 ± 0.08	6.49 ± 0.93	n.d.	12.53 ± 1.42	42.64 ± 0.69	3.35 ± 0.09	19.60–47.50	13.02–15.52

n.d.: not determined; <sup>1</sup>g CaCO<sub>3</sub> L<sup>-1</sup> or g CaCO<sub>3</sub> kg<sup>-1</sup>; <sup>2</sup>expressed as percentage; <sup>3</sup>measured as equivalent glucose; <sup>4</sup>measured as equivalent syringic acid; <sup>5</sup>values from Cayuela et al. (2006); López-Piñeiro et al. (2008); Ntougias et al. (2013); <sup>6</sup>values from Martin et al. (2018); Zema et al. (2018); Rokaya et al. (2019); Jiménez-Castro et al. (2020).

### Biochemical Methane Potential assays

The results of the BMP assays (expressed as mL CH<sub>4</sub> g VS<sub>added</sub><sup>-1</sup>) concerning the Northern part of Greece (namely the feedstocks of corn silage, cattle manure and malt) are presented in Table 2. The ratios of fresh matter and the corresponding VS ratios of the tested substrates, which were added to the vials after the DOE, are also presented in the same Table. In addition, the results of the BMP assays are illustrated in Fig. 1.

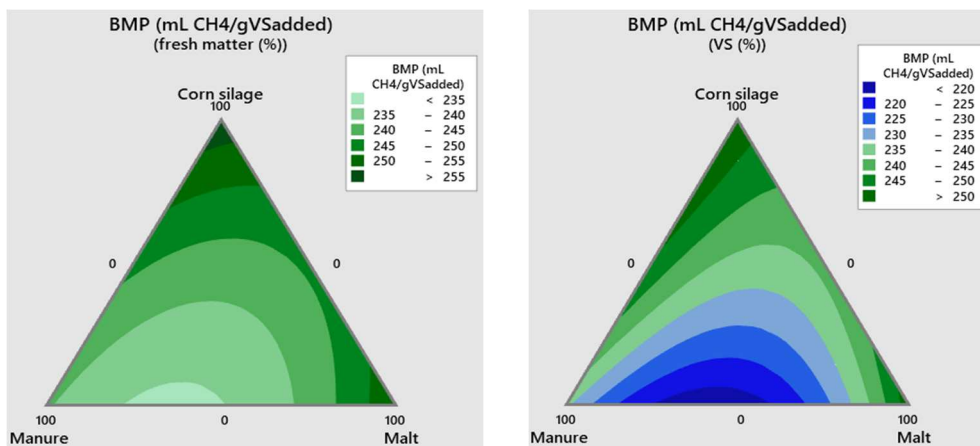
**Table 2.** Volume and VS ratios of mixtures, experimental and expected BMP values, expressed as mL CH<sub>4</sub> g VS<sub>added</sub><sup>-1</sup>

Corn silage	Cattle manure	Malt	Corn silage	Cattle manure	Malt	Measured BMP (mL CH <sub>4</sub> g VS <sub>added</sub> <sup>-1</sup> ± SD)	Expected BMP (mL CH <sub>4</sub> g VS <sub>added</sub> <sup>-1</sup> )
(%w/w fresh matter)			(%VS)				
0	0	100	0	0	100	255.23 ± 16.40	-
100	0	0	100	0	0	262.40 ± 34.37	-
0	100	0	0	100	0	236.08 ± 3.36	-
0	50	50	0	12.14	87.86	239.35 ± 11.17	252.90
50	0	50	62.14	0	37.86	259.25 ± 10.04	259.68
50	50	0	92.23	7.77	0	254.60 ± 7.28	260.36
33.33	33.33	33.33	59.05	4.97	35.98	238.60 ± 5.87	258.51
16.67	16.67	66.67	28.40	2.39	69.21	232.65 ± 10.96	256.81
66.67	16.67	16.67	85.22	1.79	12.98	226.70 ± 32.53	260.99
16.67	66.67	16.67	51.39	17.31	31.31	243.03 ± 8.94	255.60

The BMP assays for Northern Greece using residues of corn silage, malt and cattle manure indicate that the BMP of the mono-substrates are in agreement to other published works in literature. Specifically for corn silage, other values found in literature range from 204 to 410 mL CH<sub>4</sub> g VS<sub>added</sub><sup>-1</sup> (Bruni et al., 2010; Labatut et al., 2011; Mayer et al., 2014; Menardo et al., 2015; Roj-Rojewski et al., 2018), with the highest value being presented for experiments in which whole corn grains are used. Concerning the results of the current study, the spoilage of the corn silage combined with its long storage duration might have led to partial degradation of the easily biodegradable organic compounds, resulting thus in a decreased BMP yield. In addition, the literature values for malt varied from 64 mL CH<sub>4</sub> g VS<sub>removed</sub><sup>-1</sup> to 366 mL CH<sub>4</sub> g VS<sub>added</sub><sup>-1</sup> (Peces et al., 2015; Diego- Díaz et al., 2018), with the values of the present study being close enough to the aforementioned yields (approximately 255 mL CH<sub>4</sub> g VS<sub>added</sub><sup>-1</sup>). Regarding the experimental yield of cattle manure, the value of 236 mL CH<sub>4</sub> g VS<sub>added</sub><sup>-1</sup>, obtained in this study, is in accordance with other references (Krishania et al., 2013; Strömberg et al., 2014; Thygesen et al., 2014; Cu et al., 2015; Diaz et al., 2016; Wijaya et al., 2020).

As can be seen in Table 2 and Fig. 1, corn silage and malt exhibited the maximum BMP value. However, there are no statistically significant differences in the produced methane between the tested substrates, as described by the *P* values (*P* > 0.05) in Table 3. For this reason, these residues can be used in practice, either as mono-substrates or in mixtures, taking into account only their regional availability and the reactor's operating conditions, such as wet, semi-dry or dry anaerobic digestion, high-rate or conventional operation etc. These results further indicate that co-digestion of residues from the three main agro-waste categories produced in Northern Greece, i.e. crop and

industrial residues as well as animal manure, can be performed and be beneficial for the process performance in terms of process parameter adjustment (such as moisture content or nutrients ratio), without, however, observing any synergistic effects as the expected BMP values of the feedstock mixtures were equal or less to the mono-substrates' performance (Table 2); moreover, the highest BMP values were observed nearly to 100% malt or corn silage (Fig. 1).



**Figure 1.** Results of the BMP assays according to dry matter (left) and volatile solids percentage (right).

**Table 3.** ANOVA table for the cumulative methane yields

Source	DF	Seq SS	Adj SS	Adj MS	F-Value	P-Value
Regression	5	499.22	499.22	99.84	0.47	0.78
Linear	2	265.55	192.40	96.20	0.45	0.66
Quadratic	3	233.67	233.67	77.89	0.37	0.78
Corn silage*Manure	1	7.41	8.13	8.13	0.04	0.85
Corn silage*Malt	1	89.41	90.76	90.76	0.43	0.55
Manure*Malt	1	136.85	136.85	136.85	0.65	0.47
Residual Error	4	846.63	846.63	211.66		
Total	9	1,345.85				

According to literature, feedstocks such as manure or maize silage have already been co-digested with other waste streams like food wastes, whey or other agro-industrial residues, exhibiting various results (Hidalgo & Martín-Marroquín, 2015; Cárdenas-Cleves et al., 2018; Valenti et al., 2018; Vivekanand et al., 2018). It is widely hypothesized that co-digestion could lead to higher methane yields and thus synergistic effects, if higher buffering capacity, more balanced C/N ratio or higher readily biodegradable organic fraction could be achieved (Xie et al., 2017). In our study, even if the buffering capacity or the C/N ratio are improved due to the presence of manure, the absence of easily biodegradable compounds, such as monomers, is considered to be equally important for the lack of synergistic effects. The recalcitrant lignocellulosic content combined with the monomers limitation of the tested mixtures can strongly affect the bacterial community functions. The most possible explanation is that, as the hydrolytic bacteria exhibit

notably higher growth rates comparing to the methanogens (Lim et al., 2020), the presence of easily biodegradable monomers could lead to the hydrolytic microbial community enrichment and therefore to prospective increased yields.

The quadratic equation fitting to the experimental methane yields resulted in the regression equation described in Eq. 2. This equation simulates the productivity of methane for any proportion of the aforementioned substrates (fresh matter). The nonlinear terms in this equation indicate whether a substrate is affected by the other. Since these terms present low values, no statistically significant differences between the substrates were obtained.

$$Y \text{ (ml CH}_4\text{/g VS}_{added}) = 2.58\text{Corn silage} + 2.41\text{Manure} + 2.55\text{Malt} - 0.001\text{Corn silage} \cdot \text{Manure} - 0.004\text{Corn silage} \cdot \text{Malt} - 0.005\text{Manure} \cdot \text{Malt} \quad (2)$$

where  $Y$  is the expected BMP (mL CH<sub>4</sub> g VS<sub>added</sub><sup>-1</sup>) and *Corn silage*, *Manure*, *Malt* refer to the percentage (% of fresh mater) of corn silage, manure, and malt, respectively.

## CONCLUSIONS

Greece generates significant amounts of agricultural residues. Even if there are many promising valorisation methods, the anaerobic digestion process has been proven not only an environmentally friendly, but also a feasible renewable energy production method, over the recent years. Concerning the available residues examined, corn silage, malt and cattle manure seemed to be the most suitable feedstocks for anaerobic digestion, in the case of Northern Greece. The BMP results obtained in this study are in agreement with the methane potential of the tested mono-substrates reported in the existing literature. There were no statistically significant differences in the produced methane nor any synergistic effects on methane production during co-digestion of the tested feedstocks, in various ratios; as a result, the decision for energy valorisation of these residues, via anaerobic co-digestion, has to be based on their regional availability and the digester's operating conditions. More studies are yet required to unravel the potential of all available feedstocks, remaining still unexploited in Greek fields and agro-industries, for energy production through anaerobic co-digestion.

**ACKNOWLEDGEMENTS.** This article has derived and financed from project SYNAGRON, a joint RT&D project under **Greece – China Call for Proposals** launched under the auspices of the **Ministry of Science and Technology (MOST)** of the People's Republic of China and the Ministry of Development & Investments / **General Secretariat of Research and Technology (GSRT)** of the Hellenic Republic. Greece: Funded under European Regional Development Fund (ERDF) and National Resources (GSRT). China: Funded under Ministry of Science and Technology of the People's Republic of China.

## REFERENCES

- Alatzas, S., Moustakas, K., Malamis, D. & Vakalis, S. 2019. Biomass potential from agricultural waste for energetic utilization in Greece. *Energies* **12**, 1095.
- Angelidaki, I., Alves, M., Bolzonella, D., Borzacconi, L., Campos, J.L., Guwy, A.J., Kalyuzhnyi, S., Jenicek, P. & van Liers, J.B. 2009. Defining the biomethane potential (BMP) of solid organic wastes and energy crops: a proposed protocol for batch assays. *Water Science and Technology* **59**(5), 927–934.

- APHA AWWA WEF, 2012. Standard Methods for the Examination of Water and Wastewater, 20th edition. American Public Health Association, Washington DC, USA.
- Bruni, E., Jensen, A.P., Pedersen, E.S. & Angelidaki, I. 2010. Anaerobic digestion of maize focusing on variety, harvest time and pretreatment. *Applied Energy* **87**, 2212–2217.
- Cárdenas-Cleves, L.M., Marmolejo-Rebellón, L.F. & Torres-Lozada, P. 2018. Improvement of the biochemical methane potential of food waste by means of anaerobic co-digestion with swine manure. *Brazilian Journal of Chemical Engineering* **35**(4), 1219–1229.
- Cayuela, M.L., Sánchez-Monedero, M.A. & Roig, A. 2006. Evaluation of two different aeration systems for composting two-phase olive mill wastes. *Process Biochemistry* **41**, 616–623.
- Chynoweth, D.P., Turick, C.E., Owens, J.M., Jerger, D.E. & Peck, M.W. 1993. Biochemical methane potential of biomass and waste feedstocks. *Biomass Bioenerg.* **5**, 95–111.
- Cu, T.T.T., Nguyen, T.X., Triolo, J.M., Pedersen, L., Le, V.D., Le, P.D. & Sommer, S.G. 2015. Biogas Production from Vietnamese Animal Manure, Plant Residues and Organic Waste: Influence of Biomass Composition on Methane Yield. *Asian-Australasian Journal of Animal Sciences (AJAS)* **28**(2), 280–289.
- Dareioti, M.A. & Kornaros, M. 2015. Anaerobic mesophilic co-digestion of ensiled sorghum, cheese whey and liquid cow manure in a two-stage CSTR system: Effect of hydraulic retention time. *Bioresour. Technol.* **175**, 553–562. doi:10.1016/j.biortech.2014.10.102
- Dareioti, M.A. 2015. *Energy valorization of agroindustrial wastes and sweet sorghum for the production of gaseous biofuels through anaerobic digestion*. PhD Thesis, Department of Chemical Engineering, University of Patras, Patras, Greece, pp. 51–52.
- Dareioti, M.A., Vavouraki, A.I. & Kornaros, M. 2014. Effect of pH on the anaerobic acidogenesis of agroindustrial wastewaters for maximization of bio-hydrogen production: a lab-scale evaluation using batch tests. *Bioresour. Technol.* **162**, 218–227. doi:10.1016/j.biortech.2014.03.149
- Díaz, I., Figueroa-González, I., Miguel, J.A., Bonilla-Morte, L. & Quijano, G. 2016. Enhancing the biomethane potential of liquid dairy cow manure by addition of solid manure fractions. *Biotechnology Letters* **38**(12), 2097–2102.
- Diego-Díaz, B., Fernández-Rodríguez, J., Vita, A.I. & Peñasa, F.J. 2018. Biomethanization of solid wastes from the alcoholic beverage industry: Malt and sloe. Kinetic and microbiological analysis. *Chemical Engineering Journal* **334**, 650–656.
- Hellenic Statistical Authority, Statistics, Annual Agricultural Statistical Survey, <https://www.statistics.gr/en/statistics/agr>
- Hidalgo, D. & Martín-Marroquín, J.M. 2015. Biochemical methane potential of livestock and agri-food waste streams in the Castilla y León Region (Spain). *Food Research International* **73**, 226–233.
- Jiménez-Castro, M.P., Buller, L.S., Zoffreo, A., Timko, M.T. & Forster-Carneiro, T. 2020. Two-stage anaerobic digestion of orange peel without pre-treatment: Experimental evaluation and application to São Paulo state. *Journal of Environmental Chemical Engineering* **8**, 104035.
- Kashi, S., Satari, B., Lundin, M., Sárvári Horváth, I. & Othman, M. 2017. Application of a mixture design to identify the effects of substrates ratios and interactions on anaerobic co-digestion of municipal sludge, grease trap waste, and meat processing waste, *Journal of Environmental Chemical Engineering* **5**, 6156–6164.
- Krishania, M., Vijay, V.K. & Chandra, R. 2013. Methane fermentation and kinetics of wheat straw pretreated substrates co-digested with cattle manure in batch assay. *Energy* **57**, 359–367.
- Labatut, R.A., Angenent, L.T. & Scott, N.R. 2011. Biochemical methane potential and biodegradability of complex organic substrates. *Bioresour. Technol.* **102**, 2255–2264.



- Lais, A., Barampouti, E.M. & Mai, S. 2017. Challenges and opportunities of anaerobic digestion of agricultural residues and livestock manure in the region unit of Florina. In Athens: *proceedings of the 5th International Conference on Sustainable Solid Waste Management*, Greece, pp. 1–13.
- Lim, J.W., Park, T., Tong, Y.W. & Yu, Z. 2020. The microbiome driving anaerobic digestion and microbial analysis. *Advances in Bioenergy* **5**, 1–61.
- López-Piñeiro, A., Albarrán, A., Rato Nunes, J.M. & Barreto, C. 2008. Short and medium-term effects of two-phase olive mill waste application on olive grove production and soil properties under semiarid mediterranean conditions. *Bioresource Technology* **99**, 7982–7987.
- Martín, M.A., Fernández, R., Gutiérrez, M.C., Siles, J.A. 2018. Thermophilic anaerobic digestion of pre-treated orange peel: Modelling of methane production. *Process Safety and Environmental Protection* **117**, 245–253.
- Martín, M.A., Fernández, R., Gutiérrez, M.C., Siles, J.A. 2018. Thermophilic anaerobic digestion of pre-treated orange peel: Modelling of methane production. *Process Safety and Environmental Protection* **117**, 245–253.
- Mayer, F., Gerin, P.A., Noo, A., Foucart, G., Flammang, J., Lemaigre, S., Sinnaeve, G., Dardenne, P. & Delfosse, P. 2014. Assessment of factors influencing the biomethane yield of maize silages. *Bioresource Technology* **153**, 260–268.
- Menardo, S., Balsari, P., Tabacco, E. & Borreani, G. 2015. Effect of conservation time and the addition of lactic acid bacteria on the biogas and methane production of corn stalk silage. *BioEnergy Research* **8**, 1810–1823.
- Moustakas, K., Parmaxidou, P. & Vakalis, S. 2020. Anaerobic digestion for energy production from agricultural biomass waste in Greece: Capacity assessment for the region of Thessaly. *Energy* **191**, 116556.
- Nikolaïdou, E., Iossifidou, M., Tataki, V., Eftaxias, A., Aivasidis, A. & Diamantis, V. 2016. Energy Recovery and Treatment of Winery Wastes by a Compact Anaerobic Digester. *Waste Biomass Valor.* doi 10.1007/s12649-016-9541-1
- Ntougias, S., Bourtzis, K. & Tsiamis, G. 2013. The Microbiology of Olive Mill Wastes. *BioMed Research Internationl.* <http://dx.doi.org/10.1155/2013/784591>
- Owen, W.F., Stuckey, D.C. & Healy Jr., J.B. 1979. Bioassay for monitoring biochemical methane potential and anaerobic toxicity. *Water Res.* **13**, 485-492.
- Peces, M., Astals, S., Mata-Alvarez, J. 2015. Effect of moisture on pretreatment efficiency for anaerobic digestion of lignocellulosic substrates. *Waste Management* **46**, 189–196.
- Roj-Rojewski, S., Wysocka-Czubaszek, A., Czubaszek, R. & Banaszuk, P. 2018. Does Wetland Biomass Provide an Alternative to Maize in Biogas Generation? *Renewable Energy Sources: Engineering, Technology, Innovation.* Springer, Cham, 127–137.
- Rokaya, B., Kerroum, D., Hayat, Z., Panico, A., Ouafa, A. & Pirozzi, F. 2019. Biogas production by an anaerobic digestion process from orange peel waste and its improvement by limonene leaching: Investigation of H<sub>2</sub>O<sub>2</sub> pre-treatment effect. *Energy Sources, Part A: Recovery, Utilization, and Environmental Effects.* doi: 10.1080/15567036.2019.1692975
- Sagani, A., Hagidimitriou, M. & Dedoussis, V. 2019. Perennial tree pruning biomass waste exploitation for electricity generation: The perspective of Greece. *Sustainable Energy Technologies and Assessments* **31**, 77–85.
- Skoulou, V. & Zabaniotou, A. 2007. Investigation of agricultural and animal wastes in Greece and their allocation to potential application for energy production. *Renewable and Sustainable Energy Reviews* **11**, 1698–1719.
- Sluiter, A., Hames, B., Ruiz, R., Scarlata, C., Sluiter, J., Templeton, D. & Crocker, D. 2011. Determination of Structural Carbohydrates and Lignin in Biomass. National Renewable Energy Laboratory (NREL). *Laboratory Analytical Procedure (LAP).*

- Strömberg, S., Nistor, M. & Liu, J. 2014. Towards eliminating systematic errors caused by the experimental conditions in Biochemical Methane Potential (BMP) tests. *Waste Management* **34**, 1939–1948.
- Thygesen, O., Sommer, S.G., Shin, S.G. & Triolo, J.M. 2014. Residual biochemical methane potential (BMP) of concentrated digestate from full-scale biogas plants. *Fuel* **132**, 44–46.
- Tsigkou, K., Sakarika, M. & Kornaros, M. 2019. Inoculum origin and waste solid content influence the biochemical methane potential of olive mill wastewater under mesophilic and thermophilic conditions. *Biochemical Engineering Journal*. <https://doi.org/10.1016/j.bej.2019.107301>
- Tsigkou, K., Zaglis, D., Tsafarakidou, P., Zapanti, P., Manthos, G., Karamitou, K., Zafiri, C. & Kornaros, M. 2021. Expired food products and used disposable adult nappies mesophilic anaerobic co-digestion: Biochemical methane potential, feedstock pretreatment and two-stage system performance. *Renewable Energy* **168**, 309–318.
- Valenti, F., Zhong, Y., Sun, M., Porto, S.M.C., Toscano, A., Dale, B.E., Sibilla, F. & Liao, W. 2018. Anaerobic co-digestion of multiple agricultural residues to enhance biogas production in southern Italy. *Waste Management* **78**, 151–157.
- Vivekanand, V., Mulat, D.G., Eijsink, V.G.H. & Horn, S.J. 2018. Synergistic effects of anaerobic co-digestion of whey, manure and fish ensilage. *Bioresource technology* **249**, 35–41.
- Vlyssides, A., Mai, S. & Barampouti, E.M. 2015. Energy generation potential in Greece from agricultural residues and livestock manure by anaerobic digestion technology. *Waste Biomass Valor* **6**, 747–757.
- Wijaya, A.S., Jariyaboon, R., Reungsang, A. & Kongjan, P. 2020. Biochemical Methane Potential (BMP) of Cattle Manure, Chicken Manure, Rice Straw, and Hornwort in Mesophilic Mono-digestion. *International Journal of Integrated Engineering* **12**(3), 1–8.
- Xie, S., Wickham, R. & Nghiem, L.D. 2017. Synergistic effect from anaerobic co-digestion of sewage sludge and organic wastes. *International Biodeterioration & Biodegradation* **116**, 191–197.
- Zema, D.A., Fòlino, A., Zappia, G., Calabrò, P.S., Tamburino, V. & Zimbone, S.M. 2018. Anaerobic digestion of orange peel in a semi-continuous pilot plant: An environmentally sound way of citrus waste management in agro-ecosystems. *Science of the Total Environment* **630**, 401–408.
- Zhao, C., Yan, H., Liu, Y., Huang, Y., Zhang, R., Chen, C. & Liu, G. 2016. Bio-energy conversion performance, biodegradability, and kinetic analysis of different fruit residues during discontinuous anaerobic digestion. *Waste Management* **52**, 295–301.

## Theoretical research into directional stability of trailed tandem- type disk harrow

V. Bulgakov<sup>1</sup>, J. Olt<sup>2,\*</sup>, V. Nadykto<sup>3</sup>, V. Volskiy<sup>4</sup>, S. Polishchuk<sup>5</sup>,  
A. Aboltins<sup>6</sup> and H. Beloev<sup>7</sup>

<sup>1</sup>National University of Life and Environmental Sciences of Ukraine, 15 Heroyiv Oborony Str., UA 03041 Kyiv, Ukraine

<sup>2</sup>Estonian University of Life Sciences, Institute of Technology, 56 Kreutzwaldi Str., EE 51006 Tartu, Estonia

<sup>3</sup>Dmytro Motorny Tavria State Agrotechnological University, 18<sup>B</sup> Khmelnytsky Ave, UA 72310 Melitopol, Zaporozhye Region, Ukraine

<sup>4</sup>National Scientific Centre, Institute for Agricultural Engineering and Electrification, 11 Vokzalna Str., Glevakcha 1, Vasylykiv District, UA 08631 Kyiv Region, Ukraine

<sup>5</sup>National Scientific Centre, Institute of Agriculture of NAAS of Ukraine, 2<sup>b</sup>, Mashinobudivnikiv Str., Chabany vil., Kyiv-Svyatoshin Dist., UA 08162, Kyiv Region, Ukraine

<sup>6</sup>Latvia University of Life Sciences and Technologies, Cakstes Blvd. 5, LV 3001 Jelgava, Latvia

<sup>7</sup>University of Ruse “Angel Kanchev”, 5, Studentska Str., BG 7017, Ruse, Bulgaria

\*Correspondence: [jyri.olt@emu.ee](mailto:jyri.olt@emu.ee)

Received: August 27<sup>th</sup>, 2021; Accepted: October 6<sup>th</sup>, 2021; Published: October 7<sup>th</sup>, 2021

**Abstract.** Disking is one of the methods of soil cultivation, provides its effective crumbling, loosening, partial mixing and soil inversion. This ensures that crop residues on the soil surface are shredded and intermixing with loosened soil particles. Since, in addition to crop stubble, weeds are also counted as crop residues, soil disking, along with the use of herbicides, is often regarded as the most effective method of controlling the weediness of the agricultural background. Despite the fact that numerous studies on the disk harrow working process are available, insufficient attention has been paid to the study of the stability of harrow machine-tractor units, especially trailed ones. The purpose of this study is to establish the theoretical patterns that would provide for selecting the trailed disk harrow parameters that ensure the desired directional stability of the implement, which, in its turn, helps to achieve the desired qualitative performance of the disk harrowing machine-tractor unit. The principles of the theory agricultural machine, analytical mechanics, higher mathematics, as well as methods of PC-assisted numerical calculations have been used. According to the results of the study, it has been established that sufficient directional stability of the trailed disk harrow can be ensured if its working width  $B$ , the distance from the hitch point to the centre of resistance (parameter  $d$ ) and the operating speed  $V_0$  are properly selected. Determining the above-mentioned parameters of the disk harrow with the use of the obtained new analytical relations ensures achieving just their optimal combination, which provides for the maximum field productivity of the harrow machine-tractor unit with the satisfactory stability of disk harrow movement in the horizontal plane.

**Key words:** disk harrow, dissipation; quasi-elasticity, speed, stability, working width.

## INTRODUCTION

One of the methods of soil cultivation, providing good crumbling, loosening, partial mixing and soil inversion, is disking operation. If there are plant residues on the soil surface, they are effectively shredded and involved in the process of intermixing with loosened soil particles. Since, in addition to crop stubble, crop residues include weeds, soil disking, along with the use of herbicides, is often seen as a method of controlling the weediness of agricultural background (Knezevic et al., 2003; Balsari et al., 2021).

Soil disking, as is known, is performed by trailed or mounted (sometimes semi-mounted) disk harrows. Scientists all over the world pay a lot of attention to the rational choice of their design parameters. After careful analysis, the bulk of the results obtained in the completed research can be divided into two groups.

The first and more numerous of them are studies of the influence of the design parameters and operating mode of the disk harrow on the draft-energy performance of the tillage unit.

Ranjbar et al. (2013) studied the effect of disk harrow speed on its draft resistance. The speed of the tillage unit varied from 0.80 to 1.98 m s<sup>-1</sup>. In addition, soil moisture (11–23%) and tillage depth (4–16 cm) were variables.

The same goal was pursued by Kogut et al. (2016). The researchers changed the angle of the harrow discs in the horizontal (12–20°) and vertical (7–15°) planes at different values of tillage depth and working speed of the tillage unit.

The influence of the disk harrow tool setting angle in the horizontal plane (when installed up to 30°), the operating speed (2.1–3.1 m s<sup>-1</sup>) and the disk depth (6–18 cm) on the disk draft resistance was studied by Bulgakov et al. (2019).

In a study by Priporov & Priporov (2021) when measuring the draft resistance of harrows, the authors determined the specific value of this parameter per meter of the working width of the tillage tool. Similar results were obtained by Serrano et al. (2008) and Serrano & Peça, 2008. The working width of the disk harrow did not exceed 4 m, and its operating speed started from a rather small value - 0.8 m s<sup>-1</sup>.

In addition to estimating the draft resistance of the disk harrow, researchers have studied the effect of changes in its parameters and mode of operation on the fuel consumption of the wheeled tractor used and the slipping of its wheels (Serrano et al., 2003 and 2007; Salokhe et al., 2010).

In addition to the traditional arrangement of the disk harrow, variants of combining different working tools in one design have been investigated. For example, in Javadi & Hahiahmad (2006) the option of combining disks with rollers was considered. There have been studies of harrow designs, in which the front row of the tools has an active drive and the rear row has a passive drive (Upadhyay & Raheman, 2018). The disk harrow parameters studied were the angles of inclination of the tools in the horizontal plane, as well as the depth of tillage and soil hardness (cone index). The presence of actively driven disks in some harrow designs made it necessary to study the effect of the mode of their rotation on the draft resistance of the harrow, as well as the torque and power required to drive these working tools.

In addition to harrows, the use of spherical working tools was investigated in disk ploughs (Ranjbarian et al., 2017). The tillage depth did not exceed 23 cm, and the movement speed of the ploughing unit was, in our opinion, extremely low: 0.5–1.1 m s<sup>-1</sup>.

The second direction of research on disk harrows is devoted to the study of the influence of the design parameters and operating modes of these implements on the quality of tillage. In the work (Damanauskas et al., 2019) the process of quality of chopping and incorporation winter rape stubble into the soil was investigated. The studied parameters were disk setting angles in horizontal plane (10–20°), tillage depth (5–8 cm) and working speed of the harrow (1.4–3.6 m s<sup>-1</sup>). The results of almost similar research problem were presented in the article (Aykas et al., 2005).

The positioning of disk working tools on the harrow frame provides for their movement in the soil with a certain overlap. The value of this parameter in relation to the angles of inclination of the disk tool in the horizontal and vertical projection planes is analysed in the work (Zhuk & Sokht, 2018).

From the above analysis, it is easy to see that among the numerous scientific studies devoted to disk implements, there are almost no works aimed at substantiating the optimal value of their working width (parameter *B*). Especially in combination with the establishing the optimal relation between this design parameter and the desired value of the working speed of the disking machine-tractor unit (parameter *V*). While that is very important, because the right combination of parameters *B* and *V* allows you to achieve optimum field productivity of the tillage machine (*W*).

The attempt to increase the *W* value by increasing the value of the *B* parameter encourages engineers to create trailed machines. And it is quite logical, because an increase in the working width of any agricultural machine is associated with a corresponding increase in its weight. And the greater the value of the latter is, the more problematic it is to use such a machine in the tractor-mounted configuration.

It should be emphasized that the use of wide-span trailed agricultural machines requires a careful study of their stability in the horizontal plane (Bulgakov et al., 2016, 2017), especially at relatively high (more than 2.5 m s<sup>-1</sup>) speeds of the machine-tractor unit.

The problem is that the increase in the linear dimensions and the resulting increase in the masses, moments of inertia of trailed machines together with the increase in working speeds of their movement leads to a significant change in the dynamic properties of the entire machine-tractor unit. In some cases, the latter can acquire the properties of a mechanical oscillating system with reduced directional stability. As a result, this definitely leads to a decrease in the quality of the technological operation performed by this machine-tractor unit. When disking the soil, this can manifest itself in the presence of blunders in the field, increased overlap of the cultivated area, undesirable type of the course stability of the used aggregate tractor and the associated increased fuel consumption, etc.

Once again emphasizing and understanding the importance of this problem, the authors, however, could not find the scientific research results related to the study of the stability of harrow machine-tractor units, first of all, trailed ones.

In view of the above, the purpose of this study is to establish theoretical patterns that allow to select the values of speed and working width of the trailed disk harrow that ensure its desired directional stability. The solution of such a problem is one of the main

conditions ensuring the high-quality performance of the technological process carried out by the machine.

## MATERIALS AND METHODS

Initially, the assumption is made that the trailed tandem type (with an X frame) disk harrow as a dynamic system performs plane-parallel motion only in the horizontal plane. For analytical study of the trailed disk harrow movement, it is necessary to generate the differential equation of its movement relative to the point of its attachment to the carrying tractor. Fig 1 shows the equivalent diagram of such disk harrow movement, considering the movement of all its points in the horizontal plane. In this case, in first approximation, it is assumed that the point of connection of the disk harrow to the wheeled tractor (point  $S$ ), with which the movable reference system  $YOX$ , is connected, moves linearly and uniformly at speed  $\vec{V}_o$ , the modulus of which is  $V_o = \text{const}$  (Fig. 1).

All external forces acting on a given dynamic system are represented by the resultant vector  $\vec{R}$ . It is applied at the centre of resistance of the harrow, i.e., at point  $K$  (Fig. 1) and determines the direction of the absolute velocity  $\vec{V}_a$  of this point.

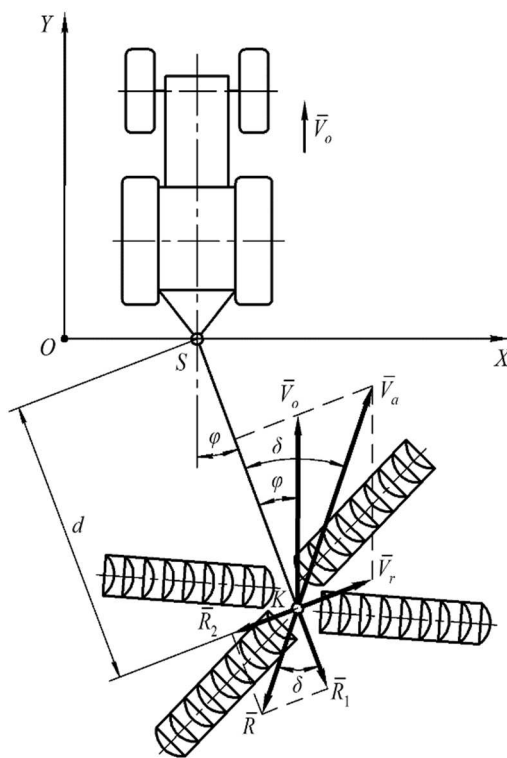
In the vector representation  $\vec{V}_a$  is the geometric sum of the translational  $\vec{V}_o$  and relative  $\vec{V}_r$  speeds of the disk harrow resistance centre movement. The modulus of the latter is equal to:

$$V_r = \dot{\varphi} \cdot d, \quad (1)$$

where  $d$  – the distance between the disk harrow's hitching point (point  $S$ , Fig. 1) and the centre of its resistance (point  $K$ ).

The result of the relative movement of the point  $K$  is the horizontal rotation of the harrow relative to the point of its attachment to the aggregating tractor. A quantitative measure of this rotation is the angle  $\varphi$  (Fig. 1).

As follows from the analysis of Fig. 1, the vector of absolute speed of the disk harrow's centre of resistance  $\vec{V}_a$  makes an angle  $\delta$  with its trailing device (line  $SK$ ). It is easy to see that, given the smallness of the angles  $\varphi$  and  $\delta$  and using expression (1), the value of  $\tan \delta$  will be equal to:



**Figure 1.** Equivalent diagram movement performed by trailed tandem type disk harrow in the horizontal plane.

$$\tan \delta \approx \delta \approx \frac{V_r + V_o \cdot \sin \varphi}{V_o \cdot \cos \varphi} = \frac{\dot{\varphi} \cdot d + V_o \cdot \varphi}{V_o} = \frac{\dot{\varphi} \cdot d}{V_o} + \varphi. \quad (2)$$

The resultant force vector  $\bar{R}$  (Fig. 1) is conveniently represented as the geometrical sum of two components: longitudinal  $\bar{R}_1$  and transverse  $\bar{R}_2$ . The first can be expressed by the following composition:

$$R_1 = K_s \cdot B, \quad (3)$$

where  $K_s$  – specific draft resistance of the harrow,  $\text{kN m}^{-1}$ ;  $B$  – disk harrow working width, m.

As for the force  $\bar{R}_2$ , it can be determined from the following relation (Fig. 1):

$$R_2 = R_1 \cdot \tan \delta. \quad (4)$$

Taking into account relations (2), (3) and (4), we finally have:

$$R_2 = K_s \cdot B \cdot \left( \frac{\dot{\varphi} \cdot d}{V_o} + \varphi \right). \quad (5)$$

The differential equation that describes the independent rotational motion of the disk harrow relative to the point  $S$  of its attachment to the aggregating tractor is:

$$J_o \cdot \ddot{\varphi} = \Sigma \bar{M}_{(S)}, \quad (6)$$

where  $J_o$  – moment of inertia of the disk harrow relative to the vertical axis passing through the point  $S$ ;  $\Sigma \bar{M}_{(S)}$  – sum of moments of external forces acting on the harrow relative to the point  $S$ .

As follows from the equivalent diagram shown in Fig. 1:

$$\Sigma \bar{M}_{(S)} = -R_2 \cdot d, \quad (7)$$

or taking into account relation (4):

$$\Sigma \bar{M}_{(S)} = -K_s \cdot B \cdot d \cdot \left( \frac{\dot{\varphi} \cdot d}{V_o} + \varphi \right). \quad (8)$$

The value of the moment of inertia  $J_o$  can be calculated with sufficient accuracy from the following relationship:

$$J_o = \frac{m}{3} \cdot (13d^2 + 4b^2 + a^2), \quad (9)$$

where  $m, b, a$  – mass (kg), length (m) and width (m) of one section of the disk harrow, respectively.

After substituting the obtained expressions (8) and (9) into (6) and performing appropriate transformations, we finally obtain the differential equation of motion, i.e. the mathematical model of the trailed disk harrow rotary motion, in the following form:

$$\ddot{\varphi} + 2n \cdot \dot{\varphi} + k^2 \cdot \varphi = 0, \quad (10)$$

where  $n = \frac{K_s \cdot B \cdot d^2}{2J_o \cdot V_o}$ ;  $k^2 = \frac{K_s \cdot B \cdot d}{J_o}$ .

It should be noted that the coefficient  $n$  characterizes the dissipative properties of the dynamic system and the coefficient  $k^2$  – characterizes the quasi-elastic ones. Since the values of these coefficients are always positive, the oscillatory motion of the trailed harrow, as a dynamic system, is stable. However, this stability can be various. First of

all, it depends on the roots of the characteristic Eq. (10). In this case there can be three variants of them. Namely:

$$\lambda_{1,2} = -n \pm i\sqrt{n^2 - k^2} : \text{if } n^2 < k^2; \quad (11)$$

$$\lambda_{1,2} = -n \pm \sqrt{n^2 - k^2} : \text{if } n^2 > k^2; \quad (12)$$

$$\lambda_{1,2} = -n : \text{if } n^2 = k^2, \quad (13)$$

where  $i = \sqrt{-1}$ .

Let us consider these three cases one by one. Due to the presence of the complex component, the solution of relation (11) represents a stable (i.e., damped), but still oscillatory motion of the trailed harrow relative to its equilibrium position.

The roots defined by expressions (12) and (13) belong to the solution of Eq. (10) in this form:

$$\varphi = e^{-nt} \cdot (K_1 \cdot e^{\sqrt{n^2 - k^2}t} + K_2 \cdot e^{-\sqrt{n^2 - k^2}t}), \quad (14)$$

where  $K_1, K_2$  – integration constants;  $t$  – time.

From the analysis of Eq. (14), it follows that at time  $t = 0$  some initial angle  $\varphi_0$  of disk harrow's deviation from the equilibrium state is related to the integration constants  $K_1$  and  $K_2$  in accordance with the following expression:

$$\varphi = \varphi_0 = K_1 + K_2. \quad (15)$$

At the same moment of time (i.e., at  $t = 0$ ) another relation is also true:

$$\dot{\varphi} = K_1 \cdot (\sqrt{n^2 - k^2} - n) - K_2 \cdot (\sqrt{n^2 - k^2} + n) = 0. \quad (16)$$

The joint solution of equations (15) and (16) allows us to determine the integration constants:

$$K_1 = \varphi_0 \cdot \frac{\sqrt{n^2 - k^2} + n}{2 \cdot \sqrt{n^2 - k^2}}; \quad K_2 = \varphi_0 \cdot \frac{\sqrt{n^2 - k^2} - n}{2 \cdot \sqrt{n^2 - k^2}}.$$

After substituting these constants into Eq. (14), we obtain the solution to the mathematical model (10) in the following form:

$$\varphi = \frac{\varphi_0}{2 \cdot A} \cdot e^{-nt} \cdot [(A + n) \cdot e^{At} + (A - n) \cdot e^{-At}], \quad (17)$$

where  $A = \sqrt{n^2 - k^2}$ .

Relation (17) describes the damped aperiodic motion of the considered dynamic system. Obviously, it is more preferable, than the oscillatory motion.

The roots defined by expression (12) of Eq. (17) will occur if the following condition is met:

$$n^2 = \frac{(K_s \cdot B)^2 \cdot d^4}{4J_o^2 \cdot V_o^2} \geq k^2 = \frac{K_s \cdot B \cdot d}{J_o}. \quad (18)$$

From the analysis of the obtained expression (18), it follows that the movement speed  $V_o$  of the disk harrow tilling unit should not exceed the value determined by this expression:

$$V_o \leq \frac{d}{2} \cdot \sqrt{\frac{3K_s \cdot B \cdot d}{m \cdot (13d^2 + 4b^2 + a^2)}}. \quad (19)$$



The obtained Eq. (19), as we see, includes such an important construction parameter of the disk harrow as its working width  $B$ . In this case, in conjunction with the speed  $V_o$  of working movement, it also determines such an indicator as the field productivity  $W$  of this tillage machine. In analytical form it looks as follows (Boson et al., 2019):

$$W = 0.36 \cdot B \cdot V_o. \quad (20)$$

The optimal value of the disk harrow working width  $B$  can be determined by taking into account the following relation of partial derivatives:

$$\frac{\frac{\partial W}{\partial V_o}}{\frac{\partial N_e}{\partial V_o}} = \frac{\frac{\partial W}{\partial B}}{\frac{\partial N_e}{\partial B}}, \quad (21)$$

where  $N_e$  – engine power of the used aggregating tractor, kW.

It is known from tractor theory (Macmillan, 2002) that:

$$N_e = \frac{(K_s \cdot B + f \cdot G) \cdot V_o}{\eta_t \cdot (1 - \delta)}, \quad (22)$$

where  $f$  – rolling resistance coefficient;  $G$ ,  $\eta_t$ ,  $\delta$  – operating gravity force (kN), transmission efficiency and drive wheel slip of the used wheeled tractor, respectively.

According to the up-to-date approaches to the determination of the value of the parameter  $\delta$  (Nadykto et al., 2015), we take the linear pattern of its change in the following form is assumed:

$$\delta = k + k_1 \cdot \frac{K_s \cdot B}{G}, \quad (23)$$

where  $k$ ,  $k_1$  – approximation constants of relation of slipping of the tractor wheels and the draft force generated by the tractor.

Taking into account expression (23), relation (22) has the following form:

$$N_e = \frac{(K_s \cdot B + f \cdot G) \cdot V_o \cdot G}{\eta_t \cdot [G(1 - k) - k_1 \cdot K_s \cdot B]}. \quad (24)$$

After determining the partial derivatives  $\frac{\partial W}{\partial V_o}$ ,  $\frac{\partial W}{\partial B}$ ,  $\frac{\partial N_e}{\partial V_o}$ ,  $\frac{\partial N_e}{\partial B}$ , then substituting these expressions into (21) and performing appropriate transformations, we obtain a relationship that allows us to determine the optimal working width  $B$  of the disk harrow. We have:

$$C_3 \cdot B^3 + C_2 \cdot B^2 + C_1 \cdot B + C = 0, \quad (25)$$

where  $C_3 = K_s^3 \cdot k_1^2 \cdot G$ ;

$$C_2 = -(K_s \cdot G)^2 \cdot (1 - k);$$

$$C_1 = -K_s \cdot k_1 \cdot f \cdot G^3 \cdot (1 - k);$$

$$C = G^4 \cdot f \cdot (1 - k)^2.$$

Thus, all the analytical expressions determine the relations between the parameters of the considered dynamic system have been obtained. The application of these expressions make it possible in practice to determine the optimal values of the said parameters.

As an example of applying the obtained theoretical results, let us consider a machine-tractor unit for soil disking on the basis of the aggregating wheeled tractor of class 3 with a nominal drawbar pull of 30 kN. Such tractor with 4WD wheel arrangement and 23.1R26 tires has the following parameters: operational gravity  $G = 81$  kN; engine

power  $N_c = 135$  kW; transmission efficiency  $\eta_{tr} = 0.93$ ; approximation constants of tractor wheels slipping vs. drawbar pull  $k = 0.001$  and  $k_1 = 0.450$ .

The disk harrow considered in the theoretical studies has the following values of its design parameters:  $m = 850$  kg;  $d = 4.8$  m;  $a = 2.2$  m;  $b = 0.8$  m. These design parameters are averaged for the family of those trailed disk harrows that in practice are used with the aforementioned tractor with a nominal drawbar pull of 30 kN.

Many years of practice have shown that the disking machine-tractor unit is most often used on agricultural background, for which the average value of the coefficient of to rolling resistance is  $f = 0.12$ . In this case, the specific resistance coefficient of disk harrow  $K_s$  can vary within range of 5.5-7.0  $\text{kN m}^{-1}$ . In principle, this corresponds to the experimental data presented in (Serrano & Peça, 2008).

Numerical solution of received analytical expressions (17), (18), (19) and (25) has been carried out with the use of the PC program developed by authors. This made it possible to plot the graphical relations between the parameters of the considered dynamic system, as presented in Fig. 2 – Fig. 7.

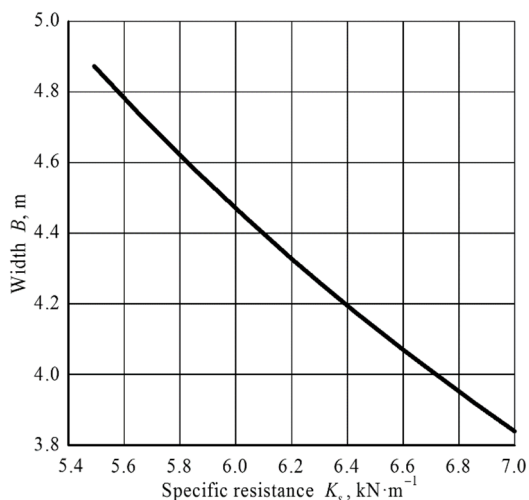
In the theoretical calculations of the relation (17), the initial deviation of the trailed harrow from the state of equilibrium was taken equal to  $\varphi_0 = 3^\circ$ . As is known from practice, in the real conditions of operating this tillage tool, the value of this angle does not exceed  $5^\circ$ .

## RESULTS AND DISCUSSION

The analysis of solution of equations (18) and (22) shows that with increase of  $K_s$  from 5.5 to 7.0  $\text{kN m}^{-1}$  the optimal value of disk harrow working width  $B$  decreases (Fig. 2).

But the change in the parameter  $B$  occurs in such a way that the value of the product ( $B \cdot K_s$ ), which is the draft resistance of the disc harrow, remains almost at the same level. In this connection, the operating speed  $V_o$  of forward movement of the disk tillage machine, which satisfies the condition (19), is also constant and equal to  $2.86 \text{ m s}^{-1}$  (i. e.  $10.3 \text{ km h}^{-1}$ ). The required tractor engine power is 132 kW. This is quite realizable, because the nominal power of the tractor engine with a nominal drawbar pull of 30 kN can, as noted above, be 135.0 kW.

Increasing the speed  $V_o$  of the working movement of the tractor with disk harrow to a level of more than  $2.86 \text{ m s}^{-1}$  is technically possible, due to the consequent change in the value of the condition (18), the very nature of the relative motion performed by the trailed tillage implement under consideration as a dynamic system will change (Fig. 3).



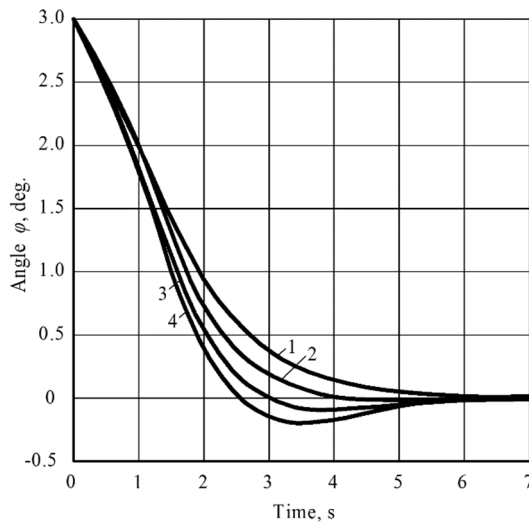
**Figure 2.** Relation of the working width  $B$  of the disc harrow on the value of  $K_s$ .

For example, condition (18) is fulfilled at speed equal to  $V_0 = 2.86 \text{ m s}^{-1}$ . Since in this case dissipative properties of the dynamic system, represented by the parameter  $n^2$ , prevail over quasi-elastic ones, then after the initial deviation of the harrow from the equilibrium state by  $3^\circ$  its aperiodic movement back to the initial position takes place.

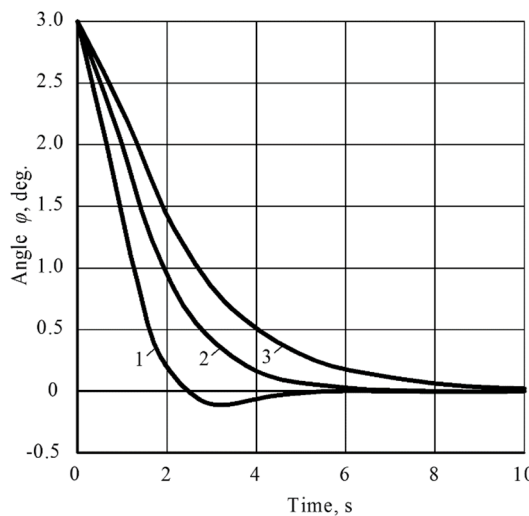
After increasing the working speed of the tillage machine up to  $V_0 = 3.36 \text{ m s}^{-1}$  condition (18) is violated. This means that the quasi-elastic properties of the system, represented by the coefficient  $k^2$ , become predominant in the considered dynamic system. As a result, the movement of the trailed disk harrow in relation to the point  $S$  (Fig. 1) becomes oscillatory. The higher the working speed of the cultivation unit (Fig. 3) is, the more these oscillations occur.

Analysis of equations (18) and (19) shows that the nature of the relative motion of the disc harrow is influenced to some extent, in addition to its working width  $B$ , by the moment of inertia  $J_0$ . The latter, as can be seen from expression (9), in its turn depends on such parameters as  $d$ ,  $m$ ,  $b$  and  $a$ . Of these, according to the results of our calculations, the first two (i.e.,  $d$  and  $m$ ) have a significant influence on the value of  $J_0$ . In this case, the influence of the parameter  $d$  is more tangible if changes in the mass of the harrow are considered within such limits, which do not lead to changes in its working width  $B$ .

It should be noted that the trailed disk harrow in terms of mechanics is essentially a physical pendulum, the swing radius of which represented by the parameter  $d$  – the distance between the hitch point of the disk harrow (point  $S$ , Fig. 1) and the centre of its resistance (point  $K$ ). As the value of this parameter  $d$  decreases, the character of the relative motion of the disk harrow trends to change from asymptotically stable to oscillatory one (Fig. 4).



**Figure 3.** Dynamics of change in the disk harrow deviation angle  $\varphi$  at different forward speeds  $V_0$ : 1 –  $V_0 = 2.86 \text{ m s}^{-1}$ ; 2 –  $V_0 = 3.36 \text{ m s}^{-1}$ ; 3 –  $V_0 = 3.86 \text{ m s}^{-1}$ ; 4 –  $V_0 = 4.36 \text{ m s}^{-1}$ .



**Figure 4.** Dynamics of change in disk harrow deviation angle  $\varphi$  at different values of the parameter  $d$ : 1 –  $d = 2.8 \text{ m}$ ; 2 –  $d = 4.8 \text{ m}$ ; 3 –  $d = 6.8 \text{ m}$ .

This result is quite logical. As noted above, increasing the value of the parameter  $d$  leads to an increase in the moment of inertia of the disk harrow  $J_o$ . However, at first glance, it would seem that according to Eq. (18), this should cause a corresponding decrease in the values of the parameters  $n^2$  and  $k^2$ .

In reality, this is true only for the quasi-elastic coefficient (i.e.  $k^2$ ). For it, an increase in the parameter  $d$  leads to such an outstripping growth of the moment of inertia  $J_o$ , which eventually causes an intensive decrease in the value of the  $k^2$  (Fig. 5).

The nature of the change in the square of the dissipative parameter  $n^2$  in this case is quite different. Here, a similar increase in the value of the design parameter  $d$ , raised to the fourth degree [see expression (18)], significantly outpaces the growth of the value of the moment of inertia of the harrow  $J_o$ . As a result, as the value of  $d$  increases, the value of the parameter  $n^2$  also increases accordingly (Fig. 5). Because of the predominance of dissipative (i.e., scattering) properties in the dynamical system we are considering, it becomes more prone to asymptotic motion after receiving an external deflecting perturbation.

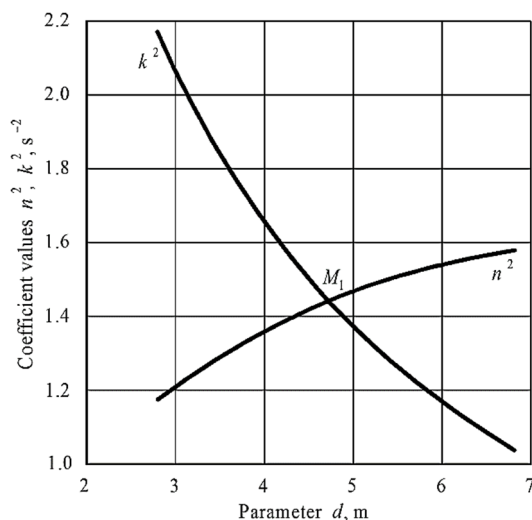
Conversely, reducing the distance between the hitch point and the centre of resistance of the disk harrow (parameter  $d$ ) can result in, as shown in Fig. 4, although stable, but still oscillatory nature of its relative motion in the horizontal plane of projections.

The limit value for the reduction of the parameter  $d$  can be easily determined by using the characteristic point  $M_1$  (Fig. 5). Its coordinates correspond to the conditions movement of the trailed disk harrow, in which the condition  $n^2 = k^2$  is true. In this case solving the Eq. (10) results in obtaining the roots defined by expression (13).

In fact, the abscissa of the point  $M_1$  reflects the value of the design parameter  $d$ , the decrease of which can cause the oscillatory behaviour of the trailed disk harrow, when it returns from the perturbed state to the position of stable equilibrium.

However, it this does not imply that in the real design of this tilling implement, the link length  $SK$  (Fig. 1) should be as long as possible. It should be remembered that an increase in the parameter  $d$  inevitably leads to an increase in the turning radius of the unit (Bulgakov et al., 2018) and its longitudinal dimension. And this is already an undesirable situation.

Moreover, a significant increase in the value of  $J_o$  as a result of increasing the value of the parameter  $d$  can lead to a deterioration in the damping conditions of the harrow angular oscillations during its return from the perturbed position to the initial equilibrium one.



**Figure 5.** Relation between coefficients  $n^2$  and  $k^2$  and parameter  $d$ .

Finding a compromise in this solution lies in selecting the value of  $d$  with due account for the condition (19), meeting which ensures the asymptotic character of trailed disk harrow's angular displacement in the horizontal plane.

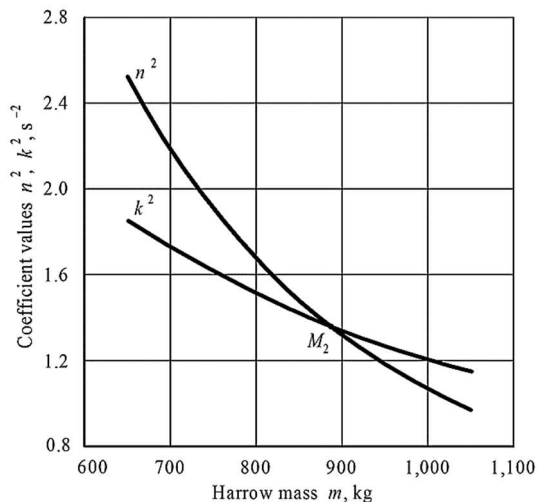
As emphasized above, increasing the value of the parameter  $m$  also affects the moment of inertia of the harrow  $J_o$ . However, as calculations show, it's effect is not as significant as that of the parameter  $d$ .

The effect of mass  $m$  on the coefficients  $n^2$  and  $k^2$  is qualitatively the same, but quantitatively it is different. As calculations show, in the whole range of the accepted values of the parameter  $m$ , the dissipative properties of the trailed harrow  $n^2$  decrease more intensively than the quasi-elastic ones  $k^2$  (Fig. 6).

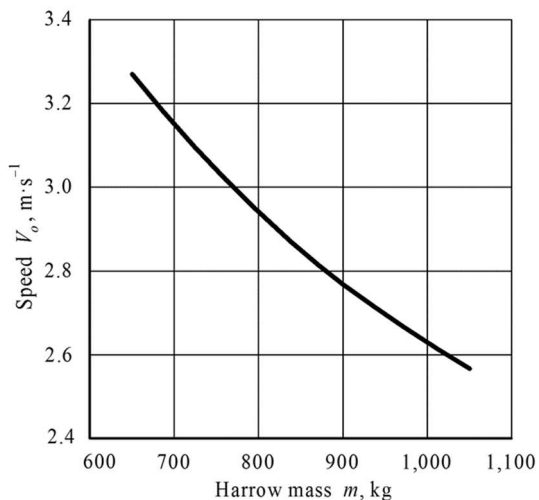
This results in obtaining the characteristic point  $M_2$ , which characterizes the condition  $n^2 = k^2$  and separates the zones of asymptotic and oscillatory character of the trailed harrow motion after its return from the deflected state to the initial equilibrium state. It is quite obvious that the first and more preferable of these zones is situated to the left of point  $M_2$ , since in it this zone the dissipative properties of the dynamical system in question prevail over the quasi-elastic ones. That causes the situation, where external disturbances are unable to generate the unwanted oscillatory character of the relative motion of the trailed disk harrow.

As follows from the analysis of the graphical dependences presented in Fig. 6, to ensure the asymptotic character of the perturbed motion of the considered trailed harrow, its design parameter  $m$ , defined by abscissa of the point  $M_2$ , should not exceed 880 kg. Otherwise, i.e., when selecting a larger value of mass  $m$ , the speed  $V_o$  of forward movement of the disk harrow should be reduced. The graphical representation of this process is shown in Fig. 7.

When making the final selection of disk harrow mass, it should be kept in mind that increasing the value of this parameter increases the inertial properties of this dynamic system. In a



**Figure 6.** Relation between coefficients  $n^2$  and  $k^2$  and parameter  $m$ .



**Figure 7.** Relation between optimum speed  $V_o$  of the disk harrow on its mass.

certain way, this increases its resistance to the influence of external disturbing (deviating) factors. At the same time, a dynamic system with a large mass is much more difficult to bring out of the state of oscillatory motion.

## CONCLUSIONS

The satisfactory directional stability of the trailed disk harrow can be ensured by proper selection of its working width  $B$ , the distance from the hitch point to the centre of resistance (parameter  $d$ ) and the operating speed  $V_0$ .

The optimum combination of the disk harrow parameters  $B$ ,  $d$  and  $V_0$ , which provides for the maximum field productivity of the harrow machine-tractor unit with satisfactory stability of the disk harrow movement in the horizontal plane, is achieved, when these parameters are determined using the obtained new analytical relations (18), (19) and (25).

The theoretically obtained mathematical relations (18), (19) and (25) can be used for solving similar problems in case of any other symmetrical machine-tractor unit with a trailed process part.

## REFERENCES

- Aykas, E., Cakir, E. & Gulsoylu, E. 2005. The effect of tillage parameters on the performance of the heavyduty offset disk harrow. *Asian J. Plant Sci.* **3**, 425–428.
- Balsari, P., Biglia, A., Comba, L., Sacco, D., Eloi Alcatrão, L., Varani, M., Mattetti, M., Barge, P., Tortia, C., Manzone, M., Gay, P. & Ricauda Aimonino, D. 2021. Performance analysis of a tractor - power harrow system under different working conditions. *Biosystem Engineering* **202**, 28–41. <https://doi.org/10.1016/j.biosystemseng.2020.11.009>
- Boson, E.S., Verniaev, O.V., Smirnov, I.I. & Sultan-Shach, E.G. 2019. *Theory, Construction and Calculation of Agricultural Machines*. 2<sup>nd</sup> Ed., Scientific Publisher, 810 pp. ISBN: 9789388399838
- Bulgakov, V., Adamchuk, V., Arak, M., Nadykto, V., Kyurchev, V. & Olt, J. 2016. Theory of vertical oscillations and dynamic stability of combined tractor-implement unit. *Agronomy Research* **14**(3), 689–710.
- Bulgakov, V., Adamchuk, V., Nadykto, V., Kistechok, O. & Olt, J. 2017. Theoretical research into the stability of motion of the ploughing tractor-implement unit operating on the ‘push-pull’ principle. *Agronomy Research* **15**(4), 1517–1529. doi: 10.15159/AR.17.069
- Bulgakov, V., Pascuzzi, S., Ivanovs, S. & Volskyi, V. 2019. Experimental Investigations in Draft Resistance of Spherical Working Tool of Disk Harrow. *Engineering for Rural Development* **18**, 144–152. <https://doi.org/10.22616/ERDev2019.18.N171>
- Bulgakov, V., Pascuzzi, S., Nadykto, V. & Ivanovs, S. 2018. A mathematical model of the plane-parallel movement of an asymmetric machine-and-tractor aggregate. *Agric.* **8**. <https://doi.org/10.3390/agriculture8100151>
- Damanauskas, V., Velykis, A. & Satkus, A. 2019. Efficiency of disc harrow adjustment for stubble tillage quality and fuel consumption. *Soil Tillage Res.* **194**, 104311. <https://doi.org/10.1016/J.STILL.2019.104311>
- Javadi, A. & Hahiahmad, A. 2006. Effect of a New Combined Implement for Reducing Secondary Tillage Operation. *Int. J. Agric. Biol.* **8**, 725–727.
- Knezevic, M., Đurkic, M. & Knezevic, I. 2003. Effects of pre-and post-emergence weed control on weed population and maize yield in different tillage systems. *Plant soil environ* **49**(5), 223–229.

- Kogut, Z., Sergiel, L. & Zurek, G. 2016. The effect of the disc setup angles and working depth on disc harrow working resistance. *Biosyst. Eng.* **151**, 328–337. <https://doi.org/10.1016/j.biosystemseng.2016.10.004>
- Macmillan, R.H. 2002. *The Mechanics of Tractor Implement Performance*. Theory and Worked Examples. University of Melbourne, 165 pp.
- Nadykto, V., Arak, M. & Olt, J. 2015. Theoretical research into the frictional slipping of wheel-type undercarriage taking into account the limitation of their impact on the soil. *Agronomy Research* **13**(1), 148–157.
- Priporov, E.V. & Priporov, I.E. 2021. Justification of parameters of a four-row disk harrow using the experiment planning method. *IOP Conf. Ser. Earth Environ. Sci.* **659**, 8–13. <https://doi.org/10.1088/1755-1315/659/1/012013>
- Ranjbar, I., Rashidi, M., Lehmal, H.F., Mirmoradi, M. & Abdolizadeh, E. 2013. Modeling of double action disc harrow draft force based on tillage depth and forward speed. *Middle East J. Sci. Res.* **17**, 1061–1067.
- Ranjbarian, S., Askari, M. & Jannatkah, J. 2017. Performance of tractor and tillage implements in clay soil. *J. Saudi Soc. Agric. Sci.* **16**, 154–162. <https://doi.org/10.1016/j.jssas.2015.05.003>
- Salokhe, V.M., Soni, P., Nalavade, P.P. & Niyamapa, T. 2010. Performance of Free Rolling and Powered Tillage Discs. *Soil Tillage Research* **109**, 87–93. <https://doi.org/10.1016/j.still.2010.05.004>
- Serrano, J.M. & Peça, J.O. 2008. The forward speed effect on draught force required to pull trailed disc harrows. *Spanish J. Agric. Res.* **6**, 182–188. <https://doi.org/10.5424/sjar/2008062-309>
- Serrano, J.M., Peça, J.O., Marques da Silva, J., Pinheiro, A. & Carvalho, M. 2007. Tractor energy requirements in disk harrow systems. *Biosyst. Eng.* **98**, 286–296. <https://doi.org/10.1016/j.biosystemseng.2007.08.002>
- Serrano, J.M., Peça, J.O., Pinheiro, A., Carvalho, M., Nunes, M., Ribeiro, L. & Santos, F. 2003. The Effect of Gang Angle of Offset Disc Harrows on Soil Tilth, Work Rate and Fuel Consumption. *Biosyst. Eng.* **84**, 171–176. [https://doi.org/10.1016/S1537-5110\(02\)00261-1](https://doi.org/10.1016/S1537-5110(02)00261-1)
- Serrano, J.M., Peça, J.O., Pinheiro, A.C. & Carvalho, M. 2008. Short communication. Evaluation of the energy requirements in tractor-disc harrow systems. *Spanish J. Agric. Res.* **6**, 205–209. <https://doi.org/10.5424/sjar/2008062-321>.
- Upadhyay, G. & Raheman, R. 2018. Performance of combined offset disc harrow (front active and rear passive set configuration) in soil bin. *Journal of Terramechanics* **78**, 27–37. <https://doi.org/10.1016/j.jterra.2018.04.002>
- Zhuk, A.F. & Sokht, K.A. 2018. Arrangement of Spherical Disks for Frontal Harrows. *Agric. Mach. Technol.* **12**, 41–43. <https://doi.org/10.22314/2073-7599-2018-12-4-53-56>

## **Evaluation of carbon, nitrogen, and oxygen isotope ratio measurement data for characterization of organically and conventionally cultivated spring barley (*Hordeum vulgare* L.) grain**

L. Buša<sup>1,\*</sup>, M. Bērtiņš<sup>1</sup>, A. Vīksna<sup>1</sup>, L. Legzdiņa<sup>2</sup> and D. Kobzarevs<sup>1</sup>

<sup>1</sup>University of Latvia, Faculty of Chemistry, Department of Analytical Chemistry, Jelgavas street 1, LV-1004 Riga, Latvia

<sup>2</sup>Institute of Agricultural Resources and Economics, Priekuli Research Centre, 2 Zinatnes street, LV-4126 Priekuli, Latvia

\*Correspondence: lauma.busa@lu.lv

Received: March 1<sup>st</sup>, 2021; Accepted: June 7<sup>th</sup>, 2021; Published: June 16<sup>th</sup>, 2021

**Abstract.** With the growing interest of public in the quality of their consumed food, organic produce has been steadily gaining an important place in everyday menus of our society. The growing demand has boosted organic farming and we have also seen the price difference between organic products and their conventional counterparts. It is important to the public to have security, that the food labelled ‘organic’ has really been grown according to the good practices of organic farming and that it has not received any chemical pesticides, herbicides, and synthetic fertilizers. Stable isotope ratios of crops from different crop management systems can help to answer these questions, as these values depend on the growing conditions, fertilizers used etc. In this study, 10 barley grain samples from conventional and organic crop management systems have been studied. Carbon, nitrogen and oxygen isotope ratios have been determined and the element content in the samples has been calculated. Student’s *t*-test has been performed to evaluate whether the differences between various parameters are significant. For potential clustering and discrimination of organic and conventional grains principal component analysis has been carried out. The PCA showed that no significant clustering can be observed, however the Student’s *t*-test for  $\delta^{15}\text{N}$  values confirmed that barley grown with green-manure fertilizers are significantly ( $p < 0.01$ ) enriched with the heavier nitrogen isotope. Furthermore, it has been concluded that the total element content of carbon and nitrogen in barley grains does not correlate with the stable isotope ratios and cannot help with discriminating of these samples.

**Key words:** barley, organic farming, grain, principal component analysis, stable isotopes, stable isotope ratio mass spectrometry.

### **INTRODUCTION**

With the growing world population, an important matter is providing enough food for affordable price. Cereal crops are a major food group that on average provides up to 50% of total everyday calorie intake worldwide (Hawkesford, 2014). To ensure the price



remains low enough, the crop yield needs to be elevated. This can be accomplished by developing new ways of fertilization of the land, in order to increase the yield (Zhang et al., 2017). The easiest way to achieve elevated crop yields is to use specifically designed fertilizers that contain all the key nutrients plants need. However, there is a growing demand for organically grown food, especially in wealthy countries. This growing interest in organic food has spiked both organic food production and its prices (Pawlewicz, 2020). From these factors comes also the interest of consumers to have confidence in the fact that the products being marketed as organically grown, really have not received any unwanted chemical fertilizers and pesticides. Therefore, novel analytical techniques are being used to characterize and differentiate between the conventionally and organically grown crops (Laursen et al., 2013).

Barley (*Hordeum vulgare* L.) is a member of the grass family and belongs to one of the most important groups of plants in the world, the *Triticeae* tribe, along with other important crops, such as wheat, rye and triticale (Von Bothmer & Komatsuda, 2011). Barley is one of the top five crops in the world, with the average production reaching over 140 million tons per year (Shewry & Ullrich, 2014). In the EU the barley production has been stable at around 60 million metric tons per year (European Union, 2021). Barley can be considered one of the most versatile crops, as it can be grown in areas with moderate average temperatures and precipitation and is considered to be a very tolerant crop towards drought (Shewry & Ullrich, 2014). Barley can be grown using different farming approaches, with the most popular being conventional farming where synthetic fertilizers, containing nutrients essential for plants, are used and organic farming where soil fertilization can be ensured in various ways. In this study, in the organic crop management system, green manure of legumes has been used. Because of the legumes ability to fix atmospheric nitrogen via roots and their substantial biomass, they are widely used as plants for green manure. The use of green manure can increase crop productivity and growth, along with reducing nitrate-nitrogen leaching risk (Dabin et al., 2016).

A very promising novel analytical technique used for the identification of organic production in the last decades has been stable isotope ratio mass spectrometry (SIRMS), as it allows to evaluate the input of fertilizers on the plants. Analysis of bulk  $\delta^{15}\text{N}$  in organically grown crops has shown the capability to discriminate between crops from conventional and organic farming (Novak et al., 2019). The  $\delta^{15}\text{N}$  values in fertilizers depend on their way of production. The synthetic fertilizers have nitrogen isotope ratios close to 0 ‰ since they have been produced from atmospheric nitrogen. While the nitrogen isotope ratios of various organic fertilizers (animal manure, compost etc.) are within the range of 4–6‰. Subsequently, the  $\delta^{15}\text{N}$  values change in the crops and can be determined using SIRMS (Mihailova et al., 2014). Previous studies have shown that depending on the fertilizer used, the stable isotope ratios of plants reflect the fertilizer  $\delta^{15}\text{N}$  values (higher  $^{15}\text{N}$  content in the fertilizer results in higher nitrogen isotope ratios of plants). However, the previous studies have mainly focused on the differences between synthetic and animal origin fertilizers (Bol et al., 2005; Mihailova et al., 2014). In this research, the organic produce was fertilised with green-manure (peas) that is less enriched with  $^{15}\text{N}$  if compared to animal manure, compost, etc.

In this study barley grain samples from conventional and organic crop management systems have been analysed to evaluate the possibility to discriminate between organically and conventionally grown grain based on their stable isotope ratio values and total carbon, nitrogen and oxygen content.

## MATERIALS AND METHODS

### Description of samples

The barley grain samples were cultivated and collected at Institute of Agricultural Resources and Economics, Priekuli Research Centre, during the year 2017. The field trials were established in two crop management systems - organic and conventional (hereinafter - B and C, respectively) in four replicates, the cultivation plots were positioned in a lattice pattern with an area of 12 m<sup>2</sup> each. Sowing rate was 400 germinating seeds per m<sup>2</sup>. The organic cultivation plot used in this study was established in the year 2015 when all use of synthetic fertilizers and pesticides was discontinued. In 2015 the organic cultivation plot was left fallow, followed by cultivation of rye as the forecrop and peas for green manure in 2016. No other types of fertilizers have been used in the organic cultivation plot. The conventional cultivation plot has been established for several decades. To characterise the soil, the pH<sub>KCl</sub> was measured, available potassium and phosphorus content assessed, and soil granulometric composition determined. The soil characteristics, forecrops and applied fertilizers are summarized in Table 1.

**Table 1.** Summary of soil characteristics and fertilizers used in the conventional and organic barley farming experimental fields at Priekuli Research Centre

Parameter	Crop management system	
	Conventional	Organic
pH <sub>KCl</sub>	5.3	5.9
Organic matter content, %	1.8	2.3
Available potassium (K <sub>2</sub> O), mg kg <sup>-1</sup>	143	167
Available phosphorus (P <sub>2</sub> O <sub>5</sub> ), mg kg <sup>-1</sup>	120	177
Soil group, granulometric composition	Sod-podzolic, sandy loam	Sod-podzolic, sandy loam
Forecrop	Potatoes	Peas for green manure
Complex fertilizer	N15-P15-K15	–
Nitrogen fertilizer	N33-P3	–
Nutrient doses in pure substance, kg ha <sup>-1</sup>	N108-P70-K66	–

Altogether 5 conventionally grown barley samples (BarlA-C to BarlE-C) and 5 organically grown barley samples (BarlA-B to BarlE-B) were analysed, where A, B, C, D, E is the same genotype (variety, mixture or population). A pooled sample of 100 grams was obtained by mixing equal parts of barley grains collected from each of four subplots of the crop management system. Before analysis, the samples were air-dried at 60 °C for 24 hours until constant mass of the samples was achieved. Five grams of each barley grain sample (including husk and bran) were dry ground using mixer mill (MM-400, Retsch, Germany) with steel balls at the frequency of 15 s<sup>-1</sup> for 5 minutes.

### Stable isotope analysis

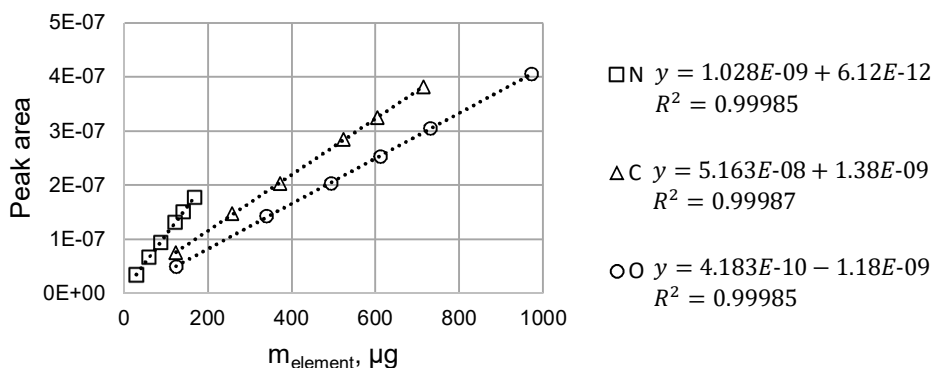
All samples were analysed by elemental analyser-continuous flow-stable isotope ratio mass spectrometry (EA-CF-SIRMS) using a Nu Horizon (Nu Instruments, United Kingdom) stable isotope mass spectrometer interfaced with an EA3024 (EuroVector, Italy) elemental analyser to determine carbon and nitrogen isotope ratios. For the determination of oxygen isotope ratios, the elemental analyser was additionally interfaced with HT-PyrOH unit (EuroVector, Italy).

1 mg of the milled barley grains were weighed into a small tin capsule (5 mm × 3.5 mm). Afterwards, the capsule was folded and compressed to a ball shape, in order to contain the sample and minimise air presence. An auto-sampler was used to introduce the prepared sample into elemental analyser. The stable carbon, nitrogen and oxygen isotopic composition were measured relative to the Vienna Pee Dee Belemnite (VPDB), atmospheric air (AIR) and Vienna Standard Mean Ocean Water (VSMOW) standards respectively. Each sample was analysed in duplicates and the average is reported.

The reference materials used for  $\delta^{13}\text{C}$  and  $\delta^{15}\text{N}$  measurements were L-glutamic acid USGS-40 ( $\delta^{13}\text{C}_{\text{VPDB}} = -26.39\text{‰}$ ;  $\delta^{15}\text{N}_{\text{AIR}} = -4.52\text{‰}$ ) and USGS-41 ( $\delta^{13}\text{C}_{\text{VPDB}} = 37.63\text{‰}$ ;  $\delta^{15}\text{N}_{\text{AIR}} = 47.57\text{‰}$ ), and benzoic acid IAEA-601 ( $\delta^{18}\text{O}_{\text{VSMOW}} = 23.14\text{‰}$ ) and IAEA-602 ( $\delta^{18}\text{O}_{\text{VSMOW}} = 71.28\text{‰}$ ) for the  $\delta^{18}\text{O}$  analysis.

### Determination of carbon, nitrogen and oxygen content

In order to determine the weight fraction of carbon, nitrogen and oxygen in barley grain samples, a calibration curve was constructed using the laboratory standards with known elemental composition: L-glutamic acid ( $w_{\text{C}}\% = 40.82\%$ ;  $w_{\text{N}}\% = 9.52\%$ ) and sucrose ( $w_{\text{O}}\% = 51.41\%$ ). The mass of an element in a sample is directly correlated with the peak area of gas produced during the combustion ( $\text{CO}_2$ ,  $\text{N}_2$  and  $\text{CO}$  for carbon, nitrogen and oxygen respectively). Calibration curves and their respective equations are summarized in Fig. 1.



**Figure 1.** Calibration curves and their respective equations for determination of carbon, nitrogen and oxygen weight fractions in cereal grains using data from EA-CF-IRMS.

Student's *t*-tests (two-pair two-tailed *t*-test) were conducted to determine whether the differences of various parameters are significant. The principal component analysis (PCA) was applied to the obtained results using CAT software (Chemometric Agile Tool) in order to describe the probable clustering of samples from different crop management systems.

## RESULTS AND DISCUSSION

The obtained values of stable isotope ratios and weight fractions of carbon, nitrogen and oxygen content in barley samples from different crop management systems are summarized in Tables 2 and 3.

**Table 2.** Stable carbon, nitrogen and oxygen isotope ratios ( $\delta$ ) of barley grain from conventionally and organically cultivated land

Crop management system	Sample	$\delta^{13}\text{C}_{\text{VPDB}}$ , ‰	$\delta^{15}\text{N}_{\text{AIR}}$ , ‰	$\delta^{18}\text{O}_{\text{VSMOW}}$ , ‰
Conventional	BarlA-C	$-28.24 \pm 0.03$	$2.36 \pm 0.16$	13.0*
	BarlB-C	$-28.33 \pm 0.08$	$2.28 \pm 0.06$	$13.47 \pm 0.06$
	BarlC-C	$-28.75 \pm 0.04$	$1.6 \pm 0.3$	$14.6 \pm 1.5$
	BarlD-C	$-28.72 \pm 0.09$	$2.03 \pm 0.06$	$16.0 \pm 0.6$
	BarlE-C	$-27.99 \pm 0.03$	$2.0 \pm 0.3$	$16.24 \pm 0.17$
Organic	BarlA-B	$-27.464 \pm 0.026$	$4.01 \pm 0.16$	$17.21 \pm 0.19$
	BarlB-B	$-28.499 \pm 0.017$	$3.63 \pm 0.06$	$16.47 \pm 0.16$
	BarlC-B	$-28.48 \pm 0.02$	$3.27 \pm 0.06$	$17.8 \pm 0.4$
	BarlD-B	$-28.26 \pm 0.05$	$2.7 \pm 0.4$	$17.0 \pm 0.4$
	BarlE-B	$-28.190 \pm 0.007$	$3.5 \pm 0.2$	$17.8 \pm 0.4$

mean  $\pm$  SD, ‰; \* – a single measurement was performed.

The  $\delta^{13}\text{C}$  values show that for barley grain samples from both conventional and organic farming systems the values are within the range from  $-28.75\text{‰}$  to  $-27.46\text{‰}$  and do not differ significantly for grains from different crop management systems ( $p > 0.05$ ). That corresponds with previous research stating that barley is a  $\text{C}_3$  crop and the  $\delta^{13}\text{C}$  values for this type of plants can vary from  $-37\text{‰}$  to  $-20\text{‰}$  (Kohn, 2010). The reason for the broad  $\delta^{13}\text{C}$  value range is the effect of different factors on the photosynthesis taking place in  $\text{C}_3$  plants, for example, the water use efficiency, isotopic composition of the atmospheric  $\text{CO}_2$  etc. (Vogado et al., 2020). Therefore, the  $\delta^{13}\text{C}$  values alone are not suitable for discrimination between barley grains from different crop management systems.

**Table 3.** The nitrogen, carbon, and oxygen weight fraction in barley grain from conventionally and organically cultivated land

Crop management system	Sample	$w_{\text{C}}$ , %	$w_{\text{N}}$ , %	$w_{\text{O}}$ , %
Conventional	BarlA-C	$41.6 \pm 1.0$	$1.25 \pm 0.05$	7.8*
	BarlB-C	$43.0 \pm 1.3$	$1.57 \pm 0.04$	$40.3 \pm 1.3$
	BarlC-C	$42.0 \pm 0.4$	$1.3 \pm 0.03$	$42.5 \pm 0.5$
	BarlD-C	$44 \pm 4$	$1.6 \pm 0.2$	$42 \pm 2$
	BarlE-C	$41 \pm 2$	$1.53 \pm 0.16$	$42.5 \pm 1.4$
Organic	BarlA-B	$42.0 \pm 0.7$	$1.02 \pm 0.18$	$41.7 \pm 1.3$
	BarlB-B	$41.0 \pm 0.4$	$1.18 \pm 0.06$	$43.4 \pm 1.0$
	BarlC-B	$41.0 \pm 0.4$	$1.15 \pm 0.02$	$40 \pm 2$
	BarlD-B	$42.9 \pm 0.5$	$1.21 \pm 0.19$	$41.2 \pm 1.7$
	BarlE-B	$42.1 \pm 0.2$	$1.29 \pm 0.02$	$41.55 \pm 0.04$

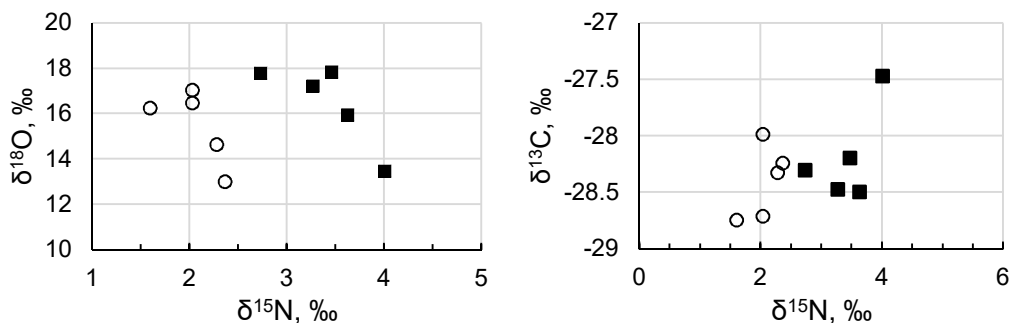
mean  $\pm$  SD, ‰; \* a single measurement was performed.

When considering the  $\delta^{15}\text{N}$  values measured in this study, a difference between the mean values for conventionally grown ( $2.1 \pm 0.3\text{‰}$ ) and organically grown barley ( $3.4 \pm 0.5\text{‰}$ ) grains can be observed. When performing the Student's  $t$ -test on  $\delta^{15}\text{N}$  values of organic and conventional barley grains, the difference shows to be significant ( $p < 0.01$ ). The main reason for the difference is the types of fertilizers used. For the conventional crop management system, a synthetic complex fertilizer (NPK) was

used, while for the organic crop management system the nitrogen content in soil was increased with the help of green manure - peas (Table 1), which is a plant of the legume family with high natural capacity to bind atmospheric nitrogen due to the rhizobia bacteria hosted on the roots of these plants. Previous research has shown that synthetic fertilizers are more depleted in  $^{15}\text{N}$  isotope if compared to the fertilizers that can be used in organic farming systems (Bateman & Kelly, 2007). However, it should be taken into consideration that legumes used as green-manure bind the atmospheric nitrogen and therefore their stable nitrogen isotope ratios should be close to the  $\delta^{15}\text{N}_{\text{AIR}}$  of 0‰ (Choi et al., 2017). Our study shows that the mean  $\delta^{15}\text{N}$  values of grains fertilized with green manure are lower than the values of other fertilizers permitted in organic cultivation systems (Bateman & Kelly, 2007). Therefore, additional research should be carried out to understand the fractionation processes taking place during the atmospheric nitrogen fixation and transfer to different parts of cereal crops. The plot of organic crop management system used in this study was established only two years prior to the harvest of samples and therefore the effects of green-manure use might be hindered by the effect of previous land use.

Stable oxygen isotope ratio in plants can change due to various reasons, for example, the variation of source water  $\delta^{18}\text{O}$  values, the different leaf water evaporation rate, etc (Barbour et al., 2005). For the barley grain from different crop management systems the mean  $\delta^{18}\text{O}$  values are higher for organically grown grain ( $17.3 \pm 0.6\text{‰}$ ) if compared to the conventionally grown ( $14.7 \pm 1.4\text{‰}$ ). When performing Student's *t*-test on  $\delta^{18}\text{O}$  values of organic and conventional barley grains, the difference shows to be not significant ( $p > 0.05$ ). Mainly the non-significant difference can be explained by the natural oxygen isotope abundance that is related to the global water cycle (Gat, 2010). Stable oxygen isotope ratio values in cereal grains are influenced by many factors, the geographic location and water contribution being more significant than fertilizer, growing condition and other effects. As the organic and conventional plots used in this study were situated near each other, the  $\delta^{18}\text{O}$  values are not significantly different.

Fig. 2. displays the relationship between nitrogen and oxygen or carbon stable isotope ratio values. As discussed previously, the grains from different crop management systems can be distinguished based on the  $\delta^{15}\text{N}$  values, while  $\delta^{18}\text{O}$  and  $\delta^{13}\text{C}$  values do not depend on the type of fertilizers used in this study.

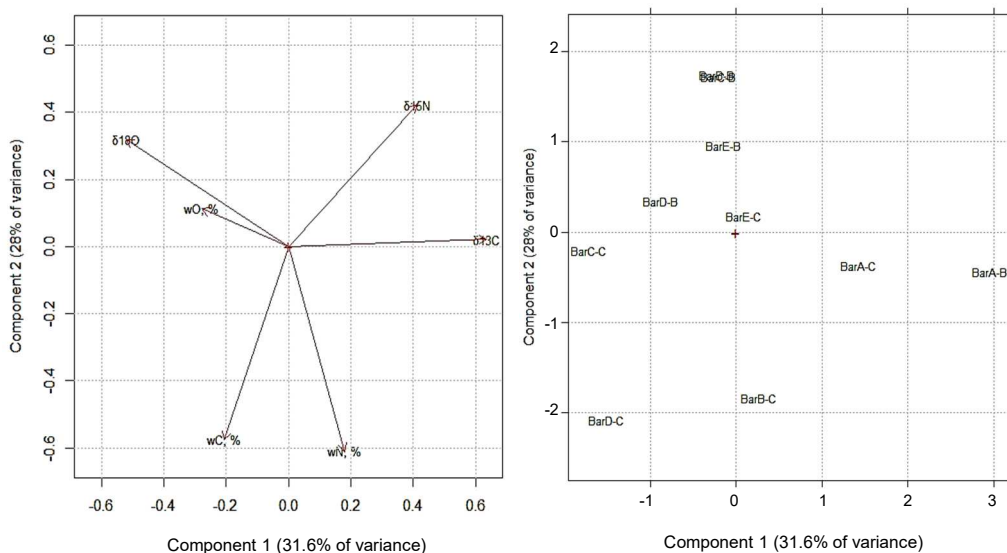


**Figure 2.** Relationship between  $\delta^{15}\text{N}/\delta^{18}\text{O}$  and  $\delta^{15}\text{N}/\delta^{13}\text{C}$  values of barley grains from different crop management systems (white circles - conventional, black squares - organic).

When evaluating the possible discrimination between organic and conventional barley grain samples in this study, it is important to bear in mind that organic produce is characterized not only by the use of appropriate fertilizers but also by the absence of any pesticides used. The results of this study classify the crop management system used only based on the fertilizers. In case of investigation of an unknown sample, additional methods for pesticide residue testing must be applied (Laursen et al., 2013).

When considering the total carbon, nitrogen and oxygen content in the barley samples, it clearly shows that the element content is not dependent on whether the grains have been grown using conventional or organic fertilizer. The carbon content in barley samples varies between 41.0–43.0%, the nitrogen content between 1.0–1.6‰ and the oxygen content between 37.8–43.4%.

To differentiate barley grain from conventional and organic crop management systems, principal component analysis (PCA) was carried out, based on the stable isotope ratios and element weight fractions in the samples analysed. The results of PCA are shown in Fig. 3.



**Figure 3.** Two-dimensional PCA Loading and Score plots for conventional and organic barley grain, total variance explained by PC1 and PC2 is 59.6%.

The loading plot of PCA shows that 31.6% of the total variance is explained by principal component 1 (PC1) and 28% by principal component 2 (PC2). The highest loadings along the PC1 are the ones of  $\delta^{13}\text{C}$  and  $\delta^{18}\text{O}$ , while along the PC2 the highest ones are of  $\delta^{15}\text{N}$ ,  $\delta^{18}\text{O}$  and total nitrogen and carbon content. The loading plot also gives us insight into the correlation between the variables. The  $\delta^{18}\text{O}$  values are positively correlated with total oxygen content in the samples, while in every other case - both for carbon and nitrogen, the stable isotope ratios of these elements are not correlated with the total content of the element in the barley grain samples.

In the score plot of the PCA four out of five organically grown barley grain samples are located closer to each other (Fig. 2). These samples are distributed along the axis of PC2 which means that the main variables to be considered when distinguishing between

conventional and organic barley grains are the stable isotope ratios of oxygen and nitrogen, as discussed before. One of the organically grown barley grain samples Bar1A-B is situated to the right, along the axis of PC1. The reason for this is the different  $\delta^{13}\text{C}$  value of this sample. The small number of analysed samples and the weak clustering of both organic and conventional samples indicates that stable isotope ratios and total element content do not provide sufficient data for discrimination between barley grains produced using synthetic and green-manure fertilizers. Additional variables must be evaluated for better distinguishing between conventional and organic barley grain samples.

## CONCLUSIONS

The study showed that  $\delta^{13}\text{C}$  of barley grains do not differ between samples from different crop management systems, agreeing with previous research that fractionation of stable carbon isotopes is not dependent on the fertilization of the cereals, but only dependent on the photosynthetic pathway characteristic for barley.

The stable isotope ratios of nitrogen and oxygen vary depending on the crop management system of barley. The barley grains from organic (green-manure) crop management system have significantly ( $p < 0.01$ ) higher  $\delta^{15}\text{N}$  values than the grains from conventional (synthetic fertilizer) crop management system.

The PCA of obtained data showed that with two principal components 59.6% of the total variance can be explained. When using principal components 1 and 2, the main loading to components is from  $\delta^{13}\text{C}$  and  $\delta^{18}\text{O}$  for the component 1 and from  $\delta^{15}\text{N}$ ,  $\delta^{18}\text{O}$  and total nitrogen and carbon content for component 2, respectively.

When plotting PC1 against PC2, four out of five organic barley samples are located closer to each other, but no real clustering is observed. The authors conclude that additional variables on a bigger sample group should be measured and incorporated in the multivariate model to improve the ability to distinguish between barley grains from different crop management systems.

## REFERENCES

- Barbour, M.M., Cernusak, L.A. & Farquhar, G.D. 2005. Factors Affecting the Oxygen Isotope Ratio of Plant Organic Material. In *Stable Isotopes and Biosphere - Atmosphere Interactions: Processes and Biological Controls*, edited by Flanagan, L.B., Ehleringer, J.R. and Pataki, D.E. Elsevier, pp. 9–28.
- Bateman, A.S. & Kelly, S.D. 2007. Fertilizer Nitrogen Isotope Signatures. *Isotopes in Environmental and Health Studies* **43**(3), 237–47. doi: 10.1080/10256010701550732.
- Bol, R., Eriksen J., Smith, P., Garnett, M.H., Coleman, K. & Christensen, B.T. 2005. The Natural Abundance of  $^{13}\text{C}$ ,  $^{15}\text{N}$ ,  $^{34}\text{S}$  and  $^{14}\text{C}$  in Archived (1923-2000) Plant and Soil Samples from the Askov Long-Term Experiments on Animal Manure and Mineral Fertilizer. *Rapid Communications in Mass Spectrometry* **19**(22), 3216–26. doi: 10.1002/rcm.2156.
- Von Bothmer, R. & Komatsuda, T. 2011. Barley Origin and Related Species. In *Barley: Production, Improvement, and Uses*. Wiley-Blackwell, pp. 14–62.

- Choi, W.J., Kwak, J.H., Lim, S.S., Park, H.J., Chang, S.X., Lee, S.M., Arshad M.A., Yun, S.I. & Kim, H.Y. 2017. Synthetic Fertilizer and Livestock Manure Differently Affect  $\Delta^{15}\text{N}$  in the Agricultural Landscape: A Review. *Agriculture, Ecosystems and Environment* **237**, 1–15. doi: 10.1016/j.agee.2016.12.020
- Dabin, Z., Pengwei, Y., Na, Z., Changwei, Y., Weidong, C. & Yajun, G. 2016. Contribution of Green Manure Legumes to Nitrogen Dynamics in Traditional Winter Wheat Cropping System in the Loess Plateau of China. *European Journal of Agronomy* **72**, 47–55. doi: 10.1016/j.eja.2015.09.012.
- European Union (EU-27) Barley Production by Year (1000 MT). <https://www.indexmundi.com/agriculture/?country=eu&commodity=barley&graph=production>. Accessed 22.02.2021.
- Gat, J.R. 2010. The Isotopes of Oxygen and Hydrogen. In *Isotope Hydrology: A Study of the Water Cycle*, edited by Wei, T.K. Imperial College Press, pp. 9–21.
- Hawkesford, M.J. 2014. Reducing the Reliance on Nitrogen Fertilizer for Wheat Production. *Journal of Cereal Science* **59**(3), 76–83. doi: 10.1016/j.jcs.2013.12.001
- Kohn, M.J. 2010. Carbon Isotope Compositions of Terrestrial C3 Plants as Indicators of (Paleo)Ecology and (Paleo)Climate. *Proceedings of the National Academy of Sciences of the United States of America* **107**(46), 19691–95. doi: 10.1073/pnas.1004933107
- Laursen, K.H., Mihailova, A., Kelly, S.D., Epov, V.N., Beraï, S., Schjoerring, J.K., Donard, O.F.X., Larsen, E.H., Pedentchouk, N., Marca-Bell, A.D., Halekoh, U., Olesen, J.E. & Husted, S. 2013. Is It Really Organic? - Multi-Isotopic Analysis as a Tool to Discriminate between Organic and Conventional Plants. *Food Chemistry* **141**(3), 2812–20. doi: 10.1016/j.foodchem.2013.05.068
- Mihailova, A., Pedentchouk, N. & Kelly, S.D. 2014. Stable Isotope Analysis of Plant-Derived Nitrate – Novel Method for Discrimination between Organically and Conventionally Grown Vegetables. *Food Chemistry* **154**, 238–45. doi: 10.1016/j.foodchem.2014.01.020
- Novak, V., Adler, J., Husted, S., Fromberg, A. & Laursen, K.H.. 2019. Authenticity Testing of Organically Grown Vegetables by Stable Isotope Ratio Analysis of Oxygen in Plant-Derived Sulphate. *Food Chemistry* **291**, 59–67. doi: 10.1016/j.foodchem.2019.03.125
- Pawlewicz, A. 2020. Change of Price Premiums Trend for Organic Food Products: The Example of the Polish Egg Market. *Agriculture (Switzerland)* **10**(2), 14–18. doi: 10.3390/agriculture10020035
- Shewry, P.R. & Ullrich, S.E. 2014. *Barley : Chemistry and Technology, Second Edition*. Elsevier Science & Technology.
- Vogado, N.O., Winter, K., Ubierna, N., Farquhar, G.D. & Cernusak, L.A. 2020. Directional Change in Leaf Dry Matter  $\delta^{13}\text{C}$  during Leaf Development Is Widespread in C3 Plants. *Annals of Botany* **126**(6), 981–90. doi: 10.1093/aob/mcaa114
- Zhang, M., Tian, Y., Zhao, M., Yin, B. & Zhu, Z.. 2017. The Assessment of Nitrate Leaching in a Rice–Wheat Rotation System Using an Improved Agronomic Practice Aimed to Increase Rice Crop Yields. *Agriculture, Ecosystems and Environment* **24**, 100–109. doi: 10.1016/j.agee.2017.03.002



## China food security assessment

V.Yu. Chernova<sup>1,2,\*</sup> and B.A. Kheyfets<sup>3,4</sup>

<sup>1</sup>People's Friendships University of Russia, Moscow, Russia, Faculty of Economics, Department of International Economic Relations, 6 Miklukho-Maklaya Str., RU117198 Moscow, Russia

<sup>2</sup>State University of Management, Institute of Marketing, 99 Ryazanskiy Prospect, RU109542 Moscow, Russia

<sup>3</sup>Institute of Economics of the Russian Academy of Sciences, 32 Nakhimovskiy Prospect, RU117218 Moscow, Russia

<sup>4</sup>Financial University under the Government of the Russian Federation, 49 Leningradsky Prospekt, RU125993 Moscow, Russia

\*Correspondence: [veronika.urievna@mail.ru](mailto:veronika.urievna@mail.ru)

Received: February 13<sup>th</sup>, 2021; Accepted: June 11<sup>th</sup>, 2021; Published: July 8<sup>th</sup>, 2021

**Abstract.** Ensuring food security is a strategic goal of any state, especially in the face of population growth. A review of the academic literature showed the presence of problems in ensuring a high level of food security in China: the rigidity of demand for food, limited land resources, structural contradictions between supply and demand. This study proposes an approach to assessing the level of food security, based on the calculation of an integral index consisting of four units of indicators: the sub-index of provision of crop products, the sub-index of productivity, the sub-index of provision of livestock products, and the sub-index of food import dependence. The results show that, in general, the level of food security in China has increased over the period under review, but there are problems in self-sufficiency in crop and dairy products, as well as in an increase in food import dependence. A forecast of the dynamics of the integral index of the food security level and its sub-indices was constructed, which showed that a decrease in the integral index might occur due to a decrease in self-sufficiency in livestock products and import dependence, while the availability of crop products and yields will increase. The study showed that the measures taken by the Chinese government led to some positive changes, but it is necessary to take a comprehensive approach to this problem, to solve which it is necessary to use the potential of all sectors of the food industry.

**Key words:** food security, COVID-19 restrictions, food markets, agriculture, import dependence, government support.

## INTRODUCTION

Food security is one of the most important conditions for national security. To ensure it, it is necessary to solve a set of issues, including an increase in the area of arable land, an increase in the production of crop and livestock products without environmental damage (Vervoort et al., 2014), lean food production and minimizing food waste

(Kubule et al., 2019; Andersson et al., 2020). Obviously, when food production reaches its technological peak, the lack of arable land will become a key factor limiting its production (Van Dijk & Meijerink, 2014; Pöldaru et al., 2018). In recent decades, worldwide, population growth has outpaced food production growth, which has led to a decrease in food availability per capita, has created new risks for a number of countries.

China is the most populous country in the world. China's food production per capita is currently above the world average of about 470 kg per person, facing an increase of 14% over more than 22 years (414 kg per person in 1996). The total food production is growing steadily, in 2018 this figure was about 660 million tons (State Council Information Office of the People's Republic of China, 2019). However, the active growth of production creates threats in the use of land resources (Zhou et al., 2015). More than 20% of the world's population lives in China, with less than 10% of arable land. The availability of food in China is important not only because it affects a large part of the world's population and consumption, but also because rapid industrialization has led to competition for resources between agricultural and non-agricultural sectors, strong income growth, rapid urbanization, and population growth (Zhanga et al., 2018). All this stimulates the demand for agricultural products.

One can agree that in the context of active socio-economic development, China's food security in the future is of increasing concern (Jiang et al., 2019). First, although food production in China has increased, significant year-to-year fluctuations in supply and prices remain. Market stabilization and food price inflation have been among the main goals of government policy since the late 1980s, and the problem has not yet been resolved and is exacerbated by external global trends. Second, food security and access to food are mainly problems of poverty. China's economic growth as a whole is unevenly manifested in its regions. Incomes in the central and eastern regions of China continue to grow at a faster rate than in the western and southwestern regions. Income inequality between regions and between rural and urban areas continues to grow (Mukhopadhyay et al., 2018). Third, the COVID-19 outbreak, which became a global pandemic in early 2020, continues to impact agricultural supply chains. This is mainly reflected in the supply of grain, as many exporting countries have announced export bans. Disruption to supply chains has already driven up global food prices (Marchisio, 2020).

These and other reasons are more and more relevant to the topic of ensuring food security in China. That is why the purpose of this study is to assess food security and justify measures to stabilize it. To do this, the authors studied the current state of the Chinese agricultural industry; identified new trends in its development manifested against the backdrop of the COVID-19 pandemic; analyzed the effectiveness of food security measures taken by the Chinese government at the national and regional levels.

The paper consists of several sections. In the introduction, the authors substantiate the relevance of the issue, determine the purpose and tasks of the research. The literature review considers the concepts of food security, clarifies the difference between the categories of food security and food self-sufficiency, poses the problems of China's food security, and identifies approaches to its assessment. Materials and methods present the authors' approach to assessing food self-sufficiency based on an integral indicator comprising four sub-indices. The results of the study present an assessment of food self-sufficiency based on the proposed approach, as well as an explanation of the revealed import dependence of China based on the self-sufficiency level. The dynamics of the integral index of the food security level and its components are forecasted. The

discussion section compares the results obtained with other studies and analyzes the food self-sufficiency situation. The conclusion contains findings concerning China's food security prospects in the medium term.

## LITERATURE REVIEW

Food security is a priority in the political agenda for many countries' governments. Achieving food security supposes that the country's population has stable access from economic, physical, and social perspectives to the volume of safe and nutritious food products that meets their nutritional needs (Food and Agriculture Organization of the United Nations, 2017).

It is important to note that food security is not synonymous with food self-sufficiency. The concept of food security does not consider the origin of food products or the country's ability to produce food products, provided that they are affordable, nutritious, high-quality, and safe. According to FAO's concept, food self-sufficiency is the degree to which a country can meet its food needs through its own domestic production (Food and Agriculture Organization of the United Nations, 1999). This definition concerns a situation when a country practices complete autarky and has closed its borders for international food trade. In FAO's modern interpretation, food self-sufficiency is defined as a country's production of agri-food products satisfying the predominant part of its need for food, which approaches or exceeds 100% of domestic food consumption. This definition does not exclude the possibility of international trade. Countries that are self-sufficient in food may to some extent specialize their food production and import, as well as export, food products (Puma et al., 2015; Clapp, 2017).

Let us discuss the case of China. With the advancement of industrialization, food security in China is facing new challenges, including increased demand for food, resource constraints, and structural contradictions. Despite the measures taken, there are still many unresolved problems. According to Van Meijla et al. (2020), the government should rationally address food security issues, based on such aspects as the establishment of a system for protecting food prices, improving the agricultural business model, increasing food subsidies, etc.

Hasegawa et al. (2018) pointed out that China's food security should focus on agricultural infrastructure, key links in food logistics, food markets, food subsidy policies, and other areas. To protect China's food security, a reproduction reserve system should be developed. That is, food security should enhance the comprehensive potential of food production, as it is based on the organic integration of food production, distribution, and consumption (Godfray & Robinson, 2015).

As one can see, the issue of ensuring food security is very urgent and requires an early solution, which predetermines the importance of assessing its level.

Many indicators have been proposed to identify which countries need to improve their food security status (Melgar-Quinonez et al., 2005; Kuyvenhoven, 2012; Food and Agriculture Organization of the United Nations, 2013; Jones et al., 2013; Pérez-Escamilla, 2013; Kuzmin, 2015). However, the lack of consensus on how to compare and rank countries has prompted international institutions to create composite indices to summarize information. The index building process includes several options that obviously affect the result. This review aims to understand how relevant and discretionary the choice of

algorithms can be for calculating composite food security indices. Table 1 presents a systematization of approaches to assessing the level of food security.

**Table 1.** Approaches to assessing the level of food security

Method	Description
Anthropometric indices	Initial data: Weight, height, body size and other information on food provision, preparation, food composition and consumption. <b>Result:</b> The proportion of the population that is undernourished. Features: Mapping of food security can be done both nationally and locally. It takes a long time to directly measure food security.
Household expenditure survey	Initial data: Household information on spending on food and other necessities. <b>Result:</b> Per capita calorie intake. Features: Allows identifying the determinants of consumption. Converting available food to calories involves basic assumptions that can cause measurement errors. Measures the amount of food available (ignores consumption in a given period).
Survival strategy evaluation indices of different levels	Initial data: Respondents' answers (on how households respond to food shortages). <b>Result:</b> A vision of how households are responding and/or adapting to the presence or threat of food shortages. Features: Subjective assessment. Household comparisons are problematic.
Scales based on food insecurity experiences	Initial data: A scale containing elements that reflect the conceptual and multidimensional nature of food security. <b>Result:</b> Various algorithms for transforming food security assessment scales. Features: Measures food security according to individual experience.
Food intake assessment indices	Initial data: Food consumption by an individual/household over a given period. <b>Result:</b> The amount of food consumed. Features: Directly measures consumption, not food availability.

Based on the approaches presented, one can conclude that it is advisable to assess the level of food security taking into account the context of the study. In this case, it is important to assess the dynamics of changes in the level of food security, taking into account the production and imports of food.

The review showed that most researchers agree that ensuring national food security is essential for agricultural sustainability (Fang et al., 2018; Morea & Balzarini, 2018; Raymond et al., 2018; Pakravan-Charvadeh et al., 2020). They are also concluded that the issues of the sustainability of supply chains, the subject of responsibility, and the area of food security were widely discussed in the literature, but they have not formed a general analytical basis for studying the level of food security, taking into account import dependence, natural conditions, productivity, consumer relations, and other factors (Ray et al., 2013; Valešová et al., 2017; Ceballos et al., 2020; Nicola et al., 2020). As a result, many studies (for example, Ghose, 2014; Wu et al., 2016) treat food security as food self-sufficiency. Zou & Guo (2015) consider food security as self-sufficiency and reduce it to self-sufficiency in grain as the main agricultural crop. Based on this, Zou & Guo have developed an index system for the quantitative assessment of food security.

## MATERIALS AND METHODS

To assess food security, the authors propose to use an integral approach through calculating the corresponding food security index, which includes four units of assessment indicators: the sub-index of provision of crop products, the sub-index of productivity, the sub-index of provision of livestock products, and the sub-index of food import dependence. The proposed integral index includes indicators with different dimensions to ensure the commensurability of different indicators, their values were normalized using the ‘maximum-minimum’ method.

First, the sub-indices of indicators, the greater value of which characterizes a higher level of food security, were calculated as follows:

$$i_{FSi} = 100 + \frac{i_i - V_{av}}{(V_{max} - V_{min})/2} \cdot \quad (1)$$

Second, the sub-indices of indicators, the greater value of which characterizes a lower level of food security, were calculated using the formula:

$$i_{FSi} = 100 + \frac{V_{av} - i_i}{(V_{max} - V_{min})/2} \cdot \quad (2)$$

where  $i_{FSi}$  – the sub-index for the  $i$ -th year;  $V_{av}$  – the average value of the indicator for the period;  $V_{max}$  – the maximum value of the indicator for the period;  $V_{min}$  – the minimum value of the indicator for the period.

The integral index of the level of food security  $I_{FSi}$  was calculated as follows:

$$I_{FSi} = \frac{\sum_{m=1}^M i_{FSi}}{M} \cdot \quad (3)$$

where  $M$  – the number of units for assessing the level of food security (in the studied case,  $M = 4$ , since the assessment examined four units of indicators).

Units of indicators of the integral index of food security:

1. Sub-index of provision of crop products. Production of the most commonly consumed crop products. The production of such crops as corn, rice, green corn, oil palm fruits, soybeans, wheat was assessed per capita.

2. Sub-index of productivity, which includes indicators of the productivity of the most frequently consumed crop products.

3. Sub-index of provision of livestock products. Production of the most commonly consumed livestock products. The production of such types of meat as pork, goat, lamb, poultry, goose/guinea fowl, duck meat per population was assessed.

4. Sub-index of food import dependence, which includes such indicators as the coefficient of dependence on grain imports, the cost of food imports in total exports of goods, the variability of food production per capita, the ratio of food imports to the population, the prevalence of undernourishment (in % of the population).

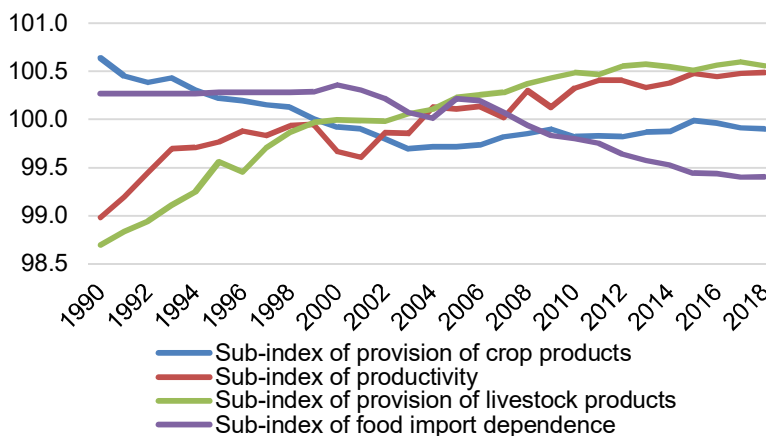
The advantage of the proposed integral index of the level of food security is wide coverage of various aspects of agriculture. The approach provides a high degree of accuracy and identifies weaknesses in food security.

In the course of the study, a forecast of the dynamics of the integral index and its sub-indices was constructed using the least-squares method. The paper used statistical

data on agriculture and trade in China of the Food and Agriculture Organization of the United Nations (2020) for 1990–2018.

## RESULTS

Using the proposed approach for calculating the integral index of food security, the authors calculated all of its components. Fig. 1 presents the data for four sub-indices.



**Figure 1.** Sub-indices of the level of food security in China in 1990–2018.

Source: (Food and Agriculture Organization of the United Nations, 2020).

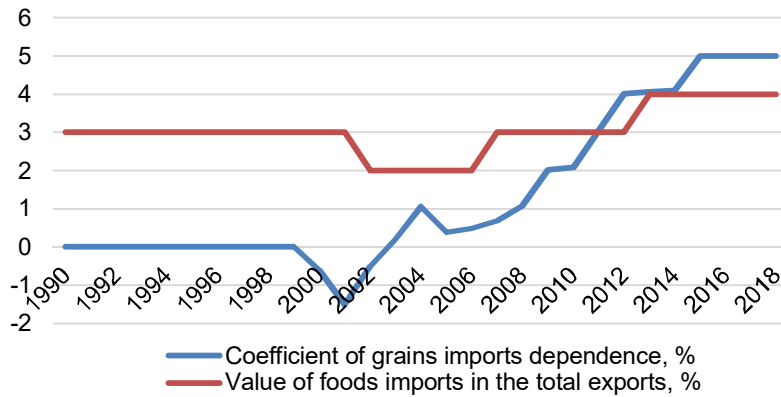
The dynamics of the sub-index of provision of livestock products demonstrate steady growth. This indicates the use of innovative technologies in agriculture, which affects the total volume of livestock production. Increased competitiveness becomes a logical consequence of innovation (Batkovskiy et al., 2020). Growth for chicken meat in 1990–2018 was 2.53 times; for pork - 0.51 times; for lamb - 1.16 times, for duck - 1.54 times, for goat and goose/guinea fowl - 1.13 and 1.32 times, respectively (Food and Agriculture Organization of the United Nations, 2020). The results of calculating the productivity index showed an increase in all the products under consideration: the yield of corn increased by 34.9%, rice - by 22.9%, corn - by 27.5%, oilseeds - by 4.9%, soybeans and wheat - by 22.3% and 69.6%, respectively.

Despite the increase in productivity, the indicators of the sub-index of provision of crop products are characterized by unstable trends. According to the data obtained, only the production of corn per capita shows an increase over the period of 1990–2018 by 26.7%, while the production of rice, wheat, soybeans, and oil palm fruits decreased by 41.3%, 49.1%, 32%, and 21.9%, respectively (Food and Agriculture Organization of the United Nations, 2020). A strong decrease is observed in the specific indicator of production of particular crops per capita (with an accompanying increase in the population of China over the period under review).

The sub-index of food import dependence also shows a decrease, which is associated with an increase in imports of particular types of products, primarily, this concerns crop production (wheat, rice, soybeans). Thus, the coefficient of dependence on grain imports increased more than 10-fold, the value of food imports in total exports

increased by 33.3%, the variability of food production per capita increased almost 2-fold (by 96.3%), a positive trend is shown by the index of undernourishment (in % of the population) - it decreased by 52%.

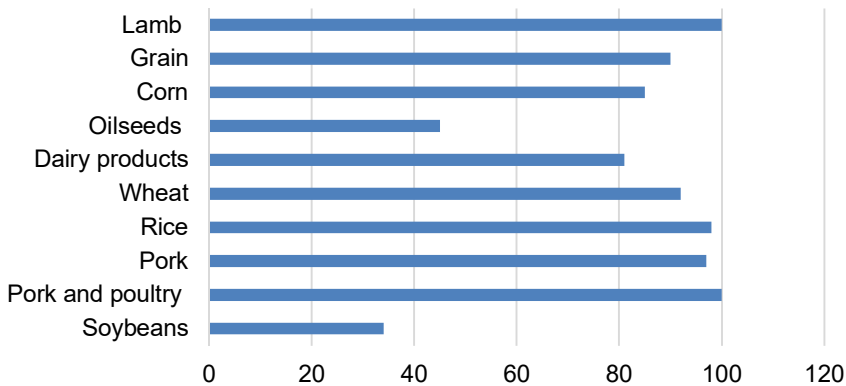
The coefficient of the level of China’s dependence on grain imports and the specific cost of food imports in the total exports of goods and services are shown in Fig. 2. The data show that the minimum value of the coefficient of dependence on grain imports was observed in 2001, after which its annual increase began. The value of food imports in the total exports of goods and services show a similar trend: in the early 2000s, this indicator was minimal, after which its value began to grow.



**Figure 2.** Indicators of China’s food import dependence for 1990–2018.

Source: (Food and Agriculture Organization of the United Nations, 2020).

To understand the components of food import dependence, let us consider China’s self-sufficiency coefficient for some particular types of food products (Fig. 3). As one can see, the greatest dependence on imports is observed in the production of soybeans (34%), oilseeds (45%).

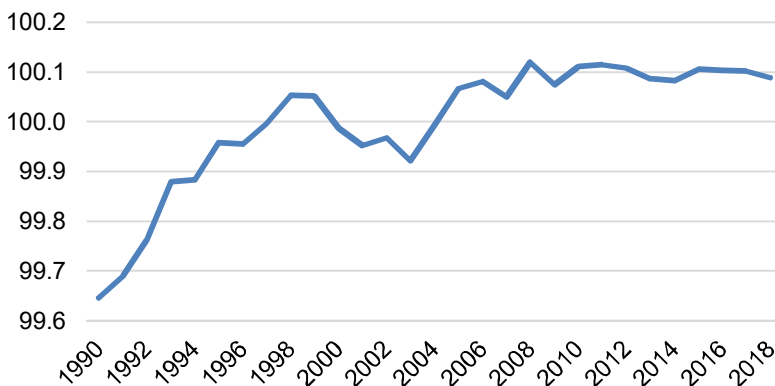


**Figure 3.** Coefficients of China’s self-sufficiency for certain types of agricultural products in 2018, %.

Source: (Food and Agriculture Organization of the United Nations, 2020).

Self-sufficiency data indicate that the lowest values are related to crop and dairy products. The self-sufficiency goal set by the authorities (for a long time China applied the 95% rule: domestic supply must be able to cover at least 95% of domestic demand (Organisation for Economic Co-operation and Development, 2018)) is becoming more difficult to fulfill every year: the main reason is associated with the increasing volume of agricultural products supplied to meet demand, continuing to grow, causing, as a result, a significant increase in imports of grain, as well as soybeans and other staple foods. China’s sharply widening trade deficit in agriculture and agri-food is proof of this. Local production of grains (rice (98%), wheat (92%), corn (85%)) met 90% of the national needs in 2018, compared to more than 100% in the early 2000s. Since 2018, rice production in China has shown negative growth for two consecutive years, while consumption and therefore demand has continued to rise, putting pressure on domestic production. China’s rice self-sufficiency is relatively high, but the balance between domestic demand and supply is fragile. China also imports 19% of its dairy needs.

These trends are confirmed in the course of this research: the results of calculating the integral index of the level of food security show that in recent years the level of self-sufficiency in China has been declining (Fig. 4).



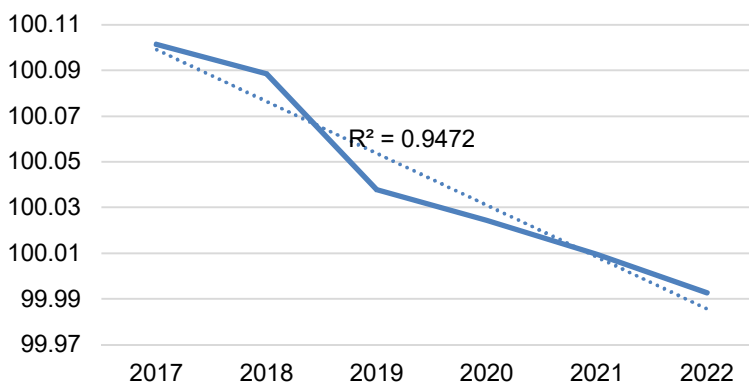
**Figure 4.** Integral index of the level of food security in China for 1990–2018.

Source: (Food and Agriculture Organization of the United Nations, 2020).

For the period of 1990–2015, the integral index increased by 0.46%, while from 2015 to 2018 it decreased by 0.02%. As mentioned above, the growth in food imports had a significant impact on this dynamics. To avoid overdependence on international markets, China’s strategy is to secure its supply, control production in other countries, and limit the number of intermediaries.

To understand the further development of the situation in the field of food self-sufficiency, the authors built a forecast of the dynamics of the integral index of the level of food security and its sub-indices (Fig. 5).





**Figure 5.** Forecast of the dynamics of the integral index of the level of food security in China.

The integral index is expected to decline by 0.1% over the next three years, suggesting an acceleration in the rate of loss of food security in China. In the medium term, this will be facilitated by a decrease in self-sufficiency in livestock products and import dependence, while the provision of crop products and productivity will increase (Table 2).

**Table 2.** Forecast of the dynamics of China's food security sub-indices

Sub-indices	Fact		Forecast*			
	2017	2018	2019	2020	2021	2022
Sub-index of provision of crop products	99.92	99.90	100.06	100.11	100.18	100.24
Sub-index of productivity	100.48	100.49	100.46	100.48	100.49	100.50
Sub-index of provision of livestock products	100.60	100.56	100.56	100.54	100.51	100.48
Sub-index of food import dependence	99.41	99.40	99.17	99.08	98.98	98.88

Note: \* – taking into account the time lag in the formation of statistics.

The results obtained differ slightly from the common point of view in other studies - that the most negative situation is observed in the field of crop production. As one can see, a one-sided policy in relation to certain sectors of agricultural production can lead to the fact that livestock indicators will decline, which, in turn, will lead to an even greater dependence on food imports.

## DISCUSSION

Due to the unprecedented growth of imports in 2020, the key purpose of China's economic policy for 2021–2025 has become to maintain stable food production (Bloomberg News, 2021). For this, the Chinese government has developed the national food security strategy based on self-sufficiency through domestic production, guaranteed food production capacity, moderate imports, and technological support. However, the increasing dependence on imports and the export ban on food grains due to the

COVID-19 pandemic is highly likely to exacerbate the global food crisis and could have serious implications for China. China's food security currently faces three major challenges - severe resource constraints, complex structural contradictions, and supply lags in agricultural logistics.

It should be noted that, on the one hand, China's agricultural policy of the year was not always aimed at meeting the needs of the population for food, at the same time, the rural sector was not always a priority of economic policy. Therefore, the very structure of China's agriculture has changed very little, the share of grains in agricultural land in the added value of agriculture has largely remained. To maintain stable food production, China is going to focus on increasing the yields of rice, wheat, soybeans, and corn to improve national food self-sufficiency. The current production volumes of Chinese grain do not cover the growing demand of animal farming for feed crops. In China's agri-food sector, the consumption of fodder grain exceeds the consumption of cereals for food purposes, which, given the limited growth potential of total grain production, exerts great pressure on China's food supply (Lin et al., 2014). Price volatility and geopolitical tensions have complicated the situation in the global feed grain market and forced China to diversify its import sources (Wang, 2021).

Another limiting factor is population growth: since 1990, the population of China has increased by 60% to 1,401 million people, the average life expectancy over the same period has increased by 11.5%, reaching 77.1 years (Food and Agriculture Organization of the United Nations, 2020). These events lead to a huge increase in the demand for food. It is forecasted that following the intensification of urbanization processes and changing diets, the consumption of main crops per capita will decrease, while demand for meat and fish products will grow (Donley, 2021).

China has about 8% of arable land to feed 19% of the world's population (Food and Agriculture Organization of the United Nations, 2020). However, not only two-thirds of China's territory is located at an altitude of more than 1,000 meters, but urbanization and desertification also limit the possibilities of land cultivation. The Chinese authorities have set a minimum cropping area of 120 million hectares to ensure 95% self-sufficiency in grain. The growth of crop production efficiency in the previous years due to the increased use of fertilizers and pesticides has reached its limit and resulted in a considerable deterioration of the soil condition. The next surge in agricultural production efficiency should be based on scientific innovation.

These demographic, land, and water barriers are limiting production growth, so China is focusing agriculture on strategic products and is looking outside the country for other foods it needs.

In addition, Chinese purchases are based on a limited number of suppliers, further increasing the country's dependence. Three countries - the United States (23%), Brazil (19%), and Australia (7%) - supply half of the agricultural and agri-food products imported by China (Food and Agriculture Organization of the United Nations, 2020). Therefore, one of China's strategies is to diversify supplies.

The implementation of the Household Responsibility System, which provided every rural household with a plot of agricultural land, made an important contribution to improving agricultural efficiency in the early 1980s. The next step was market liberalization. Policies to stimulate the development of rural enterprises have contributed to employment and increased income for rural residents. The share of non-agricultural farmers increased from 15% in 1980 to over 40% in 2018. China has over 200 million

farm households (or rural households with land contracts). Reforms in agricultural technology have also made important contributions, in particular to increased yields.

In addition, during the period of preparation for accession to the WTO, China has weakened access to import and export markets. After accession to the WTO, the aggregate indicator of support for domestic producers fell to less than 8.5% of the value of agricultural products. The most important agricultural policy measures are the minimum purchase price that applies to rice and wheat, the Temporary Storage Program, which was launched in 2008 for maize, soybeans, and rapeseed. Although the aforementioned price support measures have increased crop production, the shortage of some commodities is still high and even increasing.

It is very difficult to predict China's future food import needs. On the one hand, self-sufficiency or near-self-sufficiency in food has always been an important strategic goal of Chinese agricultural policy, especially with respect to staple crops. In recent years, China has maintained an overall food self-sufficiency rate of 95%. If it adheres to the same policy, its food imports are unlikely to change significantly in the future - at least it is certain that they will not increase significantly (according to this study, China's self-sufficiency level will decline slightly in the medium term). However, there is still a risk that the COVID-19 pandemic, poverty, and food insecurity in other countries will lead to increased protectionism and restriction of food exports. Other factors, such as dietary changes (imports of foods such as meat, milk, and sugar may increase) and demographics (consumption may stabilize as China's population approaches a peak), may also determine future levels of food imports.

Despite the strengthened measures aimed at achieving food self-sufficiency, many researchers believe that China's food self-sufficiency will decrease from 94.5% in 2015 to about 91% by 2025. However, this additional volume of imports is not expected to result in serious damage (Huang et al., 2017).

The results obtained by the authors of this paper are in line with other researchers' assessments of China's self-sufficiency. For example, Cui & Shoemaker (2018) showed that China's self-sufficiency in three main crops (wheat, rice, and corn) was about 95%, and even after the pandemic, their imports were less than 10% of domestic consumption (Wang, 2021), while about 80% of the soybean consumed in China was imported. Similar conclusions are drawn in Donley (2021), which states that by 2025, China will be almost entirely self-sufficient in main crops such as rice and wheat, but will remain the largest importer of soybeans.

A factor analysis of food security carried out by Zou & Guo (2015) showed that its level in China was permanently declining. Zou & Guo believe that these changes are caused by the growth of the population's incomes and changes in the structure of food consumption. They conclude that demand for grain is expected to grow in China, but do not specify whether it concerns grain for food or grain for livestock fodder. The main problem of food security is considered to be the gap between the production and consumption of grain.

The analytical report of Hang Seng Bank China (Wang, 2021) states that despite the priority of food self-sufficiency, an increase in the imports of a number of crops is unavoidable. Achieving self-sufficiency comes at a high cost for the Chinese economy. The problems include rising payroll costs, land depletion, and water deficiency in many regions of China. Due to low production efficiency and high production costs, grain cost prices in China are usually higher than in the global market. In the past five years,

average domestic prices for wheat, rice, corn, and soybeans have been higher than world prices.

We believe it would be advisable to adopt a strategy aimed at maintaining a balance between a comfort level of self-sufficiency in basic food products and the share of imported food products. However, the definition of the ‘comfort level’ ultimately depends on political considerations, in particular, it will be the question of achieving food security in other countries.

## CONCLUSION

The study examined China’s food security prospects over the medium term. China continues to be the main contributor to global food production and consumption. Food consumption in China will continue to grow in the coming years, driven by economic growth and urbanization. The proposed approach to assessing the level of food security in China, based on the calculation of the integral index, consisting of four units of assessment indicators, made it possible to prove that, in general, the level of food security has increased. However, the forecast for the dynamics of the integral index shows that in the medium term, there will be a reduction due to a decrease in self-sufficiency in livestock products and import dependence. China will remain self-sufficient for rice and wheat, but it will continue to depend on other countries for soybeans and corn. The dynamics will also be influenced by the restrictions associated with the COVID-19 pandemic, the decisions of some countries to restrict food exports, and the rise in food prices. To eliminate the existing restrictions, China needs to take a comprehensive approach to this problem, helping to realize the potential of all sectors of the food industry.

ACKNOWLEDGEMENTS. This study has been supported by the RUDN University Strategic Academic Leadership Program.

## REFERENCES

- Andersson, K., Eklund, J. & Rydberg, A. 2020. Lean-inspired development work in agriculture: Implications for the work environment. *Agronomy Research* **18**(2), 324–345. <https://doi.org/10.15159/AR.20.043>
- Batkovskiy, A.M., Fomina, A.V. & Sudakov, V.A. 2020. Developing the toolkit for evaluating innovative activities of enterprises to improve their competitiveness. In Bogoviz, A. & Ragulina, Y. (eds.). *Industry Competitiveness: Digitalization, Management, and Integration*. Springer, pp. 362–369. [https://doi.org/10.1007/978-3-030-40749-0\\_43](https://doi.org/10.1007/978-3-030-40749-0_43)
- Bloomberg News. 2021. *China Reaffirms Goal to Bolster Food Security as Imports Swell*. <https://www.bloomberg.com/news/articles/2021-01-04/china-reaffirms-goal-to-bolster-food-security-as-imports-swell>
- Ceballos, F., Kannan, S. & Kramer, B. 2020. Impacts of a national lockdown on smallholder farmers’ income and food security: Empirical evidence from two states in India. *World Development* **136**, 105069. <https://doi.org/10.1016/j.worlddev.2020.105069>
- Clapp, J. 2017. Food self-sufficiency: Making sense of it, and when it makes sense. *Food Policy* **66**, 88–96.
- Cui, K. & Shoemaker, S.P. 2018. A look at food security in China. *npj Science of Food* **2**, 4. <https://doi.org/10.1038/s41538-018-0012-x>

- Donley, A. 2021. *Report: China to be Nearly Self-Sufficient in Wheat, Rice by 2025*. <https://www.world-grain.com/articles/15341-report-china-to-be-nearly-self-sufficient-in-wheat-rice-by-2025>
- Fang, S.T., Ji, X., Ji, X.H. & Wu, J. 2018. Sustainable urbanization performance evaluation and benchmarking: an efficiency perspective. *Management of Environmental Quality* **29**(2), 240–254. <https://doi.org/10.1108/MEQ-07-2017-0063>
- Food and Agriculture Organization of the United Nations. 1999. *Implications of Economic Policy for Food Security: A Training Manual*. <http://www.fao.org/docrep/004/x3936e/x3936e03.htm>
- Food and Agriculture Organization of the United Nations. 2013. *New Metrics to Measure and Monitor Performance in Agriculture and Food Security, held on December 5, 2012 in Rome*.
- Food and Agriculture Organization of the United Nations. 2017. *Global Strategic Framework for Food Security and Nutrition*. <http://www.fao.org/3/MR173RU/mr173ru.pdf>
- Food and Agriculture Organization of the United Nations. 2020. *Crops*. <http://www.fao.org/faostat/ru/#data/QC>
- Ghose, B. 2014. Food security and food self-sufficiency in China: from past to 2050. *Food and Energy Security* **3**(2), 86–95.
- Godfray, H.C.J. & Robinson, S. 2015. Contrasting approaches to projecting long-run global food security. *Oxford Review of Economic Policy* **31**(1), 26–44. <https://doi.org/10.1093/oxrep/grv006>
- Hasegawa, T., Fujimori, S., Havlik, P., Valin, H., Bodirsky, B.L., Doelman, J.C. & Fellmann, T. 2018. Risk of increased food insecurity under stringent global climate change mitigation policy. *Nature Climate Change* **8**(8), 699–703. <https://doi.org/10.1038/s41558-018-0230-x>
- Huang, J., Wei, W., Cui, Q. & Xie, W. 2017. The prospects for China's food security and imports: Will China starve the world via imports? *Journal of Integrative Agriculture* **16**(12), 2933–2944. [https://doi.org/10.1016/S2095-3119\(17\)61756-8](https://doi.org/10.1016/S2095-3119(17)61756-8)
- Jiang, X., Chen, Y. & Wang, L. 2019. Can China's agricultural FDI in developing countries achieve a win-win goal? Enlightenment from the literature. *Sustainability* **11**, 41. <https://doi.org/10.3390/su11010041>
- Jones, A.D., Ngunjiri, F.M., Pelto, G. & Young, S.L. 2013. What are we assessing when we measure food security? A compendium and review of current metrics. *Advances in Nutrition: An International Review Journal* **4**(5), 481–505. <https://doi.org/10.3945/an.113.004119>
- Kubule, A., Indzere, Z. & Muizniece, I. 2019. Modelling of the bioeconomy system using interpretive structural modelling. *Agronomy Research* **17**(4), 1665–1678. <https://doi.org/10.15159/AR.19.170>
- Kuyvenhoven, A. 2012. International Food Policy Research Institute: 2011 Global Food Policy Report. *Food Security* **4**, 679–681. <https://doi.org/10.1007/s12571-012-0216-x>
- Kuzmin, E.A. 2015. Food security modelling. *Biosciences Biotechnology Research Asia* **12**, 773–781. <https://doi.org/10.13005/bbra/2095>
- Lin, H., Li, R., Jin, C., Wang, C., Wei, M. & Ren, J. 2014. China's new problems of food security revealed by the Food Equivalent Unit. *Frontiers of Agricultural Science and Engineering* **1**(1), 69–76. <https://doi.org/10.15302/J-FASE-2014023>
- Marchisio, M. 2020. *The Potential Impact of COVID-19 on China's Food Security: Prospects for Food Imports*. <https://www.ifad.org/en/web/latest/blog/asset/41937713>
- Melgar-Quinonez, H., Zubieta, A.C., Valdez, E., Whitelaw, B. & Kaiser, L. 2005. Validation of an instrument to monitor food insecurity in Sierra de Manantlan, Jalisco. *Salud Publica Mex* **47**(6), 413–422. <https://doi.org/10.1590/S0036-36342005000600005>
- Morea, D. & Balzarini, M. 2018. Financial sustainability of a public-private partnership for an agricultural development project in Sub-Saharan Africa. *Agricultural Economics (Czech Republic)* **64**, 389–398. <https://doi.org/10.17221/161/2017-AGRICECON>
- Mukhopadhyay, K., Thomassin, P.J. & Zhang, J. 2018. Food security in China at 2050: a global CGE exercise. *Journal of Economic Structures* **7**, 1. <https://doi.org/10.1186/s40008-017-0097-4>

- Nicola, M., Alsafi, Z., Sohrabi, C., Kerwan, A., Al-Jabir, A., Iosifidi, C. & Agha, R. 2020. The socio-economic implications of the coronavirus pandemic (COVID19): A review. *International Journal of Surgery* **78**, 185–193. <https://doi.org/10.1016/j.ijso.2020.04.018>
- Organisation for Economic Co-operation and Development. 2018. *OECD Food and Agricultural Reviews, Innovation, Agricultural Productivity and Sustainability in China*. <https://www.oecd-ilibrary.org/sites/9789264085299-8-en/index.html?itemId=/content/component/9789264085299-8-en>
- Pakravan-Charvadeh, M.R., Khan, H.A. & Flora, C. 2020. Spatial analysis of food security in Iran: associated factors and governmental support policies. *Journal of Public Health Policy* **41**, 351–374. <https://doi.org/10.1057/s41271-020-00221-6>
- Pérez-Escamilla, R. 2013. Can experience-based household food security scales help improve food security governance? *Global Food Security* **1**, 120–125. <https://doi.org/10.1016/j.gfs.2012.10.006>
- Pöldaru, R., Viira, A.-H. & Roots, J. 2018. Optimization of arable land use to guarantee food security in Estonia. *Agronomy Research* **16**(4), 1837–1853. <https://doi.org/10.15159/AR.18.161>
- Puma, M.J., Bose, S., Chon, S.Y. & Cook, B.I. 2015. Assessing the evolving fragility of the global food system. *Environmental Research Letters* **10**(2), 024007.
- Ray, D.K., Mueller, N.D., West, P.C. & Foley, J.A. 2013. Yield trends are insufficient to double global crop production by 2050. *PloS One* **8**(6). <https://doi.org/10.1371/journal.pone.0066428>
- Raymond, J., Kassim, N., Rose, J.W. & Morris, A. 2018. Context-specific food-based approach for ensuring nutrition security in developing countries: A review. *International Journal of Food Sciences and Nutrition* **69**, 410–416. <https://doi.org/10.1080/09637486.2017.1373751>
- State Council Information Office of the People's Republic of China. 2019. *Food Security in China*. <http://www.scio.gov.cn/zfbps/32832/Document/1666228/1666228.htm>
- Valešová, L., Herák, D., Shinoda, K., Mazancová, J. & Verner, V. 2017. The nexus between food insecurity and socioeconomic characteristics of rural households in Western Indonesia identified with Food and Nutrition Technical Assistance's approach by USAID. *Agronomy Research* **15**(3), 921–934.
- Van Dijk, M. & Meijerink, G.W. 2014. A review of global food security scenario and assessment studies: results, gaps and research priorities. *Global Food Security* **3**(3–4), 227–238. <https://doi.org/10.1016/j.gfs.2014.09.004>
- Van Meijla, H., Shutesa, L., Valin, H., Stehfest, E., van Dijk, M., Kuiper, M., Tabeau, A., van Zeist, W.-J., Hasegawa, T. & Havlik, P. 2020. Modelling alternative futures of global food security: Insights from FOODSECURE. *Global Food Security* **25**, 15. <https://doi.org/10.1016/j.gfs.2020.100358>
- Vervoort, J.M., Thornton, P.K., Kristjanson, P., Förch, W., Ericksen, P.J., Kok, K. & Ingram, J.S.I. 2014. Challenges to scenario-guided adaptive action on food security under climate change. *Global Environmental Change* **28**, 383–394. <https://doi.org/10.1016/j.gloenvcha.2014.03.001>
- Wang, D. 2021. *Is China on the Brink of Food Crisis? China's Food Security, Feed Security and Seed Security*. Hang Seng Bank China. [https://www.hangseng.com.cn/1/PA\\_esf-ca-app-content/content/pws/home/pdf/monthly\\_report\\_Mar\\_EN.pdf](https://www.hangseng.com.cn/1/PA_esf-ca-app-content/content/pws/home/pdf/monthly_report_Mar_EN.pdf)
- Wu, J., Zhang, J., Wang, S. & Kong, F. 2016. Assessment of food security in china: a new perspective based on production-consumption coordination. *Sustainability* **8**(3), 183. <https://doi.org/10.3390/su8030183>
- Zhanga, J., He, C., Chen, L. & Caoa, S. 2018. Improving food security in China by taking advantage of marginal and degraded lands. *Journal of Cleaner Production* **171**(10), 1020–1030. <https://doi.org/10.1016/j.jclepro.2017.10.110>
- Zhou, D., Yu, X. & Herzfeld, T. 2015. Dynamic food demand in urban China? *China Agricultural Economic Review* **7**, 27–44. <https://doi.org/10.1108/CAER-02-2014-0016>
- Zou, J. & Guo, S. 2015. China's food security evaluation based on factor analysis. *American Journal of Industrial and Business Management* **5**(6), 447–456.

## **Application of pineapple fiber in the development of sustainable mortars**

A.R.G. de Azevedo<sup>1</sup>, H.A. Rocha<sup>1</sup>, M.T. Marvila<sup>1</sup>, D. Cecchin<sup>2,\*</sup>, G.C. Xavier<sup>3</sup>, R.C. da Silva<sup>2</sup>, P.F.P. Ferraz<sup>4</sup>, L. Conti<sup>5</sup> and G. Rossi<sup>5</sup>

<sup>1</sup>UENF - State University of the Northern Rio de Janeiro, LAMAV - Advanced Materials Laboratory, Av. Alberto Lamego, 2000, PO Box 28013-602, Campos dos Goytacazes, Brazil

<sup>2</sup>UFF - Federal Fluminense University, TER - Department of Agricultural and Environmental Engineering; Rua Passo da Pátria, 156, PO Box 21065-230, Niterói, Brazil

<sup>3</sup>UENF - State University of the Northern Rio de Janeiro, LECIV - Civil Engineering Laboratory, Av. Alberto Lamego, 2000, PO Box 28013-602, Campos dos Goytacazes, Brazil

<sup>4</sup>UFPA - Federal University of Lavras, Department of Agricultural Engineering, Campus Universitário, PO Box 3037, Lavras, Minas Gerais, Brazil

<sup>5</sup>University of Firenze, Department of Agriculture, Food, Environment and Forestry (DAGRI), Via San Bonaventura 13, PO Box 50145 Firenze, Italy

\*Correspondence: [daianececchin@id.uff.br](mailto:daianececchin@id.uff.br)

Received: January 27<sup>th</sup>, 2021; Accepted: May 12<sup>th</sup>, 2021; Published: October 5<sup>th</sup>, 2021

**Abstract.** Due to the great worldwide increase in pineapple production, countries like Brazil and India have problems regarding the correct disposal of residues from the production of this fruit. One of the possibilities is the reuse of these residues in the form of fibers in cementitious materials, as is the case with mortars. As a result, the objective of this work is to evaluate the application of pineapple fibers in mortars in the proportion of 1: 4 (cement: sand) with addition of fiber treated in NaOH in the proportion of 3 and 6%. The properties of mechanical resistance, water absorption, mass density and adhesion were evaluated, aiming to apply the mortar in coatings of rural environments. The results indicate that the fibers reduced the mortar density and increased the mechanical strength. However, there was a reduction in adherence, especially with the use of 6% fiber, in addition to an increase in water absorption. Based on the results, it is concluded that it is feasible to use 3% of pineapple fiber for the production of coating mortars in rural environments because the results obtained in the investigation are compatible with this application and with the established normative limits.

**Key words:** rural constructions, agro-industrial wastes, sustainability, reuse.

### **INTRODUCTION**

Pineapple (*Ananas comosus*) is one of the main fruits produced in Brazil, being consumed internally and also being one of the main agricultural products exported in the

country (Braga et al., 2020). The average annual production between the years 2012 and 2018 was 1.7 billion, making Brazil the second largest producer of this fruit in the world (Scherer et al., 2015; Braga et al., 2020).

The major problem in this fruit production, in Brazil and worldwide, is the waste generated by its, mainly due to the peel and crown of the fruit (Wasserbauer et al., 2019). These wastes are disposed of without any prior care, even with great potential for reuse. Among the known ways to reuse this residue, we can mention: fuel (Chen et al., 2020), cellulose (Faria et al., 2020), spray drying (Braga et al., 2020) and as natural fiber for composites (Ramesh et al., 2016; Ramesh et al., 2017).

About this last application, some research carried out with fibers similar to pineapple, proved the feasibility of applying the material as reinforcement in cementitious matrices (Ramesh Kumar & Kesavan, 2020; Ramesh et al., 2020; Singh & Gupta, 2020). It is known that composite materials have two phases mainly: the matrix phase, which is responsible for the volume of the material, and the dispersed phase, or reinforcement, in general with application of fibers (Castoldi et al., 2019; Ryabchikov et al., 2020). This phase improves or reinforces the mechanical behavior of the matrix. In the case of cementitious materials, fibers are used for two purposes, to increase ductility and improve the tensile strength of the material (Du et al., 2021; Men et al., 2021).

The following works are mentioned as an example of the application of natural fibers: (Akinyemi & Dai, 2020) studied the application of banana fibers in cementitious mortars in the proportion 1: 3 (cement: sand) with 1.5% of banana fibers in relation to the cement mass. They observed that the fiber increases the mechanical performance of the mortar and ductilizes the material. Similar conclusions are obtained by (Elbehiry et al., 2020) in concrete.

(Sabarish et al., 2020) studied the incorporation of sisal fibers in concrete using a percentage of 1.5% in cement. The authors observed that the use of fibers improved the properties of compressive and flexural strength, in addition to discussing considerably the breaking behavior of the studied concrete elements. The results are confirmed by (de Klerk et al., 2020). Marvila et al. (2020) and de Azevedo et al. (2021) studied the application of açai fiber in cementitious matrices, applying in mortars. The results obtained by the authors prove the possibility of applying natural fibers. The results highlighted in these researches indicate a potential for the application of pineapple fibers, whose composition is cellulose such as banana, sisal and açai fibers, in cementitious matrices. (Bambi et al., 2019) studied the application of bamboo fiber in sustainable mortars for sound insulation, obtaining important results that prove the feasibility of applying the material.

In this context, the objective of this work is to evaluate the application of pineapple fiber, in contents of 3 and 6%, in the properties of the hardened state of a sustainable cement-based mortar. For this, mass density tests were performed in the hardened state, water absorption, flexural tensile strength, compressive strength and adhesion.

## **MATERIALS AND METHODS**

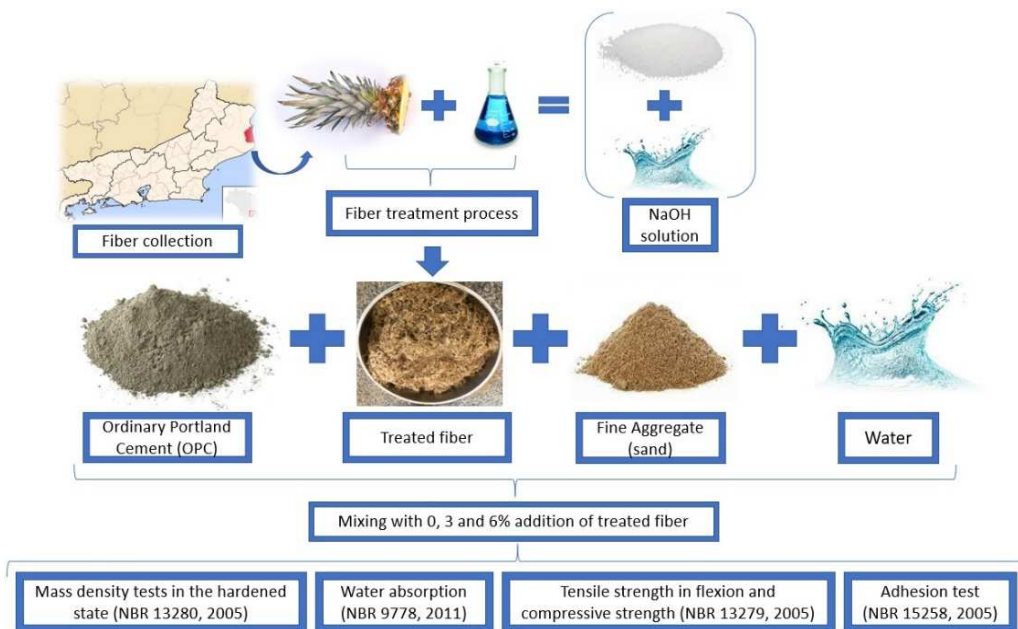
### **Materials**

The pineapple fibers were extracted from an agricultural industry located in São João da Barra - RJ - Brazil. The fibers used come from the crown of the fruit, being dried in an oven at 60 °C after extraction for a period of 24 h. The fibers were treated in a



NaOH solution with 10% mass concentration, being immersed in the treatment solution for 30 minutes. After immersion in sodium hydroxide, the fibers were washed with running water and HCl, to neutralize the pH. They were again dried in greenhouses at 60 °C for 24 h, being thus ready for application.

In addition to the fibers, ordinary Portland cement (OPC) and river washed sand collected in Campos dos Goytacazes - RJ- Brazil were used. The sand used has granulometry with a maximum diameter of 2.4 mm, standardized through the analysis of other studies (de Azevedo et al., 2018; Marvila et al., 2019). Fig. 1 presents the schematic flowchart on the methodology used in this article.



**Figure 1.** Schematic flowchart of the methodology.

### Methods

To evaluate the effects of incorporating pineapple fibers treated in mortars, specimens were produced in the proportion 1:4:1.5 (cement: sand: water), using percentages of 0, 3 and 6% of fiber in relation to cement mass. The specimens produced were in prismatic geometry 40×40×160 mm, according to the Brazilian norms (NBR 13276, 2016). In the mortar mixing stage, the pineapple fiber is added together with water, aiming at greater homogenization of the material, according to some published works (Marvila et al., 2020; A.R.G. de Azevedo et al., 2021).

After being produced, the specimens were stored at room temperature, of approximately 25 °C, for a period of 28 days. Afterwards, the samples were submitted to mass density tests in the hardened state (NBR 13280, 2005), water absorption (NBR 9778, 2011), tensile strength in flexion and compressive strength (NBR 13279, 2005), and adhesion test (NBR 15258, 2005). The tests performed are extremely important to verify the feasibility of applying sustainable mortars. In all studies, 3 samples were used

for each mortar composition studied, enabling the calculation of average and standard deviations, indicated in the figures that present the results of each property. Table 1 shows the amounts of mass applied in the study.

**Table 1.** Mortar compositions used

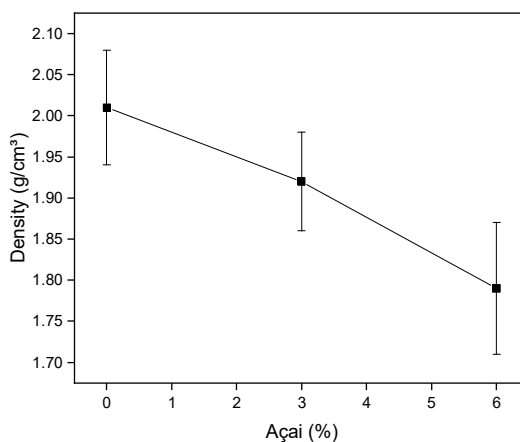
Composition	Cement (g)	Sand (g)	Water (g)	Pineapple Fiber (g)
0%	250	1,000	375	0
3%	250	1,000	375	7.5
6%	250	1,000	375	15

## RESULTS AND DISCUSSION

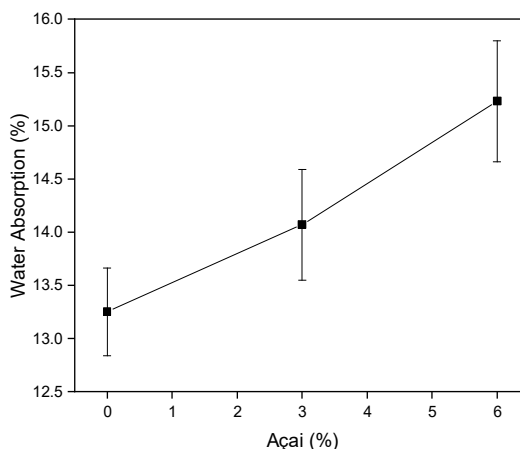
Fig. 2 shows the density of mortars in the hardened state. It is observed that there was a reduction in density as the pineapple fiber content increased. The density dropped from  $2.01 \text{ g cm}^{-3}$  (composition 0%) to  $1.79 \text{ g cm}^{-3}$  (composition with 6%). The reduction in density is due to the characteristic of fibers to increase the volume of mortars, even with little variation in the mass of the material. This information was reported by other researchers, who conducted research with natural fibers in cementitious matrices. (Quiñones-Bolaños et al., 2021) reported a drop in density from  $2.06 \text{ g cm}^{-3}$  in the reference composition to  $1.56 \text{ g cm}^{-3}$  in the composition containing 15% coconut fiber. (Sathiparan et al., 2017) obtained a reduction in density from  $2.02 \text{ g cm}^{-3}$  (0% of coconut fiber) to approximately  $1.91 \text{ g cm}^{-3}$  with 0.75% of fiber.

In other words, the results obtained are coherent when compared to other studies with natural cellulose fibers. In addition, the reduction of density with the use of fibers is beneficial for coating mortars, as they help to reduce the structure's own weight and relieve the structural loads on the building.

Fig. 3 shows the water absorption of the evaluated mortars. There is an almost linear increase in water absorption as the fibers are incorporated. Absorption increased from 13.25% (reference composition) to 15.23% (with 6% fiber). This is due to the hygroscapillary nature of the fiber, which absorbs water more



**Figure 2.** Results of mass density in the hardened state of mortars with pineapple fibers.

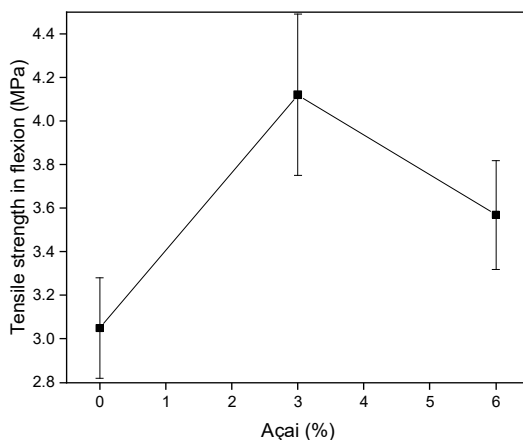


**Figure 3.** Results of water absorption of mortars with pineapple fibers.

easily than the cementitious matrix. The chemical composition of the fiber, which is predominantly cellulosic, is responsible for this behavior. Some authors who studied cementitious composites with natural fiber obtained the same pattern. This is the case of (Azevedo et al., 2020), who observed an increase in water absorption from 15% (reference composition) to 16.2% in mortars containing curauá fiber. The same pattern was observed by (Sathiparan et al., 2017), whose water absorption increased from 10% to 15% using 0.75% of coconut fiber. The results obtained, therefore, are consistent.

The increase in water absorption caused by the fibers is bad because it can cause pathologies and cracks in the coating to occur. On the other hand, increasing the water absorption can help increase the mechanical resistance due to the greater amount of water available for hydrating the cement, as will be seen in Figs 4 and 5. Thus, the analysis of the water absorption result contributes to the conclusions on the behavior of pineapple fibers, especially when correlated to the other parameters discussed in this study.

Fig. 4 shows the results of tensile strength in flexion. It is observed that there was an increase in the resistance of the composition from 0% to 3%, going from 3.05 to 4.12 MPa containing 3% of fibers. The composition with 6% pineapple fiber has a flexural tensile strength of 3.57 MPa, higher than the reference composition, but lower than the composition with 3% fiber. This is because the use of excess fibers compromises the wettability of the matrix, causing a saturation of the reinforcement phase and creating points of weakness in the material. As a result, it is recommended that the pineapple fiber content used in cementitious materials be a maximum of 3%, so as not to compromise the wettability of the composite.



**Figure 4.** Results of tensile strength flexion of mortars with pineapple fibers.

In addition to the increase in tensile strength in flexion, the use of 3 and 6% fibers improved the ductility of the material, increasing the propagation of cracks before rupture. This information had already been highlighted by other authors who studied natural fibers, as is the case of the works by Azevedo et al. (2020), de Azevedo et al. (2021). It is known that the rupture of cementitious materials is catastrophic and fragile. The use of pineapple fibers is a cheap and ecological alternative to increase the ductility of the cementitious matrix, making the material safer from a structural point of view and proving the importance of using the pineapple fibers studied in this research.

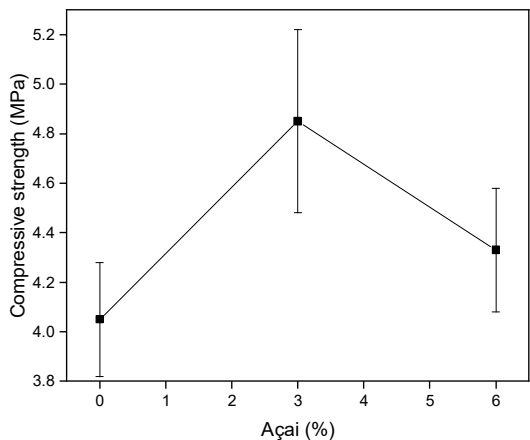
Fig. 5 shows the results of compressive strength. There is a pattern very similar to the results obtained for tensile strength in compression, where the use of 3% fiber improved the strength, when compared to the compositions of 0% and 6%. The same pattern was observed, for example, in the work of (de Azevedo et al., 2021), in which the compressive strength of compositions with 0% was 3.52 MPa, with an increase in

strength for compositions with 1.5 and 3% açai fiber to 3.84 and 4.23 MPa, respectively. The composition with 5% açai fiber, however, dropped to 3.83 MPa. Therefore, the results obtained are consistent.

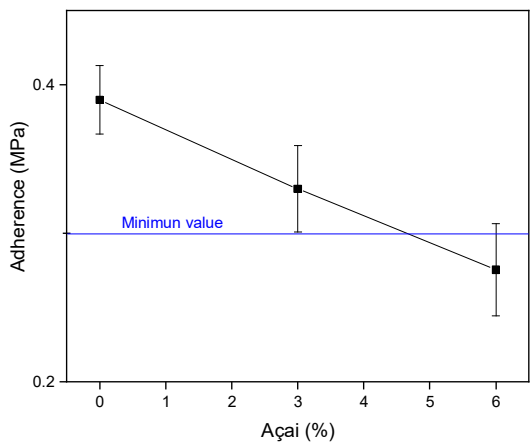
Fig. 5 shows that the compressive strength was 4.05 MPa in the 0% composition to approximately 4.8 MPa in the 3% composition. This increase of 18.5% is attributed to the better crack propagation provided by the application of pineapple fibers in the cementitious composite and prove the feasibility of applying these vegetable fibers, proposed in this article.

Fig. 6 shows the results of adherence. A drop in adherence is observed for the 3% and 6% pineapple fiber compositions, justified by the lack of penetration of the mortar in the standard substrate. The pineapple fiber, although individually increases the strength of the mortar, acts as a barrier to the penetration of the mortar cement into the substrate, impairing adherence. The Brazilian standard (NBR 15258, 2005) recommends a minimum value of 0.3 MPa for mortar adherence. It is observed that the composition of 3% of pineapple fiber meets this requirement and can be applied for the production of sustainable mortar.

The results obtained are similar to those highlighted by other authors who evaluated the application of natural fibers in coating mortars. The work of Azevedo et al. (2020), de Azevedo et al. (2021) stands out, where the authors observed that the use of vegetable fibers provided mortars with adhesion greater than 0.30 MPa.



**Figure 5.** Results of compressive strength of mortars with pineapple fibers.



**Figure 6.** Results of adherence of mortars with pineapple fibers.

## CONCLUSIONS

The main conclusions obtained in the research are:

The density results demonstrate a reduction of this property with the incorporation of fibers, attributed to the greater volume provided by the pineapple fibers. This is beneficial because it reduces the weight of the hardened material.

Water absorption increased with the incorporation of fibers, due to the hygroscopic nature and the cellulose content in the material. Although this is negative, the increase in water absorption was not high.

The compressive strength and flexural strength of compositions containing 3% fiber are superior to compositions 0% and 6% fiber. This is because the wettability point of the fiber has been reached. As a result, the incorporation of 3% fibers is indicated, which in addition to better resistance, improves the ductility of the material.

Adhesion decreased with the use of 3 and 6% of pineapple fibers, however that the use of 3% met the minimum of the Brazilian norm, of 0.3 MPa. Therefore, it is concluded by the feasibility of applying pineapple fibers in cementitious matrices for the production of sustainable mortars, in a maximum of 3%.

ACKNOWLEDGEMENTS. The authors thank the Brazilian agencies: CNPq, an FAPERJ, proc. No. E-26/210.150/2019 and E-26/010.001953/2019, for supporting this investigation.

## REFERENCES

- ABNT, 2011. NBR 9778 – Hardened mortar and concrete - Determination of water absorption, voids index and specific mass. Assoc. Bras. Normas Técnicas. (in Portuguese).
- ABNT, 2005a. ABNT NBR 13280 - Mortar for laying and cladding walls and ceilings - Determination of bulk density in the hardened state. Assoc. Bras. Normas Técnicas. (in Portuguese).
- ABNT, 2005b. NBR 13279 - Mortar for laying and covering walls and ceilings - Determination of tensile strength in flexion and compression. Assoc. Bras. Normas Técnicas. (in Portuguese).
- ABNT NBR 15258:2005. Mortar for lining walls and ceilings - Determination of potential tensile bond strength. Bras. Normas Técnicas. (in Portuguese).
- Akinyemi, B.A. & Dai, C. 2020. Development of banana fibers and wood bottom ash modified cement mortars. *Constr. Build. Mater.* **241**, 118041. <https://doi.org/10.1016/j.conbuildmat.2020.118041>
- Azevedo, A.R.G. de, Klyuev, S., Marvila, M.T., Vatin, N., Alfimova, N., Lima, T.E.S. de, Fediuk, R. & Olisov, A. 2020. Investigation of the Potential Use of Curauá Fiber for Reinforcing Mortars. *Fibers* **8**, 69. <https://doi.org/10.3390/fib8110069>
- Bambi, G., Ferraz, P.F.P., Ferraz, G.A.S., Pellegrini, P. & Giovanntonio, H.D. 2019. Measure of thermal transmittance of two different infill wall built with bamboo cultivated in Tuscany. *Agronomy Research* **17**(S1), 923–934. <https://doi.org/10.1515/AR.19.130>
- Braga, V., Guidi, L.R., de Santana, R.C. & Zotarelli, M.F. 2020. Production and characterization of pineapple-mint juice by spray drying. *Powder Technol.* **375**, 409–419. <https://doi.org/10.1016/j.powtec.2020.08.012>
- Castoldi, R. de S., Souza, L.M.S. de, & de Andrade Silva, F. 2019. Comparative study on the mechanical behavior and durability of polypropylene and sisal fiber reinforced concretes. *Constr. Build. Mater.* **211**, 617–628. <https://doi.org/10.1016/j.conbuildmat.2019.03.282>
- Chen, A., Guan, Y.J., Bustamante, M., Uribe, L., Uribe-Lorío, L., Roos, M.M. & Liu, Y. 2020. Production of renewable fuel and value-added bioproducts using pineapple leaves in Costa Rica. *Biomass and Bioenergy* **141**, 105675. <https://doi.org/10.1016/j.biombioe.2020.105675>
- de Azevedo, A.R.G., Alexandre, J., Xavier, G. de C. & Pedroti, L.G. 2018. Recycling paper industry effluent sludge for use in mortars: A sustainability perspective. *J. Clean. Prod.* <https://doi.org/10.1016/j.jclepro.2018.05.011>

- de Azevedo, Afonso R.G., Marvila, M.T., Tayeh, B.A., Cecchin, D., Pereira, A.C. & Monteiro, S.N. 2021. Technological performance of açai natural fibre reinforced cement-based mortars. *J. Build. Eng.* **33**, 101675. <https://doi.org/10.1016/j.jobe.2020.101675>
- de Klerk, M.D., Kayondo, M., Moelich, G.M., de Villiers, W.I., Combrinck, R. & Boshoff, W.P. 2020. Durability of chemically modified sisal fibre in cement-based composites. *Constr. Build. Mater.* **241**, 117835. <https://doi.org/10.1016/j.conbuildmat.2019.117835>
- Du, H., Hu, X., Han, G. & Shi, D. 2021. Experimental and analytical investigation on flexural behaviour of glulam-concrete composite beams with interlayer. *J. Build. Eng.* 102193. <https://doi.org/10.1016/j.jobe.2021.102193>
- Elbehiry, A., Elnawawy, O., Kassem, M., Zaher, A., Uddin, N. & Mostafa, M. 2020. Performance of concrete beams reinforced using banana fiber bars. *Case Stud. Constr. Mater.* **13**, e00361. <https://doi.org/10.1016/j.cscm.2020.e00361>
- Faria, L.U.S., Pacheco, B.J.S., Oliveira, G.C. & Silva, J.L. 2020. Production of cellulose nanocrystals from pineapple crown fibers through alkaline pretreatment and acid hydrolysis under different conditions. *J. Mater. Res. Technol.* **9**, 12346–12353. <https://doi.org/10.1016/j.jmrt.2020.08.093>
- Marvila, M.T., Alexandre, J., de Azevedo, A.R.G. & Zanelato, E.B. 2019. Evaluation of the use of marble waste in hydrated lime cement mortar based. *J. Mater. Cycles Waste Manag.* **21**. <https://doi.org/10.1007/s10163-019-00878-6>
- Marvila, M.T., Azevedo, A.R.G., Cecchin, D., Costa, J.M., Xavier, G.C., de Fátima do Carmo, D. & Monteiro, S.N. 2020. Durability of coating mortars containing açai fibers. *Case Stud. Constr. Mater.* **13**, e00406. <https://doi.org/10.1016/j.cscm.2020.e00406>
- Men, P., Zhou, X., Zhang, Z., Di, J. & Qin, F. 2021. Behaviour of steel–concrete composite girders under combined negative moment and shear. *J. Constr. Steel Res.* **179**, 106508. <https://doi.org/10.1016/j.jcsr.2020.106508>
- NBR 13276, 2016. Argamassa para assentamento e revestimento de paredes e tetos - Determinação do índice de consistência. Assoc. Bras. Normas Técnicas. <https://doi.org/10.1080/01080101322099>
- Quiñones-Bolaños, E., Gómez-Oviedo, M., Mouthon-Bello, J., Sierra-Vitola, L., Berardi, U. & Bustillo-Lecompte, C. 2021. Potential use of coconut fibre modified mortars to enhance thermal comfort in low-income housing. *J. Environ. Manage.* **277**, 111503. <https://doi.org/10.1016/j.jenvman.2020.111503>
- Ramesh Kumar, G.B. & Kesavan, V. 2020. Study of structural properties evaluation on coconut fiber ash mixed concrete. *Mater. Today Proc.* **22**, 811–816. <https://doi.org/10.1016/j.matpr.2019.10.158>
- Ramesh, M., Deepa, C., Rajesh Kumar, L., Sanjay, M.R. & Siengchin, S. 2020. Life-cycle and environmental impact assessments on processing of plant fibres and its bio-composites: A critical review. *Journal of Industrial Textiles* (2021). <https://doi.org/10.1177/1528083720924730>
- Ramesh, M., Gopinath, A. & Deepa, C. 2016. Machining Characteristics of Fiber Reinforced Polymer Composites: A Review. *Indian Journal of Science and Technology* **9**(42), 1–7. <https://doi.org/10.17485/ijst/2016/v9i42/101978>
- Ramesh, M., Palanikumar, K. & Reddy, K.H. 2017. Plant fibre based bio-composites: Sustainable and renewable green materials. *Renewable and Sustainable Energy Reviews* **79**, 558–584. <https://doi.org/10.1016/j.rser.2017.05.094>
- Ryabchikov, A., Kiviste, M., Udras, S.M., Lindpere, M., Vassiljev, A. & Korb, N. 2020. The experimental investigation of the mechanical properties of steel fibre-reinforced concrete according to different testing standards. *Agronomy Research* **18**(S1), 969–979. <https://doi.org/10.15159/AR.20.070>

- Sabarish, K.V., Paul, P., Bhuvaneshwari, Jones, J. 2020. An experimental investigation on properties of sisal fiber used in the concrete. *Mater. Today Proc.* **22**, 439–443. <https://doi.org/10.1016/j.matpr.2019.07.686>
- Sathiparan, N., Rupasinghe, M.N. & Pavithra, B. 2017. Performance of coconut coir reinforced hydraulic cement mortar for surface plastering application. *Constr. Build. Mater.* **142**, 23–30. <https://doi.org/10.1016/j.conbuildmat.2017.03.058>
- Scherer, R.F., Olkoski, D., Souza, F.V.D., Nodari, R.O. & Guerra, M.P. 2015. Gigante de Tarauacá: A triploid pineapple from Brazilian Amazonia. *Sci. Hortic.* (Amsterdam). **181**, 1–3. <https://doi.org/10.1016/j.scienta.2014.10.052>
- Singh, H. & Gupta, R. 2020. Influence of cellulose fiber addition on self-healing and water permeability of concrete. *Case Stud. Constr. Mater.* **12**, e00324. <https://doi.org/10.1016/j.cscm.2019.e00324>
- Wasserbauer, M., Herak, D., Mizera, C. & Hrabec, P. 2019. Utilization of image analysis for description of drying characteristics of selected tropical fruits. *Agronomy Research* **17**(S2), 1495–1500. <https://doi.org/10.15159/AR.19.072>

## Slow-release fertilization and *Trichoderma harzianum*-based biostimulant for the nursery production of young olive trees (*Olea Europaea* L.)

C. Di Vaio<sup>1</sup>, A. Testa<sup>1,2,\*</sup>, A. Cirillo<sup>1,\*</sup> and S. Conti<sup>1</sup>

<sup>1</sup>Department of Agricultural Sciences, University of Naples Federico II, Portici, IT80055 Naples, Italy

<sup>2</sup>Institute for Sustainable Plant Protection, National Research Council, Portici, IT80055, Naples, Italy

\*Corresponding author: [aurora.cirillo@unina.it](mailto:aurora.cirillo@unina.it); [antonino.testa@unina.it](mailto:antonino.testa@unina.it)

Received: May 8<sup>th</sup>, 2021; Accepted: July 30<sup>th</sup>, 2021; Published: October 5<sup>th</sup>, 2021

**Abstract.** Valorization of local olive cultivars is a key factor for the medium-term development strategy of the Italian olive agroindustry. This involves enhancements in both, cultural practices and nursery techniques. The aim of this research was the evaluation in nursery, on vegetative growth and root development of young olive plants, of two different treatments: substrate enrichment with Osmocote®, a slow-release fertilizer, and Trianum-P a *Trichoderma harzianum* based biostimulant applied as foliar spray. The trial was carried out on Rotondella and Salella, two autochthonous olive cultivars from the Campania region (southern Italy). Central axis height, number and length of lateral shoots, leaf number and trunk base diameter were monitored during the experiment. Eight months later, all plants were uprooted, and further parameters were measured: total leaf area, trunk cross sectional area (TCSA), fresh and dry weight of the leaves, shoots, trunk, roots, and total dry matter. The canopy/root ratio (C/R) was also determined. Overall, the Osmocote® treatment caused a significant increase in the vegetative growth parameters for both cultivars, with a more evident effect on the development of the canopy organs. The observation reported in the present work can represent a convenient piece of information particularly in relation to stress resilience in nursery production.

**Key words:** germplasm, nursery, Osmocote, *Trichoderma harzianum*, plant biostimulants.

### INTRODUCTION

According to recent estimates, 95% of the olive trees cultivated worldwide are concentrated in the Mediterranean area (Catalano et al., 2019). Italy ranks second as the world largest producer of olives and exporter of olive oil, after Spain (FAOSTAT, 2010–2018). On the other hand, in terms of quality, Italy ranks first with 47 certified geographical indication (PDO - Protected Designation of Origin or PGI - Protected Geographical Indication). Furthermore, Italian extra virgin olive oil represent 40% of the certified quality labels produced in Europe (Sarnari, 2020).



Along with olive oil worldwide demand continuously increasing, the medium-term growth strategy for the Italian olive agroindustry will be based on the pursuing the constant enhancement of the products quality (Sarnari, 2020). This will stimulate olive grower to move toward modern production systems, improved pest management and updated cultural practices with a focus on the exploitation of the abundant patrimony of local genetic resources estimated to include more than 800 cultivars (Muzzalupo, 2012).

Olive cultivars neglected, maybe because undesirable characteristics such as low vigor, early and abundant production, high branching, resistance to low temperatures or to heat waves, salinity tolerance, adaptability to low pruning systems, etc., may play today a crucial role in matter of biodiversity, to meet the challenges of modern olive growing, improving olive and olive oil quality (Muzzalupo, 2012; Rosati et al., 2018a and 2018b). Within this framework, nurseries are the starting point for the propagation of high-quality olive plants, making use of the rich genetic diversity of the Italian olive germplasm. The development of innovative nursery technologies aimed to better support plant growth in the nursery and/or to improve recovery from the transplant shock when the young plants are transferred to the field, should be regarded as an important research approach in this sector.

In this context, a great interest is addressed to the use of innovative sustainable practices of plant raising. In the last decades, there has been an increasing attention for a more sustainable agriculture which could increase yields and product quality, while reducing the negative impact of agrochemicals on the environment (Ventorino et al., 2016; Almadi et al., 2020; Parfeniuk et al., 2020). All these points may be fostered using plant biostimulants (PB) (Ventorino et al., 2013; López-Bucio et al., 2015; Parillo et al., 2017). Plant biostimulants are defined as ‘materials, other than fertilizers, that promote plant growth when applied in low quantities’ (du Jardin, 2015; Rouphael & Colla, 2020). According to this definition, different types of PBs have constantly played an important role in agriculture: to cite just a few examples, mycorrhizal soil fungi that establish symbiotic associations with most crop plants improving plant performance and soil health (Loit et al., 2018), nitrogen fixing rhizobia or humic substances have long been recognized as essential contributors to soil fertility (du Jardin, 2015). More recently, a number of biotic (Briccoli et al., 2009; Tataranni et al., 2009) or abiotic (Molina Soria, 2006) biostimulants have been reported to promote plant growth and defense against pathogens throughout the whole life cycle, from seed germination to plant maturity (Krouk et al., 2011) as well as increasing nutrient use efficiency and opening new routes of nutrients acquisition by plants therefore acting as biofertilizers (du Jardin, 2015).

Among the different categories of PBs, *Trichoderma* spp. are widely studied fungi and commonly used in agriculture as biological control agents (Harman et al., 2004; Prisa et al., 2013, Poveda & Baptista, 2021). *Trichoderma*-based preparations are marketed worldwide and utilized in crop protection against various plant pathogens (Woo et al., 2014). Moreover, *Trichoderma* spp. are known to improve plant resistance to environmental stresses such as salinity and drought by increasing the branching capacity of the root system, thus improving nutrient status and water acquisition (López-Bucio et al., 2015). The most common methods of application of *Trichoderma* are soil and foliar application. Soil is a repertoire of both beneficial and pathogenic microbes.

Delivering of *Trichoderma* spp. to soil will increase the population dynamics of augmented fungal antagonists and thereby would suppress the establishment of pathogenic microbes onto the infection court, this is the most effective method of application of *Trichoderma* particularly for the management of soil-borne diseases. The efficacy of biocontrol agents for foliar diseases is greatly affected by the fluctuation of microclimate. Phyllosphere is subjected to diurnal and nocturnal, cyclic and non-cyclic variation in temperature, relative humidity, dew, rain, wind and radiation. Hence, water potential of phylloplane microbes will be varying constantly. It will also vary between leaves or the periphery of the canopy and on sheltered leaves. Higher relative humidity could be observed in the shaded, dense region of the plant than that of peripheral leaves. Though foliar application of *Trichoderma* reduces the severity of diseases under field conditions, it is not technically feasible due to increased dosage and economy realized from the crop. Consequently, dosage and frequency of application has to be standardized based on the crop value, which could be as a reliable and practical approach (Kumar et al., 2014).

Based on the above knowledge, we conducted an experiment to compare the effects on the vegetative growth and root development of young olive plants raised in nursery of two different treatments, a substrate enrichment applying Osmocote®, a slow-release fertilizer (Poole & Conover, 1989) and a foliar spray, Trianum-P, a *Trichoderma harzanium*-based biostimulant (Barker, 1988). Two ancient olive cultivars Rotondella, an oil variety, and Salella a double purpose variety for both oil and table consumption, were selected for this study.

## MATERIALS AND METHODS

### Plant material and growth conditions

The trial was carried out in 2018 at the experimental site of the University of Naples in Portici (province of Naples, Southern Italy, 40°48'53.9"N, 14°20'52.8"E, 37 m a.s.l.), in a Mediterranean or Csa climate, according to Köppen classification (Peel et al., 2007). Two olive (*Olea europaea L.*) cultivars Rotondella, an oil variety, and Salella, a double purpose variety for both oil and table consumption, autochthonous of the Campania Region were chosen (Di Vaio et al., 2013b). For each cultivar, a total of thirty young plants obtained from semi-woody cuttings, uniform in size and vegetative activity, were transplanted in April into 3-liter square pots, containing a substrate obtained mixing equal volumes of peat, sand, and soil (1:1:1 v/v). Plants were grown in a nursery area, under UV stabilized high density polyethylene (PEHD) black shading net, 50% relative shading. Drip irrigation was automatically activated every two days with a flow rate of 2 liters per hour. Plants were irrigated with water equal to 100% of the evapotranspiration (ET) calculated by weight.

### Experimental treatments

For each of the two cultivars, three treatments were compared: (1) untreated Control; (2) potting substrate enriched with 3 g per liter of Osmocote® 15/9/12, a slow-release granular fertilizer commercialized by ICL Specialty Fertilizers (ICL Italia Treviso srl, Italy); (3) foliar spray application of 'Trianum-P' by Koppert Biological Systems (Koppert Italia, Bussolengo (VR), Italy) at the dose of 50 mL per liter. According to the producer's description, 'Trianum-P' is a combination of spores and

mycelium of saprophytic soil, mainly *Trichoderma harzianum*, with the addition of appropriate enzymatic mixtures to enhance its biological activity. The treatments were performed only once, at the beginning of the test (23 April) and each treatment was replicated on 10 potted plants.

### Data collection

The effect of the experimental treatments on vegetative growth was assessed at monthly intervals during one whole growing season, starting from 23 April until the end of the vegetative growing season (30 November). At each sampling date, the following measurements were recorded: height of the primary axis; number and length of the lateral shoots; diameter at the stem base; number of leaves. At the end of the vegetative growing season the plants were uprooted, and the following measurements were recorded: leaf area; leaves, shoots, trunk, roots and total fresh and dry matter weight. The total leaf area per plant was measured using a bench top Li-Cor 3100 leaf area meter (LI-COR Inc. Nebraska USA), the trunk cross sectional area (TCSA) was calculated by standard formula ( $\text{girth}^2/4\pi$ ). Following these measurements, the fresh weights were recorded for each individual replicate sample. Then the fresh samples were dehydrated under vacuum, in stove at 70°C until reached constant weight, consequently the dry weight of the samples was recorded. The canopy/root ratio (C/R) was also calculated.

### Statistical analysis

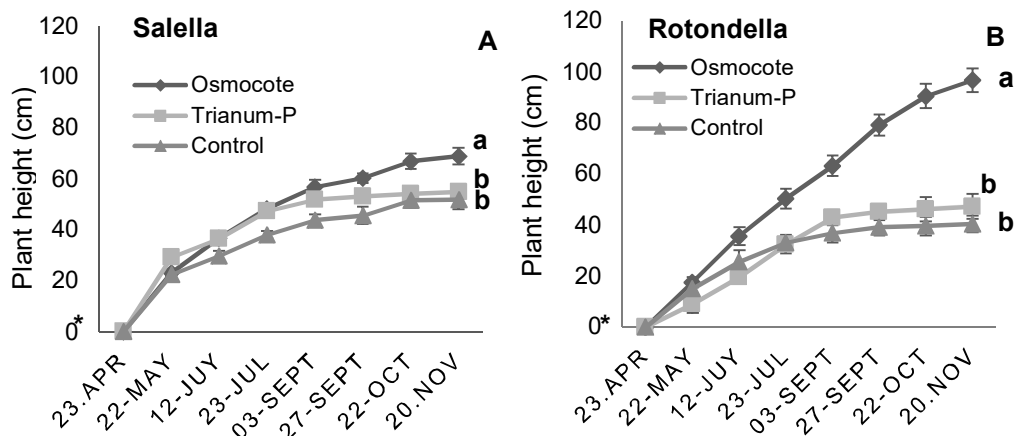
The data of parameters analyzed were normally distributed and they were processed by analysis of variance (ANOVA) and mean separations were performed through the Duncan multiple range test ( $P < 0.05$ ), using the XL-STAT version 2012 statistics software package (Addinsoft, Paris, France)

## RESULTS AND DISCUSSION

Fig. 1 reports the height increase during the vegetative season for both cultivars. Overall, the control plants of cv. Rotondella (Fig. 1, A) showed a more vigorous growth over the season compared with cv. Salella in agreement with Di Vaio et al. (2013b) (Fig. 1, B). In fact, in this neutral condition the increase in height of cv. Salella moved from 22.40 cm, one month after the beginning of the test, to 51.90 cm, at the end of the growing season. Through the same time the cv. Rotondella increase was from 15 cm to 40.30 cm. The Osmocote treatment resulted in an enhanced shoot growth in both cultivars: the growth of the primary axis of the Osmocote treated trees was 19.1% taller for cv. Salella and 58.3% for cv. Rotondella. These results converge with previously published reports confirming the effectiveness of slow-release fertilizers on the growth of olive nursery plants (Fernandez-Escobar et al., 2004; Meddad-Hamza et al., 2010). In contrast, no significant differences in shoot height were recorded for the plants treated with Trianium-P. Our results do not confirm the observations by Hermosa et al., 2013 that reported enhances in plant growth based on similar *Trichoderma* spp. treatments.

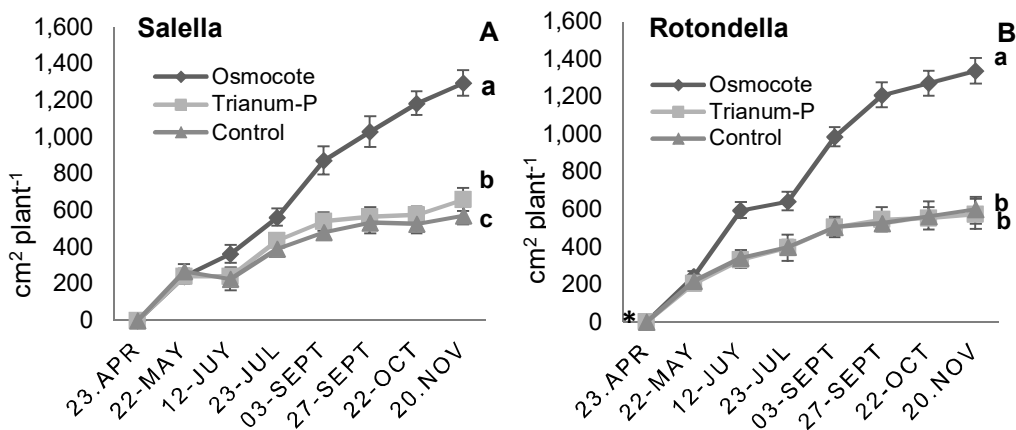
The total leaf area of the Osmocote treated plants also resulted significantly larger than control in both cultivars (Fig. 2). In the case of cv. Salella (Fig. 2, A), at the last sampling date the total leaf area per plant was 573.34 cm<sup>2</sup> per plant for the control and 1,293.45 cm<sup>2</sup> per plant for the Osmocote treated plants, corresponding to 55.7%

enhancement of the surface. Similar effect was recorded for the cv. Rotondella (Fig. 2, B), leaf area was 123.1% compared to control.



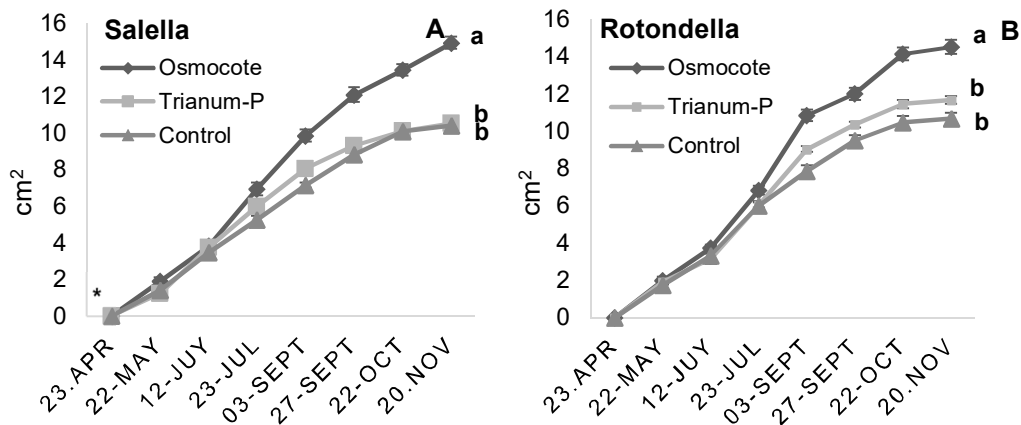
**Figure 1.** Effect of treatments on plant height increase of cvs Salella (A) and Rotondella (B) during the growing season (mean  $\pm$  SE). Means with the different letters are significantly different using Duncan's test ( $P < 0.05$ ). \*Indicates the application of Osmocote® and *Trichoderma harzianum* (Trianum-P).

The Trianum-P treatment caused in cv. Salella 13.1% increase for leaf area compared to control, means were significantly different according to the Duncan's test at the 0.05% probability level. The leaf area increase resulting from *Trichoderma* treatments has previously documented in cucumber (Yedidia et al., 2001) and in tomato (Vinale et al., 2008; Azarmi et al., 2011). On the other hand, in the case of cv Rotondella the same Trianum-P treatment did not produce any significant difference in total leaf area compared to control.

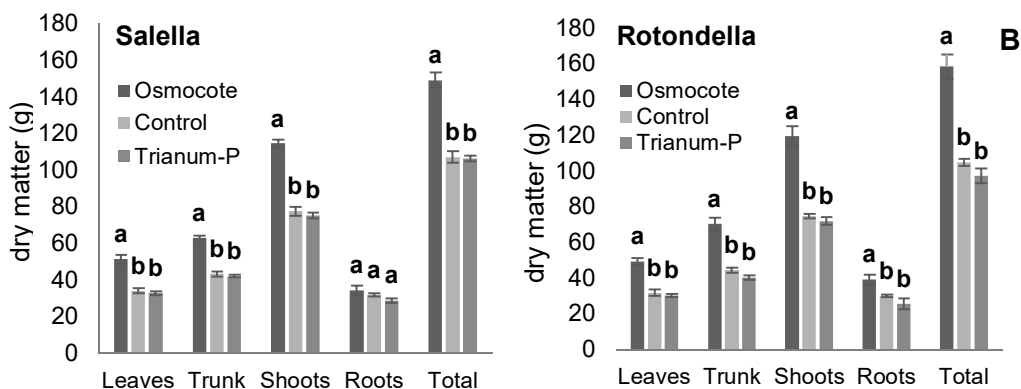


**Figure 2.** Effect of treatments on plant leaf area increase of cvs Salella (A) and Rotondella (B) during the growing season (mean  $\pm$  SE). Means with the different letters are significantly different using Duncan's test ( $P < 0.05$ ). \*Indicate the application of Osmocote® and *Trichoderma harzianum* (Trianum-P).

As regards to TCSA (trunk cross sectional area), control plants of both cultivars showed similar increases: 10.41 mm<sup>2</sup> for Salella and 10.68 mm<sup>2</sup> for Rotondella, at the end of the growing season (Fig. 3, A-B). Osmocote treated plants exhibited a larger growth, an average of 14.92 mm<sup>2</sup> TCSA for cv. Salella, corresponding to 30.2% increase compared to control. In the same experiment the cv. Rotondella plants had a final TCSA of 14.52 mm<sup>2</sup>, 26.4% more than the respective control. Only a small, statistically non-significant, increase TCSA was recorded for the Triamum-P treatment in both cultivars.



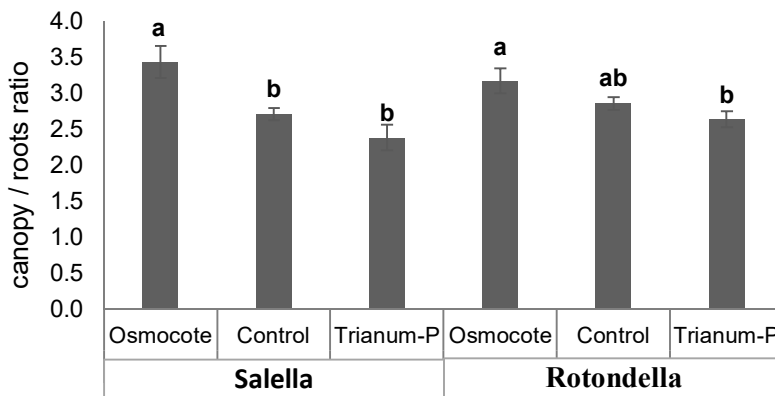
**Figure 3.** Effect of treatments on trunk cross sectional area (TCSA) increase of cvs Salella (A) and Rotondella (B) during the growing season (mean ± SE). Means with the different letters are significantly different using Duncan’s test ( $P < 0.05$ ). \*Indicate the application of Osmocote® and *Trichoderma harzianum* (Triamum-P).



**Figure 4.** Effect of treatments on dry matter accumulation and partitioning (leaves, trunk, canopy, roots and total) of cvs Salella and Rotondella (mean ± SE). Means with the different letters are significantly different using Duncan’s test ( $P < 0.05$ ).

At the end of the growing season, the dry biomass data were recorded for each plant: leaves, trunk, shoots, and roots were weighed separately, Fig. 4. Compared to control, the supplement of Osmocote to the potting substrate significantly increased the final weight of each part of the plant, with the only exception of the root weight in cv. Salella.

In terms of total biomass, the dry weight was higher than control for both the cvs. Salella and Rotondella, 28.1% and 33.9% respectively. Although, other studies found that *Trichoderma* increased yield and total dry matter like in potatoes (Mohsin et al., 2010). Rakibuzzaman et al. (2021) reported an experimental settings where the increase in the total dry matter due to *Trichoderma* treatment can be attributed to the cumulative effect of increased leaf area index, increased nutrient uptake, and increased rate of photosynthesis.



**Figure 5.** Effect of treatments on canopy/roots ratio of cvs Salella and Rotondella (mean ± SE). Means with the different letters are significantly different using Duncan’s test ( $P < 0.05$ ).

The canopy/root ratios, based on the dry mass data are presented in Fig. 5, reveal significant effects of the different treatments on both cultivars. Osmocote treatment favored the canopy growth in both cultivars and this effect was statistically significant in the case of the more vigorous cv. Salella (+21%). An analogous effect was reported by Worrall et al., 1987 in a previously published research. Conversely, the Trianium-P treatment resulted in a significantly lower canopy to root ratio compared with the Osmocote treatment (-30.6%), showing that this treatment favored the growth of the root system. A similar effect on the canopy to root ratio in olive plants, has also been reported as an effect of mycorrhizal inoculum (Citernes et al., 1998; Meddad-Hamza et al., 2010) or water deficit as observed by Di Vaio et al. (2012 and 2013a) on Leccino and Racioppella cultivars. This effect can be interpreted as a reduction of the evapo- transpirant surface relative to the root surface, increasing the tolerance to drought conditions (Dichio et al., 2002). Our results diverge from previous studies showing a positive effect of *Trichoderma* treatment on the development of the plant root system (Tataranni et al., 2009; López-Bucio et al., 2015). Contrasting studies on the effects of *Trichoderma* are reported also in the bibliography, as some studies report the *Trichoderma* efficacy in symbiosis with mycorrhizal fungi, while others report inhibition of effects in the presence of these symbiotic fungi (Green et al., 1999).

## CONCLUSIONS

Olive plants clearly responded to the substrate slow-release fertilizers application, in fact fertilized plants increased significantly in terms of leaf area per plant, central axis height, trunk diameter, and dry mass production compared to control plants; this product can improve the performance of young olive trees in the nursery.

Otherwise, plants treated with foliar spray containing a *Trichoderma harzianum* - based biostimulant, had a vegetative growth not statistically dissimilar to the control. Based on our results, we can say that a single application of foliar spray (*Trichoderma harzianum*) could be less effective compared to the direct effect on roots, when it is added to the potting substrate, where *Trichoderma* species behave as a free-living organism, common in soil and root ecosystems. Here it determines root colonization and, consequently, enhances growth and development, crop productivity, resistance to biotic and abiotic stresses, uptake and use of nutrients.

Numerous studies are available about *Trichoderma* application on the plant canopy, although not defined reliable protocols are available. This work represents a preliminary test of applications with products *Trichoderma*-based and slow-release fertilizer, on the two Campania autochthonous cultivars. Our results suggest a larger deepening, particularly in the use of the sprays products to improve the productive performance of nurseries and quality and quantity of young olive trees.

**Author Contributions:** Conceptualization, Claudio Di Vaio; methodology, Claudio Di Vaio, Stefano Conti, and Antonino Testa; data processing and software, Aurora Cirillo; validation, Claudio Di Vaio, Stefano Conti, and Antonino Testa; writing original draft preparation, Claudio Di Vaio, Stefano Conti, Antonino Testa, and Aurora Cirillo; writing review and editing, Claudio Di Vaio, Stefano Conti, and Antonino Testa; funding acquisition, Claudio Di Vaio. All authors have read and agreed to the published version of the manuscript.

## REFERENCES

- Almadi, L., Paoletti, A., Cinosi, N., Daher, E., Rosati, A., Di Vaio, C. & Famiani, F. 2020. A Biostimulant Based on Protein Hydrolysates Promotes the Growth of Young Olive Trees. *Agriculture* **10**(12), 618. doi: 10.3390/agriculture10120618
- Azarmi, R., Hajjehgari, B. & Giglou, A. 2011. Effect of *Trichoderma* isolates on tomato seedling growth response and nutrient uptake. *African Journal of Biotechnology* **10**(31), 5850–5855.
- Barker, R. 1988. *Trichoderma* spp. as plant stimulants. *Critical Reviews in Biotechnology* **7**(2), 97–106.
- Briccoli Bati, C., Santilli, E., Varlaro, M.E. & Alessandrino, M. 2009. Effects of a commercial arbuscular mycorrhizal fungi inoculum on vegetative growth of three young olive cultivars, *XXXIII CIOSTA - CIGR V Conference*, Reggio Calabria (Italy). 17–19 June, pp. 2015–201.
- Catalano, L., Shoki, A.-D., Boscia, D. & Martelli, G.P. 2019. Guidelines for the prevention, eradication and containment of *Xylella fastidiosa* in olive-growing areas. FAO, Cairo, Egypt, pp. 64.
- Citernes, A.S., Vitagliano, C. & Giovannetti, M. 1998. Plant growth and root system morphology of *Olea europaea* L. *Olea europaea* L. rooted cuttings as influenced by arbuscular mycorrhizas. *The Journal of Horticultural Science and Biotechnology* **73**(5), 647–654. doi: 10.1080/14620316.1998.11511028
- Di Vaio, C., Marallo, N., Marino, G. & Caruso, T. 2013a. Effect of water stress on dry matter accumulation and partitioning in pot-grown olive trees (cv Leccino and Racioppella). *Scientia Horticulturae* **164**, 172–177. doi: 10.1016/j.scienta.2013.09.008
- Di Vaio, C., Marra, F.P., Scaglione, G., La Mantia, M. & Caruso, T. 2012. The effect of different vigour olive clones on growth, dry matter partitioning and gas exchange under water deficit. *Scientia Horticulturae* **134**, 72–78. doi: 10.1016/j.scienta.2011.11.001

- Di Vaio, C., Nocerino, S., Paduano, A. & Sacchi, R. 2013b. Characterization and evaluation of olive germplasm in Southern Italy. *Journal of the Science of Food and Agriculture* **93**(10), 2458–2462. doi: 10.1002/jsfa.6057
- Dichio, B., Romano, M., Nuzzo, V. & Xiloyannis, C. 2002. Soil Water Availability and Relationship between Canopy and Roots in Young Olive Trees (cv Coratina). *In IV International Symposium on Olive Growing* **586**, 255–258. doi: 10.17660/ActaHortic.2002.586.48
- Du Jardin, P. 2015. Plant biostimulants: Definition, concept, main categories and regulation. *Scientia Horticulturae* **196**, 3–14. doi: 10.1016/j.scienta.2015.09.021
- FAOSTAT. Food and Agriculture Organization of the United Nations. Statistics Division, Available at: <http://faostat3.fao.org> (Accessed: August 3, 2020).
- Fernandez-Escobar, R., Benlloch, M., Herrera, E. & Garcia-Novelo, J.M. 2004. Effect of traditional and slow-release N fertilizers on growth of olive nursery plants and N losses by leaching. *Scientia Horticulturae* **101**(1–2), 39–49. doi: 10.1016/j.scienta.2003.09.008
- Green, H., Larsen, J., Olsson, P.A., Jensen, D.F. & Jakobsen, I. 1999. Suppression of the biocontrol agent *Trichoderma harzianum* by mycelium of the arbuscular mycorrhizal fungus *Glomus intraradices* in root-free soil. *Applied and Environmental Microbiology* **65**(4), 1428–1434.
- Harman, G.E., Howell, C.R., Viterbo, A., Chet, I. & Lorito, M. 2004. *Trichoderma* species - opportunistic, avirulent plant symbionts. *Nat. Rev. Microbiol.* **2**(1), 43–56. doi: 10.1038/nrmicro797
- Hermosa, R., Rubio, M.B., Cardoza, R.E., Nicolás, C., Monte, E. & Gutiérrez, S. 2013. The contribution of *Trichoderma* to balancing the costs of plant growth and defense. *Int. Microbiol.* **16**(2), 69–80.
- Krouk, G., Ruffel, S., Gutiérrez, R.A., Gojon, A., Crawford, N.M., Coruzzi, G.M. & Lacombe, B. 2011. A framework integrating plant growth with hormones and nutrients. *Trends in plant science* **16**(4), 178–182. doi: 10.1016/j.tplants.2011.02.004
- Kumar, S., Thakur, M. & Rani, A. 2014. *Trichoderma*: Mass production, formulation, quality control, delivery and its scope in commercialization in India for the management of plant diseases. *African journal of agricultural research* **9**(53), 3838–3852.
- Loit, K., Soonvald, L., Kukk, M., Astover, A., Runno-Paurson, E., Kaart, T. & Öpik, M. 2018. The indigenous arbuscular mycorrhizal fungal colonisation potential in potato roots is affected by agricultural treatments. *Agronomy Research* **16**, 510–522. doi.org/10.15159/ar.18.063
- López-Bucio, J., Pelagio-Flores, R. & Herrera-Estrella, A. 2015. *Trichoderma* as biostimulant: exploiting the multilevel properties of a plant beneficial fungus. *Scientia Horticulturae* **196**, 109–123. doi: 10.1016/j.scienta.2015.08.043
- Meddad-Hamza, A., Beddiar, A., Gollotte, A., Lemoine, M.C., Kuszala, C. & Gianinazzi, S. 2010. Arbuscular mycorrhizal fungi improve the growth of olive trees and their resistance to transplantation stress. *African Journal of Biotechnology* **9**(8), 1159–1167. doi: 10.5897/AJB09.1282
- Mohsin, T., Sumera, Y. & Fauzia Hafeez, Y. 2010. Biological control of potato black scurf by rhizosphere associated bacteria. *Brazilian Journal of Microbiology* **41**, 439–451. <https://doi.org/10.1590/S1517-83822010000200026>
- Molina Soria, C. 2006. Olive tree (*Olea europaea* L. *Olea europaea* L.) response to the application of biostimulants. *Agris.fao.org*. 82–91.
- Muzzalupo, I. 2012. Olive Germplasm - Italian Catalogue of Olive Varieties, IntechOpen, London, UK. doi.org/10.5772/3577
- Parfeniuk, A., Mineralova, V., Beznosko, I., Lishchuk, A., Borodai, V. & Krut, V. 2020. Mycobiota of the rhizosphere of raspberry plants (*Rubus idaeus* L.) under the influence of varieties and new fertilizers in conditions of organic production. *Agronomy Research* **18**, 2550–2558.



- Parillo, R., Ventorino, V., Pepe, O., Rivas, P.C. & Testa, A. 2017. Use of Compost from Chestnut Lignocellulosic Residues as Substrate for Tomato Growth. *Waste Biomass Valorization* **8**, 2711–2720. doi: 10.1007/s12649-016-9761-4
- Peel, M.C., Finlayson, B.L. & McMahon, T.A. 2007. Updated world map of the Koppen-Geiger climate classification. *Hydrol. Earth Syst. Sci.* **11**(5),1633–1716. doi: 10.5194/hess-11-1633-2007.
- Poole, R.T. & Conover, C.A. 1989. Fertilization of four indoor foliage plants with Osmocote or Nutricote. *Journal of Environmental Horticulture* **7**(3), 102–108. doi: 10.24266/0738-2898-7.3.102
- Poveda, J. & Baptista, P. 2021. Filamentous fungi as biocontrol agents in olive (*Olea europaea* L.) diseases: mycorrhizal and endophytic fungi. *Crop Protection* **146**, 105672. doi.org/10.1016/j.cropro.2021.105672
- Prisa, D., Sarrocco, S., Forti, M., Burchi, G. & Vannacci, G. 2013. Endophytic ability of *Trichoderma* spp. as inoculants for ornamental plants innovative substrates. *Biocontrol of plant pathogens in sustainable agriculture IOBC/wprs Bulletin* **86**, 169–174.
- Rakibuzzaman, M., Akand, M.H., Siddika, M. & Uddin, A.J. 2021. Impact of *Trichoderma* application as bio-stimulator on disease suppression, growth and yield of potato. *Journal of Bioscience and Agriculture Research* **27**, 2252–2257. doi.org/10.18801/jbar.270121.274
- Rosati, A., Paoletti, A., Al Hariri, R. & Famiani, F. 2018a. Fruit production and branching density affect shoot and whole-tree wood to leaf biomass ratio in olive. *Tree Physiology* **38**, 1278–1285. doi: 10.1093/treephys/tpy009
- Rosati, A., Paoletti, A., Al Hariri, R., Morelli, A. & Famiani, F. 2018b. Resource investments in reproductive growth proportionately limit investments in whole-tree vegetative growth in young olive trees with varying crop loads. *Tree Physiology* **38**, 1267–1277. doi: 10.1093/treephys/tpy011
- Rouphael, Y. & Colla, G. 2020. Editorial: Biostimulants in Agriculture’, *Frontiers in plant science* **11**(40), 1–7. doi: 10.3389/fpls.2020.00040
- Sarnari, T. 2020. Scheda di settore: olio di oliva. ISMEA Mercati. Available at: <http://www.ismeamercati.it> (Accessed: August 3, 2020).
- Tataranni, G., Santilli, E., Briccoli Bati, C. & Dichio, B. 2009. The influence of mycorrhizae on the vegetative growth of five *Olea europaea* L. *Olea europaea* L. cultivars. *Acta Italus Hortus* **1**,72–75.
- Ventorino, V., Parillo, R., Testa, A., Aliberti, A. & Pepe, O. 2013. Chestnut Biomass Biodegradation for Sustainable Agriculture. *Bioresources* **8**(3), 4647–4658. doi: 10.15376/BIORES.8.3.4647-4658
- Ventorino, V., Parillo, R., Testa, A., Viscardi, S., Espresso, F. & Pepe, O. 2016. Chestnut green waste composting for sustainable forest management: Microbiota dynamics and impact on plant disease control. *Journal of environmental management* **166**, 168–177. doi: 10.1016/j.jenvman.2015.10.018
- Vinale, F., Sivasithamparam, K., Ghisalberti, E.L., Marra, R., Barbetti, M.J., Li, H., Woo, S.L. & Lorito, M. 2008. A novel role for *Trichoderma* secondary metabolites in the interactions with plants. *Physiol. Physiological and molecular plant pathology* **72**(1–3),80–86. doi.org/10.1016/j.pmpp.2008.05.005
- Woo, S. L., Ruocco, M., Vinale, F., Nigro, M., Marra, R., Lombardi, N., ... & Lorito, M. 2014. *Trichoderma*-based products and their widespread use in agriculture. *The Open Mycology Journal* **8**(1).
- Worrall, R.J., Lamont, G.P., O’Connell, M.A. & Nicholls, P.J. 1987. The Growth Response of Container-Grown Woody Ornamentals to Controlled-Release Fertilizers. *Scientia horticulturae* **32**(3–4), 275–286. doi: 10.1016/0304-4238(87)90093-8
- Yedidia, I., Srivastva, A.K., Kapulnik, Y. & Chet, I. 2001. Effect of *Trichoderma harzianum* on microelement concentrations and increased growth of cucumber plants. *Plant Soil* **235**, 235–242. doi: 10.1023/A:1011990013955

## Enrichment of the winter triticale gene pool under intergeneric hybridization

I. Diordiieva<sup>1,\*</sup>, V. Kochmarskyi<sup>2</sup>, Ia. Riabovo<sup>3</sup>, L. Riabovo<sup>1</sup> and O. Serzhyk<sup>1</sup>

<sup>1</sup>Uman National University of Horticulture, Uman, Ukraine, Faculty of Agronomy, Department of Genetics, Plant Breeding and Biotechnology, 1 Institytska Str., UA20300 Uman, Ukraine

<sup>2</sup>State Enterprise “Experimental Farm “Elite” of Mironovskyi Institute of Wheat named after V.N. Remeslo NAAS of Ukraine, v. Central, UA08853 Mironovskyi region, Ukraine

<sup>3</sup>Uman National University of Horticulture, Uman, Ukraine, Faculty of Agronomy, Department of Plant Growing, 1 Institytska Str., UA20300 Uman, Ukraine

\*Correspondence: diordieva201443@gmail.com

Received: May 31<sup>st</sup>, 2021; Accepted: August 3<sup>rd</sup>, 2021; Published: September 10<sup>th</sup>, 2021

**Abstract.** The purpose of the research was to expand the genetic diversity of winter triticale under intraspecific and remote hybridization and to obtain new valuable forms for their involvement in the breeding process of creating high-yielding crop varieties. For this purpose interspecific and remote hybridization of different species of wheat, rye, triticale, *Elimus arenarius* L. and evaluation of obtained hybrids were carried out from 2013 to 2020. According to the results of our research it is proved that the species *Triticum spelta* L. and *Triticum petropavlovskyi* Udacz. had dominant genes of incompatibility with rye. Crossing *Triticum compactum* Host. and *Triticum sphaerococcum* Perciv. species with rye allowed obtaining a higher level of seed setting, but the grain obtained with the participation of *Triticum sphaerococcum* Perciv. species was not viable. Compatibility of triticale with spelt and *Elimus arenarius* L. was low. The level of seed formation in F<sub>1</sub> hybrids under artificial pollination was higher than under spontaneous pollination. Seed germination obtained from pollination of F<sub>1</sub> hybrids by fertile forms of triticale - was low. It was found that hybridization of three-species triticale with spelt had a positive effect on grain quality indicators in the offspring. Crossing triticale with *Elimus arenarius* L. led to ear elongation, but caused a significant reduction in all indicators of grain quality in the offspring. As a result of remote hybridization of three-species triticale and spelt wheat, winter triticale varieties Navarra and Strateh were created and included in the State register of plant varieties suitable for distribution in Ukraine since 2018.

**Key words:** initial material, hexaploid wheat, rye, crosses, varieties.

### INTRODUCTION

Triticale is an artificially created biological species that does not have a natural center of origin and a long process of evolution (Lonbani & Arzani, 2011). Therefore, a necessary condition for successful breeding work is the constant production of new initial material involving a wide variety of available forms and remote species, in

particular, wheat and rye with the best characteristics in terms of economic-and-valuable features and properties (Gorianina, 2015; Kang et al., 2016).

Synthesis of new materials is possible using different methods, in particular: 1) synthesis of primary octaploid and hexaploid triticale for wheat and rye hybrids and subsequent doubling of the number of chromosomes under the action of polyploidizing substances. This is the main method of introducing wheat and rye germplasm into the triticale gene pool (Sechniak & Sulyma, 1984; Lule et al., 2014); 2) synthesis of secondary hexaploid triticale, based on pollination of F<sub>1</sub> hybrids of different origins by pollen of hexaploid triticale. This method is technically simple and allows creating new forms of crop on a large scale on the basis of highly productive local, selection and foreign samples of wheat, rye and triticale (Sisodia & McGinnis, 1970). The basis of both methods is obtaining of remote hybrids between wheat and rye. Since the genetic diversity of parental forms is great, the number of theoretically possible combinations can be significant (Sechniak & Sulyma, 1984; Sisodia & McGinnis, 1970).

The lack of study of the problem of wheat and rye hybridization and the diversity of scientists' opinions in this regard confirms the relevance, theoretical and applied significance of the scientific field.

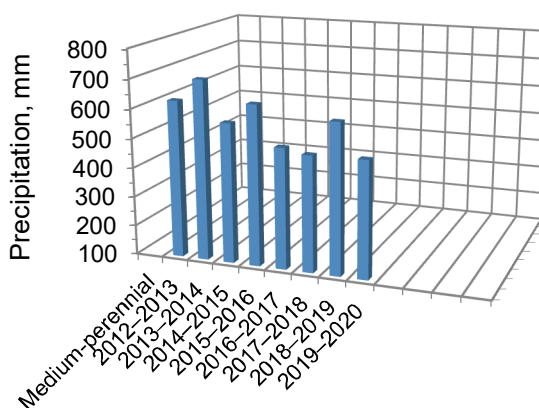
**The purpose** of the research was to expand the genetic diversity of winter triticale samples under intraspecific and remote hybridization and to obtain new valuable forms for their involvement in the selection process of creating high-yielding crop varieties.

## MATERIALS AND METHODS

The research was conducted during 2013–2020 at the plots of land of the Department of genetics, plant selection and biotechnology of Uman National University of Horticulture located in the Right-Bank Forest-Steppe zone of Ukraine. The region belongs to the subzone of unstable humidity (there are droughts once in 2–3 years). The average long-term precipitation rate for the region is 633 mm, the average annual air temperature is + 6.7 °C (Figs 1, 2).

In some years significant fluctuations in moisture supply, both in the direction of excessive moisture and in the direction of precipitation deficit during the period of research under the general increase in temperature regime with regard to the average long-term indicators were observed. The years of 2015 and 2016 were the most optimal in terms of moisture supply and temperature regime.

The soil of the experimental field was chernozem podzolized heavy loam low-humus on loess. The content of humus in the arable layer was 3.2–3.4%, the level of saturation of the bases in the range of 90–93%, the reaction of the soil solution was



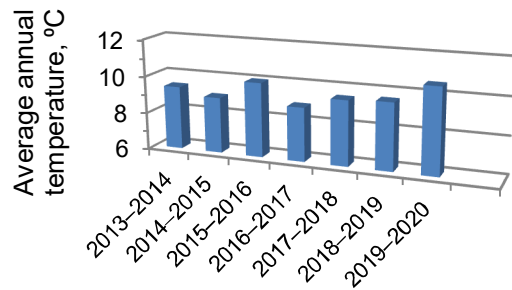
**Figure 1.** Precipitation (mm) for the period of research.

medium acid (pHKCl 5.7), hydrolytic acidity was 1.9–2.3 mmol kg<sup>-1</sup> of soil, the content of mobile compounds of phosphorus and potassium (according to DSTU 4115-2002) was 125–150 mg kg<sup>-1</sup>.

The initial material for hybridization was five species of winter hexaploid wheat, in particular, *Triticum spelta* L. (Zoria Ukrainy, Yevropa varieties), *Triticum sphaerococcum* Perciv. (Sharada variety), *Triticum aestivum* L. (Podolianka, Artemida, Freia, Artaplot varieties), *Triticum petropavlovskyi* Udacz., *Triticum compactum* Host.; samples of winter rye 193, 169 and 330 of Uman NUH selection and lines 308, 309 created at Nosivka selection-and-research station; samples of hexaploid triticale of own selection and varieties of Rozivska 6, Ladne, Khlibodar Kharkivsky, Beta, Alkid, Suvenir, Rarytet; samples of octaploid triticale UA0602463 and UA0601654 provided by the National center for plant genetic resources of Ukraine; wild forms of *Elimus arenarius* L.

Hybridization was performed by emasculation (removal of anthers) of maternal flowers and their forced pollination by parental pollen form. After the seed maturing, the mother inflorescences were cut, the number of emasculated flowers and formed seed were counted, and the percentage of seed setting and the level of progamous incompatibility were determined. Pollen fertility was determined using dyes (methylene blue or iodine lugol solution). F<sub>1</sub> hybrids were sown in the field conditions and determined the field germination of seeds. F<sub>2-5</sub> hybrids were sown in four repetitions at the rate of 10 grains in a row of 1 m in length with a row spacing of 25 cm. The numbers were placed in blocks, where every 10<sup>th</sup> number was the control variant. In the control varietal testing, the best samples were sown on the plots with the estimated area of 10 m<sup>2</sup> in four repetitions. A systematic method of plots placement was used in the research.

Hybrid progeny was analyzed by measuring morphological and economically valuable features, including plant height, lodging resistance, ear length, grain weight from the main ear and 1,000 grains weight, protein and gluten content in grain and its quality indicators, yield, etc. A systematic method of plots placement was used in the research. The numbers were arranged in blocks with a plant density of 400 thousand pcs ha<sup>-1</sup> under four-time repetition. All accounting, observation and control variety testing of the created varieties were carried out in accordance with the 'Methodology of the State scientific-and-technical examination of plant varieties' (2012). State scientific-and-technical examination of the varieties of Navarra and Strateh was conducted during 2015–2018 at the State agricultural centers for examination of plant varieties in 17 regions of Ukraine. The reliability of research, the degree of features variation and the significance of differences between indicators of laboratory tests (protein and gluten content) were determined at the level of significance of  $P \leq 0.01$ , for field studies -  $P \leq 0.05$  using statistical analysis program (SAS) v. 9.1.3. The variation coefficient



**Figure 2.** Average annual temperature (°C) for the period of research.

(V, %), standard deviation (S) and experimental error (Sx) were determined by the method of E. R. Ehrmantraut et al. (2000) and the use of MS Excel program.

## RESULTS AND DISCUSSION

**Hybridization of hexaploid wheat species with diploid rye.** It was proved that combining disability due to the display of progamous incompatibility and death of hybrid embryos at different stages of their formation under intergeneric hybridization of wheat with rye was observed (Raina, 1984; Hills et al., 2007). This complicated the work of obtaining the primary forms of triticale.

It is known that soft wheat has genes that inhibit intergeneric compatibility, in particular, Kr<sub>1</sub> gene located in chromosome 5B, and Kr<sub>2</sub> gene located in chromosome 5A (Raina, 1984; Hua & Liu, 2012). Only 7% of the world's varieties of soft wheat cross well with rye (genotype kr<sub>1</sub>kr<sub>1</sub>kr<sub>2</sub>kr<sub>2</sub>, has setting of hybrid grains at the level of 50%), 14% - have a satisfactory level of compatibility (genotype Kr<sub>1</sub>Kr<sub>1</sub>kr<sub>2</sub>kr<sub>2</sub>, provides seed setting at the level of 10–30%, and genotype kr<sub>1</sub>kr<sub>1</sub>Kr<sub>2</sub>Kr<sub>2</sub> - 30–50%), and 80% of varieties have low compatibility under crossing (genotype Kr<sub>1</sub>Kr<sub>1</sub>Kr<sub>2</sub>Kr<sub>2</sub> – setting up to 10%). In addition, it is believed that there are other genes localized in D and R genomes that are responsible for intergeneric hybridization (Qi et al., 1999). The value of the cytoplasm is not eliminated (Hsam & Larter, 1974). Data on genetic control of species compatibility of *Triticum spelta* L., *Triticum compactum* Host. and *Triticum petropavlovskyi* Udacz. with rye in the scientific literature is not found. Since these species have identical genomic formula with soft wheat and chromosomal composition of individual subgenomes, it is possible to assume the presence of Kr-genes of different allelic state in their genome.

The success of crossing under remote hybridization depends on the level of progamic and postgamous incompatibility of the initial maternal and paternal forms. It can be determined in different ways, including: 1. By the ratio of the number of setting hybrid seed to the number of pollinated flowers. This gives an idea of the level of progamic incompatibility of the original forms, which varies significantly and depends not only on genotypes, but also on the technique of crossing, pollination time, pollen quality, weather conditions, etc. (Sechniak & Sulyma, 1984). 2. By the similarity of hybrid grains (the ratio of the number of similar seed to the total number of formed seed, expressed in a percentage), which characterizes the level of postgamous incompatibility of the original forms. This indicator varies less and depends on the parents' genotypes (Sechniak & Sulyma, 1984). 3. By the ratio of the number of similar hybrid grains to the total number of pollinated flowers, expressed in a percentage (Sechniak & Sulyma, 1984). 4. By the ratio of the number of hybrid plants that survived at the time of harvest to the number of wheat flowers pollinated with rye, expressed in a percentage (Manickavelu et al., 2009).

In the course of research, the analysis of the level of progamic and postgamous incompatibility of different types of hexaploid wheat under hybridization with diploid rye was carried out. The first and fourth methods to analyze the success of crossing were used. In 2015, samples of winter rye 193 and 169 were the pollinators. Spelt wheat of Zoria Ukrainy variety had a low level of seed setting under intergeneric hybridization, which indicates the presence of dominant alleles of incompatibility genes in the genome (Table 1).

**Table 1.** The level of seed setting under hybridization of different types of hexaploid wheat with rye, 2015–2017

Maternal form (wheat)			Paternal form (rye)			
Species	Variety	Probable combination of wheat genes	Level of seed setting, %	Survival of hybrid plants, %	Level of seed setting, %	Survival of hybrid plants, %
2015			Sample 193	Sample 169		
<i>Triticum spelta</i> L.	Zoria Ukrainy	Kr <sub>1</sub> Kr <sub>1</sub> Kr <sub>2</sub> Kr <sub>2</sub>	8.8	0.0	9.5	0.0
	Yevropa	Kr <sub>1</sub> Kr <sub>1</sub> kr <sub>2</sub> kr <sub>2</sub>	15.2	1.9	18.2	0.0
<i>Triticum sphaerococcum</i> Perciv.	Sharada	Kr <sub>1</sub> Kr <sub>1</sub> kr <sub>2</sub> kr <sub>2</sub>	18.7	0.0	21.2*	0.0
<i>Triticum aestivum</i> L.	Freia	kr <sub>1</sub> kr <sub>1</sub> Kr <sub>2</sub> Kr <sub>2</sub>	31.1*	10.7*	35.2*	9.5*
	Artaplot	Kr <sub>1</sub> Kr <sub>1</sub> kr <sub>2</sub> kr <sub>2</sub>	20.8	3.7	21.1*	0.0
2016			Line 308	Line 309		
<i>Triticum spelta</i> L.	Zoria Ukrainy	Kr <sub>1</sub> Kr <sub>1</sub> Kr <sub>2</sub> Kr <sub>2</sub>	6.5	0.0	4.2	0.0
	Yevropa	Kr <sub>1</sub> Kr <sub>1</sub> kr <sub>2</sub> kr <sub>2</sub>	12.8	4.7	13.8	4.9
<i>Triticum sphaerococcum</i> Perciv.	Sharada	Kr <sub>1</sub> Kr <sub>1</sub> kr <sub>2</sub> kr <sub>2</sub>	15.6	0.0	19.2	0.0
<i>Triticum aestivum</i> L.	Artemida	kr <sub>1</sub> kr <sub>1</sub> Kr <sub>2</sub> Kr <sub>2</sub>	32.5*	6.1	32.7*	5.8
	Podolianka	Kr <sub>1</sub> Kr <sub>1</sub> kr <sub>2</sub> kr <sub>2</sub>	25.8*	4.2	27.2*	4.1
<i>Triticum petropavlovskiy</i> Udacz.		Kr <sub>1</sub> Kr <sub>1</sub> Kr <sub>2</sub> Kr <sub>2</sub>	5.1	0.0	4.5	0.0
<i>Triticum compactum</i> Host.		Kr <sub>1</sub> Kr <sub>1</sub> kr <sub>2</sub> kr <sub>2</sub>	11.2	9.4	10.7	9.1
2017			Line 308	Line 330		
<i>Triticum spelta</i> L.	Zoria Ukrainy	Kr <sub>1</sub> Kr <sub>1</sub> Kr <sub>2</sub> Kr <sub>2</sub>	5.8	0.0	5.2	0.0
	Yevropa	Kr <sub>1</sub> Kr <sub>1</sub> kr <sub>2</sub> kr <sub>2</sub>	10.7	0.0	11.1	0.0
<i>Triticum sphaerococcum</i> Perciv.	Sharada	Kr <sub>1</sub> Kr <sub>1</sub> kr <sub>2</sub> kr <sub>2</sub>	18.2	0.0	20.2	0.0
<i>Triticum petropavlovskiy</i> Udacz.		Kr <sub>1</sub> Kr <sub>1</sub> Kr <sub>2</sub> Kr <sub>2</sub>	4.8	0.0	5.1	0.0
<i>Triticum compactum</i> Host.		Kr <sub>1</sub> Kr <sub>1</sub> kr <sub>2</sub> kr <sub>2</sub>	12.2	9.5*	12.8	9.7*

Note: \* – the difference is relevant at the significance level of  $P < 0.05$ .

Spelt varieties of Yevropa, soft wheat of Artaplot and round grain wheat of Sharada had a higher level of compatibility with rye (setting in the range of 15.2–21.2%), which suggested the presence of kr<sub>2</sub> genes in the genome in a recessive homozygous state. The highest level of seed setting was recorded in soft winter wheat of Freia variety (over 30%), indicating its probable combination of kr<sub>1</sub>kr<sub>1</sub>Kr<sub>2</sub>Kr<sub>2</sub> genes. The sample of winter rye 169 was more easily crossed with hexaploid wheat compared to sample 193. However, the higher combination ability was recorded when pollinating with sample 193.

In 2016, crossing of different types of hexaploid wheat was performed with winter rye lines 308 and 309, which were characterized by stunting ( $h = 72–74$  cm), long ear (10–12 cm), and line 309 - by erectile arrangement of leaf blade. *Triticum petropavlovskiy* Udacz. species showed a low level of seed setting (4.5–5.1%) when crossing with diploid rye. Probably its genome is filled with dominant incompatibility genes. According to our data, spelt wheat variety of Zoria Ukrainy also had dominant incompatibility genes, as a small amount of seed (4.2–6.5%) was formed under hybridization with rye. However, under hybridization of spelt wheat variety of Yevropa with rye, a larger number of hybrid seed (12.8–13.8%) was obtained, which indicated the presence of the recessive kr<sub>2</sub> gene

in the genome. This variety was created under hybridization of spelt with soft wheat (Polyanetska, 2012; Diordiieva et al., 2018a). Maybe, it inherited the recessive alleles of  $Kr_2/k_r2$  gene from soft wheat. *Triticum compactum* Host. and *Triticum sphaerococcum* Perciv. species probably have  $Kr_1Kr_1k_r2k_r2$  genotype, because seed setting under hybridization with rye was at the level of 10.7–21.2%. The highest rate of seed formation (32.5–32.7%) was recorded when crossing winter soft wheat of Artemida variety with rye. A possible combination of the variety genes was  $kr1kr1Kr2Kr2$ .

In 2017, winter rye line 308 and sample 330 which was created under hybridization of the maternal component of the hybrid by Dünger with self-pollinated line 149 were used as pollinators. The research results indicated the presence of dominant incompatibility genes in the genome of *Triticum petropavlovskiyi* Udacz. species and in spelt wheat variety of Zoria Ukrainy, as seed setting for their crossing with rye was low. These results were confirmed by data from previous years. It was established the level of seed setting in the range of 10.7–20.2% for *Triticum compactum* Host., *Triticum sphaerococcum* Perciv. species and spelt wheat variety of Yevropa which indicated the presence of the recessive gene  $Kr_2/k_r2$  in the genome.

Winter rye sample 330 was better crossed with hexaploid types of wheat than line 308 and provided a higher percentage of seed formation. Viable seed was obtained only in the combination of *Triticum compactum* Host. × sample 330 crossing, but hybrid plants could not be separated and propagated because hybrid generation did not set the seed even after hybridization with the fertile form of winter triticale.

**Overcoming the sterility of wheat-and-rye  $F_1$  hybrids.** Wheat-and-rye  $F_1$  hybrids are distinguished by sterility due to the lack of chromosome homology of the paternal species. Therefore, further work with them involves overcoming sterility. Currently, a number of ways to overcome the sterility of wheat-and-rye  $F_1$  hybrids, in particular: 1) pollination of hybrid flowers with pollen of one of the paternal forms; 2) pollination of hybrid flowers with pollen of the third species with the same number of chromosomes; 3) method of meiotic polyploidization, which consists of pollination of hybrid flowers with pollen of hexaploid triticale; 4) providing optimal conditions for meiosis, gametogenesis, flowering, pollination and fertilization of hybrid plants (Grauda, 2010); 5) method of mitotic polyploidization, which consists of doubling the number of chromosomes in  $F_1$  hybrids under the action of colchicine (Sechniak & Sulyma, 1984; Fu et al., 2010; Giacomini et al., 2015).

In our studies, seed obtained from plants of wheat-and-rye  $F_1$  hybrids was sown on the plots. The method of meiotic polyploidization, which involves pollination of first-generation hybrids with pollen of hexaploid triticale, was chosen as the most optimal to overcome the pollen sterility. The chosen method allowed expanding the genetic diversity of hexaploid triticale. During such crosses, gradual elimination in hybrids of D genome of soft wheat and formation of constant genotypes with the genomic formula AABRR were occurred, that is secondary hexaploid triticale was formed (Han et al., 2003). The recombination potential of triticale was wide because of the influence under its formation of soft and durum wheat species with genomes of different quality (Kwiątek et al., 2015; Diordiieva et al., 2018a; Kwiątek & Nawracała, 2018).

In order to overcome the sterility of plants in the remote  $F_1$  hybrids, they were pollinated with pollen of different samples of hexaploid triticale. Some wheat-and-rye hybrids of the first generation were easily crossed with hexaploid forms (Freia × sample 169, *Triticum compactum* Host. × line 308), some of them did not cross at all, did not

set seed, and, as a result, they eliminated (Yevropa × line 308, *Triticum compactum* Host. × line 309, Yevropa × line 309) (Table 2). Scientists (Sechniak & Sulyma, 1984) indicate a higher percentage of seed setting under spontaneous pollination of sterile remote hybrids. However, according to our research results, better setting was provided by controlled forced pollination. Ears that were not placed under the isolator for artificial pollination (50% of spikes of each plant) in the vast majority of cases did not form seed. As an exception, it was recorded only one case of seed setting under spontaneous plants pollination ♀ Yevropa variety × ♂ winter rye line 308 when two seeds were formed, and they turned out to be non-viable.

**Table 2.** Results of pollination of the obtained wheat-and-rye F<sub>1</sub> hybrids with pollen of hexaploid triticale, 2016–2018

Combination of crossing ♀ F <sub>1</sub> (wheat × winter rye) × ♂ 6x triticale	Number of, pcs.				Level of seed setting, %	Germination capacity, %
	Pollinated ears	Pollinated flowers	Formed seed	Obtained plants		
(Yevropa variety × sample 193) × Alkid variety	3	62	8	1	12.9	12.5
(Yevropa variety × line 308) × Suvenir variety	1	23	0	0	0.0	0.0
(Yevropa variety × line 309) × Suvenir variety	1	23	2	0	0.0	0.0
(Freia variety × sample 169) × Alkid variety	3	65	10	2	15.4	20.0
(Freia variety × sample 193) × pollen mixture of 6x triticale**	2	45	8	2	17.8*	25.0*
(Artaplot variety × sample 193) × Suvenir variety	1	27	0	0	0.0	0.0
(Artemida variety × line 308) × pollen mixture of 6x triticale	1	28	4	1	14.3	25.0
(Artemida variety × line 309) × Alkid variety	1	28	3	0	0.0	0.0
(Podolianka variety × line 308) × pollen mixture of 6x triticale	1	27	6	1	22.2*	16.7
(Podolianka variety × line 309) × pollen mixture of 6x triticale	1	26	6	2	23.1*	33.3*
( <i>Triticum compactum</i> Host. × line 308) × Alkid variety	2	65	10	2	15.4	20.0
( <i>Triticum compactum</i> Host. × line 309) × pollen mixture of 6x triticale	1	23	0	0	0.0	0.0
( <i>Triticum compactum</i> Host. × sample 330) × pollen mixture of 6x triticale	1	24	5	1	20.8*	20.0

Note: \* – the difference is relevant at the significance level of  $P \leq 0.05$ ;

\*\* the pollen donors were varieties of winter triticale Alkid and Suvenir at the ratio of 50:50.

Increase in the level of seed setting under pollination of wheat-and-rye F<sub>1</sub> hybrids was observed. In hybrids, the influence of incompatibility genes disappears, which probably leads to the increase in the level of seed setting. The largest number of grains



(10 pieces) was formed by F<sub>1</sub> hybrids obtained in the combination of crossing (Freia × sample 169) × Alkid and (*Triticum compactum* Host. × line 308) × Alkid. Hybrid seed had low germination capacity (in most cases, one or two seeds were viable).

Seed setting and its field germination increased under saturating crosses of wheat-and-rye F<sub>2</sub> hybrids with pollen of hexaploid triticales.

In addition, in three combinations of crossing, seed formation as a result of free pollination by an unknown parental form was recorded. At the same time, the level of seed setting under free pollination was 5–10% higher than under controlled crossing. In plants obtained from the pollination of wheat-and-rye F<sub>2</sub> hybrids with pollen of hexaploid triticales, restoration of pollen fertility was usually observed. In the future, individual selection and analysis of elite plants among the obtained samples, which will allow choosing a valuable original material and sources of economically valuable features for selection improvement of hexaploid triticales, can be carried out.

**Hybridization of octa- and hexaploid triticales with spelt wheat and *Elimus arenarius* L.** The compatibility of triticales with wheat, in particular spelt, is determined by the genotypes of the original forms included in the crossing scheme, and depends on meteorological conditions (Li et al., 2015). A broad formative process in hybrids of hexaploid triticales with spelt wheat was observed; in the result of which recombinant forms that can be used in the selection work by genes donors of economically valuable features were formed (Diordiieva et al., 2018b).

It was found that seed setting under triticales crossing with spelt wheat was low, regardless of the octaploid (2.8–3.2%) or hexaploid (1.2–8.0%) level of crop ploidy (Table 3).

**Table 3.** Level of seed setting under crossing octa- and hexaploid forms of triticales with spelt wheat and *Elimus arenarius* L., 2014

Maternal form	Paternal form	Number of, pcs.		Level of seed setting, %	
		Castrated flowers	Formed grains		
Octaploid forms	UA0602463*	Zoria Ukrainy variety	687	22**	3.2
	UA0601654*	Zoria Ukrainy variety	632	18**	2.8
	UA0602463*	<i>Elimus arenarius</i>	250	3	1.2
Hexaploid forms	Rozivska variety 6	Zoria Ukrainy variety	350	16	4.6
	Ladne variety	Zoria Ukrainy variety	324	17**	5.2**
	Rarytet variety	Zoria Ukrainy variety	287	14	4.9
	Rarytet variety	<i>Elimus arenarius</i>	285	4	1.4
	Suvenir variety	Zoria Ukrainy variety	315	18	5.7**
	Khibodar kharkivsky variety	Zoria Ukrainy variety	452	20**	4.4
	Alkid variety	Zoria Ukrainy variety	560	22**	3.9
	Alkid variety	<i>Elimus arenarius</i>	290	6	2.1
Beta variety	Zoria Ukrainy variety	187	15	8.0**	

Note: \* – sample number according to the catalogue of the National Center for Plant Genetic Resources of Ukraine; \*\* – the difference is relevant at the significance level of  $P \leq 0.05$ .

Number of researches showed that the lack of homologous conjugation between chromosomes of the genomes *R* of triticales and *D* of wheat leads to abnormalities in the embryonic development of hybrids (Badaev et al., 1985; Khanna, 1990; Kalinka & Achrem, 2018).

We can expect the same deviations under hybridization of triticale with spelt wheat because spelt wheat has a genomic composition similar to soft wheat. As a result, deformed and thin grains with different shapes of hybrid caryopsis were formed.

F<sub>1</sub> hybrids from crossing hexaploid triticale with spelt by the morphological structure of the ear and the general habit of plants are of the same type. Characteristic features of F<sub>1</sub> hybrids were the presence of a long fluffy bald ear, coarse glume and complicated grain threshing, which is probably inherited from spelt wheat. F<sub>1</sub> hybrids from crossing octaploid triticale with spelt by the morphology of plants and ears approached wheat, because their genotype was quantitatively dominated by wheat genomes in a ratio of 3:1, which was qualitatively supplemented by the spelt genetic material. Their ear is bald or semi-bald, of medium length (11–13 cm) and density.

Awnless of hexaploid wheat species is controlled by *B1*, *B2*, *Hd* genes which are localized in *5A*, *6B* and *4A* chromosomes. Baldness in first-generation hybrids while crossing barbate hexaploid triticale with bald forms of soft wheat is dominated. In subsequent generations, the expression of the baldness feature is significantly reduced to its complete absence. The reasons for such changes have not been clearly determined (Johnson et al., 2008). Spelt wheat contains a recessive allele *q* in a homozygous state, which controls the formation of the speltoid type of ear, and the dominant *TgTg* alleles, which control the presence of coarse glume. The presence of at least one of these alleles leads to ear elongation and complication of threshing in hybrid offspring (De Faris et al., 2006). Hybrids of triticale × spelt wheat are heterozygous by these alleles in the first generation, which explains the homogeneity of the morphological structure of the ear and the phenotypic manifestation of spelt wheat features.

Hybridization of triticale with *Elimus arenarius* L. provided a lower level of seed setting, that was 1.2%, for crossing combinations with octaploid forms, and - 1.4–2.1% with hexaploid ones. Hybrids obtained under the participation of *Elimus arenarius* L. were characterized by a long (20–22 cm) ear with a significant number of spikelets and flowers. The phenotype of the plants was similar to triticale. The presence of a waxy coating and dove-colored plants, which, apparently, was inherited from *Elimus arenarius* L. was their distinct difference from the original varieties of triticale. Triticale hybrids obtained under the participation of spelt wheat and *Elimus arenarius* L. were sterile. Only a few cases of formation of fertile pollen grains were recorded. Spontaneous pollination of the first generation hybrids gave low indicators of ear grain content of F<sub>1</sub> plants, which was 0.0–2.5% for octaploid triticale and 0.0–3.0% for hexaploid triticale (Table 4).

It was observed a higher level of seed setting under isolation and artificial pollination of ears of the F<sub>1</sub> hybrid plants obtained under the participation of spelt wheat with hexaploid triticale pollen, which was 5.2–8.7% for crossing combinations with octaploid triticale, and 3.5–9.0% with hexaploid one. Seed did not set under artificial pollination of F<sub>1</sub> hybrids (octaploid triticale × *Elimus arenarius* L.) with pollen of the maternal seed form. Six seeds under hybrids re-crossing (hexaploid triticale × *Elimus arenarius* L.) with hexaploid triticale were obtained, but only one of them was germinable.

**Table 4.** Level of seed setting of remote hybrids under spontaneous and artificial pollination, 2015

Crossing combination	Spontaneous pollination			Artificial pollination with pollen of hexaploid triticales		
	Number of formed seed, pcs.	Level of seed Setting, %	Germination Capacity, %	Number of formed seed, pcs.	Level of seed setting, %	Germination Capacity, %
♀ UA0602463 × ♂ Zoria Ukrainy variety	4	2.5	0.0	12	5.2	16.7*
♀ UA0601654 × ♂ Zoria Ukrainy variety	0	0.0	0.0	14*	8.7*	14.3
♀ UA0602463 × ♂ <i>Elimus arenarius</i> L.	0	0.0	0.0	0	0.0	0.0
♀ Rozivska variety 6 × ♂ Zoria Ukrainy variety	7	2.7*	14.3	8	3.5	0.0
♀ Ladne variety × ♂ Zoria Ukrainy variety	0	0.0	0.0	9	6.0	11.0
♀ Rarytet variety × ♂ Zoria Ukrainy variety	6	2.1	16.7	10	7.1	10.0
♀ Rarytet variety × ♂ <i>Elimus arenarius</i> L.	0	0.0	0.0	2	1.1	0.0
♀ Suvenir variety × ♂ Zoria Ukrainy variety	8	3.0*	25.0*	12	7.5	16.7
♀ Khlibodar kharkivsky variety × ♂ Zoria Ukrainy variety	6	2.1	0.0	14*	8.8*	7.1
♀ Alkid variety × ♂ Zoria Ukrainy variety	9	2.5	11.0	14*	9.0*	14.2
♀ Alkid variety × ♂ <i>Elimus arenarius</i> L.	0	0.0	0.0	4	1.5	25.0*
♀ Beta variety × ♂ Zoria Ukrainy variety	8	2.7*	25.0*	10	8.5*	10.0

Note: \* – the difference is relevant at the significance level of  $P \leq 0.05$ .

Seeds obtained by both methods of pollination (artificial and spontaneous) were thin and deformed. Most grains were not viable, the germination capacity ranged from 0.0 to 25.0% Octa- and hexaploid triticales (genomic formula, ABDR and ABR, respectively), although they have genomes related to spelt wheat (genomic formula ABD), but they differ in the presence of rye genome R. This leads to a lack of homologous conjugation between the chromosomes of the parental forms causing abnormalities in embryonic development in hybrids. A wider range of abnormalities in embryonic development in hybrids under hybridization of triticales with *Elimus arenarius* L. can be observed, because these species do not have related genomes at all. This explains the formation of deformed and slender seed with different forms of hybrid karyopses and low viability.

Further work with the obtained hybrids consisted in backcrossing with their pollen of certain varieties of triticales and resowing of the obtained seed. Plants of the formed populations differed in height, morphological features of an ear, pollen fertility, etc. They were characterized by a high level of pollen sterility, which led to a small number of productive plants.

**Analysis of triticales samples by indicators of grain productivity and quality.** New samples of winter triticales were synthesized under hybridization of octa- and hexaploid triticales with spelt wheat and *Elimus arenarius* L., different types of wheat with winter rye. A number of new materials due to the intensive form-building process, which were analyzed by morphobiological properties and economically valuable features, were obtained. As a result of research, it was identified samples that exceeded the standard in terms of yield and elements of ear productivity.

Breeding materials obtained with the participation of spelt wheat were characterized by a significant range of variability in plant height ( $V = 25\%$ ) (Table 5). According to this indicator, all samples were divided into short-stemmed ( $h = 60\text{--}80$  cm), low-stemmed ( $h = 81\text{--}100$  cm) and medium-stemmed ( $h = \text{more than } 100$  cm). All samples obtained with the participation of *Elimus arenarius* L. were classified as medium-stemmed ( $h = 110\text{--}118$  cm).

**Table 5.** Indicators of economically valuable features of winter triticale samples created under remote hybridization, 2018–2020

Breeding material	Plant height, cm	Lodging		Ear length, cm	Grain mass from the ear, gr	Yield, $t\ ha^{-1}$	1,000 seeds mass, gr	Content of, %	
		%	Resistance points					Gluten	Protein
Group standard*	110	4	8	12.2	2.03	6.48	48.5	24.2	11.8
Samples obtained with participation of spelt wheat									
28	112	12	6	14.2	2.08	5.87	49.1	26.6**	13.0**
35	115	4	8	13.2	2.35**	6.81**	48.5	23.8	12.4**
61	95	3	8	12.0	2.10	6.92	49.4	26.0**	12.4**
68	87	3	8	12.8**	2.22**	6.95**	50.5**	27.8**	12.8**
85	118**	8	7	12.5	2.01	5.77	45.1	26.8**	12.5**
92	110	6	7	13.0**	1.87	5.92	48.7	25.4**	12.2**
112	108	2	8	14.1	2.12**	6.95**	46.8	23.8	12.2**
254	92	15	5	13.2	1.75	5.56	47.2	22.4	11.5
455	108**	3	8	12.0	1.98	6.15	48.0	30.2**	14.2**
481	87	3	8	12.8**	2.20**	6.85**	48.2	20.8	11.1
484	85	5	7	12.5	2.18	6.74	50.2**	21.9	11.5
491	110	5	7	13.4**	2.25**	6.53	48.2	26.4**	12.5**
x	102	–	–	12.9	2.09	6.42	48.3	25.2	12.4
S	12	–	–	0.7	0.17	0.53	1.5	2.7	0.8
$LSD_{0.95}$	4	–	–	0.4	0.09	0.27	1.6	0.2	0.1
V, %	25	–	–	8	12	18	13	8	6
Sx, %	4	–	–	3.7	4.2	4.3	3.5	0.8	0.9
Samples obtained with participation of <i>Elimus arenarius</i> L.									
5	118**	10	6	20.8**	1.58	5.35	42.2	22.1	11.1
8	115**	8	7	22.4**	1.75	5.58	43.1	23.6	11.6
10	110	12	6	19.5**	1.62	5.41	40.8	22.5	11.2
13	114	13	6	20.2**	1.47	5.18	41.2	22.8	11.4
x	114	–	–	20.7	1.61	5.38	41.8	22.8	11.3
S	3	–	–	1.2	0.12	0.17	1.0	0.6	0.2
$LSD_{0.95}$	4	–	–	0.7	0.06	0.20	1.6	0.2	0.1
V, %	9	–	–	11	15	16	7	10	8
Sx, %	4	–	–	3.5	4.0	4.1	3.7	0.8	0.9

Note. \*Group standard – winter triticale varieties of Alkid, Rarytet, Suvenir; \*\* – the difference is relevant, higher than group standard at the significance level of  $P \leq 0.05$ .

Species *Triticum spelta* L. and *Elimus arenarius* L. were characterized by a long ear (*Triticum spelta* – up to 20 cm, *Elimus arenarius* L. - up to 30 cm) (Gabel, 1984; Gulyas et al., 2012). Hybridization of three-species triticale with these species led to ear elongation in the offspring. In such a case, crossing with spelt caused a slight (0.4–1.9 cm) ear elongation, and hybridization with *Elimus arenarius* L. contributed to

the production of offspring with an ear length in the range of 19.5–22.4 cm, which significantly exceeded the group standard and samples obtained with the participation of spelt wheat.

However, the materials obtained under hybridization of triticale with *Elimus arenarius* L. were characterized by a decrease in grain mass from the ear and a decrease in yield compared to the group standard. There were identified seven samples (35, 61, 68, 481, 484 and 491) among the ones obtained with the participation of spelt wheat, which significantly exceeded the group standard by yielding capacity.

It was found that hybridization of three-species triticale with spelt wheat had a positive effect on the indicators of offspring grain quality, in particular, on the protein and gluten content.

Nine of the 12 samples that had spelt in the generation, significantly exceeded the group standard by protein content in the grain, seven of which were characterized by a significant increase in gluten content and two -by the essential increase in 1,000 seed mass. Increase in protein and gluten content in grain indicates a positive effect of crossing triticale with spelt wheat, which is characterized by a high level of these indicators manifestation (protein - up to 25%, gluten - up to 50%) and a high coefficient of inheritance of these criteria in hybrids. Hybridization of these two species was carried out in order to create new triticale with high grain quality.

The great weight of 1,000 grains in sample 484 is obviously inherited from the maternal form of the variety of three-species triticale Alkid, which is one of the most productive in Ukraine and is characterized by a weight of 1,000 grains at the level of 50.5–51.0 g. Hybridization of three-species triticale with *Elimus arenarius* L. led to the great decrease in all grain quality indicators in the offspring, which was expected because *Elimus arenarius* L. is a wild species that has no production value. It was involved in the hybridization system as a donor of high indicators of ear productivity.

**The results of winter triticale breeding.** Hexaploid winter triticale varieties of Navarra and Strateh in the result of hybridization of three-species triticale and spelt wheat and multiple individual selections were created, and they were included in the State register of plant varieties suitable for distribution in Ukraine since 2018.

Varieties by the method of remote hybridization of three-species forms of triticale and spelt wheat, followed by individual selections in  $F_{2-4}$  and repeated improving selections in terms of productivity and grain quality in  $F_{5-6}$  were created. Navarra variety (sample 491) was created by hybridization of three-species triticale of Rozivska 6 variety with a sample of spelt wheat from the submontane regions of the Carpathians, followed by crossing of the first generation hybrids with spring triticale variety Khlibodar Kharkivsky. Strateh variety (sample 455 awnless) was created by crossing winter triticale varieties Rozivska 6 and Alkid and pollination of the first generation hybrid with pollen of spelt wheat sample from the submontane regions of the Carpathians. During their creation, an important task was set - to increase protein and gluten content in grain due to the introgression of genetic material of spelt wheat into the hexaploid triticale genotype. Their genotype combined the genetic material of the varieties of three-species triticale, which was created in selection institutions located in remote ecological-and-geographical areas of Ukraine. The best samples analyzed in the selection nursery by displaying of economically valuable features with the help of multiple individual selections were chosen. Five numbers after a severe rejection of families in terms of productivity, grain quality and lodging resistance were chosen. After materials

approbation, high-yielding samples 491 and 455 (awnless), which were analyzed in a competitive variety testing, were separated. These samples were selected as constant genotypes characterized by high yields (sample 491) and high protein and gluten content (sample 455). In addition, sample 455 was characterized by awnless, which was quite rare in winter triticale. Sample 491, except for spelt wheat, contains the genetic material of triticale of different developmental types (winter and spring) in its genome.

In the course of research it was established that the average yield of 491 sample for the period of competitive variety testing (2013–2015) in the conditions of Uman NUH was 5.97 t ha<sup>-1</sup>, which significantly exceeded the group standard (Table 6). The average yield of sample 455 (awnless) was 4.96 t ha<sup>-1</sup>, which was not significantly inferior to the group standard. Sample 491 was characterized by a high level of displaying of economically valuable features; in particular, it was significantly inferior to the group standard by the plants height (102 cm) and significantly exceeded it in terms of lodging resistance. It did not differ significantly from the control variant indicators in terms of grain quality (gluten content - 21.7%, grain unit - 690 g L<sup>-1</sup>, 1,000 seeds mass - 47.8 g).

**Table 6.** Productivity indicators of winter triticale samples 491 and 455 (awnless) under competitive variety testing in the conditions of Uman NUH, 2013–2015

Indicators	Group standard*	Genotype (factor A)		<i>LsD</i> <sub>0.95</sub>		
		Sample 491	Sample 455	A	B	AB
Year (factor B) 2013						
Yield, t ha <sup>-1</sup>	5.02	5.75**	4.78	<u>0.12***</u>	<u>0.09</u>	<u>0.19</u>
				30.0	22.5	47.5
Plant height, cm	108	100	103	<u>4.12</u>	<u>1.25</u>	<u>3.25</u>
				47.8	14.5	37.7
Lodging, %	19.8	5.4	32.1	–		
resistance points	5	7	5			
Gluten content, %	21.5	21.7	29.8**	<u>0.65</u>	<u>0.15</u>	<u>0.68</u>
				43.9	10.2	45.9
Grain unit, g L <sup>-1</sup>	685	690	685	<u>21.2</u>	<u>12.2</u>	<u>30.8</u>
				33.0	18.9	48.0
1,000 seed mass, g	47.1	47.1	46.2	<u>2.12</u>	<u>0.74</u>	<u>2.35</u>
				40.7	14.2	45.1
2014						
Yield, t ha <sup>-1</sup>	5.35	6.12**	5.14	<u>0.14</u>	<u>0.12</u>	<u>0.21</u>
				29.8	25.5	44.7
Plant height, cm	112	104	109	<u>4.25</u>	<u>1.28</u>	<u>3.58</u>
				46.7	14.1	39.3
Lodging, %	29.1	10.2	48.5	–		
resistance points	5	6	3			
Gluten content, %	20.1	20.5	28.1**	<u>0.58</u>	<u>0.21</u>	<u>0.75</u>
				37.7	13.6	48.7
Grain unit, g L <sup>-1</sup>	680	680	680	<u>20.1</u>	<u>12.1</u>	<u>30.2</u>
				32.2	19.4	48.4
1,000 seed mass, g	48.5	48.6	45.4	<u>2.15</u>	<u>1.28</u>	<u>2.40</u>
				36.9	21.9	41.2

Table 6 (continued)

2015						
Yield, t ha <sup>-1</sup>	5.15	6.04**	4.96	<u>0.12</u>	<u>0.10</u>	<u>0.20</u>
				28.6	23.8	47.6
Plant height, cm	110	102	108	<u>4.18</u>	<u>1.25</u>	<u>3.47</u>
				47.0	14.0	39.0
Lodging, %	26.4	8.9	43.9	–		
resistance points	5	7	3			
Gluten content, %	22.8	22.8	31.4**	<u>0.61</u>	<u>0.22</u>	<u>0.71</u>
				37.2	13.4	49.4
Grain unit, g L <sup>-1</sup>	690	700	690	<u>20.5</u>	<u>11.8</u>	<u>30.5</u>
				32.6	18.8	48.6
1,000 seed mass, g	48.0	47.8	47.5	<u>2.21</u>	<u>1.21</u>	<u>2.75</u>
				35.8	19.6	44.6

Note: \*Group standard – varieties of winter triticale Alkid, Rarytet, Suvenir; \*\* – the difference is relevant, higher than standard at the significance level of  $P < 0.05$ ; \*\*\* above the line –  $LsD_{05}$  by factors, under the line – % influence of the factor on the feature manifestation.

Dispersion analysis showed relevant differences between genotypes, environments and their interaction by all features, as well as the difference in the influence of these factors on the formation of the level of features manifestation. Thus, the main factor in yield dispersion, gluten content, grain unit and mass of 1,000 seed was the interaction of genotype-environment. Genotype determined dispersions of plant height throughout all years of research.

According to the results of a three-year competitive variety testing, sample 491 in 2015 was submitted to the State scientific-and-technical examination under the name of Navarra variety. Sample 455 (awnless) successfully combined high yield and high indicators of grain quality (gluten content - 29.8%, protein - 13.0%, grain unit - 685 g L<sup>-1</sup>). 1,000 seeds mass was 48.2 g. According to the results of a three-year competitive variety testing, sample 455 (awnless) in 2015 was submitted to the State scientific-and-technical examination under the name of Strateh variety.

The state scientific-and-technical examination of the created varieties passed during 2015–2018 in 17 regional State centers of plant varieties examination. During this period, the average yield of Navarra variety in the Polissia zone was 5.46 t ha<sup>-1</sup>, which exceeded the zone average indicators by 1.0 t ha<sup>-1</sup> (Table 7).

Navarra variety was characterized by high grain quality, in particular, by protein content - 13.1%, 1,000 seeds mass - 48.6 g and was characterized by high resistance (8.3–9.0 points) to adverse environmental factors (fall, drought, fungal diseases). A slight lodging (resistance point - 6.5) should be noted among the negative characteristics of the variety.

The variety yield in the Forest-Steppe zone was lower and was to 5.29 t ha<sup>-1</sup>. However, it should be mentioned its higher resistance to adverse biotic and abiotic environmental factors, which was not inferior to the group standard in this area (8.5–9.0 points). It should be noted that a decrease in plant height to 94 cm in the Forest-Steppe zone in Navarra variety compared to the same indicator in the Polissia zone (114 cm) was recorded. This had a positive effect on its resistance to lodging (7.5 points).

**Table 7.** Productivity indicators of winter triticale variety of Navarra according to the results of the State scientific-and-technical examination, 2015–2018

Indicator	Forest-Steppe			Polissia		
	Average by zone	Navarra	Strateh	Average by zone	Navarra	Strateh
Yield, t ha <sup>-1</sup>	5.59	5.26	5.13	4.46	5.46*	5.03
Fall	8.9	9.1	9.1	9.1	8.8	8.8
Drought	8.5	8.5	8.5	8.5	8.8	8.5
Lodging	8.1	7.5	8.6	8.6	6.5	7.0
Resistance (points) to						
root rot	9.0	9.0	9.1	9.1	9.0	9.0
Fusariosis	9.0	9.0	9.1	9.1	8.5	8.5
powdery mildew	9.0	9.0	9.1	9.1	9.0	9.0
brown rust	9.0	9.0	9.1	9.1	8.3	8.8
Plants height, cm	104	94	109	113	114	140*
Unseeded ear, %	12.7	20.0	19.0	16.6	12.3	14.7
1,000 seeds mass, g	47.8	48.3	49.2	46.6	48.6	48.9*
Protein content, %	–	13.0	14.3*	–	13.1	14.0*

Note: \* – the difference is relevantly higher than the average by the indicators area at the significance level of  $P < 0.05$ .

The yield of Strateh variety in the Polissia zone averaged 5.03 t ha<sup>-1</sup> which exceeded average indicators by zone by 0.57 t ha<sup>-1</sup>. The variety was characterized by high grain quality, by protein content - 14.0%. It had a complex high resistance (8.5–9.0 points) to adverse environmental factors and it was characterized by low plants lodging (7.0 points), which was obviously due to the average height of the plant stand of 140 cm. 1,000 seeds mass - 48.9 g. The yield of Strateh variety (5.13 t ha<sup>-1</sup>) in the Forest-Steppe zone was lower in comparison with the average indicators of the zone (5.59 t ha<sup>-1</sup>) However, the variety was characterized by a high content of protein in grain (14.3%) and an average plant height of 109 cm, which had a positive effect on lodging resistance (8.6 points).

According to the results of the State scientific-and-technical examination, Navarra and Strateh varieties were included in the State register of plant varieties suitable for distribution in Ukraine in 2018 and recommended for cultivation in the Polissia zone.

## CONCLUSIONS

1. It is proved that the species *Triticum spelta* L. and *Triticum petropavlovskyi* Udacz. had dominant genes of incompatibility with rye, their hybridization and seed formation process was difficult, and hybrid seed did not germinate in the field conditions. Crossing *Triticum compactum* Host. and *Triticum sphaerococcum* Perciv. species with rye allowed obtaining a higher level of seed setting, but the grain obtained with the participation of *Triticum sphaerococcum* Perciv. species was not viable. Pollination of remote wheat-and-rye hybrids with hexaploid triticale pollen led to partial stabilization of the chromosome set and restoration of pollen fertility.

2. Compatibility of triticale with spelt wheat and *Elimus arenarius* L. was low regardless of the level of triticale ploidy. The level of seed formation in F<sub>1</sub> hybrids under artificial pollination was higher than under spontaneous pollination. Seed germination



obtained from pollination of F<sub>1</sub> hybrids by fertile forms of triticale, regardless of the method of pollination and pollinator - was low.

3. It was found that hybridization of three-species triticale with spelt wheat had a positive effect on grain quality indicators in the offspring, in particular, on protein and gluten content. Crossing triticale with *Elimus arenarius* L. led to ear elongation, but caused a significant reduction in all indicators of grain quality in the offspring.

4. As a result of remote hybridization of three-species triticale and spelt wheat, winter triticale varieties of Navarra and Strateh were created, which were included in the State register of plant varieties suitable for distribution in Ukraine since 2018.

## REFERENCES

- Badaev, N.S., Badaeva, E.D., Bolsheva, N.L., Maximov, N.G. & Zelenin, A.V. 1985. Cytogenetic analysis of forms produced by crossing hexaploid triticale with common wheat. *Theoretical and Applied Genetics* **70**, 536–541.
- De Faris, J., Simons, K.J., Zhang, Z. & Gill, B.S. 2006. The wheat super domestication gene Q. II *Wheat Information Service* **100**, 129–148.
- Diordiieva, I.P., Riabovol, Ia.S., Riabovol, L.O., Poltoretskii, S.P. & Kotsiuba, S.P. 2018a. *Breeding improvement of triticale with use of spelt wheat*. VPC «Vizavi», Uman, Ukraine, 214 pp. (in Ukrainian).
- Diordiieva, I., Riabovol, L., Riabovol, I., Serzhyk, O., Novak, A. & Kotsiuba, S. 2018b. The characteristics of wheat collection samples created by *Triticum aestivum* L./*Triticum spelta* L. hybridisation. *Agronomy research* **16**(5), 2005–2015. doi.org/10.15159/AR.18.181
- Ehrmantraut, E., Shevchenko, I. & Nenyn, P. 2000. Mathematical analysis and interpretation of research. Coll. Science. works Institute for Sugar Beet UAAS, **2**, 189–205. (in Ukraine).
- Fu, S, Tang, Z. & Ren, Z. 2010. Inter- and intra-genomic transfer of small chromosomal segments in wheat-rye allopolyploids. *Journal of Plant Research* **123**(1), 97–103. <https://doi.org/10.1007/s10265-009-0264-2>
- Gabel, M. 1984. A Biosystematic Study of the Genus *Elymus* (Gramineae: Triticeae) in Iowa. *Proceedings of the Iowa Academy of Science* **91**(4), 140–146.
- Giacomin, R.M., Assis, R., Brammer, S.P., Nascimento, J.A. & Da-Silva, P.R. 2015. Backcrossing to increase meiotic stability in triticale. *Genetics and Molecular Research* **14**(3), 11271–11280. <https://doi.org/10.4238/2015.September.22.21>
- Gorianina, T.A. 2015. Breeding results on triticale. *Yang scientist* **22**, 14–18 (in Russian).
- Grauda, D., Lepse, N., Strazdiņa, V., Kokina, I., Lapiņa, L., Miķelsons, A., Ļubinskis, L. & Rashal, I. 2010. Obtaining of doubled haploid lines by anther culture method for the Latvian wheat breeding. *Agronomy research* **8** (Special Issue III), 545–552.
- Gulyas, G., Rakszegi, M., Bogнар, Z., Lang, L. & Bedö, Z. 2012. Evaluation of genetic diversity of spelt breeding materials based on AFLP and quality analyses. *Cereal Res. Commun* **40**, 185–193.
- Han, F., Fedak, G., Ouellet, T. & Liu, B. 2003. Rapid genomic changes in interspecific and intergeneric hybrids and allopolyploids of Triticeae. *Genome* **46**, 716–723.
- Hills, M., Hall, L., Messenger, D., Graf, R., Beres, B. & Eudes, F. 2007. Evaluation of crossability between triticale (x *Triticosecale* Wittmack) and common wheat, durum wheat and rye. *Environ Biosafety Res.* **6**(4), 249–57.
- Hsam, S.L.K. & Larter, E.N. 1974. Influence of source of wheat cytoplasm on the synthesis and plant characteristics of hexaploid triticale. *Canadian Journal of Genetics and Cytology* **16**, 333–340.
- Hua, C. & Liu, Q. 2012. Characterizing the sequences of Kr gene in common wheat. *Triticeae Genomics and Genetics* **3**(4), 418–422. doi: 10.5376/tgg.2012.03.0004

- Johnson, E.R., Nalam, V.J., Zemetra, R.S. & Riera-Lizarazu, O. 2008. Mapping the compactum locus in wheat (*Triticum aestivum* L.) and its relationship to other spike morphology genes of the Triticeae. *Euphytica* **163**, 193–201. doi: 10.1007/s10681-007-9628-7
- Kalinka, A. & Achrem, M. 2018. Reorganization of wheat and rye genomes in octoploid triticale ( $\times$  Triticosecale). *Planta* **247**, 807–829.
- Kang, H., Wang, H., Huang, J., Wang, Y., Li, D., Diao, C., Zhu, W., Tang, Y., Wang, Y., Fan, X., Zeng, J., Xu, L., Sha, L., Zhang, H. & Zhou, Y. 2016. Divergent development of hexaploid triticale by a wheat-rye-*Psathyrostachys huashanica* trigenic hybrid method. *PLoS One*, **11**(5), e0155667. doi:10.1371/journal.pone.0155667
- Khanna, V.K. 1990. Germination, pollen fertility and crossability between triticale and wheat and reversion patterns in early segregating generations. *Cereal Res. Commun* **18**, 359–362.
- Kwiatek, M., Majka, M., Wiśniewska, H., Apolinarska, B. & Belter, J. 2015. Effective transfer of chromosomes carrying leaf rust resistance genes from *Aegilops tauschii* Coss. into hexaploid triticale ( $\times$  *Triticosecale* Witt.) using *Ae. tauschii*  $\times$  *Secale cereale* amphiploid forms. *J. Appl. Genet.* **56**, 163–168. doi: 10.1007/s13353-014-0264-3
- Kwiatek, M.T. & Nawracała, J. 2018. Chromosome manipulations for progress of triticale ( $\times$ Triticosecale) breeding. *Plant Breeding* **137**, 823–831. doi: 10.1111/pbr.12652.
- Li, H., Guo, X., Wang, C. & Ji, W. 2015. Spontaneous and divergent hexaploid triticales derived from common wheat  $\times$  rye by complete elimination of D-Genome chromosomes. *PLOS ONE* **10**(3). e0120421. <https://doi.org/10.1371/journal.pone.0120421>
- Lonbani, M. & Arzani, A. 2011. Morpho-physiological traits associated with terminal droughtstress tolerance in triticale and wheat. *Agronomy research* **9**(1–2), 315–329.
- Lule, D., Tesfaye, K. & Mengistu, G. 2014. Genotype by environment interaction and grain yield stability analysis for advanced triticale (x. *Triticosecale* Wittmack) genotypes in Western Oromia, Ethiopia. *Ethiop. Journal. Sci.* **37**(1), 63–68.
- Manickavelu, A., Koba, T., Mishina, K. & Sassa, H. 2009. Molecular characterization of crossability gene *Kr* for intergeneric hybridization in *Triticum aestivum* (Poaceae: Triticeae). *Plant Systematics and Evolution* **278**(1–2), 125–131.
- Polyanetska, I.O. 2012. Breeding-genetic improvement of *Triticum spelta* (L.) and its use breeding of *Triticum aestivum* (L.). PhD. Thesis, Kyiv, Institute of Agriculture, 189 pp. (in Ukrainian).
- Qi, Z.J., Li, Q.Q. & Wang, H.G. 1999. Crossability of some land wheat races from Shandong with rye, Huabei Nongxuebao. *Acta Agriculturae Boreali-Sinica* **14**(2), 15–19.
- Raina, S.K. 1984. Crossability and in vitro development of hybrid embryos of *Triticum durum*  $\times$  *Secale cereale*. *Indian Journal of Genetics and Plant Breeding* **44**(3), 429–437.
- Sechniak, L.K. & Sulyma, Yu.G. 1984. *Triticale*. Kolos, Moscow, 317 pp. (in Russian).
- Sisodia, N.S. & McGinnis, R.C. 1970. Importance of hexaploid wheat germplasm in hexaploid triticale breeding. *Crop Science* **10**(2), 161–162.
- State qualification methodology of plant varieties expertise on definition of suitability for distribution in Ukraine (grains, grouts, and leguminous species) 2012. Kyiv, Ukraine institute of plant varieties expertise, pp. 81. (in Ukrainian).
- State register of plant varieties suitable for dissemination in Ukraine 2021. Kyiv, Ukraine institute of plant varieties expertise, 524 pp.

## **Comparison of spatial-temporal analysis modelling with purely spatial analysis modelling using temperature data obtained by remote sensing**

L.M. dos Santos<sup>1,\*</sup>, G.A.S. Ferraz<sup>1</sup>, H.J.P. Alves<sup>2</sup>, J.D.P. Rodrigues<sup>3</sup>,  
S. Camiciottoli<sup>4</sup>, L. Conti<sup>4</sup> and G. Rossi<sup>4</sup>

<sup>1</sup>Federal University of Lavras, Department of Agricultural Engineering, University Campus, BR37.200-000 Lavras-MG, Brazil

<sup>2</sup>Institute of Applied Economic Research- IPEA, Rio de Janeiro, BR 20071-900 Rio de Janeiro, Brazil

<sup>3</sup>Geoprocessing Analyst, Bracell, Lençóis Paulistas, BR17120-000 São Paulo, Brazil

<sup>4</sup>University of Firenze, Department of Agriculture, Food, Environment and Forestry, Via San Bonaventura, 13, Firenze, Italy

\*Correspondence: [luanna\\_mendess@yahoo.com.br](mailto:luanna_mendess@yahoo.com.br)

Received: March 25<sup>th</sup>, 2021; Accepted: May 20<sup>th</sup>, 2021; Published: October 5<sup>th</sup>, 2021

**Abstract.** Variations in climatic elements directly affect the productivity of agricultural activities. Temperature is one of the climatic elements that varies in space and time. Therefore, understanding spatial variations in temperature is essential for many activities. Given the above, the objective of this work was to compare the performance of the proposed spatiotemporal analysis model with that of purely spatial analysis using temperature data obtained by remote sensing. The experimental data were arranged in a grid with 403 spatial locations, with 22 samples collected in a 24-hour period. The statistical software R Core Team (2020) was used to perform the analysis. The packages used in the analyses were ‘geoR’, ‘CompRandFld’, ‘scatterplot3d’, and ‘fields’. For making the maps, the software ArcGIS was used. The behavioural analysis of spatiotemporal dependence indicated, through the covariogram graph of the data, that there is a strong spatial dependence. For the cases of purely spatial analysis of phenomena, a separate spatial model for each time is justified because this type of model presents a smaller prediction error and requires simpler processing than the space-time model. It was possible to compare the space-time analysis with the purely spatial analysis using temperature data obtained by remote sensing images. The data modelled with the purely spatial analysis had, on average, lower error than those with the space-time model.

**Key words:** climatic elements, geostatistics, mathematical modelling.

### **INTRODUCTION**

Agricultural activities are always susceptible to the variations in climatic elements and consequently to risks. Temperature is one of the climatic elements that varies in space and time, and this parameter participates in several physiological processes in

plants and animals. Thus, understanding this element is important and relevant for evaluating studies on crop adaptation and agricultural planning (Coelho et al., 1973; Medeiros et al., 2005). Temperature is also important for the indication of the sowing time, irrigation, determination of yield potential, credit, and agricultural insurance (Cargnelutti Filho et al., 2008).

According to Viana et al. (2019), the temperature has strong temporal dependence, causing the energy received by Earth to vary mainly due to the rotational (variation in the day) and translational (variation in the year) movements of the Earth, in addition to having spatial variations, depending, for example, on the movements of air masses and variations in the surface, such as soil cover, albedo, altitude, and humidity.

Understanding the spatiotemporal dependence of temperature is essential for many activities. However, meteorological data are usually acquired in an ad hoc and isolated manner through automatic weather stations (Hartkamp, 1999). According to Varejão-Silva (2006), although there are large air temperature data series available for some locations in certain regions, there may be no records for the exact location one is interested in studying. In addition, according to Medeiros et al. (2015), there are a small number of weather stations, making the density of available temperature data low and making it difficult to characterize the thermal field. These situations are very common in practice and promote the development of techniques that seek to estimate the temperature in locations for which there are no data (Medeiros et al., 2015).

Thus, it is possible to obtain temperature data from satellite images. The series of geostationary satellites Meteosat Second Generation (MSG), in orbit since 2002, uses the spinning enhanced visible and infrared imager (SEVIRI) sensor and produces images in 12 spectral channels with a spatial resolution of 3 km at nadir, a temporal resolution of 15 minutes, and a radiometric resolution of 10 bits (Schmetz et al., 2002). MSG is useful for data acquisition and subsequent spatialization with good temporal resolution. However, satellite image data must be subjected to radiometric corrections to reduce the influence of the atmosphere (Geiger et al., 2008). Another factor that interferes with image acquisition is the weather conditions. On cloudy days, for example, the passage of solar energy is blocked by clouds, with the consequent loss of surface data (Honkavaara et al., 2013).

Given the loss of information, the spatialization of this variable can be performed using interpolation techniques in which values are estimated in unsampled locations, and maps can be created with continuous data in space; these procedures are part of geostatistics.

Currently, geostatistical methods facilitate the interpretation of data randomness, in addition to being an efficient tool for spatializing climatic elements (Pessanha et al., 2020), predicting noise from agricultural machinery (Santos et al., 2020), and predicting data within animal facilities (Curi et al., 2014; Cemek et al., 2016, Ferraz et al., 2016; Damasceno et al., 2019; Ferraz et al., 2019; Oliveira et al., 2019), among other applications in which the maps generated by this method facilitate data interpretation. However, these studies, although working with spatiotemporal data, performed purely spatial analyses and did not concomitantly explore the interaction between the spatial and temporal components.

The application of spatiotemporal geostatistics, through covariance structure modelling, is one of the procedures for spatiotemporal data analysis that takes into account the interactions between the spatial and temporal components and allows

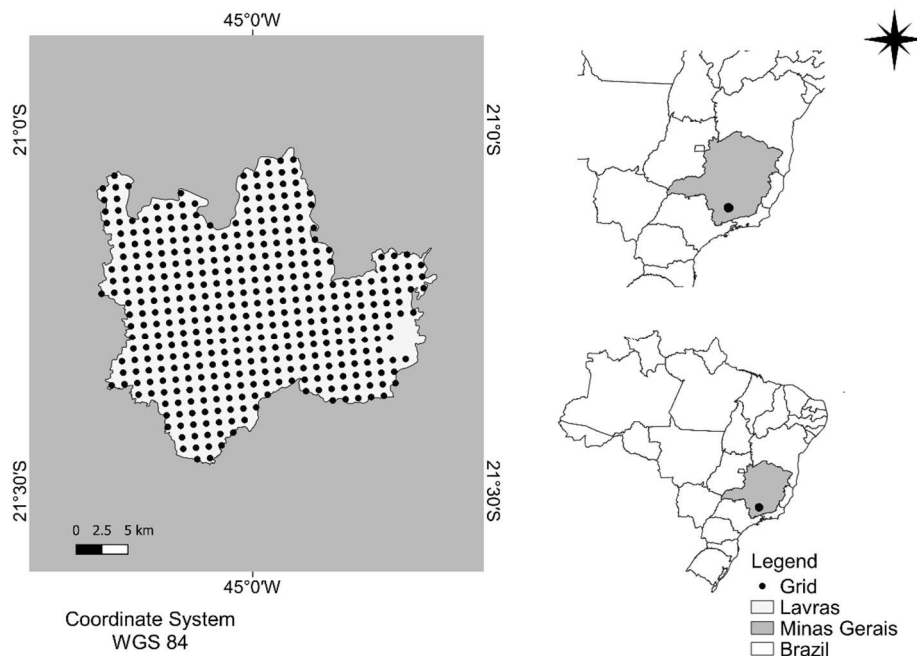
interpolations in time and space (Viana et al., 2019). This procedure was proposed by Gneiting (2002) and allows the simultaneous performance of spatial and temporal analyses.

Thus, the objective of this study was to compare the performance of the proposed spatiotemporal analysis with that of purely spatial analysis using temperature data obtained by remote sensing.

## MATERIALS AND METHODS

### Data Acquisition

The study area (Fig. 1) is located in the municipality of Lavras, in the state of Minas Gerais (MG), in the southeastern region of Brazil between latitude  $21^{\circ} 14' 45''$  south and longitude  $45^{\circ} 00'$  W of Greenwich, with a maximum altitude of 918 m above sea level (ASL). The municipality of Lavras is in an ecotone of the Cerrado and Atlantic Forest domains, where remnants of seasonal semideciduous forest, grassland, montane savanna, and cerrado (Brazilian savanna) are found (Souza et al., 2003; Dalanesi et al., 2004; Pereira et al., 2010). The climate of the region, according to the Koppen classification, is of the Monsoon-influenced humid subtropical climate (Cwa) type, characterized by a dry season in the winter and a rainy season in the summer. The average annual precipitation is 1,460 mm, and the average annual temperature is  $20.4^{\circ}\text{C}$ , with a minimum of  $17.1^{\circ}\text{C}$  in July and a maximum of  $22.8^{\circ}\text{C}$  in February (Dantas et al., 2007).



**Figure 1.** Location of the municipality of Lavras, MG.

Data were obtained with images from the MSG series of geostationary satellites of the European Organization for the Exploitation of Meteorological Satellites (EUMETSAT). These satellites have instruments such as the geostationary earth radiation budget (GERB) radiometer, communication instruments such as geostationary search and rescue (GEOS&R), the data collection system (DCS) data storage platform, and the SEVIRI sensor.

The SEVIRI sensor is equipped with 12 spectral channels, ranging from visible wavelengths to far-infrared wavelengths, including absorption bands of water vapor, ozone (O<sub>3</sub>), and carbon dioxide (CO<sub>2</sub>), with a spatial resolution between 1 km and 3 km at nadir (Fensholt et al., 2006). MSG stands out as the first series of geostationary satellites in the world with red and near infrared (NIR) bands, which are very useful for monitoring the Earth's surface at high temporal resolution (Schmetz et al., 2002).

With this temporal resolution, meteorological images can be obtained every 15 minutes in nominal mode or every 5 minutes in rapid scan mode. Thus, the values obtained every 15 minutes by MSG can be acquired 96 times a day. However, in this study, we used 22 observations of mean temperature values collected during the 1 July 2013, thus obtaining the temperature from time 1 to time 22, in which time 1 corresponded to 00 h and time 22 corresponded to 5 h 15 AM of the chosen day. These parameters were randomly selected to test the models under study.

The images were corrected following the methodology proposed by Geiger et al. (2008). The correction of atmospheric effects is important due to the dynamics of atmospheric components (aerosols, gases and clouds). For this, the SMAC (Simplified Method for Atmospheric Correction) technique is used, which demands less time. The data were arranged in a grid with 403 spatial locations spaced 1 km apart. A total of 403 locations were used to cover the entire study region (Fig. 1).

### Space-time random fields

Let  $Z(s,t)$  be a random variable measured at position  $s$  in  $R_d$ , and at time  $t$  in  $R$ ,  $R_d$  is the space,  $R$  is the time, and  $R_d \times R$  is the domain of the random field defined in space-time. In this sense, a space-time random field is defined as  $Z(s,t)$ , where  $s$  is in  $R_d$  and  $t$  is in  $R$ . In this article,  $d = 2$  is considered such as in the study by Rodrigues et al. (2019). However, note that  $d$  can be any positive integer.

### Kriging

The linear kriging predictor is defined as  $Z(s_0,t) = \mu_z + \sigma' \Sigma^{-1} (Z - \mu_z)$ . The case where  $\mu$  is constant but unknown denotes ordinary kriging. This estimator must meet the following criteria:

$[Z(s_0,t_0) - \hat{Z}(s_0,t_0)] = 0$ ; that is, it should be unbiased;

$\text{Var} [Z(s_0,t_0) - \hat{Z}(s_0,t_0)]$  is minimal.

Generally, sampling is performed with a set of points distributed sparsely throughout the region. The objective is to continuously describe the process throughout the region. However, for the case of the prediction of space-time random fields, obtaining theoretical models of semivariograms can be very complicated. A simpler method is to consider theoretical models of the stationary covariance functions that are valid.

### Covariance functions

In geostatistics, for each sampled location spatially and temporally located, there is only one realization, and the number of observations is always finite. This condition usually makes it impossible to infer the probability distribution of the location. Therefore, some hypotheses are necessary, including one commonly called the hypothesis of stationarity. Assuming this second-order hypothesis, the covariance is a tool that can be used for the autocorrelation between pairs of measured values separated by a distance  $h$ . According to Sherman (2011), a moments estimator for the covariance is defined according to equation (1):

$$\widehat{C}(h,u) = \frac{1}{N(h,u)} \sum_{N(h,u)} \{[Z(s_1,t_1) - \mu][Z(s_2,t_2) - \mu]\}^2 \quad (1)$$

where  $N(h,u)$  is the number of points that are within the distance  $h$  in each time lag  $u$  and  $\mu$  is the mean of the random field.

### Gneiting's model (2002)

Gneiting (2002) proposes the direct construction of classes of nonseparable stationary space-time covariance functions in the space-time domain. Consider two conveniently chosen functions  $\varphi(r)$ ,  $r \geq 0$  and  $\psi(r)$ . The first is a completely monotone function, and the second is a positive function with a completely monotone derivative. These definitions can be seen in Gneiting (2002), which presents the following model given by Eq. (2):

$$C(h,u) = c_0 + \frac{\sigma^2}{(a|u|^{2\alpha+1})^{\delta+\beta}} \exp\left(-c \frac{\|h\|^{2\gamma}}{(a|u|^{2\alpha+1})^{\beta\gamma}}\right) \quad (2)$$

where  $\|h\|$  is the spatial distance,  $|u|$  is the time lag,  $\sigma^2$  is the variability present in the random field, and  $c_0 = \frac{\sigma_{h=0}^2}{a|u|^\delta}$  is the nugget effect that is defined as an uncontrollable sampling error. Eq. (2) is implemented in the 'CompRandFld' package available in the R software and is used in the data analysis, where  $a$ ,  $c$ , and  $\sigma^2 > 0$  and  $\alpha, \gamma, \beta \in (0, 1]$ . Here,  $a$  and  $\alpha$  are the scaling and smoothness parameters of the process in time;  $c$  and  $\gamma$  are the scale and smoothness parameters of the process in space. The parameter  $\beta$  measures the strength of the space-time interaction.

### Software used

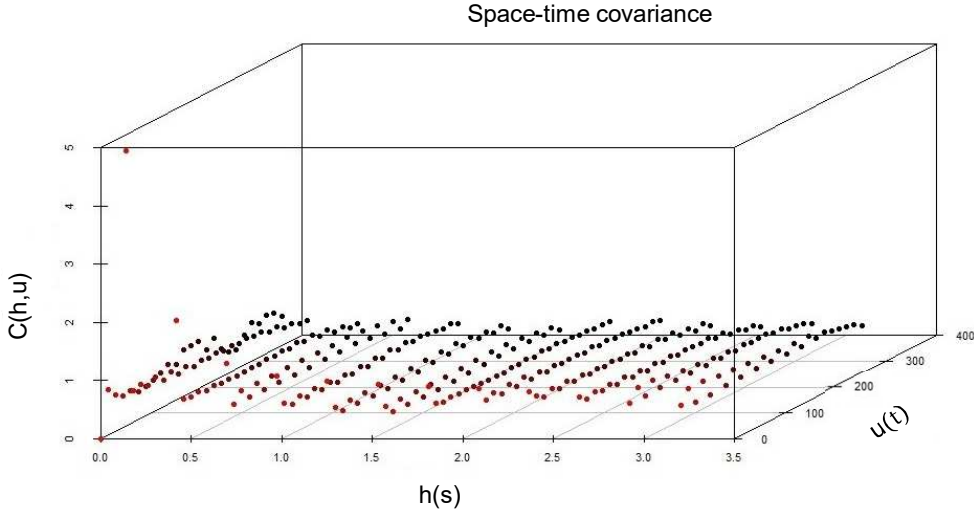
The free statistical software R version 3.5.0 (Team, 2020) was used to perform the geostatistical analyses. The packages used in the analyses were 'geoR' (Ribeiro Júnior & Diggle 2020), 'CompRandFld' (Padoan & Bevilacqua, 2020), 'scatterplot3d' (Ligges et al., 2020), and 'fields' (Nychka et al., 2020); these packages are essential for working with spatiotemporal geostatistics. The standard format of a spatiotemporal database has coordinates ( $x$ ,  $y$ ) of the locations, with values of the attribute ( $z$ ), in this case, the average temperature in addition to the times/dates of the measurements.

The calculated values of kriging prediction and variance were exported in text format (.txt) to ArcGIS to prepare the maps. The universal transverse Mercator (UTM) coordinate system, datum WGS 84, zone 23 south, was used with the intention of adaptation to the field data.

## RESULTS AND DISCUSSION

### Spatiotemporal behaviour

The existence of a spatiotemporal relationship in the data is the key point for the use of the space-time covariance function models proposed, as observed in Fig. 2.



**Figure 2.** Sample covariogram.

### Spatiotemporal analysis

The space-time covariance function model proposed by Gneiting (2002) is given by Eq. (3):

$$C(h,u) = 1.728e^{-7} + \frac{2.002}{(2.082|u|^{7.084e-01} + 1)^1} \exp\left(1.468 \frac{0.008634||h||^{6.685e-01}}{(2.082|u|^{7.084e-01} + 1)^1}\right) \quad (3)$$

Table 1 shows the estimated parameters for the covariance model according to Eq. (3):

**Table 1.** Estimated parameters of Gneiting’s model (2002)

$C_0$	$\sigma^2$	$a$	$\alpha$	$c$	$\gamma$	$\beta$
0.0000001728	2.002	2.082	1	1.468	1	1

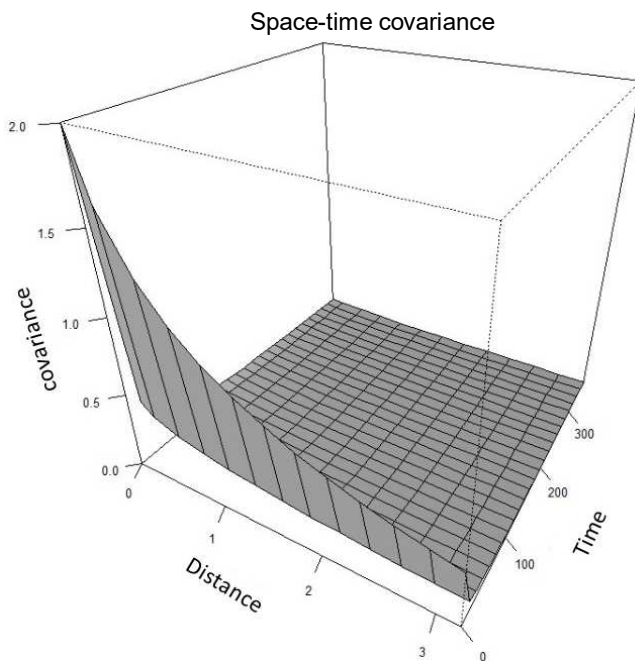
$C_0$  is the nugget effect;  $\sigma^2$  is the random field variance,  $a$  is the scale parameter in time;  $\alpha$  is the smoothness parameter in time;  $c$  is the scale parameter in space;  $\gamma$  is the smoothness parameter in space, and  $\beta$  is the parameter that measures the strength of the space-time interaction.

In the analysis of the behaviour of the spatiotemporal dependence between the data, a covariogram plot is a useful tool. Fig. 3 shows the spatiotemporal covariogram fitted to the data. Strong spatial dependence is perceived because  $\beta = 1$ , and this parameter measures the strength of the space-time interaction.

With classical statistics, the interaction between space and time cannot be obtained; i.e., the variability in the space and time dimensions cannot be collectively captured (Bicalho, 2008). With the spatiotemporal model, the covariogram shows that the spatiotemporal dependence is short-range. This means that this dependence is strong, indicating that the influence between the points ceases to exist within short distances in



space and time in the study area; that is, when travelling 1.48 km in space and 34.7 hours in time, there is no longer a dependence.



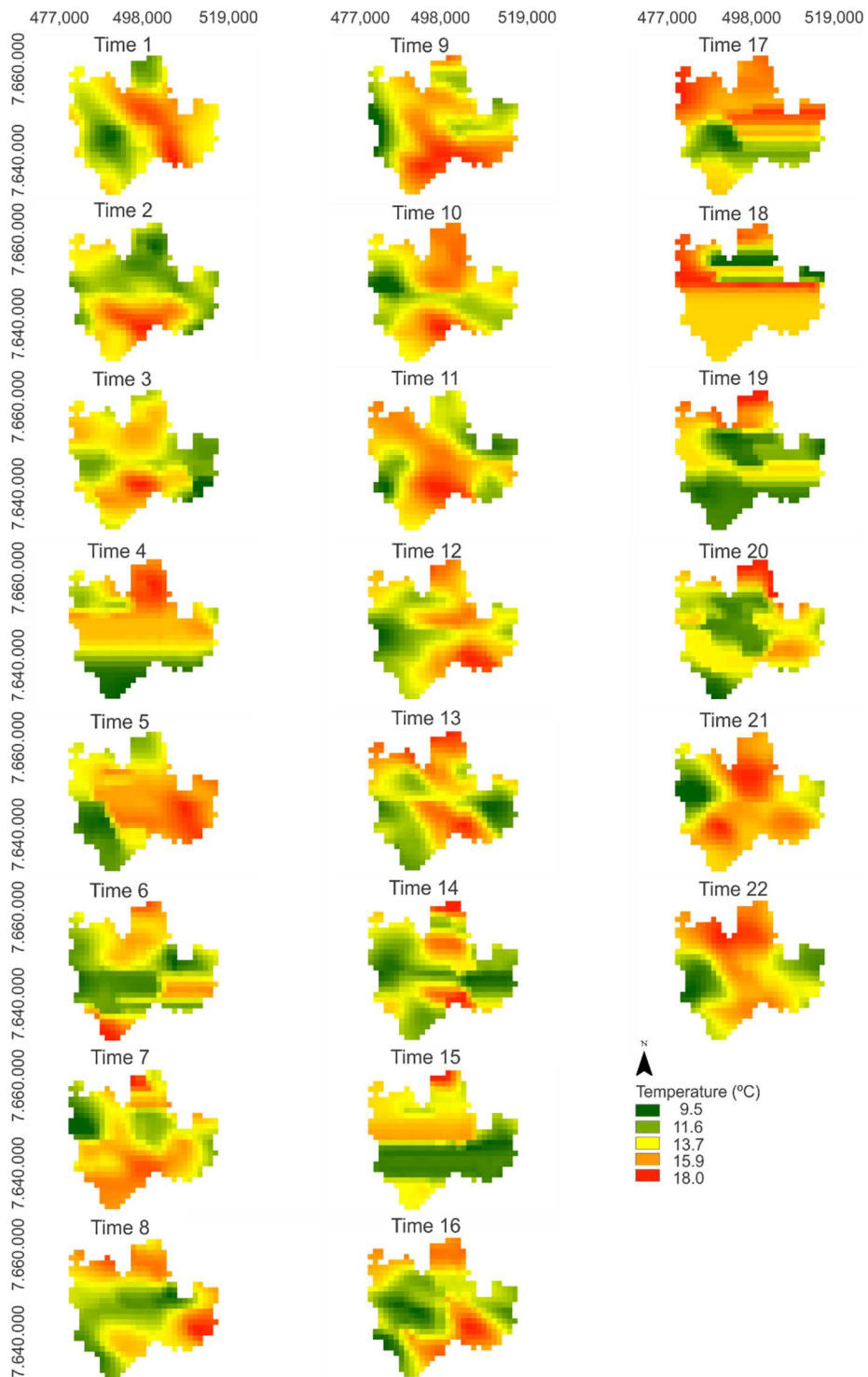
**Figure 3.** Spatiotemporal covariogram fitted to the data.

The ordinary kriging technique is a linear predictor that requires continuity in the study area to be applied, which assumes that there is a mean in the random field studied but that it is unknown. This provides the maps that generally serve as a visual information instrument to continuously investigate patterns of occurrence of some phenomena in the study area. The maps obtained over the period of the studied day show the temperature variation and the interaction that occurs between the phenomenon in space and time.

The maps show the daily evolution of the temperature of the city of Lavras, MG, over a day. Fig. 4 shows that the temperature ranged from a minimum of 9.5 °C to 18 °C because it considers a winter day, in which the temperature ranges from 11 °C to 25 °C. In addition, the analyses and maps were prepared with temperature data from 00:00 to 05:15 AM in the morning of the studied day. Thus, the resulting temperature is characterized as mild in this period. A temperature classification table was proposed in this study to help identify the thermal sensation at the study site (Table 2). This table classified temperature ranging from 0 °C to 7 °C as very cold; from 7 °C to 13 °C as cool; from 13 °C to 18 °C as mild; from 18 °C to 24 °C as pleasant; from 24 °C to 29 °C as warm; from 29 °C to 35 °C, as hot, and above 35 °C as scorching.

**Table 2.** Characterization of the mean hourly temperatures

	Temperature (°C)	Characterization
Classes	0 to 7	Very cold
	7 to 13	Cool
	13 to 18	Mild
	18 to 24	Pleasant
	24 to 29	Warm
	29 to 35	Hot
	> 35	Scorching

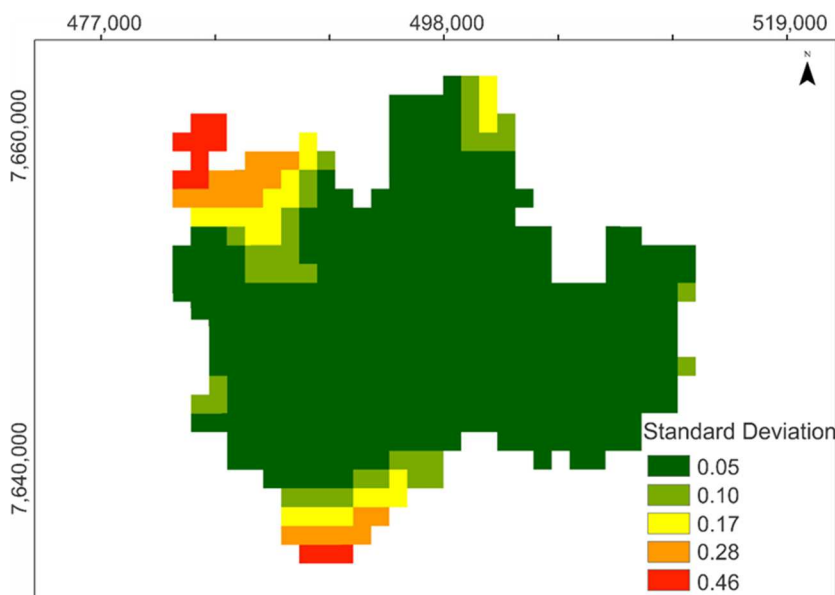


**Figure 4.** Interpolation maps of the mean air temperature using ordinary kriging from time 1 to time 22 for the studied day.

Fig. 4 shows that from time 1 (00 h) to time 3 (00 h 30), the temperature can be classified according to Table 2 as mild, as most of the area stayed between 13 °C and 18 °C. From time 4 (00 h 45) to time 22 (5 h 15 AM), the temperature can be classified according to Table 2 as cool, ranging from 7 °C to 13 °C, showing some transition regions with mild temperature.

The warmest zones, i.e., the red- and orange-coloured areas of the maps, especially at times 2, 3, and 18, were observed in the central region where the highest population density is found. The boundary regions are farm regions with greater vegetation, so the temperature in these areas were predominantly shaded green.

The maps presented in Fig. 4 may contain errors, and a way to assess whether the proposed model fits the data well is to evaluate its residuals (Fig. 5). They should be well-behaved with minimum values. The residual is defined as  $E[\widehat{Z}_{(s,t)} - Z_{(s,t)}]$ , where  $\widehat{Z}_{(s,t)}$  is the value estimated by the model and  $Z_{(s,t)}$  is the real value.



**Figure 5.** Residuals map.

When the error maps are presented, they are consistent, which indicates little variation in errors between the measured times. This is a great result. The intention is not to determine if this is the best model for these data but to compare the performance of this model with another model and to determine which is the best option for data analysis: stationary space-time covariance functions or a purely spatial model, separated by each time.

### Purely spatial analysis

In this study, we did not seek to produce kriging maps but rather a descriptive analysis of the standard deviations of the prediction errors. It is reasonable to assume that the model with the smallest prediction error is the best choice. The purely spatial dependence model with best fit to the data was the exponential model, taking into

account the criterion of greater range, the nugget effect, and the spatial contribution. These results were used in the construction of Table 3. This choice is usually made ‘by feeling’ because there are no statistical tests that indicates which model should be fitted. The respective parameters were estimated using the least squares method.

**Table 3.** Comparison between the two models, where the descriptive measures of the minimum, mean, and maximum were evaluated for the standard deviations of the prediction errors

Time	Space-time			Purely Spatial		
	Minimum	Mean	Maximum	Minimum	Mean	Maximum
Time 01	0.0381	0.0488	0.0828	0.0003	0.0139	0.0657
Time 02	0.0381	0.0422	0.0827	0.0003	0.0149	0.0675
Time 03	0.0381	0.0477	0.0820	0.0003	0.0155	0.0701
Time 04	0.0381	0.0477	0.0817	0.0002	0.0089	0.0457
Time 05	0.0381	0.0477	0.0816	0.0002	0.0094	0.0470
Time 06	0.0381	0.0477	0.0816	0.0003	0.0141	0.0712
Time 07	0.0381	0.0477	0.0815	0.0005	0.0234	0.1035
Time 08	0.0381	0.0477	0.0815	0.0004	0.0199	0.0922
Time 09	0.0381	0.0477	0.0815	0.0003	0.0153	0.0723
Time 10	0.0381	0.0477	0.0815	0.0005	0.0214	0.0802
Time 11	0.0381	0.0477	0.0815	0.0005	0.0224	0.0838
Time 12	0.0381	0.0477	0.0815	0.0003	0.0164	0.0728
Time 13	0.0381	0.0477	0.0815	0.0004	0.0177	0.0764
Time 14	0.0381	0.0477	0.0815	0.0003	0.0157	0.0740
Time 15	0.0381	0.0477	0.0815	0.0003	0.0164	0.0758
Time 16	0.0381	0.0477	0.0815	0.0003	0.0135	0.0744
Time 17	0.0381	0.0477	0.0815	0.0003	0.0137	0.0655
Time 18	0.0381	0.0477	0.0815	0.0003	0.0133	0.0660
Time 19	0.0381	0.0477	0.0815	0.0002	0.0093	0.0493
Time 20	0.0381	0.0477	0.0816	0.0001	0.0079	0.0424
Time 21	0.0381	0.0477	0.0816	0.0019	0.0099	0.0509
Time 22	0.0381	0.0477	0.0817	0.0002	0.0084	0.0443

According to Table 3, one can opt for purely spatial modelling because, on average, this type of modelling has the smallest error. However, it is necessary to consider that the space-time model of Gneiting (2002) takes into account both the existing spatial dependence and temporal dependence, in addition to the possibility of making predictions for unsampled times. Table 1 shows that choosing the model of Gneiting (2002) does not result in much loss of information in the process of predicting values, which is the goal of geostatistics.

The space-time model is extremely useful for predicting unsampled values and is advantageous for obtaining missing data in the case of sensor failures or even cloud cover, showing a low magnitude of prediction error. The interpolation of unknown values is associated with the prediction, whereas the forecast is associated with the extrapolation of unknown values, so with the model proposed by Gneiting (2002), it is possible to forecast and predict these temperature values as a tool to concomitantly monitor the behaviour of phenomena over time and space. However, because this model is complex and requires software with the capacity to store and process complex and intense calculations, its use must be analysed, and resources for this processing should be obtained.

For the cases of the pure spatial analysis of phenomena, a separate spatial model for each time is justified by the fact this type of model yields a smaller prediction error and requires a simpler processing than the space-time model.

Most studies found in the literature for temperature spatialization used multiple linear regression (Medeiros et al., 2005; Bardin et al., 2010; Castro et al., 2010; Lyra et al., 2011, Gomes et al., 2014), which is a low-accuracy model for estimating values, showing the potential of both the purely spatial model and the space-time model for the spatialization of climatic elements, where the former has lower error and the latter has forecasting and prediction abilities.

## CONCLUSIONS

It was possible to compare the space-time analysis with the purely spatial analysis using temperature data obtained by remote sensing images. The data modelled with the purely spatial analysis had, on average, lower error than those with the space-time model.

ACKNOWLEDGEMENTS. The authors thank, the Foundation for Research of the State of Minas Gerais (FAPEMIG), the National Council for Scientific and Technological Development (CNPq), the Coordination for the Improvement of Higher Education Personnel (CAPES), the Federal University of Lavras (UFLA) and University of Firenze (UniFI).

## REFERENCES

- Bardin, L., Pedro Júnior, M.J. & De Moraes, J.F. 2010. Estimation of maximum and minimum air temperatures for the 'Circuito das Frutas' region (São Paulo State, Brazil). *Revista Brasileira de Engenharia Agrícola e Ambiental* **14**(6), 618–624 (in Portuguese).
- Bicalho, B.C. 2008. *Space-Time Models: Case Studies*. Masters dissertation, Federal University of Minas Gerais, Belo Horizonte, Brazil, 176 pp.
- Cargnelutti Filho, A., Maluf, J.R.T. & Matzenauer, R. 2008. Geographic coordinates in the ten-day maximum and mean air temperature estimation in the State of Rio Grande do Sul, Brazil. *Ciência Rural* **38**(9), 2448–2456 (in Portuguese).
- Castro, F.D.S., Pezzopane, J.R., Cecílio, R.A. & Pezzopane, J.E. 2010. Use of radar images to estimate air temperature. *Idesia* **28**(3), 69–79 (in Portuguese).
- Cemek, B., Kucuktopcu, E. & Demir, Y. 2016. Determination of spatial distribution of ammonia levels in broiler houses. *Agronomy Research* **14**(2), 359–366.
- Coelho, D.T., Sediya, G. & Vieira, M. 1973. Estimates of average monthly and annual temperatures in the state of Minas Gerais. *Revista Ceres* **20**(112), 455–459 (in Portuguese).
- Curi, T.M.R. de C., Vercellino, R. do A., Massari, J.M., Souza, Z.M. & Moura, D.J. de. 2014. Geostatistic to evaluate the environmental control in different ventilation systems in broiler houses. *Engenharia Agrícola* **34**(6), 1062–1074 (in Portuguese).
- Dalanesi, P.E., Oliveira-Filho, A.T. & Fontes, M.A.L. 2004. Flora and structure of the arboreal component of the forest of the Parque Ecológico Quedas do Rio Bonito, Lavras, Minas Gerais State, and correlations between species distribution and environmental variables. *Acta Botanica Brasílica* **18**(4), 737–757 (in Portuguese).
- Damasceno, F.A., Oliveira, C.E.A., Ferraz, G.A.S., Nascimento, J.A.C., Barbari, M. & Ferraz, P.F.P. 2019. Spatial distribution of thermal variables, acoustics and lighting in compost dairy barn with climate control system. *Agronomy Research* **17**(2), 385–395. <https://doi.org/10.15159/ar.19.115>

- Dantas, A.A.A., Carvalho, L.G. & Ferreira, E. 2007. Climatic classification and tendencies in Lavras region, MG. *Ciência e Agrotecnologia* **31**(6), 1862–1866 (in Portuguese).
- Fensholt, R., Sandholt, I., Stisen, S. & Tucker, C. 2006. Analysing NDVI for the African continent using the geostationary meteorological second generation SEVIRI sensor. *Remote Sensing of Environment* **101**(2), 212–229.
- Ferraz, P.F., Yanagi Junior, T., Ferraz, G.A., Schiassi, L. & Campos, A.T. 2016. Spatial variability of enthalpy in broiler house during the heating phase. *Revista Brasileira de Engenharia Agrícola e Ambiental* **20**(6), 570–575.
- Ferraz, P.F.P., Ferraz, G.A.S., Schiassi, L., Nogueira, V.H.B., Barbari, M. & Damasceno, F.A. 2019. Spatial variability of litter temperature, relative air humidity and skin temperature of chicks in a commercial broiler house. *Agronomy Research* **17**(2), 408–417. <https://doi.org/10.15159/ar.19.112>
- Geiger, B., Carrer, D., Franchisteguy, L., Roujean, J.L. & Meurey, C. 2008. Land surface albedo derived on a daily basis from Meteorological second generation observations. *IEEE Transactions on Geoscience and Remote Sensing* **46**(11), 3841–3856.
- Gneiting, T. 2002. Nonseparable, stationary covariance functions for space-time data. *Journal of the American Statistical Association* **97**(458), 590–600.
- Gomes, D.P., Carvalho, D.F., de Oliveira Neto, D.H. & dos Santos, C.A. B. 2014. Estimated air temperature and reference evapotranspiration in the state of Rio de Janeiro. *Irriga* **19**(2), 302–314 (in Portuguese).
- Hartkamp, A.D., De Beurs, K., Stein, A. & White, J.W. 1999. *Interpolation techniques for climate variables*. NRG-GIS Series 99-01. Mexico, D.F.: CIMMYT.
- Honkavaara, E., Saari, H., Kaivosoja, J., Pölonen, I., Hakala, T., Litkey, P., Mäkynen, J. & Pesonen, L. 2013. Processing and assessment of spectrometric, stereoscopic imagery collected using a lightweight UAV spectral camera for precision agriculture. *Remote Sensing* **5**(10), 5006–5039.
- Ligges, U., Maechler, M. & Schnackenberg, S. 2020. Scatterplot3d: 3D Scatter Plot R package version 0.3–41, URL <https://cran.r-project.org/web/packages/scatterplot3d/scatterplot3d.pdf> Accessed 23 april 2020
- Lyra, G.B., Santos, M.J.D., Souza, J.L.D., Lyra, G.B. & Santos, M.A.D. 2011. Mapping annual air temperature in Alagoas state, Brazil, with different digital elevation models and spatial resolutions. *Ciência Florestal* **21**(2), 275–287 (in Portuguese).
- Medeiros, R.M., Francisco, P.R.M., Santos, D., da Silva, L.L., Bandeira, M.M. & AESA, C.G.P. 2015. Variability of the Temperature Range of Air in the Paraíba State-Brazil. *Revista Brasileira de Geografia Física* **8**(01), 128–135 (in Portuguese).
- Medeiros, S.S., Cecílio, R.A., Melo Junior, J.C.F. & Silva Junior, J.L. C. 2005. Estimation and spatialization of minimum, mean and maximum air temperatures for the Northeast region of Brazil. *Revista Brasileira de Engenharia Agrícola e Ambiental* **9**(2), 247–255 (in Portuguese).
- Nychka, D., Furrer, R., Paige, J. & Sain, S. 2020. Fields: Tools for Spatial Data. R package version 9.6, URL <https://cran.r-project.org/web/packages/fields/fields.pdf>. Accessed 23 april 2020
- Oliveira, C.E.A., Damasceno, F.A., Ferraz, P.F.P., Nascimento, J.A.C., Ferraz, G.A.S. & Barbari, M. 2019. Geostatistics applied to evaluation of thermal conditions and noise in compost dairy barns with different ventilation systems. *Agronomy Research* **17**(3), 783–796.
- Padoan, S. & Bevilacqua, M. 2020. CompRandFld: Composite-Likelihood Based Analysis of Random Fields. R package version 1.0.3–5, URL <https://cran.r-project.org/web/packages/CompRandFld/CompRandFld.pdf>. Accessed 23 april 2020.

- Pereira, I.M., Berg, E.V.D., Pinto, L.V.A., Higuchi, P. & Carvalho, D.A. 2010. Evaluation and proposal of connectivity of remnant fragments in the campus of Universidade Federal de Lavras, Minas Gerais. *Cerne* **16**(3), p. 305–321 (in Portuguese).
- Pessanha, M.S., dos Santos, L.M., Lyra, G.B., Lima, A.O., Lyra, G.B. & de Souza, J.L. 2020. Interpolation methods applied to the spatialisation of monthly solar irradiation in a region of complex terrain in the state of Rio de Janeiro in the southeast of Brazil. *Modeling Earth Systems and Environment*, [online], p. 1–14. <https://doi.org/10.1007/s40808-020-00878-8>
- R Core Team. 2020. R: A Language and Environment for Statistical Computing. Vienna, Austria. Disponível em: <<https://www.R-project.org/>>.
- Ribeiro Júnior, P.J. & Diggle, P.J. 2020. GeoR: analysis of geostatistical data.R package version 1.7–5.2.1 URL <https://cran.r-project.org/web/packages/geoR/geoR.pdf>. Accessed 23 april 2020
- Rodrigues, J.D.P., Alves, M.C., Freitas, A.S., Pozza, E.A., Oliveira, M.S. & Alves, H.J.P. 2019. Geostatistical stationary space-time covariance functions modeling of Yellow Sigatoka progress in banana crop. *Australasian Plant Pathology* **48**(3), 233–244.
- Santos, L.M.D., Ferraz, G.A.S., Batista, M.L., Martins, F.B.S. & Barbosa, B.D.S. 2020. Characterization of noise emitted by a low-profile tractor and its influence on the health of rural workers. *Anais da Academia Brasileira de Ciência* [online], **92**(3). <https://doi.org/10.1590/0001-3765202020200460>
- Schmetz, J., Pili, P., Tjemkes, S., Just, D., Kerkmann, J., Rota, S. & Ratier, A. 2002. An Introduction to Meteosat Second Generation (MSG). *Bulletin of the American Meteorological Society* **83**(7), 977–992.
- Sherman, M. *Spatial Statistics and Spatio-Temporal Data: Covariance Functions and Directional Properties*. [S.l.]: Library of Congress Cataloging, 2011
- Souza, J.S., Espirito-Santo, F.D.B., Fontes, M.A.L., Oliveira-Filho, A.T. & Botezelli, L. 2003. Analysis of the floristic and structural variations of a tree community in a tropical semideciduous forest fragment on the margins of the Capivari river, Lavras, southeastern Brazil. *Revista Árvore* **27**(2), pp. 185–206 (in Portuguese).
- Varejão-Silva, M.A. 2006. *Meteorology and Climatology*. Recife: INMET.
- Viana, R.S.M., dos Santos, G.R., Moreira, D.S., Louzada, J.M. & Rosa, L.M.F. 2019. The Use of Space-Temporal Geostatistics in the Prediction of Maximum Air Temperature. *Revista Brasileira de Geografia Física* **12**(1), pp. 096–111 (in Portuguese).

## Morphology of *Camellia Sinensis* L. leaves as marker of white tea authenticity

N. Durnova<sup>1</sup>, M. Simakova<sup>1</sup>, D. Isaev<sup>1</sup>, I. Simakova<sup>2,\*</sup> and A. Simakov<sup>2</sup>

<sup>1</sup>Saratov State Medical University named after V.I. Razumovsky, Faculty of Pharmacy, B. Kazach'ya Str., 112, RU410012 Saratov, Russia

<sup>2</sup>Saratov State Agrarian University named after N.I. Vavilova, Department of Veterinary Medicine, Biotechnology and Food Technology, B. Sadovaya Str., 220, RU410005 Saratov, Russia

\*Correspondence: [simakovaiv@yandex.ru](mailto:simakovaiv@yandex.ru)

Received: February 1<sup>st</sup>, 2021; Accepted: April 24<sup>th</sup>, 2021; Published: August 18<sup>th</sup>, 2021

**Abstract.** Tea is one of the most common drinks in the world. Classic tea is obtained by brewing the leaves of the *Camellia sinensis* L plant in hot water. However, even the leaves collected from the same branch of the same tea bush can have completely different anatomical, biochemical and taste characteristics. White tea is the youngest, immature apical leaves of the tea bush (fleshes) together with leaf buds (tips) which are is considered the most valuable parts of teaplant.

The chemical composition of tea is studied in sufficient detail, however, there are still no uniform criteria for determining the authenticity of white tea leaves, which creates great preconditions for falsifying this most valuable type of raw material. The aim of this study was to study the macro- and microstructure of white tea leaves from different manufacturers and to determine the morphological markers of the authenticity of white tea leaves.

The objects of research were white tea from the Nandana Tea Factory (Sri Lanka) and white tea from an unknown manufacturer, purchased from a local tea shop.

The study of raw materials was carried out in accordance with the requirements of GF XIV OFS 1.5.1.0003.15 ‘Leaves’ and OFS 1.5.3.0003.15 ‘Technique of microscopic and microchemical examination of medicinal plants and herbal medicinal products.’

The work was carried out on the basis of the laboratories of the Department of Food Technologies of FGBOU VO Saratov GAU named after N.I. Vavilov, and the Department of General Biology, Pharmacognosy and Botany, Saratov State Medical University named after V.I. Razumovsky Ministry of Health of Russia.

Studies of the structure of white tea leaves from various manufacturers have shown that the structure and presence of morphological elements of leaves, such as hairs, stomata, leaf edge, druses, sclereids, differ markedly and can serve as reliable markers for identifying the variety of tea.

**Key words:** white tea, morphological signs, tea grade, tips.

### INTRODUCTION

Tea is one of the most common drinks in the world. Classic tea is obtained by brewing the leaves of *Camellia sinensis* L. in hot water. However, even leaves harvested



from the same branch of the same tea bush can have completely different anatomical, biochemical and taste characteristics. The most valuable is white tea made from the youngest, immature apical leaves of a tea bush (fleshes) together with leaf buds (tips). Different studies have found many health beneficial properties of white tea extract such as antioxidant (Dias et al., 2013), antimutagenic (Rusak, 2008; Mao et al., 2010), hypolipidemic (Söhle et al., 2009), antidiabetic (Anderson & Polansky, 2002), vasoprotective and antihypertensive (Curin & Andriantsitohaina, 2005), antimicrobial (Chou et al., 1999). Such an impressive list of positive effects on the human body greatly increases both the value of white tea among consumers and the interest of producers in its procurement, despite the labour-consuming nature of this process.

White tea represents unexpanded leaf buds or buds with 1–2 top young leaves. It is called white because of the large number of hairs that give the leaves a characteristic shade. While being processed, white tea undergoes only 2 technological steps: withering and drying. This allows one to maximally preserve the original chemical composition of the leaves and determines a large number of medicinal effects of white tea (Yoshino et al., 1994; Chou et al., 1999; Anderson & Polansky, 2002; Curin & Andriantsitohaina, 2005; Gramza et al., 2005; Evstigneeva et al., 2016).

G. Santana-Rios et al. (Santana-Rios et al., 2001) noted the similarity of the chemical composition of white and green tea, namely, nine main components of white tea (catechin, epicatechin, epigallocatechin, epicatechingallate, epigallocatechin-3-gallate, theobromine, theophylline, caffeine, gallic acid) are also found in green tea, and the total amount of catechins in white and green tea is about the same. At the same time, the research results show that white tea is superior to green tea in terms of its antimutagenic activity (Santana-Rios et al., 2001).

Similar results were obtained by T. R. Dias et al (Dias et al., 2014). It was found that the main component that determines the antioxidant potential of white and green tea is epigallocatechin-3-gallate (EGCG). Its content in white and green tea from the same manufacturer is very different - in white tea it is twice as much EGCG as in green tea. Accordingly, the antioxidant activity of white tea is more pronounced.

In the research work by U.J. Unachukwu et al. (Unachukwu et al., 2010) contradictory data were obtained: the amount of total catechins in white tea, depending on the variety, can be less, more or comparable to different varieties of green tea. Moreover, even within one type of white tea, produced by different companies, the content of common catechins can be more than 10 times as different.

Such significant differences in the chemical composition of white tea can be associated, among other factors (like climate, soil composition, intensive or organic agriculture, altitude, even the southern or northern part of the slope), with the lack of markers of the authenticity of the tea leaf. The chemical composition of tea has been studied in sufficient detail, however, there are still no uniform criteria for determining the authenticity of white tea leaves, which creates great preconditions for the falsification of this most valuable type of raw material. Thus, the aim of this research article was to study the macro- and microstructure of white tea leaves from different manufacturers to determine the morphological markers of authenticity of white tea leaves.

**The objects of research** were white tea from the Nandana Tea Factory (Sri Lanka) and white tea purchased from a tea shop in Saratov. It should be clarified that white tea from the Nandana Tea Factory was produced, packaged and purchased at the factory, the labeling corresponded to the requirements of TR CU 022/2011 Technical

Regulations of the Customs Union 'Food products in terms of their labeling'. Tea bought in a teashop in Saratov was sold by weight, there was no labeling.

## MATERIALS AND METHODS

The study of raw materials was carried out on a Carl Zeiss Primo Star microscope in accordance with the requirements of GF XIV OFS 1.5.1.0003.15 'Leaves' and OFS 1.5.3.0003.15 'Technique of microscopic and microchemical study of medicinal plant materials and herbal medicines.'

For the analysis, whole leaves or pieces of a leaf blade with an edge and a vein, pieces of a leaf from the base and apex, and pieces of a petiole (if the leaf has a petiole) were taken.

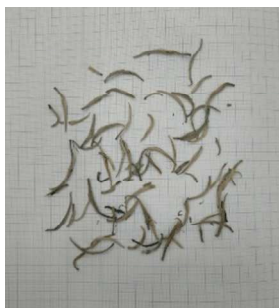
They were bleached in the following way: several pieces of raw material were placed into a flask or a test tube, a sodium hydroxide solution of 5% diluted with water (1:1) was added and boiled for 2–5 min, depending on the thickness and density of the objects, avoiding strong softening. Then the contents were poured into a glass, the liquid was poured through 2–4 layers of gauze, which was used to cover the glass, and the raw materials were thoroughly washed with water, each time the water was drained through the same gauze. The content of the glass was transferred in a small amount of water into a Petri dish. The particles of raw material remaining on the gauze were washed off into the same Petri dish. The pieces were removed from the water with a scalpel or spatula and placed on a glass slide in a drop of a 33% glycerin solution. Pieces of raw material, bleached and placed on a glass slide, were divided into two parts with a scalpel or dissecting needles, one of them was carefully turned over. A piece of petiole was placed on a glass slide. The thin petioles were crushed with a scalpel or the reverse end of a dissecting needle to release the epidermis. The epidermis was removed from the thick petioles using dissecting needles or a razor, removing the coarse inner parts of the petiole, which prevented us from obtaining a good epidermal micropreparation. The object was covered with a cover glass, if necessary, slightly pressed down from above with a clean reverse end of the dissecting needle and slightly heated until air bubbles were removed, after cooling, the leaf and the epidermis of the petiole were examined from both sides under a microscope, first at low, then at high magnification. The upper and lower epidermis, as well as deep leaf structures located under the epidermis (parenchyma, inclusions, vessels, etc.) were examined at different magnifications, using a macro- and microscrews.

The preparation of cross-sections of petioles was carried out as follows. Slices were made from the soaked petioles, by clamping pieces of the petiole into a bottle cork or elderberry core. When using a bottle cap, it was preliminarily boiled in water for 15 minutes. A piece of elderberry or bottle cap was cut into halves and a piece of leaf was clamped between the two halves. To make cross sections, the surface of the piece should be prepared so that it is strictly perpendicular to the axis of the petiole or leaf vein. The finished sections were placed in a Petri dish with water, from where the sections were taken out and examined under a microscope; the most relevant samples were selected.

## RESULTS AND DISCUSSION

Dried raw white tea A (tea sample from the factory) is represented by whole leaves of a silvery-green color with a petiole, with abundant pubescence on the underside of the leaf. The leaf blade (lamina) is turned inward from the edges through the ventral side. A leaf measuring 1.2–3.0 cm in length and up to 0.5 cm in width has a dorsal crescent-shaped bend. The main vein on the underside of the leaf is absolutely visible. Broken leaves are rarely found. Inside some leaves, there are tips that are morphologically similar to the rest of the leaves, but smaller and coiled into a tube (Fig. 1).

The raw material of tea B (tea sample from the store) contains less than half of these leaves. Most of them are almost whole leaves up to 5 cm in length and parts of leaf blades (lamina) are quite large (up to 1.5×1.5 cm), unfolded. The upper side of the leaf blade is black and almost without hairs, the lower side is similar in appearance to tea A. There are also a large number of small parts of leaves up to 2×2 mm in size, sometimes branches up to 2 cm long are found (Fig. 2).



**Figure 1.** White tea A.



**Figure 2.** White tea B.

Raw tea A does not change its shape after brewing, but the color of the leaves changes from silvery green to dark green, almost black. Tips are clearly visible. The leaf is rather thick and fragile; when we try to take a sample for a micropreparation, the upper and lower epidermis are easily peeled off, and the leaf itself breaks apart (Fig. 3).

After boiling, tea B leaves unfold, become slightly transparent, green in color. It should be noted that the leaves strongly stain the water even after several washes. Quite a large number of branches are also visible (Fig. 4).



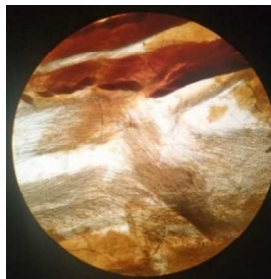
**Figure 3.** Tea A after boiling.



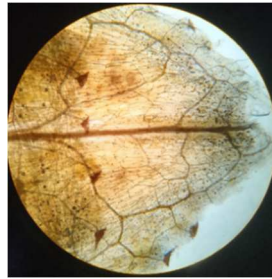
**Figure 4.** Tea B after boiling.

Figs 5 and 7 show a very high density of hairs and numerous outgrowths of the edge of the leaf blade, which are not easily visible.

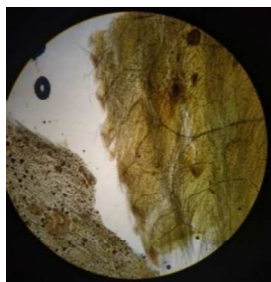
In Figs 6 and 8, a much smaller number of hairs are noted, and the outgrowths of the leaf edge are filled with extractive substances or are absent (the points of their attachment are visible).



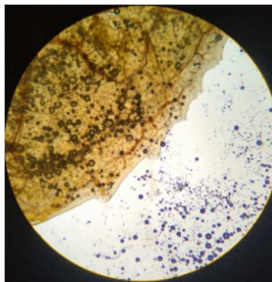
**Figure 5.** Tea A leaf plate. Magnification 10×4.



**Figure 6.** Tea B leaf plate. Magnification 10×4.

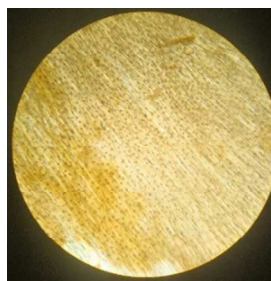


**Figure 7.** Tea A leaf plate. Magnification 10×4.



**Figure 8.** Tea B leaf plate. Magnification 10×4.

The photograph of the lower epidermis of tea A (Fig. 9) shows such a high density of hairs that they completely block the view of the underlying structures. Fig. 11 shows where the hairs are attached to the epidermis. Epidermal cells with some cellular structures and hair attachment points are clearly visible. You can see that between the adjacent hairs there are from 1 to 3 cells of the epidermis.

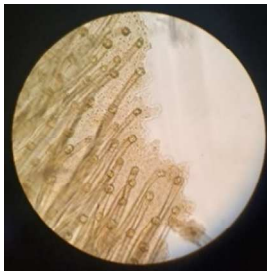


**Figure 9.** Tea A trichomes. Magnification 10×10.

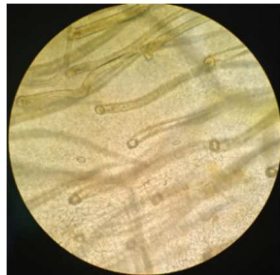


**Figure 10.** Tea B trichomes. Magnification 10×10.

Tea B is characterized by a significantly lower hair density (Fig. 10). Moreover, the length of the hairs B is shorter (Fig. 12).



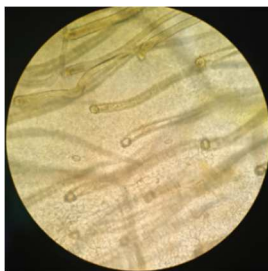
**Figure 11.** Tea A trichomes. Magnification 10×40.



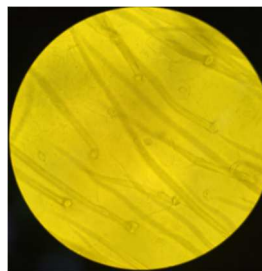
**Figure 12.** Tea B trichomes. Magnification 10×40.

The stomata on tea A could not be seen due to the very high density of hairs.

The stomata on tea B are clearly visible (Fig. 13). In addition, cuticle folds are visible in Fig. 14.



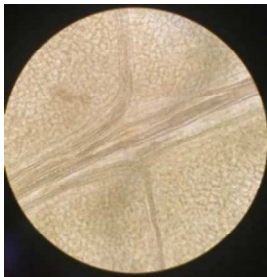
**Figure 13.** Tea B stomata. Magnification 10×40.



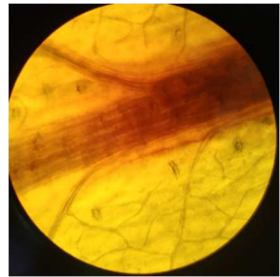
**Figure 14.** Tea B cuticle. Magnification 10×40.

Fig. 15 shows conductive bundles (fasciculus) of white tea A, which have a typical structure. The spiral thickening of the vessel wall is clearly visible. Thicker vessels are located in the center of the vascular bundle, the diameter of the vessels decreases towards the periphery.

Conductive bundles of tea B have an identical structure, with the exception of the central vein - sclereids are randomly scattered around it (Fig. 16).



**Figure 15.** Tea A conductive bundles. Magnification 10×40.



**Figure 16.** Tea B central vein. Magnification 10×10.

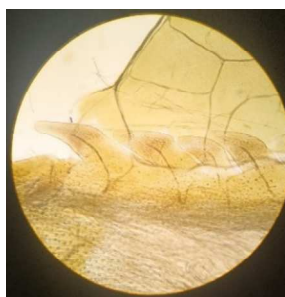
Along the entire edge of the leaf of tea A, in the middle part of the leaf blade, there are outgrowths of the leaf edges closely spaced to each other with vessels approaching them. Morphologically, these outgrowths are similar to the top of the leaf blade. It is noticeable that the formations of the leaf edge can be heterogeneous in size and shape, but have the same general structure (Figs 17, 19, 21).



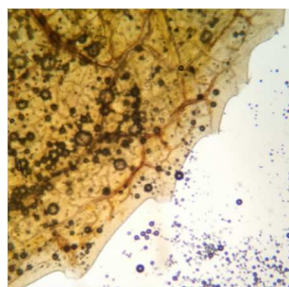
**Figure 17.** Tea A leaf edges outgrowths. Magnification 10×10.



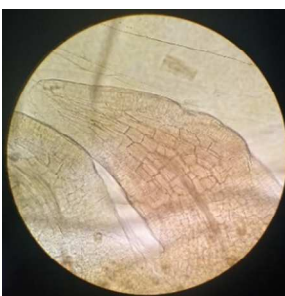
**Figure 18.** Tea B leaf edges outgrowths. Magnification 10×10.



**Figure 19.** Tea A leaf edges outgrowths. Magnification 10×10.



**Figure 20.** Tea B leaf edges outgrowths. Magnification 10×10.



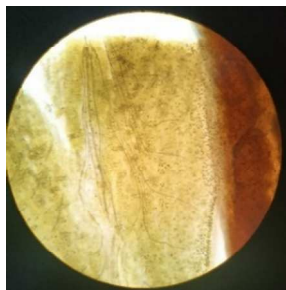
**Figure 21.** Tea A leaf edges outgrowths. Magnification 10×40.



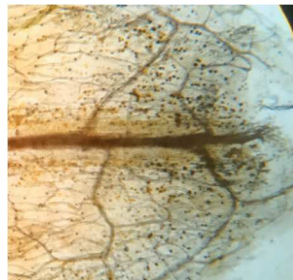
**Figure 22.** Tea B leaf edges outgrowths. Magnification 10×40.

In tea B, these outgrowths are located slightly less densely (Fig. 18). They, as was previously mentioned, are filled with extractive substances and come off, and the edge of the leaf in the points of their attachment gradually overgrows and levels out (Figs 20, 22).

Sclereids in the leaves of tea A are found near the top of the leaf; in the rest of the leaf blade, they are not found. The leaf edge near the top is solid. Druses are also found only near the top and are concentrated at the edge of the leaf (Fig. 23).



**Figure 23.** Tea A sclereids and druses. Magnification 10×4.



**Figure 24.** Tea B sclereids and druses. Magnification 10×4.

Druses in tea leaf B are found not only at the top of the leaf blade, but also along the edge of the leaf. Sclereids are not concentrated at the apex either, but begin to spread along the central vein into the main part of the leaf blade (Fig. 24).

### CONCLUSION

Studies of the structure of white tea leaves from various manufacturers have shown that the structure and presence of morphological elements of leaves, such as hairs, stomata, leaf edge, druses, sclereids, differ significantly and can be markers of tea raw materials (Table 3).

**Table 3.** The results of the study of the tea raw materials

Characteristic	Tea A	Tea B
Appearance	Silver-green folded dryish fleshes and individual tips	Silver-green below, black above, partially unfolded leaves and small pieces of leaves
Hairs	Long, very high density	Short, low density
Stomata	Not detected	Found everywhere
Conducting bundles	Without sclereids on the periphery	With sclereids around the central vein
Leaf edge	Living outgrowths, high density	The number of outgrowths is reduced, the initial stage of lignification or absence
Sclereids	At the top of the leaf blade	At the top of the leaf blade and along the central vein
Druses	At the top of the leaf blade	At the top of the leaf blade and along the edge of the leaf

It should be noted that in the works of various scientists, unfortunately, no attention is paid to the morphological characteristics of tealeaves. However, there is a sufficient number of scientific studies, difficult to carry out in certain conditions, on the chemical composition of tea and its effect on the body (Yi Chen et al., 2014; Dias et al., 2016; Pastoriza et al., 2017; Junjie Zhang et al., 2019).

Nowadays, the development of white tea authenticity markers is a relevant topic. The Covid-19 pandemia makes it even more topical, since it raises the issues of food quality and safety. Consumers must be confident not only in the quality, but in the authenticity of food products, especially those that have a beneficial effect on the immune system of the human body.

Taking into account the results of the previous study of the structure of the leaves of white and black tea (Isaev et al., 2020), it can be noted that white tea bought in a store by weight has an intermediate structure between a young and a mature leaf, which indicates a greater age and, thus, such tea cannot be called white.

ACKNOWLEDGEMENTS. The authors express gratitude to the Nandana Tea Factory and personally to Mr. Gunasoma Wanigasekara for the tea samples provided for the study.

## REFERENCES

- Anderson, R.A. & Polansky, M.M. 2002. Tea enhances insulin activity. *Journal of Agricultural and Food Chemistry* **50**(24), 7182–7186.
- Chen, Y., Deng, J., Wang, Y., Boping, L., Jian, D., Xuejin, M., Juan, Z., Haitao, H. & Jing, L. 2014. Study on discrimination of white tea and albino tea based on near-infrared spectroscopy and chemometrics. *Comparative Study J Sci Food Agric.* **94**(5), 1026–33. doi: 10.1002/jsfa.6376. Epub 2013 Oct 2.
- Chou, C.C., Lin, L.L. & Chung, K.T. 1999. Antimicrobial activity of tea as affected by the degree of fermentation and manufacturing season. *International Journal of Food Microbiology* **48**(2), 125–130.
- Curin, Y. & Andriantsitohaina, R. 2005. Polyphenols as potential therapeutical agents against cardiovascular diseases. *Pharmacological Reports* **57**, pp. 97–107.
- Dias, T., Tomás, G. & Teixeira, N. 2013. White tea (*Camellia sinensis* (L.)): antioxidant properties and beneficial health effects. *International Journal of Food Science, Nutrition and Dietetics* **2**(2) pp. 19–26.
- Dias, T.R., Marco, G.A., Gonçalves, D.T., Socorro, S., Silva, B.M. & Oliveira, P.F. 2014. White Tea as a Promising Antioxidant Medium Additive for Sperm Storage at Room Temperature: A Comparative Study with Green Tea. *Journal of Agricultural and Food Chemistry* **62**(3), 608–617. doi: 10.1021/jf4049462
- Dias, T.R., Alves, M.G., Casal, S., Silva, B.M. & Oliveira, P.F. 2016. The single and synergistic effects of the major tea components caffeine epigallocatechin-3-gallate and L-theanine on rat sperm viability. *Food Funct* **7**(3),1301–5. doi: 10.1039/c5fo01611h. PMID: 26902467
- Evstigneeva, T., Skvortsova, N. & Yakovleva, R. 2016. The application of green tea Extract as a source of antioxidants in the processing of dairy products. *Agronomy Research* **14**(S2), 1284–1298.
- Gramza, A. & Karczák, J. 2005. Tea constituents (*Camellia sinensis* L.) as antioxidants in lipid systems. *Trends in Food Science & Technology* **16**, 351–358.
- Isaev, D.S., Durnova, N.A., Simakova, M.A. & Simakov, A.N. 2020. Morphological characteristics of the *Camellia sinensis* l. leaves as markers of the white tea authenticity. *Collection of abstracts of the Sixth Interdisciplinary Conference "Molecular and Biological Aspects of Chemistry, Pharmaceuticals and Pharmacology"* edited by Kudryavtseva K.V. & Panina E.M. M.: Pero, pp. 42.
- Junjie, Z., Xuehong, W., Weidong, D. & Zhi, L. 2019. Study of enrichment difference of 64 elements among white tea subtypes and tea leaves of different maturity using inductively coupled plasma mass spectrometry. *Food Res. Int.* **126**, 108655. doi: 10.1016/j.foodres.2019.108655. Epub 2019 Sep 3.



- Mao, J.T., Nie, W.X. & Tsu, I.H. 2010. White tea extract induces apoptosis in non-small cell lung cancer cells: the role of peroxisome proliferator-activated receptor- and 15-lipoxygenases. *Cancer Prevention Research* **3**(9), 1132–1140.
- Pastoriza, S., Mesías, M, Cabrera, C. & Rufián-Henares, J.A. 2017. Healthy properties of green and white teas: an update. *Food Funct.* **8**(8), 2650–2662. doi: 10.1039/c7fo00611j. Epub 2017 Jun 22. PMID: 28640307 Review.
- Rusak, G., Komes, G. & Sasa, L. 2008. Phenolic content and antioxidative capacity of green and white tea extracts depending on extraction conditions and the solvent - used. *Mutation Research/Genetic Toxicology and Environmental Mutagenesis* **110**, pp. 852–858.
- Santana-Rios, G., Orner, G.A. & Amantana, A. 2001. Potent antimutagenic activity of white tea in comparison with green tea in the Salmonella assay // *Mutation Research/Genetic Toxicology and Environmental Mutagenesis* **495**(1–2), 61–74.
- Söhle, J., Knott, A. & Holtzmann, U. White 2009. Tea extract induces lipolytic activity and inhibits adipogenesis in human subcutaneous (pre)-adipocytes. *Nutrition & Metabolism* **6**, 1–10.
- Unachukwu, U.J., Ahmed, S. & Kavalier, A. 2010. White and Green Teas (*Camellia sinensis* var. *sinensis*): Variation in Phenolic, Methylxanthine, and Antioxidant Profiles. *Journal of Food Science* **75**(6), 541–548.
- Yoshino, K., Tomita, I. & Sano, M. 1994. Effects of longterm dietary supplement of tea polyphenols on lipid peroxide levels in rats. *GeroScience* **17**, 79–85.

## Acoustic analysis of cement composites with lignocellulosic residues

P.F.P. Ferraz<sup>1,\*</sup>, D.H.S. Abreu<sup>2</sup>, B.N. Huallpa<sup>1</sup>, L.S. Santana<sup>1</sup>, D. Cecchin<sup>3</sup>,  
G.F. Rabelo<sup>4</sup>, G. Rossi<sup>5</sup> and M. Barbari<sup>5</sup>

<sup>1</sup>Federal University of Lavras, Agricultural Engineering Department, Campus Universitário, PO Box 3037, CEP 37200-000 Lavras, Minas Gerais, Brazil

<sup>2</sup>University of Campinas, School of Electrical and Computer Engineering (FEEC), Communication Department, Av. Albert Einstein – 400, Cidade Universitária Zeferino Vaz, District Barão Geraldo, Campinas, São Paulo, Brazil

<sup>3</sup>Federal Fluminense University, Campus Praia Vermelha, Rua Passo da Pátria, 156, Niterói, Rio de Janeiro, Brazil

<sup>4</sup>Federal University of Lavras, Automatic Department, Campus Universitário, PO Box 3037, CEP 37200-000 Lavras, Minas Gerais, Brazil

<sup>5</sup>University of Florence, Department of Agriculture, Food, Environment and Forestry, Via San Bonaventura, IT13-50145 Firenze, Italy

\*Correspondence: [paricia.ponciano@ufla.br](mailto:paricia.ponciano@ufla.br)

Received: January 19<sup>th</sup>, 2021; Accepted: May 20<sup>th</sup>, 2021; Published: October 5<sup>th</sup>, 2021

**Abstract.** The concept of environmental sustainability has been seeking a way to develop projects that reduce the impacts provided by agricultural development and the excessive consumption of natural resources. However, there is still little knowledge about the acoustic insulation/absorption behaviour of lignocellulosic materials. Hence, this study aimed to evaluate the acoustic properties of five cement panels reinforced with the following lignocellulosic materials: eucalyptus, sugarcane bagasse, coconut shell, coffee husk, and banana pseudostem, which ones have as a reference a commercial plaster used as sealing in civil constructions. The proposed panels were produced with each lignocellulosic material residue. It was produced three replicates for each type including plaster (being 18 panels in total). The sound insertion loss (SIL) measurement of the above-mentioned panels have been performed using an acoustical treated inexpensive facility developed based on the literature. The characterization of the acoustic behaviour of the studied materials were analysed according to the IEC (61260-1). The acoustic measurements have been done in the range of 20 Hz to 20 kHz and the analysis in octave bands have been performed. To make the analysis easier, the overall range of frequencies mentioned above was divided as ‘low’, ‘middle’ and ‘high’ ranges. Additionally, the measurement of thickness, density and porosity structure parameters of the lignocellulosic samples have been performed. According to the results and doing a trade-off analysis, the eucalyptus presented the overall best performance considering the overall range of analysis, being the banana pseudostem and sugarcane bagasse materials as good competitors.

**Key words:** alternative building material, lignocellulosic panels, sound insertion loss, residue materials.

## INTRODUCTION

The concept of environmental sustainability has been seeking a way to develop projects that reduce the impacts provided by agricultural development and the excessive consumption of natural resources. All waste produced by industry and agriculture must be treated correctly, avoiding harmful consequences for the environment (Arruda Filho et al., 2012).

The use of organic waste has been developed for different applications worldwide, due to the idea of mitigating environmental pollution, as well as proposing recycling alternatives (Prusty et al., 2016). The engineering design of rural and civil buildings must take the availability of the local materials into account, encouraging wherever possible the use of natural materials that can be regenerated (Bambi et al., 2019). Natural fibers, with their porous cell structure and relatively low density, are becoming popular because they are renewable, non-abrasive, economic, available in abundance and pose lower health risks during handling and processing (Sari et al., 2016). According to César et al. (2017), most of the lignocellulosic materials can be used in panel production. Besides, these panels produced with raw materials present the following advantages: good fire resistance, good thermal and acoustic insulation, good resistance to fungus and insects attack, and they can be considered as good materials to work (Iwariki & Prata, 2008). Nevertheless, using natural fibres has some disadvantages, because they do not have uniform properties. It is because the values of their properties greatly vary as these properties are directly related to the composition of their constituents, such as cellulose, hemicellulose and lignin (Azevedo et al., 2021).

The civil construction industry is one of the biggest consumers of natural resources and energy, and this fact has encouraged researches in sustainable development area. The introduction of the concept of 'sustainability' in the building sector gradually led to the production of insulation products made of natural or recycled material; some of them are already present in the market while others are still at an early stage of production or study (Asdrubali et al., 2015).

One option to use the lignocellulosic materials in building solutions is the use of cement-bonded particle boards/panels. According to Mendes et al. (2017) these panels are products manufactured from a mixture of Portland cement, chemical additives and particles generated from lignocellulosics. Cement-bonded panels could be used in building construction improving the performance on fire resistance and thermal/acoustic insulation. However, there is still little knowledge about the acoustic insulation/absorption behaviour of lignocellulosic materials. In order to absorb sound, materials should have high porosity to allow the sound to enter in their matrix, and for dissipation (Berardi & Iannace, 2015).

According to Ghofrani et al. (2016) in general, there are two main ways to control noise: The first one is to control/reduce the sources of noises. The second one is to control/reduce the noise through the transmission path. Hence, it is important to evaluate the acoustic properties of panels produced with lignocellulosic materials. These approaches could be particularly important and useful in developing countries, which do not have well-defined recycling policies and are affected by disposal issues due to large quantities of agricultural and industrial by-products (Asdrubali et al., 2015).

Commercial plaster board is a widely used building material that can be used for indoor applications. Plaster boards are inexpensive materials and easy to use with a

whole bunch of advantageous attributes. Plaster boards are considered as materials with good properties in terms of heat insulation, comply with the standards for fire safety and provide a pleasant room climate (De Korte, 2015; Butakova & Gorbunov, 2016; Schug et al., 2017).

Therefore, this paper aims to evaluate acoustically cement panels produced with lignocellulosic residues. The panels are compared with a reference commercial plaster board that is frequently most common material used as walls and roofs in civil constructions.

## MATERIALS AND METHODS

The experiment was carried out at the Federal University of Lavras (UFLA), Lavras, Brazil. For the production of lignocellulosic panels, the following lignocellulosic materials were used: Eucalyptus (*Eucalyptus grandis*), sugarcane bagasse (*Saccharum officinarum*), coconut shell (*Cocos nucifera*), coffee husk (*Coffea arabica*), banana pseudostem (*Musa acuminata*) and a commercial plaster board. Three repetitions for each kind of lignocellulosic material have been made, totalizing 15 panels (5 treatments and 3 repetitions). And, three commercial reference plasterboards were bought at specialized stores in the city.

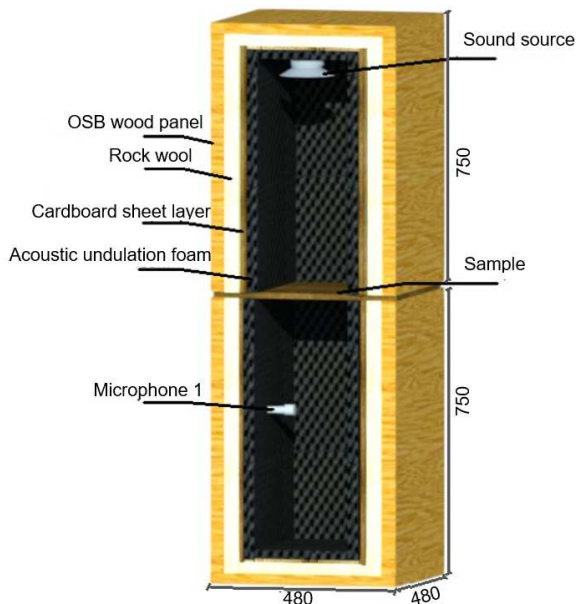
Lignocellulosic cement composites have been developed with high initial resistance Portland cement (CPV-ARI), as mineral binder and calcium chloride ( $\text{CaCl}_2$ ), used as an accelerator of the cement cure process. For the calculations of the components of each panel (lignocellulosic material, cement, water and  $\text{CaCl}_2$ ), the methodology suggested by Souza (1994) was used to determine the equivalent mass of components. In the production of panels, the following parameters were applied: material and cement ratio, 1:2.75; water and cement ratio, 1:2.5; hydration water rate of 0.25; additive, 4% (based on cement mass); percentage of losses, 6%. The calculations were performed for nominal panel density of  $1.2 \text{ g cm}^{-3}$  (Souza, 1994).

In order to produce each panel, components were weighed and then mixed in a concrete mixer for eight minutes. The total mass of components for three panels equivalent to each treatment (at the same time) was mixed. After mixing, the mass of each panel was properly separated, weighed and randomly distributed in aluminium moulds of  $480 \times 480 \times 150 \text{ mm}$ . The moulding and stapling were carried out in a cold process for 24 hours and then panels were kept in a climatic room at a temperature of  $20 \pm 2 \text{ }^\circ\text{C}$  and  $65 \pm 3\%$  relative humidity to ensure uniform drying for 28 days.

To measure the thickness (mm) of each panel, it was used as a calliper in four different points in each sample of the panels. The dimensional size and weight measured were used to calculate the thickness and density of the composites. Density ( $\text{kg m}^{-3}$ ) was calculated by the relationship between the panel mass (Kg) and the panel size ( $\text{m}^3$ ). All of these analyses were developed based on the ASTM standard method (ASTM D1037, 2016) and Deutsches Institut fur Normung - DIN (1982) standards.

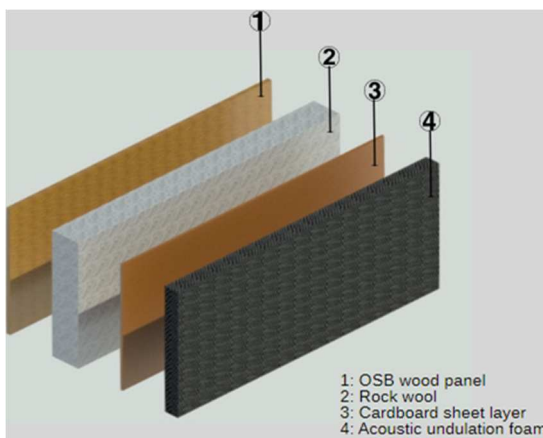
The acoustic evaluations have been performed using insertion loss measurements of the samples. The measurements have been done using a low-cost acoustic treated facility developed based on the work of Piedrahita & Fajardo (2012). A schematic representation of the mentioned facility can be seen in Fig. 1. The chamber is divided in two identical parts. It can be observed that each chamber has 750 mm height and 480 mm side of the base. The source is placed in the first chamber and the microphone in the

second chamber after the sample. The samples are placed in the intersection of the two parts and the chamber has been sealed by means of clips.



**Figure 1.** Facility developed for sound insertion loss measurement. Facility measurements are in mm.

The facility consists mainly of an external box made with oriented strand board (OSB wood panel) with 8 mm of thickness and internal layers of different materials. The outer box is basically used to guarantee the vibro-acoustic insulation from the external environment. The inner box was coated using three layers in the following order: rock wool, cardboard sheet and acoustic undulation. The thickness of these layers were, 50 mm for rock wool, 5 mm for cardboard sheet 25 mm for undulated foam, which ones are illustrated in Fig. 2 in order to have an idea in terms of thickness. It is important to mention, that the acoustic foam with undulations is to help to mitigate the sound reflection into the chamber.



**Figure 2.** Internal layers of the used facility built for sound insertion loss measurement.

The sound source was located in the first chamber, and the response was measured in the second chamber through a microphone. As an excitation was used a sine-sweep signal, and through a microphone the response was measured. Through the relation

output/input was obtained the frequency transfer functions, following the works of Farina (2000, 2007) and Müller & Massarani (2001). These measurements have been performed using a system composed by: a class-D amplifier, sound reproduction system, ECM-8000 and an audio interface with Phantom power using a sampling frequency of 192 kHz.

To turn possible the characterization of the acoustic behaviour of the proposed materials, the sound insertion loss of the different panels produced were analysed according to the IEC 61260-1.

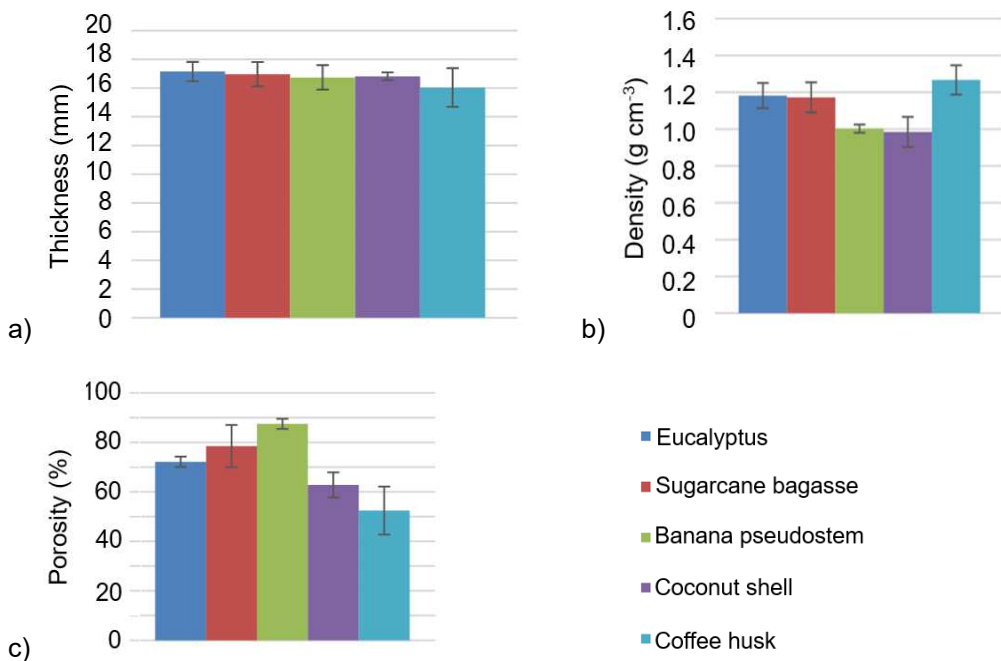
During the acoustic measurements, the background noise of the room was monitored by a hot wire anemometer model HM-385<sup>®</sup>, measurement scale 0 °C to 50 °C ± 1.0 °C.

The physical structure data analysis of the cement composites (thickness in mm, density in kg m<sup>-3</sup> and porosity %) were evaluated in a randomized design. The results were submitted to Analysis of variance (ANOVA) and Tukey test tools, both at a 5% significance level.

### RESULTS AND DISCUSSION

The factors that determine the ability of a material to resist sound transmission include the thickness, density, and porosity of the specimen (Karlinsari et al., 2012).

In the proposed work, the thickness and porosity properties have been measured also besides the density in order to add and improve the information of the samples Fig. 3).



**Figure 3.** Physical properties of the lignocellulosic panels: a) Thickness (mm); b) Density (g cm<sup>-3</sup>); c) Porosity (%) of Eucalyptus, sugarcane bagasse, banana pseudostem, coconut shell and coffee husk.

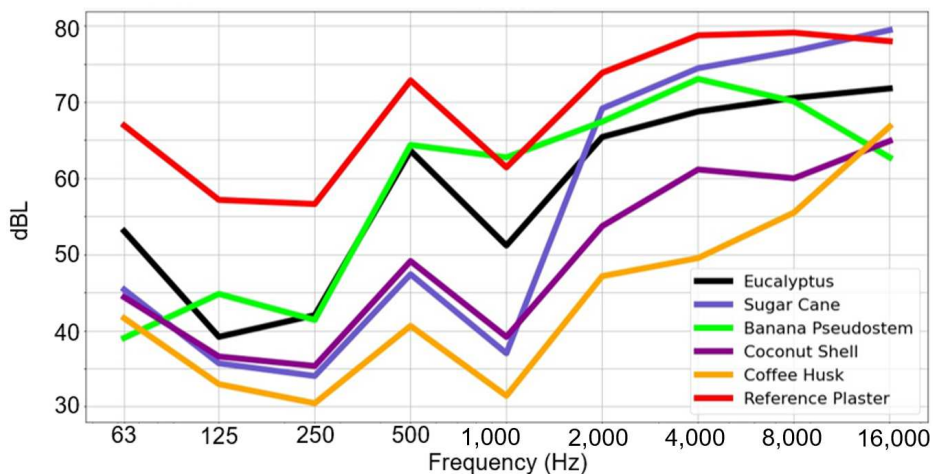
Large differences were observed in the physical properties of the lignocellulosic samples because of their different microstructures composition as a result of the chemical treatment of the raw fibres. This diversity is very interesting because it can provide considerably different porous microstructure characteristics and thus different acoustic properties.

The lignocellulosic panels thickness are similar, and all of the evaluated samples presented thickness around 17 mm. The density can be associated with the cement penetration into the permeable pores from the gaps and lumens found in the particles (Savastano et al., 2009). In our experiment, the highest density value of the composites was obtained from the panels reinforced with coffee husk followed by eucalyptus and sugar cane panels.

Pores isolated from other adjacent pores are also called ‘closed’ pores that allow some level of sound absorption, but only ‘open’ pores, which guarantee a continuous channel of communication with the external surface of the material, allow higher sound absorption characteristic (Berardi & Iannace, 2015).

For acoustic analysis through the sound insertion loss, and in order to make easier the interpretation of the data, it was proposed three groups of ranges named as ‘low’ (63 Hz, 125 Hz and 250 Hz), ‘middle’ (500 Hz, 1,000 Hz and 2,000 Hz) and ‘high’ (4,000 Hz, 8,000 Hz and 16,000 Hz).

The results of insertion loss analysis of the five kinds of samples and reference are shown in Fig. 4. It is important to mention, that for this metric, higher is better, and consequently the insertion loss of the reference sample is the highest one for ‘low’, ‘middle’ and ‘high’ frequencies. To turn possible to characterize the acoustic behaviour of the studied materials, they were analysed according to the IEC (61260-1). The acoustic measurements have been done in the range of 20 Hz to 20 kHz and the analysis in octave bands.

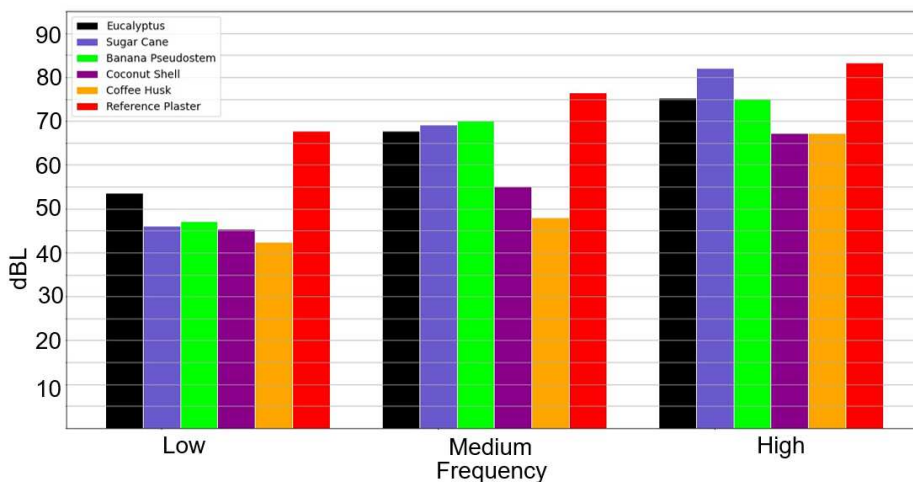


**Figure 4.** Acoustic behaviour of the studied materials.

In the range of frequencies considered as ‘low’, the eucalyptus (54 dB) followed by banana pseudostem (47 dB) and sugar cane (46 dB) presented good performance compared with the others, being the reference 67 dB; in the ‘middle’ range, the banana

pseudostem (70 dBL), sugar cane (69 dBL) and eucalyptus (68 dBL) presented better performance in comparison with the others and being the reference 76 dBL; and finally, in the range of ‘high’ range of frequencies, the sugar cane (82 dBL) followed by eucalyptus (75 dBL) and banana pseudostem (75 dBL) presented better performance compared with the others, being the reference 83 dBL. The coffee husk and the coconut shell presented lower performance of SIL in the ranges analysed. It can be observed that as a trade-off analysis, the eucalyptus presented the overall best performance considering overall range, and there is considerable difference between the reference compared with the samples proposed in ‘low’ range. However, in the ‘middle’ and ‘high’ range this difference has been reduced.

It was expected to find any acoustic difference in some frequency band correlated to the coffee husk density (Fig. 5). However, the values of insertion loss didn’t characterize this difference. Consequently, it is necessary to investigate more deeply about it.



**Figure 5.** Acoustic behaviour of the studied materials separated in ranges of frequency (low, medium, high frequency).

Summarizing, the eucalyptus shows the best performance in ‘low freq’ frequencies. the banana pseudosterm was better in ‘middle’ frequencies and sugar cane in ‘high’ frequencies. However, in a trade-off analysis, if the interest is ‘low’ and ‘middle’ frequencies, the eucalyptus and banana pseudosterm could be considered as good candidates, and if the interest is ‘high’ range, definitely the sugar cane could be a good candidate.

## CONCLUSIONS

Physical properties of the lignocellulosic materials have been measured, and the results show that for the thickness property, the high value belongs to eucalyptus, followed by sugar cane and banana pseudosterm; for the property of density, the high value belongs to coffee husk, followed by eucalyptus and sugar cane, and finally for the



property of porosity, the high value belongs to banana pseudostem, followed by eucalyptus and sugar cane. Using the insertion loss acoustic analysis, explored in results and discussion section, the eucalyptus has had better performance, followed by banana pseudostem and sugar cane in 'low' and 'middle' range of frequencies, and the sugar cane has had better performance, followed by eucalyptus and banana pseudostem. In spite of having a high value of density, the coffee husky didn't show any interesting insertion loss acoustic performance, and needs to be studied more deeply. However, the other materials of eucalyptus, banana pseudostem and sugar cane have shown interesting acoustic characteristics. The next step is proposed to improve the acoustic facility in order to explore with two or three microphones, which will permit data for acoustic absorption coefficient and transmission loss studies.

ACKNOWLEDGEMENTS. The authors would like to thank the Minas Gerais State Agency for Research and Development (FAPEMIG Grant n. CAG-APQ-01100-15).

## REFERENCES

- Arruda Filho, N., Dantas, C.P., Leal, A.F., Barbosa, N.P., Silva, C.G. & Alexandre, M.V. 2012. Mechanical strength of light cementitious composites using industrial waste and sisal fibers. *Revista Brasileira de Engenharia Agrícola e Ambiental* **16**(8), 894–902 (in Portuguese).
- Asdrubali, F., D'Alessandro, F., & Schiavoni, S. 2015. A review of unconventional sustainable building insulation materials. *Sustainable Materials and Technologies* **4**(1), 1–17.
- Azevedo, A.R.G.; Marvila, M.T.; Tayeh, B.A.; Cecchin, D.; Pereira, A.C. & Monteiro, S.N. 2021. Technological performance of açaí natural fibre reinforced cement-based mortars. *Journal of Building Engineering* **33**(1), 1–11.
- Bambi, G., Ferraz, P.F.P., Ferraz, G.A.S., Pellegrini, P. & Di Giovannantonio, H. 2019. Measure of thermal transmittance of two different infill wall built with bamboo cultivated in Tuscany. *Agronomy Research* **17**(S1), 923–934.
- Berardi, U. & Iannace, G. 2015. Acoustic characterization of natural fibers for sound absorption applications. *Building and Environment* **94**(1), 840–852.
- Butakova, M.D. & Gorbunov, S.P. 2016. Study of the Influence of Complex Additives on Properties of the Gypsum-Cement-Puzzolan Binder and Concretes on its Basis. *Procedia engineering* **150**(1), 1461–1467.
- César, A.A.D.S., Bufalino, L., Mendes, L.M., Mesquita, R.G.D.A., Protásio, T.D.P., Mendes, R.F. & Andrade, L.M.F. 2017. Transforming rice husk into a high-added value product: potential for particleboard production. *Ciência Florestal* **27**(1), 303–313.
- De Korte, A.C.J. 2015. *Hydration and thermal decomposition of cement/calcium-sulphate based materials*. Doctoral dissertation, Ph.D. Thesis, Eindhoven University of Technology. <https://research.tue.nl/en/publications/hydration-and-thermal-decomposition-of-cementcalcium-sulphate-bas>
- Farina, A. 2007. Advancements in impulse response measurements by sine sweeps. *Audio Engineering Society*. Audio Engineering Society Convention 122. Vienna, Austria, 1–21. Available: <http://www.aes.org/elib/browse.cfm?elib=14106>
- Farina, A. 2000. Simultaneous measurement of impulse response and distortion with a swept-sine technique. *Audio Engineering Society Convention 108*. Audio Engineering Society. Convention, Paris, France, 19–22. Available: <https://www.aes.org/elib/browse.cfm?elib=10211>
- Ghofrani, M., Ashori, A., Rezvani, M.H. & Ghamsari, F.A. 2016. Acoustical properties of plywood/waste tire rubber composite panels. *Measurement* **94**(1), 382–387.

- Iwariki, S. & Prata, J.G. 2008. Utilização da madeira de *Eucalyptus grandis* e *Eucalyptus dunnii* na produção de painéis cimento-madeira. *Cerne* **14**(1), 68–74.
- Karlinasari, L., Hermawan, D., Maddu, A., Bagus, M., Lucky, I.K., Nugroho, N. & Hadi, Y.S. 2012. Acoustical properties of particleboards made from betung bamboo (*dendrocalamus asper*) as a building construction material. *BioResources* **7**(4), 5700–5709.
- Mendes, R.F., Vilela, A.P., Farrapo, C.L., Mendes, J.F., Tonoli, G.H.D. & Mendes, L.M. 2017. Lignocellulosic residues in cement-bonded panels. In *Sustainable and Nonconventional Construction Materials using Inorganic Bonded Fiber Composites*. Woodhead Publishing, pp. 3–16.
- Müller, S. & Massarani, P. 2001. Transfer-function measurement with sweeps. *Journal of the Audio Engineering Society* **49**(6), 443–471.
- Piedrahita, Y. & Fajardo, F. 2012. Construcción de uma Câmara Anecoica para la Caracterización de la Pérdida de Transmisión Sonora, *Revista Brasileira de Ensino de Física* **34**(4), 1–9.
- Prusty, J.K., Patro, S.K. & Basarkar, S.S. 2016. Concrete using agro-waste as fine aggregate for sustainable built environment—A review. *International Journal of Sustainable Built Environment* **5**(2), 312–333.
- Sari, N.H., Wardana, I.N.G., Irawan, Y.S. & Siswanto, E. 2016. Physical and acoustical properties of corn husk fiber panels. *Advances in Acoustics and Vibration*, 2016. <http://dx.doi.org/10.1155/2016/5971814>
- Savastano, H. Jr., Santos, S.F. & Agopyan, V. 2009. *Sustainability of Construction Materials*. Elsevier, Amsterdam, pp. 55–81.
- Schug, B., Mandel, K., Schottner, G., Shmeliov, A., Nicolosi, V., Baese, R., ... & SEXTL, G. 2017. A mechanism to explain the creep behavior of gypsum plaster. *Cement and Concrete Research* **98**(1), 122–129.
- Souza, M.R. 1994. *Durability of cement-bonded particle board made conventionally and carbon dioxide injection*. These (Doctor of Philosophy), University of Idaho, Idaho, 123 pp.

## **Bibliometric analysis on the use of natural fibers in construction materials**

G.M.G. Ferreira<sup>1</sup>, D. Cecchin<sup>1,\*</sup>, A.R.G. de Azevedo<sup>2</sup>, I.C.R.P. Valadão<sup>1</sup>,  
K.A. Costa<sup>3</sup>, T.R. Silva<sup>4</sup>, F. Ferreira<sup>5</sup>, P.I.S. Amaral<sup>6</sup>, C.M. Huther<sup>1</sup>,  
F.A. Sousa<sup>7</sup>, J.O. Castro<sup>8</sup>, P.F.P. Ferraz<sup>8</sup> and M.A. Teixeira<sup>1</sup>

<sup>1</sup>Federal Fluminense University (UFF), Department of Agricultural Engineering and Environment, Street Passo da Pátria, n. 156, Boa Viagem, Niterói-RJ, Brazil

<sup>2</sup>North Fluminense State University (UENF), Civil Engineering Department, Campos dos Goytacazes, RJ, Brazil

<sup>3</sup>Federal Fluminense University (UFF), Production Engineering Department, Avenida dos Trabalhadores, n. 420, Vila Santa Cecília, Volta Redonda-RJ, Brazil

<sup>4</sup>North Fluminense State University (UENF), Advanced Materials Laboratory (LAMAV), Av. Alberto Lamego, 2000, 28013-602 Campos dos Goytacazes-RJ, Brazil

<sup>5</sup>Federal Fluminense University (UFF), Metallurgical Engineering Department (VMT), Volta Redonda-RJ, Brasil

<sup>6</sup>José do Rosário Vellano University (UNIFENAS), Department of Veterinary Medicine, Rodovia Mg-179 km 0, s/n - Bairro Trevo, BR 37130-000 Alfenas-MG, Brazil

<sup>7</sup>SEMAG/Aracruz, Av. Morobá, n. 20, BR 29192-733 Bairro Morobá-ES, Brazil

<sup>8</sup>Federal University of Lavras (UFLA), Campus Universitário, postal scode 3037 Lavras, MG, Brazil

\*Correspondence: [daianececchin@id.uff.br](mailto:daianececchin@id.uff.br)

Received: February 2<sup>nd</sup>, 2021; Accepted: August 3<sup>rd</sup>, 2021; Published: August 30<sup>th</sup>, 2021

**Abstract.** Due to the increasing interest of the population in the sustainability theme, there was a consequent growth in publications related to the theme in the area of civil construction. Agro-industrial waste has become an environmental problem, and with that natural fibers have found space in the reuse of waste due to its characteristics and possibilities of improving the mechanical properties of its products. In order to achieve sustainable construction demand, along with the need to reuse waste, studies have begun to analyze the application of natural fibers in construction materials. The documents provided by the Web of Science (WOS) database through research carried out with the search for the terms ‘Natural Fibers’ and ‘Building materials’ restricted to the period 2010–2020 in the main WOS collection. The institutions involved with the publications, the countries of origin of the documents, the year of publication, the keywords used by the authors and the number of citations for each document were analyzed using bibliometrics in the VOSVIEWER (VOS) software. The result of the analysis shows an increase in documents related to the theme over the years, and that the countries with the most studies in the area are China (16), USA (14) and Brazil (11), respectively. The results presented after analysis of the keywords show that natural fiber (61 occurrences), mechanical properties (44 occurrences) and composites (31 occurrences) are the words with the highest occurrence among the analyzed

documents. The present study shows the growth of research related to the theme, in addition to discriminating countries, institutions and authors, which allows monitoring the scientific expansion of the theme and guiding future studies.

**Key words:** research, civil construction, building materials; sustainability, co-occurrence analysis.

## INTRODUCTION

The growing interest in studies related to sustainability in the civil construction sector has mainly highlighted construction materials (da Silva et al., 2021). Thereby, the focus on the use of renewable sources of raw materials has been aimed at, for example, applications in composite materials of natural fibers in the construction sector, which has been presenting alternatives regarding the use of recycled fibers and reinforcements of natural fibers (organic and inorganic) in building materials (Fan, 2017; Asim et al., 2020; Erkmen et al., 2020).

The world production of natural fibers corresponds to around 32 million and 200 thousand tons, allowing us to state that most of the production of these fibers comes from cotton, which corresponds to approximately 80% of the total production weight, followed by jute, kenaf and allied fibers with about 10% of the total production weight. Wool and coconut fiber represent about 1 million tons each, and the sum of other natural fibers corresponds to 1 million and 530 thousand tons (Townsend & Sette, 2020). Bartolini et al. (2019) evidently show the growth in the number of articles published on the subject between the years 2014 and 2018 when compared to the stability presented in the period from 2006 to 2014.

Natural fibers are considered a renewable and easily obtainable resource, which can enhance the technological properties of composite materials, as well as the improvement of their mechanical and thermoacoustic characteristics, thus replacing synthetic fibers (Reddy et al., 2020). Sathish et al. (2021) also emphasize the need to reduce the use of petroleum-based synthetic fibers, allowing natural fiber to meet this need, in addition to reducing energy consumption and having high availability.

In this context, several studies have been developed for the application of natural fibers in construction materials such as Ferreira et al. (2020), who evaluated the influence of carboxylated styrene butadiene rubber coating on the mechanical performance of plant fibers and on their interface with the cementitious matrix. The authors highlighted that to reduce or mitigate interferences in the hydration of cementitious matrices, treatments for these fibers are necessary, such as reducing the fiber's dimensional variation, providing a greater interaction between the fiber surface and the hydration reactions, densifying the transition zone of the interface. The authors found that after addition of the polymer, all fibers showed an increase in tensile strength and better adhesion. The treatment reduced the water absorption capacity of all studied fibers (curauá, jute and sisal). From this perspective, it was possible to affirm that the fiber treatment provided a better interaction between the fibers and the cementitious matrix.

Azevedo et al. (2021a) evaluated the technological performance of natural açai fiber reinforced in cement-based mortars. Different fiber additions under natural conditions and after surface treatment with NaOH were studied. The authors concluded that the addition of açai fiber to mortar worked by filling part of the internal pores and as a reinforcing material for the cementitious matrix to absorb and redistribute internal

stresses. Furthermore, they emphasize that the açai fiber must be properly treated with a NaOH solution due to the loss of durable properties found in its untreated use. The authors also state that high proportions of natural fibers in cementitious composites can be harmful, thus confirming that the addition of 3.0% of natural fibers treated with NaOH in mortars is recommended to balance adequate technology and durability.

Wang & Chen (2017) studied the development of bamboo-based composites and showed that bamboo has more than ten cell layers in its cell structure, with each microfibril different and orientation with thick layers and thin layers in alternating arrangements on the cell wall. The results presented verified that bamboo-based composites are a combination of high strength, dimensional stability, durability, with reliable structural properties, having high modulus of elasticity and well dispersed through a matrix of low modulus of elasticity, thus presenting the modulus of composites greater than that of the matrix. Hamad et al. (2017) evaluated the microstructure properties and their bond with the tensile strength of different natural fibers (linen, jute, ramie and sisal fibers) and identified that jute and sisal fibers exhibit less variation in terms of fiber cross-sectional area, shape, inner lumen size and cell wall thickness compared to linen and ramie fibers, which ultimately reflects on the fibers' tensile properties. They also verified that the stress-strain behavior presented two distinct regimes. The authors found that this variation was linked to differences in fiber microstructure. When studying the development of mortar for laying and coating with natural pineapple fibers Azevedo et al. (2020) tested different percentages of fiber incorporation, as treatment (NaOH) and without fiber treatment. The authors observed that the treatment with NaOH solution and the percentage of natural pineapple fiber incorporated in up to 5% in relation to the cement mass form mortars with technological feasibility of application. Valášek & Habrová (2017) studied the hardness and abrasive wear resistance of epoxy resins filled with unordered short sisal fibers. They observed that the surface treatment of the fibers led to the removal of the surface layers of fiber, increasing surface segmentation. As for the hardness, there was a decrease in the same in the composites as the fiber addition increased.

In order to optimize the geopolymer matrix produced with Fired Clay Brick Powder Silva et al. (2020) studied the reinforcement of the material using the application of jute and sisal fibers. The authors observed that the increase in fiber content provides a linear increase in flexural strength, whereas in relation to the compression and tensile tests an optimal fiber content was presented, which varies according to the type of fiber used.

Wongsa et al. (2020) evaluated the performance of sisal fiber and coconut fiber as reinforcement of fly ash-based geopolymer mortar with high calcium content. The authors studied ten different mortar mixes, with sisal fibers, coconut fiber and glass fiber, in proportions of 0%, 0.50%, 0.75% and 1.00% of the volume of the mixture. The authors found a significant improvement in tensile and bending strength when compared to the control sample, and similar to the synthetic fiber sample. The authors observed a trend towards a decrease in compressive strength, workability, dry density and ultrasonic pulse velocity, in addition to no significant effect of the fiber on thermal conductivity and water absorption. Therefore, the authors conclude that geopolymer composites can use coir and sisal fibers as reinforcement material.

Study by Azevedo et al. (2021b) evaluated the physical and mechanical characteristics of geopolymer materials reinforced with natural fibers and geopolymer materials reinforced with synthetic fibers. They observed the need for a pre-treatment in natural fiber for better mechanical performance due to their sensitivity to alkaline environment and low adhesion to the matrix caused by substances present on its surface. When fiber pre-treatment is combined with improved traceability and ideal curing conditions, the application of natural fibers in geopolymer materials allows the replacement of synthetic fibers without harming their performance. However, the particular characteristic of each fiber must be analyzed, since the variation between different types of natural fibers can make the polymer matrix not ideally incorporated.

Tan et al. (2019) studied the application of 15 vegetable fibers from agricultural and forestry residues chosen due to their potential as a raw material for the manufacture of geopolymeric panels. The authors observed good compatibility of the studied vegetable fibers (without additives), with wood fibers being more compatible with the material than non-wood fibers in general. Zhang et al. (2021) studied the manufacture of geopolymer mortar with natural fiber as reinforcement. The authors observed good compatibility of the geopolymer matrix with the pre-treatment of natural fiber with  $\text{CaCl}_2$ , in addition to an increase in flexural strength and tenacity according to the increase in the proportion of fiber. However, it was also observed a decrease in the compressive strength of the material due to the increase in voids caused by the fiber.

With this in mind, it is possible to affirm that the incorporation of natural fibers in construction materials has been constantly the focus for new researches aimed at the application of these fibers. Thus, using bibliometric analysis to enhance the incidence of these researches is very relevant (Hamdaoui et al., 2020). According to Aziz et al. (2020), bibliometrics is related to the quantitative study of the properties of scientific productions, incorporating new understandings about a given topic to the literature.

The purpose of bibliometric analysis is to measure production, impact and collaboration, using different information as indicators, with a broad coverage of information by the database being important (Mallig, 2010). As presented by Ye et al. (2020), the bibliometric analysis allows finding a knowledge map related to certain research metrics. Databases provide valuable bibliometric data for providing global academic information (Xie et al., 2020). The Web of Science (WOS) database is widely known as one of the main sources in the academic world, where research metrics are used taking into account publication and impact algorithms, which made it a reliable and recognized source for conducting research scientific (Powell & Peterson, 2017).

Thus, the aim of this study was to carry out a bibliometric analysis of works regarding the use of natural fibers in construction materials in the period from 2010 to 2020.

## **MATERIALS AND METHODS**

Between the 21<sup>st</sup> and 22<sup>nd</sup> of January 2021, a bibliographic search was carried out in the WOS database. The search metrics used in the survey were the keywords 'Natural Fiber' and 'Building Materials', with the years 2010–2020 being adopted with a search criterion. The analysis was made through the main collection of the WOS database, adopting a broad scope of research, considering all the searchable fields available for

consultation. The documents resulting from the research were exported in a text file (TXT) in tab format (Windows), with the contents of the complete record and references cited.

The institutions involved with the publications found were analyzed with VOS through the co-authored analysis, with the metric ‘organizations’, considering all documents with at least one occurrence. From the results obtained, the three institutions with the highest occurrence were considered. The countries involved in the research were verified through VOS analysis, considering the co-authorship of the documents restricting to the countries. At least one quote per country was considered.

The information obtained through the database was placed in the Excel software, discriminating the documents by year of publication. To obtain information regarding co-occurrence parameters, countries and institutions linked to the documents, the VOS tool was used. Vosviewer (VOS) is open access software for creating and viewing bibliometric networks, which also allows analysis of text data.

To analyze the co-occurrence of keywords, initially, the metric of at least one occurrence of the keyword was used, which allowed obtaining all the keywords found in the analyzed documents. The search result was exported to a text file and opened in Excel, where equivalent and repeated words with different writing were unified through a model text file provided by VOS and later added to the program. The analysis was redone with the updated information, where the number of occurrences was defined as 5, and the keyword graph was subsequently generated.

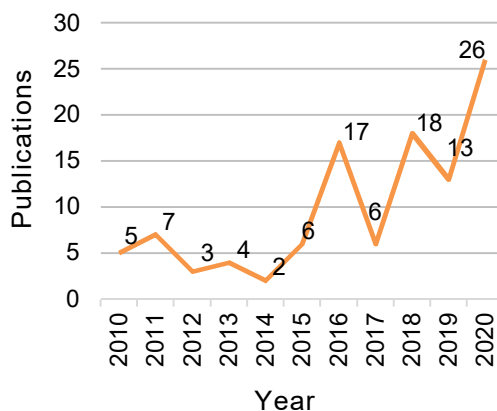
The number of citations obtained by the publications was obtained through co-occurrence analysis of the VOS in the ‘citations’ type with the ‘documents’ analysis unit, where the 9 most cited documents were considered.

## RESULTS AND DISCUSSION

Among the documents found in the WOS database, 107 were found for the period and research metrics analyzed, as shown in Fig. 1.

When analyzing the countries involved in the publications found in the WOS for the period from 2010 to 2020, a total of 43 countries were observed, the results can be seen in Fig. 2. The countries with the highest number of publications were: China (16 publications), United States (14 publications), Brazil (11 publications) and India (10 publications).

When analyzing the keywords resulting from the search in the VOS software, 34 keywords were found and presented in Fig. 3. Among them, natural fiber (61 key-words), mechanical properties (44 key-words) and composites (31 key-words).



**Figure 1.** Number of publications per year.





natural fibers in construction materials such as Princeton University (New Jersey - USA) and University of São Paulo (São Paulo - Brazil), with 4 documents each.

**Table 1.** The 10 most cited documents

Author	Residue	Citations
Pacheco-Torgal & Jalali, 2011	Bagasse, Banana leaf, Banana trunk, Coconut coir, Coconut tissue, Eucalyptus e Sisal	213
Mahjoub et al., 2014	Kenaf	134
Yan et al., 2016	Coconut fiber	91
Karade, 2010	Wheat straw, Rice straw, Coir, Hazelnut shell, Oil palm residues, Cork granules, Bark, Bagasse, Arhar stalks, Construction demolition wastes, Waste timber, Waste MDF e Furniture industry waste	85
Elsaid et al., 2018	Kenaf	71
Senthilkumar et al., 2018	Sisal	70
Ferreira et al., 2015	Sisal	51
Hamza et al., 2013	Alfa leaves, rush stems, palm leaflets and date palm wood	40
Lertwattanaruk & Suntijitto, 2015	coconut coir and oil palm	39

The increase in interest in the use of natural fibers in civil construction by researchers is evident with the increase in research related to the theme over the years, as an example we can mention the study by Khasawneh & Alyaseen (2020) in which they analyzed the use of coconut fiber in bituminous mixtures for road materials, Alavez-Ramirez et al. (2012) analyzed the use of the same fiber, however in fiber cement sandwich panels. However, Freire et al. (2017) studied the application of agro-industrial waste in the manufacture of medium-density fiberboard (MDF) and high-density fiberboard (HDF) panels in order to add value to waste and reduce the demand for wood and by-products from the production of the panels.

Representing 47.66% of the publications found in the database used, in the studied period, are China, USA, Brazil and India. Pakistan (1 post), Vietnam (1 post), South Korea (1 post), Arab Emirates (1 post), Malaysia (5 post), Indonesia (2 post), Iran (1 post), Iraq (1 post), Jordan (1 publication), Taiwan (2 publications), Turkey (1 publication), Saudi Arabia (6 publication), India (10 publication) and Thailand (6 publication), countries belonging to the Asian continent, as observed in the analysis, also demonstrate great interest in research involving the topic, resulting in 46.70% of publications, which is justified by the fact that the continent is a major agricultural producer and most of the fibers from waste in the sector. In South America, research in the area is concentrated in Brazil, with 11 publications, followed by Colombia (2 publications), Argentina (1 publication), Chile (1 publication) and Peru (1 publication).

Asian countries are benchmarks for the strength of scientific research related to sustainability Det Udomsap & Hallinger (2020). The results are consistent with the studies by Li et al. (2018), which shows the growth of China in research related to the reuse of solid waste, where the country reaches the first place surpassing the USA in production in the area.

The residues obtained between the keywords were sisal, with 14 co-occurrences, followed by wood with 8 co-occurrences and coconut fiber with 7 occurrences. Also found during waste keyword analysis such as date palm (6), Fly Ash (5 occurrences),

Hemp (4 occurrences), Jute (4 occurrences), Kenaf (4 occurrences), Bagasse (4 occurrences), bamboo (3 occurrences) and rice straw (2 occurrences).

Hemp, jute, sisal, kenaf and coconut (coconut) residues are also recurrent keywords in WOS studies, such as Bartol & Mackiewicz-Talarczyk (2015), in relation to publications related to fiber studies. The potential of using Coffee husk, Coconut shell, and Banana pseudostem in scientific composites is presented in studies by Ferraz et al. (2020). Study by Kochova et al. (2020), demonstrates that coconut fiber has in its structure characteristics with adequate thermal and mechanical conditions, and can provide several applications in the construction industry. However, De Azevedo et al. (2021a) draws attention to the fact that some materials with cementitious matrix are not suitable for application of natural fibers due to the pH in the pore region of the matrix.

The use of agricultural by-products (natural fibers) in composite materials made with soil matrix and cement / lime has shown results of improved physical, mechanical and durability properties Danso & Manu (2020). The keywords also showed the occurrence of words related to material properties, such as mechanical properties (44) and thermal properties (7). The result showed the occurrence of behavior (26), strength (26), performance (18), tensile (6), physical properties (5), flexural strength (6), which analyze the properties of the material.

The mechanical performance of materials is the target of many studies, the term 'Mechanical Properties' was one of the ten most cited keywords in the study by Liu (2013), with 3,687 citations, with 'Building materials' being the second most cited with 6344 quotes.

The analyzes carried out by Alao et al. (2019) with marijuana fiber in polypropylene composites used tests of traction, compression, flexion, water absorption and expansion, air permeability and spectroscopy.

It is clear from the results presented by Karade (2010), the need for further research to better understand the durability property, a keyword with 18 occurrences in the publications from 2010 to 2020 analyzed in this article.

The literature review work by Pacheco-Torgal & Jalali (2011) reinforced the fact that mechanical properties, one of the keywords, are the focus of much of the available literature. The study by Slebi-Acevedo et al. (2019) draws attention to the lack of information regarding porous mixtures with addition of fibers, in addition to the need for studies on the mixture of two or more fibers to improve the mechanical properties of the composite.

There is a change in the need for studies over time, due to the emergence of new research in the area. The present work allows the monitoring of the scientific expansion of the theme through the bibliometric analysis carried out, allowing then to guide future studies.

## CONCLUSIONS

Bibliometric analysis allowed an in-depth study of the number of documents referring to the use of natural fibers in construction materials, showing a considerable increase in the last eleven years, with a total of 26 publications in 2020. Among the countries identified in the documents are China, the United States, Brazil and India. The study found as keywords with the highest occurrence the words natural fiber, mechanical properties and composites.

The present study showed the growing interest in research related to the theme ‘Natural Fibers’ and ‘Building Materials’, in addition to presenting institutions and countries more closely linked to the theme and the relevance of the authors, in addition to allowing to follow the scientific expansion of the theme and guide future studies.

## CHALLENGES AND FUTURE PERSPECTIVES

Based on this study, it is possible to affirm that the topic is very relevant, but it also needs to advance in certain issues, especially with regard to the emergence of new unconventional fibers. It was evidently possible to verify that materials produced with natural fibers contribute to improve the development of construction materials in terms of performance and sustainability. However, it is necessary to point out that the search for this theme should not be limited only to these parameters, but also to be sought considering that there is a large market behind it for these materials to be applied, not only to develop them.

Materials that incorporate natural fibers can offer a number of advantages over the traditional ones used in construction, however, the challenges continue to move towards the replacement of conventional materials by those that can exert a structure and function comparable to traditional ones, as well as presenting durability to long term, in addition to the cost and design of the material. Thus, it is possible to list some of these challenges that should be considered for future perspectives for the development of building materials using natural fibers: Mechanical property variability and stiffness; Standardization of these new materials; Long term durability; Cost reduction; Market acceptance.

## REFERENCES

- Alao, P.F., Kallakas, H., Poltimäe, T. & Kers, J. 2019. Effect of hemp fibre length on the properties of polypropylene composites. *Agronomy Research* **17**(4), 1517–1531. doi: 10.15159/AR.19.146
- Alavez-Ramirez, R., Chiñas-Castillo, F., Morales-Dominguez, V.J. & Ortiz-Guzmana, M. 2012. Thermal conductivity of coconut fibre filled ferrocement sandwich panels. *Construction and Building Materials* **37**, 425–431. doi: 10.1016/j.conbuildmat.2012.07.053
- Asim, M., Uddin, G.M., Jamshaid, H., Raza, A., Tahir, Z. ul R., Hussain, U., Satti, A.N., Hayat, N. & Arafat, S.M. 2020. Comparative experimental investigation of natural fibers reinforced light weight concrete as thermally efficient building materials. *Journal of Building Engineering* **31**, 101411. doi: 10.1016/j.job.2020.101411
- Azevedo, A.R.G. de; Cruz, A.S.A., Marvila, M.T., Oliveira, Leandro B., Monteiro, S.N., Vieira, C.M.F., Fediuk, R., Timokhin, R., Vatin, N. & Daironas, M. 2021b. Natural Fibers as an Alternative to Synthetic Fibers in Reinforcement of Geopolymer Matrices: A Comparative Review. *Polymers* **13**(15), 493. doi: 10.3390/polym13152493
- Azevedo, A.R.G. de; Marvila, M.T., Tayeh, B.A., Cecchin, D., Pereira, A.C. & Monteiro, S.N. 2021a. Technological performance of açai natural fibre reinforced cement-based mortars. *Journal of Building Engineering* **33**, 101675. doi: 10.1016/j.job.2020.101675
- Azevedo, A.R.G., Marvila, M.T., Zanelato, E.B., Alexandre, J., Xavier, G.C. & Cecchin, D. 2020. Development of mortar for laying and coating with pineapple fibers. *Revista Brasileira de Engenharia Agrícola e Ambiental* **24**(3), 187–193. doi: 10.1590/1807-1929/agriambi.v24n3p187-193

- Aziz, E., Mustapha, H. & Jamila, E.A.A 2020. bibliometric study of the recent advances in open innovation concept. *Procedia Computer Science* **175**, 683–688. doi: 10.1016/j.procs.2020.07.100
- Bartol, T. & Mackiewicz-Talarczyk, M. 2015. Bibliometric Analysis of Publishing Trends in Fiber Crops in Google Scholar, Scopus, and Web of Science. *Journal of Natural Fibers* **12**(6), 531–541. doi: 10.1080/15440478.2014.972000
- Bartolini, M., Bottani, E. & Grosse, E.H. 2019. Green warehousing: Systematic literature review and bibliometric analysis. *Journal of Cleaner Production* **226**, 242–258. doi: 10.1016/j.jclepro.2019.04.055
- da Silva, T.R., de Azevedo, A.R.G., Cecchin, D., Marvila, M.T., Amran, M., Fediuk, R., Vatin, N., Karelina, M., Klyuev, S. & Szelag, M. 2021. Application of Plastic Wastes in Construction Materials: A Review Using the Concept of Life-Cycle Assessment in the Context of Recent Research for Future Perspectives. *Materials* **14**, 3549. doi: 10.3390/ma14133549
- Danso, H. & Manu, D. 2020. Influence of coconut fibres and lime on the properties of soil-cement mortar. *Case Studies in Construction Materials* **12**, e00316., doi: 10.1016/j.cscm.2019.e00316
- Det Udomsap, A. & Hallinger, P. 2020. A bibliometric review of research on sustainable construction, 1994–2018. *Journal of Cleaner Production* **254**. doi: 10.1016/j.jclepro.2020.120073.
- Elsaid, A., Dawood, M., Seracino, R. & Bobko, C. 2011. Mechanical properties of kenaf fiber reinforced concrete. *Construction and Building Materials* **25**(4), 1991–2001. doi: 10.1016/j.conbuildmat.2010.11.052
- Erkmen, J., Yavuz, H.I., Kavci, E. & Sari, M. 2020. A new environmentally friendly insulating material designed from natural materials. *Construction and Building Materials* **255**, ISSN: 09500618. doi: 10.1016/j.conbuildmat.2020.119357
- Fan, M. 2017. Future scope and intelligence of natural fibre based construction composites. *Advanced High Strength Natural Fibre Composites in Construction* 545–556. doi: 10.1016/B978-0-08-100411-1.00022-4
- Ferraz, P., Mendes, R., Ferraz, G., Carvalho, V., Avelino, M., Narciso, C., Eugênio, T., Cadavid, V. & Bambi, G. 2020. Thermal analysis of cement panels with lignocellulosic materials for building. *Agronomy Research* **18**(S1), 797–80. doi: 10.15159/AR.20.124
- Ferreira, S.R., Neto, A.R.S., Silva, F. de A., de Souza Jr, F. G. & Filho, R. D. T. 2020. The influence of carboxylated styrene butadiene rubber coating on the mechanical performance of vegetable fibers and on their interface with a cement matrix. *Construction and Building Materials* **262**, 15–36. doi: 10.1016/j.conbuildmat.2020.120770
- Ferreira, S.R., Silva, F.A., Lima, P.R.L. & Toledo Filho, R.D. 2015. Effect of fiber treatments on the sisal fiber properties and fiber-matrix bond in cement based systems. *Construction and Building Materials* **101**, 730–740. ISSN: 09500618, doi: 10.1016/j.conbuildmat.2015.10.120
- Freire, A., Júnior, C., Rosa, M.O., Almeida Neto, J. & Figueirêdo, M. 2017. Environmental assessment of bioproducts in development stage: The case of fiberboards made from coconut residues. *Journal of Cleaner Production* **153**, 230–241. doi: 10.1016/j.jclepro.2017.03.100
- Hamad, S.F., Stehling, N., Holland, C., Foreman, J.P. & Rodenburg, C. 2017. Low-Voltage SEM of Natural Plant Fibers: Microstructure Properties (Surface and Cross-Section) and their Link to the Tensile Properties. *Procedia Engineering* **200**, 295–302. doi: 10.1016/j.proeng.2017.07.042
- Hamdaoui, O., Limam, O., Ibos, L. & Mazioud, A. 2020. Thermal and mechanical properties of hardened cement paste reinforced with Posidonia-Oceanica natural fibers. *Construction and Building Materials* **269**, 121339. doi: 10.1016/j.conbuildmat.2020.121339
- Hamza, S., Saad, H., Charrier, B., Ayed, N., Charrier-El, F. & Charrier - El Bouhtoury, F. 2013. Physico-chemical characterization of Tunisian plant fibers and its utilization as reinforcement for plaster-based composites. *Industrial Crops and Products* **49**, 357–365. doi: 10.1016/j.indcrop.2013.04.052

- Karade, S.R. 2010. Cement-bonded composites from lignocellulosic wastes. *Construction and Building Materials* **24**(8), 1323–1330. doi: 10.1016/j.conbuildmat.2010.02.003
- Khasawneh, M.A. & Alyaseen, S.K. 2020. Analytic methods to evaluate bituminous mixtures enhanced with coir/coconut fiber for highway materials. *Materials Today: Proceedings* **33**, 1752–1757. doi: 10.1016/j.matpr.2020.04.870
- Kochova, K., Gauvin, F., Schollbach, K. & Brouwers, H.J.H. 2020. Using alternative waste coir fibres as a reinforcement in cement-fibre composites. *Construction and Building Materials* **231**, 117121. doi: 10.1016/j.conbuildmat.2019.117121
- Krishnasamy, S., Saba, N., Rajini, N., Muthukumar, C., Jawaid, M., Siengchin, S. & Alothman, O. 2018. Mechanical properties evaluation of sisal fibre reinforced polymer composites: A review. *Construction and Building Materials* **174**, 713–729. doi: 10.1016/j.conbuildmat.2018.04.143
- Lertwattanaruk, P. & Suntijitto, A. 2015. Properties of natural fiber cement materials containing coconut coir and oil palm fibers for residential building applications. *Construction and Building Materials* **94**, 664–669. doi: 10.1016/j.conbuildmat.2015.07.154
- Li, N., Han, R. & Lu, X. 2017. Bibliometric analysis of research trends on solid waste reuse and recycling during 1992–2016. Resources, *Conservation and Recycling* **130**, 109–117. doi: 10.1016/j.resconrec.2017.11.008
- Liu, T. 2013. A bibliometric analysis of the performance of Advanced Materials Research from 2005 to 2012. *Advanced Materials Research* **803**, 165–168. doi: 10.4028/www.scientific.net/AMR.803.165
- Mahjoub, R., Yatim, J., Mohd.Sam, A.R. & Hashemi, S.H. 2014. Tensile properties of kenaf fiber due to various conditions of chemical fiber surface modifications. *Construction and Building Materials* **55**, 103–113. doi: 10.1016/j.conbuildmat.2014.01.036
- Mallig, N. 2010. A relational database for bibliometric analysis. *Journal of Informetrics* **4**(4), 564–580. doi: 10.1016/j.joi.2010.06.007
- Pacheco-Torgal, F. & Jalali, S. 2011. Cementitious building materials reinforced with vegetable fibres: A review. *Construction and Building Materials* **25**(2), 575–581. doi: 10.1016/j.conbuildmat.2010.07.024
- Powell, K.R. & Peterson, S.R. 2017. Coverage and quality: A comparison of Web of Science and Scopus databases for reporting faculty nursing publication metrics. *Nursing Outlook* **65**(5), 572–578. doi: 10.1016/j.outlook.2017.03.004
- Reddy, P.V., Reddy, S., Jeeru, L.R., Krishnu, D.M. & Rajendra Prasad, P. 2020. An overview on natural fiber reinforced composites for structural and non-structural applications. *Materials Today: Proceedings* **45**, 6210–6215. doi: 10.1016/j.matpr.2020.10.523
- Sathish, S., Karthi, N., Prabhu, L., Gokulkumar, S., Balaji, D., Vigneshkumar, N., Ajeem Farhanb, T.S., AkilKumar, A. & Dinesh, V.P. 2021. A review of natural fiber composites: Extraction methods, chemical treatments and applications. *Materials Today: Proceedings*, **45**, 8017–8023. doi: 10.1016/j.matpr.2020.12.1105
- Silva, G., Kim, S., Bertolotti, B., Nakamatsu, J. & Aguilar, R. 2020. Optimization of a reinforced geopolymer composite using natural fibers and construction wastes. *Construction and Building Materials* **258**, 119697. doi: 10.1016/j.conbuildmat.2020.119697
- Slebi, C., Lastra-González, P., Pascual-Muñoz, P. & Castro-Fresno, D. 2019. Mechanical performance of fibers in hot mix asphalt: A review. *Construction and Building Materials* **200**, 756–769. doi: 10.1016/j.conbuildmat.2018.12.171
- Tan, J., Lu, W., Huang, Y., Wei, S., Xua, X., Liu, L. & Zheng, G. 2019. Preliminary study on compatibility of metakaolin-based geopolymer paste with plant fibers. *Construction and Building Materials* **225**, 772–775. doi: 10.1016/j.conbuildmat.2019.07.142
- Townsend, T. & Sette, J. 2016. *Natural Fibres and the World Economy. Natural Fibres: Advances in Science and Technology Towards Industrial Applications*, 381–390. doi: 10.1007/978-94-017-7515-1\_30

- Valášek, P. & Habrová, K. 2017. Influence of sisal fibres on tribological properties of epoxy composite systems. *Agronomy Research* **15**(S1), 1242–1250.
- Wang, G. & Chen, F. 2017. *Development of bamboo fiber-based composites. Advanced High Strength Natural Fibre Composites in Construction*, pp. 235–255. doi: 10.1016/b978-0-08-100411-1.00010-8
- Wongsa, A., Kunthawatwong, R., Naenudon, S., Sata, V. & Chindaprasirt, P. 2020. Natural fiber reinforced high calcium fly ash geopolymer mortar. *Construction and Building Materials* **241**, 118143. doi: 10.1016/j.conbuildmat.2020.118143
- Xie, H., Zhang, Y. & Duan, K. 2019. Evolutionary overview of urban expansion based on bibliometric analysis in Web of Science from 1990 to 2019. *Habitat International* **95**, 102100. doi: 10.1016/j.habitatint.2019.102100
- Yan, L., Chouw, N., Huang, L. & Kasal, B. 2016. Effect of alkali treatment on microstructure and mechanical properties of coir fibres, coir fibre reinforced-polymer composites and reinforced-cementitious composites. *Construction and Building Materials* **112**, 168–182. doi: 10.1016/j.conbuildmat.2016.02.182
- Ye, N., Kueh, T., Liu, L., Yongxin, H. & Yu, H. 2020. A bibliometric analysis of corporate social responsibility in sustainable development. *Journal of Cleaner Production* **272**, 122679. doi: 10.1016/j.jclepro.2020.122679
- Zhang, N., Ye, H., Pan, D. & Zhang, Y. 2021. Effects of alkali-treated kenaf fiber on environmentally friendly geopolymer-kenaf composites: Black liquid as the regenerated activator of the geopolymer. *Construction and Building Materials* **297**, 123787. doi: 10.1016/j.conbuildmat.2021.123787

## **Wheat cultivars exposed to high temperature at onset of anthesis for yield and yield traits analysis**

R. Goher and M. Akmal\*

Department of Agronomy, Faculty of Crop Production Sciences, The University of Agriculture, Peshawar-25130, Pakistan

\*Correspondence: [akmal@aup.edu.pk](mailto:akmal@aup.edu.pk)

Received: April 16<sup>th</sup>, 2021; Accepted: July 26<sup>th</sup>, 2021; Published: August 16<sup>th</sup>, 2021

**Abstract.** Temperature fluxes at some critical growth stages adversely affect the crop yield. Heat stress (HS) of limited duration shows mild to marked effects on crop yield. The study focused on evaluating HS of limited durations on wheat crop effective from anthesis. Four wheat cultivars (Pirsabak-2005, Pakhtunkhwa-2015, Pakistan-2013, and DN-84) and three advanced lines (P-2, P-12, and P-18) were subjected to HS for 48, 72, and 96 h evaluating changes in the yield and yield contributing traits. The experiment was conducted in a randomized complete block design during 2017–18 and 2018–19 at Agronomy Research Farm, the University of Agriculture Peshawar Pakistan. At the onset of anthesis, plants were exposed to HS in the plastic tunnel for limited durations. The temperature inside and outside tents was recorded periodically. The mean across the years showed a significant effect on yield traits by HS imposition at anthesis stage. The mean data across the two years showed a significant effect of HS on yield and yield contributing traits. In comparison with control, spike weight (g) reduced by 29, 40, and 49% under limited HS of 48, 72, and 96 h, respectively. Grains per spike were decreased by 45, 61, and 69% and grain weight by 29, 36, and 45% from control to imposed HS of 48, 72, and 96 h, respectively. Overall grain yield decreased by 44, 61, and 70% upon exposed to 48, 72, and 96 h of HS, respectively. The differences among the cultivars for yield and yield contributing traits were different under various HS conditions. The study concluded that HS effective from anthesis has an adverse effect on grain weight and number and hence the grain yield. Among the cultivars, Pakistan-2013 showed better resistance to HS of limited duration when exposed at the anthesis stage of the crop growth.

**Key words:** heat stress, heat-stress duration, grain weight, grain number, wheat yield.

### **INTRODUCTION**

Wheat is susceptible to heat stress at critical growth stages (Gupta et al., 2013) resulting in yield losses. Plant growth is adversely affected by heat stress through the sudden increase in temperature, particularly at the start of the reproductive stages of plant growth (Asseng et al., 2015). Yield loss has been reported up to 6% with 1 °C rise in temperature from optimum at critical growth stages (Akter & Islam, 2017). An increase in temperature has shown adverse effects on plant meristem, which resulted in a decrease in leaf photosynthetic activity (Haque et al., 2014) but an increase in leaf fall was also

observed (Kosova et al., 2011). Change in daily temperature has shown adverse effects on the flag leaf of the wheat crop, which resulted in yield loss (Zhao et al., 2007). Senescence of the leaf has also increased due to high temperature with structural changes in the chloroplast, breakdown of vacuoles, damaging cell membrane, and intrusion of cellular stability (Khanna-Chopra, 2012). Some common adverse effects were also observed under heat stress like reduction in the photosynthetic process, changes in stomatal behavior, reduction in flag leaf area, premature leaf fall, and loss of pollen viability, etc. (Asseng et al., 2011).

Research has confirmed rapid spike growth at a temperature over 20 °C (Semenov, 2009) with complete pollen sterility in wheat at above 30 °C (Kumar et al., 2020). The reason for pollen sterility was due to the disintegration of the pollen cell and microspore (Anjum et al., 2008). The structure of cell endosperm and aleurone layer has shown changes by differences in the day and night temperatures (Dias et al., 2008). Heat stress for more than 3 days effective from anthesis has resulted in abnormal anther and functionally futile florets (Hedhly et al., 2009; Yu et al., 2014). Heat stress (+ 1–2 °C) has caused a reduction in grain size and numbers due to limited grain fill duration in wheat (Lukac et al., 2012). The high temperature at the post-anthesis stage of wheat has also resulted in early maturity, limited grain fill period, loss in grain number, and weight (Nasehzadeh & Ellis, 2017; Mazurenko et al., 2020). Heat stress also decreased biomass (Akter & Islam, 2017) due to the limited source accumulation rate (Prasad & Djanaguiraman, 2014). Heat stress at anthesis has shown about a 23% reduction in the above-ground biomass of wheat crops (Banerjee & Krishnan, 2015). Considering the available weather data in Pakistan (1960 to 2010) for future projection through model approach for future climate change (2030 and 2040) a temperature rise is expected from 1 to 2 °C that may affect the wheat crop (Hanif & Ali, 2014).

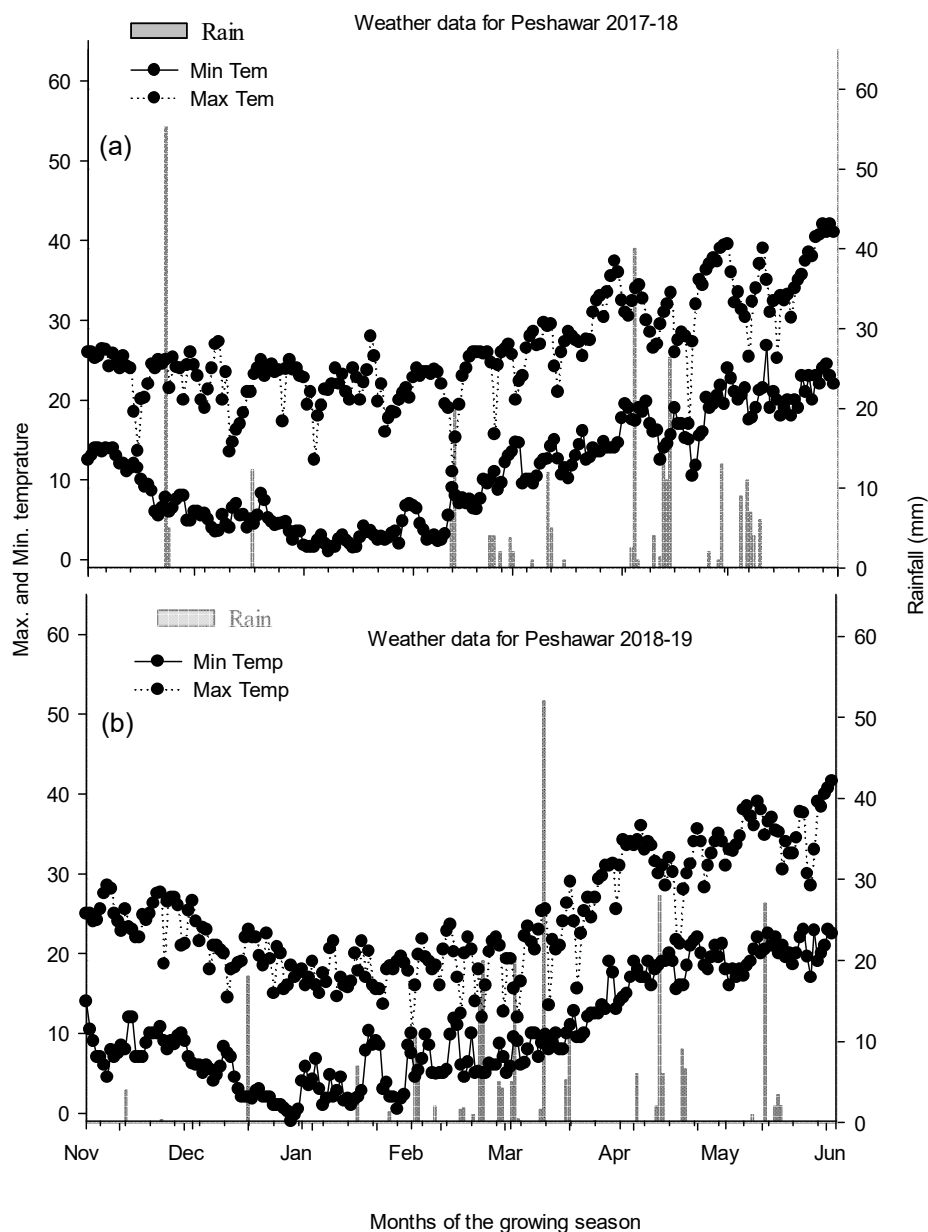
This study aimed to expose plants to heat stresses by artificially raising the growth temperature for limited durations by making temporary polyethylene plastic tents over the plants effective from the onset of the anthesis stage of the crop. We want to estimate the change that has taken place in the primary yield traits that adversely affect the grain yield of the promising wheat cultivars. It has been observed that in changing climate the abnormal HS is frequently observed in the field during the crop entered from vegetative to reproductive stages of growth.

## MATERIALS AND METHODS

### Site description

A 2-year field experiment was conducted during winter 2017–18 and 2018–19 at Agronomy Research Farm, the University of Agriculture Peshawar-Pakistan. The location of the experimental site was at 34° 1'13.50 "N" and 71° 28'53.02 "E", 350 m above sea level. Climate is subtropical, received 500–700 mm annual precipitation, with daily mean temperature varying from  $24 \pm 6.24$  °C to  $40.7 \pm 6.29$  °C during the wheat crop growth (November to May). The soil of the experimental site was silt loam having pH > 7.6, organic matter < 1%. Sand (18.13%) silt (71.23%) and clay (10.64%), and classified as *Ustocrept* based on USDA classification (Anonymous, 2007). Data regarding seasonal temperature (Max. and Min.) and rainfall of the crop growth period were obtained from the local Metrological Department (Fig. 1).





**Figure 1.** Temperature and rainfall of the crop growth seasons are presented in the separate windows during the experimental years (a) 2017–18 and (b) 2018–19 with bars for rainfall (mm) and lines for temperature minimum (T Min °C) and maximum (T Max °C).

### Experimental design and treatments

The experiment was conducted in a randomized complete block design (RCBD) using three replications. Seven wheat cultivars/lines were exposed to three heat stress (HS) durations by raising the growth temperature in plastic tents for limited durations (48, 72, and 96 h) effective from the anthesis stage of the crop growth. Seeds were sown

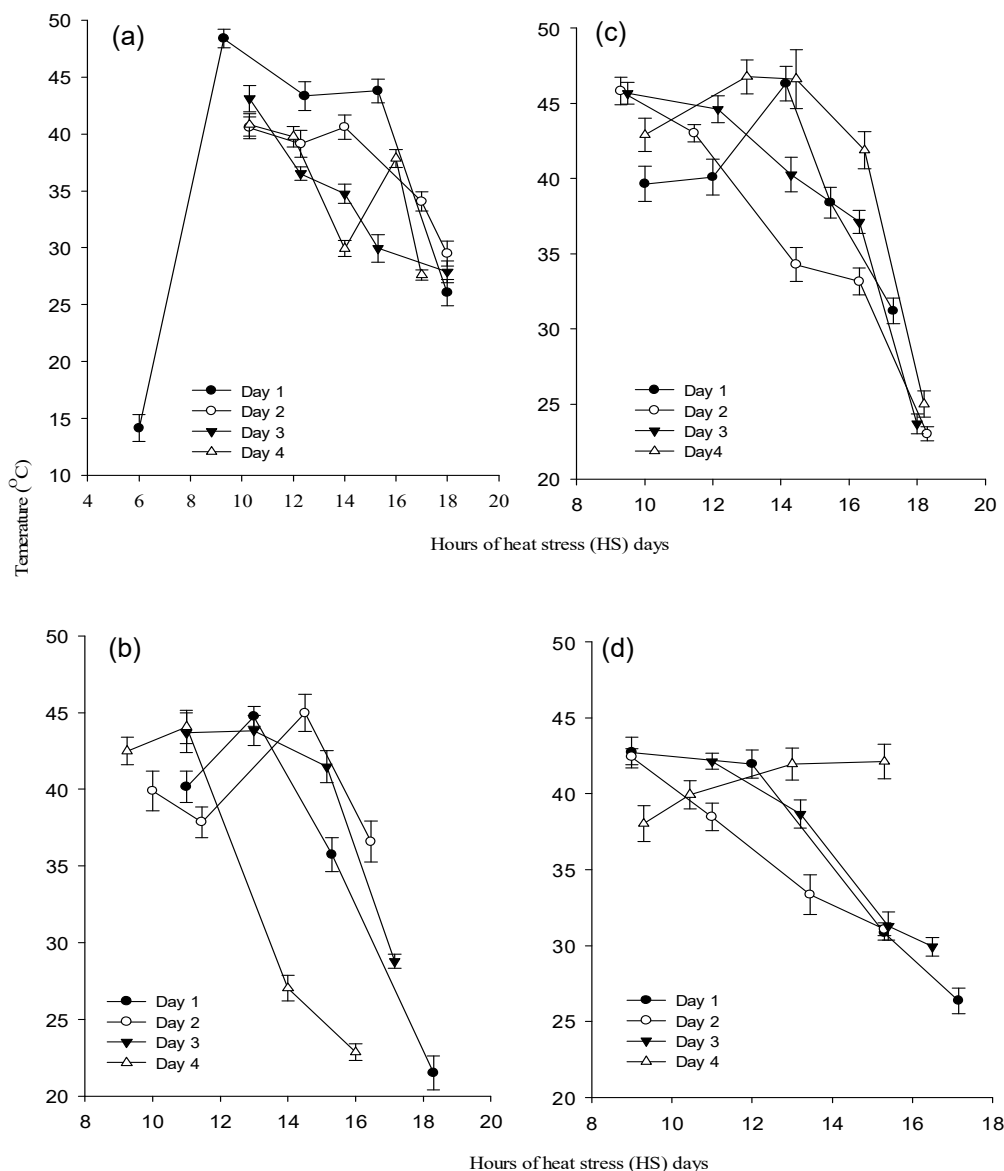
on Nov. 30, 2017, and Nov. 10, 2018, at Agronomy Research Farm, the University of Agriculture, Peshawar with the recommended rate ( $100 \text{ ha}^{-1}$ ) for all cultivars. Sowing was done with the help of a hand drill in 6 rows, 5 m long and 30 cm apart. The field was prepared as recommended for wheat sowing. Fertilizers including urea (46% N), single superphosphate (20%  $\text{P}_2\text{O}_5$ ), and murate of potash (60% K) were added during seedbed preparation to provide fixed amounts of  $120 \text{ kg ha}^{-1}$  N,  $80 \text{ kg ha}^{-1}$  P, and  $50 \text{ kg ha}^{-1}$  K, respectively. Nitrogen was applied in two equal splits at sowing and 50 days after sowing (DAS). Four high yielding wheat cultivars (Pirsabak-2005, Pakhtunkhwa-2015, Pakistan-2013, and DN-84) including three advanced lines (P-2, P-12, and P-18) were exposed to heat stress (HS) through artificially raising the temperature inside the tents for limited durations (48, 72, and 96 h) effective at the onset of anthesis stage. One control treatment with normal growth (no HS) was also included.

### Heat stress (HS)

Temporal heat stress (HS) was established by raising the inside plastic tents temperature for the plant growth effective from the crop anthesis stage. Four high-yielding wheat cultivars such as Pirsabak-2005, Pakhtunkhwa-2015, Pakistan-2013, and the DN-84 (as a check) along with three selected lines (P-2, P-12, and P-18) were evaluated. All 4 cultivars including the P-12 line were uniform in anthesis except lines (P-2 and P-18), which were relatively late to start anthesis and maturity. The pedigree of the check is the Mexico line from CIMMYT (Siddiq et al., 2006). Plants in 2 rows of the limited length in an experimental unit were covered under a plastic tent made over steel rods and 2-ply transparent polyethene sheets for higher HS imposition. An auto-measuring temperature clock (*Humidity/Clock HTC- 01*) was also installed within and outside tents for temperature. On completion of HS for the defined duration, plastic sheets were removed and the crop was allowed to grow as a normal crop for the rest of the growth period. Control plots were not treated with HS for the entire crop growth duration in the field.

The temperatures inside and outside the tents were periodically recorded four times a day during the HS durations. All readings were averaged for a single mean. Mean differences of all the readings within tents from outside temperature were  $+3.08$ ,  $+4.04$ , and  $+4.41$  °C in the year 2017–18 and  $+2.42$ ,  $+3.18$ , and  $+3.53$  °C in the year 2018–19 for all cultivars (Pirsabak-2005, Pakhtunkhwa-2015, Pakistan-2013, DN 84, and P-12) and  $+7.16$ ,  $+7.23$  and  $+7.37$  °C for the year 2017–18 and  $+5.47$ ,  $+5.91$  and  $+6.25$  °C for the year 2018–19 for the relatively late anthesis cultivars (P-2 & P18) for the duration of 48, 72, and 96 h HS, respectively. Differences in temperatures inside from the outside within the plastic tent vary for the different hours of the HS durations and are shown in Fig. 2. The absolute mean temperatures for 48, 72, and 96 h during the HS within the tents were  $36.0 \pm 10.2$ ,  $35.4 \pm 8.8$  and  $35.4 \pm 8.1$  (2017–18),  $37.7 \pm 7.38$ ,  $38.3 \pm 7.04$ , and  $37.2 \pm 7.93$  (2018–19) for all cultivars,  $37.5 \pm 7.21$ ,  $37.8 \pm 7.48$ , and  $38.5 \pm 7.74$  (2017–18), and  $35.9 \pm 6.31$ ,  $35.8 \pm 5.90$  and  $37.0 \pm 5.54$  (2018–19) for the late anthesis cultivars during HS of 48, 72, and 96 h, respectively.

All other cultural operations such as irrigation, fungicide, weeding, and nutrients, etc. were applied uniformly as recommended for the wheat crop in the area. Harvesting was done manually at the crop maturity on May 4, 2018, for normal cultivars and May 10, 2018, for late-maturing advanced lines in 2017–18, and May 5, 2019, for normal and May 13, 2019, for relatively advanced lines in 2018–19.



**Figure 2.** Periodic temperature change observed during heat stress (HS) from inside and outside the plastic tents over plants in the field. Figures (a and b) for cultivars (Pirsabak-2005, Pakhtunkhuwa-2015, Pakistan-2013, DN-84 and P-12) and windows (c and d) for late anthesis cultivars (P-2 & P-18) during 2017–18 2018–19, respectively.

### Sampling and measurements

Days to anthesis were counted from sowing to 80% tillers in an experimental unit that reached the stage of anthesis. Maturity was counted from sowing to the stage when peduncle turned yellow and grain in spikes was hard. Ten spikes from an experimental unit were randomly selected and preserved. Data of spike length (cm), spike weight (g), grain weight (g), and grain number were recorded in the lab after properly drying the

samples. To record the above-ground biomass and yield, two rows of one-meter length in an experimental unit were harvested, bundled, and sun-dried for 10 days. Biomass was weighed and threshed using a mini-lab thresher. Both biomass and grain yield were subsequently adjusted with samples taken and oven-dry in a forced circulating hot air oven for about 46 h at 70 °C. Grains were separately weighed for each plot and expressed in kg ha<sup>-1</sup>. Harvest index (HI) was determined as the ratio of grain to biomass. Data were statistically analyzed using the Fisher's analysis of variance technique and the mean found significant ( $p < 0.05$ ) were separated using the least significant difference (*LSD*) test (Steel et al., 1997).

## RESULTS AND DISCUSSION

### Days to anthesis and maturity

Days to anthesis were significantly affected by different cultivars (C; Table 1).

**Table 1.** Days to anthesis and -maturity of wheat cultivars as influenced by the heat stress durations effective from anthesis stage of the crop growth

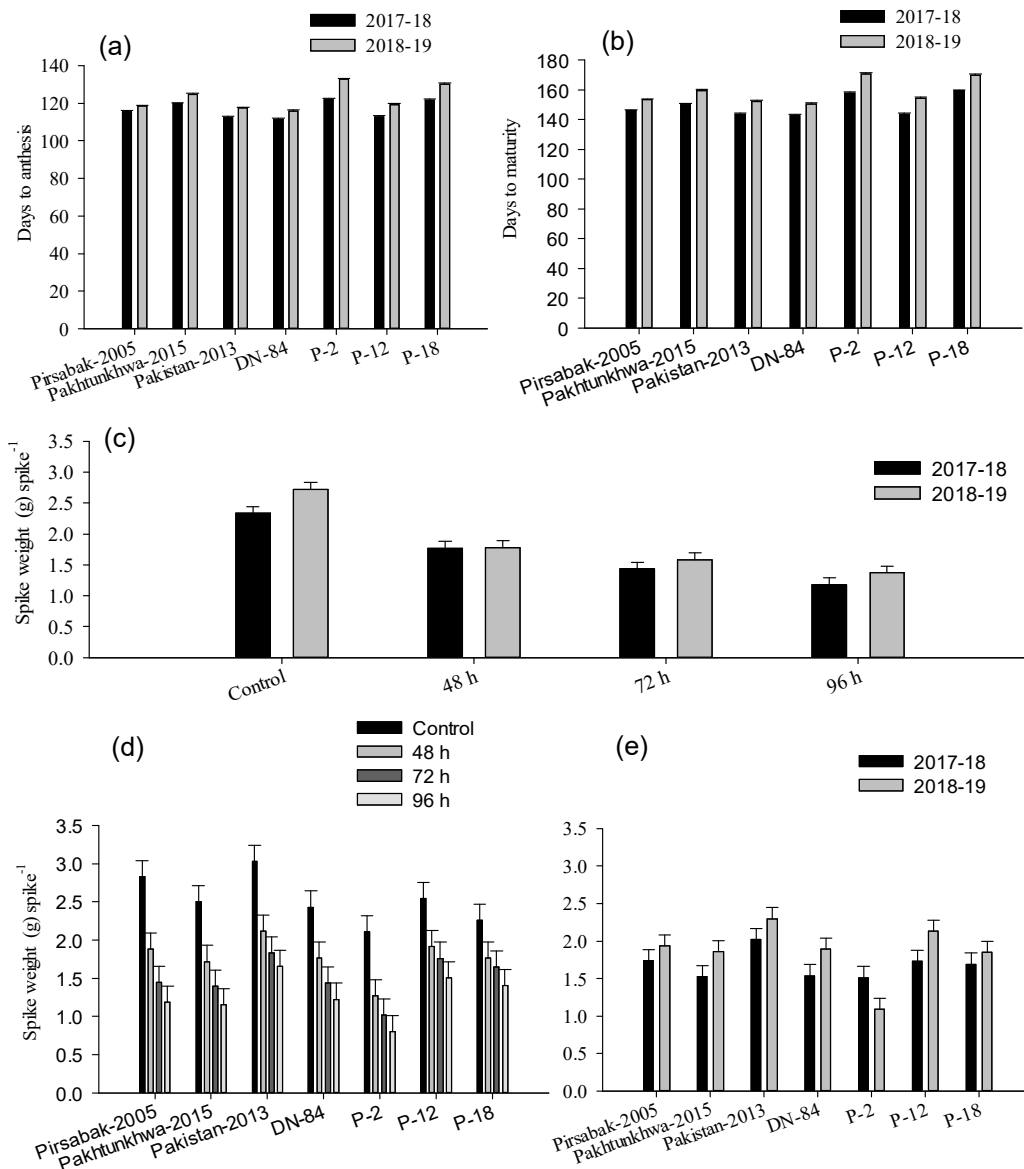
Cultivars (C)	Days to anthesis			Days to maturity		
	2017–18	2018–19	Mean	2017–18	2018–19	Mean
Pirsabak-2005	115.3	118.3	116.8 d	146.0	153.3	149.7 c
Pakhtunkhwa-2015	119.7	124.7	122.2 c	150.0	159.7	154.8 b
Pakistan-2013	112.3	117.3	114.8 f	143.7	152.3	148.0 e
DN-84	111.3	115.7	113.5 g	142.7	150.7	146.7 f
P-2 (Line)	122.0	132.7	127.3 a	157.7	170.7	164.2 a
P-12 (Line)	112.7	119.3	116.0 e	143.7	154.3	149.0 d
P-18 (Line)	121.7	130.0	125.8 b	159.3	170.0	164.7 a
<i>LSD</i> (0.05) for C	0.4	0.7	0.4	0.6	0.9	0.5
Heat stress (HS)						
Control	116.4	122.6	119.5	149.0	158.7	153.9
48 h	116.4	122.6	119.5	149.0	158.7	153.9
72 h	116.4	122.6	119.5	149.0	158.7	153.9
96 h	116.4	122.6	119.5	149.0	158.7	153.9
<i>LSD</i> (0.05) for HS	NS	NS	NS	NS	NS	NS
Year mean	116.4 b	122.6 a	**	149.0	158.7	**
Level of significance ( $p < 0.05$ ) for treatment interaction						
HS x Y	-	-	ns	-	-	ns
C x HS	-	-	ns	-	-	ns
C x Y	-	-	**	-	-	**
C x HS x Y	-	-	ns	-	-	ns

Means followed by different letters within a category of treatments are statistically dissimilar using the least significant difference (*LSD*) test ( $p < 0.05$ );

\* and \*\* represents the significance at ( $p < 0.05$ ) and ( $p < 0.01$ ) probability, NS = Non-significance.

The average across the years showed the maximum days to anthesis for P-2, followed by P-18, Pakhtunkhwa-2015, Pirsabak-2005, P-12, and Pakistan-2013. Minimum days to anthesis were observed for DN-84. Cultivars differed in anthesis due to the growth cycle (Cossani & Reynolds, 2015). In contrast, days to anthesis did not differ from control to heat stress (HS) imposed for about 48, 72, or 96 h. Days to anthesis were greater in the year 2018–19. It might be due to that crop in year 2017–18 was planted

late and cumulative temperatures of growth were greater in year 2017–18 than 2018–19. It needs to be clarified here that temporary plastic tents made over the crop fully covering it, have subsequently increased the humidity within tents, which contrary to HS promoted rust infection on the plants. To avoid this high humidity within tents, in 2018–19 plastic length of the tents was restricted about 25cm above the ground surface over the plants. Interaction (Y x C) revealed a marked change in days to anthesis in all cultivars with greater magnitude in 2018–19 (Fig. 3, a).



**Figure 3.** Interactions of treatments (a) cultivars x years for days to anthesis (b) cultivars x years for days to maturity (c) heat stress x years (d) cultivars x heat stress (e) cultivars x years for weight (g) spike<sup>-1</sup> of the cultivars.

Days to maturity showed significant changes for cultivars (Table 1). On two years' averages, the maximum days to maturity were recorded for P-2, which was statistically similar to P-18, followed by Pakhtunkhwa-2015, Pirsabak-2005, P-12, and Pakistan-2013. Minimum days to maturity were noted for cultivar DN-84. Changes in days to maturity of cultivars are based on their genetic differences as reported earlier (Sikder, 2009; Bhattarai et al., 2017). They observed that different cultivars of the same species differed in days to maturity within a similar climate. Moreover, changes in seed size make them different to imbibe and hence to emerged. This created differences of about 1–4 days irrespective of the same planting date. Days to maturity did not differ from control to HS of any duration. Days to maturity were higher in 2018–19, which might be due to changes in mean daily temperature of duration between seasons and also due to timely planting of crop unlike 2017–18, where sowing was delayed due to heavy rains. Treatment interaction (Y x C) showed significant changes in days to maturity among the cultivars with markedly more days were observed in 2018–19 (Fig. 3, b).

### **Spike weight**

A significant difference was found in spike weight ( $\text{g spike}^{-1}$ ) for cultivars and HS (Table 2). On two years averages, the spike weight was markedly higher in Pakistan-2013, followed by P-12 with similar ( $p < 0.05$ ) in Pirsabak-2005. The lowest spike weight was noted in P-2. Philipp et al. (2018) observed differences in spike weight of the different cultivars, which was due to changes in grain number, grain sizes, and grain weight. Spike weight was reduced from control to the imposing HS for 48, 72, and 96 h. A similar finding of the reduction in spike weight under HS was observed by Semenov et al. (2014). They explained that spike weight associates with HS, as a decline in fertile spikelet was noted, which resulted in a decrease in the grain number and their weight. According to them, it was common that grains growth in HS situation resulted in shrivelled and smaller grains with lighter weight. Grain number per spikelet has reduced which decreased grains per spike (Philipp et al., 2018). Spike weight was observed higher in 2018–19, which was due to differences in the climatic conditions of the seasons. Similar changes in yield contributing traits due to variations in the environment have been reported earlier (Sikder, 2009; Nasehzadeh & Ellis (2017).

Interaction (HS x Y) exhibited a reduction in the spike weight in 2017–18, which was observed in comparison with control for any of the HS treatments (Fig. 3, c). This may be due to frequently abrupt changes in the absolute temperature due to unexpected rainfalls at the stage of the crop anthesis, and thereafter, in the grain development stage. The crop was sown late and availed less time to complete its growth cycle hence spike growth followed by grain number and weight were affected upon exposed to HS. Our results are in line with the published literature on the wheat crop (Semenov et al., 2014). They explained that overall the seasonal changes have an adverse effect on grain growth and especially in the early development stages. Interaction (C x HS) was also found significant in spike weight (Fig. 3, d). Spike weight showed a reduction in a linear fashion with extending HS (i.e. 48, 72, and 96 h) duration on crop effective from anthesis when compared with control. Nevertheless, Pakistan-2013, P-12, and P-18 were found relatively better to reduce spike weight in HS. Wheat grain fill duration may be attributed to sink-limiting for sources under the HS. These results are supported by the earlier study (Abdelrahman et al., 2020), explaining that the source-limited condition during the grain development is important to bring a change in spike weight by adversely affecting grain

number and size. Mohammadi (2012) already observed differences among genotypes to maintain higher seed weight, despite passing through HS for a limited duration. However, it should not couple with the crop-sensitive stages of plant growth. The HS effect can be classified as a high level of heat tolerance when there is no significant effect by HS on yield traits. This might be possible that the crop is not at the critical stage of growth and/or the HS is not so severe that adversely affects the yield traits.

Interaction of treatment (C x Y) showed a relatively higher spike weight in all cultivars during 2018–19 except P-2 (Fig. 3, e). The HS was found higher in 2017–18, which might have caused differences in the spike weight of wheat due to surpassing from a critical stage of the crop growth such as early developing grains. A similar severe adverse effect of the HS in fertilization and/or initial grain growth has caused losses to a complete failure of grains in developing spike (Mohammadi, 2012).

### **Grain weight**

Grain weight (g spike<sup>-1</sup>) differed for cultivars and HS (Table 2). On two years averages, Pakistan-2013 showed the highest grain weight, followed by P-12, DN-84, and the lowest grain weight was observed in P-2. Rates of weight losses in the developing grain differed in different cultivars. Cultivar possessing stability in grain weight under HS did not affect but those found sensitive to HS has greatly lost grain weight (Hossain et al., 2013). Grain weight showed marked reduction when compared with the control for every next degree of the imposed HS such as 48, 72, and 96 h, respectively. Heat stress has adversely affected grain growth and development. At the onset of anthesis and/or early grain developing, increasing HS duration has shown almost a linear reduction in the wheat grain size and number. It might be due to adversely affecting the assimilate translocation for grain set, which showed a reduction in grain growth rate and duration (Akter & Islam, 2017). Our results were supported by the findings of Dias & Lidon (2009) who explained that HS, in general, has speed-up the grain-fill rates by curtailing the grain-fill duration, which resulted in lower grain weight. A higher grain weight was noted in 2017–18. The prevailing cumulative temperature has played a significant role in grain growth; therefore, we found differences between the years. Moreover, the time of anthesis for the cultivars differed within seasons and the timing of imposing HS within seasons and cultivars have shown variations in the grain weights.

Interaction (HS x Y) showed higher grain weight in 2018–19 for control treatment and lower for the crop exposed to HS for about 48, 72, and 96 h (Fig. 4, a). Increase HS duration has reduced the translocation of assimilates which outcomes in a gradual reduction in grain weight with extending HS durations on the crop. The HS index was noted higher during 2018–19 as the temperature on imposition of the HS to crop was +35 °C for the maximum of the reading recorded in HS. This might have led to a drop in grain weight and the development of a higher number of smaller shrivelled grains and/or higher empty florets due to pollen abortion. Dias et al. (2008) reported similar results that wheat crops subjected to HS of 31/20 °C in day/night temperatures have shown marked changes in the structure of endosperm cells and aleurone layers, which resulted in the shriveled grains. Treatment interaction (C x HS) also showed significant changes in grain weight for the years (Fig. 4, b). As expected, extended HS duration has resulted a significant loss in grain weight of all cultivars. However, Pakistan-2013 showed relatively a lower reduction in grain weight by extending the HS durations from control to every next level of the HS. This pattern was more or less mimicked for the

other cultivar like P-12. The formation and translocation of assimilates reduced in the prolonged HS and/or extending its duration, hence all cultivars have shown an adverse effect on grain weight leading to smaller grain and low yield under HS (Abdelrahman et al., 2020). Thus, extending HS duration at any critical stage of the plant growth has resulted in significant loss to complete failure of grain growth.

**Table 2.** Spike weight and grain weight (g) spike<sup>-1</sup> of wheat cultivars as affected by heat stress duration effective from anthesis stage of the crop growth

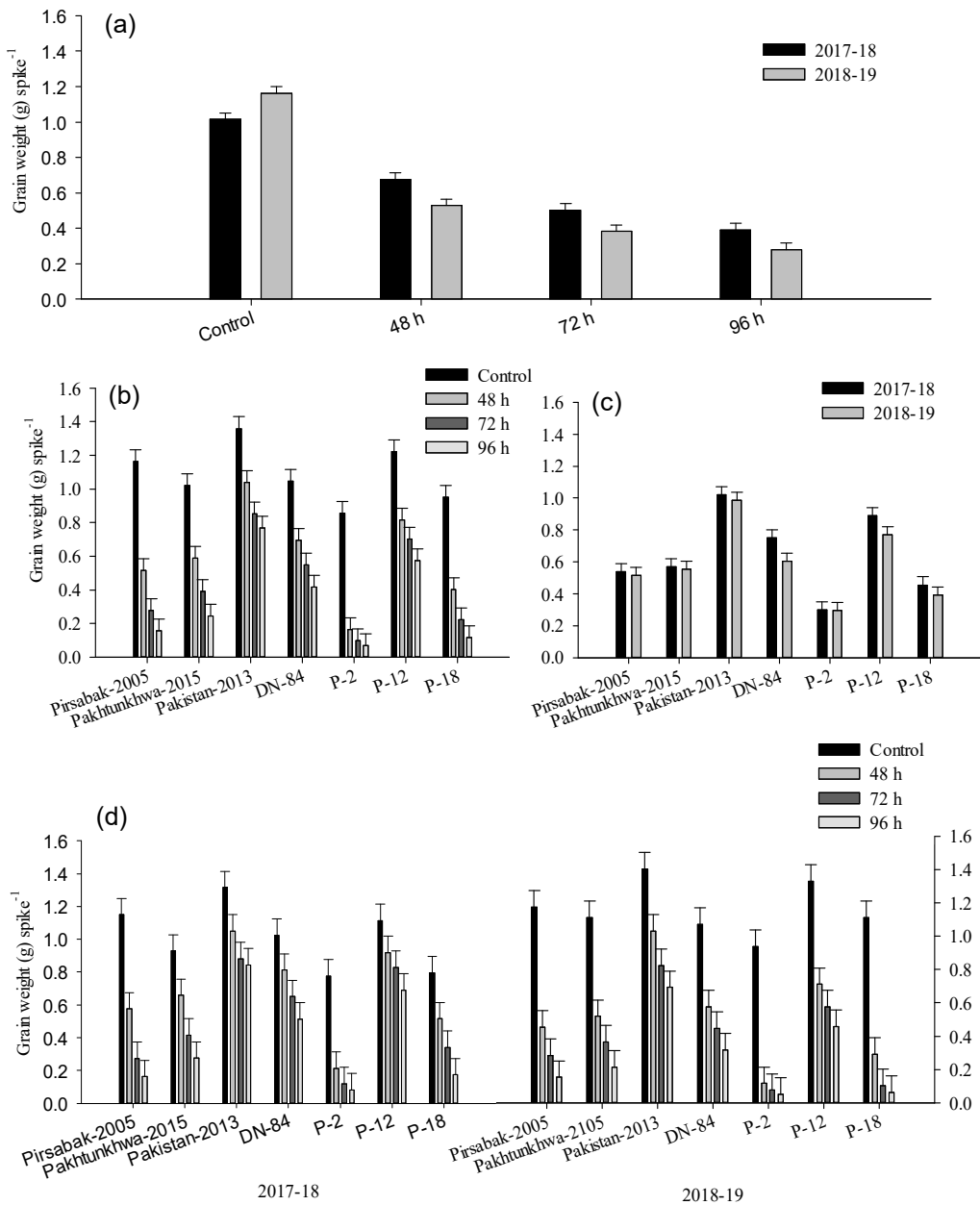
Cultivars (C)	Spike weight (g) spike <sup>-1</sup>			Grain weight (g) spike <sup>-1</sup>		
	2017–18	2018–19	Mean	2017–18	2018–19	Mean
Pirsabak-2005	1.74	1.94	1.84 bc	0.54	0.52	0.53 d
Pakhtunkhwa-2015	1.53	1.86	1.69 d	0.57	0.55	0.56 d
Pakistan-2013	2.02	2.30	2.16 a	1.02	0.99	1.01 a
DN-84	1.54	1.90	1.72 d	0.75	0.60	0.68 c
P-2 (Line)	1.51	1.09	1.30 e	0.30	0.30	0.30 f
P-12 (Line)	1.72	2.13	1.93 b	0.89	0.77	0.83 b
P-18 (Line)	1.69	1.85	1.77 cd	0.46	0.39	0.42 e
<i>LSD</i> (0.05) for C	0.15	0.15	0.11	0.06	0.05	0.04
Heat Stress (HS)						
Control	2.34	2.72	2.53 a	1.02	1.16	1.09 a
48 h	1.77	1.79	1.78 b	0.68	0.53	0.60 b
72 h	1.43	1.58	1.51 c	0.50	0.38	0.44 c
96 h	1.18	1.37	1.28 d	0.39	0.28	0.33 d
<i>LSD</i> (0.05) for HS	0.12	0.11	0.08	0.04	0.03	0.03
Year mean	1.68	1.86	**	0.65	0.59	*
Level of significance ( $p < 0.05$ ) for treatment interaction						
HS x Y	-	-	**	-	-	**
C x HS	NS	**	**	**	**	**
C x Y	-	-	**	-	-	**
C x HS x Y	-	-	NS	-	-	**

Means followed by different letters within a category of treatments are statistically dissimilar using the least significant difference (*LSD*) test ( $p < 0.05$ );

\* and \*\* represents the significance at ( $p < 0.05$ ) and ( $p < 0.01$ ) probability, NS = Non-significance.

Interaction of treatments (C x Y) showed the same trend for cultivars, with higher grain weight in 2017–18 but a relatively marked variations for DN-84 and P-12 between seasons (Fig. 4, c). The relative absolute temperature in 2018–19 at the anthesis stage of the wheat crop was quite higher than 2017–18, and hence HS inside plastic tents were severe, which has negatively affected the grain growth due to disruption of the photosynthetic machinery in the top leaves particularly the flag leaf that resulted in partially filled florets with fewer grains and hence reduced the grain size and grain weight in most cultivars. Three-way interaction (C x HS x Y) also showed a marked reduction in grain weight of the cultivars by extending HS durations in both years with higher reductions observed for 2018–19 (Fig. 4, d). Pakistan-2013 and P-12 were found relatively stable to resist the imposed HS, however, P-2 was found more susceptible. It has been explained earlier that HS has adversely affected the grain formation in florets and hence the growth (Semenov et al., 2014). Imposed HS in 2018–19 was relatively stronger in intensity and had shown marked variations in wheat grain weight.





**Figure 4.** Interactions of treatment (a) heat stress x year, (b) cultivars x heat stress, (c) cultivars x year, (d) cultivars x heat stress x year for grain weight (g) spike<sup>-1</sup> of cultivars.

### Grain number

Grain number (spike<sup>-1</sup>) exhibited marked variations in wheat cultivars and HS (Table 3). The higher numbers were observed in Pakistan-2013, followed by P-12 and DN-84 with non-significant changes. The lowest grain number was noted in P-2. It has been confirmed that grain number reduced with HS but varied among wheat cultivars. Plants treated with HS have shown a reduction in the grain number (Lukac et al., 2012;

Mazurenko et al., 2020), whereas, cultivars did differ to stand with HS. A temperature of +20 °C, at the time of anthesis, has accelerated spike growth which has reduced the grain number and hence resulted in a limited spikelet size (Semenov, 2009). Grain number has shown a reduction in all wheat cultivars with increment in HS from control to every next stage such as 48, 72, and 96 h, which are in line with the findings of Anjum et al. (2008). They reported that high temperature at anthesis is harmful to pollen survival. It caused pollen sterility and hence limited with grain number. The difference in grain number of the cultivars is obvious in the rate of sterility in florets when the temperature exceeds +30 °C. The rates of sterility may differ within cultivars due to differences in the timing of their anthesis (Kumar et al., 2020). Both structure and function of anthers are poorly affected under the mild HS and severely when HS undergoes a prolonged duration of +3-days at the critical growth stage of the crop like anthesis or grain development (Hedhly et al., 2009). Grains number did not show any statistical change between the years of this study.

**Table 3.** Grain number spike-1 and grain yield (kg ha<sup>-1</sup>) of wheat cultivars as affected by heat stress duration at anthesis stage of the crop growth

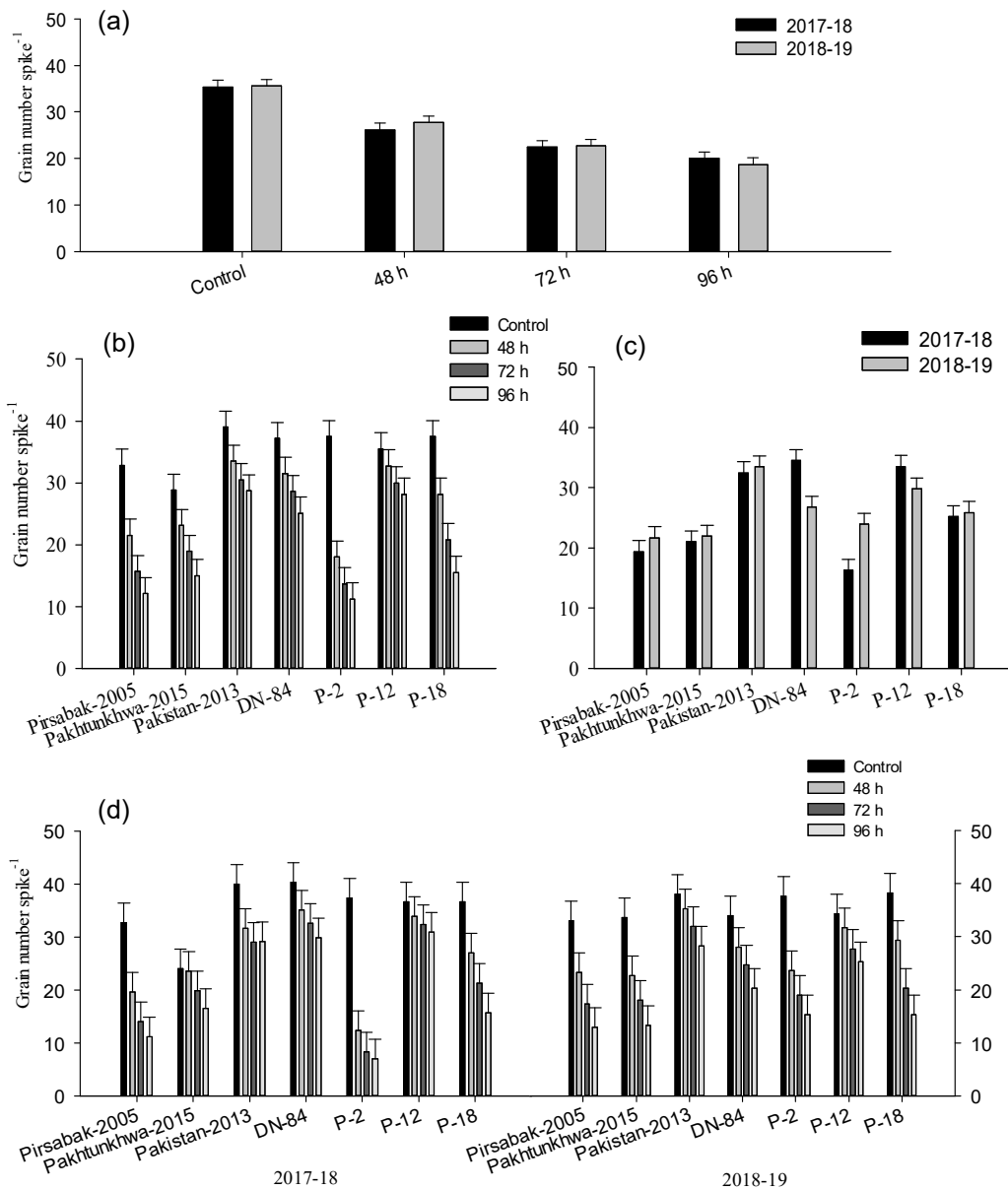
Cultivars (C)	Grain number spike <sup>-1</sup>			Grain yield (kg ha <sup>-1</sup> )		
	2017–18	2018–19	Mean	2017–18	2018–19	Mean
Pirsabak-2005	19.37	21.67	20.52 de	1,489	1,481	1,484 d
Pakhtunkhwa-2015	21.00	21.92	21.46 d	1,522	1,468	1,495 d
Pakistan-2013	32.45	33.42	32.93 a	2,907	2,848	2,878 a
DN-84	34.47	26.75	30.61 b	2,039	1,797	1,918 c
P-2 (Line)	16.27	23.92	20.09 e	813	796	805 f
P-12 (Line)	33.45	29.75	31.60 b	2,439	2,308	2,373 b
P-18 (Line)	25.17	25.82	25.49 c	1,268	1,037	1,153 e
<i>LSD</i> (0.05) for C	2.17	1.49	1.30	170.1	113.6	101.1
Heat stress (HS)						
Control	35.38	35.56	35.47 a	2,885	3,303	3,094 a
48 h	26.16	27.71	26.94 b	1,870	1,562	1,716 b
72 h	22.5	22.71	22.60 c	1,351	1,059	1,205 c
96 h	20.06	18.71	19.39 d	1,024	0.781	0.902 d
<i>LSD</i> (0.05) for HS	1.64	1.13	0.99	128.60	86.9	76.5
Year mean	26.0	26.2	NS	1,782	1,676	*
Level of significance ( $p < 0.05$ ) for treatment interaction						
HS x Y	-	-	*	-	-	**
C x HS	**	**	**	**	**	**
C x Y	-	-	**	-	-	ns
C x HS x Y	-	-	**	-	-	ns

Means followed by different letters within a category of treatments are statistically dissimilar using the least significant difference (*LSD*) test ( $p < 0.05$ );

\* and \*\* represents the significance at ( $p < 0.05$ ) and ( $p < 0.01$ ) probability; NS = Non-significance.

Interaction (HS x Y) showed marked reductions in grain number during 2017–18 at 48 h HS but no changes thereafter for extending HS to 72 h. Control treatments did not show any changes in grain number between the years (Fig. 5, a). A significant difference between the years was noticed in prevailing temperature at anthesis and hence has caused variations for HS. Similarly, cultivars and various HS durations showed a clear difference

for grain number in both years. The interaction (C x HS) also exhibited a marked reduction in the grain number of cultivars exposed to HS but at different rates (Fig. 5, b).



**Figure 5.** Interaction of treatments (a) heat stress x year, (b) cultivars x heat stress, (c) cultivars x years, (d) cultivars x heat stress x year for grain number spike<sup>-1</sup> of cultivars.

Grain number per spike decreased with the HS but, was almost at a stable rate for the cultivar Pakistan-2013, P-12, and DN-84 as compared to the rest of the cultivars. It showed that cultivars were stable to resist HS at anthesis. The pollen viability is an important factor not to be affected with HS within cultivars (Semenov et al., 2014). Otherwise, a

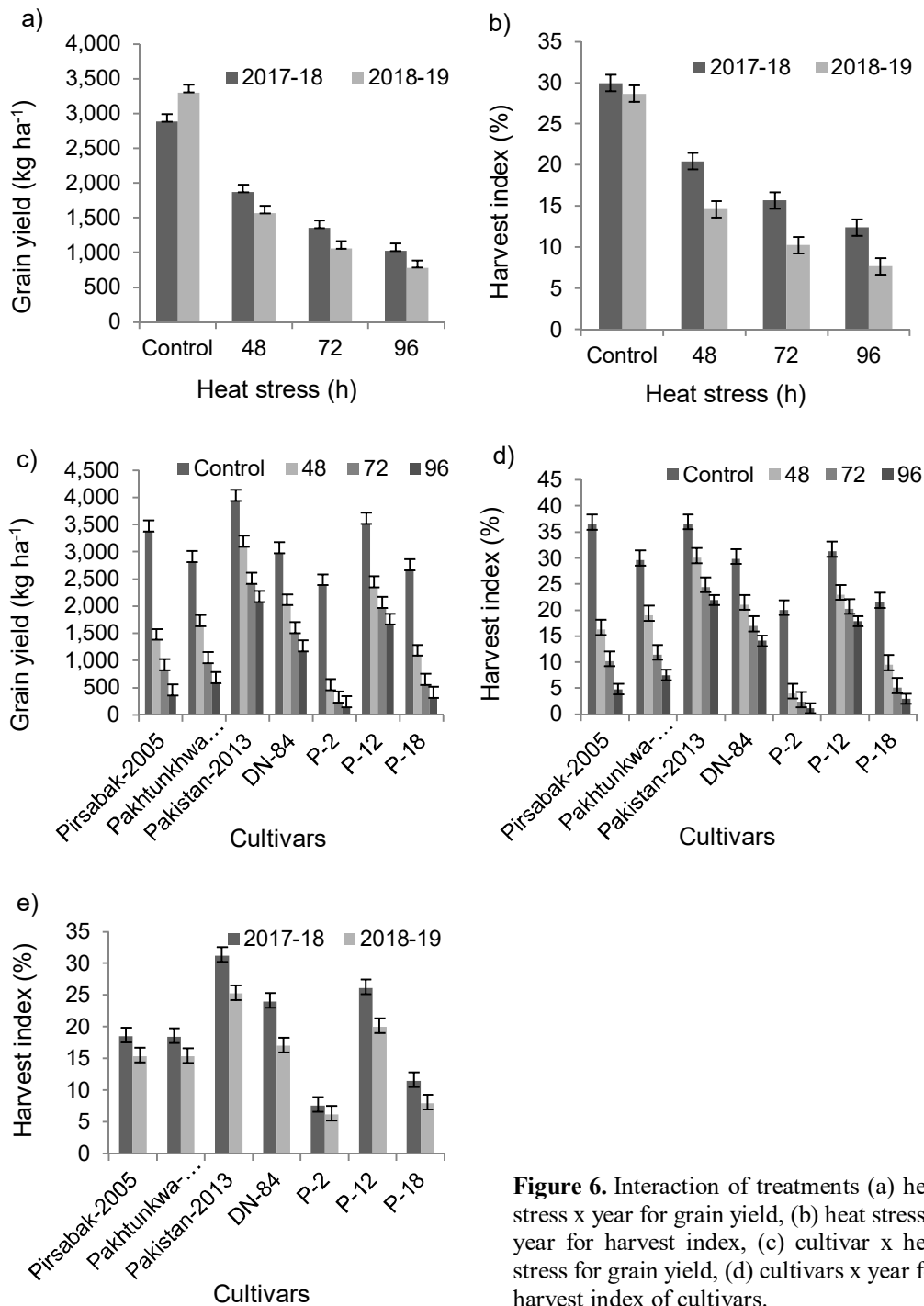
decrease in grain number in wheat spike may accelerate to a complete failure of the grains (Kumar et al., 2020). Relatively faster variations in grain number within spikes exposed to HS from control have shown the rate of susceptibility of the cultivar facing HS at the crop critical growth stages. The interaction (C x Y) has revealed higher grain numbers within the spikes of all cultivars except DN-84 and P-12 in 2018–19 (Fig. 5, c). Cultivars did vary in grain number within spikes by prevailing temperature and its critical stage of the growth when plants undergo anthesis or grain development (Moshatati et al., 2017). The interaction (C x HS x Y) showed a gradual reduction in grain number of the cultivars but with different rates between seasons (Fig. 5, d). An unusual variation in the grain number was noticed in wheat cultivar Pakhtunkhwa-2015 and P-2, which reflects their susceptibility to HS exposed at the anthesis stage of the crop growth. Similar variations in grain number within wheat spikes under temporarily elevated HS have been reported by Mohammadi (2012) which were due to loss in pollen fertility (Bhattarai et al., 2017).

### **Grain yield**

As observed from the yield traits, grain yield ( $\text{kg ha}^{-1}$ ) exhibited changes within cultivars and HS (Table 3). Grain yield was reported the highest for Pakistan-2013, followed by P-12, DN-84, and Pakhtunkhwa-2015. The lowest grain yield was recorded in P-2. The HS starting from the anthesis stage of the crop growth which reflected marked reductions in the yield. It was due to the limited duration of the resource utilization for grain fill periods and their accumulation as grain within spikes (Dias & Lidon, 2009; Yin et al., 2009). A higher yield of wheat cultivars might be due to a relative delay in the senescence phase of the cultivar with a relatively higher grain filling rate under the HS. It has been observed that assimilates partitioning is limited in the adverse growth conditions for grains development (Farooq et al., 2011). Grain yield showed a reduction when compared with control to any HS imposed on plants for 48, 72, and 96 h. Marked reduction in yield observed with exposing plants to a temperature above 24 °C at the crop anthesis stage (Prasad & Djanaguiraman, 2014), which were due to a significant effect on yield contributing traits of the plants. The anthesis stage is one of the most critical factors of the grain yield. From anthesis to grain development stages, the climate photoperiod expands, and the daily temperature increases relatively at a very faster rate for the next few days in comparison with the previous growth duration such as stem elongation. This showed an adverse effect on grain number and weight which resulted in a marked reduction of grain yield (Nasehzadeh & Ellis, 2017; Bergkamp et al., 2018). Grain yield was observed higher in 2017–18 as mean temperatures of two years differed and HS was probably found less fatal in 2017–18 which resulted in a higher yield. The absolute temperature in 2017–18 was comparatively low at the anthesis stage, which might have decreased the severity of HS effects and therefore have better yield.

Interaction (HS x Year) reflected a better yield of the control treatment in 2018–19. Nonetheless, a decrease in yield was observed with imposing HS on wheat, which raised the surrounding temperature in a plastic tent and it might become fatal for the pollen sterility as well as assimilates accumulation in grains by extending the HS duration (Fig. 6, a). Grain yield in 2018–19 was reported higher despite the higher absolute temperature. The reason could be that crops were infected with rust due to HS and the rainy season in the month of April-May which resulting higher variations

in yield under controlled conditions in 2017–18. Treatments interaction (C x HS) exhibited a significant change in grain yield across average of the two years (Fig. 6, c).



**Figure 6.** Interaction of treatments (a) heat stress x year for grain yield, (b) heat stress x year for harvest index, (c) cultivar x heat stress for grain yield, (d) cultivars x year for harvest index of cultivars.

Grain yield markedly reduced for wheat cultivars with extending the HS duration with a relatively higher reduction in lines P-2 and P-18 than the rest of the cultivars. Each cultivar responded differently to changes in HS which depending on its potential and coinciding with the growth. Similar findings have been already observed by Nasehzadeh & Ellis (2017). According to them, the susceptible cultivars showed greater losses in yield when exposed to HS by adversely affecting their pollen fertility and decreasing their rate of assimilates accumulation in grains. Temperature changes have been noted within years at the crop anthesis stages, which have shown differences in the yield of the cultivars. The cumulative effect of the HS corresponds to critical stages of growth of the cultivar which has created mild to marked variations in the cultivars subjected to HS between years. The higher ambient temperature is directly related to HS. It is also obvious that as the HS duration prolonged the adverse effect on yield would be greater.

### **Biomass yield**

Above-ground biomass ( $\text{kg ha}^{-1}$ ) also reflected a significant variation for wheat cultivars and HS treatment (Table 4). The highest biomass was recorded in the advanced line P-18, which was statistically similar with the line P-2, followed by P-12, and Pakistan-2013. Our findings are in line with the published reports (Banerjee & Krishnan, 2015; Rakutko et al., 2020). They observed differences in biomass among the cultivars. It is estimated that a reduction of 23.5% biomass is expected when plants are subjected to HS at the start of anthesis, which limits the growth of flag leaf within HS conditions (Bergkamp et al., 2018). The plant biomass decreased with increasing HS as compared to the control for every next level of the HS such as 48, 72, and 96 h but varying greatly among cultivars. Imposing HS (+40 °C) may have also lead to scorching on leaves and sunburn, reducing branches, twigs, and stems elongation, starting early senescence and greater leaf abscission, which reflected significant losses in plant biomass (Moshatati et al., 2017). Biomass was recorded higher in 2018–19, which might be due to the reason that the crop had enjoyed the optimum growth period and hence has gathered the maximum assimilates to produce higher biomass. However, uneven changes at maturity stages of the cultivars were noted between years with differences for the same cultivar in 2018–19. Rust infestation has also damaged the plants within tents in 2017–18 due to higher humidity created by the fully covered tents. However, all other possible treatment combinations for the interactions were found non-significant in yielding the above-ground biomass production.

### **Harvest index**

Harvest index (%), which is the ratio of grain yield to above-ground biomass, was significant for the cultivars and HS treatment (Table 4). Better harvest index was derived for the cultivar Pakistan-2013, followed by P-12, and DN-84. Increased HS at the start of the crop anthesis stage has shown marked reductions in grain filling durations within the cultivars, and has reflected a lower grain as well as biomass yield followed by a lower harvest index. Prasad & Djanaguiraman (2014) also observed that higher temperature (+24 °C) around the plant anthesis stages may lead to floret sterility, which resulted in a lower grain yield than total biomass and has shown a reduction in harvest indices. Harvest index consistently decreased with extending HS duration from the control treatment to any HS duration. Harvest index is directly related to grain production, which was reduced under the HS due to declining both grain weight and the grain number.

Similar results were also published by Prasad et al. (2011). They reported that the imposition of short duration HS for a limited period has adversely affected grains as compared to the total above-ground biomass, and has shown a reduction in harvest index. A higher harvest index was noted in 2017–18 as the absolute temperature was different between years and was relatively stable at the time of the crop anthesis and early grain filling in 2017–18. Plants have responded with an effect on the transportation of assimilates from source to sink, which might have resulted in more filled grains and a higher harvest index. This is clearly explained by Reynolds et al. (2005) and also by Farooq et al. (2011). Interaction (HS x Y) also reflected a better harvest index in 2017–18 for control as compared to the rest of the treatments (Fig. 6, b). The intensity of temperature during grain development is the main factor affecting grain weight.

**Table 4.** Biomass yield (kg ha<sup>-1</sup>) and harvest index (%) of wheat cultivars as affected by heat stress effective from the anthesis stage of the crop growth

Cultivars (C)	Biomass yield (kg ha <sup>-1</sup> )			Harvest index (%)		
	2017–18	2018–19	Mean	2017–18	2018–19	Mean
Pirsabak-2005	7,746	9,199	8,472 d	18.51	15.36	16.93 d
Pakhtunkhwa-2015	8,077	9,177	8,627 d	18.41	15.33	16.87 d
Pakistan-2013	9,256	11,176	102,156 b	31.2	25.24	28.22 a
DN-84	8,407	10,460	9,434 c	23.97	17.00	20.49 c
P-2	10,606	12,174	11,390 a	7.57	6.18	6.88 f
P-12	9,246	11,322	10,284 b	26.14	20.04	23.09 b
P-18	10,787	12,548	11,668 a	11.5	7.94	9.72 e
<i>LSD</i> (0.05) for C	631.1	340.5	354.5	2.10	1.02	0.93
Heat stress (HS)						
Control	9,823	11,683	10,753 a	29.93	28.67	29.30 a
48 h	9,448	10,977	10,212 b	20.45	14.6	17.53 b
72 h	8,765	10,582	9,673 c	15.68	10.23	12.95 c
96 h	8,606	10,218	9,412 c	12.4	7.69	10.04 d
<i>LSD</i> (0.05) for HS	477.1	257.4	268.0	1.59	0.77	0.71
Year mean	9,161	10,865	***	19.61 a	15.30 b	**
Level of significance ( $p < 0.05$ ) for treatment interaction						
HS x Y	-	-	ns	-	-	**
C x HS	ns	ns	ns	**	**	**
C x Y	-	-	ns	-	-	**
C x HS x Y	-	-	ns	-	-	ns

Means followed by different letters within a category of treatments are statistically dissimilar using the least significant difference (*LSD*) test ( $p < 0.05$ ).

\* and \*\* represents the significance at ( $p < 0.05$ ) and ( $p < 0.01$ ) probability, NS = Non-significance.

The temperature in 2018–19 was higher than 2017–18 for all HS durations and hence has shown markedly adverse effects on the yield traits, which resulted in a decrease in harvest index. A lower grain yield was reported in 2018–19, followed by a lower harvest index compared to 2017–18. Treatment interaction (C x HS) exhibited a significant reduction in harvest index of cultivars subjected to the HS at a critical stage of the plant growth, but with varying rates due to resistances of the cultivars for pollen fertility and/or timing of crop anthesis during the day temperature (Fig. 6, d). Harvest index markedly reduced with the imposition of HS in P-2 and P-18 relative to the rest of the cultivars in this study as their grain yield was also lower. Similar differences within cultivars in the

harvest index on exposing the crop to HS at the time of its growth and development were also noted by Gupta et al. (2015). Gibson & Paulsen (1999) also reported marked changes in the crop harvest index on exposure to HS (+20 °C) from anthesis to maturity. The crop harvest index was decreased at a faster rate on facing HS during the growth and development, subject to the climate and crop growth stage, which resulted in a faster declining the grain yield than the biomass (Gupta et al., 2015). Grain yield decreased with changes in the number and weight of the developing grains within spikes. This is due to a decrease in the rate of starch synthesis at the grain filling duration (Hogy et al., 2013), hence lost food reserves stored in grains. Interaction (C x Y) reflected a higher harvest index in all cultivars during 2017–18 (Fig. 6, e). The cultivar with better grain yield has shown healthy traits with relatively marked HS in 2018–19 showing a higher harvest index. Heat stress is the main factor affecting grain growth and development and it was observed relatively higher in 2018–19, which adversely affected the growth, yield, and yield traits and finally the harvest index.

## CONCLUSIONS

It is concluded that the period between anthesis to grain filling is the most critical stage of the wheat crop. Plants when undergoes heat stress for a shorter duration during this critical stage of the plant growth, resulted in marked losses in the grain weight (45, 61, and 69%) and grain number (29, 36, and 45%) of spike with extending HS duration from control to 48 h, to 72 h, and thereafter from 72 to 96 h, respectively. This showed a considerable reduction in the grain yield and subsequently increased production cost. Extending the duration of HS during the critical stages of plant growth has resulted in a marked reduction in wheat productivity. However, cultivars differed in yield losses under the imposed HS which shows that potential exists within cultivars for future breeding to make available the best resistant cultivar that could be planted in areas facing adverse weather effects in terms of heat stress on yield losses.

**ACKNOWLEDGMENTS.** The authors acknowledged the partial financial support of the Higher Education Commission (HEC) Islamabad for the completion of the research through funds available in NRP 20-5178. Equal thanks are also extended to the Climate Change Center, the University of Agriculture Peshawar and Inter-Cooperation (IC) project water for livelihood sponsored by the SDC for living expenses of the scholar during her study at the university leading to a Ph.D. degree. Sincere thanks are on record for Mr. Nawab Ali and Gul Roz to help in experimental arrangements.

## REFERENCES

- Abdelrahman, M., Burritt, D.J., Gupta, A., Tsujimoto, H. & Tran, L.S.P. 2020. Heat stress effects on source sink relationships and metabolome dynamics in wheat. *Journal of Experimental Botany* **71**(2), 543–554.
- Akter, N. & Islam, M.R. 2017. Heat stress effects and management in wheat. A review. *Agronomy for sustainable development* **37**(5), 37.
- Anjum, F., Wahid, A., Javed, F. & Arshad, M. 2008. Influence of foliar applied thiourea on flag leaf gas exchange and yield parameters of bread wheat (*Triticum aestivum* L) cultivars under salinity and heat stresses. *International Journal of Agriculture and Biology* **10**(6), 619–626.



- Anjum, S.A., Xie, X.Y., Wang, L.C., Saleem, M.F., Man, C. & Lei, W. 2008. Morphological, physiological and biochemical responses of plants to drought stress. *African journal of agricultural research* **6**(9), 2026–2032.
- Anonymous. 2007. Soil Survey of Pakistan. Land resources inventory and agricultural land use plan of Peshawar district, pp. 102.
- Asseng, S., Ewert, F., Martre, P., Rotter, R.P., Lobell, D.B., Cammarano, D., Kimball, B.A., Ottman, M.J., Wall, G. & White, J.W. 2015. Rising temperatures reduce global wheat production. *Nature climate change* **5**(2), 143–147.
- Asseng, S., Foster, I. & Turner, N.C. 2011. The impact of temperature variability on wheat yields. *Global Change Biology* **17**(2), 997–1012.
- Banerjee, V. & Krishnan, P. 2015. Effect of high temperature stress on biomass partitioning in wheat (*triticum aestivum* L.) at different growth stages. *Journal of Agricultural Physics* **15**(2), 122–126.
- Bergkamp, B., Impa, S., Asebedo, A., Fritz, A. & Jagadish, S.K. 2018. Prominent winter wheat varieties response to post-flowering heat stress under controlled chambers and field based heat tents. *Field Crops Research* **222**, 143–152.
- Bhattarai, R.P., Ojha, B.R., Thapa, D.B., Kharel, R., Ojha, A. & Sapkota, M. 2017. Evaluation of elite spring wheat (*Triticum aestivum* L.) genotypes for yield and yield attributing traits under irrigated condition. *International journal of applied sciences and biotechnology* **5**(2), 194–202.
- Cossani, C.M. & Reynolds, M.P. 2015. Heat stress adaptation in elite lines derived from synthetic hexaploid wheat. *Crop Science* **55**(6), 2719–2735.
- Dias, A. & Lidon, F. 2009. Evaluation of grain filling rate and duration in bread and durum wheat, under heat stress after anthesis. *Journal of Agronomy and Crop Science* **195**(2), 137–147.
- Dias, A.S., Bagulho, A.S. & Lidon, F.C. 2008. Ultrastructure and biochemical traits of bread and durum wheat grains under heat stress. *Brazilian Journal of Plant Physiology* **20**(4), 323–333.
- Farooq, M., Bramley, H., Palta, J.A. & Siddique, K.H. 2011. Heat stress in wheat during reproductive and grain filling phases. *Critical Reviews in Plant Sciences* **30**(6), 491–507.
- Gibson, L. & Paulsen, G. 1999. Yield components of wheat grown under high temperature stress during reproductive growth. *Crop Science* **39**(6), 1841–1846.
- Gupta, N., Agarwal, S., Agarwal, V., Nathawat, N., Gupta, S. & Singh, G. 2013. Effect of short-term heat stress on growth, physiology and antioxidative defence system in wheat seedlings. *Acta Physiologiae Plantarum* **35**(6), 1837–1842.
- Gupta, N., Khan, A., Maheshwari, A., Narayan, S., Chhapola, O., Arora, A. & Singh, G. 2015. Effect of post anthesis high temperature stress on growth, physiology and antioxidative defense mechanisms in contrasting wheat genotypes. *Indian Journal of Plant Physiology* **20**(2), 103–110.
- Hanif, M. & Ali, J. 2014. Climate scenarios 2011–2040 districts Haripur, Swabi, Attock and Chakwal Pakistan. *Study conducted by Climate Change Centre, University of Agriculture, Peshawar*, pp. 27.
- Haque, M.S., Kjaer, K.H., Rosenqvist, E., Sharma, D.K. & Ottosen, C.O. 2014. Heat stress and recovery of photosystem II efficiency in wheat (*Triticum aestivum* L.) cultivars acclimated to different growth temperatures. *Environmental and Experimental Botany* **99**, 1–8.
- Hedhly, A., Hormaza, J.I. & Herrero, M. 2009. Global warming and sexual plant reproduction. *Trends in plant science* **14**(1), 30–36.
- Hogy, P., Poll, C., Marhan, S., Kandeler, E. & Fangmeier, A. 2013. Impacts of temperature increase and change in precipitation pattern on crop yield and yield quality of barley. *Food chemistry* **136**(3–4), 1470–1477.
- Hossain, A., Sarker, M., Saifuzzaman, M., Teixeira da Silva, J., Lozovskaya, M. & Akhter, M. 2013. Evaluation of growth, yield, relative performance and heat susceptibility of eight wheat (*Triticum aestivum* L.) genotypes grown under heat stress. *International Journal of Plant Production* **7**(3), 615–636.
- Khanna-Chopra, R. 2012. Leaf senescence and abiotic stresses share reactive oxygen species-mediated chloroplast degradation. *Protoplasma* **249**(3), 469–481.

- Kosova, K., Vitamvas, P., Prasil, I.T. & Renaut, J. 2011. Plant proteome changes under abiotic stress contribution of proteomics studies to understanding plant stress response. *Journal of proteomics* **74**(8), 1301–1322.
- Kumar, A., Chhaya, R., Singh, V.P. & Singh, L. 2020. Exploitation of heterosis for grain yield and quality traits in wheat. *Journal of Pharmacognosy and Phytochemistry* **9**(2), 1465–1468.
- Lukac, M., Gooding, M.J., Griffiths, S. & Jones, H.E. 2012. Asynchronous flowering and within plant flowering diversity in wheat and the implications for crop resilience to heat. *Annals of botany* **109**(4), 843–850.
- Mazurenko, B., Kalenska, S., Honchar, L. & Novytska, N. 2020. Grain yield response of facultative and winter triticale for late autumn sowing in different weather conditions. *Agronomy Research* **18**(1), 183–193.
- Mohammadi, M. 2012. Effects of kernel weight and source-limitation on wheat grain yield under heat stress. *African Journal of Biotechnology* **11**(12), 2931–2937.
- Moshatati, A., Siadat, S., Alami Saeid, K., Bakhshandeh, A. & Jalal Kamali, M. 2017. The impact of terminal heat stress on yield and heat tolerance of bread wheat. *International Journal of Plant Production* **11**(4), 549–560.
- Nashezadeh, M. & Ellis, R.H. 2017. Wheat seed weight and quality differ temporally in sensitivity to warm or cool conditions during seed development and maturation. *Annals of botany* **120**(3), 479–493.
- Philipp, N., Weichert, H., Bohra, U., Weschke, W., Schulthess, A.W. & Weber, H. 2018. Grain number and grain yield distribution along the spike remain stable despite breeding for high yield in winter wheat. *PLoS One* **13**(10), e0205452.
- Prasad, P., Pisipati, S., Momcilovic, I. & Ristic, Z. 2011. Independent and combined effects of high temperature and drought stress during grain filling on plant yield and chloroplast EF-Tu expression in spring wheat. *Journal of Agronomy and Crop Science* **197**(6), 430–441.
- Prasad, P.V. & Djanaguiraman, M. 2014. Response of floret fertility and individual grain weight of wheat to high temperature stress: sensitive stages and thresholds for temperature and duration. *Functional Plant Biology* **41**(12), 1261–1269.
- Rakutko, S., Avotiņš, A., Berzina, K., Rakutko, E. & Alsina, I. 2020. Radiation use efficiency by tomato transplants grown under extended photoperiod. *Agronomy Research* **18**(S3), 1853–1859.
- Reynolds, M., Pellegrineschi, A. & Skovmand, B. 2005. Sink limitation to yield and biomass: a summary of some investigations in spring wheat. *Annals of Applied Biology* **146**(1), 39–49.
- Semenov, M., Stratonovitch, P., Alghabari, F. & Gooding, M. 2014. Adapting wheat in Europe for climate change. *Journal of Cereal Science* **59**(3), 245–256.
- Semenov, M.A. 2009. Impacts of climate change on wheat in England and Wales. *Journal of the Royal Society Interface* **6**(33), 343–350.
- Siddiq, M., Ahmad, I., Rehman, S. & Ahmad, N. 2006. Pirsabak Barani-05, A New Wheat Variety for Cultivation in. *Asian Journal of Plant Sciences* **5**(3), 566–569.
- Sikder, S. 2009. Accumulated heat unit and phenology of wheat cultivars as influenced by late sowing heat stress condition. *Journal of Agriculture & Rural Development* **7**, 59–64.
- Steel, R.G.D., Torrie, J.H. & Dickey, D.A. 1997. *Principles and procedures of statistics: a biometrical approach*. 3<sup>rd</sup> Edition ed. McGraw-Hill, New York, USA, pp. 352–358.
- Yin, X., Guo, W. & Spiertz, J.H. 2009. A quantitative approach to characterize sink-source relationships during grain filling in contrasting wheat genotypes. *Field Crops Research* **114**(1), 119–126.
- Yu, Q., Li, L., Luo, Q., Eamus, D., Xu, S., Chen, C., Wang, E., Liu, J. & Nielsen, D.C. 2014. Year patterns of climate impact on wheat yields. *International Journal of Climatology* **34**(2), 518–528.
- Zhao, H., Dai, T., Jing, Q., Jiang, D. & Cao, W. 2007. Leaf senescence and grain filling affected by post-anthesis high temperatures in two different wheat cultivars. *Plant Growth Regulation* **51**(2), 149–158.

## **Some mechanisms of winter resistance in apricot flower buds in the period of ecodormancy**

A.M. Golubev\*, N.A. Alyoshina, V.E. Anfalov, A.A. Kulikov and  
V.S. Vdovenko

Laboratory of Molecular Genetic Selection of Fruit Crops, Federal State Budgetary Scientific Institution "Federal Agrarian Scientific Center of Agriculture of The South-East" (FSBSI "FASCA South-East". 7 Tulaikov Str., RU410010 Saratov, Russia  
\*Correspondence: biotechnoalgot@mail.ru

Received: March 27<sup>th</sup>, 2021; Accepted: July 6<sup>th</sup>, 2021; Published: August 30<sup>th</sup>, 2021

**Abstract.** The accelerated development of flower buds during the thaw in apricots and almonds during the ecodormancy period leads to significant damage to the flower elements during return frosts and loss of future crops. The aim of the research was to identify the mechanisms of delay in the rate of development of flower buds during the ecodormancy period, their relationship with the degree of frost resistance and the timing of flowering in apricots. The following indicators of flower buds were analyzed: the degree of exit from endodormancy, frost resistance at temperatures of -18 °C and -31 °C, the degree of morphological development of flower elements, the activity of  $\alpha$ -amylases at temperatures of +15 °C and +60 °C, total content water, phenolcarboxylic acids, flavonoids and free proline. A significant positive correlation was revealed between the percentage of death of flower buds at a temperature of -18 °C and the percentage of buds emerging from endogenous dormancy (0.64\*), the percentage of death of buds at a temperature of -31 °C and the degree of development of flower elements (0.70\*), water content and the degree of development of flower elements (0.76\*\*), amylase activity at +60 °C and amylase activity at +15 °C (0.76\*\*), the content of phenolcarboxylic acids in the bark of shoots and flower buds (0.61\*). For the first time, psychrophilic forms of  $\alpha$ -amylases have been discovered in apricot flower buds.

**Key words:** frost resistance of flower buds, psychrophilic  $\alpha$ -amylase, thermal stability of  $\alpha$ -amylases,  $\alpha$ -amylase inhibitors, phenolic compounds.

### **INTRODUCTION**

Winter hardiness of flower buds is the main problem of stone fruit crops in the northern hemisphere (Yablonskiy & Markovich, 1970a; Sholokhov & Savvina, 1975). The greatest winter hardiness of flower buds corresponds to the endodormancy period, as buds break from endodormancy their winter hardiness is also lost (Glozer, 2010). The mechanism of endodormancy has not yet been fully understood, but it is known that its duration depends on both the genotype (Olukolu, 2010) and the number of low positive temperatures in the autumn-winter period (Viti et al., 2010). There is also evidence that plant break endodormancy can be produced not only by low positive temperatures, but

also by respiration inhibitors (Walton et al., 2009; Hegazi, 2012; El Masri et al., 2018), producers of active oxygen radicals, or strong oxidants (Bailly et al., 2008; Sarath & Mitchell, 2008). Without break endodormancy, the plant is incapable of further development. This problem arises in hot countries, where, for some cultivars with long-term dormancy, there is a lack of low positive temperatures to exit endodormancy (Rouse et al., 2006). If a plant approaches the growing season with incomplete exit from dormancy, then it develops very slowly and, as a rule, drops flower buds (Albuquerque et al., 2003). During endodormancy, both hydrolytic and synthetic processes are blocked (Seif El-Yazal & Seif El-Yazal, 2013), no new gene products capable of breaking dormancy arise (Gumilevskaya & Azarkovich, 2007; Dogramaci et al., 2010), but allowed oxidative polymerization of reserve substances - carbohydrates (Cooke et al., 2012; Fadon et al., 2018), fatty acids (Porta & Rocha-Sosa, 2002), phenolic compounds (Ji et al., 2015). After break endodormancy, hydrolytic processes are gradually activated. One of the first events in cells after break endodormancy is the hydrolysis of a very hydrophilic protein, dehydrin (Yamane et al., 2006).

Hydrolysis of 1,3- $\beta$ -glucan (callose) in the plasmodesmata and sieve tube (lat. *tuboli cribrosi*) of the vascular bundles, after break endodormancy, opens the way for tissue watering (Leubner-Metzger & Meins, 2001; Leubner-Metzger, 2003; Cilia & Jackson, 2004) and creating conditions for the activity of other hydrolases. Then starch (Fadon et al., 2018), oligosaccharides (Yablonskiy & Markovich, 1970), and lipids (Seif El-Yazal & Seif El-Yazal, 2013) are gradually hydrolyzed. In different apricot varieties, the endodormancy period can vary from 300 chill units for varieties - 'A.1740' and 'Gold Kist' (Bradley & Maurer, 2002; Olukolu et al., 2009), to 1,266 and 1,450 chill units for varieties - 'Orangered'® and 'Zard' (Kostina, 1969; Guerriero et al., 2002).

Modern apricot varieties, in a temperate climate zone, lack endodormancy for the entire frosty period, which reduces their winter hardiness. In Central Russia, the maximum duration of endodormancy (up to the 1<sup>st</sup>-2<sup>nd</sup> decade of February) in such apricot varieties as: 'Zavodskoy No. 1', 'Saratov ruby'® (Golubev et al., 2020), 'Manitoba 604' (Licznar-Małańczuk & Sosna, 2005), but even their rest is not enough for resistance to thaws. Most of the varieties of Central Russia come out of dormancy by mid-January. After the endodormancy is over, the sum of positive temperatures (Razavi et al., 2011) and the maximum values of thaw temperatures are of greatest importance for the development of flower buds. In the more southern regions of the country, where there are many thaws in the second half of winter and the ambient temperature can reach +15 – +20 °C, internal factors that restrain the rapid development of flower buds are of particular importance. Studies show that the rate of development of flower buds during the endodormancy period and their winter hardiness depend on the sensitivity of the genotype to the photoperiod (Stirling et al., 2002; Avdeev, 2014), the time of differentiation of flower buds (Tuz, 1960; Nemeth et al., 2008), the rate of development elements of the flower (Yablonskiy, 1970), the intensity of the breakdown of carbohydrates, indirectly indicating the activity of hydrolytic enzymes (Yablonskiy & Markovich, 1970; Seif El-Yazal & Seif El-Yazal, 2013), the content of phenolic inhibitors (Morozova, 1970; Korableva, 1974; Nenko et al., 2018; Paliy et al., 2018), sensitivity to thaw temperatures (Genkel & Oknina, 1964), biosynthesis of stress proteins (Levit et al., 1990). During the endodormancy period, flower buds develop especially rapidly in almonds (*Amygdalus communis* L.) (Prudencio et al., 2020) and apricots (*Prunus Armeniaca* L.) (Tuz, 1960). Our research is aimed at identifying the

mechanisms of delaying the rate of development of flower buds during the ecodormancy period, their relationship with the degree of frost resistance and flowering periods, as well as the classification of apricot genotypes according to the mechanisms of protection against premature awakening of flower buds, which will help combine several resistances in the created variety and prevent them death from recurrent frosts.

## MATERIALS AND METHODS

The material for the research was a collection of apricot varieties and hybrid forms (h.f.) of the private breeding nursery Golubevs, Saratov (Table 1).

**Table 1.** Characteristics of the studied samples

Genotype	Origin	Delayed or acceleration flowering
‘Zavodskoy No. 1’	local form	very late, +3 days
‘LXVI-09-1’	‘XV-03-1’ x ‘Late blooming №4’	very late, +3 days
‘7589’	<i>P. brigantiaca</i> x <i>P. armeniaca</i> ‘Makhtobi’	very late, +3 days
Plum ‘Svetlana’	unknown	very late, +3 days
‘VII-05-1’	Plum ‘Svetlana’ x apricot h.f. ‘Original’	very late, +3 days
‘Late blooming EM’	local form	very late, +3 days
‘Saratov ruby’ ®	sibirian h.f. ‘Handsome’ x h.f. ‘Pharaon’	middle (23.04.2020)
‘Manitoba 604’	‘Scout’ x ‘McClure’	early-middle, -0.5 days
‘Zhigulevsky souvenir’	unknown	early, -1 day
‘Gonsi Magyar kajszi’	‘Magyar Kajszi’ clone	early, -1 day
‘Generous’	h. f. ‘Pharaoh’ x h.f. of Baikalov	very early, -2 days
‘ <i>P. sibirica</i> No. 1’	unknown	superearly, -3 days

The analyzed plants grow in one area, without differences in microrelief, soil fertility and microclimate. Breeding forms - ‘Zavodskoy No. 1’, ‘LXVI-09-1’, ‘VII-05-1’, ‘Saratov ruby’ ®, ‘Generous’, ‘*P. sibirica* No. 1’ grow on their roots, genotypes - ‘7589’, ‘Late blooming EM’, ‘Manitoba 604’, ‘Zhigulevsky souvenir’, ‘Gonsi Magiyar kaiszi’ are grafted onto the same seminal rootstocks of apricot, the eastern plum ‘Svetlana’ is grafted onto a seedling home plum (*Prunus domestica*). Samples were taken from the southeastern side from the middle part of the crown, simultaneously for all analyzes (except for determining the release of flower buds from dormancy) from the same trees at the age of 12 years.

The winter hardiness of fruit buds was determined in mid-February (February 16, 2020) (the third component of winter hardiness is frost resistance during thaws), after holding for 24 hours at temperatures of -18 °C or -31 °C (rapid cooling) and the 3<sup>rd</sup> days at a temperature of +25 °C. The winter hardiness of fruit buds was analyzed in 2 replicates, 100 buds each. The number of dead buds was counted on longitudinal sections under an MBS-10 binocular microscope and expressed as a percentage of the total number of buds.

The stages of morphophysiological development of apricot flower buds were studied under an MBS-10 binocular microscope with a Levenhuk M300 BASE Microscope digital camera. The degree of development of flower elements was assessed using 12 photographs of longitudinal sections of flower buds of each cultivar for each sampling date (12/18/2019, 01/22/2020, 02/16/2020). The delay or acceleration of

flowering was assessed visually by the difference in the dates of mass flowering (more than 80% of open flowers) in the studied genotypes in comparison with the apricot cultivar 'Saratov Ruby'® with an average flowering period (04/23/2020).

The degree of interruption of dormancy of flower buds in the studied genotypes was determined by the percentage of flowers capable of blooming after 15 days on cut branches placed in water at +25 °C, guided by Richardson's method (Richardson et al. 1974). For analysis, three branches of each variety were cut off (01/22/2020) with at least 120–150 flower buds each. The water was changed every 3 days. All flower buds capable of developing into a flower to the white bud stage were classified as dormancy breaking.

The  $\alpha$ -amylase activity was determined using 3,5-dinitrosalicylic acid (DNSA) (Miller, 1959). The flower buds stored at -20 °C were ground in a porcelain mortar with the addition of quartz sand. The extract for analysis was obtained as follows: 0.5 g of crushed flower buds were added with 5 mL of phosphate buffer (pH 6.8), and then incubated for 1 hour at 4 °C with constant shaking. Then the samples were centrifuged at 10,000 rpm for 10 minutes. Further, all parameters were determined in the supernatant fluid.

The calibration graph was built for maltose, in triplicate.

Substrate for fermentolysis: 15 mL of phosphate buffer (pH 6.8) and 5 mL of 0.9% sodium chloride solution were heated to 80–90 °C, a suspension consisting of soluble starch 0.5 g and 20 mL of distilled water was added, boiled for 1.5–2 minutes, brought to 50 mL, and then cooled.

Enzymatic hydrolysis was carried out as follows: 1 mL of the extract (supernatant) was incubated with 1 mL of the substrate at 60 °C for 120 minutes or at 15 °C for 24 hours. To determine the amylase activity, 0.1 mL of the enzyme mixture was taken, 0.3 mL of 3,5-dinitrosalicylic acid reagent was added to it and incubated for 10 minutes at 100 °C in a water bath. Then 3 mL of distilled water cooled to +4 °C was added.

The optical density (D) of the colored solution was determined on a spectrophotometer Model - 752N 190–960 nm (China) at a wavelength of 530 nm. Calculation of  $\alpha$ -amylase activity was performed using a calibration curve. The  $\alpha$ -amylase activity was expressed in mg of maltose released per minute per 100 mg wet weight of the sample. The determination was carried out in three biological and three analytical replicates.

Phenolic compounds were extracted three times from the bark of annual apricot shoots or flower buds with 70% ethanol at 80 °C in a flask with a reflux condenser. The extraction was carried out as follows: 300 mg of plant material dried at 110 °C (flower buds or bark of annual shoots) was poured for the first time with 10 mL of 70% ethanol and heated in a water bath (80 °C) for 30 minutes. It was re-extracted with 10 mL of 70% ethanol under the same conditions for 20 minutes. The third time was extracted with 5 mL of 70% ethanol for 10 min. The extracted material and extracts were combined, transferred quantitatively to centrifuge tubes, and centrifuged at 6,000 rpm for 10 minutes. The supernatant was made up to 25 mL with 70% ethanol.

The study was carried out in 3 biological and 3 analytical replicates. The aliquot for analysis was 0.2 mL.

The total content of phenolcarboxylic acids was determined by the method developed for plant raw materials (Petukhova & Mirovich, 2019), spectrophotometrically at a wavelength of 325 nm. For the quantitative determination of flavonoids, we used the method (Methods for assessing..., 2012), based on the ability of flavonoids to form a stable complex with a citrate-boric reagent with an absorption maximum at 420 nm.

The content of flavonoids and phenolcarboxylic acids (PCA) in flower buds or bark of annual shoots on February 16, 2020 in apricot, plum, and plum-apricot hybrids was expressed in mg per 1 g of dry weight. The calibration graph for determining the concentration of phenolcarboxylic acids was built using gallic acid, and for flavonoids, using quercetin.

Thin layer chromatography of flavonoids was carried out in an upward flow of solvents toluene - acetone - formic acid at a ratio of 40: 30: 6 or on an OPTLC 'Chrompress-25' instrument using plates for HPTLC / OPTLC Silica Gel Pre-coated Aluminum Sheets.

The proline content in flower buds was determined by colorimetric or spectrophotometric methods at  $\lambda$  530 nm, in glass cuvettes, using a ninhydrin reagent and sulfosalicylic acid (Bates et al., 1973). The concentration of proline in the samples was expressed in mg per 1 g of dry weight of the sample. Proline was determined in 3 biological and 5 analytical replicates. The weighed amount was 200 mg.

The water content in flower buds was determined by the gravimetric method, after drying to constant weight in a thermostat at 110 °C. For the analysis, a sample of 1 g of plant material was taken in 3 replicates.

All experimental data were processed statistically using the AGROS program, version 2.09.

## RESULTS AND DISCUSSION

Freezing of apricot branches with flower buds in mid-February during a thaw at a temperature of -18 °C showed the distribution of genotypes according to the degree of damage, from 8.20% to 91.07% (Table 2).

**Table 2.** The degree of frost resistance of flower buds, their release from dormancy and the timing of flowering

Genotype	Percent death at temperature, as of		Percent of flower buds recovery from dormancy on 01/22/2020	Degree of development of flower elements	Water content in flower buds (%)
	-18 °C	-31 °C			
'Zavodskoy No. 1'	8.20	100.00	8.77	6	52.12
'LXVI-09-1'	9.06	100.00	10.68	5	53.93
'7589'	12.05	97.78	14.48	2	44.30
Plum 'Svetlana'	15.19	46.00	41.88	1	48.46
'VII-05-1'	20.01	95.18	33.62	3	48.37
'Late blooming EM'	25.00	99.00	49.61	4	46.73
'Saratov ruby' ®	30.11	97.02	49.15	4	47.72
'Manitoba 604'	34.50	100.00	83.36	6	55.81
'Zhigulevsky souvenir'	19.17	100.00	69.52	5	54.03
'Gonci Magyar Kajsz'i'	74.54	100.00	54.64	6	52.07
'Generous'	91.07	100.00	89.09	6	55.54
' <i>P. sibirica</i> No. 1'	19.61	100.00	67.75	6	51.11
<i>LSD</i> 0.05	17.672	7.033	21.244		2.513

There is a tendency to an increase in the death of flower buds with an increase in the percentage of their exit from endodormancy (Correlation coefficient 0.64\*). The available feature correlations are shown in Table 3.

The Table 2 shows that in all very late flowering genotypes, the death of buds at -18 °C does not exceed 25%, whereas in early ('Gonsi Magyar kaiszi') and very early ('Generous') flowering genotypes, death can reach 74.54 and 91.07%, respectively. Late blooming genotypes differed quite strongly in the percentage of flower buds coming out of dormancy - from 8.77% to 49.61%. Late flowering genotypes differed even more in the degree of development of flower elements. Fig. 1 shows the degree of development of floral elements in the most contrasting genotypes.

In our study, all genotypes could be divided into 6 groups according to the degree of development of flower elements (Table 2, Fig. 1). The first degree of development of flower elements was characterized by small, poorly formed anthers with a high degree of transparency, a small transparent pistil, transparent petals, and the presence of free space in the bud. From the first to the sixth degree, there was an increase in the size of the bud as a whole and all the elements of the flower, the formation of their typical structure, a decrease in transparency and free space. The sixth degree of bud development was characterized by well-formed all structural elements of the flower with large, opaque anthers, a large pistil with a rounded basal part and a formed stigma.

A particularly strong lag in the morphophysiological development of flower buds was observed in the eastern plum 'Svetlana' and a distant hybrid '7589' of the alpine plum and apricot (*P. brigantiaca* x *P. armeniaca* 'Makhtobi'). It is known from the literature that the degree of winter hardiness of flower buds depends on the stage of morphophysiological development; the more advanced the morphophysiological stage of flower bud, the lower its hardiness (Sholokhov & Savvina, 1975). Flower buds of varieties and hybrids created on the basis of Siberian genotypes ('Manitoba 604', 'Generous', '*P. sibirica* No. 1') are characterized by an accelerated rate of morphophysiological development of flower buds (5 и 6 degree of development of flower elements). Flower buds after emerging from endogenous dormancy, in order to maintain viability at critical temperatures (in our case, -31 °C), require additional protective mechanisms aimed at curbing the development of floral elements and the accumulation of water content in the buds. The very low correlation coefficient between the percentage of flower bud deaths at -31 °C and the percentage of awakened flower buds (0.1) indicates that not all late flowering genotypes have mechanisms to inhibit the rapid rate of bud development during the ecodormancy period. When flower buds are exposed to a critically low temperature of -31 °C during the ecodormancy period, it is not the degree of dormancy or even the flowering period of the genotype that comes to the fore, but the stage of morphophysiological development of flower buds (correlation






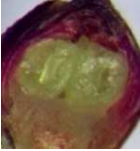


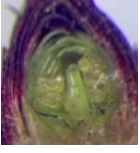









**Table 3.** Correlation analysis between frost resistance and some other characteristics of flower buds

Correlation coefficient matrix					
	1	2	3	4	5
1	1.00				
2	0.20	1.00			
3	0.64*	0.10	1.00		
4	0.43	0.70*	0.41	1.00	
5	0.41	0.27	0.50	0.76**	1.00

\* Significant at 5% level; \*\* Significant at 1% level; 1 – percent death of flower buds at -18 °C; 2 – percent death of flower buds at -31 °C; 3 – percentage of awakened buds; 4 – degree of development of flower elements; 5 – Water content in flower buds, %.



coefficient 0.70\*) and the water content in cells. In very late flowering genotypes ‘Zavodskoy No. 1’ and ‘LXVI-09-1’ with the lowest percentage of buds coming out of dormancy (8.77 and 10.68%, respectively), but with more advanced stages of development of floral elements (6 and 5, respectively), at extremely low temperatures (-31 °C), the death of flower buds was 100%. The highest (statistically significant) frost resistance (death of only 46%) was shown by the oriental plum variety ‘Svetlana’, in which the average percentage of recovery from dormancy of flower buds (41.88%), but the greatest lag in the development of the structural elements of the flower (underdeveloped anthers, unformed stigma pistil; see Table 2 and Fig. 1). The total water content in the buds of more than 50% was critical for all genotypes, regardless of the timing of flowering.

Variety, hybrid, shape	Flower buds morphology on:			Degree of development of flower elements
	12/18/2019	01/22/2020	02/16/2020	
Plum ‘Svetlana’				1
7589’				2
‘VII-05-1’				3
‘Late blooming EM’				4
‘LXVI-09-1’				5
‘Manitoba 604’				6

**Figure 1.** The degree of development of floral elements in the most contrasting genotypes at different periods of rest.

The correlation between the degree of development of flower elements and water content is statistically significant and amounts to 0.76\*\* at the 1% significance level. All genotypes with earlier flowering than the apricot variety 'Saratov Ruby' had a more developed morphophysiological stage of flower buds (well-formed, opaque, anthers; pistil with a rounded base and a formed stigma), increased water content (more than 50%) and 100% flower buds death after exposure to temperatures of -31 °C. It is possible that active protection mechanisms are more important at critical temperatures, for example, osmoprotectors (Arora et al., 1996; Arora R. 1996; Liu et al., 2007; Szabados & Savoure, 2009; Chen et al., 2012), antifreeze proteins (Griffith et al., 1992; Yeh et al., 2000; Griffith et al., 2005; Provesi et al., 2016), cold shock proteins (Perras & Sarhan, 1989; Gong et al., 2002; Nakaminami et al., 2009; Takahashi et al., 2013) and chaperones (Samuel et al., 2000; Karlson & Imai, 2003; Piszczek et al., 2005; Shimosaka & Ozawa, 2015).

So, studies have shown that a delay in the stage of morphophysiological development of flower buds is an essential adaptive mechanism in increasing winter hardiness.

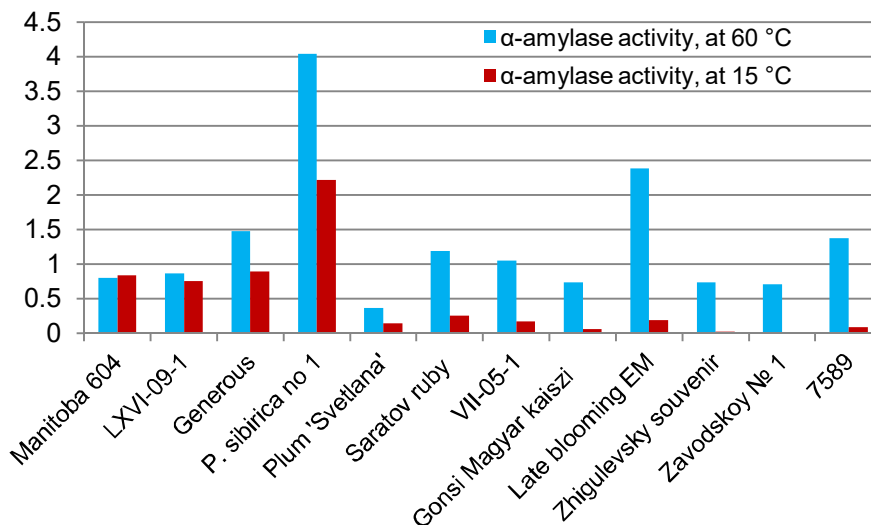
To identify the reasons for the accelerated rate of development of apricot flower buds during the ecodormancy, the activity of  $\alpha$ -amylase, as one of the thermolabile enzymes, was studied. Consider the existing prerequisites for such research. During the endodormancy period, the maximum accumulation of starch was found in flower buds (Fadon et al., 2018), and as it emerges from dormancy, its amount decreases. The enzyme hydrolyzing native starch is  $\alpha$ -amylase (Manners, 1974). An important role of  $\alpha$ -amylase in plant life is that, with the participation of this enzyme, such a storage organic matter as starch is converted from a non-transportable form into transport sugars, heading to growth points. Other amylolytic enzymes are also involved in the degradation of starch, but the contribution of  $\alpha$ -amylase is to initiate this process. Only  $\alpha$ -amylase is able to break down intact starch granules (Manners, 1974). Apricot, in contrast to plum, is considered a 'starchy' breed, that is, in its tissues, part of the starch accumulated in the autumn period remains throughout the entire endodormancy period (Bosieva & Nartikoeva, 2014). In addition, an increase in amylase activity largely characterizes the intensity of the processes of 'physiological swelling' associated with the accumulation of osmotically active substances (Obrucheveva & Antipova, 1997). Some researchers (Carginale et al., 2004) associate damage to flower buds in apricot during thaws with the presence of its own temperature threshold in each genotype - the threshold of sensitivity to positive temperatures. When warming, varieties with a low temperature threshold react quickly, initiating biochemical reactions leading to the hydrolysis of reserve nutrients and the formation of substances that promote growth. Cultivars with a high temperature threshold require more heat to initiate similar reactions. There is evidence (Wagner et al. 2017) that the developmental processes of the male gametophyte in plants blooming in winter and early spring are able to adapt to low temperatures during evolution.

To study the activity of  $\alpha$ -amylase at contrasting temperatures, genotypes of all flowering periods were selected - from super early to very late, different sensitivity to thaws and frost resistance of flower buds. The experiments were carried out on 9 apricot genotypes, 2 apricot-plum hybrids and one oriental plum variety (Table 4). Amylase activity was tested at 2 temperatures - +60 °C and + 15 °C, and the enzymatic lysis at 60 °C was carried out for 120 minutes, and at 15 °C - during the day.

**Table 4.** Activity of  $\alpha$ -amylase, (mg of maltose released per minute per 100 mg of wet weight of the sample), content of flavonoids (mg per 1 g of dry buds), the content of phenol carboxylic acids (PCA) (mg per 1 g of dry buds) and proline (mg per 1 g wet weight of flower buds) in February buds (16.02.2020) apricot, plum and plum-apricot hybrids

Genotype	$\alpha$ -amylase activity in flower buds, at		Flavonoid content in flower buds	Content of PCA		Proline content in flower buds
	60 °C	15 °C		in the shoot bark	in flower buds	
‘Zavodskoy No. 1’	0.71	0.02	34.56	6.82	11.87	1.05
LXVI-09-1	0.87	0.76	41.92	7.28	12.91	1.25
‘7589’	1.38	0.09	2.57	11.85	16.39	1.46
Plum Svetlana	0.37	0.15	41.99	9.54	12.68	1.21
VII-05-1	1.05	0.17	26.17	6.91	13.01	1.06
‘Late blooming EM’	2.39	0.19	38.20	9.51	12.79	2.01
‘Saratov ruby’®	1.19	0.26	35.23	7.58	9.68	0.68
‘Manitoba 604’	0.80	0.84	37.76	9.23	12.79	0.70
‘Zhigulevsky souvenir’	0.74	0.03	10.01	7.25	9.43	1.12
‘Gonsi Magyar kaiszi ‘	0.74	0.06	39.49	5.90	10.63	1.12
‘Generous’	1.48	0.90	32.79	7.73	9.23	1.21
<i>P. sibirica</i> no 1	4.04	2.22	5.53	7.98	7.5	0.93
LSD 0.05	0.637	0.092	3.320	0.619	1.039	0.063

Studies have shown that genotypes rapidly awakening in the thaw, with an advanced stage of morphophysiological development of flower buds (‘Manitoba 604’, ‘Generous’, ‘*P. sibirica* No. 1’), created on the basis of Siberian forms, have  $\alpha$ -amylase activity at low temperatures (15 °C) was several times higher than in genotypes with delayed development of flower buds (‘Saratov Ruby’, ‘Svetlana’ plum, ‘VII-05-1’, ‘Late blooming EM’) (Fig. 2).



**Figure 2.** The activity of  $\alpha$ -amylase (the amount of formed maltose (mg) per minute per 100 mg of raw buds) at different temperatures.

The graph shows that genotypes created with the participation of Siberian forms ('*P. sibirica* No. 1', 'Generous', 'Manitoba 604') have increased  $\alpha$ -amylase activity both at high incubation temperatures (60 °C) and at low temperatures (15 °C). From which it can be concluded that in the genotypes '*P. sibirica* No. 1', 'Manitoba 604' and 'Generous' hydrolytic enzyme  $\alpha$ -amylase is more adapted to low temperatures and is able to start working already in thaws, which entails hydrolysis of starch, saturation of tissues with water, more intensive development of flower buds and, as a result, a decrease in their frost resistance. It is known from the literature (Gianese et al., 2001; D'Amico et al., 2001; D'Amico et al., 2002) that is sufficient a point mutation in the structural gene of  $\alpha$ -amylase, leading to the replacement of only one amino acid in protein molecule so that this enzyme becomes cold-resistant and begins to work at lower temperatures. With the Siberian forms of apricot, similar mutations apparently occurred and psychrophilic isoforms of  $\alpha$ -amylases were formed. After exposure to low-temperature refrigeration (-31 °C) on flower buds of genotypes with high amylase activity at +15 °C - '*P. sibirica* No. 1' (2.22 mg min<sup>-1</sup> per 100 mg wet weight), 'Manitoba 604' (0.84), 'Generous' (0.90), 'LXVI - 09-1' (0.76) mortality was 100%, and in genotypes with low enzyme activity - plum 'Svetlana' (0.15), VII-05-1 (0.17), 'Saratov Ruby' (0.26), mortality was 46%, 95.18% and 97.02%, respectively. Thus, the temperature sensitivity of  $\alpha$ -amylase is an important indicator in the characterization of the genotype - the physiological activity of its flower buds during the thaw. Measurement of  $\alpha$ -amylase activity at different temperatures can serve as a kind of marker, with the help of which it will be possible to isolate genotypes that are least sensitive to thaws and have the highest winter hardiness flower buds.

Based on the literature data (Sholokhov & Savvina, 1975) that varieties with the same rate of morphogenesis when crossing do not always give the same picture of inheritance of this trait in the offspring, it can be concluded that there are several mechanisms of restraining the development of flower buds. Phenolic compounds may be one of the factors regulating the rate of morphogenesis. The maximum accumulation of phenolic compounds in the scales of flower buds is observed in the autumn-winter period, and at the time of blooming, their number is minimal (Zhang et al., 2020). Phenolic compounds are powerful antioxidants and inhibitors, both in plants and in other organisms. The group of phenolic compounds is not homogeneous in their biological action, some of them are Indoleacetic acid (IAA) oxidase inhibitors (phenolcarboxylic acids: vanillic acid, ferulic acid; flavonoids: luteolin, quercetin, etc.), the other part, on the contrary, are IAA oxidase stimulants (phenolcarboxylic acids: p-coumaric acid, p-hydroxybenzoic acid; flavonoids: apigenin, kaempferol, etc.) (Volynets, 2013). A number of articles (Wang et al., 2010; Chen et al., 2013; Li et al., 2014; Yuan et al., 2014) showed the inhibitory activity of phenolic compounds, primarily flavonoids, on  $\alpha$ -amylases and  $\alpha$ -glycosidases human. We assume that the premature awakening of flower buds depends on hydrolytic enzymes -  $\alpha$ -amylases,  $\alpha$ -glycosidases,  $\beta$ -glucosidases, 1,3- $\beta$ -glucanases. The presence of inhibitors of these enzymes in flower buds or bark of annual shoots will increase the winter hardiness of genotypes. So, when studying the effect of biologically active substances on the activity of alpha-amylase and frost resistance of winter wheat (Atimoshoae & Titika, 1990), it turned out that substances that reduce the level of enzyme activity during the period of hardening of plants increase their frost resistance. A more significant decline in alpha-amylase activity corresponds to a higher frost resistance.

We studied two groups of phenolic compounds - phenol carboxylic acids (PCA) and flavonoids, in flower buds (in mid-February) and bark (in late October) in apricot, plum and their hybrids. Studies have shown (Table 4) that the greatest amount of PCA in the bark of annual shoots accumulates in the genotypes with the latest flowering - hybrid '*P. brigantiaca* x *P. armeniaca* Makhtobi' (11.85 mg g<sup>-1</sup> dry weight of bark), 'Late blooming EM' (9.51), Plum 'Svetlana' (9.54). The 'Manitoba 604' cultivar (9.23 mg) has a slightly lower, but rather high PCA content in bark, which, although it does not have a flowering delay, showed restrained amylase activity at 60 °C. The highest content of PCA in flower buds is observed in late flowering genotypes: 'Late blooming EM' (18.36 mg g<sup>-1</sup> d.w.), '*P. brigantiaca* x *P. armeniaca* Makhtobi' (16.39 mg), VII-05-1 (13.01 mg), Late blooming LXVI-09-1 (12.91 mg), early flowering forms showed a significantly lower content - '*P. sibirica* No. 1' (7.5 mg), 'Generous' (9.23 mg), that is, the same trend has remained. A positive correlation (0.61\*) was found between the PCA content in bark and flower buds (Table 5).

**Table 5.** Correlation analysis of flower buds  $\alpha$ -amylase activity and its potential inhibitors

Correlation coefficient matrix								
	1	2	3	4	5	6	7	8
1	1.00							
2	0.20	1.00						
3	-0.03	0.30	1.00					
4	0.09	0.19	0.76**	1.00				
5	0.25	-0.27	-0.48	-0.28	1.00			
6	-0.31	-0.28	0.15	-0.01	-0.31	1.00		
7	-0.40	-0.18	-0.41	-0.52	0.08	0.61*	1.00	
8	-0.07	-0.05	0.17	-0.28	0.00	0.39	0.41	1.00

\* Significant at 5% level; \*\* Significant at 1% level; 1 – % death of flower buds at -18 °C; 2 – % death of flower buds at -31 °C; 3 – amylase activity at 60 °C; 4 – amylase activity at 15 °C; 5 – flavonoids in flower buds; 6 – PCA in the bark of shoots; 7 – PCA in flower buds; 8 – proline in flower buds.

Since each genotype has its own set of PCA, which can act in different directions, it is difficult to find the dependence of the  $\alpha$ -amylase activity on the total PCA. Correlation analysis still showed, albeit a small (mathematically insignificant) negative relationship between the total PCA content in flower buds and  $\alpha$ -amylase activity both at 60 °C (-0.41) and at 15 °C (-0.52). The component analysis of phenol carboxylic acids should provide more convincing data. A similar pattern was observed in the total content of flavonoids. The highest content of flavonoids was found in late blooming genotypes - 'Svetlana' plum (41.99 mg g<sup>-1</sup> of dry weight of buds), 'LXVI-09-1' (41.92) and 'Late blooming EM' (38.20). In early flowering forms, for example, '*P. sibirica* No. 1', the content of flavonoids was only 5.53 mg g<sup>-1</sup> of dry weight of buds, in another early flowering variety 'Zhigulyovskiy souvenir' there were 10.01 mg of them. It is interesting to trace the relationship between the sum of flavonoids and the activity of  $\alpha$ -amylase. There is a slight inverse relationship (correlation coefficient -0.48) between the  $\alpha$ -amylase activity and the accumulation of flavonoids: the more there are, the lower the  $\alpha$ -amylase activity for most genotypes. It should also be noted that not all flavonoids and their glycosides inhibit  $\alpha$ -amylases with the same potency (Wang et al., 2010; Chen et al., 2013; Li et al., 2014; Yuan et al., 2014).

Preliminary data from chromatographic analysis of flavonoids on silica gel plates show that the number of components in different genotypes varies from 2 to 10. For the time being, 3 flavonoids have been identified - rutin, naringenin and quercetin. Research in this direction continues.

The next line of research is to test the role of free proline in the delay of flowering and the formation of frost resistance of stone fruit buds. There are data in the literature on osmoregulation and competitive inhibition of hydrolases by L-proline - in the struggle for free water (Kiyosue et al., 1996; Nakashima et al., 1998). The analysis showed that the highest proline concentrations in mid-February accumulated flower buds of late flowering genotypes - 'Late blooming EM' (2.01 mg g<sup>-1</sup> flower buds wet weight) and '*P. brigantiaca* x *P. armeniaca* Makhtobi' (1.46), and the smallest ones are 'Saratov ruby' (0.68), 'Manitoba 604' (0.70) and *P. sibirica* No.1 (0.93). There is a weak (insignificant) inverse dependence of the  $\alpha$ -amylase activity on the accumulation of free proline - the more the hydrophilic amino acid itself, the lower the enzyme activity (correlation coefficient -0.28).

Multiple mechanisms of flowering delay and protection from low temperatures complicate the understanding of the role of one or another component, but comprehensive studies will make it possible to isolate genotypes with one mechanism or another, combine them in one genotype, and create flower buds with high winter hardiness. For breeding purposes, the most valuable genotypes should combine a low dormancy rate of flower buds, low free water content, low  $\alpha$ -amylase activity during thaws, and high accumulation of proline and flavonoids. Out of the studied samples, only 2 genotypes correspond to these characteristics - 'Svetlana' plum and 'Late blooming EM' apricot, which will be used in further breeding work.

## CONCLUSIONS

The study showed the complex nature of the formation of not only the winter hardiness trait of apricot flower buds, but also the timing of flowering of genotypes. All studied genotypes were characterized by the flowering period, the degree of recovery from dormancy, the rate of morphogenesis of flower buds, their frost resistance, cold resistance of  $\alpha$ -amylases, the accumulation of phenol carboxylic acids, flavonoids and proline, and water content.

As a result of this study, the following genotypes valuable for breeding were identified that showed the least flower buds death at -18 °C: 'Zavodskoy No. 1' (8.2%), 'LXVI-09-1' (9.06%), '*P. brigantiaca* x *P. armeniaca* Makhtobi' (12.05%), 'Svetlana' plum (15.19%), 'VII-05-1' (20.01%). The genotype with the highest winter hardiness of flower buds at a critical temperature of -18 °C was revealed - 'Svetlana' plum.

Correlations were revealed between the frost resistance of apricot flower buds at a temperature of -18 °C and the percentage of buds break from endodormancy (0.64\*), the percentage of flower buds death at a temperature of -31 °C and the degree of development of flower elements (0.70\*), water content and the degree of development of flower elements (0.76\*\*).

For the first time, psychrophilic forms of  $\alpha$ -amylases were found in apricot flower buds. Genotypes with adaptation of  $\alpha$ -amylases to low temperatures - *P. sibirica* No. 1' and 'Generous', 'Manitoba 604', 'LXVI-09-1' are needed for further comparative studies.

## REFERENCES

- Albuquerque, N., Burgos, L. & Egea, J. 2003. Apricot flower bud development and abscission related to chilling, irrigation and type of shoots. *Scientia Horticulturae* **98**, 265–276.
- Arora, R. 1996. Accumulation of a 60-kD Dehydrin Protein in Peach Xylem Tissues and Its Relationship to Cold Acclimation. *HortScience* **31**(6), 923–925.
- Arora, R., Wisniewski, M. & Rowland, L.J. 1996. Cold Acclimation and Alterations in Dehydrin-like and Bark Storage Proteins in the Leaves of Sibling Deciduous and Evergreen Peach. *J. Amer. Soc. Hort. Sci.* **121**(5), 915–919.
- Atimoshoae, M.V. & Titika, M.D. 1990. Changes in the activity of alpha-amylase in germinating wheat grain – a criterion for assessing bioregulators of frost resistance. *Exogenous regulation of water exchange, drought and frost resistance of plants*. Chisinau: Shtiintsa, pp. 86–89. (in Russian).
- Avdeev VI, 2014. Problems of resistance of fruit plants to hypothermia. *Bulletin of the Orenburg State Pedagogical University* **3**(11), 25–29.
- Bailly, C., Bouteau, H.El M. & Corbineau, F. 2008. Role of signaling by reactive oxygen species in seed germination and dormancy. *Journal de la Societte de Biologie* **202**(3), 241–248. doi: 10.1051/jbio:2008025
- Bates, L.S., Waldren, R.P. & Teare, I.D. 1973. Rapid determination of free proline for water-stress studies. *Plant and Soil* **39**, pp. 205–207.
- Bosieva, O.I. & Nartikoeva, R.R. 2014. Seasonal Dynamics of Starch Content in Woody Plants. *News of the Gorsk State Agrarian University* **51**(4), pp. 407–410.
- Bradley, L. & Maurer, M., 2002. *Deciduous Fruit & Nuts for the Low Desert*. The University of Arizona College of Agriculture and Life Sciences. Iss.March.
- Carginale V, Trinchella F, Capasso C, Scudiero R. & Parisi E. 2004. Gene amplification and cold adaptation of pepsin in Antarctic fish. *Gene*, Jul 21, **336**(2), pp.195–205.
- Chen, K., Fessehaie, A. & Arora, R. 2012. Dehydrin metabolism is altered during seed osmopriming and subsequent germination under chilling and desiccation in *Spinacia oleracea* L. cv. Bloomsdale: Possible role in stress tolerance. *Plant Science* **183**, 27–36.
- Chen, L., Wang, C., Yi Wei, Q-Y., Ning, Z. & Yuan, E., 2013. Interaction of dihydromyricetin and  $\alpha$ -amylase. *Natural product communications* **8**(3), 339–342.
- Cilia, M.L. & Jackson, D. 2004. Plasmodesmata form and function. *Current Opinion in Cell Biology* **16**, 500–506.
- Cooke, J.K., Eriksson, M.E. & Olavi Junttila, O., 2012. The dynamic nature of bud dormancy in trees: environmental control and molecular mechanisms. *Plant, Cell and Environment* **35**, 1707–1728. doi: 10.1111/j.1365-3040.2012.02552.x
- D'Amico, S., Gerday, C. & Feller, G. 2001. Structural Determinants of Cold Adaptation and Stability in a Large Protein. *The J. of Biol. Chem* **276**(28), of July 13, pp. 25791–25796.
- D'Amico, S., Gerday, C. & Feller, G. 2002. Dual Effects of an Extra Disulfide Bond on the Activity and Stability of a Cold-adapted  $\alpha$ -Amylase. *The Journal of Biological Chemistry* **277**(48), Iss. of November 29, pp. 46110–46115.
- Dogramaci, M., Horvath, D.P., Chao, W.S., Foley, M.E., Christoffers, M.J. & Anderson, J.V. 2010. Low temperatures impact dormancy status, flowering competence, and transcript profiles in crown buds of leafy spurge. *Plant Mol Biol* **73**, 207–226. DOI 10.1007/s11103-010-9621-8
- El Masri, I.Y., Rizkallah, J. & Sassine, Y.N. 2018. Effects of Dormex (Hydrogen Cyanamide) on the performance of three seedless table grape cultivars grown under greenhouse or open-field conditions. *Agronomy Research* **16**(5), 2026–2036. <https://doi.org/10.15159/AR.18.191>
- Fadon, E., Herrero, M. & Rodrigo, J. 2018. Dormant Flower Buds Actively Accumulate Starch over Winter in Sweet Cherry. *Frontiers in Plant Science* **9**, article 171.
- Genkel, P.A., Oknina, E.Z. 1964. Dormancy and frost resistance of fruit plants. M.: *Science*. 242 pp. (in Russian).

- Gianese, G., Argos, P. & Pascarella, S. 2001. Structural adaptation of enzymes to low temperatures. *Protein Engineering* **14**(3), 141–148.
- Glozer, K. 2010. Dormancy, chill accumulation, rest-breaking and freeze damage – what are the risks. [fruitsandnuts.ucdavis.edu/files/73907.pdf](http://fruitsandnuts.ucdavis.edu/files/73907.pdf). (Accessed 09/05/2013).
- Golubev, A.M., Bodrov, B.V., Anfalov, V.E. & Aleshina, N.A., 2020. Scientific and Methodical Approaches in the Creation of the Gene Pool of Stone Grain Crops. *Bulletin KrasGAU* **7**, 38–46 (in Russian, English abstr.).
- Gong, Z., Lee, H., Xiong, L., Jagendorf, A., Stevenson, B. & Zhu, J.-K. 2002. RNA helicase-like protein as an early regulator of transcription factors for plant chilling and freezing tolerance. *PNAS*. August 20, **99**(17), 11507–11512. [www.pnas.org/cgi/doi/10.1073/pnas.172399299](http://www.pnas.org/cgi/doi/10.1073/pnas.172399299)
- Griffith, M., Ala, P., Yang, D.S.C., Hon, W.-C. & Moffatt, B.A. 1992. Antifreeze Protein Produced Endogenously in Winter Rye Leaves. *Plant Physiol* **100**, 593–596.
- Griffith, M., Lumb, C., Wiseman, S.B., Wisniewski, M., Johnson, R.W. & Marangoni, A.G. 2005. Antifreeze Proteins Modify the Freezing Process In Planta. *Plant Physiology*, May, vol. **138**, pp. 330–340. [www.plantphysiol.org/cgi/doi/10.1104/pp.104.058628](http://www.plantphysiol.org/cgi/doi/10.1104/pp.104.058628)
- Guerriero, R., Vin, R., Monteleone, P. & Gentili, M., 2002. La valutazione della dormienza nell'albicocco: tre metodi a confronto. *Frutticoltura* **3**, 73–77.
- Gumilevskaya, N.A. & Azarkovich, M.I., 2007. Transcriptional and translational events in the embryos of dormant recalcitrant horse chestnut seeds during stratification. In the collection: *VI Congress of the Society of Plant Physiologists of Russia and the International Conference 'Modern Plant Physiology: from Molecules to Ecosystems.'* June 18–24, Syktyvkar, vol. **1**, abstracts, pp. 180–182 (in Russian).
- Hegazi, A.A. 2012. Effects of Some Dormancy Breaking Agents on Flowering, Fruiting and Fruit Characteristics of 'Canino' Apricot Cultivar. *World Journal of Agricultural Sciences* **8**(2), 169–173.
- Ji, H., Wang, Y., Cloix, C., Li, K., Jenkins, G.I., Wang, S., Shang, Z., Shi, Y., Yang, S., Li, X. 2015. The Arabidopsis RCC1 Family Protein TCF1 Regulates Freezing Tolerance and Cold Acclimation through Modulating Lignin Biosynthesis. *PLoS Genet* **11**(9), e1005471. doi:10.1371/journal.pgen.1005471.
- Karlson, D. & Imai, R. 2003. Conservation of the Cold Shock Domain Protein Family in Plants. *Plant Physiology*, January, vol. **131**, pp. 12–15.
- Kiyosue, T., Yoshida, Y., Yamaguchi-Shinozaki, K. & Shinozaki, K. 1996. A nuclear gene encoding mitochondrial proline dehydrogenase, an enzyme involved in proline metabolism, is upregulated by proline but downregulated by dehydration in Arabidopsis. *Plant Cell* **8**, 1323–1335.
- Korableva, N.P. 1974. The biochemical nature of dormancy and transition to active growth (on the example of potato tubers). *Abstract of Doctor of Biological Sciences - M.*, 58 pp. (in Russian).
- Kostina, K.F., 1969. The use of varietal resources of apricot for breeding. *GNBS* **40**, 45–63 (in Russian).
- Leubner-Metzger, G. & Meins, F.Jr. 2001. Antisense-transformation reveals novel roles for class I  $\beta$ -1,3-glucanase in tobacco seed after-ripening and photodormancy. *Journal of Experimental Botany* **52**(362), 1753–1759. doi: 10.1093/jexbot/52.362.1753
- Leubner-Metzger, G. 2003. Functions and regulation of  $\beta$ -1,3-glucanases during seed germination, dormancy release and after-ripening. *Seed Science Research* **13**, 17–34.
- Levit, T.K., Kirillov, A.F. & Kozmik, R.A. 1990. Changes in protein metabolism of grapes during low-temperature processing. *Exogenous regulation of water exchange, drought and frost resistance of plants*. Shtiintsa, Chisinau, pp. 16–27 (in Russian).
- Li, Q., Chen, L., Wei, Q.-Y., Yuan, E.-D. & Ning, Z.-X. 2014. Interaction of naringenin and  $\alpha$ -amylase. *Modern Food Science and Technology* **30**(2), 58–61+94.



- Licznar-Małańczuk, M. & Sosna, I., 2005. Evaluation of several apricot cultivars and clones in the lowers silesia climatic conditions. *J. of Fruit and Ornamental Plant Research* **13**, 49–57.
- Liu, Ji-H., Kitashiba, H., Wang, J., Ban, Y. & Moriguchi, T. 2007. Polyamines and their ability to provide environmental stress tolerance to plants. *Plant Biotechnology* **24**, 117–126.
- Manners, D.J. 1974. **In:** Plant carbohydrate biochemistry. *Proc. Phytochem. Soc. Symp.* Edinburgh, pp. 109.
- Methods for assessing the antioxidant status of plants. 2012. *Ed. Ural University*, Yekaterinburg, pp. 35–38 (in Russian).
- Miller, G.L. 1959. Use of Dinitrosalicylic Acid Reagent for Determination of Reducing Sugar. *Analytical Chemistry* **31**(3), 426–428.
- Morozova, E.V. 1970. Study of phenolic compounds in potatoes and their regulatory role in dormancy and resistance to *Phytophthora Infestans* (Mont.) De Bary. *Abstract of Cand. diss.*, M., 30 pp. (in Russian).
- Nakaminami, K., Hill, K., Perry, S.E., Sentoku, N., Long, J.A. & Karlson, D.T. 2009. Arabidopsis cold shock domain proteins: relationships to floral and silique development. *Journal of Experimental Botany* **60**(3), 1047–1062. doi:10.1093/jxb/ern351
- Nakashima, K., Satoh, R., Kiyosue, T., Yamaguchi-Shinozaki K. & Shinozaki K. 1998. A Gene Encoding Proline Dehydrogenase Is Not Only Induced by Proline and Hypoosmolarity, but Is Also Developmentally Regulated in the Reproductive Organs of Arabidopsis. *Plant Physiol.* **118**, pp. 1233–1241.
- Nemeth, Sz., Szalay, L. & Remenyi, M.L., 2008. Flower bud differentiation in apricot. *International Journal of Horticultural Science* **14**(4), 19–21.
- Nenko, N.I., Ilyina, I.A., Petrov, V.S., Sundyreva, M.A. & Skhalyakho, T.V. 2018. Influence of endogenous phenolic compounds on winter hardiness of grape varieties. Phenolic compounds: a functional role in plants. **In:** *Sat. scientific. articles on the materials of the X International Symposium 'Phenolic Compounds: Fundamental and Applied Aspects'*, Moscow, May 14–19, 2018, M., pp. 293–295 (in Russian).
- Obrucheva, N.V. & Antipova, O.V. 1997. Physiology of seed germination initiation. *Plant Physiology* **44**, 286–302 (in Russian).
- Olukolu, B. 2010. The Genetics of Chilling Requirement in Apricot (*Prunus Armeniaca* L.). *All Dissertations*. Paper 537.
- Olukolu, B.A., Trainin, T., Fan, S., Kole, C., Bielenberg, D.G., Reighard, G.L., Abbott, A.G. & Holland, D. 2009. Genetic Linkage Mapping For Molecular Dissection Of Chilling Requirement And Bud Break In Apricot (*Prunus Armeniaca* L.). *Genome Oct.*, **52**(10), 819–828.
- Paliy, I.N., Paliy, A.E., Gubanova, T.B. & Gorina, V.M. 2018. The influence of negative temperatures on the content of phenolic compounds in some varieties of apricot (*Prunus armeniaca* L.). *GNBS Bulletin*, no. **129**, pp. 101–105 (in Russian).
- Perras, M. & Sarhan, F. 1989. Synthesis of Freezing Tolerance Proteins in Leaves, Crown, and Roots during Cold Acclimation of Wheat. *Plant Physiol.* **89**, 577–585.
- Petukhova, S.A. & Mirovich, V.M. 2019. Development of a method for the quantitative determination of phenolcarboxylic acids in the herb of goat leaflet growing in the Baikal region. **In:** *Innovative technologies in pharmacy*, Irkutsk, vol. **6**, pp. 269–273. (in Russian).
- Piszczek, G., Rozycki, J., Singh, S.K., Ginsburg, A. & Maurizi, M.R. 2005. The Molecular Chaperone, ClpA, Has a Single High Affinity Peptide Binding Site per Hexamer. *The Journal of Biological Chemistry* **280**(13), Issue of April 1, pp. 12221–12230.
- Porta, H. & Rocha-Sosa, M. 2002. Plant Lipxygenases. Physiological and Molecular Features. *Plant Physiology*, September, vol. **130**, pp. 15–21.

- Provesi, J.G., Neto, P.A.V., Arisi, A.C.M. & Amante, E.R. 2016. Antifreeze proteins in naturally cold acclimated leaves of *Drimys angustifolia*, *Senecio icoglossus*, and *Eucalyptus* ssp. *Braz. J. Food Technol.*, Campinas, v. **19**, e2016110. <http://dx.doi.org/10.1590/1981-6723.11016>
- Prudencio, A.S., Martínez-Gómez, P. & Dicenta, F. 2020. Analysis of the Modulation of Dormancy Release in Almond (*Prunus dulcis*) in Relation to the Flowering and Ripening Dates and Production under Controlled Temperature Conditions. *Agronomy* **10**, 277. doi:10.3390/agronomy10020277
- Razavi, F., Hajilou, J., Tabatabaei, S.J. & Dadpour, M.R. 2011. Comparison of chilling and heat requirement in some peach and apricot cultivars. *Research in Plant Biology* **1**(2), 40–47.
- Richardson, E.A., Seeley, S.D. & Walker, D.R. 1974. A Model for Estimating the Completion of Rest for 'Redhaven' and 'Elberta' Peach Trees. *HortScience* **9**(4), 331–332.
- Rouse, R.E., Libran, M.D.C., Hernandez, E. & Cardona, L. 2006. Low-Chill Peaches Adapted to Subtropical Florida and Tropical Puerto Rico. *Proc. Fla. State Hort. Soc.* **119**, 25–28.
- Samuel, D., Kumar, T.K.S., Ganesh, G., Jayaraman, G., Yang, P.-W., Chang, M.-M., Trivedi, V.D., Wang, S.-L., Hwang, K.-C., Chang, D.-K. & Yu, C. 2000. Proline inhibits aggregation during protein refolding. *Protein Science* **9**, 344–352.
- Sarath, G. & Mitchell, R.B., 2008. Aged Switchgrass Seed Lot's Response to Dormancy-breaking Chemicals. *Seed Technology* **30**(1).
- SeifEl-Yazal, S.A. & SeifEl-Yazal, M.A., 2013. *Causes of Bud Dormancy and the New Methods for Breaking It*. LAP LAMBERT Academic Publishing, 236 pp.
- Shimosaka, E. & Ozawa, K. 2015. Overexpression of cold-inducible wheat galactinol synthase confers tolerance to chilling stress in transgenic rice. *Breeding Science* **65**, 363–371. doi:10.1270/jsbbs.65.363
- Sholokhov, A.M. & Savvina, T.M. 1975. Inheritance of the nature of morphogenesis and winter hardiness of flower buds in apricot hybrids of the first generation. *GNBS Proceedings*, **LXVI**, 137–143 (in Russian).
- Stirling, K.J., Clark, R.J., Brown, P.H. & Wilson, S.J. 2002. Effect of photoperiod on flower bud initiation and development in myoga (*Zingiber mioga* Roscoe). *Scientia Horticulturae* **95**, 261–268.
- Szabados, L. & Savoure, A. 2009. Proline: a multifunctional amino acid. *Trends in Plant Science* **15**(2), 89–97. doi:10.1016/j.tplants.2009.11.009
- Takahashi, D., Li, B., Nakayama, T., Kawamura, Y., Uemura, M. 2013. Plant plasma membrane proteomics for improving cold tolerance. *Frontiers in Plant Science* **4**(article 90), 90.
- Tuz, A.S. 1960. Development of flower buds of peach and other stone fruit in connection with their winter hardiness in Uzbekistan. *Abstract dissertation*. Ph.D, 16 p. (in Russian).
- Viti, R., Andreini, L., Ruiz, D., Egea, J., Bartolini, S., Iacona, C. & Campoy, J.A. 2010. Effect of climatic conditions on the overcoming of dormancy in apricot flower buds in two Mediterranean areas: Murcia (Spain) and Tuscany (Italy). *Scientia Horticulturae* **124**, 217–224. doi:10.1016/j.scienta.2010.01.001
- Volynets, A.P. 2013. *Phenolic compounds in the life of plants*. Minsk, Belarusian Science, 283 pp. (in Russian).
- Wagner, J., Gastl, E., Kogler, M. & Scheiber, M. 2017. Cold Tolerance of the Male Gametophyte during Germination and Tube Growth Depends on the Flowering Time. *Plants* **6**(2). doi:10.3390/plants6010002
- Walton, E.F., Wu, R.-M., Richardson, A.C., Davy, M., Hellens, R.P., Thodey, K., Janssen, B.J., Glesve, A.P., Rae, G.M., Wood, M. & Schaffer, R.J. 2009. A rapid transcriptional activation is induced by the dormancy-breaking chemical hydrogen cyanamide in kiwifruit (*Actinidia deliciosa*) buds. *Journal of Experimental Botany* **60**(13), 3835–3848. doi:10.1093/jxb/erp231

- Wang, H., Du, Y.-Ji & Song Hua-Can. 2010.  $\alpha$ -Glucosidase and  $\alpha$ -amylase inhibitory activities of guava leaves. *Food Chemistry* **123**(1), 6–13.
- Yablonskiy, E.A. & Markovich, Z.V. 1970a. Studying the dynamics of oligosaccharides for a comparative assessment of winter hardiness of varieties of stone fruit and nut crops. *GNBS Proceedings XLVI*, 62–83 (in Russian).
- Yablonskiy, E.A. & Markovich, Z.V. 1970. Growth rates of fruit buds and winter hardiness of apricot, peach and almond varieties. *GNBS Proceedings XLVI*, 50–61 (in Russian).
- Yamane, H., Kashiwa, Y., Kakehi, E., Yonemori, K., Mori, H., Hayashi, K., Iwamoto, K., Tao, R. & Kataoka, I. 2006. Differential expression of dehydrin in flower buds of two Japanese apricot cultivars requiring different chilling requirements for bud break. *Tree Physiology* **26**, 1559–1563.
- Yeh, S., Moffatt, B.A., Griffith, M., Xiong, F., Yang, D.S.C., Wiseman, S.B., Sarhan, F., Danyluk, J., Xue, Y.Q., Hew, C.L., Doherty-Kirby, A. & Lajoie, G. 2000. Chitinase Genes Responsive to Cold Encode Antifreeze Proteins in Winter Cereals. *Plant Physiology*, November, vol. **124**, pp. 1251–1263.
- Yuan, E., Liu, B., Wei, Q., Yang, J., Chen, L. & Li, Q. 2014. Structure activity relationships of flavonoids as potent alpha-amylase inhibitors. *Nat Prod Commun.*, Aug. **9**(8), 1173–6.
- Zhang, T., Yuan, Y., Zhan, Y., Cao, X., Liu, C., Zhang, Y. & Gai, S. 2020. Metabolomics analysis reveals Embden Meyerhof Parnas pathway activation and flavonoids accumulation during dormancy transition in tree peony. *BMC Plant Biol.* **20**, 484.

## Evaluation of artificial agricultural landscapes biodiversity in Stavropol Botanical Garden

L.A. Grechushkina-Sukhorukova and E.V. Peshchanskaya\*

Federal State Budget Scientific Institution "North Caucasus Federal Scientific Agricultural Center" 478 Lenin Str., RU355029 Stavropol, Russia

\*Correspondence: [ekaterina108@mail.ru](mailto:ekaterina108@mail.ru)

Received: April 24<sup>th</sup>, 2021; Accepted: July 13<sup>th</sup>, 2021; Published: August 5<sup>th</sup>, 2021

**Abstract.** The meadow steppes recreated in the Stavropol Botanical Garden, Russia, by planting sod blocks after more than 40-year period of cultivation have preserved species composition similar to zonal steppes. The aim of our research is to evaluate the restored artificial cultivated land biodiversity. A parallel measurement of species saturation per 100 m<sup>2</sup>, yield, botanical analysis by crops was conducted on model experimental sites and in nature. Systematic and biomorphological flora study, analysis of variance were carried out. Useful plant species were identified. The restored steppes represent a multispecies community including 236 species, 149 genera, and 36 families. It consists of 5 biomorphs which comprise 2.9% of phanerophytes, 3.0% of chamephytes, 74.6% of hemicryptophytes, 14.4% therophytes that have a high degree of similarity in quantity to the steppes of Central Fore-Caucasus. The cenoses are dominated by plants having life cycles of perennial ones which accounts for 81.0%, annuals, and biennials make up 19.0%, cereals and sedges amount to 32 species (13.5%), legumes represent 28 speies (11.9%), mixed herbs are 176 (74.6%). The projective cover of grass stand is 80.0–100.0%, that corresponds 73–109 species per 100 m<sup>2</sup>. An average yield of the restored steppes grass stand is 2.8–3.8 t ha<sup>-1</sup>. It exceeds the productivity of natural cenoses by 2.1–3.3 t ha<sup>-1</sup>. The botanical analysis by crops demonstrated that in the grass stands samples of cereals (19.6–43.9%) and mixed herbs (18.3–31.2%) dominated. 18 rare plants are preserved in the cenoses. 171 species have useful properties. The site of the restored meadow steppe is an exposition and serves for sightseeing and educational purposes. Lately, sod blocks planting was widely used in experimental phytocenology and landscape design. Its implementation for natural vegetation restoration on the large areas is time-consuming and expensive compared to the method of cultivated lands, therefore it can be used in small sites as a component of combined options.

**Key words:** artificial agrarian landscapes, method of sod blocks planting, biodiversity, floral analysis, yield.

### INTRODUCTION

Since the foundation of the Botanical garden in Stavropol, Russia, the most important task of its scientific team was the study, reproduction, protection and rational use of flora and vegetation of the North Caucasus. Under the leadership of V.V. Skripchinsky, artificial models of some types of natural vegetation were created on

the territory of the garden: forest - oak, pine, fir-spruce; herbaceous phytocenoses (by sod blocks planting) - meadow steppe, subalpine meadow, etc. (Skripchinsky et al., 1971; Skripchinsky, 1973). The research was the initial stage of work on experimental applied phytocenology in our region and became the basis for the creation of new technologies - the D.S. Dzybov's method of agrostepes - the theory and technology of accelerated (40–50 times) restoration of the primary steppe analogues of the zonal type compared to self-restoration. They became the basis for the transition from the depletion practice of resource use to the restoration one (Dzybov, 2010). Models of meadow-steppe cenoses restored by sod planting method has been preserved in the botanical garden till nowadays on the area of 2 hectares. They have species composition close to natural steppes and are considered to be a reserve for the conservation of biological diversity of zonal meadow steppe species including wild relatives of cultivated, forage, medicinal, food plants, and rare species (Kozhevnikov et al., 2012). The meadow steppe is the richest ecosystem by the number of species in the Eurasian area. The species saturation per 100 m<sup>2</sup> can reach 100 or more species. *Brachypodium rupestre* (Host) Roem. et Schult., 1817, *Bromus riparius* Rehmman, 1872, *Carex humilis* Leyss., 1761, *Filipendula vulgaris* Moench., 1794., *Stipa pulcherrima* K. Koch, 1848, dominate in the meadow steppes. The projective cover of grass stand is, on average, 89% (fluctuation 65-100%), the true cover is from 3 to 7%. The yield is 2,6–10.6 t ha<sup>-1</sup> (Dzybov, 2018).

In the 19<sup>th</sup>–20<sup>th</sup> centuries in Russia, the creation of demonstration areas of the steppe by the sod blocks planting method from natural steppes for scientific and educational purposes was carried out by a number of scientists such as A.N. Krasnov in Kharkiv University Botanical garden, G.I. Tanfilyev in Petersburg Botanical garden, V.N. Kononov in Stavropol (Voroshilovsk) Pedagogical Institute (Krasnov, 1890; Tanfilyev, 1901; Kononov, 1940). In the 30s–50s of the XX century in Wisconsin University, the USA, American geobotanist J. Curtis conducted experiments on prairie restoration using sod transplantation with addition of seedlings grown from direct planting of seeds in nurseries, hay distribution, transplanting plants from prairies. According to his opinion, sod method gives good results, but it is quite expensive that limits its usage in large areas (Archer & Bunch, 1955; Cottam & Wilson, 1966). In 1969–1983 in Donetsk Botanical garden a forb-fescue-feather grass steppes exposition 'Donbass Steppes' with an area of 8.5 hectares was created using seeds and sod blocks planting. Artificially created phytocenoses were rich in floristic variety including 359 species, 220 genera and 50 families. Perennial plants (63.7%), biennial plants (12.4%), annuals (12.6%), shrubs (6%) small bushes (5.3%) dominate in life-forms vegetation. Formed species resistance after the period of 20-year experiment was maintained by the wide range of species and ecological ones including grasses (Kondratyuk & Chupyrina, 1989). Since 1970s, D.S. Dzybov has grassed the sites with disturbed natural vegetation in subalpine ecoregion and in the meadow steppe of Central Caucasus. He drew attention to such method disadvantages as ecological damage of steppe biogeocenose when harvesting sod; slow overgrowing of sod harvesting sites; prolonged period of artificial cenoses creation; time-consuming of the method (Dzybov, 2010). The agrosteppe method is recognized in Russia as the most promising and technological one (Abdullin & Mirkin, 1995; Abdullin et al., 2003; Nezdymyminoga, 2010; Suyundukov et al., 2010).

Experimental restoration of natural system solves the problems of nature conservation. It also contributes into the maintenance of biodiversity of zonal vegetation

types and agricultural landscapes (species and pasture communities) (Isselstein et al., 2005; Plantureux et al., 2005).

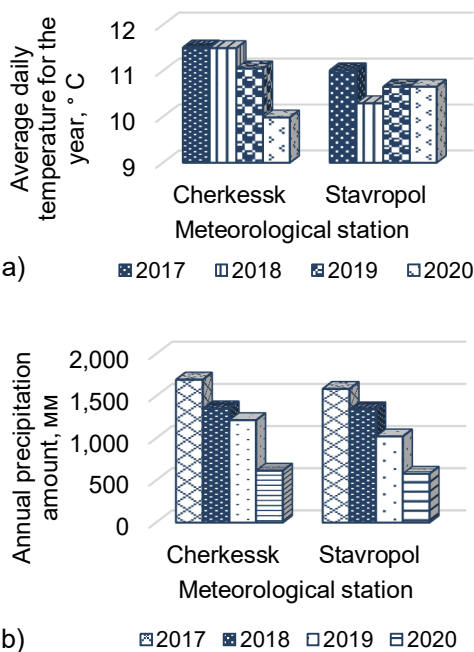
A 25-year experiment on reciprocal replanting of sod blocks following the gradient of snow cover thickness and reducing vegetation period along the slope of Mount Malaya Khatipara, Karachay-Cherkess Republic, Russia, has been conducted since 1988 in the Teberda Nature Reserve. It was studied the rate of microsuccessions that is the structure and flora saturation of alpine phytocenoses restoration. It has been shown that the higher the difference amounts between donor and acceptor communities, the higher the rate of succession in transplanted sod blocks. Abiotic conditions are also influential (Kipkeev et al., 2015).

The sod method is widely exploited in landscape design. Z.V. Dutova used forbbed-grassed steppe sod adding 20 perennial introduced species when creating landforms in city of Pyatigorsk (Dutova, 2019).

The purpose of the article is to evaluate the biodiversity of recreated artificial steppe agricultural landscape of the Stavropol Botanical garden.

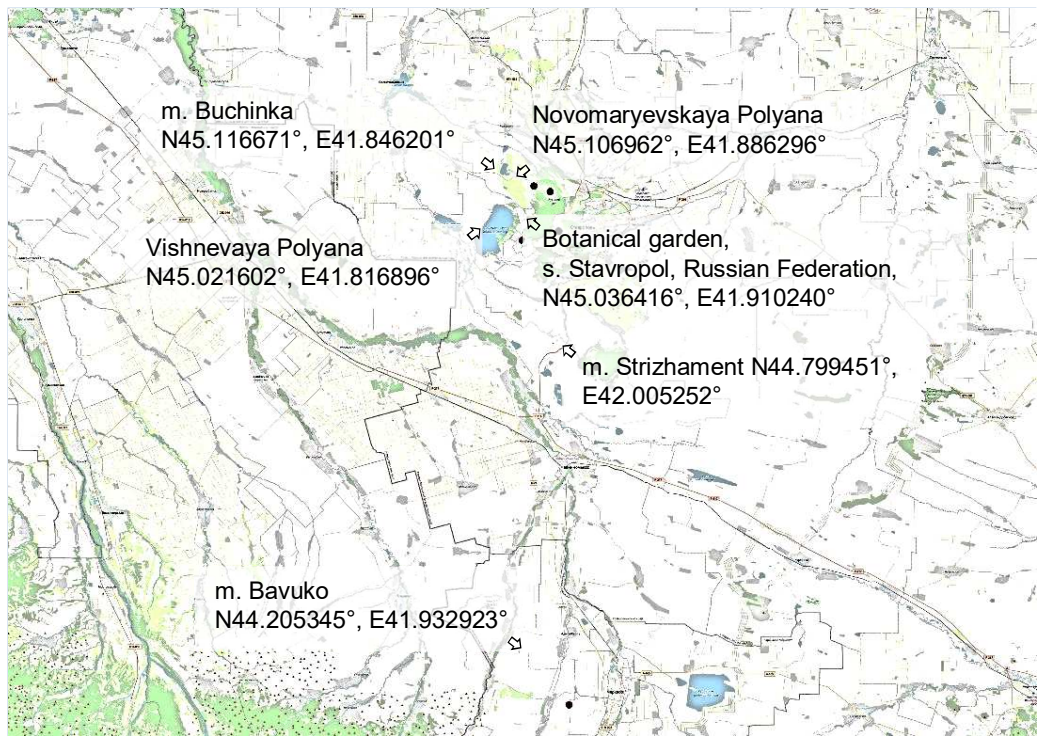
## MATERIALS AND METHODS

The recreated meadow steppe area is located in the Botanical garden in Stavropol, Russian Federation, (N45.036416°, E41.910240°) 640–660 m above sea level in unstable humidity zone HTC 1.00–1.09 with an average annual temperature 9.7–11.0 °C; the coldest month is January when the temperature reaches 4.9° below 0° degree C, the warmest month is July with the average temperature 19.6° above 0° degree C, absolute temperature minimum is 31° below 0° degree C, absolute temperature maximum is 39.7° above 0° degree C in August. The average annual precipitation is 633–720 mm. The sum of temperatures above 10 °C is 3,300–3,650 °C. The soil is leached degraded chernozems. The humus horizon depth is 31–45 cm. The upper Kholodnorodnikovsky horizon of the Stavropol Formation, which is composed of limestones, shell rocks, sandstones and sands, is located in Stavropol and its suburbs withing the research sites. Its depth varies. Thus, under the restored meadow steppes areas shell rock is found at a depth of 35 to 100 cm, while in the research sites in nature it is located at a depth of 10 to 30 cm, often with an exit to the surface. (Shalnev & Oleinikova, 2010). The weather conditions in 2017–2020 (Fig. 1) are characterized



**Figure 1.** Weather conditions of meteorological stations in the places of research performance by years (a – average annual temperature, b – total annual precipitation).

by higher daily average temperatures in Stavropol that amounts to 7.5° above C compared to average multi-year ones (+8.3 °C) in Cherkessk ranged from +9.9 °C to +11.5 °C. Total precipitation in Stavropol varies from 578.2 mm (2020) to 1,584.8 mm (2017) with the average annual norm of 720 mm. In Cherkessk precipitation ranged from 615.0 mm (2020) to 1,694.8 mm (2017) that is below the average annual norm. According to both weather stations, precipitation in 2020 was less than the multi-year average, and the summer period was characterized by prolonged droughts (SCH, 2021). The material for sod blocks planting was prepared in 1963–1984 from previously studied natural zonal meadow-steppe virgin lands with a typical floral composition located in the natural boundaries Vishnevaya (N45.021602°, E41.816896°) and Novomaryevskaya Polyana (N45,106962°, E41,886296°), mountains Strizhament (N44.799451°, E42.005252°), Buchinka (N45.116671°, E41.846201°) in Stavropolskiy Kraii and mount Bavuko (N44.205345°, E41.932923°) in the Karachay-Cherkess Republik, Russian Federation (Fig. 2). (Skripchinsky et al., 1971; Skripchinsky, 1973).



**Figure 2.** Coordinates of research sites in the Stavropol Territory and the Karachay-Cherkess Republic, Russia.

Planting was carried out in the botanical garden on a plot with soil specially prepared by dead fallow type alongside with preliminary autumn plowing followed by spring and summer peeling, and 3–4 cultivations. In the experimental field, harvested blocks of sod were planted on model plots corresponding to the origin place name: in 1963 it was ‘Vishnevaya Polyana’ with 1,210 m<sup>2</sup> area; in 1967–1968 it was ‘Strizhament’ with 5,240 m<sup>2</sup> area. The ‘Bavuko’ site (1,100 m<sup>2</sup>) was laid in 1975–1979,

‘Novomaryevskaya Polyana’ (4,000 m<sup>2</sup>) in 1967–1970, ‘Buchinka’ (2,200 m<sup>2</sup>) in 1984. The prepared blocks of sod were transported to the experimental site and placed in the appropriate size excavated holes by hand, followed by rolling and watering. Average size of harvested sod blocks was 27.9×23.5 cm with a thickness of 27.0–19.4 cm. Planting density variants were 60×60 cm, 1×1 m (with alternating uncovered sod soil in a staggered pattern), and solid arrangement (control) (Dudar, 1976). No additional replanting or reseeding was carried out. During the first two to three years after planting (until the uncultivated soil overgrown with sod), hand pulling with removal of weeds and irrigation were performed (Dudar, 1976). The total area of the recreated steppe is 2 ha. The options for maintaining recreated cenoses are: a) annual single mowing is carried out on 77.7% of the territory, b) without mowing on 22.3% (protected area). All studies cited in this article were conducted both in nature and in experimental sites. Evaluation of species saturation was carried out on 100 m<sup>2</sup> during the maximum grass stand development period. The biomorphs determination is based on the Ch. Raunkiaer classification (Raunkiaer, 1937; ‘Field geobotany’, 1964). According to the standard methodology, grass stand yield was measured once during the vegetation period on the sample area of 0.5×1.0 m in sixfold replications. Botanical analysis by crop groups was performed (Dudar, 1976; Kutuzova et al., 2015).

For statistical processing we used the package of variance analysis included in the Microsoft Excel program to calculate the null hypothesis deviation (*P-value*) at the level of significance ( $\alpha$ ) 0.05 (Kosova et al., 2015). Latin plants names are given according to ‘The Plant List’ (TPL, 2010).

## RESEARCH RESULTS

Nowadays, the formed artificial cenosis in the Stavropol Botanical garden is a multi-species community with a predominance of *Brachypodium rupestre* (Host) Roem. et Schult., 1817; *Briza media* L., 1753; *Bromus riparius* Rehm., 1872; *Carex humilis* Leyss., 1761; *Chamaecytisus ruthenicus* (Fisch. ex Wol.) Klásk., 1958; *Festuca rupicola* Heuff., 1858; *Festuca valesiaca* Schleich. ex Gaudin, 1811; *Genista tinctoria* L., 1753; *Medicago caerulea* Less. ex Ledeb., 1842; *Medicago falcata* L., 1753; *Phleum phleoides* (L.) H. Karst, 1880; *Rosa spinosissima* L., 1753; *Securigera varia* (L.) Lassen, 1989; *Stipa pulcherrima* K. Koch, 1848; *Trifolium medium* L., 1753; *Trifolium alpestre* L., 1763; *Trifolium ambiguum* M. Bieb., 1808; *Trifolium montanum* L., 1753; *Trifolium repens* L., 1753; *Vicia tenuifolia* Roth, 1788; *Vicia cracca* L., 1753.

The flora of the recreated cenoses includes 236 species belonging to 149 genera and 35 families. Of these, the share of dicotyledons (*Magnoliopsida* Brongn., 1843) accounts for 201 species (85.2%), monocotyledons (*Liliopsida* Batsch, 1802) justifies 35 species (14.8%). The largest families including more than half of the species composition are *Apiaceae* Lindl., 1836; *Asteraceae* Bercht & J.Presl, 1820; *Lamiaceae* Martinov, 1820; *Poaceae* Barnhart, 1895; *Rosaceae* Juss., 1789, which correlates with the typical spectrum of boreal territories of the Holarctic kingdom (Takhtadzhyan, 1978). Floristic groups of cenosis include cereals and sedges - 32 species (13.5%), legumes - 28 (11.9%), wild grasses - 176 (74.6%) (Table 1).



**Table 1.** Systematic analysis of the restored meadow steppes plants

No. Families	Number		Share, %	No.	Families	Number		Share, %
	genera	species				genera	species	
1. <i>Asteraceae</i> Bercht & J.Presl, 1820	27	40	17.0	19.	<i>Orchidaceae</i> Juss., 1789	2	3	1.3
2. <i>Poaceae</i> Barnhart, 1895	18	30	12.7	20.	<i>Scrophulariaceae</i> Juss., 1789	2	3	1.3
3. <i>Apiaceae</i> Lindl., 1836	12	28	11.9	21.	<i>Asparagaceae</i> Juss., 1789	2	2	0.8
4. <i>Lamiaceae</i> Martinov, 1820	14	18	7.6	22.	<i>Brassicaceae</i> Burnett, 1835	2	2	0.8
5. <i>Rosaceae</i> Juss., 1789	10	15	6.4	23.	<i>Cyperaceae</i> , Juss., 1789	1	2	0.8
6. <i>Apiaceae</i> Lindl., 1836	10	11	4.7	24.	<i>Gentianaceae</i> Juss., 1789	2	2	0.8
7. <i>Plantaginaceae</i> Juss., 1789	3	10	4.2	25.	<i>Linaceae</i> DC. ex Perleb, 1818	1	2	0.8
8. <i>Caryophyllaceae</i> Juss., 1789	5	9	3.8	26.	<i>Polygalaceae</i> Hoffmanns. et Link., 1809	1	2	0.8
9. <i>Ranunculaceae</i> Juss., 1789	4	6	2.6	27.	<i>Violaceae</i> Batsch, 1802	1	2	0.8
10. <i>Rubiaceae</i> Juss., 1789	3	7	3.0	28.	<i>Convolvulaceae</i> Juss., 1789	1	1	0.4
11. <i>Boraginaceae</i> Juss., 1789	3	6	2.5	29.	<i>Geraniaceae</i> Juss., 1789	1	1	0.4
12. <i>Caprifoliaceae</i> Juss., 1789	4	5	2.1	30.	<i>Hypericaceae</i> Juss., 1789	1	1	0.4
13. <i>Iridaceae</i> Juss., 1789	3	5	2.1	31.	<i>Liliaceae</i> Juss., 1789	1	1	0.4
14. <i>Orobanchaceae</i> Vent., 1799	5	5	2.1	32.	<i>Polygonaceae</i> Juss., 1789	1	1	0.4
15. <i>Apocynaceae</i> Juss., 1789	2	4	1.7	33.	<i>Primulaceae</i> Batsch ex Borkh., 1963	1	1	0.4
16. <i>Amaryllidaceae</i> J.St.-Hil., 1968	1	3	1.3	34.	<i>Rutaceae</i> Juss., 1789	1	1	0.4
17. <i>Campanulaceae</i> Juss., 1789	1	3	1.3	35.	<i>Santalaceae</i> R.Br., 1810	1	1	0.4
18. <i>Euphorbiaceae</i> Juss., 1789	1	3	1.3	36.	<i>Paeoniaceae</i> Raf., 1815	1	1	0.4
Total:						149	236	100

In accordance with the classification of Ch. Raunkier, the species of the restored cenoses can be attributed to five biormorphs: Ph – phanerophytes (arboreal), Ch – hamephites (shrubs), HC – hemicryptophytes (perennial grasses, rosete-forming biennials, winter-annuals), C – cryptophytes (bulbous crops, root crops, tuberous plants) and T – therophytes (annuals) (Raunkiaer, 1937) (Table 2).

The biormorph range of the of restored meadow steppes in terms of quantitative composition has a high degree of similarity with steppes of the Central Fore-Caucasus ( $r = 0.99$ ). In both cases, in the meadow steppes cenoses the hemicryptophytes dominance of grasses whose renewal buds are located near the soil surface is preserved.

**Table 2.** Comparative indices of the flora biomorphological spectrum of the restored meadow steppe and Central Fore Caucasus meadow steppes

Plants communities	Parameters	Biomorph					Total
		Ph	Ch	HK	K	T	
Restored meadow steppe	Species number	7	7	176	12	34	236
	percentage	2.9	3.0	74.6	5.1	14.4	100%
Meadow steppes of Central Caucasus	percentage	2.4	1.8	69.1	4.9	21.8	100%

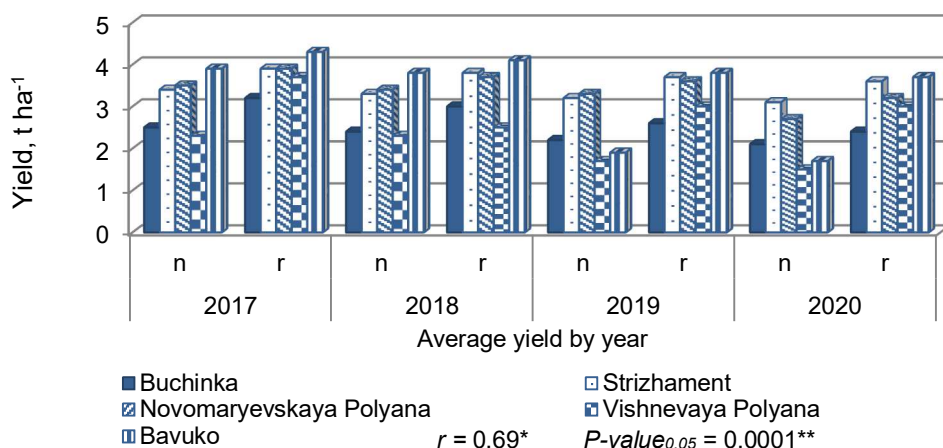
Similarity degree in species composition to the steppes of Central Caucasus  $r = 0.99^*$ ;

\* $r$  – correlation coefficient.

Another indicator of the proximity of the restored meadow-steppe cenoses flora to natural virgin lands is the predominance of perennials in its life cycles species which accounts for 81%, annuals and biennials make up only 19%. The current ratio indicates a significant phytocenotic isolation and stability of the grass stand species composition, and its ability to resist the introduction of invasive species.

The grass stand of the restored cenoses is closed with a height of 85.0–135.0 cm (in nature it reaches 65.0–95.0 cm). The projection coverage is 75–100%. There are 109 species per 100 m<sup>2</sup> of individual model cenoses: Strizhament includes 109 species; Vishnevaya Polyana has 78 species; Novomaryevskaya Polyana amounts to 79 species; Buchinka has 84 species; Bavuko accounts for 73 species.

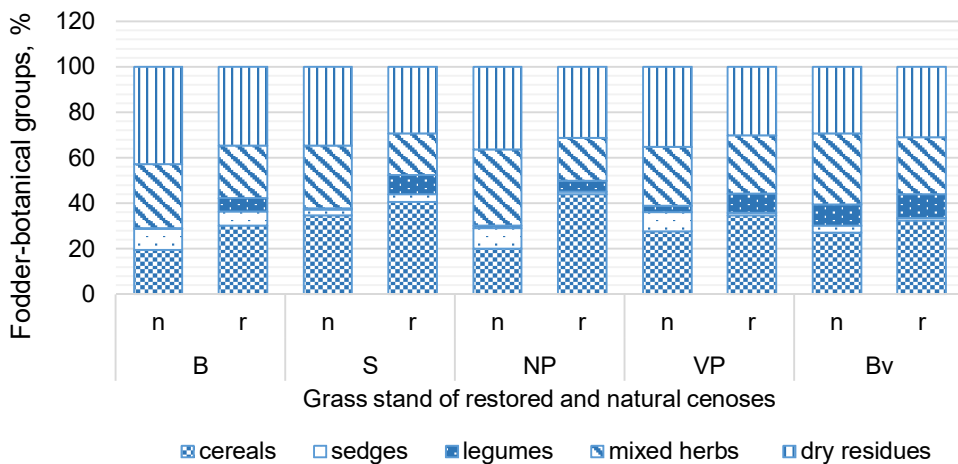
The average yield of restored steppes grass stand in 2017–2020 is 2.8 t ha<sup>-1</sup> in Buchinka and 3.8 t ha<sup>-1</sup> in Strizhament and Novomaryevskaya Polyana. It exceeds the yield indicators of similar cenoses in nature representing 2.1 t ha<sup>-1</sup> in Vishnevaya Polyana, and 3.3 t ha<sup>-1</sup> in Bavuko, the correlation coefficient is 0.69. It is shown that at the significance level ( $\alpha$ ) of 0.05 there are reliable differences between the average values in the variants (nature and restored steppe), ( $P$ -value is 0.0001). It has been noted that the amount of the grass stand yield decreases with the lowering of precipitation values from 2.3–3.9 t ha<sup>-1</sup> (nature), 3.2–4.4 t ha<sup>-1</sup> (restored) in 2017 to 1.5–3.1 t ha<sup>-1</sup> (nature), 2.4–3.7 t ha<sup>-1</sup> (restored) in 2020. The correlation coefficient is  $r = 0.9$  (Fig. 3).



\* $r$  – correlation coefficient, \*\* $P$ -value<sub>0.05</sub> – null hypothesis deviations.

**Figure 3.** An average grass stand yield in natural and restored steppes in 2017–2020 (n – natural steppes; r – restored area).

The analysis of the fodder-botanical groups in the grass stand of the restored and natural steppes showed that samples were dominated by cereals 19.6–43.9% and mixed herbs 18.3–31.2%, in all cases. Sedges make up only 1.1%, while legumes account for 0.3% (Fig. 4). The share of sedges and dry residues in natural cenoses is higher than in restored ones. While conducting the variance analysis it was found that the natural and climatic features of the restored cenoses are more significant for higher yields of cereals and legumes botanical groups (for cereals at the significance level ( $\alpha$ ) of 0.05  $P$ -value is 0.024, for legumes at the significance level ( $\alpha$ ) of 0.05  $P$ -value is 0.03. On the contrary, natural steppes conditions (at the same level of significance ( $\alpha$ ) of 0.05 the  $P$ -value is 0.009 are more significant for the value of mixed herbs productivity. No significant differences were found for the other groups.



Cereals  $P$ -value<sub>0.05</sub> = 0.024, sedges  $P$ -value<sub>0.05</sub> = 0.062, legumes  $P$ -value<sub>0.05</sub> = 0.030, mixed herbs  $P$ -value<sub>0.05</sub> = 0.009, dry residues  $P$ -value<sub>0.05</sub> = 0.095.\*

\* $P$ -value<sub>0.05</sub> – null hypothesis deviations.

**Figure 4.** Economic and botanical grass stand groups of restored and natural cenoses as a percentage of the air-dry mass sample, % (n – natural steppes; r – restored area; B – Buchinka; S – Strizhament; NP – Novomaryevskaya Polyana; V – Vishnevaya Polyana; Bv – Bavuko).

Phytocenoses with a diverse set of life forms such as shrubs, semi-shrubs, perennial and annual grasses have the highest phytomass biological productivity and yield. These communities, due to the location of above-ground organs at different heights and their roots at different depths of soil horizons, have more densely packed ecological niches, they are better adapted to the ecological features of the habitat and make better use of the environment resources (Mirkin et al., 2002).

Flora of the restored meadow steppes of the botanical garden is rich in plants with useful properties: 29 species are forage plants, 65 – medicinal, 48 – nectariferous, 6 – food, 23 – ornamental:

## Forage

**Cyperaceae:** *Carex humilis* Leyss., 1761.

**Fabaceae:** *Anthyllis vulneraria* subsp. *polyphylla* DC. 1825; *Lotus corniculatus* L., 1753; *Medicago caerulea* Less. ex Ledeb., 1842; *Medicago falcata* L., 1753; *Medicago sativa* L., 1753; *Onobrychis inermis* Steven, 1856; *Securigera varia* (L.) Lassen, 1989; *Trifolium alpestre* L., 1763; *Trifolium ambiguum* M.Bieb., 1808; *Trifolium medium* L., 1753; *Trifolium montanum* L. 1753; *Trifolium repens* L. 1753; *Vicia cracca* L. 1753; *Vicia tenuifolia* Roth, 1788.

**Poaceae:** *Brachypodium rupestre* (Host) Roem. et Schult. 1817; *Bromus inermis* Leyss., 1973; *Bromus inermis* Leyss., 1973; *Bromus riparius* Rehmann, 1872; *Dactylis glomerata* L. 1753; *Elymus hispidus* (Opiz) Melderis, 1978; *Festuca pratensis* Huds. 1762; *Festuca rupicola* Heuff., 1858; *Festuca valesiaca* Schleich. ex Gaudin, 1811; *Koeleria pyramidata* (Lam.) P.Beauv., 1812; *Phleum phleoides* (L.) H. Karst., 1880; *Phleum pratense* L., 1753; *Poa compressa* L. 1753.

## Medicinal

**Apiaceae:** *Daucus carota* L., 1753.

**Asteraceae:** *Achillea nobilis* L., 1753; *Achillea millefolium* L., 1753; *Artemisia absinthium* L., 1753; *Cichorium intybus* L., 1753; *Tanacetum vulgare* L., 1753.

**Caprifoliaceae:** *Valeriana officinalis* L., 1735.

**Fabaceae:** *Anthyllis vulneraria* subsp. *polyphylla* (DC.), 1825; *Melilotus officinalis* (L.) Pall., 1778; *Trifolium pratense* L., 1753.

**Gentianaceae:** *Gentiana cruciate* Juss, 1789; *Centaurium littorale* (Turner) Gilmour, 1937.

**Hypericaceae:** *Hypericum perforatum* L., 1753.

**Lamiaceae:** *Origanum vulgare* L., 1753; *Stachys officinalis* (L.) Trevis., 1842; *Thymus pulegioides* subsp. *pannonicus* (All.) Kerguelen, 1993.

**Orobanchaceae:** *Euphrasia tatarica* Fisch. ex Spreng., 1825.

**Paeoniaceae:** *Paeonia tenuifolia* L., 1759.

**Plantaginaceae:** *Plantago lanceolata* L., 1753; *Plantago major* L., 1753; *Veronica chamaedrys* L., 1753.

**Primulaceae:** *Primula veris* L., 1753.

**Ranunculaceae:** *Adonis vernalis* L., 1753; *Thalictrum foetidum* L. 1753; *Thalictrum minus* L., 1753.

**Rosaceae:** *Agrimonia eupatoria* L., 1753; *Crataegus curvisepala* Lindm., 1918; *Crataegus monogyna* Jacq., 1775; *Filipendula vulgaris* Moench, 1794; *Fragaria viridis* Weston, 1771; *Potentilla argentea* L., 1753; *Rosa canina* L., 1753, *Rosa spinosissima* L., 1753.

**Rubiaceae:** *Dictamnus albus* L., 1753.

**Violaceae:** *Viola arvensis* Murray, 1770.

## Nectariferous

**Asteraceae:** *Achillea millefolium*; *Achillea nobilis*.

**Boraginaceae:** *Echium vulgare* L., 1753.

**Caprifoliaceae:** *Valeriana officinalis*.

**Euphorbiaceae:** *Euphorbia iberica* Boiss., 1860; *Euphorbia stepposa* Zoz ex Prokh., 1949.

**Fabaceae:** *Anthyllis vulneraria* subsp. *polyphylla*; *Chamaecytisus ruthenicus* (Fisch. ex Wol.) Klask., 1958; *Genista tinctoria* L., 1753; *Lotus corniculatus*; *Medicago falcata*; *M. caerulea*; *M. sativa*; *Melilotus officinalis*; *Onobrychis inermis*; *Securigera varia*; *Trifolium alpestre*; *T. ambiguum*; *T. medium*; *T. repens*; *Vicia cracca*; *V. tenuifolia*.

**Lamiaceae:** *Origanum vulgare*; *Lamiun album* L., 1753; *Thymus pulegioides* subsp. *pannonicus*.

**Plantaginaceae:** *Plantago lanceolata*, *P. major*,

**Rosaceae:** *Crataegus curvisepala*; *C. monogyna*; *Crataegus pentagyna* Waldst. & Kit., 1799; *Filipendula vulgaris*; *Fragaria viridis*; *Malus orientalis* Uglitzk., 1932; *Potentilla argentea*; *Pyrus communis* Fritsch, 1892; *Rosa canina*, *Rosa spinosissima* L., 1753.

### Food

**Rosaceae:** *Crataegus curvisepala*; *Crataegus pentagyna*; *Fragaria viridis*; *Malus orientalis*; *Pyrus communis*.

### Ornamental

**Asparagaceae:** *Muscari racemosum* (L.) Lam. & DC., 1806.

**Asteraceae:** *Centaurea dealbata* Willd., 1803; *Leucanthemum vulgare* (Vail.) Lam., 1779; *Pyrethrum corymbosum* (L.) Scop., 1844;

**Caprifoliaceae:** *Dianthus armeria* L., 1753; *Dianthus capitatus* Balb. ex DC., 1813.

**Fabaceae:** *Chamaecytisus ruthenicus*; *Genista tinctoria*.

**Geraniaceae:** *Geranium sanguineum* L., 1753.

**Iridaceae:** *Crocus reticulatus* Steven ex Adam, 1805; *Crocus speciosus* M.Bieb., 1800; *Gladiolus tenuis* M. Bieb., 1808; *Iris aphylla* L., 1753.

**Lamiaceae:** *Dracocephalum austriacum* L., 1753.

**Orchidaceae:** *Orchis morio* L. subsp. *picta* (Loisel.) K. Richt. 1890; *Orchis tridentata* Scop., 1772; *Platanthera chlorantha* (Custer) Rehb., 1829.

**Paeoniaceae:** *Paeonia tenuifolia*.

**Poaceae:** *Stipa pennata* L., 1753; *Stipa pulcherrima* K. Koch, 1848.

**Primulaceae:** *Primula veris*.

**Ranunculaceae:** *Adonis vernalis*; *Anemonoides caucasica* Willd. ex Rupr., 1869.

**Rosaceae:** *Rosa canina*; *Rosa spinosissima* L.

**Rutaceae:** *Dictamnus albus*.

18 protected plant species listed in the ‘Red Book of the Stavropolskii Krai’ grow on the restored meadow-steppe cenoses (RDBSK, 2013), 10 of which are listed in the ‘Red Book of the Russian Federation’ (RDBRF, 2008) (Table 3). According to the ‘Red Book of Stavropolskii Krai’, two taxa are considered endangered (category 1). There are six vulnerable species (category 2) are six. The rest ones belong to species with decreasing numbers (category 3).

Ten rare species are also represented in the ‘Red Book of the Russian Federation’: 4 as vulnerable species, 6 as species with decreasing numbers. The most abundant rare species in the cenoses are represented by 28–40 samples. Their populations are quite vital, full-membered, most plants are in the generative phase (Rabotnov, 1950), they bloom and bear fruit, and form self-seeding.

Most of the plants are randomly located and preserved at the sites of mount Strizhament, mount Buchinka, natural boundaries Novomaryevskaya Polyana, and

Vishnevaya Polyana. Species with abundance of 5–12 specimens are predominantly found on the sites of mount Strizhament, and Vishnevaya Polyana. A number of ornamental and medicinal plants such as *Adonis vernalis*, *Gymnadenia conopsea*, *Iris aphylla*, *Paeonia tenuifolia*, *Platanthera chlorantha*, *Orchis picta* periodically reduce their amount due to being picked up by visitors.

**Table 3.** Rare and endangered species in artificially recreated cenoses

№ Species name	Predominant age groups	Amount of samples	Category of rarity status in the Red Book		Allocation to the model restored cenoses
			The Russian Federation	Stavropolskii Krai	
1. <i>Colchicum laetum</i> Steven, 1829	g <sub>2</sub>	40	3	3	Vishnevaya Polyana
2. <i>Gladiolus tenuis</i> M.Bieb., 1808	g <sub>1-2</sub>	37	-	2	Novomaryevskaya Polyana, Strizhament, Buchinka
3. <i>Anemone caucasica</i> Willd. ex Rupr., 1869	g <sub>1-2</sub>	28	-	2	Novomaryevskaya, Vishnevaya Polyana
4. <i>Diphelypaea coccinea</i> (M.Bieb.) Nicolson, 1975	g <sub>1-2</sub>	12	-	3	Strizhament, Vishnevaya Polyana
5. <i>Neotinea tridentata</i> (Scop.) R.M.Bateman, Pridgeon & M.W.Chase, 1997	g <sub>2</sub>	11	3	3	Strizhament, Novomaryevskaya Polyana,
6. <i>Crocus speciosus</i> M.Bieb., 1800	g <sub>1-2</sub>	8	2	1	Strizhament, Vishnevaya Polyana
7. <i>Iris aphylla</i> L., 1753	g <sub>1</sub>	7	2	3	Novomaryevskaya Polyana,
8. <i>Stipa pulcherrima</i> K.Koch, 1848	g <sub>1-2</sub>	6	3	2	Strizhament
9. <i>Iris spuria</i> subsp. <i>notha</i> (M.Bieb.) Asch. & Graebn., 1906	g <sub>1</sub>	6	2	2	Strizhament
10. <i>Stipa pennata</i> L., 1753	g <sub>1-2</sub>	5	3	2	Vishnevaya Polyana
11. <i>Dactylorhiza viridis</i> (L.) R.M.Bateman, Pridgeon & M.W.Chase, 1997	ss	5	-	3	Novomaryevskaya Polyana,
12. <i>Platanthera chlorantha</i> (Custer) Rchb., 1829	v	4	-	3	Novomaryevskaya Polyana,
13. <i>Gymnadenia conopsea</i> (L.) R.Br., 1813	v	4	3	3	Strizhament
14. <i>Adonis vernalis</i> L., 1753	g <sub>2</sub>	3	-	3	Novomaryevskaya Polyana,
15. <i>Orchis picta</i> Raf., 1808	g <sub>1</sub>	3	3	3	Novomaryevskaya Polyana, Strizhament
16. <i>Paeonia tenuifolia</i> L., 1759	g <sub>1-2</sub>	3	2	3	Novomaryevskaya Polyana,
17. <i>Campanula persicifolia</i> L., 1753	g <sub>2</sub>	3	-	2	Strizhament
18. <i>Crambe tatarica</i> Sebeók, 1799	g <sub>1</sub>	3	-	1	Strizhament

### **Economic efficiency**

According to the modern prices, calculation of economic efficiency of meadow steppes restoring by sod blocks planting method has shown that when performing all the required agrotechnical techniques for preparing soil, harvesting, planting and watering of the planted sod blocks the cost of establishing of 1 ha of conducted experiment (excluding further maintenance work) was €33,157.7 (at a rate of 87.0748 roubles for 1 euro under federal standards) (TUP, 2014, CRB, 2021). In accordance with our data, average hay yield per hectare is 2.8–3.8 t ha<sup>-1</sup>, which in money equivalent, at a rate of €57.4 per 1 ton of hay in Stavropolskii Krai, amounts to €160.8–218.2 a year for an annual average hay yield per 1 ha cost. Thus, estimated period of covering the performed work on the restoring meadow steppe by sod block planting method (excluding weeding and watering) is 152.0–206.3 years.

## **CONCLUSIONS**

Long-term experience on experimental phytocenology of botanical garden showed that when restoring steppe sites by planting sod blocks only zonal vegetation types should be used to preserve the biodiversity of the original natural cenosis. It is important that the area of experimental planting meets the same soil-ecological conditions in which the steppe-standard plot was formed. Some attempts to recreate in the botanical garden cenoses from other soil and climatic zones such as dry, feather-grass steppes, subalpine meadow have resulted in gradual destruction of these communities. Mesophilic species were progressively introduced into the dry steppes restored cenoses, while xerophilic species fell out.

Eventually, species of subalpine meadows also fell out, and the experimental sites were overgrown with rhizomatous grasses (FECC, 2020). Meadow steppes recreated in 1963–1984 in the Stavropol Botanical Garden by sod blocks planting on an area of 2 hectares have preserved species composition close to the zonal steppes till nowadays and are being a reserve of their biological diversity, including wild relatives of cultivated forage, medicinal, food plants, and rare species. Current flora of restored meadow steppes cenoses includes 236 species belonging to 149 genera and 35 families. Its 5 biomorphs comprise 2.9% of phanerophytes, 3.0% of chamephytes, 74.6% of hemicryptophytes, 14.4% therophytes that have a high degree of similarity in quantity to the steppes of Central Fore-Caucasus. The cenoses are dominated by plants having life cycles of perennial ones which account for 81.0%, annuals and biennials make up 19.0%, cereals and sedges amount to 32 species (13.5%), legumes represent 28 species (11.9%), mixed herbs are 176 (74.6%).

The species composition of the restored cenoses is greatly influenced by the correlation with the soil horizon heights of donor and acceptor communities. Apparently, a higher grass stand yield in experimental meadow steppe cenoses can be explained by the high thickness of the soil horizon which reaches 1 m in some places (variations of 35–100 cm). In nature it is usually equal 10–30 cm.

To prevent grass stand degradation the maintenance mode of restored steppe should include annual mowing. It is important to improve recultivation methods of sod extraction sites. The necessity of studying the natural cenoses restoration methods by scientists of Stavropolskii Krai is dictated by the high degree of economic development of its territory. The natural plant communities of the north-eastern and eastern part of the

region's lowlands are 70% or more plowed up. Significant disturbance of vegetation is noted in other zones of the area as well. The surviving remnants of virgin lands are mostly located on erosion-hazardous elements of the terrain that are not suitable for arable farming.

The sod blocks planting method has recently found an application in experimental phytocenology and landscape design. Restoration of natural vegetation by sod blocks planting in large areas is quite time-consuming and expensive compared to agropasture method. Therefore, it can only be used in a limited way in small areas as a component of combined options.

## REFERENCES

- Abdullin, M.R. & Mirkin, B.M. 1995. The experience of creating "agrosteps" in the Bashkir steppe Trans-Urals. *Bulletin of the MOIP. Department of Biology* **100**(5), 77–90 (in Russian).
- Abdullin, M.R., Mirkin, B.M. & Suyundukov, Ya.T. 2003. Restoration of the biodiversity of the steppes of Bashkortostan. *Bulletin of the Academy of Sciences of the Republic of Belarus* **8**(4), 9–15 (in Russian).
- Archer, S. & Bunch, K. 1955. Meadows and pastures of America. *Publishing House of Foreign literature*. Moscow, 106–124 (in Russian).
- Cottam, G. & Wilson, H.C. 1966. Community dynamics on an artificial prairie. *Ecology*. **47**(1), 88–96.
- Dudar, Y.A. 1976. Guidelines for the restoration and study of herbaceous plant communities. Stavropol: SNIISKH, pp. 58 (in Russian).
- Dutova, Z.V. 2019. The use of local flora species as a basis for planting in a natural style on the example of naturalistic plantings of the Perkalsky Dendrological Park. *Science news in the agro-industrial complex* **1–2**(12), 128–132 (in Russian).
- Dzybov, D.S. 2010. Agrostepes. Stavropol: *AGRUS*, pp. 265 (in Russian).
- Dzybov, D.S. 2018. Vegetation of the Stavropol Krai. Stavropol: *AGRUS*, pp. 492 (in Russian).
- Field geobotany. 1964. Moscow-Leningrad: Nauka, Vol. III. pp. 530 (in Russian).
- Isselstein, J., Jeangros, B. & Pavlu, V. 2005. Agronomic aspects of biodiversity targeted management of temperate grasslands in Europe. *Agronomy research* **3**(2), 139–151.
- Kipkeev, A.M., Cherednichenko, O.V., Tekeev, D.K. & Onipchenko, V.G. 2015. Rate of microsuccessions: Structure and floristic richness recovery after sod transplantation in alpine plant communities *Biology Bulletin Reviews* **76**(6), 461–474 (in Russian).
- Kondratyuk, E.M. & Chuprina, T.T. 1989. Creation of artificial steppe communities in the Donbass. *Recommendations*. Donetsk, pp. 21 (in Russian).
- Kononov, V.N. 1940. Spring change of aspects in the steppe areas of the vicinity of Voroshilovsk. *Proceedings of the Voroshilovsky Pedagogical Institute*. Voroshilovsk, Vol. **2**, 209–212 (in Russian).
- Kosova, E.N., Katkov, K.A., Velts, O.V., Pletukhina, A.A., Servetnik, O.L. & Khvostova, I.P. 2015. Computer technologies in scientific research. *Textbook*. Stavropol, pp. 241 (in Russian).
- Kozhevnikov, V.I., Grechushkina-Sukhorukova, L.A., Peshchanskaya, E.V. & Isaenko, T.N. 2012. Experience of meadow-steppe cenoses restoration in the Stavropol Botanical Garden by sod planting method. *Kormoproizvodstvo* **7**, 13–15 (in Russian).
- Kutuzova, A.A., Privalova, K.N. & Georgiadi, N.I. 2015. Methodology for the effective development of multivariate technologies for improving hayfields and pastures in the Northern Natural and Economic Region. *Ugreshskaya Printing House*, Moscow, pp. 67 (in Russian).



- Mirkin, B.N., Naumova, L.G. & Solomeshech, A.I. 2002. Modern science of vegetation: *Textbook. Logos*. Moscow, pp. 264 (in Russian).
- Nezdiyminoga, O.V. 2010. Results of the introduction of the agrostep method for restoring vegetation of disturbed forage lands in Central Yakutia. *Theoretical and applied problems of the use, conservation and restoration of biological diversity in grass ecosystems: Materials of the international scientific conference* Stavropol Research Institute of the Russian Agricultural Academy. *AGRUS*, Stavropol, pp. 265–267 (in Russian).
- Plantureux, S., Peeters, A. & McCracken, D. 2005. Biodiversity in intensive grasslands: Effect of management, improvement and challenges. *Agronomy research* **3**(2), 153–164.
- Rabotnov, T.A. 1950. The life cycle of perennial herbaceous plants in meadow cenoses. *Geobotany*. Moscow, Leningrad, Series 3. Iss. 6, 7–204 (in Russian).
- Raunkiaer, Ch. 1937. Plant life forms. Oxford: Clarendon Press, pp. 104.
- Red Data Book of the Russian Federation. 2008. Plants and fungi. *KMK Publishing House*. Moscow, 1, pp. 855 (in Russian).
- Red Data Book of the Stavropol Krai. 2013. Plants. Samara: *Publishing House: LLC ‘DSM’*, 1, pp. 399.
- Shalnev, V.A. & Oleinikova, D.V. 2010. Landscapes of the North Caucasus. *Textbook*. Stavropol. pp. 237 (in Russian).
- Skipchinsky, V.V. 1973. Experience of artificial recreation of destroyed phytocenoses. *Bulletin of the North-Caucasus Scientific Center of Higher School. Natural Sciences*, Rostov-on-Don, 3. 17–20 (in Russian).
- Skipchinsky, V.V., Tanfilyev, V.G., Dudar, Yu.A. & Peshkova, L.I. 1971. Artificial restoration of primary vegetation types as an integral part of natural biogeocenoses. *Botanical Journal* **56**(12), 1725–1789 (in Russian).
- Subdivisions of the Stavropol Center for Hydrometeorology and environmental monitoring. SCH. 2021. <http://stavpogoda.ru/strukt.shtml>. Accessed 26.06.2021.
- Suyundukov, Ya.T., Mirkin, B.M., Abdullin, M.R., Naumova, L.G. & Khasanova, R.F. 2010. The main results of research on the restoration of steppe ecosystems of the Trans-Urals of Bashkortostan. *Theoretical and applied problems of the use, conservation and restoration of biological diversity in grass ecosystems: Materials of the international scientific conference* Stavropol Research Institute of the Russian Agricultural Academy. *AGRUS*. Stavropol, 335–357 (in Russian).
- Takhtadzhyan, A.L. 1978. Floral areas of the Earth. Leningrad, *Science*, pp. 248 (in Russian).
- Tanfilyev, G.I. 1901. The experience of transferring the steppe to Petersburg. *Soil Science* **3**(1), 60–64 (in Russian).
- Territorial unit prices for construction and special construction works. TUP. 2014. *Stavropol Territory. Landscaping. Protective forest plantations*. Stavropol, part 47, pp. 38.
- The Central Bank of the Russian Federation. CRB. 2021. Foreign Currency Market. Available from: [https://cbr.ru/currency\\_base](https://cbr.ru/currency_base). Accessed 05.07.2021.
- The formation of the ecological-cenotic complex and the prospect of its development. FECC. 2020. Under the gen. edit. of Kozhevnikov V.I., Stavropol, pp. 192 (in Russian).
- The Plant List. TPL. 2010. Version 1. *A working list of all plant species*. Published on the Internet; <http://www.theplantlist.org>. Accessed 02.02.2021.

## Concentrations of CO<sub>2</sub> from composting under different treatments

I. Karandušovská<sup>1</sup>, P. Hlinka<sup>2</sup>, D. Páleš<sup>3</sup> and T. Szabóová<sup>1</sup>

<sup>1</sup>Slovak University of Agriculture in Nitra, Faculty of Engineering, Department of Building Equipment and Technology Safety, Tr.A. Hlinku 2, SK94976 Nitra, Slovakia

<sup>2</sup>Local Union of Ponitrie villages for separation and management of waste, Korytovská 20, SK95141 Lužianky, Slovakia

<sup>3</sup>Slovak University of Agriculture in Nitra, Faculty of Engineering, Department of Machine Design, Tr.A. Hlinku 2, SK 94976 Nitra, Slovakia

\*Correspondence: [ingrid.karandusovska@uniag.sk](mailto:ingrid.karandusovska@uniag.sk)

Received: January 28<sup>th</sup>, 2021; Accepted: July 7<sup>th</sup>, 2021; Published: July 21<sup>st</sup>, 2021

**Abstract.** The aim of this study was to analyse the production of CO<sub>2</sub> concentrations in relation to the composting technology used. Three loose piles of bio-waste (V1, V2, V3) were created with the same volume. V1 reference pile was without any treatment. The biological preparation containing probiotic bacteria was added to the pile V2. The pile V3 was treated once a week by turning and watering. The degassing shafts were installed in each pile and the Multigas Monitor 1312 gas analyser with the Multipoint Sampler 1309 were used to measure of gas concentrations during the degradation process. Continuous 24-hour measurements of carbon dioxide concentrations from each pile were performed in the first, fourth, and seventh week of the degradation process to compare the amount of concentrations between piles in those weeks. At the beginning of the process, there were no significant differences in the production of CO<sub>2</sub> concentrations from the monitored piles V1, V2 and V3. In the fourth week, significantly higher values of CO<sub>2</sub> concentrations were recorded from the pile V3 ( $P < 0.05$ ), which was turned and irrigated, than from V1 and V2. At week 7, significant differences were found between all treatments at the significance level ( $P < 0.05$ ), with the highest values from the V3 pile. It has been shown that turning and humidifying results in the highest release of CO<sub>2</sub> into the air, but in a more rapid decomposition of the microorganisms, that reducing the time required to achieve a stable compost product and increasing the efficiency of the composting plant.

**Key words:** composting technology, carbon dioxide in compost, compost properties, environmental impacts, compost moisture.

### INTRODUCTION

The increasing concern with greenhouse gas emissions and nutrients cycling creates a need for cost-effective, practical and environmentally sensible biowaste management strategies (Weidner et al., 2020). One of the easiest ways to treat biodegradable waste is composting. Plant residue material produced compost is an organic fertilizer source and it is commonly used for soil amendments (Akpınar et al., 2019). Improved soil structure

associated with the application of organic substances can help reduce water irrigation requirements during droughts and increase soil moisture retention potential (Eden, 2017). Although the benefits of composting are evident, greenhouse gases can be generated and emitted to the atmosphere during this process, contributing to global warming by producing methane (Sánchez, 2015). The importance of gaseous emissions and odor nuisances from composting plants were reported by several researchers (Nasini et al., 2016; Arriaga et al., 2017). Dhamodharan et al. (2019) have reported the intensity of gas emissions from the composting process depends on three major components, that including the feedstock materials, the composting methodology adopted and the application of final compost. These emissions could be severe if the process is not well operated with proper aeration conditions and with the final compost, when is applied to the soil. However, the proper maintenance would majorly reduce the gas emissions. Previous studies have confirmed that composting reduces, by more than 30%, the volume of organic materials ending up in already overcrowded landfill sites (Hernández-Gómez et al., 2020) and converts waste into a hygienic and valuable product (Asadu et al., 2019; Zhang et al., 2019). It is an effective strategy in terms of diverting organic solid waste from landfills and improving the heating value of feedstock in the event of energy recovery (Vaverková et al., 2020). The waste from animal production, livestock excrements, residues of various crops can be used as a starting material for biogas production (Kažimírová et al., 2018) which is understood as a source of energy with zero carbon dioxide (CO<sub>2</sub>) emissions into the atmosphere (Křištof & Gaduš, 2018). In the present study, the objective was to analyse the CO<sub>2</sub> production in relation to the composting technology used.

## MATERIALS AND METHODS

### Preparation of composting piles and measurement of CO<sub>2</sub> concentrations

An experiment to monitor carbon dioxide concentrations during the composting process was carried out in the summer period from 10<sup>th</sup> June to 2<sup>nd</sup> August 2019. The different organic raw materials (food bio-waste, green waste, garden wastes, tree clippings) were blended in certain ratios and mixed. Three loose piles of bio-waste (V1, V2, V3) were created at once and with the same volume (50 m<sup>3</sup>). In each pile, there was a different technological process of processing waste into compost. The bio-waste in the reference pile V1 was untreated. In the second pile V2, a biological preparation was used to accelerate the degradation process containing probiotic bacteria, namely probiotic cultures of lactic fermentation (*Bacillus subtilis* var natto, *Bifidobacterium animalis*, *Bifidobacterium bifidum*, *Bifidobacterium longum*, *Lactobacillus acidophilus* ...), yeasts (*Saccharomyces cerevisiae*) and organic sugar molasses. The dose was applied in a volume of 2 L m<sup>-3</sup> mixed in 20 liter of water. The V3 pile was treated once a week by turning and watering. The first turning and watering was performed on the fourth day after the pile was founded. The Multigas Monitor 1312 gas analyser, together with the Multipoint Sampler 1309 (Innova, Denmark) were used to measure gas concentrations. The measurement system is based on Photoacoustic Infrared Detection, which delivers the ability to measure virtually any gas that absorbs in the infrared spectrum. These devices were placed in a separate isolated room with a constant temperature in the range of 10–20 °C. The degassing shafts were installed in each pile, which served as places for measuring the concentrations of CO<sub>2</sub>. The PTFE sampling intake tube was introduced to

the measuring points (each degassing shaft to divert landfill gas with the average volume flow  $18 \text{ m}^3 \text{ h}^{-1}$ ) from where the air samples were delivered to the Multipoint sampler and analyser. Continuous 24-hour measurements of carbon dioxide concentrations from each pile were performed always one day in the first, fourth, and seventh weeks of the degradation process to compare the concentrations of  $\text{CO}_2$  between piles in those weeks.

Measuring points:

V1 – measurement in a pile without any treatment

V2 – measurement in a pile with addition of the biological preparation

V3 – measurement in a pile with optimization of process by turning and watering.

We hypothesized that there is no significant difference in  $\text{CO}_2$  concentrations depending on the biowaste treatment technology used during the degradation process.

### **Physical-chemical properties**

During the experiment, the temperature inside each pile was monitored manually every day. The Pfeuffer GT 1 needle thermometer was used to measure compost temperature. The average temperature was determined by taking three measurements at the left, middle, and right side in each pile at 30, 60 and 90 cm depths.

Determination of the compost moisture, pH and C/N nutrient ratio were performed in a certified laboratory. Samples were collected from the left, middle, and right side of each pile at 30, 60 and 90 cm depths. These samples were combined and mixed into one composite sample. The composite samples were collected from each pile at day 7, 28 and 49.

### **Determination of the weight of the final products**

At the end of the composting process, the piles were sieved and weighed to examine the efficiency of each composting process. A Pezzolato drum sorter with a mesh size of 40 mm was used for sieving. The sorter has two belts, where one product falls out, which has been sieved with a fraction smaller than 40 mm and the fraction larger than 40 mm falls up on the other belt. A reinforced concrete bridge scale with a measuring accuracy of 20 kg was used to determine the weight.

### **Statistical analysis**

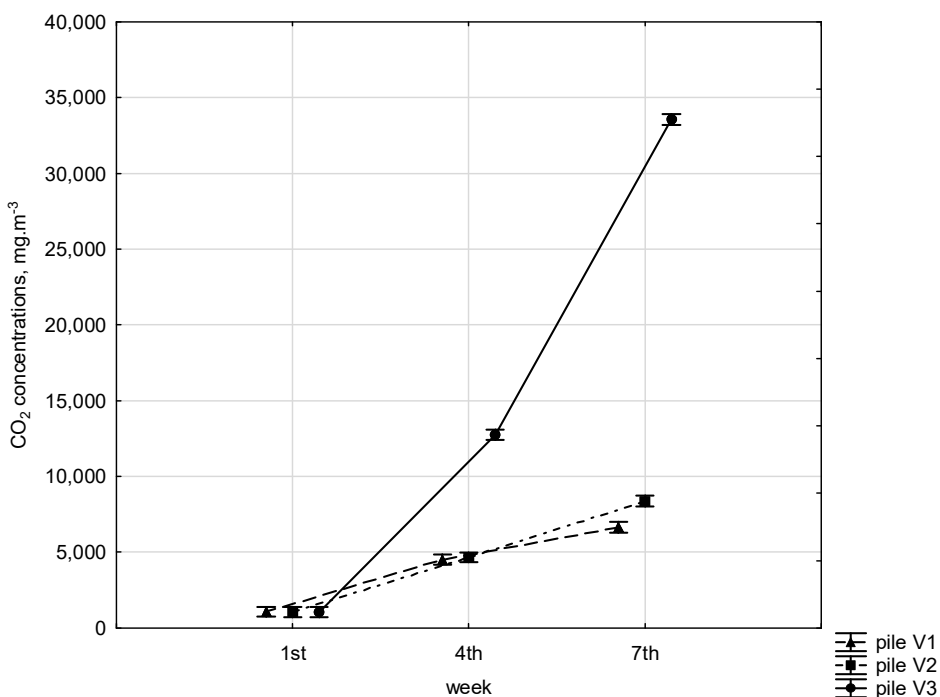
All measured data were subjected to analysis of variance (ANOVA) test in Statistica 10. Post-hoc analysis by Tukey's test (HSD) was used to verify the significance of the differences with a probability level  $\alpha = 0.05$ .

## **RESULTS AND DISCUSSION**

### **$\text{CO}_2$ concentrations from composting**

The range of  $\text{CO}_2$  concentrations varied considerably during the composting period. During the seven-week composting period, the minimum and maximum range of  $\text{CO}_2$  concentrations from the pile V1 were  $955.63 \text{ mg m}^{-3}$  in the first week and  $8,172.20 \text{ mg m}^{-3}$  in the seventh week. From the pile V2, the range of  $\text{CO}_2$  concentrations were from  $986.35 \text{ mg m}^{-3}$  at week 1<sup>st</sup> to  $10,061 \text{ mg m}^{-3}$  at week 7<sup>th</sup>. From the pile V3, the minimum  $\text{CO}_2$  value was  $969.22 \text{ mg m}^{-3}$  at week 1<sup>st</sup> and the maximum was  $37,462.00 \text{ mg m}^{-3}$  at week 7<sup>th</sup>. Fig. 1 shows the average results of a 24-hour continuous measurement of  $\text{CO}_2$  production from three piles V1, V2 and V3 observed in the first, fourth and seventh weeks of compost maturation. The measurements showed that the

amount of gas concentrations gradually increased during the process. In the first week, the production of CO<sub>2</sub> concentrations from the monitored piles did not differ significantly ( $P < 0.05$ ) (Table 1). The mean values were 1,071.86 mg m<sup>-3</sup> ± 57.66 (V1); 1,052.09 mg m<sup>-3</sup> ± 28.12 (V2) and 1,053.94 mg m<sup>-3</sup> ± 27.37 (V3). In the fourth week, statistically significantly higher gas concentrations were recorded from the V3 pile ( $P < 0.05$ ), which was turned and irrigated, than from the pile of V1 and V2 (Table 1). The mean CO<sub>2</sub> concentrations were 4,498.80 mg m<sup>-3</sup> ± 394.56 (V1); 4,651.96 mg m<sup>-3</sup> ± 452.32 (V2) and 12,757.06 mg m<sup>-3</sup> ± 1,673.52 (V3). These values were 2.8 times higher than from piles V1 and V2. In the seventh week, it was statistically proven that the highest gas concentrations were recorded from the V3 pile ( $P < 0.05$ ) (Table 1). The mean CO<sub>2</sub> values were 6,642.41 mg m<sup>-3</sup> ± 902.4 (V1); 8,359.11 mg m<sup>-3</sup> ± 1,092.93 (V2) and 33,554.94 mg m<sup>-3</sup> ± 2,619.42 (V3). The measured CO<sub>2</sub> values were 5 times higher from the V3 pile than from V1 and 4 times higher than from the V2 pile.



**Figure 1.** Two-factor analysis of variance CO<sub>2</sub> concentrations from pile V1, V2, V3 in the first, fourth and seventh week of the bio-waste decomposition ( $F$  test results,  $P = 0.0000$ ).

The CO<sub>2</sub> concentrations had an increasing trend in all three piles monitored during the process, the highest concentrations were produced from the turned V3 pile. As reported by Dhamodharan et al. (2019) the amount and characterization of the gases emitted from composting process vary and are related to the initial feedstock materials composted and the composting methodology adopted. The data agreed with the results of Nasini et al. (2016) who found an increase in the CO<sub>2</sub> concentrations during the process and the maximum concentrations of CO<sub>2</sub> occurred at the end of the process. This behaviour was expected during the oxidative phase when aerobic microorganisms were

involved. Composting is strictly an aerobic process, but however anaerobic conditions prevail in few zones of the windrow piles which are unavoidable. These zones lead to the formation of CH<sub>4</sub> due to the insufficient diffusion of oxygen from the windrow piles (Dhamodharan et al., 2019). The production of CH<sub>4</sub> concentrations during experiment were published (Hlinka et al., 2019), it was found that CH<sub>4</sub> concentrations in both V1 and V3 pile had a growing trend throughout the process. In the V2 pile with the addition of the bio-preparation, the CH<sub>4</sub> concentrations increased shortly after the pile formation and the highest CH<sub>4</sub> concentration's production was already in the fourth week.

**Table 1.** Results of significant differences in CO<sub>2</sub> concentrations between V1, V2 and V3 piles in the monitored weeks by Tukey *HSD* test; variable CO<sub>2</sub>; mg m<sup>-3</sup>, probabilities for post hoc at the level of significance  $\alpha = 0.05$

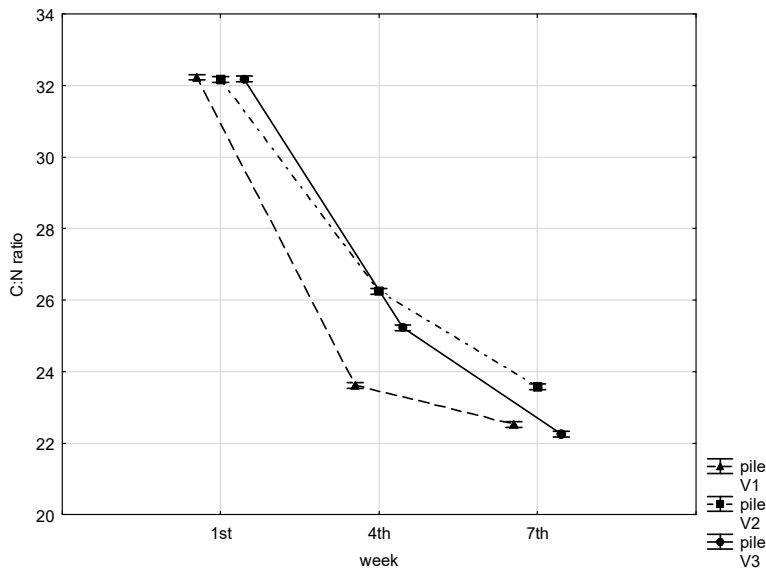
Pile	Mean CO <sub>2</sub> concentrations	<i>P</i> - value	
1 <sup>st</sup> week			
V1	1,071.86 ± 57.66 <sup>a</sup>	0.05901	0.09747
V2	1,052.09 ± 28.12 <sup>a</sup>	0.97518	
V3	1,053.94 ± 27.37 <sup>a</sup>		
4 <sup>th</sup> week			
V1	4,498.80 ± 394.56 <sup>a</sup>	0.76826	0.00002
V2	4,651.96 ± 452.32 <sup>a</sup>	<b>0.00002</b>	
V3	12,757.06 ± 1,673.52 <sup>b</sup>		
7 <sup>th</sup> week			
V1		<b>0.00024</b>	0.00010
V2	8,359.11 ± 1092.93 <sup>b</sup>	<b>0.00010</b>	
V3	33,554.94 ± 2,619.42 <sup>c</sup>		

Notes: letters a, b, and c indicate the significance of the difference, and same letters indicate the difference is not significant.

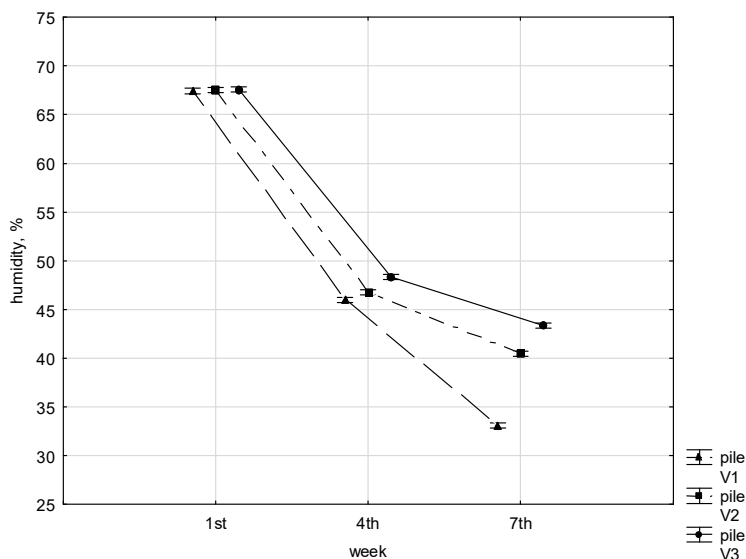
### Physical and chemical characteristics of biowaste

The main factors controlling the compost process are those characteristics of an aerobic biological process such as temperature, moisture, pH and C/N ratio (Ermolaev et al., 2015; Bohacz, 2019). The values were pH<sub>V1</sub> = 7.31 ± 0.26, pH<sub>V2</sub> = 7.54 ± 0.18 and pH<sub>V3</sub> = 7.54 ± 0.18, humidity h<sub>V1</sub> = 67.42% ± 0.30, h<sub>V2</sub> = 67.53% ± 0.28 and h<sub>V3</sub> = 67.56% ± 0.28 and a nutrient ratio C/N<sub>V1</sub> = 32.23/1 ± 0.05, C/N<sub>V2</sub> = 32.17/1 ± 0.02, C/N<sub>V3</sub> = 32.18/1 ± 0.01 from the samples of material taken at week 1<sup>st</sup> from each pile (Fig. 2, 3, 4). Referring to Reyes-Torres et al. (2018) these values can be considered satisfactory to ensure efficient decomposition. The optimal moisture content for composting depends on the waste typology, but it is often set at a 60–70% fresh weight basis. The C/N ratio is an important factor to control the microbiological metabolisms (Godwin et al., 2017). As reported by several authors (Sánchez et al., 2015; Guidoni et al., 2018), to achieve a C/N ratio of 25–30/1 in mature compost, it is necessary to optimize the C/N in fresh compost in the range 20–40/1. The C/N ratio below 20/1 produces an excess of ammonia and unpleasant odours, while the C/N ratio above 40/1 does not provide enough N for microbial growth and a fast composting process (Wang & Zeng, 2018). At week 4<sup>th</sup>, from laboratory tests of the chemical-physical properties of material samples from each pile, slightly higher pH values were found than at the beginning of the process, namely pH<sub>V1</sub> = 7.55 ± 0.25, pH<sub>V2</sub> = 7.74 ± 0.29 and pH<sub>V3</sub> = 7.77 ± 0.32. Humidity in each pile decreased to h<sub>V1</sub> = 45.98% ± 0.30, h<sub>V2</sub> = 46.78% ± 0.45 and h<sub>V3</sub> = 48.34% ± 0.32 and the C/N nutrient ratio decreased to C/N<sub>V1</sub> = 23.62/1 ± 0.23, C/N<sub>V2</sub> = 26.25/1 ± 0.07, C/N<sub>V3</sub> = 25.23/1 ± 0.06 (Fig. 2, 3, 4). From the collected samples from each pile at week 7<sup>th</sup>, optimal values of pH<sub>V1</sub> = 7.88 ± 0.26, pH<sub>V2</sub> = 7.96 ± 0.27 and pH<sub>V3</sub> = 7.92 ± 0.29 were found, which conform to the safe compost standards (Zhang et al., 2017). The humidity decreased to h<sub>V1</sub> = 33.1% ± 0.57, h<sub>V2</sub> = 40.45% ± 0.33 and h<sub>V3</sub> = 43.34% ± 0.38

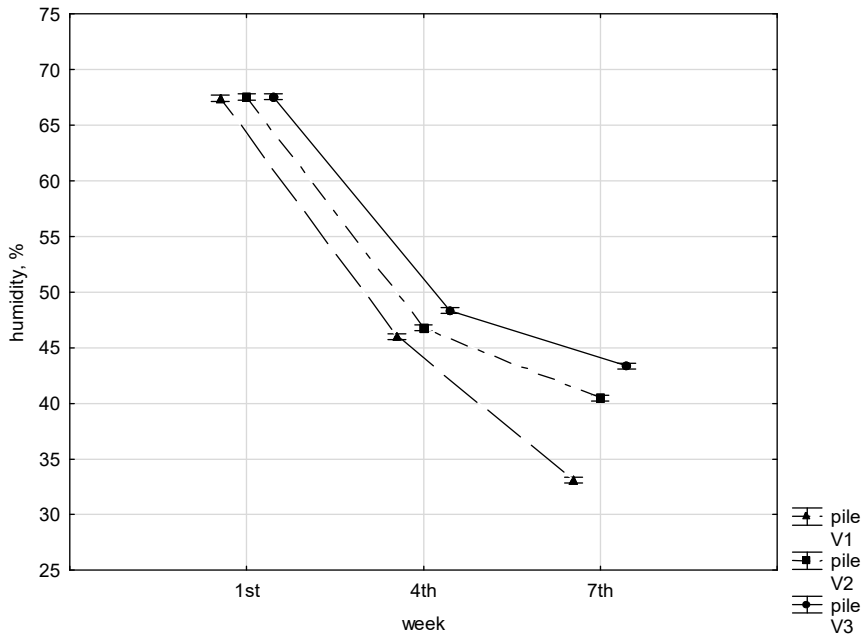
and the nutrient ratio decreased to  $C/N_{V1} = 22.53/1 \pm 0.13$ ,  $C/N_{V2} = 23.58/1 \pm 0.12$ ,  $C/N_{V3} = 22.25/1 \pm 0.13$  (Figs 2, 3, 4). These results are consistent with the knowledges of several authors (Tibu et al., 2019; Xu et al., 2020) who have been reported that during the maturation (fermentation) of compost, part of the carbon, such as carbon dioxide decreases and the C/N ratio narrows. Al-Bataina et al. (2016) stated that C/N ratio decreased with increase in compost age. These were indicative of reduction in carbon content of the treatments by microbe activities, as well as evolution of nitrogen.



**Figure 2.** Two-factor analysis of variance C/N ratio of material from piles V1, V2, V3 in the first, fourth and seventh week of the bio-waste decomposition (*F* test results;  $P = 0.0000$ ).



**Figure 3.** Two-factor analysis of variance humidity of material from piles V1, V2, V3 in the first, fourth and seventh week of the bio-waste decomposition (*F* test results;  $P = 0.0000$ ).



**Figure 4.** Two-factor analysis of variance pH of material from piles V1, V2, V3 in the first, fourth and seventh week of the bio-waste decomposition (*F* test results;  $P = 0.82856$ ).

By analysing significant differences using Tukey's *HSD* test, the values of the chemical properties of C/N biowaste did not show the significance of the differences in the first week of the composting process between the composted piles. At weeks 4 and 7, there were significant differences in C/N ratio values between treatment methods V1, V2 and V3 (Table 2). The moisture content of the composted material was not significantly different in the first week, in the fourth and seventh weeks there were already significant differences between all composting methods V1, V2 and V3 (Table 3). The pH values of the composted material were not significantly different in the first, fourth and seventh weeks between all composting methods V1, V2 and V3 (Table 4).

**Table 2.** Results of significant differences in C/N ratio between V1, V2 and V3 piles in the monitored weeks by Tukey *HSD* test; variable C/N ratio, probabilities for post hoc at the level of significance  $\alpha = 0.05$

Pile	C/N ratio	<i>P</i> - value	
<b>1<sup>st</sup> week</b>			
V1	$32.23 \pm 0.05^a$	0.10199	0.80075
V2	$32.17 \pm 0.02^a$		0.80075
V3	$32.18 \pm 0.01^a$		
<b>4<sup>th</sup> week</b>			
V1	$23.62 \pm 0.23^a$	<b>0.00013</b>	<b>0.00013</b>
V2	$26.25 \pm 0.07^b$		<b>0.00013</b>
V3	$25.23 \pm 0.06^c$		
<b>7<sup>th</sup> week</b>			
V1	$22.53 \pm 0.13^a$	<b>0.00013</b>	<b>0.00074</b>
V2	$23.58 \pm 0.12^b$		<b>0.00013</b>
V3	$22.25 \pm 0.13^c$		

Notes: letters a, b, and c indicate the significance of the difference, and same letters indicate the difference is not significant.



**Table 3.** Results of significant differences in humidity between V1, V2 and V3 piles in the monitored weeks by Tukey *HSD* test; variable humidity; %, probabilities for post hoc at the level of significance  $\alpha = 0.05$

Pile	Humidity, %	P - value	
1 <sup>st</sup> week			
V1	67.42 ± 0.30 <sup>a</sup>	0.73628	0.60895
V2	67.53 ± 0.28 <sup>a</sup>	0.97633	
V3	67.56 ± 0.28 <sup>a</sup>		
4 <sup>th</sup> week			
V1	45.98 ± 0.30 <sup>a</sup>	<b>0.00103</b>	<b>0.00013</b>
V2	46.78 ± 0.45 <sup>b</sup>	<b>0.00013</b>	
V3	48.34 ± 0.32 <sup>c</sup>		
7 <sup>th</sup> week			
V1	33.1 ± 0.57 <sup>a</sup>	<b>0.00013</b>	<b>0.00013</b>
V2	40.45 ± 0.33 <sup>b</sup>	<b>0.00013</b>	
V3	43.34 ± 0.38 <sup>c</sup>		

Notes: letters a, b, and c indicate the significance of the difference, and same letters indicate the difference is not significant.

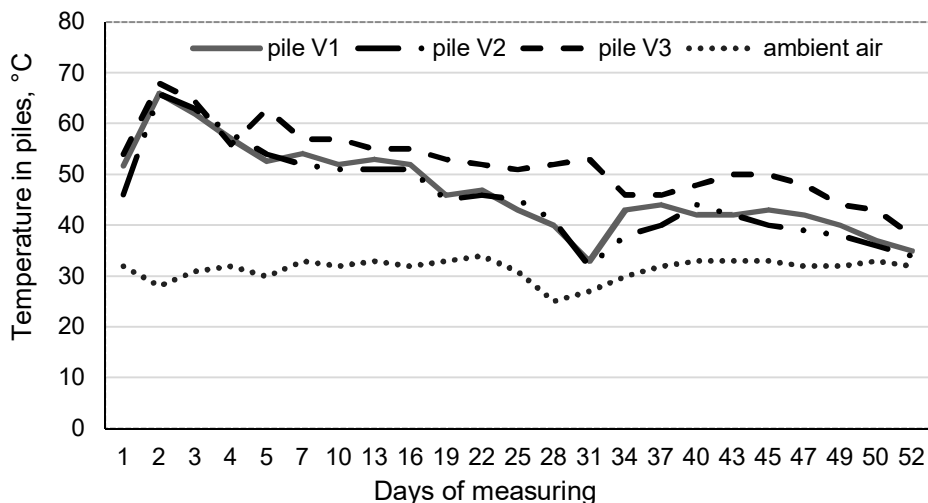
**Table 4.** Results of significant differences in pH values between V1, V2 and V3 piles in the monitored weeks by Tukey *HSD* test; variable pH, probabilities for post hoc at the level of significance  $\alpha = 0.05$

Pile	pH	P - value	
1 <sup>st</sup> week			
V1	7.31 ± 0.26 <sup>a</sup>	0.089511	0.095236
V2	7.54 ± 0.18 <sup>a</sup>	0.99952	
V3	7.54 ± 0.18 <sup>a</sup>		
4 <sup>th</sup> week			
V1	7.55 ± 0.25 <sup>a</sup>	0.396254	0.291111
V2	7.74 ± 0.29 <sup>a</sup>	0.97483	
V3	7.77 ± 0.32 <sup>a</sup>		
7 <sup>th</sup> week			
V1	7.88 ± 0.26 <sup>a</sup>	0.829846	0.951706
V2	7.96 ± 0.27 <sup>a</sup>	0.95668	
V3	7.92 ± 0.29 <sup>a</sup>		

Notes: same letters indicate the difference is not significant.

### Temperature evolution

The temperature of treatments increased rapidly after the experiments were started (Fig. 5), the maximum temperatures (68 °C, 66 °C, 65 °C) were observed at day 2.



**Figure 5.** Temperature profile in pile V1, V2, V3 and ambient air during the composting process.

Then the temperature decreased gradually during the process between 60 and 50 °C and the degradation process took place in the thermophilic phase. The thermophilic phase of all treatments was long enough to satisfy the requirement for sanitation effect. Chaher et al. (2020) stated that the maintenance of a temperature above 55 °C for two consecutive

weeks is the requirements of compost evaluation in terms of guaranteeing the removal of pathogens. The drop in temperature demonstrated that almost all the complex organic compounds were well-degraded during the mesophilic and thermophilic phases (Akyol et al., 2019; Calabi-Floody et al., 2019, Chaher et al., 2020). During the V3 treatment, there were a few small temperature fluctuations due to the mechanical turning of the compost pile. A similar trend was observed by Cook et al. (2015) and Yang et al. (2019) according to which it is possible to improve the structure of the matrix and to displace biodegradable substances to reactivate the microbial activity when the composting piles were turned.

### Weight of the final products

At the end of the degradation process, sieving and weighing of each pile were performed to determine the weights of the resulting products in terms of the processing technology used. Table 5 gives an overview of the weights of each pile before sieving, after sieving and the percentage of compost produced from each pile. It was found that turning and irrigation in the V3 pile had a significant effect on the degradation of organic matter. This may be attributed to the increased oxygen provided by turning the windrow and by higher temperature that enhanced microbial activity. Weight loss in the V3 pile was lowest (18.44%, V1 = 23.26% and V2 = 21.85%) which means that due to the treatment, the highest rate of waste degradation was achieved, and we achieved the highest percentage of the final product in the form of compost (Table 2). These results suggest that the decomposition rate in the turned pile proceeded much faster than the unturned ones. The composting process, with its requirements for turning and aeration is one of the important steps to produce a good quality compost product (He et al., 2020). As reported (Han et al., 2018; Reyes-Torres et al., 2018), appropriate management such as turning ensure enough oxygen for microbial activities to release heat and reducing greenhouse warming potential (GWP) during aerobic composting.

**Table 5.** Weights of each pile before sieving and after sieving

Pile	Mass (kg)		Percentage of the initial mass at the end of experiment	
	Whole pile	Seedlings	Compost	
V1	2,580	600	1,980	76.74%
V2	3,020	660	2,360	78.15%
V3	2,820	520	2,300	81.56%

## CONCLUSIONS

The measurements showed that the production of monitored CO<sub>2</sub> concentrations in the summer period was the lowest at the beginning of composting process. The amount of gas concentrations gradually increased during the process. The aim of this study was to analyse the production of CO<sub>2</sub> in relation to the composting technology used. Our assumption that there is no significant difference in CO<sub>2</sub> concentrations depending on the biowaste treatment technology has only been partially confirmed using statistical methods. At the beginning of the process, in the first week, there were no significant differences in the production of CO<sub>2</sub> concentrations from the monitored piles. In the fourth week, significantly higher values of CO<sub>2</sub> concentrations were recorded from the V3 pile ( $P < 0.05$ ), which was turned and irrigated, than from the V1 and V2 piles. At

week 7, significant differences were found between all treatments at the level of significance ( $P < 0.05$ ) with the highest values from the V3 pile. Turning affected several important physical and chemical parameters such as temperature, carbon loss and the resulting amount of product. The final product from the three composting treatments was significantly different in terms of C/N ratio and compost moisture. The results suggest that using a technological process, we can produce a higher amount of quality compost. It has been shown that turning and humidifying results in the highest release of CO<sub>2</sub> into the air, but in a more rapid decomposition of the microorganisms, thus reducing the time required to achieve a stable compost product and increasing the efficiency of the composting plant.

**ACKNOWLEDGMENTS.** This publication was supported by the Operational Program Integrated Infrastructure within the project: Demand-driven research for the sustainable and innovative food, Drive4SIFood 313011V336, cofinanced by the European Regional Development Fund.

## REFERENCES

- Akpinar, C., Demirbas, A. & Ortas, I. 2019. The Effect of Different Compost Compositions on Arbuscular Mycorrhizal Colonization and Nutrients Concentration of Leek (*Allium Porrum* L.) Plant. *Communications in Soil Science and Plant Analysis* **50**, 1–12. doi.org/10.1080/00103624.2019.1659299
- Akyol, C., Ince, O. & Ince, B. 2019. Crop-based composting of lignocellulosic digestates: focus on bacterial and fungal diversity. *Bioresour Technology* **288**, 121549. doi.org/10.1016/j.biortech.2019.121549
- Al-Batiana, B.B., Young, T.M. & Ranieri, E. 2016. Effects of compost age on the release of nutrients. *International Soil and Water Conservation Research* **4**(3), 230–236. doi.org/10.1016/j.iswcr.2016.07.003
- Arriaga, H., Viguria, M., López, D.M. & Merino, P. 2017. Ammonia and greenhouse gases losses from mechanically turned cattle manure windrows: A regional composting network. *Journal of Environmental Management* **203**, 557–563. doi.org/10.1016/j.jenvman.2017.06.006
- Asadu, C.O., Egbuna, S.O., Chime, T.O., Eze, Ch.N., Kevin, D., Mbah, G.O. & Ezema, A.C. 2019. Survey on solid wastes management by composting: optimization of key process parameters for biofertilizer synthesis from agro wastes using response surface methodology (RSM). *Artificial Intelligence in Agriculture* **3**, 52–61. doi.org/10.1016/j.aiaa.2019.12.002
- Bohacz, J. 2019. Changes in mineral forms of nitrogen and sulfur and enzymatic activities during composting of lignocellulosic waste and chicken feathers. *Environ Sci Pollut Res* **26**, 10333–10342. doi.org/10.1007/s11356-019-04453-2
- Calabi-Floody, M., Medina, J., Suazo, J., Ordiqueo, M., Aponte, H., Mora, M.L.L. & Rumpel, C. 2019. Optimization of wheat straw co-composting for carrier material development. *Waste Management* **98**, 37–49. doi.org/10.1016/j.wasman.2019.07.041
- Cook, K.L., Ritchey, E.L., Loughrin, J.H., Haley, M., Sistani, K.R. & Bolster, C.H. 2015. Effect of turning frequency and season on composting materials from swine high-rise facilities. *Waste Management* **39**, 86–95. doi.org/10.1016/j.wasman.2015.02.019
- Dhamodharan, K., Varma, V.S., Veluchamy, Ch., Pugazhendhi, A. & Rajendran, K. 2019. Emission of volatile organic compounds from composting: A review on assessment, treatment and perspectives. *Science of The Total Environment* **695**, 133725. doi.org/10.1016/j.scitotenv.2019.133725

- Eden, M., Gerke, H.H. & Houot, S. 2017. Organic waste recycling in agriculture and related effects on soil water retention and plant available water: a review, *Agron. Sustain. Dev.* **37**, 11. <https://doi.org/10.1007/s13593-017-0419-9>
- Ermolaev, E., Jarvis, A., Sundberg, C., Smars, S., Pell, M. & Jönsson, H. 2015. Nitrous oxide and methane emissions from food waste composting at different temperatures. *Waste Management* **46**, 113–119. [doi.org/10.1016/j.wasman.2015.08.021](https://doi.org/10.1016/j.wasman.2015.08.021)
- Godwin, C.M., Whitaker, E.A. & Cotner, J.B. 2017. Growth rate and resource imbalance interactively control biomass stoichiometry and elemental quotas of aquatic bacteria. *Ecology* **98**(3), 820–829. [doi.org/10.1002/ecy.1705](https://doi.org/10.1002/ecy.1705)
- Guidoni, L.L.C., Marques, R.V., Moncks, R.B., Botelho, F.T., da Paz, M.F., Corrêa, L.B. & Corrêa, É.K. 2018. Home composting using different ratios of bulking agent to food waste. *J Environ Manag* **207**, 141–150. [doi.org/10.1016/j.jenvman.2017.11.031](https://doi.org/10.1016/j.jenvman.2017.11.031)
- Han, Z., Sun, D., Wang, H., Li, R., Bao, Z. & Qi, F. 2018. Effects of ambient temperature and aeration frequency on emissions of ammonia and greenhouse gases from a sewage sludge aerobic composting plant. *Bioresource Technology* **270**, 457–466. [doi.org/10.1016/j.biortech.2018.09.048](https://doi.org/10.1016/j.biortech.2018.09.048)
- He, X., Han, L. & Huang, G. 2020. Analysis of regulative variables on greenhouse gas emissions and spatial pore gas concentrations with modeling during large-scale trough composting. *Journal of Cleaner Production* **277**, 124066. [doi.org/10.1016/j.jclepro.2020.124066](https://doi.org/10.1016/j.jclepro.2020.124066)
- Hernández-Gómez, A., Calderón, A., Medina, C., Sanchez-Torres, V. & Oviedo-Ocaña, E.R. 2020. Implementation of strategies to optimize the co-composting of green waste and food waste in developing countries. A case study: Colombia. *Environmental Science and Pollution Research*. [doi.org/10.1007/s11356-020-08103-w](https://doi.org/10.1007/s11356-020-08103-w)
- Hlinka, P., Karandušovská, I. & Mihina, Š. 2019. Monitoring of gas production during the biowaste composting. *Acta technologica agriculturae* **22**(3), 75–79. [doi.org/10.2478/ata-2019-0014](https://doi.org/10.2478/ata-2019-0014)
- Chaher, N.E h., Chakchouk, M., Abdallah, N., Nelles, M. & Hamdi, M. 2020. Potential of windrow food and green waste composting in Tunisia. *Environmental Science and Pollution Research*. [doi.org/10.1007/s11356-020-10264-7](https://doi.org/10.1007/s11356-020-10264-7)
- Kažimírová, V., Gaduš, J. & Giertl, T. 2018. Verification of suitability of substrate composition for production and quality of biogas. *Acta technologica agriculturae* **21**(3), 115–118. [doi.org/10.2478/ata-2018-0021](https://doi.org/10.2478/ata-2018-0021)
- Křištof, K. & Gaduš, J. 2018. Effect of alternative sources of input substrates on biogas production and its quality from anaerobic digestion by using wet fermentation. *Agronomy Research* **16**(3), 769–783. [doi.org/10.15159/AR.18.146](https://doi.org/10.15159/AR.18.146)
- Nasini, L., De Luca, G., Ricci, A., Ortolani, F., Caselli, A., Massaccesi, L., Regni, L., Gigliotti, G. & Proietti, P. 2016. Gas emissions during olive mill waste composting under static pile conditions. *International Biodeterioration & Biodegradation* **107**, 70–76. [doi.org/10.1016/j.ibiod.2015.11.001](https://doi.org/10.1016/j.ibiod.2015.11.001)
- Reyes-Torres, M., Oviedo-Ocaña, E.R., Dominguez, I., Komilis, D. & Sánchez, A. 2018. A systematic review on the composting of green waste: feedstock quality and optimization strategies. *Waste Management* **77**, 486–499. [doi.org/10.1016/j.wasman.2018.04.037](https://doi.org/10.1016/j.wasman.2018.04.037)
- Sánchez, A., Artola, A., Font, X., Gea, T., Barrena, R., Gabriel, D., Sánchez-Monedero, M.A., Roig, A., Cayuela, M.L. & Mondini, C. 2015. Greenhouse gas emissions from organic waste composting. *Environmental Chemistry Letters* **13**, 223–238. [doi.org/10.1007/s10311-015-0507-5](https://doi.org/10.1007/s10311-015-0507-5)
- Tibu, C., Annang, T.Y., Solomon, N. & Yirenya-Tawiah, D. 2019. Effect of the composting process on physicochemical properties and concentration of heavy metals in market waste with additive materials in the Ga West Municipality, Ghana. *International Journal of Recycling of Organic Waste in Agriculture* **8**, 393–403. [doi.org/10.1007/s40093-019-0266-6](https://doi.org/10.1007/s40093-019-0266-6)

- Vaverková, M.D., Adamcová, D., Winkler, J., Koda, E., Petrželová, L. & Maxianová, A. 2020. Alternative method of composting on a reclaimed municipal waste landfill in accordance with the circular economy: benefits and risks. *Science of The Total Environment* **723**, 137971. doi.org/10.1016/j.scitotenv.2020.137971
- Wang, S. & Zeng, Y. 2018. Ammonia emission mitigation in food waste composting: a review. *Bioresour Technology* **248**, 13–19. doi.org/10.1016/j.biortech.2017.07.050
- Weidner, T., Graça, J., Machado, T. & Yang, A. 2020. Comparison of local and centralized biowaste management strategies – A spatially-sensitive approach for the region of Porto, *Waste Management* **118**, 552–562. doi.org/10.1016/j.wasman.2020.09.013
- Xu, Z., Li, G., Huda, N., Zhang, B., Wang, M. & Luo, W. 2020. Effects of moisture and carbon/nitrogen ratio on gaseous emissions and maturity during direct composting of cornstalks used for filtration of anaerobically digested manure centrate, *Bioresource Technology* **298**, 122503. doi.org/10.1016/j.biortech.2019.122503
- Yang, F., Li, Y., Han, Y., Qian, W., Li, G. & Luo, W. 2019. Performance of mature compost to control gaseous emissions in kitchen waste composting. *Science of The Total Environment* **657**, 262–269. doi.org/10.1016/j.scitotenv.2018.12.030
- Zhang, D., Luo, W., Yuan, J., Li, G. & Luo, Y. 2017. Effects of woody peat and superphosphate on compost maturity and gaseous emissions during pig manure composting. *Waste Management* **68**, 56–63. doi.org/10.1016/j.wasman.2017.05.042
- Zhang, S., Wen, J., Hu, Y., Fang, Y., Zhang, H., Xing, L., Wang, Y. & Zeng, G. 2019. Humic substances from green waste compost: an effective washing agent for heavy metal (Cd, Ni) removal from contaminated sediments. *Journal of Hazardous Materials* **366**, 210–218. doi.org/10.1016/j.jhazmat.2018.11.103

## Identification of the effectiveness of associative rhizobacteria in spring wheat cultivation

L.E. Kolesnikov<sup>1,\*</sup>, A.A. Belimov<sup>2</sup>, E.Y. Kudryavtseva<sup>3</sup>, B.A. Hassan<sup>4</sup> and Yu.R. Kolesnikova<sup>3</sup>

<sup>1</sup>Saint-Petersburg State Agrarian University, Faculty of Agrotechnologies, Soil science and Ecology, Department of Plant Protection and Quarantine, Petersburgskoe Shosse, 2, RU196601, St. Petersburg - Pushkin, Russia

<sup>2</sup>Federal State Budgetary Scientific Institution “All-Russian Research Institute for Agricultural Microbiology”, Laboratory of rhizosphere microflora, sh. Podbelskogo, 3, RU196608, St. Petersburg, Pushkin-8, Russia

<sup>3</sup>Federal Research Center N.I. Vavilov All-Russian Institute of Plant Genetic Resources (VIR), genetic resources of wheat department, plant introduction department, Bolshaya Morskaya Str. 42–44, RU190000, St. Petersburg, Russia

<sup>4</sup>Ministry of Agriculture, Agricultural Research Office, Abo-Ghraib, St. Al-Zaytun, H. IQ10081, Baghdad, Iraq

\*Correspondence: kleon9@yandex.ru

Received: January 31<sup>st</sup>, 2021; Accepted: October 5<sup>th</sup>, 2021; Published: October 19<sup>th</sup>, 2021

**Abstract.** The maximum increase in wheat yield (by 67% to the control), associated with a decrease in the root rot development by 19%, an increase in the productive bushiness by 18%, the spike weight by 26%, in the grains number per spike by 8% was noted when using the *Bacillus subtilis* strain 124-11; the strain effect on leaf diseases was insignificant (2–5%). The plants differed in the maximum changes (to control) in the total bushiness by 59%, the plants vegetative part weight by 27%, the flag leaf area by 21%, the pre-flag leaf area by 28%, the roots numbers and weight by 20% and 62%. After plants treatments with the *Pseudomonas fluorescens* strain SPB2137, the wheat maturation period was reduced by 9% (to the control), wheat yield increased by 58% due to a decrease in the development of root rot and septoria by 18%, the yellow rust pustules area by 44%; the productive bushiness and plant height increased by 25% and 19%, the plant vegetative weight by 21%, the spike length by 4%. The most expressed protective and growth-stimulating effect was shown by the *Sphingomonas* sp. K1B, which caused a maximum decrease (to the control) in the root rot and yellow rust development by 22% and 7%, the strips length by 22%, the pustules number in the strip by 29%, brown rust by 10%, septoria by 11%. Wheat plants were characterized by a large number and length of roots by 17% and 13%, root weight by 49%, a maximum increase in the nodal roots number and length by 15% and 17%; total bushiness by 34.5%; a maximum increase in plant vegetative weight by 37%; the spike length by 3%.

**Key words:** associative rhizobacteria, biocontrol of phytopathogens, productivity, soft wheat, yield structure.

## INTRODUCTION

The bacteria that stimulate plant growth (Plant Growth Promoting Bacteria - PGPB) relate to different groups, with most species belonging to the genera, *Azospirillum*, *Bacillus*, *Enterobacter*, *Gluconacetobacter*, *Paenibacillus*, *Pseudomonas*, *Rhizobium*, *Streptomyces* and *Agrobacterium* (Kumar et al., 2015; Kalantari et al., 2018; Tabande et al., 2020). Stimulating effects of the majority of PGPB are traditionally associated with three main mechanisms: phytohormones production, an increasing nutrients availability and water for crops, and plant protection from diseases (Asaf et al., 2017a).

One of the most studied phytohormones, found in a large number of metabolites of microorganisms - is auxins (Tsavkelova et al., 2006). Auxins synthesis is a process which depends on carbon and nitrogen sources, temperature, pH, and tryptophan presence in soils (Mohite, 2013). The application of *Bacillus amyloliquefaciens* S-134 with the ability of secreting indolyl-3-acetic acid in an amount of 26 mcg mL, could stimulate wheat growth and gave an increase in yield by 34% (Raheem et al., 2018).

One of the key elements of antagonistic mechanisms of PGPB activity, is the synthesis of biologically active compounds of various nature, such as antibiotics, lytic enzymes, siderophores and etc. (Sharma et al., 2009; Naseri & Younesi, 2021). A large and diverse group of antibiotics that are effective against phytopathogenic microorganisms is produced by spore-forming gram-positive bacteria *Bacillus subtilis*. One of the first antibiotics isolated from culture fluid of *Bacillus subtilis* was subtilin (Housusright, 1948), which is a short peptide, then lipopeptide antibiotics of several classes were isolated from various strains of *B. subtilis*: subsporins (Loeffler et al., 1986), bacillomycins L and D (Peypoux et al., 1987), phengicins (Loeffler et al., 1986) and others, and also Fe<sup>3+</sup> siderophores were identified (Hofemeister et al., 2004).

The study of the genus *Pseudomonas* as typical representatives of the rhizosphere microflora aroused great interest for researchers. In addition to its antagonistic abilities against phytopathogenic fungi (Naseri, 2019), the genus *Pseudomonas* exhibits other interesting properties: improving phosphorus nutrition for plants (Satyaprakash et al., 2017), synthesizing plant growth stimulators (Selvakumar et al., 2011; Pham et al., 2017), producing siderophores responsible for iron transport (Trapet et al., 2016), as well as substances responsible for inducing resistance to phytopathogens (Strunnikova et al., 2007; Pieterse et al., 2014). Pseudomonads, as typical soil bacteria, are able to synthesize a whole complex of antibiotics. The best studied antibiotics are phenazines (Briard et al., 2015), phloroglucins (Kidarsa et al., 2011), as well as pyoluteorin (Hu HBO et al., 2005) and pyrrolnitrin (Park et al., 2011). The protective action of PGPB-based biopreparation is also explained by the presence of the enzyme 1-aminocyclopropane-1-carboxylate deaminase (ACC-deaminase), which reduces the concentration of ethylene phytohormone in plants (Nadeem et al., 2013).

Inoculation of wheat seeds with a pseudomonas-based preparation leads to increase root and stem growths, increase germination energy thus, enhancing yield amount, especially under the circumstances of low doses of phosphorous fertilizers (Ali et al., 2011). Wheat seeds treatment with *Pseudomonas putida* 108 strain combined with of 50% phosphorus application caused an increase in wheat yield by 37% (Zabihi et al., 2011), and with *Pseudomonas fluorescens* Pf strain - by 16% (Naiman et al., 2009).

There is little information in the literature about rhizospheric bacteria belonging to the genus *Sphingomonas*. The strain *Sphingomonas spiritivorum* 38-22 had a high growth-stimulating activity, which provided an increase in yield of winter wheat at the level of 21% (Pukhaev et al., 2009). The *Sphingomonas* S11 strain had a greater antagonistic activity against eight *Fusarium* strains that cause wheat diseases (Wachowska et al., 2013a). Treating soybean with *Sphingomonas* sp. LK11 significantly increased plant height and biomass, photosynthetic pigments, glutathione, amino acids (proline, glycine, and glutamate) and primary sugars, compared to control plants (Asaf et al., 2017b).

The scientific novelty of this work consists in a comprehensive assessment of the impact of associative rhizobacteria strains (*Bacillus subtilis* 124-11, *Pseudomonas fluorescens* SPB2137 and *Sphingomonas* sp. K1B) on a wide range of indicators that characterize morphological characteristics of plants, grain yield and wheat resistance to the most dangerous diseases, namely root rot, powdery mildew, brown and yellow rust.

The purpose of the research is to obtain the data that indicate the possibility of developing an environmentally friendly technology for wheat cultivation, which provides an increase in its productivity and a decrease in the pathogens' harmfulness, with reducing the cost of plant protection measures.

## MATERIALS AND METHODS

The place of experimental work is Laboratory of Rhizosphere Microflora of the All-Russian Research Institute of Agricultural Microbiology (ARRIAM, Saint Petersburg) and Department of Plant Protection and Quarantine of Saint-Petersburg State Agrarian University SPbGAU (Saint Petersburg). The effectiveness of associative rhizobacteria strains on *Triticum aestivum* cultivars study was carried out in the experimental field of Federal research centre "The N.I. Vavilov All-Russian Institute of Plant Genetic Resources" (VIR) from 2017 to 2019 (Fig. 1).

**Bacterial samples.** The object of the study was the strains *Bacillus subtilis* 124-11 (growth inhibitor of phytopathogenic fungi according to unpublished data of Laboratory of Rhizosphere Microflora of the ARRIAM), *Sphingomonas* sp. K1B (hyper-producer of auxins according to unpublished data of Laboratory of Rhizosphere Microflora of the ARRIAM) and *Pseudomonas fluorescens* SPB2137 (producer of auxins, contains ACC deaminase, growth inhibitor of phytopathogenic fungi (Kravchenko et al., 2003). Strains were obtained from the Russian Collection of Agricultural Microorganisms (All-Russia Research Institute for Agricultural Microbiology, Saint-Petersburg), and information on their properties have not been published.



**Figure 1.** Spring wheat sowing in the experimental field of the VIR, 2019.



**Wheat experiment.** Plant material of the study were *Triticum aestivum* cultivars Trizo, k-64981 and Sudarynya, k-66407. In the field experiment, seeds were inoculated and sprayed with the strains *Bacillus subtilis* 124-11, *Sphingomonas* sp. K1B and *Pseudomonas fluorescens* SPB2137. For this purpose, strains were grown for two days on a Potato Dextrose Broth (P6685, Sigma-Aldrich, USA). Then, seeds were dipped with a suspension of bacteria ( $10^8$  cells mL<sup>-1</sup>) at the rate of 2 mL suspension per 10 g seeds and kept for an hour as previously described (Kozhemyakov & Tikhonovich, 1998). Prophylactic spraying of plants with a culture liquid of bacteria ( $10^9$  cells mL<sup>-1</sup>) was carried out in the phases of stem extension and the beginning of flowering.

The experiments were arranged on a randomized complete block designed with four replicates. For one variant of the experiment, plot area was 1.0 m<sup>2</sup>, treatments for plots in replicates were arranged systematically. The experiment samples was sown manually on plots in an ordinary way of sowing with a distance between rows of 15 cm and the distance between seeds in a row was 1–2 cm. The seeding depth was 5–6 cm.

Wheat productivity was studied in the phases: development of the germ shoot (stage 3-leaves), earing-flowering and maturation according to a set of indicators that characterize morphological characteristics and yield structure (Kolesnikov et al., 2019). In the ear-flowering phase, a complex of plant indicators: productive and total bushiness (pieces), plant phase (score, according to the Zadok's Scale (Zadoks, 1974) flag and pre-flag leaf area (cm<sup>2</sup>), plant height (cm), spike length (cm), spikelets number per spike (pieces), spike weight (g) was studied. In addition, number and length of roots (main embryonic root, embryonic coleoptile and roots) extending from the epicotyl were calculated. Number and length of nodal roots, root weight, plants vegetative part weight were taken into account. In the maturation phase (stage of full ripeness), structure of wheat yield was studied according to the following indicators: spikelets number per spike, pieces; spike length, cm; weight of an spike with grain; grains number per spike, pieces; grains weight per spike, 1,000 grains weight. The potential (biological) yield of a single wheat plant was calculated in accordance with data about reproductive tillering and grain weight per an spike of one plant (Kolesnikov, Kremenevskaya et al., 2020; Kolesnikov, Novikova et al., 2020).

**Analysis of the development of wheat diseases.** Assessment of plants damage degree caused by root rot disease was carried out in laboratory in the phases of tillering (complete tillering) and earing-flowering in accordance with generally accepted scale (Popov, 2011). The flag and pre-flag leaves damage intensity caused by powdery mildew (*Blumeria graminis* Speer.), was calculated according to the generally accepted indicator- conditional degree of plant damage (Geshele, 1978), as well as additional indicators - number and area of spots with plaque. Affection of wheat flag and pre-flag leaves by the causative agent of brown rust (*Puccinia recondita* Rob. ex Desm. f. sp. tritici Eriks.) was taken into account on the R. F. Peterson scale (Geshele, 1978). As additional phytopathological parameters, pustules number per leaf and pustule area were used.

The wheat damage intensity caused by yellow rust pathogen was evaluated according to the generally accepted Manners scale, and, also, the pathogenesis indicators were used: pustules number (total per leaf), number of stripes with pustules, length of stripes with pustules, pustule area and their number in the strip.

The size of infectious structures of pathogens formed on leaves during pathogenesis (spots, pustules, etc.) was determined using an ocular micrometer. The values of pustules

and spots with plaque area were calculated on the assumption of their elliptical shape (Kolesnikov, Kremenevskaya et al., 2020; Kolesnikov, Novikova et al., 2020).

**Statistical analyses.** The algorithm for statistical processing of field experiment data was based on the creation of an electronic database, first in Microsoft Excel spreadsheets, then in IBM SPSS Statistics software platform was utilized. Methods of parametric statistics based on calculation of mean and standard errors (SEM), 95% confidence intervals, and the Student's *t*-test were used in the calculations. In addition, methods of ANOVA using the Scheffe test to compare and verify the likeness of sample variances were applied (Lemeshko & Ponomarenko, 2006).

## RESULTS AND DISCUSSION

At the first stage of study, wheat productivity indicators were compared in the experimental variants: when plants were treated with associative rhizobacteria strains and without treatment (control group).

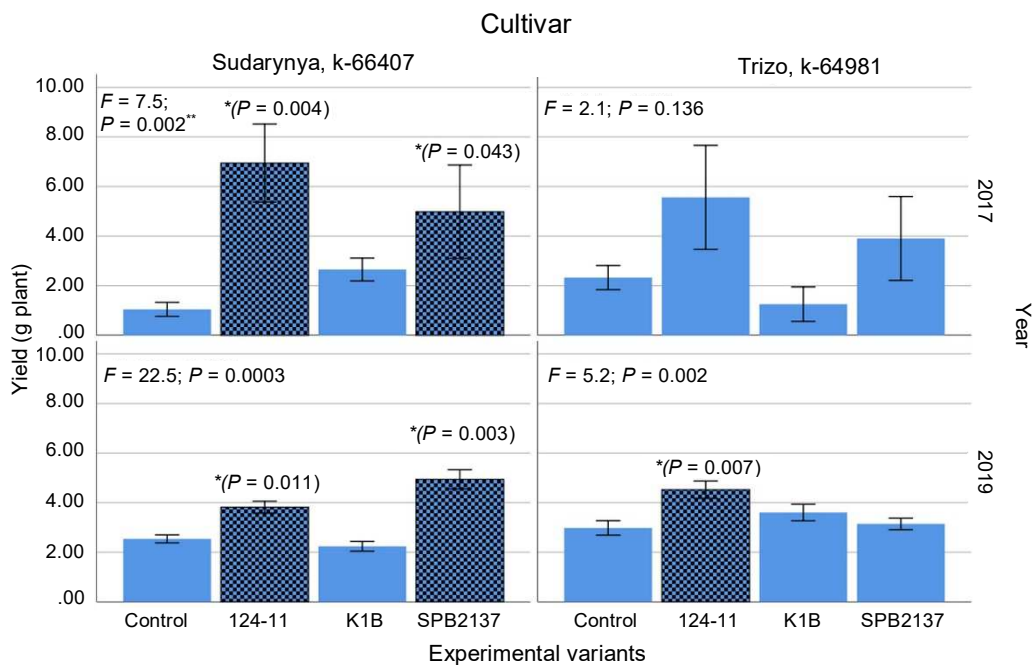
Yield is an integral feature that depends on the values of wheat productivity and the grains weight per one spike. Table 1 shows the data of multivariate analysis of wheat yield variance from inoculants, wheat cultivars, replicates, years. A significant effect of the inoculants and the years of research on wheat yield was revealed. A significant change in the wheat yield was defined from the interaction of Inoculant \* Year factors was determined\* Wheat cultivar\* Replicate.

**Table 1.** Multivariate analysis of variance wheat yield, the 2017–2019

Source	Type III Sum of Squares	<i>Df</i>	Mean Square	<i>F</i>	Sig.
Corrected Model	1,601.24	55	29.11	16.40	0.000
Intercept	2,179.83	1	2,179.83	1,228.26	0.000
Inoculant	138.81	3	46.27	26.07	0.000
Year	901.55	2	450.78	254.00	0.000
Wheat cultivar	5.70	1	5.70	3.21	0.074
Replicate	8.03	2	4.02	2.26	0.105
Inoculant * Year	143.72	6	23.95	13.50	0.000
Inoculant* Wheat cultivar	16.64	3	5.55	3.13	0.025
Inoculant* Replicate	53.53	6	8.92	5.03	0.000
Year * Wheat cultivar	35.51	2	17.76	10.00	0.000
Year* Replicate	14.41	2	7.21	4.06	0.018
Wheat cultivar* Replicate	21.70	2	10.85	6.11	0.002
Inoculant* Year * Wheat cultivar	60.22	5	12.04	6.79	0.000
Inoculant * Year * Replicate	17.24	6	2.87	1.62	0.139
Inoculant* Wheat cultivar* Replicate	42.02	6	7.00	3.95	0.001
Year * Wheat cultivar* Replicate	18.67	2	9.33	5.26	0.005
Inoculant * Year* Wheat cultivar* Replicate	54.56	6	9.09	5.12	0.000
Error	990.30	558	1.77		
Total	6,077.10	614			
Corrected Total	2,591.53	613			

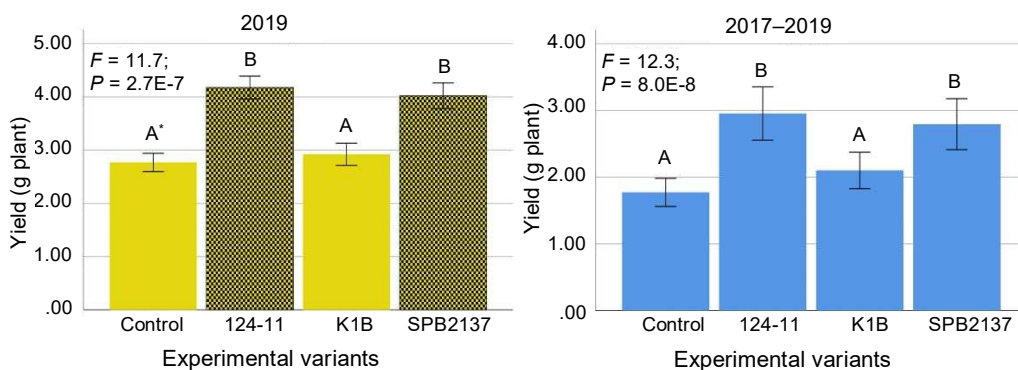
R Squared = 0.62

Based on the calculation of 95% confidence intervals for average statistically significant differences in wheat yield in the experimental variants were revealed in 2018 and 2019. In 2017, the wheat yield changed insignificantly. The greatest impact on wheat yield in 2019 was exerted by *B. subtilis* 124-11 and *Ps. fluorescens* SPB2137 (Fig. 2). When using *B. subtilis* 124-11, yield of wheat cultivars Sudarynya, k-66407 and Trizo, k-64981 in 2019 significantly increased ( $P < 0.05$ ) in comparison with the control by 50% -  $t$ -test = 3.8 (on average for the period 2017–2019 - by 88%,  $t$ -test = 4.7) and by 52% -  $t$ -test = 3.4 (2017–2019 - by 46%,  $t$ -test = 2.7), respectively. With the application of *Ps. fluorescens* SPB2137 in 2019, there was a significant increase ( $P < 0.05$ ) in the yield of Sudarynya, k-66407 cultivar by 95% -  $t$ -test = 5.7 (on average for the period 2017–2019 - by 122%,  $t$ -test = 5.3). While the yield of Trizo, k-64981 cultivar in 2019 was not significantly affected by this strain (in 2019, the yield increased by 5%, for the period 2017–2019 - by 9%).



**Figure 2.** Changes in wheat yield of cultivars Sudarynya, k-66407 and Trizo, k-64981 when using associative rhizobacteria, the 2017 and 2019. Inoculation treatments: Control - water, 124-11 – *B. subtilis* 124-11, K1B – *Sphingomonas* sp. K1B, SPB2137 – *Ps. fluorescens* SPB2137. Vertical line – standard error of mean; \* – significant values of the indicator, different from the control, according to the Scheffe criterion at a certain significance level;  $F$  – Fisher criterion according to the single-factor analysis of variance.

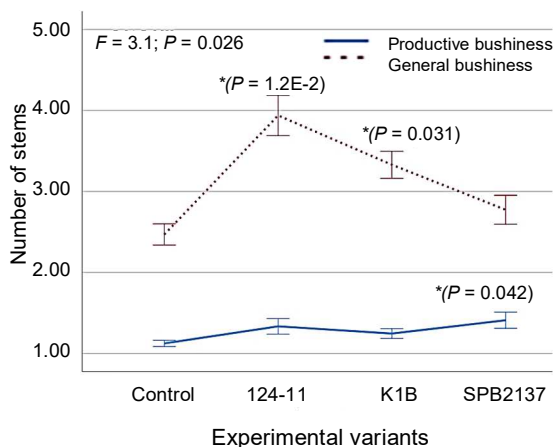
Figs. 3, 4 summarize data on biological yield of soft wheat, averaged over above-mentioned wheat cultivars and calculated based on the results of field experiment in 2019, also for the period 2017–2019. Using strains of *B. subtilis* 124-11 and *Ps. fluorescens* SPB2137 showed a statistically significant increase in wheat yield in 2019 at  $P < 0.05$  by 51% ( $t$ -test = 5.1) and 45% ( $t$ -test = 4.2), and for the time 2017–2019 - by 67% ( $t$ -test = 5.2) and 58% ( $t$ -test = 4.6), respectively.



**Figure 3.** Average yield of soft wheat when using associative rhizobacteria, the 2017–2019. Variants of inoculation: Control – water, 124-11 – *B. subtilis* 124-11, K1B – *Sphingomonas* sp. K1B, SPB2137 – *Ps. fluorescens* SPB2137. The graphs show the average values of the indicators and 95% confidence intervals, \* the same letters mark the values of the indicator that are not significantly different.

In 2019, the use of *B. subtilis* 124-11 strain caused an increase in the values comparing with the control ( $P < 0.05$ ) in the indicators: rate of plant development in the phases of ontogenesis (by 11%;  $t$ -test = 2.2), plant height (by 22%;  $t$ -test = 2.8), the number of roots (by 25%;  $t$ -test = 2.7), pre-flag leaf area (by 31%;  $t$ -test = 3.3). In the experimental variant, where *Sphingomonas* sp. K1B was applied, an increase in the values of following indicators ( $P < 0.05$ ) were noticed: rate of plant development in the phases of ontogenesis (by 11%;  $t$ -test = 2.6), plant height (by 16%;  $t$ -test = 2.2), roots number (by 23%;  $t$ -test = 2.9), root length (35%;  $t$ -test = 3.7), nodal root length (21%;  $t$ -test = 2.8). The use of *Ps. fluorescens* SPB2137 influenced plant development rate in the phases of ontogenesis (by 12%;  $t$ -test = 3.0), plant height (by 24%;  $t$ -test = 3.8), number of roots (by 20%;  $t$ -test = 2.8), pre-flag leaf area (by 29%;  $t$ -test = 3.3).

The strains of associative bacteria had the greatest impact on the wheat productive and total bushiness (Fig. 4). In particular, for the period 2017–2019, it was noticed that the application of *B. subtilis* 124-11



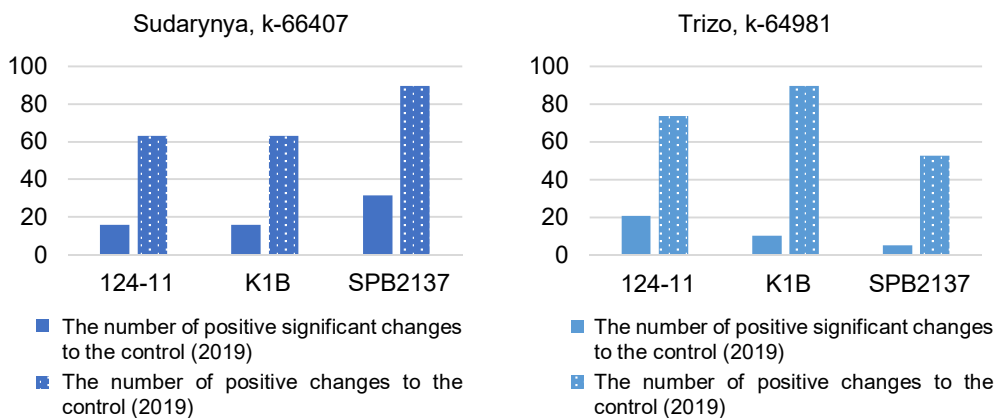
**Figure 4.** Total and productive bushiness of soft wheat when using associative rhizobacteria, the 2017–2019. Variants of inoculation: Control – water, 124-11 – *B. subtilis* 124-11, K1B – *Sphingomonas* sp. K1B, SPB2137 – *Ps. fluorescens* SPB2137. Vertical line – standard error of mean; \* – significant values of the indicator, different from the control, according to the Scheffe criterion at a certain significance level;  $F$  – Fisher criterion according to the single-factor analysis of variance.

and *Sphingomonas* sp. K1B strains resulted in a significant increase in the total bushiness at  $P < 0.05$  by 59% ( $t$ -test = 5.2) and 35% ( $t$ -test = 4.1). Using *Ps. fluorescens* SPB2137 led to an increase in the productive bushiness by 25% ( $t$ -test = 2.6). Strains of *B. subtilis* 124-11 and *Sphingomonas* sp. K1B did not significantly affect the productive bushiness (the change to the control was 18% and 10%, respectively,  $P > 0.05$ ).

For the period 2017–2019, a significant effect of the studied strains ( $P < 0.05$ ) on the increase in the plants vegetative weight was noted (*B. subtilis* 124-11 - by 27%;  $t$ -test = 2.6, *Sphingomonas* sp. K1B - by 37%;  $t$ -test = 3.1, *Ps. fluorescens* SPB2137 - by 21%;  $t$ -test = 2.3).

The greatest influence on grain number per spike increasing by 8% ( $t$ -test = 2.5), compared with control, for the period 2017–2019 was exerted by *B. subtilis* 124-1 strain. In the variant of the experiment, where the strain *Sphingomonas* sp. K1B was tested, a decrease in grain number per spike by 12% was noticed ( $t$ -test = 3.9).

Fig. 5 shows the positive changes ( $P > 0.05$ ) and significantly positive changes ( $P < 0.05$ ) in the values of wheat cultivars productivity indicators (Sudarynya, k-66407 and Trizo, k-64981) when using strains of associative rhizobacteria comparing with the control. In 2019, the greatest number of significant positive changes in productivity indicators (32%) was registered in the variant of experiment where *Ps. fluorescens* SPB2137 strain was used on the Sudarynya, k-66407 cultivar. Also, *B. subtilis* 124-11 strain had highest efficiency in relation to the productivity of Trizo, k-64981 cultivar (22% of significant positive changes in productivity indicators).

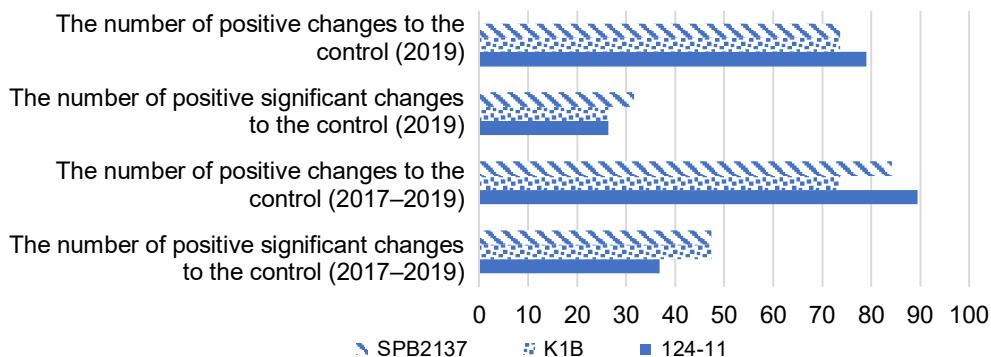


**Figure 5.** The number of changes (%) in the values of wheat productivity indicators when using strains of associative rhizobacteria comparing with control. 2019 Inoculation variants: 124-11 – *B. subtilis* 124-11, K1B – *Sphingomonas* sp. K1B, SPB2137 – *Ps. fluorescens* SPB2137.

For the period 2017–2019, the greatest number of significant positive changes in productivity indicators (47% of the total number of indicators) were registered in the experimental variants where *Sphingomonas* sp. K1B and *Ps. fluorescens* SPB2137 strains were used (Fig. 6).

At the second stage of study, influences of associative rhizobacteria strains on wheat pathogens development intensity were studied.

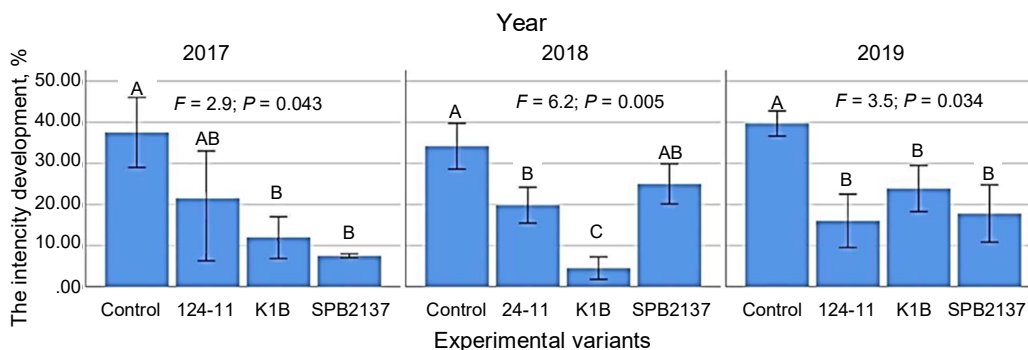
In 2019, the Trizo, k-64981 and Sudarynya, k-66407 cultivars were almost equally affected by root rot ( $R_g = 40\%$ ). The fungus *Bipolaris sorokiniana* (Sacc.) Shoem as the causative agent of wheat helminthosporium root rot, was identified by microscopic analysis.



**Figure 6.** The number of changes (%) in the values of productivity indicators of two wheat cultivars (Sudarynya, k-66407 and Trizo, k-64981) when using strains of associative rhizobacteria comparing with control, the 2017–2019. Inoculation variants: 124-11 – *B. subtilis* 124-11, K1B – *Sphingomonas* sp. K1B, SPB2137 – *Ps. fluorescens* SPB2137.

In 2019, the most pronounced statistically significant decrease in disease development  $P < 0.05$  was recorded on Sudarynya, k-66407 cultivar in the experimental variants when using *B. subtilis* 124-11 - by 21%,  $t$ -test = 6.6 and *Ps. fluorescens* SPB2137 - by 27%,  $t$ -test = 2.5.

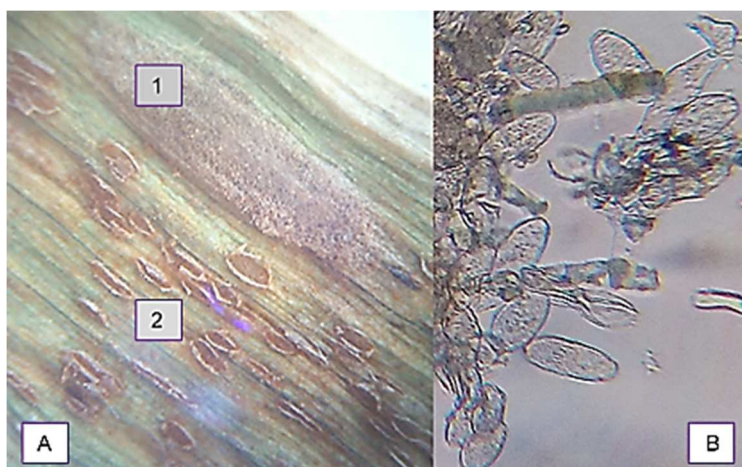
The results of a comparative analysis of root rot development for the period 2017–2019 in the experiment variants with using of strains of associative rhizobacteria and without using (control), on average on two wheat cultivars (Trizo, k-64981 and Sudarynya, k-66407) are shown in Fig. 7.



**Figure 7.** Development of wheat root rot in experimental variants with using associated rhizobacteria strains and without using (control) on wheat cultivars (Trizo, k-64981 and Sudarynya, k-66407) 2017–2019. Variants of inoculation: Control – water, 124-11 – *B. subtilis* 124-11, K1B – *Sphingomonas* sp. K1B, SPB2137 – *Ps. fluorescens* SPB2137. The graphs show average values of the indicator and 95% confidence intervals; \* – the same letters mark values of the indicator that are not significantly different.

In accordance with the Fischer criterion (F), the strongest differences in the experimental variants were revealed in 2018. The *Sphingomonas* sp. K1B had the greatest effectiveness against wheat root rot, in 2018 it caused the disease development significant decreasing - by 86.8% compared to the control (from  $34.2 \pm 5.6\%$  - in the control to  $4.5 \pm 2.7\%$ ). In 2017 and 2019, in this experimental variant, the root rot development decreased by 68.0% and 39.8%, respectively. The greatest decrease in the disease development - by 80% compared to the control, when using the *Pseudomonas fluorescens* SPB2137 was revealed in 2017, and in the variant with the 124-11 *Bacillus subtilis* strain - in 2019 (by 59.6%).

Powdery mildew is one of the most common and harmful diseases in wheat, causing significant losses in its yield. The causative agent of this disease is the microscopic fungus *Blumeria graminis* (DC.) Speer f. sp. *tritici* March (Fig. 8).



**Figure 8.** Symptoms of mixed infection on leaves of Trizo wheat cultivar, k-64981: A – spots with plaque of powdery mildew (1) and uredopustule of brown rust (2), an increase of 16X; B – conidia of the causative agent of powdery mildew, an increase of 800X (orig.).

In 2019, only *Sphingomonas* sp. K1B strain had an insignificant effectiveness in reducing intensity development of powdery mildew. In this variant of experiment, the decrease in disease development was 6% and the number of spots with plaque decreased by 27%. However, for the period 2017–2019, a significant decrease in the area of spots with plaque of powdery mildew after the treatments of Sudarynya, k-66407 cultivar was marked (with *Sphingomonas* sp. K1B. - by 58%,  $t$ -test = 2.3; with *Ps. fluorescens* SPB2137 - by 60%,  $t$ -test = 2.3; with *B. subtilis* 124-11 - by 64%;  $t$ -test = 2.5).

The causative agent of wheat brown rust, *Puccinia recondita* Rob. ex Desm f. sp. *tritici*, which causes the formation of many uredopustules on leaves during the growing season (Fig. 10). In 2019, the most significant plants damage caused by brown rust was registered on the Trizo cultivar, k-64981 ( $R_b = 28.8 \pm 6.9\%$ , pustules number  $N_p = 295.8 \pm 126.3$ ). The intensity of disease affection of wheat cultivar Sudarynya, k-66407 was:  $R_b = 6.9 \pm 1.8\%$ , pustules number  $N_p = 48.0 \pm 20$ . A small decrease in disease development from 7% to 8% comparing with a control, was recorded in the experimental variants where strains of *B. subtilis* 124-11, *Sphingomonas* sp. K1B. and

*Ps. fluorescens* SPB2137 were used. While for the period 2017–2019, a significant decrease in brown rust development on average for both wheat cultivars when using *Sphingomonas* sp. K1B strain (by 10%,  $t$ -test = 2.6), in comparison with the control, was revealed.

The international scientific name of the causative agent of yellow rust is *Puccinia striiformis* West. f. sp. *tritici*. In 2019, the most significant damage caused by yellow rust was registered on Sudarynya, k-66407 cultivar ( $R_b = 21.7 \pm 6.6\%$ , pustules number  $N_p = 857.2 \pm 242.5$ ). The intensity of disease affection of Trizo, k-64981 cultivar was:  $R_b = 8.0 \pm 4.0\%$ , pustules number  $N_p = 242.0 \pm 122.4$ . The greatest decrease in the wheat damage by yellow rust in comparison with the control was registered in Sudarynya, k-66407 cultivar when using *Sphingomonas* sp. K1B strain (unreliable for disease development at  $P > 0.05$  - by 12%; strips number - by 13% and reliable at  $P < 0.05$ , pustules number in the strip - by 34%,  $t$ -test = 2.7; pustules number per leaf - by 35%,  $t$ -test = 3.0). No symptoms of yellow rust were detected in 2019 after the treatments by *B. subtilis* 124-11 on Trizo, k-64981 cultivar. Using *Ps. fluorescens* SPB2137 on Trizo, k-64981 cultivar caused a slight ( $P > 0.05$ ) decrease in the disease development intensity by 7%, the stripes number by 13%, and a significant decrease ( $P < 0.05$ ) in the stripe length by 50% ( $t$ -test = 2.2), the pustules number per stripe by 75%, ( $t$ -test = 2.5) the pustules number per leaf - by 80% ( $t$ -test = 2.7). On average, for the above-mentioned cultivars for the period 2017–2019, the strain *Sphingomonas* sp. K1B had the highest efficiency against yellow rust, the use of which led to a decrease in the strip length at  $P < 0.05$  by 22% ( $t$ -test = 2.6), the pustules number per strip by 29% ( $t$ -test = 2.5). A significant decrease in the pustule area by 44% ( $t = 4.7$ ) was marked in the experiment variant with the using *Ps. fluorescens* SPB2137.

## CONCLUSIONS

The greatest potential yield of wheat in 2019 was revealed in the experimental variants with using *B. subtilis* 124-11 strains ( $Y_r = 4.2 \pm 0.2$  g plant, when recalculated per 1 ha  $Y = 6.19 \pm 0.33$  t ha) and *Ps. fluorescens* SPB213 ( $Y_r = 4.0 \pm 0.2$  g plant,  $Y = 5.9 \pm 0.4$  t ha), and for the period 2017–2019 - when using *B. subtilis* 124-11 ( $Y_r = 3.0 \pm 0.2$  g plant,  $Y = 6.2 \pm 0.3$  t ha). At the same time, in 2019, the maximum number of significant positive changes in productivity indicators was recorded when using *Ps. fluorescens* SPB2137 (32%), and for the period 2017–2019 when using *Sphingomonas* sp. K1B and *Ps. fluorescens* SPB2137 (47%). For the period 2017–2019, it was noticed that only with the application of *Ps. fluorescens* SPB2137 revealed a significant increase in the productive bushiness by 25% ( $t$ -test = 2.6,  $P < 0.05$ ). Although, the treatments with *B. subtilis* 124-11 and *Sphingomonas* sp. K1B strains did not significantly affect the productive bushiness, but had a protective effect against the pathogens of wheat, particularly helminthosporium root rot. The maximum decrease in the disease development intensity by 26% was registered in 2017–2019 on Trizo k-64981 cultivar when using *Sphingomonas* sp. K1B. The strain of *Sphingomonas* sp. K1B showed the greatest effectiveness against the complex of leaf diseases.

The rhizobacteria high efficiency revealed in our research caused due to their growth-stimulating effect on plants and an increase in their adaptive potential to environmental factors, which is consistent with the results of studies presented in a number of scientific papers in this field (Araujo et al., 1994; Belimov et al., 2014;



Hashem et al., 2019; Naseri, 2019). The antagonistic activity of rhizobacteria against phytopathogenic fungi, its dependence on environmental factors and application methods, as well as the bacterium ability to cause induced plant resistance are widely discussed in various works (Araujo et al., 1994; Matzen et al., 2019; Wachowska et al., 2013b). Perhaps, the high efficiency of our rhizobacteria in wheat cultivation is associated with their combined application during sowing and throughout the entire growing season, as well as the diseases development inhibiting by plants preventive spraying before the first signs of disease development appearance.

The obtained data indicate the possibility of more effective cultivation and wheat protection from diseases when using bacterial strains (*B. subtilis* 124-11, *Ps. fluorescens* SPB2137, *Sphingomonas* sp. K1B), which can increase the wheat yield and its resistance to the main pathogens.

ACKNOWLEDGEMENTS. This work was carried out within the framework of the state tasks according to the VIR thematic plan for project No. 0662-2019-0006 and to the ARRIAM thematic plan for project No. 0482-2021-0001.

## REFERENCES

- Ali, S.Z., Sandhya, V., Grover, M., Linga, V.R. & Bandi, V. 2011. Effect of inoculation with a thermotolerant plant growth promoting *Pseudomonas putida* strain AKMP7 on growth of wheat (*Triticum* spp.) under heat stress. *Journal of Plant Interactions* **6**, 239–246. doi:10.1080/17429145.2010.545147
- Araujo, M.A.V., Mendonça-Hagler, L., Hagler, A. & van Elsas, J. 1994. Survival of genetically modified *Pseudomonas fluorescens* introduced into subtropical soil microcosms. *FEMS Microbiology Ecology* **13**, 205–216. 10.1111/j.1574-6941.1994.tb00067.x.
- Asaf, S., Khan, A., Khan, M., Imran, Q., Yun, B.-W. & Lee, I-J. 2017a. Osmoprotective functions conferred to soybean plants via inoculation with *Sphingomonas* sp. LK11 and exogenous trehalose. *Microbiological Research* **205**, 135–145. doi: 10.1016/j.micres.2017.08.009
- Asaf, S., Khan, M.A., Khan, A.L., Waqas, M., Shahzad, R., Kim, Ah-Yeong, Kang, Sang-Mo & Lee, In-Jung. 2017b. Bacterial endophytes from arid land plants regulate endogenous hormone content and promote growth in crop plants: an example of *Sphingomonas* sp. and *Serratia marcescens*. *Journal of Plant Interactions* **12**(1), 31–38. doi.org/10.1080/17429145.2016.1274060
- Belimov, A.A., Dodd, I.C., Safronova, V.I., Dumova, V.A., Shaposhnikov, A.I., Ladatko, A.G., & Davies, W.J. 2014. Abscisic acid metabolizing rhizobacteria decrease ABA concentrations in planta and alter plant growth. *Plant physiology and biochemistry* **74**, 84–91. doi:10.1016/j.plaphy.2013.10.032
- Briard, B., Bomme, P., Lechner, Beatrix, E., Mislin, Gaëtan, L.A., Lair, V., Prévost, Marie-Christine, Latgé, Jean-Paul, Haas, H. & Beauvais, A. 2015. *Pseudomonas aeruginosa* manipulates redox and iron homeostasis of its microbiota partner *Aspergillus fumigatus* via phenazines. *Scientific reports* **5**, 8220. doi: 10.1038/srep08220
- Geshele, E.E. 1978. Fundamentals of phytopathological assessment in plant breeding. Moscow, Kolos, pp. 53 (in Russian).
- Hashem, A., Tabassum, B., Abd, A. & Elsayed, F. 2019. *Bacillus subtilis*: A plant-growth promoting rhizobacterium that also impacts biotic stress. *Saudi Journal of Biological Sciences* **26**(6), 1291–1297. 10.1016/j.sjbs.2019.05.004

- Hofemeister, J., Conrad, B., Adler, B., Hofemeister, B., Feesche, J., Kucheryava, N., Steinborn, G., Franke, P., Grammel, N., Zwintscher, A., Leenders, F., Hitzeroth, G. & Vater, J. 2004. Genetic analysis of the biosynthesis of non-ribosomal peptide- and polyketide-like antibiotics, iron uptake and biofilm formation by *Bacillus subtilis* A1/3. *Molecular Genetics and Genomics* **272**(4), 363–378. doi: 10.1007/s00438-004-1056
- Housusright, D.R., Henry, J.R. & Berkman, S.A. 1948. Microbiological method for the assay of subtiling. *Journal of Bacteriology* **55**(4), 545–550.
- Hu, H., Xu, Y., Chen, F., Zhang, X.H. & Hu, B.K. 2005. Isolation and characterization of a new fluorescent *Pseudomonas* strain that produces both phenazine 1-carboxylic acid and pyoluteorin. *Journal of microbiology and biotechnology* **15**(1), 86–90.
- Kalantari, S., Marefat, A., Naseri, B. & Hemmati, R. 2018. Improvement of bean yield and Fusarium root rot biocontrol using mixtures of *Bacillus*, *Pseudomonas* and *Rhizobium*// *Tropical Plant Pathology* **43**, 499–505. <https://doi.org/10.1007/s40858-018-0252-y>
- Kidarsa, T.A., Goebel, N.C., Zabriskie, T.M. & Loper, J.E. 2011. Phloroglucinol mediates cross-talk between the pyoluteorin and 2, 4-diacetylphloroglucinol biosynthetic pathways in *Pseudomonas fluorescens* Pf-5. *Molecular microbiology* **81**(2), 395–414. doi: 10.1111/j.1365-2958.2011.07697.x
- Kolesnikov, L.E., Belimov, A.A. & Dones, P.M. 2019. The biological effectiveness of the associative rhizobacteria strains on soft wheat. *Proceedings of the St. Petersburg State Agrarian University* **1**(54), 57–64 (in Russian). doi: 10.24411/2078-1318-2019-11057
- Kolesnikov, L.E., Kremenevskaya, M.I., Razumova, I.E., Kolesnikova, Yu.R., Ambulatova, E.V. & Yazeva, E.O. 2020. The biological basis for the use of protein growth stimulant made from cattle split for wheat foliar feeding and disease suppression. *Agronomy Research* **18**(S2), 1336–1349 doi.org/10.15159/AR.20.082
- Kolesnikov, L.E., Novikova, I.I., Popova, E.V., Priyatkin, N.S., Zuev, E.V., Kolesnikova, Yu.R., & Solodyannikov, M.D. 2020. The effectiveness of biopreparations in soft wheat cultivation and the quality assessment of the grain by the digital x-ray imaging. *Agronomy Research* **18**(4), 2436–2448. doi.org/10.15159/AR.20.206
- Kozhemyakov, A.P. & Tikhonovich, I.A. 1998. Use of legume inoculants and biopreparations with complex action in agriculture. *Proceedings of the Russian Academy of Agricultural Sciences* **6**, 7–10.
- Kravchenko, L.V., Azarova, T.S., Leonova-Erko, E.I., Shaposhnikov, A.I., Makarova, N.M. & Tikhonovich, I.A. 2003. Root exudates of tomato plants and their effect on the growth and antifungal activity of pseudomonas strains. *Microbiology* **72**(1), 37–41.
- Kumar, A., Bahadur, I., Maurya, B.R., Raghuwanshi, R., Meena, V.S., Singh, D.K. & Dixit, J. 2015. Does a plant growth-promoting rhizobacteria enhance agricultural sustainability. *Journal of Pure and Applied Microbiology* **9**(1), 715–724.
- Lemeshko, B.Yu. & Ponomarenko, V.M. 2006. Investigation of statistical distributions of the Scheffe criterion under the laws of observation errors that differ from normal. 2006. *Proceedings of the VIII International Conference 'Actual problems of Electronic Instrumentation' APEP-2006* (**6**), 87–90.
- Loeffler, W., Tschén, Johannes S.-M., Vanittanakom, N. & Kugler, M. 1986. Antifungal Effects of Bacilysin and Fengymycin from *Bacillus subtilis* F-29-3 A Comparison with Activities of Other Bacillus Antibiotics. *Journal of Phytopathology* **115**(3), 204–213. doi: 10.1111/j.1439-0434.1986.tb00878.x
- Matzen, N., Heick, T. & Jørgensen, L. 2019. Control of powdery mildew (*Blumeria graminis* spp.) in cereals by Serenade®ASO (*Bacillus amyloliquefaciens* (former subtilis) strain QST 713). *Biological Control*. **139**, 104067. 10.1016/j.biocontrol.2019.104067
- Mohite, B. 2013. Isolation and characterization of indole acetic acid (IAA) producing bacteria from rhizospheric soil and its effect on plant growth. *Journal of soil science and plant nutrition* **13**(3), 638–649.

- Nadeem, S.M., Zahir, Z.A., Naveed, M. & Nawaz, S. 2013. Mitigation of salinity-induced negative impact on the growth and yield of wheat by plant growth-promoting rhizobacteria in naturally saline conditions. *Annals of Microbiology* **63**(1), 225–232. doi.org/10.1007/s13213-012-0465-0
- Naiman, A.D., Latronico, A. & Garcia de Salamone, I.E. 2009. Inoculation of wheat with *Azospirillum brasilense* and *Pseudomonas fluorescens*: impact on the production and culturable rhizosphere microflora. *European Journal of Soil Biology* **45**(1), 4–51. doi.org/10.1016/j.ejsobi.2008.11.001
- Naseri, B. 2019. Legume root rot control through soil management for sustainable agriculture. In: Meena, R.S., Kumar, S., Bohra, J.S., Jat, M.L. (Eds.) *Sustainable Management of Soil and Environment*, pp. 217–258. doi:10.1007/978-981-13-8832-3
- Naseri, B. & Younesi, H. 2021. Beneficial microbes in biocontrol of root rots in bean crops: A meta-analysis (1990–2020). *Physiological and Molecular Plant Pathology* **116**. doi.org/10.1016/j.pmp.2021.101712
- Park, J.Y., Oh, S.A., Anderson, A.J., Neiswender, J., Kim, J.-C. & Kim, Y.C. 2011. Production of the antifungal compounds phenazine and pyrrolnitrin from *Pseudomonas chlororaphis* O6 is differentially regulated by glucose. *Letters in applied microbiology* **52**(5), 532–537. doi.org/10.1111/j.1472-765X.2011.03036.x
- Peypoux, F., Pommier, M.T., Das, B.C., Besson, F., Delcambe, L. & Michel, G. 1984. Structures of bacillomycin D and bacillomycin L peptidolipid antibiotics from *Bacillus subtilis*. *The Journal of antibiotics* **77**(12), 1600–1604.
- Pham, V.T., Rediers, H., Ghequire, M.G., Nguyen, H.H., De Mot, R., Vanderleyden, J. & Spaepen, S. 2017. The plant growth-promoting effect of the nitrogen-fixing endophyte *Pseudomonas stutzeri* A15. *Archives of microbiology* **199**(3), 513–517. Doi 10.1007/s00203-016-1332-3
- Pieterse, Corné M.J., Zamioudis, C., Berendsen, Roeland, L., David, M.W., Van Wees, Saskia C.M. & Bakker, Peter A.H.M. 2014. Induced systemic resistance by beneficial microbes. *Annual review of phytopathology* **52**, 347–375.
- Popov, Yu.V. 2011. Method for the estimation of the root rots development in cereals. *Plant protection and quarantine* **8**, 45–47 (in Russian).
- Pukhaev, A.R., Farniev, A.T. & Kozhemyakov, A.P. 2009. Efficiency of new associative rhizobacteria strains at winter wheat sowings. *Zemledelie* **8**, 40–41 (in Russian).
- Raheem, A., Shaposhnikov, A., Belimov, A.A., Dodd, I.C. & Ali, Basharat. 2018. Auxin production by rhizobacteria was associated with improved yield of wheat (*Triticum aestivum* L.) under drought stress. *Archives of Agronomy and Soil Science* **64**(4), 574–587. doi:10.1080/03650340.2017.1362105
- Satyaprakash, M., Nikitha, T., Reddi, E.U.B., Sadhana, B. & Vani, S. Satya. 2017. Phosphorous and phosphate solubilising bacteria and their role in plant nutrition. *International Journal of Current Microbiology and Applied Science* **6**(4), 2133–2144. doi: 10.20546/ijemas.2017.604.251
- Selvakumar, G., Joshi, P., Suyal, P., Mishra, P., Joshi, G., Bisht, J.K., Bhatt, J. & Gupta, H.S. 2011. *Pseudomonas lurida* M2RH3 (MTCC 9245), a psychrotolerant bacterium from the Uttarakhand Himalayas, solubilizes phosphate and promotes wheat seedling growth. *World Journal of Microbiology and Biotechnology* **27**, 1129–1135. doi:10.1007/S11274-010-0559-4
- Sharma, R.R., Singh, D. & Singh, R. 2009. Biological control of postharvest diseases of fruits and vegetables by microbial antagonists: A review. *Biological control* **50**(3), 205–221.
- Strunnikova, O.K., Shakhnazarova, V.Yu., Vishnevskaya, N.A., Chebotar, V. & Tikhonovich, I.A. 2007. Development and relations of *Fusarium culmorum* and *Pseudomonas fluorescens* in soil. *Microbiology* **76**(5), 596–602. doi:10.1134/S002626170705013X

- Tabande, L. & Naseri, B. 2020. How strongly is rhizobial nodulation associated with bean cropping system? *Journal of Plant Protection Research* **60**, 176–184. doi: 10.24425/jppr.2020.133307
- Trapet, P., Laure, A., Agnès, K., Stéphanie, P., Sylvie, C., Christian, C., Sylvie, M., Philippe, L., David, W. & Angélique, Besson-Bard. 2016. The *Pseudomonas fluorescens* siderophore pyoverdine weakens *Arabidopsis thaliana* defense in favour of growth in iron-deficient conditions. *Plant physiology* **171**(1), 675–93. doi: 10.1104/pp.15.01537
- Tsavkelova, E.A., Klimova, S.Yu., Cherdyntseva, T.A. & Netrusov, A.I. 2006. Microbial producers of plant growth stimulators and their practical use: a review. *Applied biochemistry and microbiology* **42**(2), 117–126. doi: 10.1134/S0003683806020013 (in Russian).
- Wachowska, U., Jedryczka, M., Irzykowski, W. & Glowacka, K. 2013a. Use of *Aureobasidium pullulansto* control fusarium head blight on winter wheat ears caused by *Fusarium culmorum*. *Communications in agricultural and applied biological sciences* **78**(3), 545–549.
- Wachowska, U., Irzykowski, W., Jedryczka, M., Stasiulewicz-Paluch, A. & Glowacka, K. 2013b. Biological control of winter wheat pathogens with the use of antagonistic Sphingomonas bacteria under greenhouse conditions. *Biocontrol Science and Technology* **23**, 1110–1122. 10.1080/09583157.2013.812185
- Zabihi, H., Savaghebi, G.R., Khavazi, K., Ganjali, A. & Miransari, M. 2010. Pseudomonas bacteria and phosphorous fertilization, affecting wheat (*Triticumaestivum* L.) yield and P uptake under greenhouse and field conditions. *Acta Physiologiae Plantarum* **33**, 145–152. doi:10.1007/s11738-010-0531-9
- Zadoks, J.C., Chang, T.T. & Konzak, C.F. 1974. A Decimal Code for the Growth Stages of Cereals. *Weed Research* **14**, 415–421.

## **The biological basis for the use of acrylic hydrogel and protein growth stimulant in the soft wheat and triticale cultivation**

L.E. Kolesnikov<sup>1,\*</sup>, M.V. Uspenskaya<sup>2</sup>, M.I. Kremenevskaya<sup>2</sup>, A.G. Orlova<sup>1</sup>,  
I.E. Razumova<sup>1</sup> and Yu.R. Kolesnikova<sup>3</sup>

<sup>1</sup>Saint-Petersburg State Agrarian University, Faculty of Agrotechnologies, Soil science and Ecology, Department of Plant Protection and Quarantine, Petersburgskoe Shosse, 2, RU196601 St-Petersburg – Pushkin, Russia

<sup>2</sup>ITMO University, School of Biotechnology and Cryogenic Systems, Faculty of Food Biotechnologies and Engineering, 49 Kronverksky Pr., RU197101 St-Petersburg, Russia

<sup>3</sup>Federal Research Center N.I. Vavilov All-Russian Institute of Plant Genetic Resources (VIR), genetic resource of wheat department, plant introduction department, Bolshaya Morskaya ul. 42–44, RU190000 St-Petersburg, Russia

\*Correspondence: kleon9@yandex.ru

Received: January 29<sup>th</sup>, 2021; Accepted: November 4<sup>th</sup>, 2021; Published: November 22<sup>nd</sup>, 2021

**Abstract.** The development of technologies for the environmentally friendly biopreparations production and use including biopreparations based on acrylic hydrogel and protein growth stimulant, which is obtained by chemical hydrolysis from by-products of slaughtered animals processing is carried out as part of the optimization of the phytosanitary condition of wheat crops and creation of favourable agro-ecological conditions for its cultivation. An important feature of acrylic hydrogel is the ability to retain and release water to plants when needed. At the same time, protein hydrolysate can provide plants with an additional source of nitrogen which is a component of plant proteins, chlorophyll and it is necessary for normal growth and development of plants during the vegetation. The addition of the protein growth stimulant to acrylic hydrogel expands the potential application of Super Moisture Absorbent (SMA) due to the long-term growth-stimulating effect on plants. The acrylic hydrogel and protein growth stimulant were added to the soil when wheat sowing in the certain concentrations and proportions. Wheat productivity was studied by the indicators complex, characterized the plants morphological features and the yield structure. Assessment of the degree of plant affection caused by pathogens was carried out both according to the generally accepted phytopathological indicator - conditional intensity of development, and using additional parameters. In the research, it was found that acrylic hydrogel and protein growth stimulant provide an increase in wheat yield and reduce the pathogens harmfulness. In combined application, they can be used in agriculture for wheat cultivation as a low-cost and environmentally friendly soil conditioner.

**Key words:** acrylic hydrogel, plant diseases, productivity elements, protein growth stimulant, soft wheat, triticale.

## INTRODUCTION

Currently, research aimed at finding ways to increase the yield and quality of grain crops is becoming especially relevant, in particular, using techniques that improve the moisture supply and nutrition of plants, reduce the harmfulness of pathogens and optimize the phytosanitary state of agrocenoses (Pavlyushin et al., 2016). The production of agricultural crops in the world is accompanied by the depletion of fresh water resources as a result of irrigation of cultivated areas, chemical and biological pollution, and the growth of greenhouse gas emissions (Falkenmark & Rockström, 2014). At the same time, the annual production of cereals in the world should grow by almost a billion tons, as the world's population may exceed nine billion people by 2050 (Shewry et al., 2016). Factors that reduce the yield of grain crops are the decrease in agricultural land suitable for cultivation, climate change, unpredictable stress factors of an abiotic and biotic nature. In addition, the decline in the genetic diversity of wheat in the pursuit of elite high-yielding varieties, in particular, leads to the formation of new races of pathogens, contributes to the accumulation of the infectious potential of pathogens that lead to epiphytosis (Figueroa et al., 2018; Novakazi et al., 2020). In the world, the total loss of grain crops caused by climate change and pollution can reach 37% (Burney & Ramanathan, 2014). According to Gupta et al. (2017) an increase in the average daily maximum and minimum temperatures by 1 °C will lead to a decrease in wheat yield by 2–4%. In the conditions of global warming and aridization, in general, in Russia by 2030, grain yields may decrease by 15%, and in the Volga region, in the south of Western Siberia and the North Caucasus - by 20% (Zhuchenko, 2004). The grain shortage can reach by 27% if the increase in the aridity of the climate will appear combined with soil degradation (Gundyryn et al., 2016).

Polymer materials are widely used in various priority areas of science, technology and engineering development. They are easily processed and chemically modified, and have valuable physical and mechanical properties (Zhang et al., 2013).

Recently, among the most promising polymer materials, a special group of ‘soft’ polymer materials - hydrogels, which are usually a three-dimensional matrix consisting of linear (or branched) hydrophilic weakly cross-linked polymers with the ability to absorb large amounts of liquid, may be of great interest (Pourjavadi et al., 2004; Chang et al., 2010). The radical copolymerization of monomers in aqueous solutions using crosslinking agents containing two or more unsaturated groups is the most common method for the synthesis of chemically crosslinked acrylic hydrogels (Zoolshoev et al., 2016). The radical polymerization of acrylic monomers can be carried out in aqueous or organic medium, suspension, mass, or emulsion (Kabiri et al., 2011; Iqbal et al., 2016). Bi - or polyfunctional low-molecular-weight compounds of the acrylate type, such as divinylbenzene, methylene bis-acrylamide, guanidine methacrylate, etc., are usually used as a crosslinking agent during radical polymerization, which leads to crosslinking of the macromolecules (Chavda et al., 2012). The method of crosslinking polymer macromolecules in solution is also used to create hydrogels from natural polymers, such as cellulose or chitosan (Bigi et al., 2001; Zhang et al., 2006).

A hydrogel particle, which is a cross-linked hydrophilic polymer (superabsorbing polymer, SAP), can rapidly swell up to 1,000 times its dry volume and retains a large amount of water (Yamaguchi, 2014). In agriculture, hydrogels are mainly used as soil structure-forming agents and polymer carriers for the release of nutrients necessary for

the growth and development of crops, as well as in the production of chemical plant protection products (Guilherme et al., 2015). Hydrogel, especially in southern Russia, reducing the moisture deficit and improves the moisture availability of plants, reduces the risk of crop losses leading culture of winter wheat, and therefore, improve stability of grain production. In particular, according to Gundyryin et al. (2016), when using hydrogel, the value of the increase in wheat yield can vary from 4.0 to 24.7 c per ha (8.8–44.0%).

Advances in the synthesis of tetrazole derivatives have increased the possibility of obtaining new macromolecular compounds, which has significantly increased interest in this class of (co)polymers, since the introduction of tetrazole-containing monomers into copolymers has expanded the areas of practical application of acrylic hydrogels. The use of copolymers based on acrylic acid (AC) salts and 2-methyl-5-vinyltetrazole is possible as a medium for growing plants at high temperatures of surrounding environment (Kabakova et al., 2003). Strongly swollen acrylic copolymers, along with a high water-holding capacity, have the presence of nitrogen and potassium elements in their composition, contribute to increasing crop yields and their resistance to adverse environmental factors (Bortolin al, 2011). It should be noted that at the initial stages of wheat development, the lack of nitrogen leads to a decrease in the natural weight of the grain, and in the later stages of ontogenesis - to a decrease in its quality: the protein content (Bairwa et al., 2013b).

The properties of acrylic hydrogels resemble those of biological tissues and are due to their ability to retain and release water to plants as needed (Zohuriaan-Mehr & Kabiri, 2008). The degree of swelling in distilled water and in saline solution of acrylic hydrogel composites can reach:  $700 \text{ g g}^{-1}$  and  $75 \text{ g g}^{-1}$  (Baidakova et al., 2019b). The water absorption of hybrid hydrogels obtained by free radical polymerization in an aqueous medium from acrylamide, acrylic acid and corn starch was  $400\text{--}700 \text{ g g}^{-1}$  in distilled water and  $100\text{--}150 \text{ g g}^{-1}$  in NaCl solution at a temperature of  $20\text{--}30 \text{ }^{\circ}\text{C}$  (Long et al., 2003).

From a wide range of commercially available moisture-retaining sorbents, it can be noted: 'Soiltex L7', 'Agrosoke' (Great Britain), 'Sumikagel' (Japan), 'Arasorb' (Japan), 'Matrigel' (Germany), 'Juviderm' (France), 'Hydrat sol P' (France), etc. A moisture-absorbing agent based on hydrolyzed acrylonitrile and cellulose waste 'RAPG', had a degree of swelling up to  $750 \text{ g g}^{-1}$  (Gundyryin et al., 2016). The application doses of moisture-retaining polymer sorbents are minimal (0.3–0.5% of the soil weight), and depend on the type of soil and climate zone, the growing season of plants, the type of agricultural crop, etc. (Baran et al., 2015).

Soil conditioners can be an additional source of ammonium nitrogen for soil bacteria (Dabhi et al., 2013). In particular, the addition of wood flour to polyacrylamide hydrogel was an additional source of nutrition for soil bacteria (Entrya et al., 2002).

Acrylic hydrogels do not cause a negative impact on the environment, since they are introduced in small quantities, and decompose by microorganisms within 1–3 years, depending on their composition and production methods. At the same time, they are most advantageous economically compared to materials obtained on the basis of biopolymers in the price-properties ratio.

The inclusion of various fillers in the copolymers composition significantly expands the potential for the use of acrylic super moisture-absorbing agents by improving the physical and chemical properties of materials (Uspenskaya et al., 2005).

The use of the hydrogel matrix as a carrier of the nutrients necessary for the plant during the growing season is quite an urgent issue (Zhong et al., 2013). As nutrients for plant growth can be used secondary raw materials of meat processing secondary raw materials of meat processing for plant growth (Kremenevskaya et al., 2017). The combined use of acrylic hydrogels and hydrolyzed protein waste as fillers leads to regulated plant growth (Baidakova et al., 2019b). The use of amino acids of secondary biological raw materials makes it possible to obtain preparations with growth-stimulating properties that can compete with expensive plant growth regulators. The cost of the biopreparation, obtained by us from the cattle hides production waste is about 1.7 euros. Thus, the development of polymer hydrogels filled with the protein growth stimulant obtained from collagen-containing animal tissue waste is a very relevant and promising direction for improving the soil structure, increasing its moisture capacity and optimizing the acid-alkaline balance (Yanez-Chavez et al., 2014; Baran et al., 2015; Mellelo et al., 2019).

The purpose of this work is to study the effectiveness of a polymer hydrogel based on potassium acrylate and the protein growth stimulant, including when they are used together in the soft wheat cultivation. Materials and Methods sections should include full description of all the materials, chemicals, instrumentation, and methodologies that were used in the work.

## MATERIALS AND METHODS

Experimental studies were carried out in the experimental field of the Federal Research Center N.I. Vavilov All Russian Institute of Plant Genetic Resources (VIR). The plant material for the study included the cultivars of soft wheat and triticale: Trizo, k-64981 (Russia, Leningrad region) and Dua, k-828 (Australia). These samples were provided for study by the Department of Wheat Genetic Resources of the VIR.

The study object was a moisture-absorbing polymer hydrogel composition based on potassium acrylate and N, N' - methylenebisacrylamide as a crosslinking agent (Baidakova et al., 2019a). Divinylbenzene is used as crosslinking agent in the creation of various moisture super absorbents in concentrations of 0.01–0.001 wt.% of the entire material weight. Based on the monomers reactivity and toxicity, methylene bisacrylamide was chosen as a crosslinking agent in the work. The polymer hydrogel (Fig. 1) based on potassium acrylate was obtained using an unique technology at the International Research Institute of Bioengineering at ITMO University.

The technological scheme of the composite superabsorbent synthesis process included: preparation of the reaction mixture; polymerization; washing of the resulting hydrogel from monomers (the sol-fraction removal); drying of the resulting acrylic hydrogel composite at a temperature of no more than 40 °C; crushing. The auxiliary stage - the purification of the initial monomers and reagents: ammonium persulfate (PSA), which was previously recrystallized according to the standard method for removing impurities (Rabinovich & Khavin, 1991), acrylic acid (AA) was previously distilled under vacuum to remove the polymerization inhibitor. Next, preparation an 8N aqueous solution of potassium hydroxide. The KOH concentration was determined by titration of 0.1 N hydrochloric acid solution in the presence of phenolphthalein. As a redox system, PSA and tetramethylethylenediamine were used. Preparation of a 2%



aqueous solution of ammonium persulfate PSA. Preparation of a 1% aqueous solution of TMED (Baidakova et al., 2019a).

The protein hydrolysate (Fig. 2) was developed using a unique technology at the mega Faculty of Food Biotechnologies and Low-Temperature Systems of ITMO University from the processed products of slaughtered animals (RF Patent No. 2662782. 31.07.2018).



**Figure 1.** The polymer hydrogel composition in the dried state.



**Figure 2.** The protein growth stimulant (protein hydrolysate).

The protein hydrolysate composition includes various combinations of polypeptides with different molecular weights and amino acids that affect the yield of agricultural crops and increase their resistance to unfavorable environmental factors. The main active component in the protein hydrolysate is the amino acid - glycine, the content of which in the protein filler used is one third of the total weight of all the amino acids present in it.

The experiments were arranged on a randomized complete block designed with three replicates. For one variant of the experiment, plot area was 1.0 m<sup>2</sup>, treatments for plots in replicates were arranged systematically. The experiment samples were sown manually on plots in an ordinary way of sowing with the distance between rows by 15 cm and the distance between seeds in a row by 1–2 cm. The seeding depth was 5–6 cm. The seeding rate was 300 grains per 1 m<sup>2</sup>. These activities were carried out in accordance with the generally accepted recommendations and methods of the VIR.

The scheme of the experiment when applying a polymer hydrogel and a protein growth stimulant to the soil when sowing soft wheat and triticale was as follows:

- ‘K’ – Control (without applying biopreparations to the soil);
- ‘0.5 G’ – Hydrogel (based on the ability to bind 200 mL of water);
- ‘1G’ – Hydrogel (based on the ability to bind 400 mL of water);
- ‘0.5 G:1S’ – Hydrogel + Protein stimulant (based on the ability to bind 200 mL of water);
- ‘1G:2S’ – Hydrogel + Protein stimulant (based on the ability to bind 400 mL of water).

Polymer granules of hydrogel envelop the roots of wheat, forming a protective cover and prevent them from drying out (Fig. 3), and a protein stimulant improves plant nutrition.

Wheat productivity was described by 19 indicators that characterize the morphological features of plants and the structure of wheat yield in the earing-flowering

and maturation phases (Kolesnikov, Popova et al., 2019). In particular, the total and productive bushiness of plants, the ontogenesis phases, the flag and pre-flag leaves area (cm<sup>2</sup>), the plant vegetative part weight (g), etc. have been measured. The yield structure have been studied by the spikelets number per spike, pcs.; the spike length, cm; the spike weight, g; the grains number per spike, pcs.; the grains weight; the 1,000 grains weight. In addition, the samples' field germination was marked. The amount of sampling for each variant of the experiment was 20 plants.



**Figure 3.** The polymer granules on the roots of soft wheat.

The potential (biological) yield of a single wheat plant was calculated according to the data about the productive bushiness and the grains weight of spike per one plant (g plant<sup>-1</sup>). In relation to the area of sowing, the potential yield ( $Yp$ ) of wheat cultivars (t ha<sup>-1</sup>) was measured by the productive bushiness, the grains weight per spike and the number of plants sown per 1 m<sup>2</sup>:

$$Yp = Mk \cdot Kp \cdot Pp \cdot 10,000 \quad (1)$$

where are:  $Mk$  – the grains weight of spike per one plant (t);  $Kp$  – productive bushiness of the sample;  $Pp$  – crop density (number of plants per 1 m<sup>2</sup>), calculated using field germination data.

The intensity of wheat affection by diseases was determined using both generally accepted criteria (the disease development, the reaction type) and additional criteria (in particular, the pustules number per leaf, the pustule area for - rust fungi, the number of spots with plaque, the area of spots with plaque - for powdery mildew, etc.). The pathogenesis parameters were characterized by the results of wheat leaves measurements in the laboratory using the MBS-9 binocular and the Micromed trinocular (Kolesnikov, Novikova et al., 2018). The use of this set of pathogenesis indicators allowed to expand the range of methods of statistical data analysis applicable to the study, and to increase the accuracy of the experiment.

The degree of plant damage caused by *Bipolaris sorokiana* (Sacc.) Shoem - helminthosporous root rot was evaluated in the laboratory. (Fig. 4) in the phases of wheat tillering (the stage of finished tillering) and earing-flowering in accordance with the generally accepted method (Popov, 2011).



**Figure 4.** The conidia of the helminthosporous root rot (*Bipolaris sorokiniana* (Sacc.) Shoem.).

The affection intensity of wheat flag and pre-flag leaves by powdery mildew - *Blumeria graminis* Speer. (Fig. 5) was measured in accordance with the graphical scale of the conditional degree of plant damage

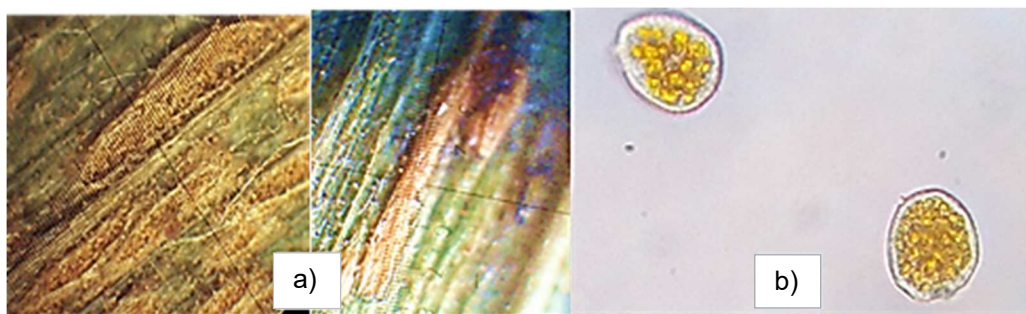
(Geshele, 1978), the number and area of spots with plaque were taken into account (Kolesnikov, Kremenevskaya et al., 2020).

The intensity of wheat damage caused by the yellow rust pathogen - *Puccinia striiformis* West. syn. *R. glumarum* Eriks. et Henn. (Fig. 6) was evaluated according to the generally accepted Manners scale, and, in addition, the total number of pustules per leaf, the number of strips with pustules, the length of the strips with pustules, the area of the pustule and their number in the strip were studied.

The values of the rust species' pustules area and powdery mildew' spots were calculated on the assumption of their elliptical shape (Kolesnikov, Kremenevskaya et al., 2020; Kolesnikov, Novikova et al., 2020).



**Figure 5.** Symptoms of the wheat powdery mildew development.



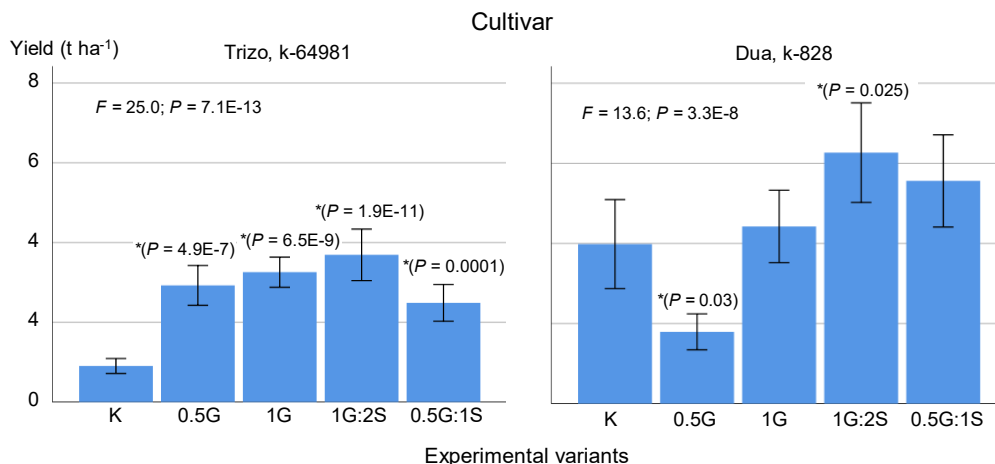
**Figure 6.** The symptoms of wheat yellow rust: uredopustules (a) and urediniospores (b).

Intensity of samples' damage, caused by septoria (*Stagonospora nodorum* (Berk.) Castellani & E.G. Germano), was determined in the phases of milk and wax ripeness of grain by the disease conditional development on the flag and pre-flag leaf surface in accordance with the James scale (James, 1971). The algorithm for statistical processing of field experience data was based on the creation of an electronic database, first in Microsoft Excel spreadsheets, then in the IBM SPSS Statistics software platform. The methods of parametric statistics based on the calculation of standard errors of the mean  $\pm SEM$ , 95% confidence intervals and the Student's *t*-test were used in the calculations. Methods of nonparametric statistics included Cohen's test (Cohen, 1988), multiple comparisons (Scheffe's method).

## RESULTS AND DISCUSSION

The polymer hydrogel, based on potassium acrylate and the protein growth stimulant, effect features on the soft wheat yield and triticale, including when used together, are shown on Fig. 7.

The maximum and statistically significant yield increase by 2.8 t ha<sup>-1</sup> (Trizo, k-64981) and by 2.3 t ha<sup>-1</sup> (Dua, k-828) was observed in the '1G:2S' experimental variant - when using the polymer hydrogel and protein growth stimulant combined.



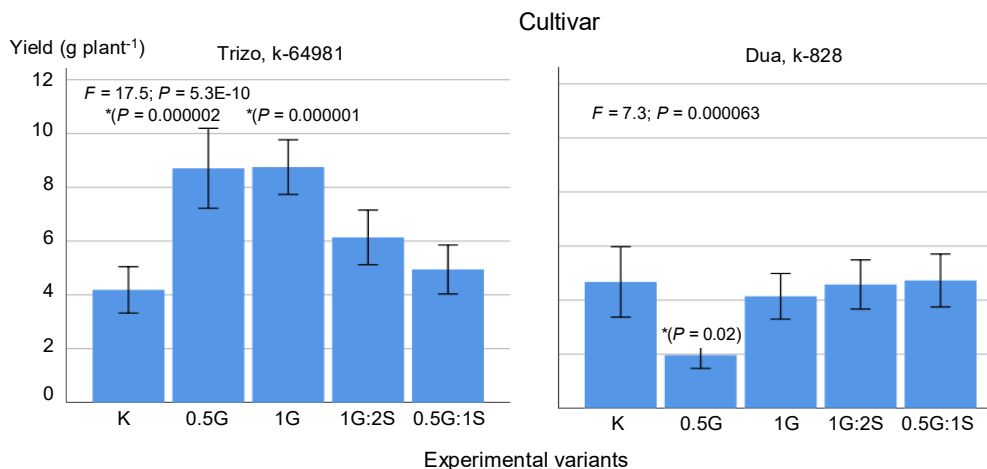
**Figure 7.** The soft wheat yield (t ha<sup>-1</sup>) when using the polymer hydrogel and the protein growth stimulant, including their combined application. K-control; 0.5 G-hydrogel based on the ability to bind 200 mL of water; 1G-hydrogel (based on the ability to bind 400 mL of water); 0.5 G:1S-hydrogel + protein stimulant (based on the ability to bind 200 mL of water); 1G:2S-hydrogel + protein stimulant (based on the ability to bind 400 mL of water). Vertical line – standard error of mean; \* – significant values of the indicator, different from the control, according to the Scheffe criterion at a certain significance level; *F* – Fisher criterion according to the single-factor analysis of variance.

Subsequently, the effect size was estimated based on the calculation of Cohen's *d* values. Based on Cohen's test, a large effect was detected when the polymer hydrogel and the protein growth stimulant were used combined in the experiment variant 0.5 G:1S compared to the control (Trizo cultivar, k-64981: *d* = 2.5; Dua cultivar, k-828: *d* = 0.8) and an average medium effect - in the 1G variant:2S (Trizo grade, k-64981: *d* = 0.7; Dua grade, k-828: *d* = 0.5).

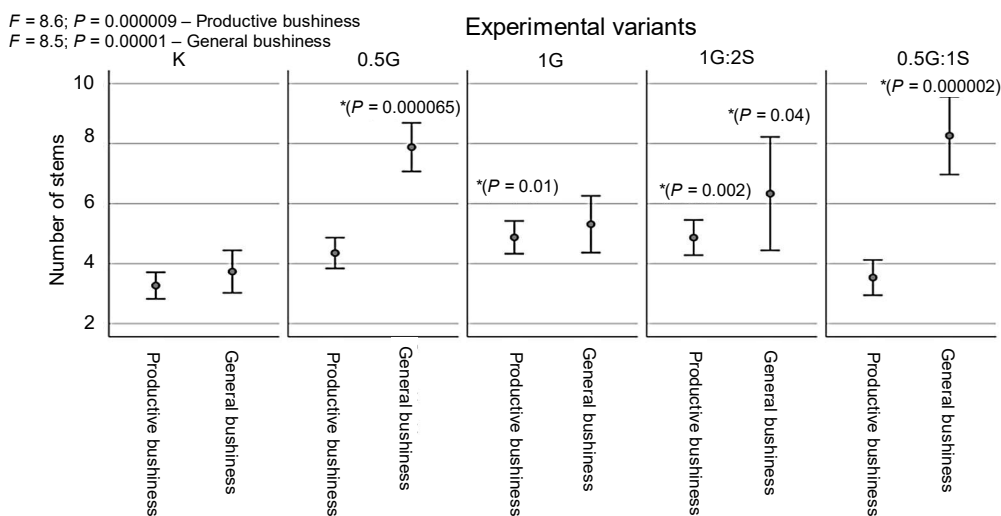
The change in the soft wheat and triticale potential yield per one plant (g plant), with the data about productive bushiness, is shown in Fig. 8. It is noted that the highest yield increase by 4.5–4.6 g was detected in the Trizo cultivar, k-64981 in the experimental variants, where the polymer hydrogel was used in the ratios of 0.5 G and 1G (0.5G – Cohen's *d* = 1.0 and 1G – Cohen's *d* = 1.1). The protein growth stimulant addition to the polymer hydrogel led to an increase in wheat yield by 18.1%.

The maximum value of *B<sub>p</sub>* when *B<sub>p</sub>* significantly increased by 26.4% (Trizo, k-64981) and by 35.8% (Dua, k-828) was registered in the experimental variant: protein growth stimulant + polymer hydrogel (1G:2S).

The highest biopreparations influence on the total and productive bushiness was registered on the Trizo cultivar, k-64981. The maximum increase in productive bushiness by 49.0–49.2% compared to the control was noted in the variants: 1G and 1G:2S (Fig. 9).



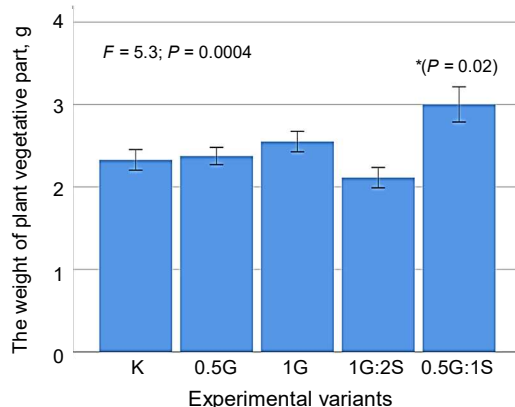
**Figure 8.** The changes in the potential yield of soft wheat (g plant<sup>-1</sup>) when using the polymer hydrogel and the protein growth stimulant, including their combined application. K-control; 0.5 G-hydrogel based on the ability to bind 200 mL of water; 1G-hydrogel (based on the ability to bind 400 mL of water); 0.5 G:1S-hydrogel + protein stimulant (based on the ability to bind 200 mL of water); 1G:2S-hydrogel + protein stimulant (based on the ability to bind 400 mL of water). Vertical line – standard error of mean; \* – significant values of the indicator, different from the control, according to the Scheffe criterion at a certain significance level;  $F$  – Fisher criterion according to the single-factor analysis of variance.



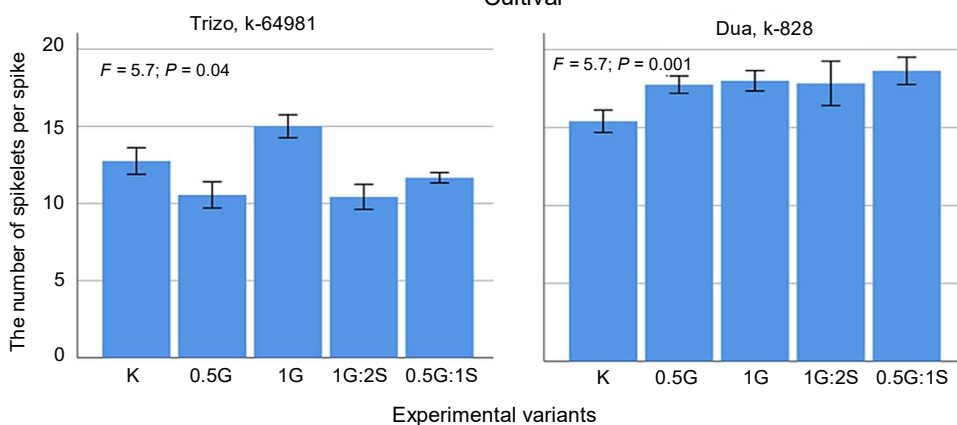
**Figure 9.** The productive and general bushiness of the Trizo soft wheat cultivar (k-64981) when using the polymer hydrogel and the protein growth stimulant, including their combined application. K-control; 0.5 G-hydrogel based on the ability to bind 200 mL of water; 1G-hydrogel (based on the ability to bind 400 mL of water); 0.5 G:1S-hydrogel + protein stimulant (based on the ability to bind 200 mL of water); 1G:2S-hydrogel + protein stimulant (based on the ability to bind 400 mL of water). Vertical line – standard error of mean; \* – significant values of the indicator, different from the control, according to the Scheffe criterion at a certain significance level;  $F$  – Fisher criterion according to the single-factor analysis of variance.

Based on Cohen's test of the wheat total bushiness, a large effect of the indicator changes was revealed in the variant: 0.5G (cultivar Trizo, k-64981:  $d = 0.9$ ) and 0.5 G:1S (cultivar Trizo, k-64981:  $d = 2.4$ ).

The change in the plants vegetative weight calculated on average for these wheat cultivars, depending on the experiment variant, is shown in Fig. 10. The largest increase in the plants vegetative weight (by 29.3%), compared with the control, was recorded in the 0.5G:1S variant. On the Trizo cultivar, k-64981 in the 1G variant, compared with the control, a significant increase by 72.4% of the nodal roots number and by 45.9% of the vegetative weight, while in the 0.5G variant - by 39.2% of the nodal roots length and by 27.4% of the vegetative mass was revealed. When the polymer hydrogel was used combined with the protein growth stimulant 0.5G:1S, the vegetative weight of plants increased by 35.6% compared to the control. However, there was no statistically significant effect of biopreparations on these parameters on Dua (k-828) triticale cultivar. Based on Cohen's test of the wheat vegetative weight in the 0.5G:1S variant, a large effect of the indicator changes was revealed in the cultivars Trizo, k-6498 ( $d = 1.0$ ) and Dua, k-828 ( $d = 0.8$ ).

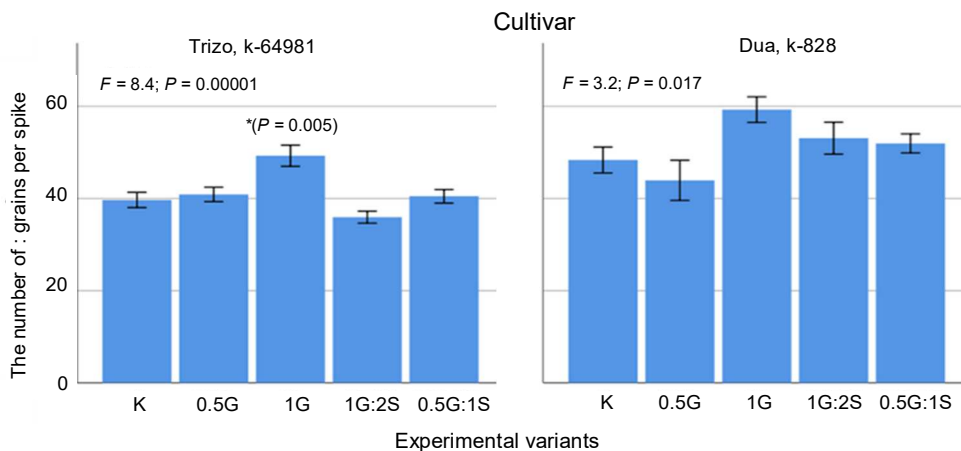


**Figure 10.** The weight of soft wheat vegetative part when using the polymer hydrogel and the protein growth stimulant, including their combined application. Vertical line – standard error of mean; \* – significant values of the indicator, different from the control, according to the Scheffe criterion at a certain significance level;  $F$  – Fisher criterion according to the single-factor analysis of variance.



**Figure 11.** Changes in the number of spikelets per spike on Trizo, k-64981 and Duo, k-828 cultivars when using the polymer hydrogel and the protein growth stimulant, including their combined application. Vertical line – standard error of mean.  $F$  – Fisher criterion according to the single-factor analysis of variance.

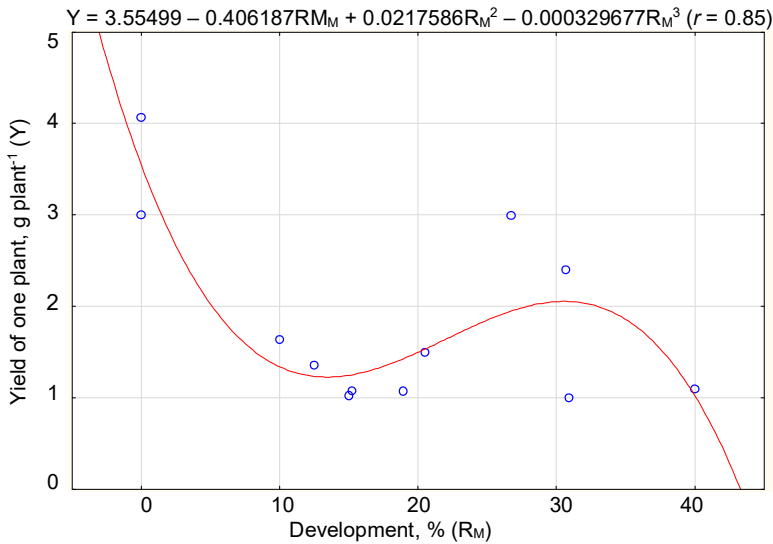
The highest values of the spikelets number per spike (Fig. 11) and the grains number per spike (Fig. 12) in the variant 1G were registered (Trizo, k-64981 - Cohen's  $d = 0.5$  and  $0.9$ ; Dua, k-828 - Cohen's  $d = 0.8$  and  $0.7$ , accordingly). The maximum effect size for the spikelets number per spike  $d = 1.3$  was registered on the Dua, k-828 cultivar in the 0.5G:1S variant. On the Trizo, k-64981 cultivar, the use of polymer hydrogel led to an increase in the number of spikelets per spike by 9.0% and in the number of grains per spike by 24.2%, while on the Dua, k-828 cultivar - by 7.0% and 22.4%, respectively.



**Figure 12.** Changes in the number of grains per spike on Trizo, k-64981 and Duo, k-828 cultivars when using the polymer hydrogel and the protein growth stimulant, including their combined application. Vertical line – standard error of mean; \* – significant values of the indicator, different from the control, according to the Scheffe criterion at a certain significance level;  $F$  – Fisher criterion according to the single-factor analysis of variance.

It is known that wheat diseases greatly reduce the crop yield. In particular, as shown in Fig. 13 the yield of wheat cultivar Trizo, k-64981 decreased depending on the intensity of the powdery mildew development. In addition, an inverse correlation was revealed between the pustules number ( $r = -0.61$ ), the number of pustules in the strip ( $r = -0.62$ ), the length of the strip with yellow rust pustules ( $r = -0.65$ ) and the area of the wheat flag leaf. The development of septoria (wheat leaf blotch) caused a decrease in the grains weight per spike ( $r = -0.61$ ).

Soft wheat (Trizo, k-64981) was affected in the most by the root rot pathogen ( $R_g = 20\%$ ) compared to triticale - (Duo, k-828) ( $R_g = 9.5\%$ ). In this regard, the biopreparations effectiveness was studied on the Trizo cultivar, k-64981. In the 0.5G experimental variant the root rot development had not detected. At the same time, only in this variant of the experiment, symptoms of powdery mildew development were revealed ( $R_m = 12.5 \pm 2.5\%$ ; number of spots with a plaque of  $N_{p.m.} = 12.0 \pm 4.0$ ; area of spots with a plaque of  $S_m = 5.9 \pm 3.0 \text{ mm}^2$ ). The decrease in the root rot development by 9% compared to the control was noted in the 0.5G:1S experimental variant. When using only the polymer hydrogel in the 1G variant, a decrease in the root rot development by 6.7% was revealed. However, when the polymer hydrogel and the protein growth stimulant were used together at the highest concentrations in 1G:2S variant, the degree of plant damage by root rot increased by 2.2%.

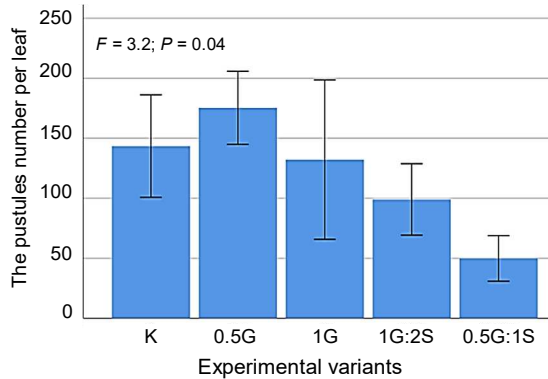


**Figure 13.** Dependence of the soft wheat (Trizo, k-64981) yield on the intensity of powdery mildew development

In accordance with Cohen's test values of root rot development on average on cultivars Trizo, k-64981 and Duo, k-828 in the 0.5G:1S variant, the greatest decrease in the disease development (by 11%) was revealed compared with the control, and the maximum scope of the effect  $d = 0.9$  was marked. In this experimental variant, field germination increased by 30.2% ( $d = 1.4$ ).

The development of wheat leaf blotch on the Trizo, k-64981 cultivar when using the polymer hydrogel in the 1G variant was the same as in the control. However, in the 0.5G experimental variant, when using the polymer hydrogel at lower concentrations and in the 1G:2S variant, when it used combined with the protein growth stimulant, the degree of wheat leaf damage by the disease decreased by 12.5% compared to the control (Cohen's test:  $d = 5.3$  and  $d = 6.1$ , accordingly).

The features of the yellow rust development, characterized by the number of pustules on the wheat flag leaf on the Trizo cultivar, k-64981 when using the polymer hydrogel and the protein growth stimulant, including their combined application, are shown in Fig. 14. In the experimental variant 0.5G:1S the smallest number of the pathogen pustules was registered (by 65.3% less than in the control, Cohen's test:  $d = 0.7$ ).



**Figure 14.** Change in the number of pustules of the yellow rust pathogen on the flag leaves of the Trizo cultivar, k-64981, when using the polymer hydrogel and the protein growth stimulant, including their combined application. Vertical line – standard error of mean;  $F$  – Fisher criterion according to the single-factor analysis of variance.



In addition to the diseases development, in spring wheat and triticale sowings, for the first time in 2020, symptoms of deviation from normal plant growth and development - deformities of unknown etiology were revealed (Fig. 15). The most notable phenotypic changes were in the curvature of the spikes and spiral twisting of the leaves in the ear formation stage. During the subsequent ontogenesis phases, the symptoms remained unchanged until the harvest.

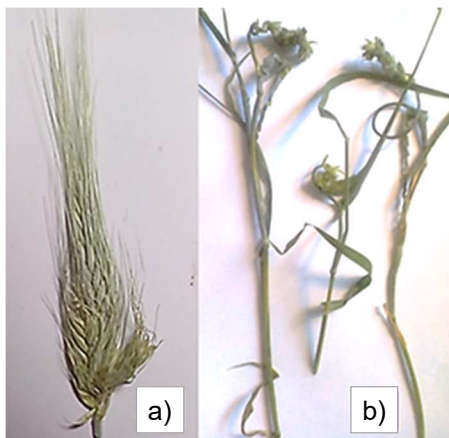
These deviations did not cause a significant decrease in yield, but their cause was not identified. Perhaps the changes were caused by some side effect during the period of action of the systemic herbicide StarTerr, BP, adverse weather conditions, as well as plant damage by phytoplasmas. Plant infestation with wheat nematode was excluded based on the results of plant material microscopy. In 2021, in the case of a return of such symptoms in cereals, we plan to study this phenomenon in detail through laboratory diagnostic methods.

The biopreparations use had an impact on the prevalence of symptoms of deviations from plants normal growth and development of unknown

etiology. The greatest effectiveness in relation to the wheat deformation was revealed in the experimental variants 1G (Cohen's test:  $d = 1.1$ ) and 1G:2S (Cohen's test:  $d = 1.3$ ), where a decrease in the occurrence proportion of plants with deviations symptoms by 16.7% compared to the control was noted.

When evaluating the revealed values of effect size (Cohen's  $d$ ) for 19 wheat productivity indicators in the above-mentioned experimental variants, the strongest effect on plants was registered for the protein growth stimulant and the polymer hydrogel combined application in the 0.5G:1S variant. A strong scope of the effect was noted for the growth of field germination, the increase in root length, the flag leaf area, the spike length, the spikelets number per spike, the spike weight, the potential yield. In this experimental variant, large effect size was revealed for reducing of the root rot development, and medium effect size - for indicators of the yellow rust development.

It should be noted that triticale has a greater adaptive potential to environmental factors than wheat. In this regard, we have identified a greater number of changes in photometric and phytopathological parameters in soft wheat in the experimental variants when using the polymer hydrogel and protein growth stimulant, including their combined application.



**Figure 15.** Symptoms of the plants' normal growth and development deviations of unknown etiology: a – deformation of triticale spikes (Dua cultivar, k-828), b –deformation of soft wheat plants (Trizo cultivar, k-64981).

## CONCLUSIONS

The stimulating treatments caused the most impact on the Trizo wheat cultivar, k-64981. The use of polymer hydrogel in the ratios 0.5G1 and 1G resulted in a statistically significant increase in 12 of the 19 indicators of wheat productivity (63.2%). The protein growth stimulant addition to the polymer hydrogel in 0.5G:1S and 1G:2S variants caused an increase by 15.8% of the indicators. However, when the protein growth stimulant and the polymer hydrogel were applied together to the soil, it was marked the greatest increase in the plants field germination - the most important indicator determining the yield of wheat: in the 1G:2S variant - by 26.4% and in the 0.5G:1S - by 20.0%, compared to other experimental variants, as well as a significant increase in the productive and total bushiness of the samples. In the 1G:2S variant of the experiment, the productive bushiness increased by 49.0%, and the total bushiness - by 69.6%. The maximum number of productivity indicators (26.3%), characterized by an increase in values compared to the control, was revealed on the triticale Dua, k-828 cultivar with the combined use of the polymer hydrogel and the protein growth stimulant in the 0.5G:1S experiment variant. In the experimental variants 1G:2S and 0.5 G:1S, in particular, a significant increase in the plants field germination by 35.8% and by 22.6%, their faster growth by 16.3% and by 11.0% (in the phase of ontogenesis) was noted. In the 0.5G:1S variant, the area of the flag and pre-flag triticale leaves, which directly affect the spike weight, increased by 80.3% and 61.2%, respectively. The maximum and statistically significant yield increase by 2.8 t ha<sup>-1</sup> (Trizo, k-64981) and by 2.3 t ha<sup>-1</sup> (Dua, k-828) was observed in the 1G:2S variant, which was mainly due to the joint statistically significant effect of the polymer hydrogel and the protein growth stimulant on field germination, while in the Trizo, k-64981 cultivar - on the productive bushiness of samples. In relation to pathogens, biopreparations acted ambiguously. The maximum decrease in the development intensity of root rot on the Trizo, cultivar k-64981 was identified in the 0.5G variant – by 20%, and the combined use of the polymer hydrogel and the protein growth stimulant (0.5G:1S) resulted in the disease development reduction by 8.9%. In addition, in the 0.5G:1S experimental variant, the minimum development of yellow rust was detected (the pustules number per leaf was less than in the control by 65.3%). The greatest effectiveness against wheat deformation of unknown etiology was revealed in the 1G and 1G:2S experimental variants, where there was a decrease in the occurrence proportion of plants with symptoms of deviations by 16.7% compared to the control.

**ACKNOWLEDGEMENTS.** This work was carried out within the framework of the state task according to the VIR thematic plan for project No. 0662-2019-0006 ‘Search, maintenance of viability and disclosure of the potential of hereditary variability of the world collection of VIR cereals and cereals for the development of an optimized genebank and rational use in breeding and crop production’.

The authors express their deep gratitude to the head of the Department of wheat genetic resources VIR E.V. Zuev for many years of productive cooperation and assistance in research.

## REFERENCES

- Baidakova, M., Sitnikova, V., Uspenskaya, M., Olekhovich, R. & Kremenevskaya, M. 2019a. Polymer acrylic hydrogels with protein filler: Synthesis and characterization. *Agricultural Research* **17**(1), 913–922.
- Baidakova, M.V., Sitnikova, V.E., Uspenskaya, M.V., Olekhovich, R.O., Kremenevskaya, M.I. & Denisov, T.S. 2019b. Study of the properties of composition hydrogels based on potassium polyacrylate and protein filler. *Izvestiya SPbGTI (TU)* **48**(74), 115–119 (in Russian).
- Bairwa, R.K., Purohit, H.S., Meena, R.H. & Jain, H.K. 2013. Phosphorus levels and phosphatic biofertilizers influenced yield, nutrient uptake and soil fertility under wheat (*Triticum aestivum* L.). *Ecology, Environment and Conservation* **19**, 757–762.
- Baran, A., Zaleski, T., Kulikowski, D. & Wieczorek, J. 2015. Hydrophysical and Biological Properties of Sandy Substrata Enriched with Hydrogel. *Polish Journal of Environmental Studies* **24**(6), 2355–2362.
- Bigi, A., Cojazzi, G., Panzavolta, S., Rubini, K. & Roveri, N. 2001. Mechanical and thermal properties of gelatin films at different degrees of glutaraldehyde crosslinking. *Biomaterials* **22**(8), 763–768.
- Bortolin, A., Aouada, F.A., Moura, M.R., de Ribeiro, C., Long, E. & Mattoso, L.H.C. 2011. Application of polysaccharide hydrogels in adsorption and controlled-extended release of fertilizers processes. *Journal of Applied Polymer Science* **123**(4), 2291–2298.
- Burney, J. & Ramanathan, V. 2014. Recent climate and air pollution impacts on Indian agriculture. *Proceedings of the National Academy of Science* **111**(46), 16319–16324.
- Chang, C., Duan, B., Cai, J. & Zhang, L. 2010. Superabsorbent hydrogels based on cellulose for smart swelling and controllable delivery. *European Polymer Journal* **46**(1), 92–100. doi.org/10.1016/j.eurpolymj.2009.04.033
- Chavda, H.V., Patel, R.D., Modhia, I.P. & Patel, C.N. 2012. Preparation and characterization of SPH and SPHCs. *International Journal of Pharmaceutical Investigation* **2**, 134–139.
- Cohen, J. 1988. *Statistical Power Analysis for the Behavioral Sciences* (2nd ed.). Hillsdale, NJ: Lawrence Erlbaum Associates, Publishers.
- Dabhi, R., Bhatt, N. & Pandit, B. 2013. Super absorbent polymers –An Innovative water saving technique for optimizing crop yield. *International Journal of Innovative Research in Science, Engineering and Technology* **2**(10), 5333–5340.
- Entrya, J.A., Sojkaa, R.E., Watwoodb, M. & Rossc, C. 2002. Polyacrylamide preparations for protection of water quality threatened by agricultural runoff contaminants. *Environmental Pollution* **120**, 191–200.
- Falkenmark, M. & Rockström, J. 2014. *Balancing Water for Humans and Nature: The New Approach in Ecohydrology*. 320 pp.
- Figuroa, M., Hammond-Kosack, K.E. & Solomon, P.S. 2018. A review of wheat diseases-a field perspective. *Molecular plant pathology* **19**(6), 1523–1536. doi: 10.1111/mpp.12618
- Geshele, E.E. 1978. *Fundamentals of phytopathological evaluation in plant breeding*. Moscow: Kolos, 53 pp.
- Guilherme, M.R., Aouada, F.A., Fajardo, A.R., Martins, A.F., Paulino, A.T., Davi, M.F.T., Rubira, A.F. & Muniz, E.C. 2015. Superabsorbent hydrogels based on polysaccharides for application in agriculture as soil conditioner and nutrient carrier: A review. *European Polymer Journal* **72**, 365–385. doi.org/10.1016/j.eurpolymj.2015.04.017
- Gundryrin, V.N., Godunova, E.I. & Shkabarda, S.N. 2016. Productivity of winter wheat with hydrogel after seeded fallow. *Achievements of Science and Technology of AIC* **30**(8), 37–39 (in Russian).

- Gupta, R., Somanathan, E. & Dey, S. 2017. Global warming and local air pollution have reduced wheat yields in India. *Climatic Change* **140**, 593–604. doi.org/10.1007/s10584-016-1878-8
- Iqbal, F.M., Ahmad, M. & Rashid, A. 2016. Synthesis and in vitro characterization of hydroxypropyl methylcellulose-graft-poly (acrylic acid/2-acrylamido-2-methyl-1-propanesulfonic acid) polymeric network for controlled release of captopril. *Acta Poloniae Pharmaceutica* **73**(1), 183–196.
- James, W.O. 1971. *Canadian Plant Disease Survey* **51**(2), 36–55.
- Kabakova, M.M., Uspenskaya, M.V., Sirotinkin, N.V. & Sanatin, E.V. 2003. Behavior of cross-linked copolymers of acrylic acid and 5-vinyltetrazole in aqueous media. *Russian Journal of Applied Chemistry* **76**(7), 1176–1178 (in Russian).
- Kabiri, K., Omidian, H., Zohuriaan-Mehr, M.J. & Doroudiani, S. 2011. Superabsorbent hydrogel composites and nanocomposites: A review. *Polymer Composites* **32**(2), 277–289.
- Kolesnikov, L.E., Novikova, I.I., Surin, V.G., Popova, E.V., Priyatkin, N.S. & Kolesnikova, Yu.R. 2018. Estimation of the Efficiency of the Combined Application of Chitosan and Microbial Antagonists for the Protection of Spring Soft Wheat from Diseases by Spectrometric Analysis *Applied Biochemistry and Microbiology* **54**(5), 546–552 (in Russian).
- Kolesnikov, L.E., Kremenevskaya, M.I., Razumova, I.E., Kolesnikova, Yu.R., Ambulatova, E.V. & Yazeva, E.O. 2020. The biological basis for the use of protein growth stimulant made from cattle split for wheat foliar feeding and disease suppression. *Agronomy Research* **18**(S2), 1336–1349. doi.org/10.15159/AR.20.082
- Kolesnikov, L.E., Novikova, I.I., Popova, E.V., Priyatkin, N.S., Zuev, E.V., Kolesnikova, Yu.R. & Solodyannikov, M.D. 2020. The effectiveness of biopreparations in soft wheat cultivation and the quality assessment of the grain by the digital x-ray imaging. *Agronomy Research* **18**(4), 2436–2448. doi.org/10.15159/AR.20.206
- Kolesnikov, L.E., Popova, E.V., Novikova, I.I., Priyatkin, N.S., Arkhipov, M.V., Kolesnikova, Yu.R., Potrakhov, N.N., Van Duijn, B. & Gusarenko, A.S. 2019. Multifunctional biologics which combine microbial anti-fungal strains with chitosan improve soft wheat (*Triticum aestivum* L.) yield and grain quality. *Agricultural Biology* **54**(5), 1024–1040 (in Russian).
- Kremenevskaya, M.I., Sosnina, O.A., Semenova, A., Udina, I. & Glazova, A.E. 2017. Meat industry by-products for berry crops and food production quality improvement. *Agronomy Research* **15**(S2), 1330–1347.
- Kremenevskaya, M.I., Kremenevskaya, V.S. & Sosnin, V.A. A method of producing a protein product. *Patent of the Russian Federation* No. 2662782. 31.07.2018. Byul. 16.
- Long, J.-Y. & Song, Zh.Q. 2003. Research on water absorbance of poly (starch-acrylic acid-acrylamide) complex superabsorbent in different mediums. *Chemistry and industry of forest products* **23**(4), 27–30.
- Mellelo, E., Samuilova, E.O., Denisov, T.S., Martynova, D.M. & Olekhnovich, R.O. 2019. Influence of the bentonite-containing acrylic humectant composite on the soil microflora. *Agronomy Research* **17**(5), 1960–1968.
- Novakazi, F., Afanasenko, O., Lashina, N., Platz, G., Snowdon, R., Loskutov, I. & Ordon, F. 2020. Genome-wide association studies in a barley (*Hordeum vulgare*) diversity set reveal a limited number of loci for resistance to spot blotch (*Bipolaris sorokiniana*). *Plant Breeding* **139**(3), 521–535. https://doi.org/10.1111/pbr.12792
- Pavlyushin, V.A., Vilkova, N.A., Sukhoruchenko, G.I. & Nefedova, L.I. 2016. Formation of agroecosystems and pest communities. *Plant Protection News* **2**, 5–15 (in Russian).
- Popov, Y.V. 2011. Method for the estimation of the root rots development in cereals. *Plant protection and quarantine* **8**, 45–47 (in Russian).

- Pourjavadi, A., Harzandi, A.M. & Hosseinzadeh, H. 2004. Modified carrageenan 3. Synthesis of a novel polysaccharide-based superabsorbent hydrogel via graft copolymerization of acrylic acid onto kappa-carrageenan in air. *European Polymer Journal* **40**(7), 1363–1370.
- Rabinovich, V.A. & Havin, Z.Ya. 1991. *Short chemical Handbook* /Edited by A. A. Potekhin, A. I. Efimov. L.: Chemistry, 432 pp.
- Shewry, P.R., Pellny, T.K. & Lovegrove, A. 2016. Is modern wheat bad for health? *Nature Plants* **2**, 1–3. doi.org/10.1038/NPLANTS.2016.97
- Uspenskaya, M.V., Sirotinkin, N.V., Yatsenko, S.V. & Masik, I.V. 2005. Formulations based on hollow glass spheres and polyurethane foams. *Russian Journal of Applied Chemistry* **78**(5), 830–833.
- Yamaguchi, T. 2014. Rapid Swelling and Pattern Formation in Hydrogel Particles// *Nihon Reoroji Gakkaishi* **42**(2), 129–33.
- Yanez-Chavez, Y., Pedroza-Sandoval, L.G., Sánchez-Cohen, A. & Samaniego-Gaxiola, J.A. 2014. Assessment of the impact of compost and hydrogel as soil moisture retainers on the growth and development of forege maize (*Zea mays* L.). *Journal of Agriculture and Environmental Sciences* **3**(4), 93–106.
- Zhang, L., Yu, P. & Luo, Y. 2006. Separation of caprolactam-water system by pervaporation through crosslinked pva membranes. *Separation and Purification Technology* **52**(1), 77–83.
- Zhang, Y., Chan, H.F. & Leong, K.W. 2013. Advanced materials and processing for drug delivery: the past and the future. *Adv. Drug Deliv. Rev.* **65**(1), 104–120. doi: 10.1016/j.addr.2012.10.003
- Zhong, K., Lin, Z.T., Zheng, X.L., Jiang, G.B., Fang, Y.S., Mao, X.Y. & Liao, Z.W. 2013. Starch derivative-based superabsorbent with integration of water-retaining and controlled-release fertilizers // *Carbohydrate Polymers* **92**(2), 1367–76. doi: 10.1016/j.carbpol.2012.10.030
- Zhuchenko, A.A. 2004. *Resource potential of grain production in Russia*. Moscow, 1109 pp. (in Russian).
- Zohuriaan-Mehr, M.J. & Kabiri, K. 2008. Superabsorbent polymer materials: a review. *Iranian Polymer Journal* **17**(3), 451–477.
- Zoolshoev, Z.F., Bobrova, N.V., Kurindin, I.S. & Vlasov, P.V. 2016. Preparation and properties of hydrogels based on polyacrylamide cross-linked with glutaric aldehyde. *Bulletin of the Tver State University. Series: Chemistry* **1**, 100–109 (in Russian).

## **Development of the mathematical model of the electric resistance baking process**

B. Kulishov<sup>1,\*</sup>, D. Minkin<sup>2</sup>, A. Fedorov<sup>1</sup> and A. Novoselov<sup>1</sup>

<sup>1</sup>ITMO University, Saint Petersburg, Faculty of Food Biotechnologies and Engineering, School of Biotechnology and Cryogenic Systems, Kronverkskiy ave.49, RU197101 St. Petersburg, Russia

<sup>2</sup>Saint Petersburg University of State Fire Service of Emercom of Russia, Department of Physical and Technical Fundamentals of Fire Safety, Moskovskiy ave.149, RU 196105 St. Petersburg, Russia

\*Correspondence: kulishov.b@list.ru

Received: March 23<sup>rd</sup> 2021; Accepted: May 25<sup>th</sup> 2021; Published: June 16<sup>th</sup>, 2021

**Abstract.** The work is dedicated to the development of the mathematical model of the electric resistance baking process for the purpose of predicting temperature changes during baking of dough pieces of arbitrary sizes. The equation for the non-stationary thermal regime of a body with an internal heat source was used with a number of assumptions. The dynamics of the dough temperature changes was determined by numerical solution of the equation in Comsol Multiphysics.

Due to the complexity of the dough baking process and the impossibility of solving the equation by analytical method only, a number of values included in the energy balance of ER baking were determined experimentally. A dough piece with dimensions of 100×50×80 mm was baked during the experiment. After the adjustment, the adequacy of the model was checked by comparing the data on the dough temperature changes during baking dough pieces of the same recipe, but of different sizes (150×49×80, 80×62×80, and 65×75×80). Statistical analysis using Fisher's criterion confirmed the adequacy of the model.

**Key words:** bread, electric resistance baking, mathematical modeling.

### **INTRODUCTION**

Currently, the process of electric resistance baking (ER baking) of bread is becoming the subject of an increasing number of studies due to its advantages over convective baking. Electric resistance baking is energy-efficient; no ovens in the conventional sense are required for ER baking, since heating occurs due to the release of heat directly inside the dough piece itself in accordance with Joule's law. In this regard the duration of the electric resistance baking process is several times shorter than that of convective baking. It must be noted that the duration of ER baking process depends significantly on the shape of the dough piece, namely, on the ratio of the distance between the electrodes and the height and width of the dough piece. Also, the dough

formula, moisture and salt content of the dough play an important role. Therefore, convective and ER baking should be compared taking into consideration all these factors. In particular, in the work (Kulishov et al., 2020) bread of the same weight was baked by two methods: convective and ER baking, wherein the duration of convective baking was 25 minutes, ER baking - 2 minutes maximum. In work (Kulishov et al., 2021) the duration of baking of toast bread by the ER method was 5 minutes, by convective method - 25 minutes.

Direct comparison of baking times using different reference sources is often difficult because ER heating is rarely used directly for baking bread. Usually, this is a tool for uniform and controlled heating of the dough in order to study its properties, as, for example, in works (Luyts et al., 2013; Masure et al., 2019).

For the practical application of the electric resistance baking process, reliable prediction of the temperature regime of baking is of great importance. The dynamics of temperature change during baking, as well as its distribution over the volume of the dough piece, depends on a number of parameters. Among these are the power of heat release, the formula of the dough piece and its thermophysical properties, the conditions of heat exchange with the surrounding objects and the walls of the container in which baking is carried out, as well as the physicochemical processes intrinsic to the baking process. To ensure the necessary behavior of the temperature of the dough piece, it is important to have a methodology for calculating and choosing the electric capacity, time of baking, formula of the dough piece, and the design of the installation.

There are a number of publications on the mathematical modeling of electrical resistance heating. In particular, estimation of the temperature distribution over the volume of the dough piece, the influence of external conditions, the designs of experimental installations and measurement techniques for various types of dough pieces and liquids are presented in works (Sastry & Palaniappan, 1992; Fryer & Li, 1993; Fu & Hsieh, 2006; Ghnimi et al., 2008; Marra et al., 2009; Gally et al., 2016; Gally et al., 2017). In the work (Gally et al., 2016) much attention is paid to the influence of the dough formula on its thermophysical properties and electrical conductivity, their dependence on temperature; a thermal model of the baking process has been developed. The key drawback of the presented materials is the absence of parameters that would make allowance for the processes of moisture evaporation during baking and the corresponding physicochemical transformations in the dough piece. These processes have a significant effect on the temperature regime of baking and electricity consumption. In addition, it is not clear from the published materials how the proposed calculation models can be applied to objects with other geometric relationships.

Thus, the purpose of this work is to develop the mathematical model (MM) of the ER baking process for the correct prediction of the temperature of the dough piece during its baking by the electric resistance method. Adequate mm will allow to determine the duration and dynamics of bread baking for various process parameters and arbitrary sizes of the dough piece.

To achieve this goal, it is necessary to solve the following tasks:

- to assess the factors affecting this thermal process, to develop physical and mathematical models of this process on the basis of the well-known literature data on the ER heating of dough pieces, as well as the results of our own experimental studies on this problem;

- to carry out numerical modeling of ER baking and provide recommendations for the optimal process parameters.

## MATERIALS AND METHODS

### Development of the physical model of ER baking

The heat transfer processes in the considered device are complex, therefore it is necessary to make a number of assumptions that simplify the solution of the problem and increase the reliability of the calculation results. In this case, the mechanism of heat transfer in the dough mass is a non-stationary thermal regime of a body with an internal heat source.

The proposed physical model is based on the following assumptions:

1. All the ingredients of the dough formula are evenly distributed throughout its volume, therefore, its thermophysical properties such as density, heat capacity and thermal conductivity are identical throughout the volume of the dough piece;
2. The temperature field of the dough piece is uniform and characterized by one volume average temperature;
3. Heat exchange with the cell walls is neglected due to the low thermal conductivity of the wall material and the relatively short baking time;
4. Heat exchange of the dough piece with the environment is carried out by means of free convection and radiation through the open surface of the piece, while the coefficient of convective-radiant heat transfer and the ambient temperature are considered constant;
5. Heat exchange surface area and the total specific heat of the dough piece are considered constant;
6. The voltage of the alternating current supplied to the electrodes is constant and equal to 220 V;
7. Resistance to the flow of electric current passing through the dough piece depends on the electrophysical properties of the dough pieces and their geometrical dimensions.

Assumption 2 is justified by the fact that the heat release, when the structure of the prepared dough piece is homogeneous, will be even throughout its volume.

Assumption 5 is justified by the fact that changes in surface area and weight of the dough piece due to the moisture evaporation during baking are insignificant in relation to the initial values before baking.

### Mathematical description of the physical model of ER baking

The task is to predict the temperature of the dough piece at any given time.

For the case of a non-stationary thermal regime of a body with an internal heat source, the differential equation will have the form:

$$\nabla^2 t + \frac{W(t)}{\lambda} = \frac{c\rho}{\lambda} \frac{dt}{d\tau}; \quad (1)$$

where  $c$  – specific heat capacity,  $J \cdot (kg \cdot K)^{-1}$ ;  $\rho$  – density,  $kg \cdot (m^3)^{-1}$ ;  $\lambda$  – thermal conductivity of the dough piece,  $W \cdot (m \cdot K)^{-1}$ ;  $W$  – power density of heat release in the dough piece,  $W \cdot (m^3)^{-1}$ .



For the case of a uniform temperature field in the body and the conditions of heat exchange with the environment, corresponding to the Newton-Richmann law, Eq. (1) will take the form:

$$\frac{dt}{d\tau} + m(t - t_c) = \frac{W(t) \cdot V}{C}; \quad (2)$$

where  $C$  – total specific heat of the dough piece,  $J \cdot K^{-1}$ ;  $m = \alpha S \cdot C^{-1}$  – heating rate,  $s^{-1}$ ;  $\alpha$  – coefficient of convective-radiant heat transfer with the environment,  $W \cdot (m^2)^{-1} \cdot K$ ;  $S$  – heat exchange surface area,  $m^2$ ;  $V$  – volume of the dough piece,  $m^3$ ;  $t_c$  – ambient temperature.

During baking, the energy supplied to the electrodes is consumed in several processes:

1. Heating the dough mass from the initial temperature to the temperature of 98–99 °C ( $W_C$ );
2. Partial evaporation of water that is present in the dough ( $W_{ev}$ );
3. Physicochemical processes taking place during baking, such as protein denaturation, starch gelatinization, etc. ( $W_{phc}$ );
4. Irreversible heat loss to the environment ( $W_{hl}$ );
5. Heat loss due to heating of the electrodes ( $W_{elh}$ );
6. Heat loss due to electrochemical reactions, which are inevitable when using stainless steel electrodes at a current frequency of 50 Hz ( $W_{el/ch}$ ).

The heat dissipation power density  $W$  undergoes significant changes during baking because this value depends on many factors: the resistance of the dough piece, humidity, temperature, physicochemical and thermophysical properties of the dough, which, in turn, depend on temperature and a number of other factors and also change during the ER heating process. As a result, the electric power supplied to the dough piece ( $W_{el}$ ) changes significantly throughout the entire process.

Taking these factors into account a heat balance equation was drawn up to determine the resulting power supplied to the dough piece:

$$W_{el}(t) = W_C(t) + W_{hl}(t) + W_{phc}(t) + W_{ev}(t) + W_{elh} + W_{el/ch}; \quad (3)$$

where  $W_{el}(t)$  – electric power;  $W_{phc}(t)$  – power spent on physical and chemical processes during baking;  $W_C(t)$  – power consumed for heating the dough mass with heat capacity  $C$ ;  $W_{elh}$  – power consumed for heating of the electrodes;  $W_{el/ch}$  – power spent on electrochemical reactions;  $W_{ev}(t)$  – power consumed for moisture evaporation;  $W_{hl}(t)$  – power lost to the environment during heating.

The solution to Eq. (2) is the expression:

$$t(\tau) = t_0 e^{-m\tau} + m e^{-m\tau} \int_0^\tau e^{m\tau} \left( t_c + \frac{W(t) \cdot V}{mC} \right) d\tau; \quad (4)$$

In view of the complexity and multifactorial nature of the processes taking place when baking a dough piece, it is a difficult task to determine the type of a functional dependence (3) analytically. Possibility to obtain the necessary relationships experimentally was considered in this work.

**Bread making technology.** A straight-dough preparation method was used. The processes were carried out in the following sequence:

- weighing components, heating water to 36 °C;
- mixing yeast with flour, dissolving salt in a portion of water;
- dosing components into the bowl of the dough mixing machine;

- kneading dough in a dough mixing machine (Bear Varimixer Teddy), kneading mode - 4 minutes at a speed of ~ 78 rpm, 1.5 minutes at a speed of ~ 208 rpm, a hook was used for kneading;
- fermentation of the dough for 2 hours, at 35 °C, with manual punching after 1 hour and 20 minutes (proofing cabinet Miwe Aero, model AE 6.06.04, Germany);
- cutting dough and forming dough pieces;
- proofing dough in a proofing cabinet at temperature of 40 °C and at relative humidity of 80% for 1 hour (Miwe Klima, type MGT, Germany)
- baking dough by the electric resistance method in the laboratory ER oven;
- cooling the bread.

The dough formula is shown in Table 1.

For successful baking a round piece of dough with a mass of  $230 \pm 1$  g was formed, its edges were cut off so that to obtain area of 50 mm that will ensure close contact of the dough piece with electrodes. The forming scheme is identical to the one described in article (Kulishov et al., 2020). The dough sample had a mass of  $150 \pm 5$  g.

Baking of bread dough and sponge cake samples after proofing was carried out at a voltage of 220 V, a frequency of 50 Hz. During baking current flowing through the dough sample was measured using an IEK 266 C ammeter and the dough temperature was measured using a chromel-alumel DTPK011-07/1.5 thermocouple. The thermocouple was connected to an analog input module, which was connected to a personal computer via the RS-485 - USB interface. Data from the input module was processed in MasterScada in real time. The thermocouple was installed in the dough sample at a certain point, in the center, at a height of  $45 \pm 5$  mm from the chamber bottom.

**Determination of the heat capacity of the dough.** The value of the specific heat capacity of the dough piece  $c = 1,600 \text{ J (kg K)}^{-1}$  was determined experimentally on the installation IT-S-400. To measure the heat capacity of materials unable to hold their shape, for example, bulk materials or liquids, the installation was equipped with a cuvette where the dough piece was placed. The description of the installation and measurement procedure is given in the reference source (Platunov et al., 1986).

**Experimental installations.** To carry out an experiment to determine the values included in the Eq. (4) the installation described in (Kulishov et al., 2020) was used.

Further, in order to check the mm by comparing the dynamics of temperature changes obtained using mm and the experiment, a number of experiments were carried out on baking dough pieces of different sizes, and in one case, a different weight. To perform these experiments another installation was used.

The main elements are the casing, the hinged bottom, and the removable electrodes. The casing elements are made of non-conductive material with a low thermal conductivity coefficient. Grooves for electrodes are cut in the side walls of the casing with a pitch of 13 mm, which makes it possible to carry out experiments with a wide range of distances between the electrodes. The electrodes are made of 3 mm thick AISI

**Table 1.** The dough formula

Ingredients	The mass of ingredients, g
Wheat flour 1 <sup>st</sup> grade	$500.0 \pm 1.0$
Salt	$5.0 \pm 0.1$
Instant yeast	$2.5 \pm 0.1$
Water	$315.0 \pm 2.0$

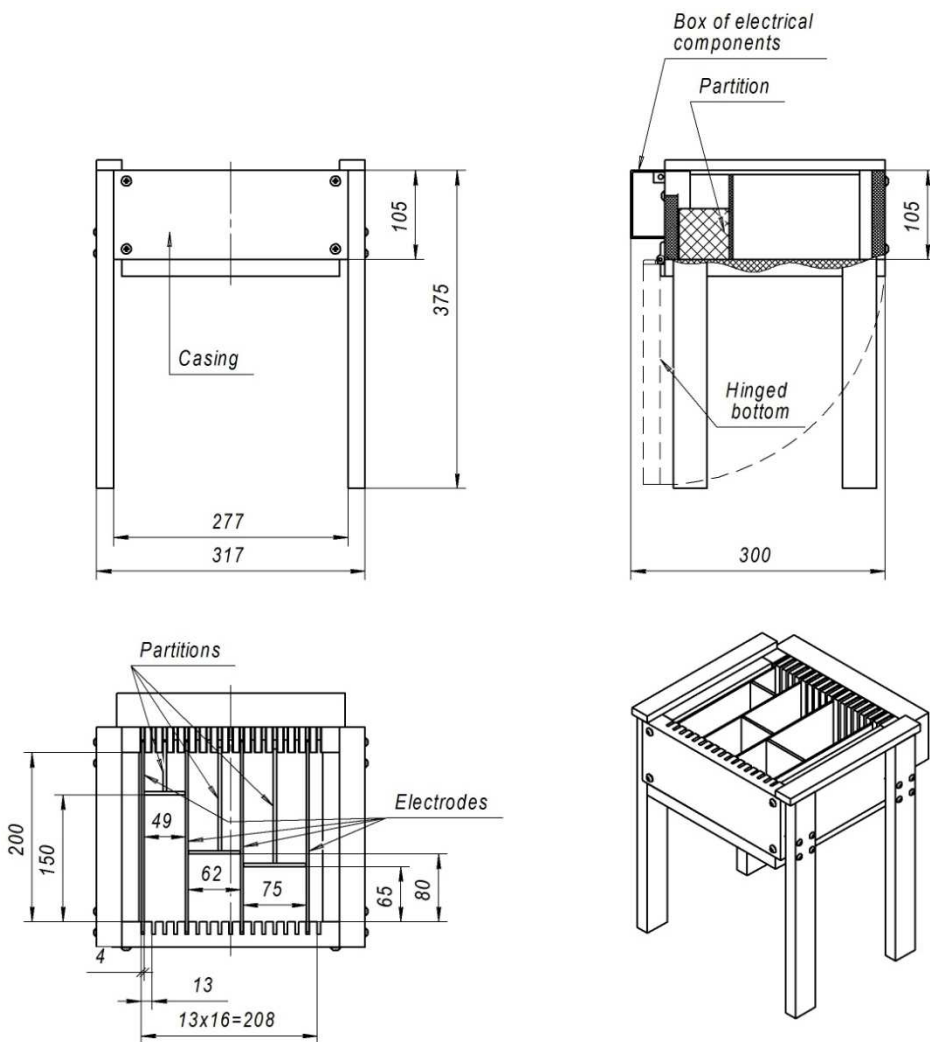
304 stainless steel. To check the mathematical model, the experiments on baking dough pieces of the following weights and sizes were carried out:

1. Dough piece L:W:H 150×49×80 mm, weight 227 g;
2. Dough piece L:W:H 80×62×80 mm, weight 150 g
3. Dough piece L:W:H 65×75×80 mm, weight 150 g.

To limit the lengths of the dough pieces, special partitions made of monolithic sheet polycarbonate 4 mm thick were installed in the chamber.

The installation drawing is shown in Fig. 1.

During the experiments on checking the mm, the same formula and technology of dough preparation and ER baking were used as in the main experiment.

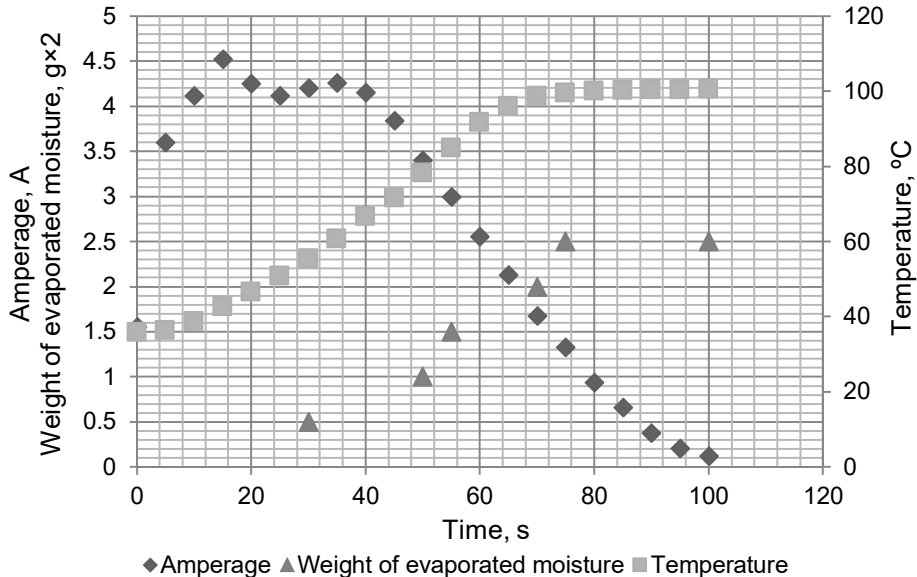


**Figure 1.** Installation drawing.

## RESULTS AND DISCUSSION

### Experimental determination of the components of a mathematical model

Curves of current, temperature and weight of evaporated moisture were obtained in the experiment and are shown in the Fig. 2.



**Figure 2.** Curves of current, temperature and weight of evaporated moisture versus time of baking.

The amount of energy spent on baking was determined by processing the data obtained during the experiment. After recalculation the specific power consumption for baking 1 kg of dough was  $397.4 \text{ kJ kg}^{-1}$ .

The temperature dynamics is represented by data from one of the temperature sensors. This is explained by the fact that the difference between the readings from other sensors does not exceed  $4 \text{ }^\circ\text{C}$ , thus confirming the assumption 1 and allowing to consider the temperature field of the dough piece uniform. The amount of evaporated moisture was 5 g, which confirms the accepted assumption 4.

The authors compared the experimental results with works on a similar subject. It is worth noting that the comparison should be made taking into account the differences in the bread formula and technology and the weights of dough pieces.

Nevertheless, there is a certain similarity of the experimental data of work (Kulishov et al., 2021) in the behavior of temperature and current during ER baking with the graphs obtained during experiments in this work.

The study (Masure et al., 2019) is rather difficult to compare with the data presented in the given work, since the object of the study in this work is gluten-free bread, its formula and technology differ significantly from those used in the article. The ER heating mode used by the authors is controlled by changing the voltage of the PID controller so as to obtain a temperature profile identical to the profile obtained when baking bread in a convection oven, while the ER baking voltage remains constant in the article.

The results of the experimental data of the study (Derde et al., 2014) are also difficult to compare with this work, since the authors investigate changes in moisture distribution and physical changes in starch of breads conventionally baked or using an ERO. At the same time, the temperature kinetics of both baking methods are the same, which is achieved by voltage regulation during ER baking (similar to the research method mentioned above).

By analyzing the curves of current strength and temperature versus time, it can be established that a significant part of the power consumed is spent on physicochemical processes. Indirectly, this can be judged by a sharp change in the electrical resistance of the dough piece. The power consumption for heating the dough piece is a small part of the power consumption:

$$Q = c \cdot (t_k - t_0) = 1600(98 - 36) = 100 \frac{\text{kJ}}{\text{kg}};$$

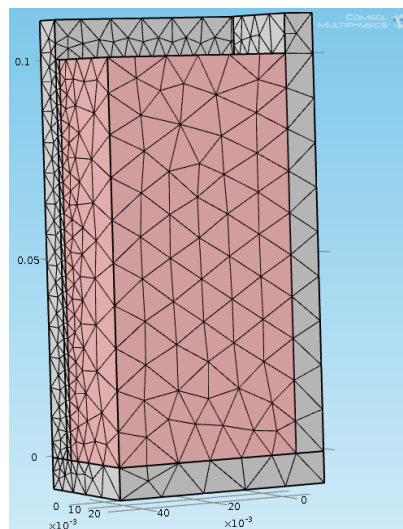
Let us trace how the temperature of the dough piece would change if all the supplied power was spent on heating it, that is  $W_c = W_{el}$ . Let us define the change in electrical power through the dependence of the specific electrical resistance  $\rho(t)$  of the dough piece on temperature:

$$W_{el}(t) = \frac{U^2}{R(t)V} = \frac{U^2}{\rho(t)l} \quad (5)$$

The dependence  $\rho(t)$  will be determined by measuring values of the current strength and voltage, the dimensions of the dough piece and the temperature during the experiment. The calculation results are given in Table 2.

**Table 2.** Temperature dependence of the parameters of the dough piece

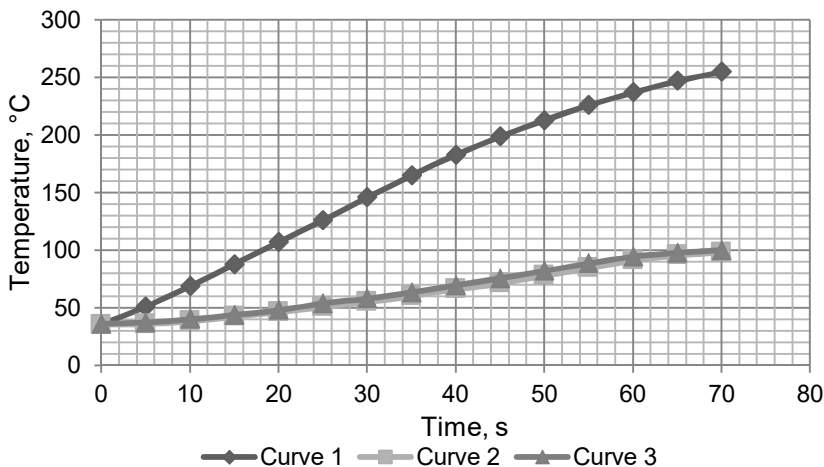
$t$ , °C	Experiment $\rho(t)$ , Ohm·m	Experiment $W_{el}(t)$ , $W \cdot (m^3)^{-1}$	Correction $W(t)$ , $W \cdot (m^3)^{-1}$	$K(t)$
35.8	17.1	1.14	0.0557	20.4
36.4	11.4	1.7	0.223	7.63
38.7	10.2	1.9	0.372	5.12
42.6	10.0	1.93	0.379	5.09
46.5	10.5	1.84	0.418	4.41
50.9	10.6	1.83	0.435	4.21
55.4	10.4	1.86	0.514	3.62
60.8	10.5	1.85	0.561	3.30
66.6	11.	1.76	0.472	3.72
71.5	12.2	1.69	0.647	2.46
78.3	13.7	1.41	0.630	2.24
84.8	15.8	1.22	0.651	1.88
91.6	18.8	1.03	0.423	2.44
96.0	23.1	0.838	0.249	3.37
98.6	29.2	0.662	0.196	3.38



**Figure 3.** Numerical model of the experimental installation.

Thus, based on the data in the Table 1 and expression (5), let us solve Eq. (3) numerically with the object model compiled in Comsol Multiphysics. The Fig. 3 shows

an image of a model compiled for ¼ part of the installation due to its symmetry. The results of numerical calculation (curve 1) and experiment (curve 2) are shown in the Fig. 4.



**Figure 4.** The results of the numerical calculation of the temperature during heating the dough piece and the experimental curve during baking.

Analyzing the discrepancy between the temperature curves 1 and 2, a correction to the initial data of the numerical model characterizing the dependence of the heat source power can be made. The calculation of the correction is carried out on the basis of the possibility to estimate the power consumed for heating the dough pieces  $W_c$  and the heat exchange with the environment  $W_{hl}$  at each of the baking stages from the experimental curve 2:

$$W_c = \frac{cM(t(\tau_{i+1}) - t(\tau_i)) \cdot (\tau_2 - \tau_1)}{V}; \tag{6}$$

$$W_{hl} = \frac{\alpha S(t(\tau) - t_f)}{V}; \tag{7}$$

where  $\tau_i, \tau_{i+1}$  are two adjacent points in time on the diagram, the Fig. 3;  $\tau_j = (\tau_i + \tau_{i+1})/2$  is a point in time characterizing one of the baking stages, s;  $M$  – weight of the dough piece, kg;  $c$  – specific heat capacity of the dough piece,  $J \cdot (kg \cdot K)^{-1}$ ;  $S$  is the area of the heat transfer surface,  $m^2$ ,  $\alpha$  is the heat transfer coefficient, determined on the basis of criterion relations for heat transfer under free convection conditions,  $W \cdot (m^2 \cdot K)^{-1}$ .

The calculation of the heat flux  $W_{hl}$  within the scope of the experiment showed that  $W_{hl} / W_{el} < 0.005$ , which makes it possible to neglect this value for this experimental installation.

Based on the results of calculations by formulas (6), (7) and the value of the total consumed electrical power  $W_{el}(t)$  calculated by formula (5), we can find the overall power consumption for components which are hardly definable by calculation, namely heat loss due to heating of the electrodes  $W_{elh}$ , heat loss due to electrochemical reactions  $W_{el/ch}$ , evaporation of liquid  $W_{ev}(t)$  and physicochemical processes  $W_{phc}(t)$ , taking place during baking. Thus, the dependence  $W(t)$  was obtained on the basis of expression (5) and presented in the column ‘Correction’ of the Table 2. It should be noted that the

values of  $W(t)$  presented in the Table 2 can be used only for dough pieces with thickness  $l$  and heat exchange surface area  $S$  corresponding to the design of this cell.

In order for the developed thermal model to be applied for different sizes of dough pieces, the following transformation was carried out:

1) connection between the consumed electric power  $W_{el}(t)$  and the initial data for the thermal model  $W(t)$  using the proportionality coefficient  $K(t)$  is established:

$$K(t) = \frac{W(t)}{W_{el}(t)}; \tag{8}$$

The result of calculating  $K(t)$  is shown in the Table 2.

2) Expression (8) is transformed to find the power density of heat release  $W(t)$  based on the temperature dependence of the specific electrical resistivity:

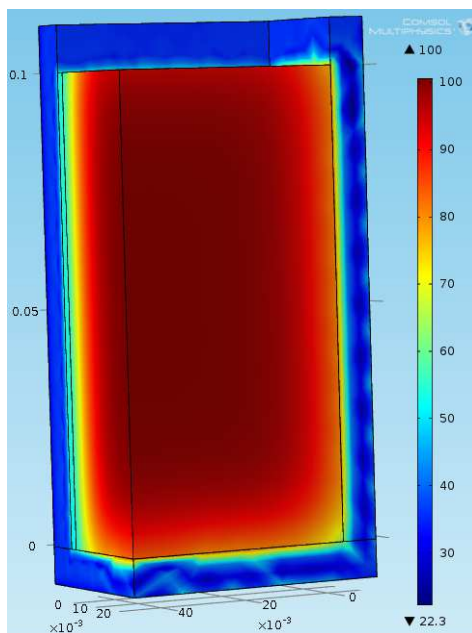
$$W_{el}(t) = \frac{U^2}{\rho(t)l^2K(t)}; \tag{9}$$

Expression (9) allows to calculate the power of heat release in a dough piece in the form of a parallelepiped with random geometric dimensions. If the contribution of the heat transfer due to the convective-radiant heat transfer has a significant effect, the value of  $W(t)$  should be increased by the value of  $W_{hl}$ , calculated by expression (7).

The results of the calculation with a numerical model with the power  $W(t)$  calculated by expression (9) are presented by the curve 3 in the Fig. 4. Comparing curves 2 and 3 in the Fig. 4, it can be noted that making a correction allows you to obtain a satisfactory convergence of the simulation and experiment results.

The Fig. 5 shows the temperature distribution in the dough piece obtained using a numerical model.

Analyzing the data obtained, it can be noted that the dough piece has a temperature field corresponding to the accepted assumption 1. However, when ensuring uniform temperature distribution in practice, it should be borne in mind that the shape of the dough piece does not fully correspond to the parallelepiped. Less electric current flows through the top of the dough piece that rises during proofing, which can lead to insufficient heating of this part of the dough piece. To reduce the influence of this factor, a cell should be manufactured with such a ratio of geometric dimensions that the area of the upper part of the cell is several times less than the area of the surfaces of the electrodes in contact with the dough piece. This solution also makes it possible to reduce the outflow of heat into the environment by reducing the heat exchange surface area.



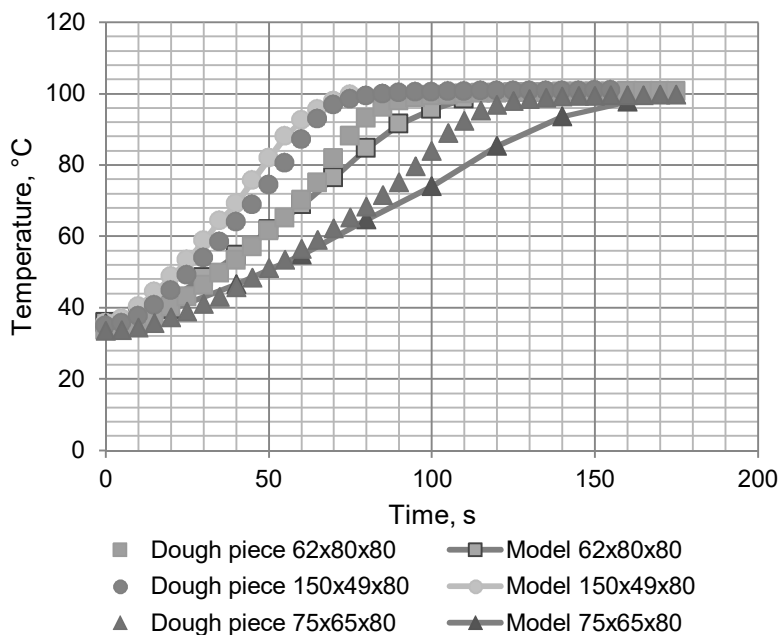
**Figure 5.** The result of numerical simulation based on the corrected power of the heat source.

In addition, to reduce the thermal interaction with the cell walls (fulfillment of assumption 2), a heat-insulating material with a thermal conductivity of less than  $0.1 \text{ W}\cdot(\text{m}\cdot\text{K})^{-1}$  should be used.

The developed thermal model also makes it possible to determine the baking time of the dough piece  $\tau$ . When performing a numerical calculation it should be stopped when the required temperature level in the dough piece is reached. Analyzing the results of experiments on dough pieces of various sizes it was found that the optimal baking parameters are obtained in the dough piece when the temperature reaches  $98 \text{ }^\circ\text{C}$ .

The developed thermal model is suitable for predicting the temperature regime of baking, provided that the formula and baking technology described in the Materials and Methods section of this work are observed. In case of using other formulations and technologies, the parameters of the model should be adjusted.

To check the reliability of the calculations made by numerical model experiments were carried out with dough pieces with the dimensions  $62\times 80\times 80$ ,  $75\times 65\times 80$  and  $49\times 150\times 80 \text{ mm}$  prepared according to the same recipe. The power  $W(t)$  was determined for a voltage of  $220 \text{ V}$  by the expression (9) as the initial data for the numerical model. Comparison of the temperature curves obtained by the model and experiment are shown in the Fig. 6.



**Figure 6.** Comparison of simulation and experiment results.

Based on the results of experiments and simulation a statistical analysis of the results was carried out using the Fisher test in Microsoft Excel software. The data on the temperature change obtained by experiment and the mathematical model are shown in Table 3. The results of one-way ANOVA test performed in Microsoft Excel are shown in Table 4.



**Table 3.** Data obtained experimentally and using the model

150×49×80			80×62×80			65×75×80		
t, c	model T, °C	experiment	t, c	model T, °C	experiment	t, c	model T, °C	experiment
0	35.7	34.99	0	35.76	33.97	0	35.73	33.6
5	36.9	35.61	10	37.8	36.33	20	39.55	37.33
10	40.4	37.57	20	42.8	41.59	40	46.68	45.77
15	44.5	40.74	30	48.4	47.76	60	54.9	56.4
20	48.7	44.85	40	54.6	55.25	80	64.8	68.24
25	53.4	49.04	50	61.8	63.8	100	74.1	83.93
30	58.9	53.97	60	68.8	73.43	120	85.4	96.88
35	64.3	58.37	70	76.4	87.55	140	93.6	99.21
40	69.2	63.94	80	84.6	95.8	160	97.8	99.58
45	75.6	68.8	90	91.47	98.82			
50	82	74.49	100	95.6	99.81			
55	88.1	80.61	110	98.44	100.26			
60	92.5	87.17						
65	95.6	92.96						
70	98	96.86						
75	99.7	98.42						

**Table 4.** The results of one-way ANOVA test

62×80×80						
Source of variation	SS	df	MS	F	P-Value	F critical
Between groups	59.85042	1	59.85041667	0.098629404	0.756439297	4.300949462
Inside groups	13,350.07	22	606.8212326			
Total	13,409.92	23				
75×65×80						
Source of variation	SS	df	MS	F	P-Value	F critical
Between groups	44.7458	1	44.7458	0.070663168	0.793768532	4.493998418
Inside groups	10,131.63	16	633.2266375			
Total	10,176.37	17				
150×49×80						
Source of variation	SS	df	MS	F	P-Value	F critical
Between groups	132.4785	1	132.4785031	0.25495387	0.617297564	4.170876757
Inside groups	15,588.53	30	519.6175423			
Total	15,721	31				

The following statement was taken as the null hypothesis: the differences between the temperature values calculated by the mm and those obtained during the experiment are caused by random factors, the averages in all classes are equal, and the method for determining the temperature - mm or experiment - does not affect the result. Based on the results of the calculation it was determined that the calculated value of the Fisher criterion is less than the value from the Table, which justifies acceptance of the null hypothesis. This fact allows to consider the model as adequate.

## CONCLUSION

The developed mathematical model based on the equation of the non-stationary thermal regime of a body with an internal heat source allows to determine the dynamics of temperature changes during baking dough pieces by the electric resistance method using numerical solution in Comsol Multiphysics with an accuracy sufficient for practical use.

## REFERENCES

- Derde, L.J., Gomand, S.V., Courtin, C.M. & Delcour, J.A. 2014. Moisture Distribution during Conventional or Electrical Resistance Oven Baking of Bread Dough and Subsequent Storage. *Journal of Agricultural and Food Chemistry* **62**(27), 6445–6453. doi:10.1021/jf501856
- Gally, T., Rouaud, O., Jury, V., Havet, M., Ogé, A. & Le-Bail, A. 2017. Proofing of bread dough assisted by ohmic heating. *Innovative Food Science and Emerging Technologies* **39**, 55–62. doi: 10.1016/j.ifset.2016.11.008
- Gally, T., Rouaud, O., Jury, V. & Le-Bail, A. 2016. Bread baking using ohmic heating technology; a comprehensive study based on experiments and modeling. *Journal of Food Engineering* **190**, 176–184. doi: 10.1016/j.jfoodeng.2016.06.029
- Ghnimi, S., Flach-Malaspinaa, N., Dresche, M., Delaplace, G. & Maingonnat, J.F. 2008. Design and performance evaluation of an ohmic heating unit for thermal processing of highly viscous liquids. *Chemical engineering research and design* **86**, 626–632. doi:10.1016/j.cherd.2008.02.005
- Fu, W.-R. & Hsieh, C.-C. 2006. Simulation and Verification of Two-Dimensional Ohmic Heating in Static System. *Journal of Food Science* **64**(6), 946–949. DOI 10.1111/j.1365-2621.1999.tb12257.x
- Fryer, P. & Li, Z. 1993. Electrical resistance heating of foods. *Trends in Food Science & Technology* **41**, 364–369. doi: 10.1016/0924-2244(93)90018-6.
- Marra, F., Zell, M., Lyng, J.G., Morgan, D.J. & Cronin, D.A. 2009. Analysis of heat transfer during ohmic processing of a solid food. *Journal of Food Engineering* **91**, 56–63. doi:10.1016/j.jfoodeng.2008.08.015
- Kulishov, B., Kulishova, K., Rudometova, N., Fedorov, A. & Novoselov, A. 2020. Advantages of electric resistance method for baking bread and flour confectionery products of functional purpose. *Agronomy Research* **18**(4), 2449–2464. doi: 10.15159/ar.20.211
- Kulishov, B.A., Soboleva, E.V., Sergacheva, E.S. & Novoselov, A.G. 2021. Electric resistance baking as a method for production of toast bread. *IOP Conference Series: Earth and Environmental Science*, 640 072007. doi:10.1088/1755-1315/640/7/072007
- Luyts, A., Wilderjans, E., Van Haesendonck, I., Brijs, K., Courtin, C.M. & Delcour, J.A. 2013. Relative importance of moisture migration and amylopectin retrogradation for pound cake crumb firming. *Food Chemistry* **141**, 3960–3966. doi:10.1016/j.foodchem.2013.06.110
- Masure, H.G., Wouters, A.G.B., Fierens, E. & Delcour, J.A. 2019. Electrical resistance oven baking as a tool to study crumb structure formation in gluten-free bread. *Food Research International* **116**, 925–931. doi:10.1016/j.foodres.2018.09.029
- Platunov, E.S., Buravoy, S.E. & Kurepin, V.V. 1986. Thermophysical measurements and devices. Mashinostroyeniye, Leningrad, 256 pp.
- Sastry, S.K. & Palaniappan, S. 1992. Mathematical modeling and experimental studies in a static heater' on ohmic heating of liquid-particle mixtures. *Journal of Food Process Engineering* **15**, 241–261. doi: 10.1111/j.1745-4530.1992.tb00155.x

## **Marginal abatement cost curve for an ammonia reduction measure in agriculture: the case of Latvia**

A. Lenerts<sup>1,\*</sup>, K. Naglis-Liepa<sup>1</sup>, D. Popluga<sup>1</sup>, Dz. Kreišmane<sup>2</sup>, E. Aplociņa<sup>2</sup>,  
L. Bērziņa<sup>3</sup> and O. Frolova<sup>3</sup>

<sup>1</sup>Latvia University of Life Sciences and Technologies, Faculty of Economics and Social Development, Institute of Economics and Regional Development, 18 Svetes street, LV-3001 Jelgava, Latvia

<sup>2</sup>Latvia University of Life Sciences and Technologies, Faculty of Agriculture, 2 Liela street, LV-3001 Jelgava, Latvia

<sup>3</sup>Latvia University of Life Sciences and Technologies, Faculty of Environment and Civil Engineering, 19 Akademijas street, LV-3001 Jelgava, Latvia

\*Correspondence: [arnis.lenerts@llu.lv](mailto:arnis.lenerts@llu.lv)

Received: January 28<sup>th</sup>, 2021; Accepted: May 26<sup>th</sup>, 2021; Published: August 24<sup>th</sup>, 2021

**Abstract.** With the production of grain and livestock-derived agricultural commodities increasing, the agricultural sector has become one of the main sources of ammonia (NH<sub>3</sub>) emissions in Latvia. In 2018, the agricultural sector contributed to 83% of the total NH<sub>3</sub> emissions originated in Latvia (15.46 kt) (LIIR 2020). The EU has already put in place measures to control NH<sub>3</sub> emissions. This includes the EU target of reducing ammonia emissions by 21% by 2030 and sets out emission reduction commitments for Latvia. Considering Latvia's indicative reduction target, the NH<sub>3</sub> emission reductions need to be achieved by 2030 (Directive 2016/2284) so that the emissions do not exceed the 2005 level (11.33 kt). Implementing no mitigation measures, Latvia has projected agricultural sector NH<sub>3</sub> emissions to be 32.4% higher than those in 2005, and therefore the mitigation of the NH<sub>3</sub> emissions from agriculture is important. The research aims to estimate cost-effective NH<sub>3</sub> emission reduction measures in agriculture in Latvia. The results of the research represent a marginal abatement cost curve (MACC) analysis, in which we have quantified the potential for reduction for selected NH<sub>3</sub> emission mitigation measures in Latvia. A list of the measures has been established taking into account the experience of good agricultural practices in the reduction of NH<sub>3</sub> emissions (UN, 2014) and of other European countries as well. The calculations carried out allowed us to group the measures according to their priorities: measures that are cost-effective and with high potential for reduction of NH<sub>3</sub>; measures that are cost-effective but with low NH<sub>3</sub> emission reduction potential; measures that are not cost-effective but with high potential for reduction of NH<sub>3</sub>; measures that are not cost-effective and with low potential for reduction of NH<sub>3</sub>. The estimated cumulative (total) reduction of NH<sub>3</sub> emissions in Latvian agriculture by 2030, with the implementation of the measures analysed, is equal to 20.08 kt.

**Key words:** NH<sub>3</sub>, emissions, measures, reduction, cost efficiency.

## INTRODUCTION

In Latvia, agricultural output measured in value (EUR) and physical volume (tonnes) showed a steady upward trend. The key growing agricultural industries were cereal and livestock production. In the period 2013–2019, the area cropped with cereals increased by 27%. The total number of dairy cows decreased by 19%, while the number of beef cows increased by 93%, thereby resulting in a constant total number of cattle in Latvia during this period (CSB, 2020). During the analysis period, productivity in the cereal and dairy industries significantly increased, as the average cereal yield increased by 27%, while the average milk yield per cow increased by 25% (CSB, 2020). The productivity in the cereal and dairy industries increased owing to agricultural intensification, which was positively related to an increase in the amount of resources used by the industries. Ineffective management of resources leads to a number of significant negative externalities of agricultural production: greenhouse gas (GHG) and ammonia (NH<sub>3</sub>) emissions as well as nitrogen (N) losses. The mentioned externalities make a significant impact on the natural environment; therefore, the EU has set a goal to significantly reduce the impacts on the natural environment (Directive 2016/2284). NH<sub>3</sub> emissions from the agricultural sector accounted for 90.5% of the total NH<sub>3</sub> emissions in the EU, and in the period 2013–2018 the emissions increased by 2% (Eurostat, 2020).

In Latvia in 2018, the total NH<sub>3</sub> emissions from agriculture amounted to 12.83 kt, and the agricultural sector accounted for 83% of the total NH<sub>3</sub> emissions. The main sources of NH<sub>3</sub> emissions from agriculture were manure management systems and the application of synthetic fertilizers and manure. The NH<sub>3</sub> emissions from the agricultural sector have increased by 13.2% since 2005 (LIIR 2020). The main factors contributing to the increase in NH<sub>3</sub> emissions were as follows: an increase in the arable land area cropped with cereals; an increase in the application of N fertilizers and the change of the manure management system in dairy farming (Priekulis et al., 2019).

The EU has already put in place measures to control NH<sub>3</sub> emissions. This includes the EU target of reducing ammonia emissions by 21% by 2030 and sets out emission reduction commitments for Latvia. Considering Latvia's indicative emission reduction target, the NH<sub>3</sub> emission reductions need to be achieved by 2030 (Directive 2016/2284) so that the emissions do not exceed the 2005 level (11.33 kt). Implementing no mitigation measures, Latvia has projected agricultural sector NH<sub>3</sub> emissions to be 32.4% higher than those in 2005. A comparative analysis of GHG and NH<sub>3</sub> emissions in the EU Member States reveals that in Latvia the emission intensity in agriculture was below the EU average (Lenerts et al., 2019). The emission reduction targets for the EU Member States are set in relative terms and must be achieved in relative terms, regardless of the absolute value; therefore, the reduction of the NH<sub>3</sub> emissions from agriculture is important. Reducing agricultural emissions is also a key issue in the recently launched EU Farm to Fork strategy, which is part of the European Green Deal (European Commission, 2019).

The research **aims** to estimate cost-effective NH<sub>3</sub> emission reduction measures in agriculture in Latvia.

To achieve the aim, the following specific **research tasks** were set: to examine a methodology for calculating and assessing a marginal abatement cost curve (MACC) for agricultural NH<sub>3</sub> emissions; to select potential theoretical NH<sub>3</sub> emission mitigation

measures for agriculture in Latvia; to perform an assessment and a MACC analysis of NH<sub>3</sub> emissions from agriculture in Latvia.

The research used the data from Central Statistical Bureau of Latvia (CSB): fertilisers and manure used (tonnes); livestock (number); land used in agriculture (hectares), Agricultural Data Centre (ADC): animal herds and holdings (feeding; manure management; intensive and extensive holding); animals (live weight; bulk; number of lactating), Latvian Rural Advisory and Training Centre (LRATR): costs of implementing and maintaining measures to reduce ammonia emissions and Eurostat databases. To process the data, the following economic **research methods** were employed: data grouping for statistical indicator calculation; time series; analysis and synthesis; induction and deduction.

## MATERIALS AND METHODS

EU Directive 2016/2284 adopted in 2016 has set an NH<sub>3</sub> emission reduction target of 1% per year for Latvia for the period 2020–2029 and the period after 2030. In order to meet the target set in the directive and taking into account forecasts (Cabinet Regulation, 2020), NH<sub>3</sub> emissions must be reduced by 4.13 kt in Latvia by 2030 (LIIR, 2020). Reaching this target is possible through introducing measures for reducing NH<sub>3</sub> emissions, which would change the production or management systems that make the largest effects on emissions. In the agricultural sector, emission reduction measures need to target the systems of cereal production, manure management and manure storage. Changing any management system, however, requires investments. Before implementing NH<sub>3</sub> emission reduction measures, it is necessary to perform a detailed assessment of the reduction measures through performing cost-effectiveness calculations and emission reduction potential calculations. One of the most suitable research methods for solving such a complex problem is marginal abatement cost curve (MACC) analysis. The method is quite widely used for analysing GHG reduction measures (Moran et al., 2011; Eory et al., 2018) and assessing NH<sub>3</sub> emission reduction measures (Buckley C. & Krol D.J. 2020) before the measures are included in policy documents.

MACC analysis provides several kinds of information, as it:

- makes it possible to assess the cost-effectiveness of certain measures for reducing NH<sub>3</sub> emissions,
- makes it possible to identify the total reduction of NH<sub>3</sub> emissions over time,
- provides information on which NH<sub>3</sub> emission reduction measures could be introduced under certain conditions.

A marginal abatement cost analysis and curve construction consists of three important steps:

- identifying measures suitable for the agricultural sector of Latvia to reduce NH<sub>3</sub> emissions,
- assessing the NH<sub>3</sub> emission reduction potential of the measures selected for the agricultural sector of Latvia,
- calculating NH<sub>3</sub> marginal abatement costs for the selected measures.

The present research analysed 16 various NH<sub>3</sub> emission reduction measures aimed at the efficient application of nitrogen (N) fertilizers, efficient off-site manure management and the expansion of organic farming. The list of the measures was based on the Code of Good Agricultural Practice for Reducing NH<sub>3</sub> Emissions (UN, 2014), the

experience of other European countries, as well as the opinions of experts from the Ministry of Agriculture and scientists from Latvia University of Life Sciences and Technologies.

The NH<sub>3</sub> emission reduction potential of the measures selected for the agricultural sector of Latvia was identified by using the guidelines and methodologies provided by the Air Pollutant Emission Inventory Guidebook (EMEP/EEA, 2016). For each category of ammonia emissions given in the relevant nomenclature, three potential levels for emission calculations were identified according to the guidelines:

- **Tier 1** methods make full use of the EMEP guidelines,
- **Tier 2** methods use the EMEP guidelines and additionally apply country-specific emission factors,
- **Tier 3** methods include country-specific calculation methodologies.

The **TIER 2** methods are mainly applied to calculate agricultural NH<sub>3</sub> emissions from the livestock industry, as there are scientifically substantiated regional differences in emission factors (VS) (LIIR, 2020). The research employed Eq. 1 to calculate NH<sub>3</sub> emissions from manure management systems.

$$NH_3 = \sum_{(T)} N_T \cdot VS_S \quad (1)$$

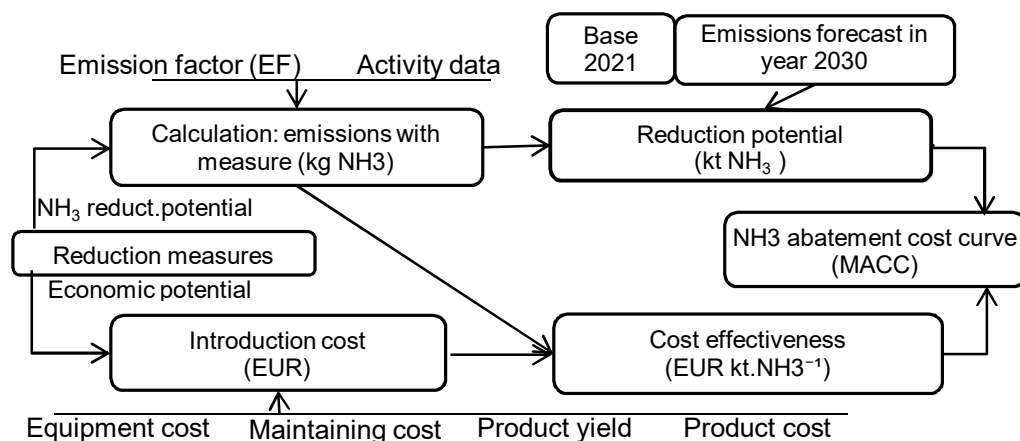
where NH<sub>3</sub> – Ammonia emissions from manure management systems, kg NH<sub>3</sub> year<sup>-1</sup>; N<sub>T</sub> – total livestock manure production for livestock group T, kg year<sup>-1</sup>; VS<sub>S</sub> – emission factor for Latvia, manure management system S, livestock group T, (kg NH<sub>3</sub>-N emissions).

Calculations of NH<sub>3</sub> emissions from soils used in agricultural production by the cereal industry were performed by using the TIER 1 methods according to Eq. 2.

$$NH_3 = \sum_{(T)} N_T \cdot EF_T \quad (2)$$

where NH<sub>3</sub> – ammonia emissions from N-containing fertilizers applied to soil, kg NH<sub>3</sub> year<sup>-1</sup>; N<sub>T</sub> – fertilizers applied to soil for group T, kg year<sup>-1</sup>; EF<sub>T</sub> – emission factor for fertilizer group T as defined in the EMEP guidelines, (kg NH<sub>3</sub>-N emissions).

The model of an algorithm for calculating the marginal abatement cost of an NH<sub>3</sub> emission reduction measure and constructing a MACC curve is shown in Fig. 1.



**Figure 1.** Model of an algorithm for calculating the marginal abatement cost of an NH<sub>3</sub> emission reduction measure and constructing a MACC curve.

The marginal abatement cost of implementing NH<sub>3</sub> emission reduction measures was calculated by using Eq. 3.

$$C_{p.c.} = \sum_{i=1}^T (Y_c \cdot P_c) - I_{p.c.} - I_{m.c.} \quad (3)$$

where  $C_{p.c.}$  – marginal abatement cost of an NH<sub>3</sub> emission reduction measure after it has been introduced, EUR;  $T$  – duration of the measure after it has been introduced,  $T = 10$  years;  $Y_c$  – average yield of product  $c$  after measure  $p$  has been introduced;  $P_c$  – 10 years average selling price of product  $c$ ;  $I_{p.c.}$  – investment cost of implementing measure  $p$  for product  $c$ ;  $I_{m.c.}$  – 10 years cost to investment maintain the implemented measure  $p$ .

The cost-effectiveness of NH<sub>3</sub> emission reduction measures was calculated according to Eq. 4.

$$MAC_p = \frac{C_{p.c.}}{NH_{3p}} \quad (4)$$

where  $MAC_p$  – cost-effectiveness of NH<sub>3</sub> emission reduction measure  $p$ , EUR/kt;  $RI_{p.c.}$  – marginal abatement cost for product  $c$  after measure  $p$  has been introduced, EUR;  $NH_{3p}$  – NH<sub>3</sub> emissions after measure  $p$  has been introduced, kt.

## RESULTS AND DISCUSSION

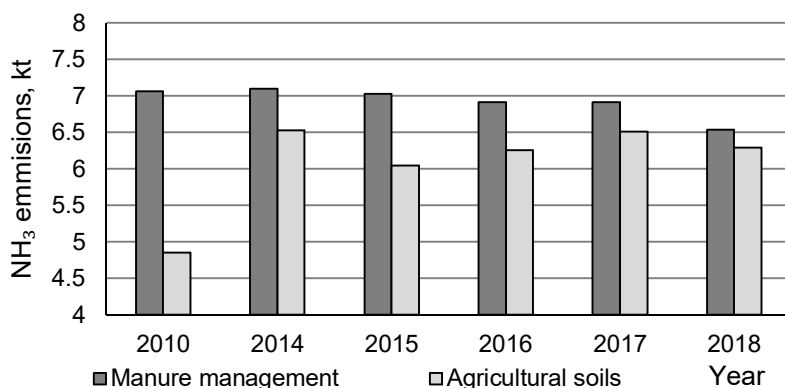
In 2018, the agricultural sector contributed to 83.0% (12.83 kt) of the total NH<sub>3</sub> emissions in Latvia (15.46 kt). The agricultural sector was the largest producer of ammonia emissions in the country. Ammonia emissions from agricultural soils and crops (including emissions from nitrogen fertilizers, manure and other organic fertilizers) accounted for 49% (6.29 kt) of the total ammonia emissions from the agricultural sector in 2018. Ammonia emissions from manure management systems accounted for 51% of the total or 6.54 kt. Changes in NH<sub>3</sub> emissions from the agricultural sector in the period 2013–2018 are summarized in Table 1.

**Table 1.** Changes in NH<sub>3</sub> emissions from the agricultural sector in Latvia in the period 2013–2018

Indicator	2010	2014	2015	2016	2017	2018
NH <sub>3</sub> , kt	11.91	13.98	13.09	13.17	13.42	12.83
Annual change rate, %	-	+15	-6.4	+0.6	+1.9	-4.4
Change from base year, %		+15	+9	+10	+12	+8

Ammonia emissions from manure management systems showed a declining trend in the period 2014–2018, while the emissions from agricultural soils (including urine and manure left on pasture by livestock during the grazing period) were volatile, i.e. both increased and decreases.

The emission trends are summarized in Fig. 2.



**Figure 2.** NH<sub>3</sub> emissions from manure management systems and soil use in Latvia in the period 2014–2018.

The NH<sub>3</sub> emission reduction measures analysed in the research were selected with the aim of improving manure and agricultural soil management systems. The reduction measures were aimed at the efficient application of fossil nitrogen (N) fertilizers, as well as efficient off-site manure management and organic farming development in the dairy industry. The measures for reducing NH<sub>3</sub> emissions adapted to conditions in Latvia and the area affected by the measures are summarized in Table 2.

**Table 2.** Measures for reducing NH<sub>3</sub> emissions adapted to conditions in Latvia and their impacts.

Measure-affected area	NH <sub>3</sub> emission reduction measure
Efficient application of nitrogen fertilizers	Precision N fertilizer application
	Fertilizer planning and practical application
	Nitrogen sequestration by including legumes in crop rotation
	Incorporation of manure directly into the soil:
	Option 1 – by means of a piping distribution system
	Option 2 – by means of a manure spreader for incorporating it directly into the soil
	Option 3 – by means of a belt spreader with hanging pipes
Efficient manure storage management	Option 4 – by means of a belt spreader with hanging pipes equipped with nozzles
	Limited liquid manure incorporation period (4 h)
	Limited litterless poultry manure incorporation period (4 h)
	Limited litter manure incorporation period (12 h)
Organic farming development	Covering liquid manure storage facilities
	Option 1 – a floating layer of expanded clay pellets
	Option 2 – a floating plastic film cover
	Option 3 – a concrete cover
	Option 4 – a tent cover
	Organic dairy farming development (extensive dairy farming with use of grazing)



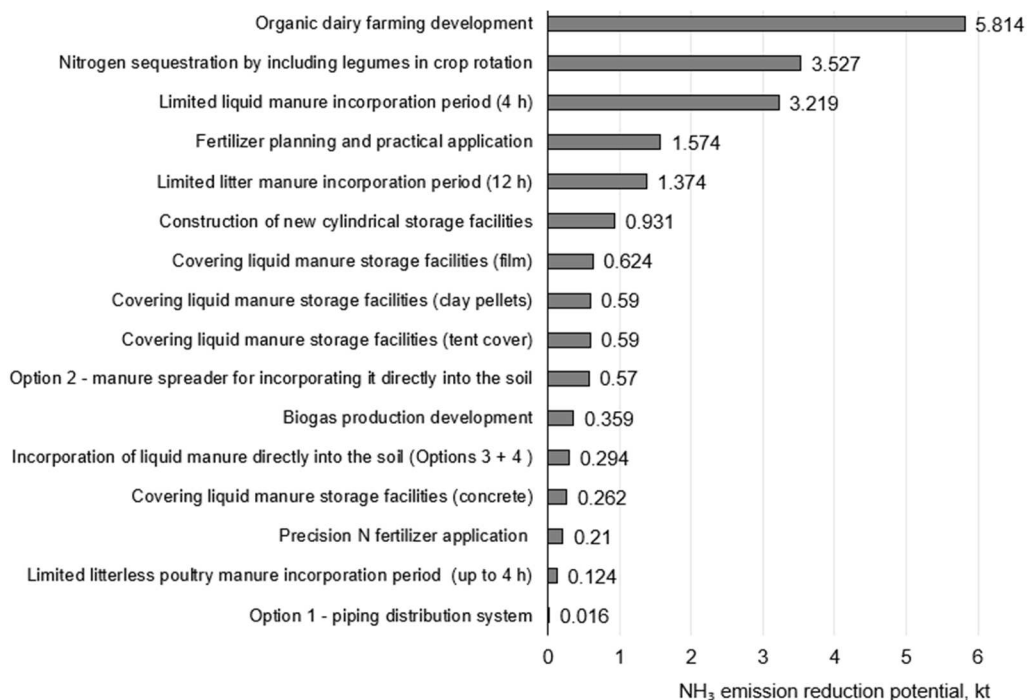
Abatement costs are associated with abatement potentials for one period of time without giving information on what happened before that period and what is assumed to happen afterwards (Kesicki, F. & Strachan, N. 2011). The emission reduction potential for the period 2021–2030 was calculated for all the selected and analysed NH<sub>3</sub> emission reduction measures.

➤ The calculations showed that the measures could be divided into three categories: **measures with high reduction potential**: organic dairy farming development; nitrogen sequestration by including legumes in crop rotation; limited liquid manure incorporation period (4 h); fertilizer planning and practical application; limited litter manure incorporation period (12 h), which together accounted for 77% of the total reduction potential,

➤ **measures with medium reduction potential**: construction of new cylindrical storage facilities; covering liquid manure storage facilities (tent cover, clay pellets, film); incorporation of liquid manure directly into the soil (Option 2); biogas production development, which together accounted for 18% of the total reduction potential,

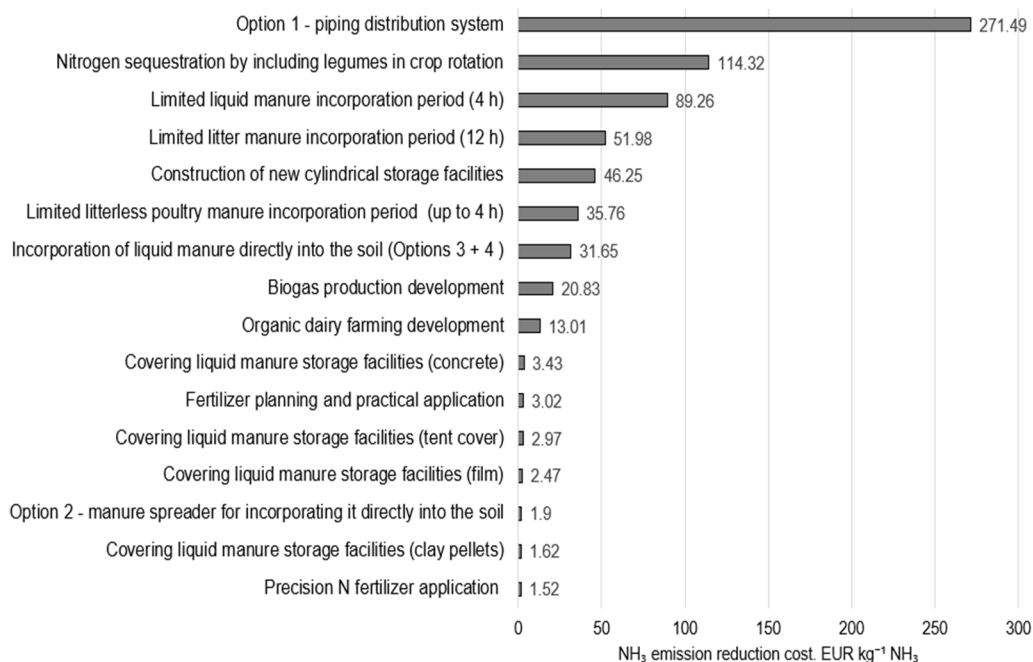
➤ **measures with low reduction potential**: incorporation of liquid manure directly into the soil (Options 1+3+4); precision N fertilizer application, covering liquid manure storage facilities (concrete), limited litterless poultry manure incorporation period (4 h), which together accounted for 5% of the total reduction potential.

The calculations results are summarized in Fig. 3.



**Figure 3.** Estimated reduction potential of the NH<sub>3</sub> emission reduction measures for the period 2021–2030.

The effectiveness of an NH<sub>3</sub> emission reduction measure is determined by calculating the unit cost (kg NH<sub>3</sub>) of reducing NH<sub>3</sub> emissions (EUR kg<sup>-1</sup> NH<sub>3</sub>). The calculation results are summarized in Fig. 4.



**Figure 4.** Rankings of measures by ammonia emission reduction cost, EUR kg<sup>-1</sup> NH<sub>3</sub>.

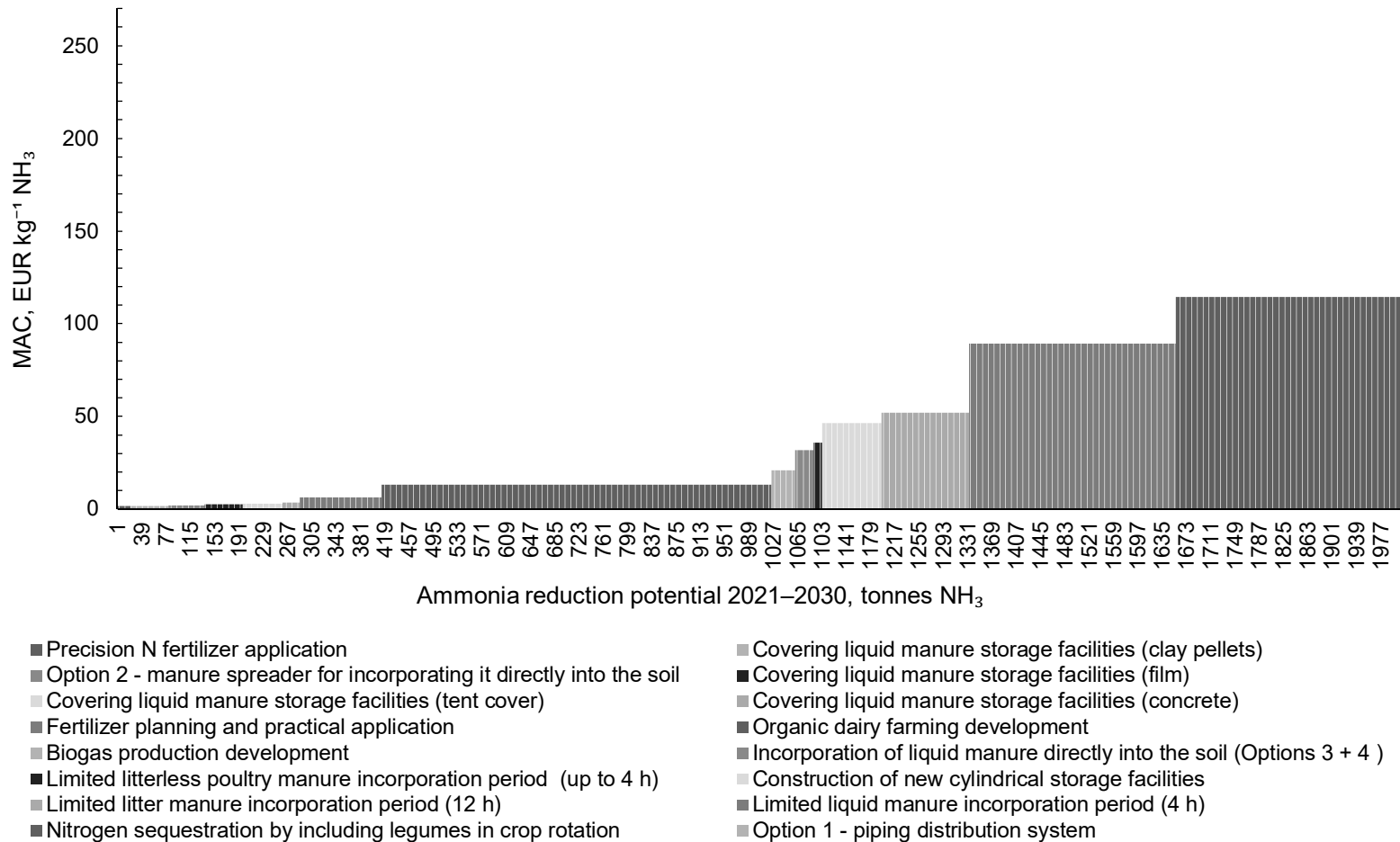
The calculations showed that the measures could be divided into three categories:

- **low cost** measures: precision N fertilizer application; covering liquid manure storage facilities (tent cover, clay pellets, tent, film); incorporation of liquid manure directly into the soil (Option 2); fertilizer planning and practical application,

- **medium cost** measures: organic dairy farming development; biogas production development; incorporation of liquid manure directly into the soil (Options 3 + 4); limited litterless poultry manure incorporation period (4 h),

- **very high cost** measures: construction of new cylindrical storage facilities; limited litter manure incorporation period (12 h); limited liquid manure incorporation period (4 h); nitrogen sequestration by including legumes in crop rotation; incorporation of liquid manure directly into the soil (Option 1).

The calculation results are summarized in Fig. 5, which shows a marginal abatement cost curve for the ammonia reduction measures (MACC). The vertical axis of the MACC curve shows the cost of reducing 1 kg of ammonia emissions (EUR kg<sup>-1</sup> NH<sub>3</sub>) and the horizontal axis shows the reduction potential of each measure (kt NH<sub>3</sub>) for a certain period of time, i.e. from 2021 to 2030.



**Figure 5.** Marginal abatement cost curve (MACC) for the ammonia reduction measures.

## CONCLUSIONS

The calculations allowed us to draw conclusions on the economic and natural environment conditions for the implementation of NH<sub>3</sub> emission reduction measures and to categorize the measures according to their priority:

1. The measures that are cost-effective and have high NH<sub>3</sub> reduction potential: fertilizer planning and practical application; organic dairy farming development. Total estimated reduction potential is 7.384 ktNH<sub>3</sub>. These measures are considered to be the most effective from both an economic and an environmental perspective and should be supported as a priority and implemented in practice.

2. The measures that are cost-effective but have low NH<sub>3</sub> emission reduction potential: precision N fertilizer application; covering liquid manure storage facilities (tent cover, clay pellets, tent, film); incorporation of liquid manure directly into the soil (Option 2); biogas production development. Total estimated reduction potential is 2.929 ktNH<sub>3</sub>. These measures are considered to be effective, yet they make low effects on reducing NH<sub>3</sub> emissions. To increase the effects, the possibilities to increase the numbers of target farms, the target area and the number of target livestock need to be considered.

3. The measures that are less cost-effective but have high NH<sub>3</sub> reduction potential: construction of new cylindrical storage facilities; limited litter manure incorporation period (12 h); limited liquid manure incorporation period (4 h); nitrogen sequestration by including legumes in crop rotation. Total estimated reduction potential is 9.051 ktNH<sub>3</sub>. These measures are considered to be economically inefficient but very effective from an environmental perspective, as they make a significant effect on reducing NH<sub>3</sub> emissions. Therefore, financial support for farms is needed to facilitate the practical implementation of these measures.

4. The measures that are not cost-effective and have low NH<sub>3</sub> reduction potential: incorporation of liquid manure directly into the soil (Options 1 + 3 + 4), limited litterless poultry manure incorporation period (4 h). Total estimated reduction potential is 0.716 ktNH<sub>3</sub>. Financial support for these measures is not a priority, as their effects on reducing NH<sub>3</sub> emissions are insignificant.

**ACKNOWLEDGEMENTS.** Adjustment of Latvian agricultural greenhouse gas and ammonia emissions as well as CO<sub>2</sub> removal (arable land and grassland) reduction cost curves (MACC) for use in agricultural, environmental and climate policy formation. Project subsidy decision No: 10.9.1-11/18/929-e.

## REFERENCES

- Buckley, C. & Krol, D.J. 2020. An Analysis of the Cost of the Abatement of Ammonia Emissions in Irish Agriculture to 2030. Teagasc. Oak Park, Carlow. ISBN: 978-1-84170-665-8.
- Cabinet Regulation 2020. Latvia's plan to reduce atmospheric pollution 2020–2030. 21 April 2020, No.197. Available: <https://likumi.lv/ta/id/314078>
- Central Statistical Bureau of Latvia (CSB) 2020. Agriculture of Latvia. Collection of Statistics. Central statistical bureau of Latvia. Available at: [www.csb.gov.lv](http://www.csb.gov.lv).
- Directive (EU) 2016/2284 of the European Parliament and of the Council of 14 December 2016 on the reduction of national emissions of certain atmospheric pollutants, amending, Directive 2003/35/EC and repealing Directive 2001/81/EC.

- EMEP/EEA. 2019. Air Pollutant Emission Inventory Guidebook 2019. EEA Report No 13/2019. European Environment Agency. Luxembourg.
- Eory, V., Pellerin, S., Garcia, G.C., Lehtonen, H., Licite, I., Mattila, H., Lund-Sørensen, T., Muldowney, J., Popluga, D., Strandmark, L. & Schulte, R. 2018. Marginal abatement cost curves for agricultural climate policy: State-of-the art, lessons learnt and future potential. *Journal of Cleaner Production* **182**, 705–716. doi: 10.1016/J.JCLEPRO.2018.01.252
- Eurostat 2020. Ammonia emissions from agriculture. Available at: <https://ec.europa.eu/eurostat/databrowser/view/tai07/default/table?lang=en>. Accessed 15.10.2020.
- European Commission COM 2019. Communication from the Commission. The European Green Deal. Brussels. Available at: <https://eur-lex.europa.eu/legal-content/EN/TXT/?qid=1596443911913&uri=CELEX:52019DC0640#document2>
- Kesicki, F. & Strachan, N. 2011. Marginal abatement cost (MAC) curves: confronting theory and practice. *Environmental Science & Policy* **14**(8), 1195–1204. doi.org/10.1016/j.envsci.2011.08.004
- Priekulis, J., Laurs, A. & Melece, L. 2019. Ammonia emission reduction measures in dairy cattle farming. In: *Engineering for Rural Development: Proceedings of the 16th International Scientific Conference*. Jelgava: LLU, pp. 83–88. doi:10.22616/ERDev2019.18.N091
- Latvia's Informative Inventory Report (LIIR) 2020. Latvian Environment Geology and Meteorology Centre. Available at: [www.meteo.lv](http://www.meteo.lv)
- Lenerts, A., Popluga, D. & Naglis-Liepa, K. 2019. Benchmarking the GHG Emissions Intensities of Crop and Livestock-derived Agricultural Commodities Produced in Latvia. *Agronomy Research* **17**(5), 1942–1952. doi.org/10.15159/ar.19.148
- Moran, D., Macleod, M., Wall, E., Eory, V., McVittie, A., Barnes, A., Rees, R., Topp, C. F.E. & Moxey, A. 2011. Marginal Abatement Cost Curves for Uk Agricultural Greenhouse Gas Emissions. *Journal of Agricultural Economics* **62**(1), 93–118. doi.org/10.1111/j.1477-9552.2010.00268.x
- UN 2014. Draft revised United Nations Economic Commission for Europe Framework Code for Good Agricultural Practice for Reducing Ammonia Emissions. United Nations Economic and Social Council. ECE/EB.AIR/2014/8, Geneva.

## **Technical and economic pre-feasibility study for the construction of septic tank-filter-sinkhole with alternative material**

P.H.N. Martins<sup>1</sup>, D. Cecchin<sup>1,\*</sup>, A.R.G. de Azevedo<sup>2</sup>, D.F. do Carmo<sup>1</sup>,  
R.A. Donagemma<sup>1</sup>, R.M.M. Waite<sup>1</sup>, N.F. Rodrigues<sup>1</sup>, F.A. Sousa<sup>3</sup>,  
P.I.S. Amaral<sup>4</sup>, C.M. Hüther<sup>1</sup>, C.R. Pereira<sup>1</sup> and V.M.F da Cruz<sup>5</sup>

<sup>1</sup>Federal Fluminense University (UFF), Department of Agricultural Engineering and Environment, Street Passo da Pátria, n.156, Boa Viagem, Niterói-RJ, Brazil

<sup>2</sup>North Fluminense State University (UENF), Civil Engineering Department, Avenida Alberto Lamego 2000 - Parque Califórnia, Campos dos Goytacazes BR28013-602 Rio de Janeiro, Brazil

<sup>3</sup>SEMAG/Aracruz, Av. Morobá, n.20, BR 29192-733 Bairro Morobá-ES, Brazil

<sup>4</sup>José do Rosário Vellano University (UNIFENAS), Department of Veterinary Medicine, Rodovia MG-179 km 0, s/n -Bairro Trevo, BR 37130-000 Alfenas-MG, Brazil

<sup>5</sup>Évora University (UE), Pólo da Mitra, PT 7002-554 Évora, Portugal

\*Correspondence: [daianececchin@id.uff.br](mailto:daianececchin@id.uff.br)

Received: February 2<sup>nd</sup>, 2021; Accepted: August 3<sup>rd</sup>, 2021; Published: August 24<sup>th</sup>, 2021

**Abstract.** The study of the different materials used in the construction of septic tanks aims to facilitate and spread the use of this sewage treatment system in places that are not assisted by municipal sewage systems and in the rural area, which despite having a smaller number of inhabitants compared to the urban area. This study aims to carry out a technical and economic evaluation of the concrete and tires using in the construction of septic tanks-filter-sinkhole. The wastewater treatment systems were built according to the recommendations in NBR 7229/93 and 13969/97. To evaluate the efficiency of each system built, the following parameters were analyzed: chemical oxygen demand (COD), the potential of hydrogen (pH), alkalinity, acidity, and temperature. In the economic evaluation, the materials and labor required to install the systems were considered using the Brazilian cost database (SINAPI), and an economic and financial feasibility study was carried out. According to the technical and economic analysis of construction, both systems showed the same technical performance, however, the concrete design proved to be more advantageous than the tire design, considering the difficulty in acquiring the tires and the high cost if it is necessary to buy them, in addition to the greater difficulty in handling and installing the tire system compared to the concrete one.

**Key words:** rural buildings, sanitary sewage, anaerobic treatment, decentralized wastewater treatment.

## INTRODUCTION

The lack of basic sanitation is a problem faced by many countries, and in Brazil, 33.5% of households do not have access to the sewage system (IBGE, 2018). The absence of sewage collection and disposal in the environment influences society in different ways, bringing negative consequences and also being one of the main causes of environmental degradation, due to the inadequate management of waste (Martinetti et al., 2007). The lack of investments in sanitation worsens the situation of soil and water contamination once, without the treatment of the generated sewage there is a continuous degradation of the springs, and consequently, limits the availability of this resource, which can lead to scarcity, due to the quality of the water resources to meet multiple uses (Sautchúck, 2004).

The 2018 data from the National Sanitation Information System (Brasil, 2019) point out that although there are 662.6 thousand kilometers of water supply networks, there are only 325.6 thousand kilometers of sewage collection networks. Sewage treatment occurs for only 46.3% of the generated sewage and not all the collected sewage is treated, which occurs for only 74.5%. In terms of the increase in households with access to the sewage network, Brazil has evolved (33.5% in 2000, to 66.5% in 2018), with a 2.9% increase in treatment, from 2017 to 2018 (Brasil, 2019). But there is still much to do, especially in rural areas. The Brazilian population living in rural areas is equivalent to 15% of the national total, there are approximately 31 million people living in almost nine million households (IBGE, 2015). Most of this rural population lives in cities where the economic base is predominantly family farming, and the basic sanitation for these residents is still insufficient, as 68.7% of households in rural areas use rudimentary systems, such as rudimentary cesspits, ditches, holes or throwing directly into rivers and soil (IBGE, 2015). According to Cheng et al. (2018), rural areas without a sewerage network depend on local sanitation services, such as septic tanks.

The use of decentralized systems for the treatment of sewage reduces the environmental footprint in rural environments, contributing to sustainability, which, as highlighted by Tihomirova et al. (2019), is one of the key factors in the management of the intelligent environment. Raukas (2010) stresses the importance of offering environmental services in rural communities contributing to the reduction of differences between urban and agrarian inhabitants.

As such, it becomes necessary studies on alternatives for the construction of decentralized sewage treatment systems, which can collect and treat sewage in rural areas or in places where the public network is unable to supply. One of the simplest systems applied, in terms of implementation and operation, is the septic tank. The cost of installing a septic tank to serve a residence with five people varies from 2,000 to 4,000 reais on average, depending on the type of material used (Habitissimo, 2020), and it can be made of polyethylene (average cost of 1,600 reais), masonry (average cost of R \$ 3,500), among other materials. However, the use of tires stands out as an alternative material for this construction, allowing the reuse of a material that is difficult to dispose of, minimizing the cost, both of the tires and domestic wastewater. This technique has been widespread by Uberlândia Department of Water and Sewage since 2014 (DMAE, 2016). In the quest for sustainability, systems such as conventional septic tanks have become a subject of critical research from all developing countries around the world (Singh et al., 2019).

Thus, this study aims to analyze the technical and economic feasibility of installing septic tanks-filter-sinkholes built with tires, compared to those of concrete treating black waters.

## MATERIALS AND METHODS

### Characteristics of the study place

Decentralized sewage treatment systems were built in two cities in the state of Rio de Janeiro, Arraial do Cabo and Nova Friburgo. The tire system was built in Nova Friburgo, a mountainous region of the state, the system was installed in holes dug in the ground. The concrete system was installed in Arraial do Cabo, a coastal town, located in the Lakes Region of Rio de Janeiro, a place with rocky soil that did not allow the excavation of the soil to install the tanks, thus the tanks were installed above ground level.

### Construction of water treatment

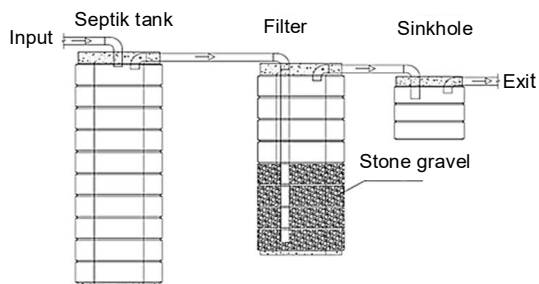
The dimensioning of both systems was based on NBR 7229 (ABNT, 1993) and NBR 13969 (ABNT, 1997), considering households with a contribution of three people (number of inhabitants in the households where the project was developed).

Only blackwaters (wastewater collected from toilets, therefore consisting of faeces, urine and toilet paper) according to Gonçalves et al. (2006) were destined for septic tanks since this segregation into smaller stations helps to stabilize the operation and lower generation of by-products, according to Gonçalves et al. (2006). According to NBR 7229 (ABNT, 1993) each person generates 150 L of domestic sewage per day, of this volume, approximately 30% is blackwater (Rebouças et al., 2007). With this information, it is estimated that the volume of sewage destined for the built systems was 135 liters per day, thus, with an estimated detention time of 17 days.

The septic tanks-filter-sinkhole systems (concrete and tires) were installed at about 15 meters away from the house, in order to avoid gases from the system, and also to prevent the pipes that would connect the house to the treatment system did not have many curves, avoiding future problems in the network.

Tires with a diameter of around 1 meter and a weight of 60 kg each were reused, such characteristics made handling and transporting the material a little difficult. Twenty bus/truck tires were required for the complete system (10 tires for the pit, 7 tires for filter and 3 tires for sinkhole, Fig. 1).

For the installation of the tires, which was made below the level of the soil surface, it was necessary to dig (with the help of diggers, hoe, and shovel) the place where the tanks would be installed. Three holes were dug with depths of 2.00; 1.70 and 1.00 m to install the septic tank, the filter, and the sinkhole respectively. Each tire is approximately 105 cm in diameter, and the excavation was carried out with a diameter of approximately



**Figure 1.** Section of the septic tank-filter-sinkhole of tires.

Source: the authors.



125 cm so that it was possible to handle the sides of the tires at the moment of inserting them in the final location.

After the excavations the tires were lowered tire by tire. The sealing between the tires was made with a cast aluminum blanket through the heat generated by a portable torch (Figs 2, a and 2, b).

For the concrete treatment system, concrete staves (Fig. 3) were used, this material is traditionally used in the construction of tanks and wells. Each stave was 120 in diameter (D120). Even with a high weight in each stave, handling it was easier than handling the tire since there were fewer units of staves per tank (three for each tank).



**Figure 2.** Overlapping tires (a), application of a bituminous layer (b).

Source: Personal collection.



**Figure 3.** Concrete staves.

Source:

<http://www.tubolarpremoldados.com.br/>

The tanks were made with overlapping precast concrete rings, joined by a 3:1 mixture of sieved sand, Portland II cement, and Sika waterproofing admixture.

Since they were installed from the ground level, it was possible to observe that some points with leakage of residue appeared during the use of the system, which occurred at the seams of the concrete rings and on the surface of the precast concrete ring, and they were repaired. It is noteworthy that this problem delayed the filling of the pit and that if the system were buried it would not be possible to identify it. Withers et al. (2011) warn about the contamination risks that these buried systems can cause to the subsoil and nearby water bodies without proper maintenance.

In both wastewater treatment systems, concreting of approximately 10 cm in height at the bottom of the tanks was carried out, in order to guarantee the tightness of the systems. For that, a 3:1 mixture of sieved sand, Portland II cement, and Sika1 waterproofing admixture was used (in the proportion suggested by the manufacturer). The concreting was carried out after the installation of the tanks, for better sealing avoiding the escape of residues.

The entrances of the systems (concrete and tire) were made through a 100 mm diameter PVC pipe that connected the sanitary of the houses to the sewage treatment systems. After the first tank was completed (septic tank), the liquid passed to the next tank through a pipe placed just below the entry level of the first tank. In the second tank (filter), the residue was taken through the pipeline to the bottom of this compartment, and through ascension, it passed through the layer of crushed stones, being filtered. When reaching almost the maximum level of this tank, the residue found the pipe and went to the sink. In this last stage of the process, the residue seeped through the bottom of the tank to the ground.

At the top of each tire tank, a 15 cm high precast concrete ring was added (Fig. 4). The sealing was done with an aluminized blanket to allow the pipes to enter/exit, as well as to support the lid. In order to close the tire tanks, lids made of precast concrete were used.

### Systems monitoring

In each system, the local temperature was monitored by consulting the data generated by the meteorological station of the National Institute of Meteorology - INMET (INMET, 2019).

The samples were collected on the surface of the septic tank and sinkhole and placed in transparent glass containers, wrapped in aluminum foil so that there was no incidence of light when carrying the samples to the laboratory. The control and care standards set out in NBR 9898 (ABNT, 1987) and at the National Guide for Collection and Samples Preservation of the National Water Agency (ANA / CETESB, 2011) were followed for storage and transportation.

The parameters analyzed in the samples was: pH, Method Electrometric 4500 B; Temperature, Method Electrometric 2550 B; Alkalinity: Titulação 2320 B; COD: Closed Reflux, Colorimetric Method. 5220 (SMEWW- 22st Edition, 2012).

The sample temperature was measured at the time of collection, with the aid of a thermometer of the Incoterm brand. The pH of each sample was measured at the time of collection with the aid of a pH measuring tape for control and reduction to values less than two, preparing them to be preserved for COD analysis, as recommended in NBR 9898 (ABNT, 1987). The pH reduction was done with 1 mol L<sup>-1</sup> sulfuric acid (H<sub>2</sub>SO<sub>4</sub>).

The system made with tires started operating on April 9, 2018, and the first sample collection was carried out with 140 days of operation, in order to characterize the effluent. The second collection of samples was performed after 196 days of this system operation. The system built with concrete, on the other hand, started operating on July 12, 2018, and after 47 days of operation, it was verified that the first tank was full and, thus, it was possible to carry out the first sample collection to characterize the effluent. The second collection was made with 103 days of operation. As in the other installed system, the first two collections were carried out only in the first tank, because there was still no residue in the third tank.

Four collection campaigns were carried out (they were carried out in August, October, February, and April), and in each one, six samples were taken per tank. To carry out the collections, it was necessary to wait for the tanks to be full.

It was not possible to install both systems in the same period, there was a gap of three months between the start of the operation of the systems. In the system made with tires, after 141 and 197 days of operation, the material was collected only from the first tank (three samples with pH adjusted for COD analysis and three samples without pH adjustment by the system). The same procedure was done in the first two campaigns



**Figure 4.** Tanks prepared to receive the lid.  
Source: Personal collection.

carried out for the concrete system when the system had 47 and 103 days operating. In the last two campaigns, both systems had residue in the three tanks, making it possible to collect material to compare between the first and last tanks of each system. The collections took place with 302 and 372 days of the experiment for the tire tank and with 208 and 278 days for the concrete tanks. Six samples were also collected from each tank, three of these samples had pH corrected, and the other three samples with no correction, a total of 48 samples. Throughout the experiment (310 days) 72 samples were collected.

The built and evaluated systems, in this study, did not have any type of inoculum to accelerate the acclimatization of organisms that act in the decomposition of organic matter.

### **Economic and financial feasibility study (EVEF)**

The costs for construction of each system were acquired, based on the National System of Costs Survey and Indexes of Construction - SINAPI widely used in Brazil, referring to March 2019 (SINAPI, 2019).

The economic and financial feasibility study (EVEF) was carried out in order to evaluate the investment plan that should be carried out before and after the installation of both systems, showing or not the feasibility of the project. For that, the following methods were used according to Waite et al. (2020): Minimum Attractive Rate; Simple Payback; Discounted Payback; Internal Rate of Return and Net Present Value.

To apply the aforementioned methods, the was necessity of the cash-flow statements of the project. By being a home effluent treatment project, and considering that the sewer and water bills come together in the state of Rio de Janeiro, the fact that the use of the system frees the owner of paying fines. Taking into account the specificity of the fine, which considers mitigating factors, among other factors, it was proposed, based on State Law No. 2661 (Rio de Janeiro, 1996), three different scenarios for the fine, namely: an optimistic scenario in which the fine would be less and therefore 10 UFIR-RJ; a normal scenario, with a fine of 50 UFIR-RJ, and a pessimistic scenario, with a larger fine, 100 UFIR-RJ. UFIR is the Fiscal Reference Unit of the state of Rio de Janeiro, considering the exercise unit in the year of 2020, which is R \$ 3.5550 (three reais and five thousand, five hundred and fifty-tenths of thousandths) according to Sefaz (2019).

In addition to the costs of installing the system, the cost of maintenance was considered, according to the analysis of current values in the market.

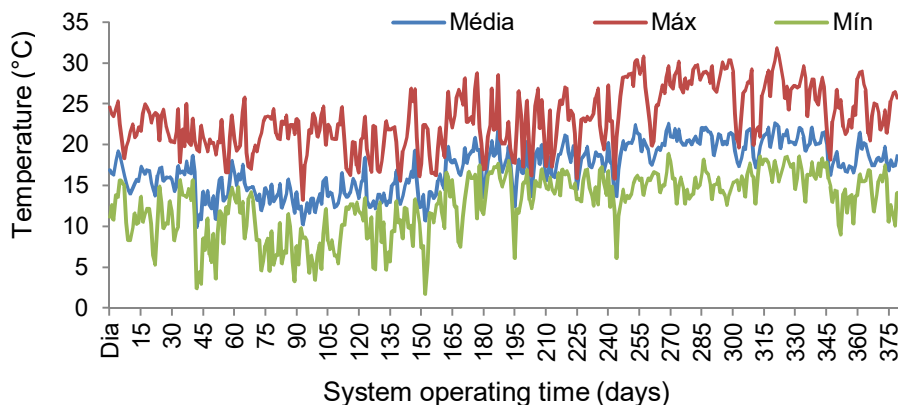
## **RESULTS AND DISCUSSION**

### **Systems monitoring**

#### Tires system

During the period of the experiment, the absolute minimum temperature (2.3 °C) was observed with 149 days of the system operation, at 9 am, the absolute maximum temperature (31.8 °C) was observed with 320 days of operation, at 6 pm. The average temperatures recorded in this period in the city of Nova Friburgo oscillated within the range of 10 °C and 25 °C, with an average in the entire period of 17.2 °C. As can be seen in Fig. 5, on some days, the average temperature was below that mentioned by Luostarinen et al. (2007) as being the ideal, considering that the microbiological activity depends on this variable, which can compromise the performance of biological reactors in the degradation of organic matter in extreme values.

Throughout the collections, the average temperature of the effluent sample in the tank outlet of the tire system was 19.7 °C. Thus, it was found that the temperature measured at the outlet of the system is within the limits allowed by CONAMA resolution 357, which establishes a temperature below 40°C of the treated effluent when released into the environment. Luostarinen et al. (2007) conducted a study comparing anaerobic systems for treating domestic sewage, at different temperatures and periods of the year. The authors found that, although there is little microbial activity in the period of low temperatures ( $5\text{ °C} < T < 13\text{ °C}$ ) these systems can be used in houses because the degradation of organic matter occurs when there is an increase in temperature.



**Figure 5.** Temperature variation during the experiment - tire system (Nova Friburgo - RJ).

The first two collections were made only in the first tank, since there was still no residue in the third tank. From the third collection, carried out with 302 days of system operation, it was possible to analyze the reduction of organic load. It can be seen in Table 1 that there was a reduction in COD of 16.69% in the third collection and 21.54% in the fourth collection. Although these values point to an increase in removal efficiency, they are still insufficient to meet the standard NBR 13969 (ABNT, 1997), which is 40 to 70% for COD removal with this type of treatment.

In the analyzes performed on the material collected at the outlet of the system (third tank), an average pH of 7.26 was observed in the first collection and 7.38 in the second collection (Table 1). Both values are in agreement with Conama Resolution 357 (Brasil, 2005) which establishes pH in the range of 6 to 9 for the discharge of effluents into bodies of water.

During the experiment period, it was also carried out alkalinity monitoring in the tanks (Table 1). The alkalinity remained relatively stable, with variation between 145 and 142 ( $\text{mgL}^{-1}\text{CaCO}_3$ ).

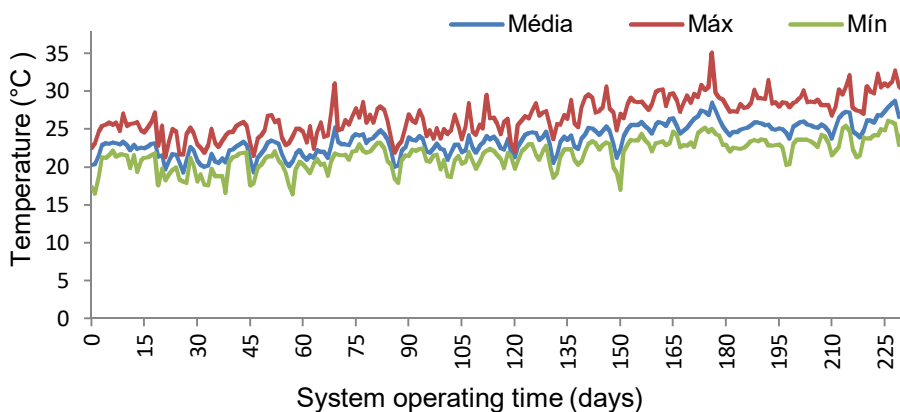
**Table 1.** Tire tanks, average results of COD ( $\text{mg O}_2\text{L}^{-1}$ ), pH and Alkalinity ( $\text{mgL}^{-1}\text{CaCO}_3$ ) analyzes

Operating time (days)	Sample results from Tank 1			Results of the Sink samples		
	COD	pH	Alcal.	COD	pH	Alcal.
141	620.00	8.07	188	-	-	-
197	656.00	7.93	201	-	-	-
302	607.00	7.69	194	505.67	7.26	145
372	705.67	7.60	216	553.67	7.38	142

The expected pH value for sanitary effluent is within the range of 6 to 9. Withers et al. (2011), and Sousa et al. (2003) treating sanitary effluents in anaerobic reactors found values in the same range.

### Concrete system

The average temperatures recorded throughout the experiment in the city of Arraial do Cabo were within the range of 15 °C to 30 °C, with an average temperature over the entire period of 22.8 °C. As can be seen in Fig. 6, most of the time the average temperature remained close to the ideal for a good functioning of the system, which is close to 25 °C (Luostarinen et al., 2007).



**Figure 6.** Temperature variation during the experiment - concrete system (Arraial do Cabo - RJ).

The minimum absolute temperature (16.4 °C) was observed with 55 days of system operation, at 10 am, while the absolute maximum temperature (35.1 °C) was observed with 170 days of operation, at 1 pm. Throughout the collections, the average temperature recorded for the effluent in the system outlet tank was 23.5 °C. Thus, as in the tire system, it was found that the temperature of the treated effluent meets the resolution of Conama 357 (Brasil, 2005), which says that the temperature of the treated effluent when released into the environment must be less than 40 °C.

The analysis of the efficiency of COD removal was made from the third collection. According to Table 6, it is noticed that there was a reduction in COD of 12.72% in the third collection

and 22.56% in the fourth collection (Table 2). The increase in removal efficiency was considerable, however, the values are still below the removal efficiency expected for the septic tank provided for in the standard NBR 13969 (ABNT, 1997), which is 40 to 70% predicted. However, the values are similar to those found by Colares & Sandri (2013) evaluating different types of post-treatment for systems with septic tanks.

**Table 2.** Concrete tanks, results of COD (mg O<sub>2</sub>L<sup>-1</sup>), pH and Alkalinity (mgL<sup>-1</sup>CaCO<sub>3</sub>) analysis

Operating time (days)	Average value of Tank 1 samples			Average value of sinkhole samples		
	COD	pH	Alcal.	COD	pH	Alcal.
47	581.67	7.50	171	-	-	-
103	617.67	7.21	185	-	-	-
208	540.00	6.86	173	471.33	7.06	130
278	670.77	7.29	204	519.33	6.95	156

Regarding the pH evaluated in the third tank, an average value of 7.06 was observed in the first analysis, and an average value of 6.95 in the second analysis (Table 2). Both values are according to CONAMA Resolution 357/05 (BRASIL, 2005) which establishes for the discharge of effluents into water bodies pH in the range of 5 to 9. Colares & Sandri (2013) when analyzing septic sink, filter, and sinkhole systems constructed of concrete treating domestic sewage found mean pH values similar to these, 7.25 and 7.41 respectively.

As in the tire system, alkalinity was monitored in the tanks. Even though the pH was lower, the alkalinity remained relatively stable, varying between 130 and 204 ( $\text{mgL}^{-1}\text{CaCO}_3$ ).

### **Comparison between the two systems**

The COD analyzes of both systems were performed with samples collected in tank 1 (after the sewage enters the system) and in tank 3 (after the sewage passes through the decanting of organic matter, microbiological decomposition, and physical filtration). The results presented in both systems show an average COD removal efficiency in the period of 17.64% for the concrete system and 19.12% for the tire system. The similarity of the effluent before the treatment occurred, as both houses where the systems were installed had the same number of inhabitants, and because of that, the volume of sewage produced in each house was similar, with an average affluent COD of  $602.53 \text{ mg L}^{-1}$  for the concrete system and  $647.17 \text{ mg L}^{-1}$  for the tire system. The built systems had the same volume, as they were dimensioned using the same calculation procedure and standards, thus storing the same amount of matter in each tank, in addition, for the collection, maintenance, and transport of samples, the same procedures were followed, providing thus a basis for comparison between analyzes. The absence of inoculation may also have contributed to the low efficiency of COD removal since there was an increase in efficiency over time in both systems. It is noticed that inoculation would provide faster acclimatization and acquisition of better results in less time, being of relevant importance (Li et al., 2014; Dhamodharan et al., 2015).

The collection of material for analysis was carried out on the surface of the tanks and because of that, there may have been interference from the input material. It is suggested for the implantation of these systems that some way of shielding be installed, preventing the incoming sample from mixing with the outgoing sample. For sampling in future studies, it is suggested to collect at different depths of the tank to increase the reliability of the analysis results, and the column sampler can be used for that, as showed by Santos (2009).

Considering the results presented in this study, it was found that there was no interference on the type of the tanks walls coating in the results found. The criterion for defining which material to use depends on the availability of tires for usage in the construction of the system, if it's necessary to purchase all material, the use of concrete rings is recommended, as the difference in the COD reduction efficiency was small, not enough to determine the choice of which material to use. However, if it is considered that the use of used tires contributes to the reduction of environmental pollution, and compatible prices in the purchase of this, of course, the recommendation would be for this option.

### Economic and financial feasibility study (EVEF)

Tables 3 and 4 detail the costs for building each system with values obtained through the National System of Costs Survey and Indexes of Construction - SINAPI (SINAPI, 2019). The system built with tires has a higher value of R\$ 2,469.29 (Table 3), due to the high value of each tire. For the development of this project, the tires were donated, which did not generate cost and made the system competitive. Without the need to pay for the purchase of tires, the system costs R\$ 1,902.31, approximately R\$ 500.00 cheaper than the concrete system. Otherwise, the cost of the system becomes higher than the concrete system, approximately twice as much. The shown value in Table 3, for the item 'used tire', was verified in the market. As it is used material there is no standard and the price may vary from region to region and/or according to the condition of the tire. The acquisition of new tires would make the construction of the sewage treatment system unfeasible. However, it should be noted that, for this purpose, used tires must have tightness, no cut or large punctures, because the tires compose the tank wall, and there can be no leakage from the stored sewage. In the region where this study was carried out, it was necessary to seek a partnership to supply the tires. In regions where tires are available at no cost for reuse in these systems, it is advisable to use this material, with a view of the economy with the most expensive part of the construction of tanks, filter and, sinkhole.

**Table 3.** Cost breakdown of the septic tank built with tires, SINAPI table values March 2019

Item	Unit	Quantity	Unit value (R\$)	Total value (R\$)	Sinapi code
Portland Cement CPII	kg	50	0.40	20.00	1379
Sand	m <sup>3</sup>	0.5	54.64	27.32	370
Gravel	m <sup>3</sup>	0.5	82.21	41.11	88549
Waterproofing Admixture	L	2	5.10	10.20	123
Concrete cover d1	m <sup>2</sup>	2.36	66.86	157.46	6171
Concrete ring h 15 cm	uni.	3	41.20	123.60	12547
Tube 100 mm	m	6	23.48	140.88	9841
Curve 100 mm	uni.	10	13.77	137.70	1966
Glue for pipe	uni.	1	53.75	53.75	122
Waterproofing membrane	m <sup>2</sup>	9	35.42	318.78	4014
<b>Subtotal (materials)</b>			<b>R\$ 526.83</b>	<b>R\$ 4,030.80</b>	
Hod carrier	h	32	19.21	614.72	88316
Used tires	uni.	20	150.00	3,000.00	Not found
Plumber Assistant	h	6	18.89	113.34	88248
Plumber	h	6	23.91	143.46	88267
<b>Subtotal (labor)</b>			<b>62.01</b>	<b>871.52</b>	
<b>Total</b>			<b>R\$ 588.84</b>	<b>R\$ 4,902.32</b>	

The system built with concrete had its consolidated advantage by presenting less value for construction, about 50% smaller than in the tire system. Among the materials presented in the cost spreadsheet of the two systems, the difference is the material that makes up the wall of the tanks, the other materials are practically the same.

**Table 4.** Cost breakdown of the septic tank built with concrete, SINAPI table values March 2019

Item	Unit	Quantity	Unit value (R\$)	Total value (R\$)	Sinapi code
Portland Cement CPII	kg	50	0.40	20.00	1379
Sand	m <sup>3</sup>	0.5	54.64	27.32	370
Gravel	m <sup>3</sup>	0.5	82.21	41.11	88549
Waterproofing Admixture	L	2	5.10	10.20	123
Concrete cover d1	m <sup>2</sup>	2.36	66.86	157.46	6171
Concrete ring D120 cm	uni.	3	128.18	384.54	12552
Concrete ring D100 cm	uni.	5	117.71	588.55	12547
Tube 100 mm	m	6	23.48	140.88	9841
Curve 100 mm	uni.	10	13.77	137.70	1966
Glue for pipe	uni.	1	53.75	53.75	122
<b>Subtotal (materials)</b>			<b>565.31</b>	<b>2,176.23</b>	
Hod carrier	h	32	19.21	614.72	88316
Plumber Assistant	h	6	18.89	113.34	88248
Plumber	h	6	23.91	14346	88267
Subtotal (labor)			42.80	256.80	
<b>Total</b>			<b>R\$ 608.11</b>	<b>R\$ 2,433.03</b>	

Based on the amount of the budget presented, and the forecast for the system maintenance about R\$ 266.00 per year, and the fine amounts for each scenario based on Rio de Janeiro UFI of R\$ 355.50 per month on the pessimist scenario, R\$ 177.75 in the normal one and R\$ 35.55 in the optimistic one, the annual cash flows were generated for each type of system, shown in Table 5 for the system built with tires and in Table 6, the one built with concrete.

**Table 5.** Septic tank cash flow built with tires

Annual cash flow - Septic tank built with tires						
Time	10-year horizon					
Scenario	Pessimistic		Normal		Optimistic	
Years	Cash-inflows (R\$)	Cash-outflows (R\$)	Cash-inflows (R\$)	Cash-outflows (R\$)	Cash-inflows (R\$)	Cash-outflows (R\$)
0	0.00	- 4,902.32	0.00	- 4,902.32	0.00	- 4,902.32
1	4,266.00	- 266.00	2,133.00	- 266.00	426.60	- 266.00
2	4,266.00	- 266.00	2,133.00	- 266.00	426.60	- 266.00
3	4,266.00	- 266.00	2,133.00	- 266.00	426.60	- 266.00
4	4,266.00	- 266.00	2,133.00	- 266.00	426.60	- 266.00
5	4,266.00	- 266.00	2,133.00	- 266.00	426.60	- 266.00
6	4,266.00	- 266.00	2,133.00	- 266.00	426.60	- 266.00
7	4,266.00	- 266.00	2,133.00	- 266.00	426.60	- 266.00
8	4,266.00	- 266.00	2,133.00	- 266.00	426.60	- 266.00
9	4,266.00	- 266.00	2,133.00	- 266.00	426.60	- 266.00
10	4,266.00	- 266.00	2,133.00	- 266.00	426.60	- 266.00
<b>Total</b>	42,660.00	- 7,562.32	21,330.00	- 7,562.32	4,266.00	- 7,562.32
Diference	R\$ 35,097.68		R\$ 13,767.68		-R\$ 3,296.32	



**Table 6.** Anual cash flow - Septic tank built with concrete

Anual cash flow - Septic tank built with concrete						
Time	10-year horizon					
Scenario	Pessimistic		Normal		Optimistic	
Years	Cash-inflows (R\$)	Cash-outflows (R\$)	Cash-inflows (R\$)	Cash-outflows (R\$)	Cash-inflows (R\$)	Cash-outflows (R\$)
0	0.00	- 2,433.03	0.00	- 2,433.03	0.00	- 2,433.03
1	4,266.00	- 266.00	2,133.00	- 266.00	426.60	- 266.00
2	4,266.00	- 266.00	2,133.00	- 266.00	426.60	- 266.00
3	4,266.00	- 266.00	2,133.00	- 266.00	426.60	- 266.00
4	4,266.00	- 266.00	2,133.00	- 266.00	426.60	- 266.00
5	4,266.00	- 266.00	2,133.00	- 266.00	426.60	- 266.00
6	4,266.00	- 266.00	2,133.00	- 266.00	426.60	- 266.00
7	4,266.00	- 266.00	2,133.00	- 266.00	426.60	- 266.00
8	4,266.00	- 266.00	2,133.00	- 266.00	426.60	- 266.00
9	4,266.00	- 266.00	2,133.00	- 266.00	426.60	- 266.00
10	4,266.00	- 266.00	2,133.00	- 266.00	426.60	- 266.00
<b>Total</b>	42,660.00	- 5,093.03	21,330.00	- 5,093.03	4,266.00	- 5,093.03
Diference	R\$ 37,566.97		R\$ 16,236.97		-R\$ 827.03	

It was considered, conservatively, that in both cases, in the first year of operation of the systems there were no cash-inflows. It can be seen that in the optimistic scenario, where the best results are implied, the worst ones are presented, in both cases. However, it should be emphasized that this was already expected, since the scenarios deal with the fine collection, and since it is a value that is expected not to pay, the higher its value, the greater the gain that the system has. Thus, in the pessimistic scenario, more optimistic results are expected for the viability of the system and vice versa. Table 7 presents the results of all methods applied to all projected scenarios, in order to facilitate the comparison of the systems presented.

**Table 7.** EVEF summary

Methods		Septic tank built with tires	Septic tank built with concrete
Pessimist	Simple Payback	2 years	1 years
	Discounted Payback	2 years	1 years
	IRR	50.03%	116.48%
	NPV	R\$ 20,531.03	R\$ 22,803.09
Normal	Simple Payback	3 years	2 years
	Discounted Payback	3 years	2 years
	IRR	20,87%	47.87%
	NPV	R\$ 7,213.60	R\$ 9,485.66
Optimist	Simple Payback	8 years	4 years
	Discounted Payback	9 years	4 years
	IRR	-10.72%	-4.51%
	NPV	-R\$ 3,440.34	-R\$ 1,168.28

The Minimum Attractiveness Rate (TMA) is a rate that varies according to the beneficiary, with no fixed rate. The Selic rate was used as the TMA, which is the basic interest rate of the economy, and considering that the investment in the Selic Treasury is one of the most stable and secure in the financial market. Therefore, considering the quotation on April 14, 020, a TMA of 4.25% was obtained.

Simple Payback is a calculation that takes into account the return time of the initial investment, where the maximum period for obtaining the recovery of the investment is established. In the pessimistic and normal scenarios, short terms of up to 3 years were

obtained for both systems, while in the optimistic one the septic tank that uses tires obtained a return time of 8 years, which is a long time, considering the value of the investment made. However, it should be noted that the purchase of tires was considered and not the donation, which has a high possibility of occurring, reducing the costs of implementation.

Discounted Payback is similar to the simple one, however, it considers an attractiveness or discount rate, so that the value of the investment in time will be considered. In the proposed analysis, large variations in the return time were not obtained when considering the variation in investment over time. Only in the pessimistic scenario of the septic tank built with tires had an increase of one year, thus repeating the same considerations obtained for the analysis of the Simple Payback.

The obtained Internal Rate of Return in the pessimistic and normal scenarios is higher than the established TMA. Thus, the project within these scenarios proves to be economically viable. In the optimistic scenario, as expected, the IRR was lower than the TMA for both systems, so in this scenario, the projects are not viable. In the comparison between both systems, we can see that the IRR value of the septic tank system built with concrete is slightly higher than the double of the septic tank system built with tires, a fact expected when it is observed that the initial investment of the septic tank built with tires is slightly more than double the septic tank built with concrete, and both have the same input value in all scenarios.

The Net Present Value (NPV) as well as the IRR obtained values above zero in the pessimistic and normal scenarios, indicating the economic viability of the projects in these scenarios, and also being below zero in the optimistic scenario, indicating the project's unfeasibility in the optimistic scenario. The NPV reinforces the conclusions obtained by the IRR, and the same observations made in the analysis of the IRR apply.

It should also be considered, that comparing these systems built with the sewage collected in the urban area, the amount invested in the construction of the concrete system corresponds to 20 months of collection and treatment of domestic sewage in a household with the same standards studied in this work. In consultation with the fee charged by the concessionaire that operates this segment in the state of Rio de Janeiro, a two-bedroom house produces an average of 30 m<sup>3</sup> of sewage per month, generating an expense for the collection and treatment service of approximately R\$ 120.00 per month.

Comparing the costs of collection and treatment between the urban area and the decentralized system proposed in the present work, the implementation of the individual system presents a greater initial investment, but the cost of maintaining the system is low (about 23 Reais monthly). It should also be noted that if, instead of the fine, this rate of 120 Reais was used as input to the EVEF, the payback amount would not be much changed compared to the normal scenario and the IRR of the concrete system would be 28.27% and NPV of R\$ 5,158.90 while the tire system would have an IRR of 11.43% and NPV of R\$ 2,886.64. Therefore, the results for both systems are attractive. It is also considered that the value used in the construction of the systems should be considered as an investment in order to guarantee people's health and quality of life. According to the World Health Organization (WHO, 2014) for every US \$ 1.00 spent on basic sanitation, US\$ 4.30 is saved in the population's health costs, a fact that alone demonstrates the importance of investing in this area.

The proposal to use tires for the construction of sewage systems emerged as an alternative solution for the reuse of a material that would be discarded. Doing that, tire reuse and sewage treatment would happen. It should be noted that tires have been used in various activities and proposals in order to reduce the impact on the environment, and they can be used in construction, in playgrounds, in the manufacture of asphalt-rubber, automotive mats, synthetic grass, among others (Lagarinhos & Tenório, 2009).

## CONCLUSIONS

Both systems can be implemented in rural homes, without major complications.

The system implementation with concrete tanks was more practical from the acquisition of materials to the installation, also showing greater economic viability.

From the perspective of technical feasibility, according to the results found during the monitoring of the systems, neither of them presented satisfactory results, to comply with the current legislation. The low efficiency may have occurred due to the way the waste was collected for analysis. As mentioned in this study, the collections took place on the surface of the first tank and, thus, it is believed that the collected material had already undergone some treatment, considering that when it reaches the tank, through the pipe, most of the organic matter deposits at the bottom of the tank. It is therefore suggested for future studies that samples should be collected over the entire depth of the tank, which can be done with the aid of a sampling column, thus obtaining a more homogeneous sample and close to the actual situation in which the sewer reaches the treatment system. Still, related to this point, it is suggested that some form of the screen should be installed so that there is no mixing of the input material with the reactor output.

The non-use of inoculum may have contributed to the low efficiency found, considering that with the use of the inoculum there is a better adaptation and development of microorganisms that act in the decomposition of organic matter.

Both projects proved to be viable in the pessimistic and normal scenarios, that is, with higher fines for the release of untreated sewage. And they proved unfeasible in the optimistic scenario, that is, with a lower fine. Even if intuitively opposed, this is the scenario in which the project would be expected to fail. The average turnaround time for the project was between one and three years, considering that a short time within the stipulated horizon. When comparing projects, it was already expected that with the same cash flow inputs, the one with the largest initial investment would have the worst viability indicators.

**RECOMMENDATIONS.** It is believed, by the results of this work can be adopted, by the public health systems of small city halls, considering in their sewage water sanitation programs.

## REFERENCES

- American Public Health Association – APHA, 2012. Standard methods for the examination of water and wastewater (SMEWW). 22th ed. Washington.
- Ana/Cetesb, 2011. National guide for collecting and preserving samples: water, sediment, aquatic communities and liquid effluents. Companhia Ambiental do Estado de São Paulo; Organizadores: Carlos Jesus Brandão et al.- São Paulo: CETESB; Brasília: ANA. (in Portuguese).

- Associação Brasileira de Normas Técnicas, 1987. NBR 9898: Preservation and sampling techniques for effluents and receiving bodies. Rio de Janeiro (in Portuguese).
- Associação Brasileira de Normas Técnicas, 1993. NBR 7229: Design, construction and operation of septic tank systems. Rio de Janeiro. (in Portuguese).
- Associação Brasileira de Normas Técnicas, 1997. NBR 13969: Septic tanks - Complementary treatment units and final disposal of liquid effluents - Design, construction and operation. Rio de Janeiro (in Portuguese).
- Brasil, 2005. Conselho Nacional do Meio Ambiente. Resolução n. 357 de 17 de março de 2005. Diário Oficial [da] União, Brasília, 18 mar., pp. 58–63.
- Brasil, 2019. Ministério do Desenvolvimento Regional. Secretaria Nacional de Saneamento – SNS. National Sanitation Information System: 24th Diagnosis of Water and Sewage Services – 2018. Brasília: SNS/MDR. 180 pp. (in Portuguese).
- Colares, C.J.G. & Sandri, D. 2013. Efficiency of sewage treatment with septic tanks followed by cultivated beds with different support media. *Ambi-Agua* **8**, 172–185.
- Cheng, S., Li, Z., Nazim Uddin, S.M., Mang, H., Zhou, X., Zhang, L., Zheng, L. & Zhang, L., 2018. Toilet revolution in China. *J. Environ. Manag.* **216**, 347–356 (in Portuguese).
- Dhamodharan, K., Kumar, V. & Kalamdhad, A.S. 2015. Effect of different livestock dungs as inoculum on food waste anaerobic digestion and its kinetics. *Bioresource Technology* **180**, 237–241.
- Dmae - Prefeitura Municipal De Uberlândia, 2016. Sustainable Septic Tank. Available in: [http://www.uberlandia.mg.gov.br/uploads/cms\\_b\\_arquivos/13916.pdf](http://www.uberlandia.mg.gov.br/uploads/cms_b_arquivos/13916.pdf) Accessed in: 10 de março de 2017 (in Portuguese).
- Gonçalves, R.F., Alves, W.C. & Zanella, L. 2006. Water conservation in urban areas. In: *Uso Racional da Água em Edificações*. Ricardo Franci Gonçalves (Coord.). Rio de Janeiro: ABES, cap. 2, pp. 29–71 (in Portuguese).
- Habitissimo, 2020. Build Septic Tank: Prices and Budgets. Available in: <https://www.habitissimo.com.br/orcamentos/construir-fossa-septica>. Acesso em abril de 2020 (in Portuguese).
- IBGE - Instituto Brasileiro de Geografia e Estatística, 2010. National Basic Sanitation Survey – PNSB, p. 40. (in Portuguese).
- IBGE - Instituto Brasileiro de Geografia e Estatística, 2015. National Household Sample Survey - PNAD, p.102 (in Portuguese).
- IBGE - Instituto Brasileiro de Geografia e Estatística, 2018. National Household Sample Survey – PNAD. Available in: Instituto Brasileiro de Geografia e Estatística <<https://agenciadenoticias.ibge.gov.br/agencia-sala-de-imprensa/2013-agencia-de-noticias/releases/24532-pnad-continua-abastecimento-de-agua-aumenta-no-centro-oeste-em-2018-mas-se-mantem-abaixo-do-patamar-de-2016>> Accessed in: 16 de julho de 2019. (in Portuguese).
- IBGE, Instituto Brasileiro de Geografia e Estatística. Synopsis of the Demographic Census. 2010. Available in: Instituto Brasileiro de Geografia e Estatística: <<https://censo2010.ibge.gov.br/sinopse/index.php?uf=33&dados=21>> Accessed in: 09 de março de 2019. (in Portuguese).
- INMET – Instituto Nacional de Meteorologia, 2019. Available in: <[www.inmet.gov.br](http://www.inmet.gov.br)> acesso em: 20 de abril de 2019 (in Portuguese).
- Lagarinhos, C. & Tenório, J., 2009. Tire recycling: discussion of the impact of Brazilian policy, *Engvista* **11**, 32–49 (in Portuguese).
- Li, Y., Hua, D., Zhang, J., Gao, M., Zhao, Y., Xu, H., Liang, X., Jin, F. & Zhang, X. 2014. Influence of inoculum to substrate ratios (ISRs) on the performance of anaerobic digestion of algal residues. *Annals of Microbiology* **64**, 955–960.

- Luostarinen, S., Sanders, W., Kujawa-Roeleveld, K., & Zeeman, G. 2007. Effect of temperature on anaerobic treatment of black water in UASB-septic tank systems. *Bioresource Technology* **98**, 980–986.
- Martinetti, T.H., Shimbo, I. & Teixeira, B.A.N. 2007. Analysis of more sustainable alternatives for local treatment of residential sanitary effluents. In: *IV Encontro Nacional e II Encontro Latino - Americano Sobre Edificações e Comunidades Sustentáveis*. Curitiba. 996–1005. Available in: [http://www.elecs2013.ufpr.br/wp-content/uploads/2007\\_artigo\\_01pdf](http://www.elecs2013.ufpr.br/wp-content/uploads/2007_artigo_01pdf). Accessed in: 29 ago. 2018 (in Portuguese).
- Organização Mundial da Saúde - OMS, 2014. Available in: [https://www.who.int/water\\_sanitation\\_health/monitoring/economics/en/](https://www.who.int/water_sanitation_health/monitoring/economics/en/) Accessed in: 06 ago de 2019 (in Portuguese).
- Rebouças, T.C. 2007. Physicochemical and microbiological characteristics of different types of residential wastewater. In.: Congresso Brasileiro de Engenharia Sanitária e Ambiental, Belo Horizonte, 24, 2007. *Anais... Minas Gerais: Associação Brasileira de Engenharia Sanitária e Ambiental* (in Portuguese).
- Rio de Janeiro (Estado). Lei 2.661, de 27 de dezembro de 1996. Constituição do Estado do Rio de Janeiro, 1996 (in Portuguese).
- Raukas, A. 2010. Sustainable development and environmental risks in Estonia. *Agronomy Research* **8**(SII), 351–356.
- Sautchúck, C. 2004. Formulation of guidelines for implementing water conservation programs in buildings. São Paulo: USP. Dissertação (Mestrado em Engenharia) - Escola Politécnica, Universidade de São Paulo, São Paulo, 303 pp. (in Portuguese).
- SEFAZ – Secretaria De Fazenda do Estado do Rio De Janeiro, 2019. Resolution 101 of December 20, 2019. Diário Oficial do Estado do Rio de Janeiro de 23 de dezembro de 2019 (in Portuguese)
- SINAPI. 2019. Civil Construction Indexes. Available in: [http://www.caixa.gov.br/site/Paginas/downloads.aspx#categoria\\_656](http://www.caixa.gov.br/site/Paginas/downloads.aspx#categoria_656). Accessed in: 19 mai 2019 (in Portuguese).
- Singh, R P., Kun, W. & Fu, D. 2019. Designing process and operational effect of modified septic tank for the pretreatment of rural domestic sewage. *Journal of Environmental Management*. **251**, 109552.
- Sousa, J.T., Van Haandel, A.C., Cavalcanti, P.F.F. & Figueiredo, A.M.F. 2003. Efluentes tratados utilizados na agricultura. In: Simpósio Brasileiro de Recursos Hídricos. 15. Anais Simpósio brasileiro de recursos hídricos. Curitiba-PR, Brasil, pp. 1–12.
- Tihomirova, K, Denisova, V., Golovko, K., Kirilina–Gutmane, O., Mezule, L. and Juhna, T. 2019. Management of wastewater from landfill of inorganic fiberglass. *Agronomy Research* **17**(S1), 1216–1226.
- Waite, R.M., Salgado, E.G. & Carmo, D.F., 2020. Economic feasibility for wastewater treatment system composed of wetlands for the wastewater reuse: a case study. *Revista agrogeoambiental* **12**(2). doi: <http://dx.doi.org/10.18406/2316-1817v12n220201461> (in Portuguese).
- Withers, P.J.A., Jarvie, H.P. & Stoate, C., 2011. Quantifying the impact of septic tank systems on eutrophication risk in rural headwater. *Environment International* **37**, 644–654.

## **Joint Business-to-Business recovery management: the moderating role of locus of failure**

N. Nik Bakhsh\* and I. Riivits-Arkonsuo

Tallinn University of Technology, School of Business and Governance, Department of Business Administration, Akadeemia Tee 3, EE19086 Tallinn, Estonia

\*Correspondence: [Naghmeh.nikbakhsh@yahoo.com](mailto:Naghmeh.nikbakhsh@yahoo.com)

Received: January 30<sup>th</sup>, 2021; Accepted: May 20<sup>th</sup>, 2021; Published: June 10<sup>th</sup>, 2021

**Abstract.** Agricultural machinery manufacturers and services providers increasingly experience failure in core products and service deliveries. Despite the importance of recovery management in context, scant research exists on studying recovery management, collaborative recovery activities, and the impact of joint recovery management on post-recovery relationship quality. More pressing is the lack of research on the impact of relationship quality on the customer's intention of future co-recovery activities. Using an experimental design with data from 30 agronomy machinery and equipment manufacturers and service providers in Iran, we investigate how customers' perception of relationship quality is influenced by the interplay of locus of failure and supplier recovery tactics (non-co-creation of recovery vs co-creation of recovery). The results reveal the locus of failure, interacts with the supplier recovery tactics to impact the customers' perceptions of relationship quality. Finally, all three dimensions of relationship quality (satisfaction, trust, and commitment) positively impact the customers' intention for future co-recovery activities.

**Key words:** business-to-business, co-creation, joint recovery management, locus of failure, relationship quality, agronomy machinery, agronomy services.

### **INTRODUCTION**

One of the industries that experience failure frequently is agricultural machinery and services. The failure in supplying of items and materials by suppliers can cause a domino effect across the customers' business network, interrupt the farm operations, cause severe damage to the farm products (Afsharnia et al., 2014), restrain the customer relationships, and threaten the long-term profitability of the supplier firm (Döscher, 2013; Zhu & Zolkiewski, 2015; Borah et al., 2019; Baliga et al., 2020). Since the supply of high-quality agricultural machinery, equipment, and services are essential for farms' production growth as the end-users (Civcisa & Grisliis, 2014; Gedzurs, 2016; Skarkova et al., 2016; Mitrofanovs et al., 2019; Buisson & Balasubramanya, 2019, Hu et al., 2020) and the manufacturers/service providers in this industry are highly dependent on their suppliers, an effective recovery management system is required to exert a positive impact on the post-failure quality of relationships and the financial performance of machinery and equipment supplier firms (Döscher, 2013; Sajtos & Chong, 2018). The recovery

management might also need the close collaboration between the suppliers and customers in the agronomy machinery industry as the supplier and customers are highly dependent and the collaborative activities might be needed to reinforce the relationship quality in this industry (Kukk & Leppiman, 2016; Franklin & Marchall, 2019; Hollebeek, 2019; Zhung et al., 2020). Up to now, however, far too little attention has been paid to the impact of joint recovery management on post-failure relationship quality in the agronomy machinery industry.

With the sensitivity of the agricultural machinery and services industry (Civcisa & Grislis, 2014; Gedzurs, 2016; Skarkova et al., 2016; Buisson & Balasubramanya, 2019; Mitrofanovs et al., 2019), the questions become: What happens to the customers' perception of relationship quality when the failure recovery is jointly created and implemented in this industry? More specially, does the customers' perception of post-failure relationship quality increase when the recovery is jointly created? Does the locus of failure impact the customers' perception of relationship quality after joint recovery management? Does the high relationship quality encourage the customer to participate in future recovery activity? These questions represent a significant gap in business marketing literature and focus on this research.

Answering these questions requires integrating two independent streams of marketing literature: research on value co-creation (Nammir et al., 2012; Chathoth et al., 2016; Kukk & Leppiman, 2016) and the B2B recovery management (Döscher, 2013; Baliga et al., 2020). Therefore, drawing on S-D logic and social exchange theory, the purpose of this research is two-folded: first to bridge the gap in the literature by investigating the relationship between the customers' perception of relationship quality and customer intention in future co-recovery in agricultural machinery and services industries environment. Second, to examine the role of locus of failure in the relationship between the joint recovery management and customers' perception of relationship quality.

## CONCEPTUAL FRAMEWORK

### **Joint recovery management and relationship quality**

We define failure as potential problems in service/product delivery and performance. Therefore, the failure in the agronomy machinery industry may be caused by different resources such as supplier-side problem (failure in upstream, internal, and downstream activities), the customer-side problem (internal customer problem, failure to provide the supplier with correct information, failure to use the service/product in a proper way) and the environmental factors such as natural disasters (Zhu & Zolkiewski, 2015). The recovery management in B2B context refers to 'A systematic approach for the development, implementation and controlling of activities by the seller firm to handle product or service failures to regain customer satisfaction and attain customer retention in the context of business-to-business markets' (Döscher, 2013, p. 18). In this definition, the failure responsibility has been attributed only to the supplier firm. Because typically, the suppliers shoulder the responsibility of failure activities based on the contractual agreement between supplier and customer (Döscher, 2013, Baliga et al., 2020). However, based on the S-D logic customers are active actors in the business processes (Grönroos, 2011; Kukk & Leppiman, 2016; Hollebeek, 2019). Under dominant service logic (S-D Logic), the value can be jointly created by customer and supplier through collaborative processes, interaction, and resources integration at different service chain

stages from service delivery to service recovery (Vargo & Lusch, 2004; Kukk & Leppiman, 2016).

One interesting example of the collaborative process is when customers engage in recovery activities or co-create the recovery activities with the supplier/service provider (Park & Ha, 2016; Bagherzade et al., 2020) through which the value can be co-created with the interaction and integration of resources. However, much less is known about joint recovery management in the agronomy machinery and services context indicating a need for a definition to develop our understanding of joint recovery management in this context. Therefore, drawing on S-D logic (Vargo & Lusch, 2004) and B2B service recovery definition (Döscher, 2013), we define the joint recovery management as:

‘The suppliers and customer’s interaction and the investment of operand and operant resources to jointly prevent, handle and resolve the product or service failures through which values are driven in the context of business-to-business market’

Besides, researchers have failed to address the impact of joint recovery management on the customers’ perception of relationship quality between supplier and customer firm in the B2B environments (e.g., Döscher, 2013; Zhu & Zolkiewski, 2015; Baliga et al., 2020), particularly in agronomy machinery settings. The relationship quality implies on the strength of the relationship between supplier and customer firms in the context of business-to-business markets (Holmlund, 2008; Grégoire et al., 2009) and conceptualized as a higher-order construct of satisfaction, trust, and commitment (Döscher, 2013; Itani & Inyang, 2015). The relationship satisfaction judgment is associated with the development of cumulative relationship satisfaction, which is substantially influenced by the occurrence of critical incidents in the relationship (Döscher, 2013). In comparison, the construct of relationship trust has been referred to the ‘Confidence in the exchange partner's reliability and integrity’ (Morgan & Hunt 1994, p. 23). Trust has been identified to be related to partner reliability, honesty, and benevolence (Winklhofer et al., 2008). Commitment is said to occur when one party believes the business relationship is sufficiently important to warrant maximum effort to maintain it indefinitely (Segarra-Moliner et al., 2013). In addition, some contingency factors might impact customer responses to the failure situations in this environment. Some of these notable factors might be the existing alternative suppliers in their network, the length of the relationship, switching cost, reciprocal supply agreement, and the locus of failure (Döscher, 2013; Baliga et al., 2020). In this paper, we focus on the role of locus of failure as the important moderating factor that might impact the relationship between joint recovery management and the post-failure relationship quality in the agronomy machinery industry.

### **Hypothesis Development**

According to S-D logic, value co-creation through collaborative activities requires a high level of interaction and resource investment from both sides of an exchange. Recovery management is essentially a social exchange (Patterson et al., 2006), and based on the social exchange theory, resource integration happens if the parties receive values from the exchange (Kotler & Zaltman, 1971). This value is related to the trade-off between the benefits driven by activities and the sacrifices of resources (Grönroos, 2011). Therefore, joint recovery management might have different relational outcomes based on the values driven from the collaborative recovery activities versus customer resource sacrifices. On the other hand, the relational outcomes of joint recovery management



might be affected by several factors (Heidenreich et al., 2015), such as the locus of failure. The locus of failure was perceived to impact the recovery management activities in the business environment (Zhu & Zolkiewski, 2015). In this paper, we argue that the locus of failure might play the moderating role in the relationship between joint recovery management and the customer perception of relationship quality. According to Döscher (2013), the recovery activities are defined in contractual agreements, and the recovery responsibility should be held on the supplier side. Also, customer firms hold less knowledge of the internal process and products/ services used in supplier firms; then they reflect the fewer competencies for identifying, analysing and resolving failures. Moreover, joint recovery management requires customer resource contribution, time, and effort.

If the problem is on the supplier side, the customer side's resource contribution might be perceived by customers as an extra loss, cost, and waste of resources. According to social exchange theory, the investment and exchange of resources happen when the exchange parties perceive the value in participation. When this value decreases, the customers might display less satisfaction, commitment, and trust in the supplier's relationship. Then, the joint recovery activities in this condition might negatively impact their perception of relationship quality. However, when the locus of failure is on the customer side, the resource contribution of supplier and their efforts into the solution of failure might increase the customers' perception of relationship quality. Since the supplier resource investment into failure recovery through the joint recovery management exceeds their contractual obligations, customers perceive a higher value driven from the recovery activities. They might display a higher level of trust, commitment, and satisfaction with the supplier and the business relationship. With the impact of the environmental factors on the service failures (Zhu & Zolkiewski, 2015), the joint recovery activities might increase the perception of relationship quality. Since the locus of failure is not from the supplier side, customers have clearer roles as participants in the recovery process, they receive an amount of control over the recovery activities and help find the optimal solution. Therefore, they perceive much more value in investing in their resources in the recovery activities and consequently perceive greater relationship quality. Based on the discussion above, we compare the customer perception of relationship quality when failure is caused by suppliers, customers themselves, and an environmental factor.

*H<sub>1a</sub>*: when the locus of failure is on the supplier end, the joint recovery activities lead to a lower perception of relationship quality rather than when the locus of failure is on the customer end.

*H<sub>2b</sub>*: when the failure is caused by an environmental factor, the joint recovery activities lead to a lower perception of relationship quality rather than when the locus of failure is on the customer end.

*H<sub>1c</sub>*: when the failure is caused by an environmental factor, the joint recovery activities lead to a higher perception of relationship quality rather than when the locus of failure is on the supplier end.

### The relationship quality and the intention for future co-creation

It has previously been observed that the relationship quality plays also a prompting role in customer engagement in business activities (Bowden, 2009; Hollebeek, 2011). This agrees with Chathoth et al. (2016), who suggest that customer engagement evolves from quality relationships between the customer and the supplier firm. The pre-established relationships based on satisfaction, commitment, and trust can also act as the antecedent to customer engagement (Hollebeek, 2011; Kumar & Pansari, 2016). According to the social exchange theory and S-D logic, we argue as the customers' satisfaction, trust and commitment with/to supplier increase they might be more eager to participate in future joint recovery activities. More specifically, with a high perception of relational values, they might be more eager to invest their resources in supplier interactions to participate in future recovery activities. Fig. 1 represents the research conceptual model.

$H_2$ : The higher perception of relationship quality is positively related to the customer intention for future joint recovery activities.

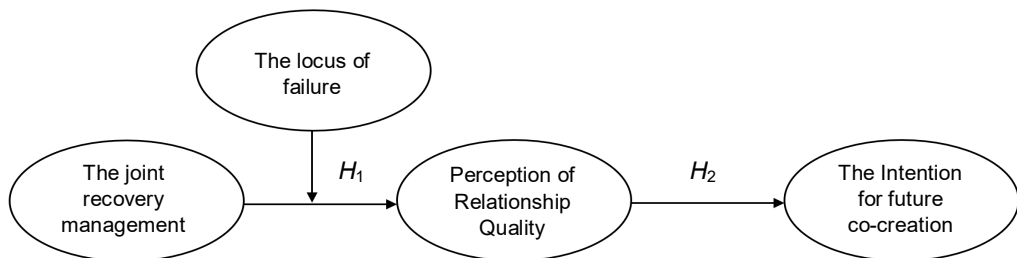


Figure 1. Conceptual model.

## MATERIALS AND METHODS

### Research design

We employed scenario-based experiments, to collect research data and test the research hypotheses. The scenario-based experimental design is currently the most popular method for evaluating service encounters involving both failure and recovery (i.e., Park & Ha, 2016; Nik Bakhsh, 2019). The scenario-based experimental design was chosen to avoid the biases associated with the retrospective self-reports, such as memory lapse and rationalization tendencies, and consistency. It is also one of the more practical ways of operationalizing the manipulations, which provides control over uncontrollable variables (Smith et al., 1999).

To test the  $H_{1a}$ ,  $H_{1b}$ , and  $H_{1c}$  hypotheses, we used three single factor 2(co-creation vs no co-creation of recovery activities)  $\times$  2 (locus of failure) experimental design. To test the  $H_2$ , a regression analysis was conducted on the pooled data gathered from all participants of the research. Multiple methods have been employed to develop the scenarios, starting with a depth qualitative interview with nine managers to generate service breakdown ideas suitable for our study, brainstorming, and small group surveys. The scenarios were evaluated based on the criticality, frequency, and similar experiences (Dong et al., 2008). The final six scenarios were different based on the locus of failure's attribution. They described a delivery situation where the customer ordered

machinery/equipment or service to the supplier when the items arrived/delivered the quantity/quality of product/service did not meet the customer expectation. In each experiment, the cause of failure varied depends on the locus of failure. In the first experiment, after the quality/quantity check from the customer side and contacting the supplier, the problem was from the supplier side and then manipulation is applied to the approach that the supplier has taken to solve the failure (co-creation vs non-co-creation). The supplier either resolved the problem themselves or asked a customer to help with the resolution with amending the items, contact other suppliers, etc. In the second experiment, the failure is caused by an environmental factor (natural disasters and unstable weather conditions); therefore, none of the parties could be held responsible for the failure situation. Again, in one scenario supplier initiate the recovery activities and, in another scenario, the customer has been asked to help with the solution. In the third experiment, it is found out the problem has been from the customer firm side themselves since they placed the wrong order or inappropriately used the items/service, then with the help of supplier they find a solution and implement it. Then, either supplier helps the customer firm to solve the failure situation, or customer's employees solved the problem themselves. We compared the customer perception of relationship quality among the experimental groups. Respondents read one of these six versions of the scenario and rated their agreement on a seven-point Likert scale, which enabled us to compare the customer perception of relationship quality among the experimental groups. Besides, including in the description of scenarios, the other contingency factors such as length of the business relationship, number of previous failures, the number of alternative suppliers in the business network, and the switching cost were similar across all experiments.

### **Sample**

The subjects in our experiments were top, middle level, and operational managers working within agricultural machinery manufacturer or service providers in Iran. We contacted 40 firms listed in a B2B services business directory, Industrial Management Institute in Iran. Most of the studied firms were medium-big sized companies with an average size > 200 full-time employees and an average age of 10 years. After identifying the target companies, 30 firms met the criteria and accepted to participate in this study.

Then we assessed all potential knowledgeable respondents through initial contact by email and ensured all 270 respondents are knowledgeable employees on the business relationship with the suppliers, have been familiarized with the concepts of failure recovery, and have experienced at least one service/product failure over previous two years. Then, the, 36% supply manager, 21% outbound preparation manager, 19% purchaser, 10% senior manager (CEO and vice president), 10% quality managers and 4% others. 60% of the respondents had over nine years of working experience; 30% had between 5 and 9 years, and 10% had less than five years. In the cover letter accompanied by the questionnaire, informants were guaranteed confidentiality. Finally, 210 usable questionnaires were received constituting a response rate of 62%. No questionnaires were returned incomplete.

### **Manipulation check**

The manipulations were pre-tested on a sample of operational and middle managers ( $n = 60$ ). The manipulation of the supplier's recovery strategy in the first and second

experiment was operationalized using the statements: ‘Customer was asked to help develop and implement the solution’ or ‘The development of solution and implementation of it all done by the supplier without customer engagement’. Moreover, the manipulation of the recovery strategy in the third experiment was operationalized using the statements ‘Supplier was asked to help develop and implement the solution’ or ‘The development of the solution and implementation of it all done by the customer without supplier engagement’. Participants read one of the two versions of the scenario and rated their agreement that the recovery was co-created on a seven-point Likert scale. The *t*-test revealed that in the first version of the scenario respondents agreed that the recovery was co-created, but not in the second version (co-created recovery: *mean* = 5.15, non-co-created: *mean* = 2.81, *t* = 10.93, *p* < .001).

### Measurement properties

The independent variable of the locus of failure was measured by three items developed by Maxham & Netemeyer (2002). This scale has been previously used to capture the attribution of failure responsibility. The dependent variable of relationship quality was captured by the three sub-constructs including the relationship trust (three items), relationship commitment (four items), and relationship satisfaction (three items) were adopted from Ulaga & Eggert (2006). Since no prior established scale was developed to measure customer intention toward future co-creation in B2B context, therefore we used the scale of ‘Repurchase intention’ introduced by Homburg et al. (2003). These 16 items were then subjected to confirmatory factor analysis (CFA) using SPSS (v. 20). After refinement, a final CFA model was estimated that demonstrated good measurement properties. *CMIN/df* = 1.06, *GFI* = 0.96, *AGFI* = 0.92, *CFI* = 0.97, *NFI* = 0.93, *IFI* = 0.97, and *RMSEA* = 0.053. The observed significant *Chi-square* = 76.280 (*df* = 35) was an appropriate Average Variance Extracted (*AVE*) > 0.63 (Fornell & Larcker, 1981) were the evidence of discriminative validity of constructs, the factor loadings were all significant (*t-values* between 11.7 and 18.3) as the evidence of convergent validity, only one item (from commitment items) being omitted (factor loading < 0.5). All construct reliabilities were acceptable (0.72–0.91) (Cronbach, 1951). Table 1 presents the result of CFA.

**Table 1.** Confirmatory factor analysis

Constructs and measures	Standardized parameters estimate	<i>T-value</i>	Average variance extracted	Reliability
Attribution of locus of failure			0.63	$\alpha = 0.87$
To high extent the supplier was responsible for the problem that we experienced	0.79	14.7		
The problem that we encountered was all supplier’s fault	0.73	12.3		
To high extent we blame the supplier for the problem	0.83	11.9		
Trust			0.66	$\alpha = 0.91$
We believe, this supplier keeps promises to us	0.71	13.5		
We believe this supplier is always concerned that our business succeeds	0.80	14.2		

Table 1 continued

We believe, this supplier is also trustworthy in future	0.91	14.8		
Commitment			0.66	$\alpha = 0.72$
Our firm genuinely cares about our business relationship with this supplier	0.88	18.3		
The relationship with this supplier deserves our business maximum effort to maintain	0.74	16.4		
Satisfaction			0.58	$\alpha = 0.75$
Despite this problem, our firm is very satisfied with this supplier	0.83	15.6		
Our firm would still make order to this supplier if we had to do it all over again	0.71	14.1		
Despite this problem, we are very pleased with what this supplier does for us	0.84	14.9		
Intention toward future co-creation			0.54	$\alpha = 0.75$
We will choose to collaborate with this supplier next time we encounter with a problem	0.71	12.3		
We collaborate this supplier and invest our resources to prevent, analysis, and solve the problem again if we had a choice	0.82	15.7		
We will choose to collaborate with this supplier next time we encounter with a problem service	0.67	11.7		

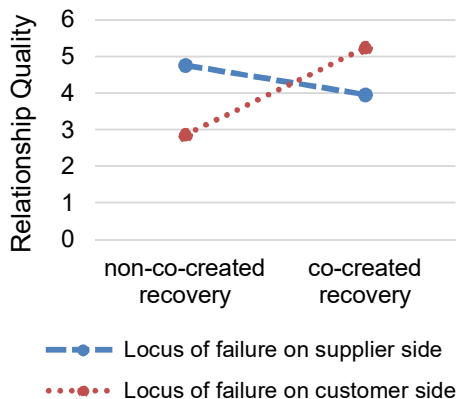
## RESULTS AND DISCUSSION

Using Excel version 2018, we conducted three ANOVAs to analyze the differences among group means in our sample and to test each hypothesis with the perception of relationship quality as the dependent measure. These experiments were designed to test the moderating impact of the locus of failure on the customers' perception of relationship quality.

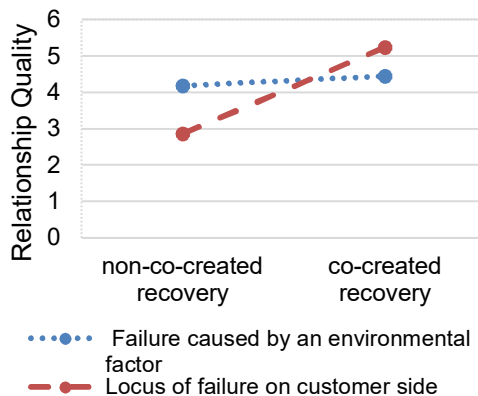
The manipulation included two recovery approaches, co-created recovery vs non-co-created recovery. Participants from the first group ( $n = 68$ ), in which the locus of failure is on the supplier side, randomly assigned to one of the two experimental conditions (co-created recovery vs non-co-created recovery). Participants from the second group ( $n = 72$ ), in which the failure caused by an environmental, randomly assigned to one of the two experimental conditions (co-created recovery vs non-co-created recovery). Similarly, participants from the third group ( $n = 70$ ), in which the locus of failure is on the customer side, randomly assigned to one of the two experimental conditions (co-created recovery vs non-co-created recovery).

The first experiment was designed to test  $H_{1a}$ . An ANOVA with the first and third groups was conducted to compare the perception of relationship quality between the first and third groups. The result ( $F(35.4) > F_{crit}(2.60)$  and  $p\text{-value} < 0.05$ ) revealed that respondents felt a greater sense of relationship quality when the locus of failure is on the customer side, and the recovery is co-created. It is apparent from Fig. 2 that as expected, the sense of relationship quality decreases when the recovery is co-created, and the locus of failure is on the supplier end. Overall, the sense of relationship quality is higher with

non-co-created recovery when the failure is caused by the supplier. The first hypothesis is supported. Fig. 2 illustrates the result of the first experiments.



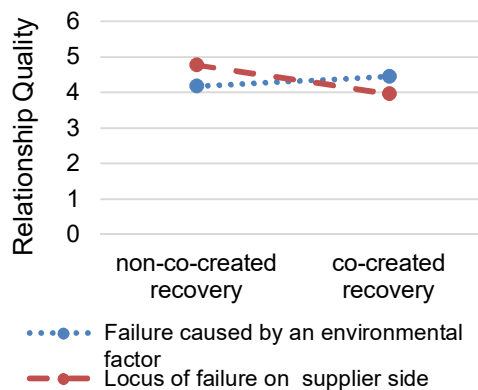
**Figure 2.** The recovery approach × The locus of failure (supplier vs customer side).



**Figure 3.** The recovery approach × The locus of failure (customer side vs environmental factor).

Similarly, in experiment two, an ANOVA with the second and third groups was conducted to test  $H_{1b}$ . The result is illustrated in Fig. 3. What is striking is the continual growth in all respondent’s sense of relationship quality when the recovery is co-created; however, the relationship quality increases sharply for the respondent who perceived the locus of failure was on the customer side rather than an environmental issue ( $F(29.2) > F_{crit}(2.60)$  and  $p\text{-value} < 0.05$ ). These results provide further support for the  $H_{1b}$ .

It is apparent from Fig. 4 that as expected, the sense of relationship quality decreases when the recovery is co-created, and the locus of failure is from the supplier side rather than an environmental issue. The figure below shows that the co-creation of recovery slightly increases the sense of relationship quality when an environmental issue causes failure. In contrast, moving toward the co-creation of recovery, the sense of relationship quality decreases when they believe that the failure is due to the internal supplier issue. The result of ANOVA ( $F(42.4) > F_{crit}(2.60)$  and  $p\text{-value} < 0.05$ ) supported the  $H_{1c}$ .



**Figure 4.** The recovery approach × The locus of failure (supplier vs environmental factor).

We analyzed the impact of relationship quality dimensions on the customers’ intention of future co-creation recovery (IFCR) on the pooled data from our respondents ( $n = 139$ ) using the regression analysis in Excel 2018. The adjusted  $R^2$  value for the IFCR equations was .61 for pooled data from all research participants. The results indicate that perceptions of trust, commitment, and satisfaction were all significantly positively

associated with IFCR. The construct trust had the largest standardized coefficient ( $\beta = 0.298$ ) followed by commitment and satisfaction ( $\beta = 0.236$  and  $0.191$ , respectively). Therefore, the result of regression provides strong evidence of a considerable amount of variance in IFCR is explained by the relationship quality constructs across all respondents: relationship trust, commitment, and satisfaction.

The findings reported here also shed new light on the role of locus of failure because of its unavoidable impact on customer response to joint recovery management in the agronomy machinery and services industry. More specifically, our study highlights the importance of locus of failure in the relationship between the co-creation of recovery and the relationship quality, which further impacts the customers' intention of future co-creation recovery. Therefore, it established a basis for promising future academic research on the recovery management in B2B environment particularly the agronomy industry.

The first question in this research was related to joint recovery management's impact on the customers' perception of relationship quality when the recovery activities were jointly created. The current study found that joint recovery management impacts the customers' perception of relationship quality. However, the type of impact (negative vs positive) depends on the attribution of locus of failure. The second question was designed to shed more light on the role of attribution of failure responsibility, which resulted in the most prominent finding from this study. According to our results, the locus of failure plays a moderating role in the relationship between joint recovery management and customers' perception of relationship quality. Therefore, in general, moving the locus of failure toward the customer side, the customers' perception of relationship quality increases significantly.

More specifically, when the locus of failure is attributed to the supplier side, customers are less likely to show a significant perception of relationship quality with joint recovery management activities. Our findings are supported by the social exchange theory and S-D Logic, as the recovery activities by the supplier reflect the contractual obligations when customer attribute the locus of failure to the supplier side activities, they hold expectations that supplier should comply with the failure handling procedures themselves as it is defined in their contractual agreements (Döscher, 2013). Therefore, the joint recovery management that required the customers' investment of their resources, might not add extra value for customers and might not be perceived by customers as increased outcomes from the exchange relationship. Since joint recovery management outcomes are not apparent to customers, their trust, commitment, and satisfaction on the relationship with the supplier decrease. The joint recovery management in the business market reflects a negative impact on the customers' perception of relationship quality. Another possible explanation for this might be that the customer firms likely hold increasingly less knowledge on the supplier's internal core procedure and products, or services used in their products or services. They believe the identification, the analysis of failures, response to the failure, resolution and controlling of them (Döscher, 2013) should largely remain with the supplier. This result also may be explained by the fact that despite the importance of failure notification, rapport of employees, feedback and explanation, and amount of cognitive control customer firms receive from the co-creation of recovery, when customers attribute failure and recovery activities more to the supplier firm than to themselves or an environmental factor, they may experience a negative impact on their role clarity and

perceived value. The yields in this study were higher than those of other studies in the consumer market that showed the positive impact of co-creation of recovery on customer post-recovery responses (Gohari et al., 2016; Park & Ha, 2016; Nik Bakhsh, 2019; Bagherzade et al., 2020). Interestingly, the customers' perception of relationship quality increases when the locus of failure is to their side. Since the supplier contribution and resource investment to failure recovery exceed the supplier's contractual obligations, customers perceive a higher value in joint recovery management as an exchange situation. Therefore, based on the social exchange theory, they see extra values driven from the supplier resource contribution to the failure recovery activities. As a result of these extra values from joint recovery management, they might have perceived higher satisfaction, commitment, and trust in the supplier's exchange relationship. Another important finding was the failure situation when an environmental factor caused the failure. Our findings revealed that, in this situation, joint recovery management increases the perception of relationship quality in customers. This result may be explained by the fact that the rapport of employees, feedback of employees of the supplier as well as the empowerment and the clarity of role can be played by the customer, are valued by the customer. This might result in a positive outcome when customers' tradeoff their investment of resources and the value driven by joint recovery management. Therefore, joint recovery management increases the perception of relationship quality in customers. Consistent with Vargo & Lusch (2004), the co-creation of recovery positively impacts the perception of relationship quality, except when the attribution of locus of failure is on the supplier side.

To answer the third research question, we tested the relationship between the relationship quality dimensions (trust, commitment, and satisfaction) and the intention for future co-creation of recovery. Strong evidence of the positive association between relationship quality and the intention for future co-creation of recovery was found from the regression analysis. This finding broadly supports other researchers' work in this area linking co-creation and engagement activities with relationship quality (e.g., Hollebeek, 2019). It is also consistent with that of Chathoth et al. (2016) who argue that customer engagement evolves from the high relationship quality relationship. These relationships may partly be explained by customer's extra value in co-creation activities driven by customer trust, commitment, and satisfaction from the business relationship with the supplier.

## CONCLUSION

The agronomy machinery manufacturers and service providers are frequently experiencing failure in their product and service delivery (Afsharnia, 2014) caused by different sources. Since the failures can make a butterfly impact on the farms and end user, there is a vital need for designing and implementing an effective recovery management system for the resolution of failure and reinforcing the relation quality after such incidents. Because of the high dependence of suppliers and customers in this industry, joint recovery management is introduced as a remedy in this study, and the moderating impact of locus failure on the relationship between joint recovery management and relationship quality is tested. Next, the authors examined how the perception of relationship quality encourages the customers to engage in future joint activities in this context.



In reviewing the agronomy literature, no data was found on joint recovery management and its relational outcome in agronomy research. Therefore, this study set out to extend our knowledge and understanding of the joint recovery management in the agronomy machinery and services market in which the high interaction between supplier and customer is essential to prevent and handle the failure situation and later avoid the failure domino effect on the farm productions.

The findings of the present research confirmed that locus of failure interacts with the supplier joint recovery efforts to impact the post-failure relationship quality. Another interesting finding is the customer perception of relationship quality impacts their intention for future co-creation of activities.

From a theoretical perspective, our research findings intend to advance the existing knowledge of agronomy industry research and the recovery management disciplines. In particular, the insights gained from this research offer four fundamental contributions to academic research associated with B2B recovery and agronomy industry literature.

First, it sheds more light on the concept of joint recovery management in the context of the agronomy machinery and services market. Existing research on co-creation of recovery mainly focused on the consumer market or other industries. Despite the sensitivity of the agronomy industry and farm operations, there remains a paucity of evidence on joint recovery management represents a significant gap in contemporary agronomy literature, and the current research represents one of the first studies on joint recovery for this context. In particular, the findings reported here focused on the condition in which the co-creation of recovery improves the relationship quality, which contributes to customers' intention for future co-creation of recovery. Therefore, our research establishes a base for future research to explore the infant domain of joint recovery management in the agronomy machinery and business markets in general.

Second, in this paper, we examined the moderation role of locus of failure on the customers' perception of the relationship's quality with the supplier in agronomy machinery industry. The present investigation responds to previous research, which has called for further research to identify the influential factors in the failure recovery (e.g., Döscher, 2013; Zhu & Zolkiewski, 2015). Therefore, the present study has gone some way towards enhancing our understanding of factors that might moderate the impact of different recovery strategies (non-co-creation vs co-creation) on the customers' perception of relationship quality.

Third, this research's findings contribute empirical evidence on the discussion about the impact of the customers' perception of relationship quality on the re-co-creation intention in recovery management in the agronomy machinery context. Therefore, the present thesis completes the previous research, which has suggested investigations on the relationship quality and customer engagement (Chathoth et al., 2016; Hollebeek, 2019). Based on these findings, the present study provides ground for further research on the role and the impact of collaborative activities in recovery management in agronomy research.

From a practical and managerial perspective, the insights derived from this study were supposed to contribute to the knowledge and practice in agronomy machinery and services industry. The findings of this study are helpful for the development of knowledge and skills of suppliers and their employees who intend to engage their customers in the failure recovery activities in the context of B2B, particularly in the agronomy machinery and services industry. The high interaction between suppliers and customers

in this industry can be used as an important tool to develop joint activities and create superior values. However, based on our findings, we propose that the value driven from the collaborative recovery management might not always be greater than the customer sacrifices (the investment of the resources) customers make, and as a result, positive relational outcomes might not always be expected. Although the feedback and rapport of suppliers play a key role in success of recovery activities in this industry, finding a solution with customer help might not increase the perceived value when the failure is on the supplier side. This research has identified that joint recovery management's effectiveness on the relationship quality varies depending on the locus of failure. This finding enables the supplier of machinery and services to understand how and to what extent the co-creation of recovery can be conducted in different failure situations to increase customer satisfaction, trust and commitment after the failure situation.

Besides, this study's findings can assist the relevant decision-makers within the supplier and customer firm in this industry about the right timing of joint recovery activities. Therefore, managers in the machinery manufacturer and service provider firm can distinguish when the co-creation and customer engagement strategies are beneficial in the failure situation and lead to a higher perception of customer relationship quality. This finding can help agronomy machinery manufacturers with improving their failure recovery systems. Although the notification, feedback, and rapport of supplier employee are essential in the industries in which the high interaction between supplier and customer is required, our empirical results show that the co-creation of recovery should only be done with caution to enhance the relationship quality when the failure is not from the supplier.

On the other hand, if the failure happens on the customer side, supplier engagement in problem-solving significantly increases the relationship quality. Therefore, the supplier should be encouraged to contribute to the failure resolution where it is possible to strengthen the relationship quality with the customer and make a higher perception of trust, commitment, and satisfaction in the customer. The joint recovery activities also can be recommended when the failure is caused by an environmental factor. When the customers have greater role clarity, require more cognitive control and feedback of recovery activities. Then customers more likely to show a greater perception of relationship quality with the joint recovery activities. For machinery suppliers and service providers in this industry, these collaborative recovery activities with the customers might be a great opportunity to open venues for building a strong relationship. More specifically, this study's results disclosed that higher satisfaction commitment and trust might increase the customers' intention for future co-creation after the recovery. Therefore, the manufacturers and service providers in the agronomy industry can take this opportunity to utilize customer resources in future recovery activities. Suppliers may use this finding for workshops and training sessions to illustrate, develop and optimize the inter-organizational process to handle the joint recovery management in agronomy machinery and services markets effectively.

## REFERENCES

- Afsharnia, F., Asoodar, M.A., Abdeshahi, A. 2014. The Effect of Failure Rate on Repair and Maintenance Cost of Four Agricultural Tractor Models. *World Academy of Science, Engineering and Technology International Journal of Agricultural and Biosystems Engineering* 8(3), 286–290.

- Bagherzadeh, R., Rawal, M., Wei, S. & Torres, J.L. 2020. The journey from customer participation in service failure to co-creation in service recovery. *Journal of Retailing and Consumer Services* **54**,102058.
- Baliga, A.J., Chawla, V., Sunder M, V. & Ganesh, L.S. 2020. Service Failure and Recovery in B2B Markets – A Morphological Analysis. *Journal of Business Research*, in press. doi: 10.1016/j.jbusres.2020.09.025
- Borah, S.B., Prakhya, S. & Sharma, A. 2019. Leveraging service recovery strategies to reduce customer churn in an emerging market. *Journal of the Academy of Marketing Science* **21**, 1–21.
- Bowden, J.L. 2009. The Process of Customer Engagement: A Conceptual Framework. *Journal of Marketing Theory and Practice* **17**(1), 63–74.
- Buisson, M.C. & Balasubramanya, S. 2019. The effect of irrigation service delivery and training in agronomy on crop choice in Tajikistan. *Land Use Policy* **81**, 175–184.
- Chathoth, P.K., Harrington, R.J. & Chan, E.S. 2016. Co-creation and higher order customer engagement in hospitality and tourism services. *International Journal of Contemporary Hospitality Management* **28**, 222–245.
- Civcisa, G. & Grislis, A. 2014. ISO/TS 16949 among Latvian production companies focused on automotive industry. *Agronomy Research* **12**, 255–262.
- Dong, B., Evans, K.R. & Zou, S. 2008. The effects of customer participation in co-created service recovery. *Academy of Marketing Science* **36**, 123–137.
- Döscher, K. 2013. *Recovery Management in Business-to-Business Markets Conceptual Dimensions, Relational Consequences and Financial Contributions*. Springer Gabler. doi:10.1007/978-3-658-05637-7
- Fornell, C. & Larcker, D.F. 1981. Evaluating structural equation models with unobservable variables and measurement error. *Journal of Marketing Research* **18**, 39–50.
- Franklin, D. & Marshall, R. 2019. Adding co-creation as an antecedent condition leading to trust in business-to-business relationships. *Industrial Marketing Management* **77**, 170–181.
- Gedzurs, A. 2016. Operation reliability of induction motors at egg processing plant ‘Balticovo’. *Agronomy Research* **14**(S1), 1161–1168.
- Gohari, A., Hamzeli, B., Pourazizi, L. & Heidarzadeh Hanzaee, K. 2016. Understanding effects of co-creation on cognitive, affective and behavioral evaluations in service recovery: An ethnocultural analysis. *Journal of Retailing and Consumer Services* **31**, 182–198.
- Grégoire, Y., Tripp, T.M., Legoux, R. & Fisher, R.J. 2009. When customer love turns into lasting hate: the effects of relationship strength and time on customer revenge and avoidance. *Journal of Marketing* **73**, 18–32.
- Grönroos, C. 2011. Value co-creation in service logic: a critical analysis. *Marketing Theory* **11**, 279–301.
- Heidenreich, S., Wittkowski, K., Handrich, M. & Falk, T. 2015. The dark side of customer co-creation: Exploring the consequences of failed co-created services. *Journal of the Academy of Marketing Science* **43**(3), 279–296.
- Hollebeek, L.D. 2011. Demystifying Customer Brand Engagement: Exploring the Loyalty Nexus. *Journal of Marketing Management* **27**, 785–807.
- Hollebeek, L. 2019. Developing business customer engagement through social media engagement-platforms: An integrative S-D logic/RBV-informed model. *Industrial Marketing Management* **81**, 89–98.
- Holmlund, M. 2008. A Definition, Model, and Empirical Analysis of Business-To-Business Relationship Quality. *Journal of Service Management* **19**, 32–62.
- Homburg, C., Giering, A. & Menon, A. 2003. Relationship Characteristics as Moderators of the Satisfaction-Loyalty Link: Findings in a Business-to-Business Context. *Journal of Business-to-Business Marketing* **10**, 35–63.

- Hu, Y., Liu, Y., Wang, Z., Wen, J., Li, J. & Lu., J. 2020. A two-stage dynamic capacity planning approach for agricultural machinery maintenance service with demand uncertainty. *Biosystems Engineering* **190**, 201–217.
- Itani, O. S. & Inyang, E. 2015. The effects of empathy and listening of salespeople on relationship quality in the retail banking industry: The moderating role of felt stress. *International Journal of Bank Marketing* **33**, 692–716.
- Kotler, P. & Zaltman, G. 1971. Social Marketing: An Approach To Planned Social Change. *Journal of Marketing* **35**(3), 3–12.
- Kukk, L. & Leppiman, A. 2016. The construct of value in knowledge-intensive business service from customer's perspective. An example of a long-term training activity. *Agronomy Research* **14**(1), 91–108.
- Kumar, V. & Pansari, A. 2016. Competitive Advantage through Engagement. *Journal of Marketing Research* **53**, 497–514.
- Maxham, J.G. & Netemeyer, R.G. 2002. A longitudinal study of complaining customers' evaluations of multiple service failures and recovery efforts. *Journal of Marketing* **66**, 57–71.
- Mitrofanovs, V., Boiko, I. & Geriņš, Ē. 2019. Management of parts and components for units and assemblies in mechanical engineering industry and its impact on the environment. *Agronomy Research* **17**(S1), 1138–1145.
- Morgan, R.M. & Hunt, S. 1994. The Commitment-Trust Theory of Relationship Marketing. *Journal of Marketing* **58**(3), 20–38.
- Nammir, D.S., Marane, B.M. & Mohammad Ali, A. 2012. Determine the Role of Customer Engagement on Relationship Quality and Relationship Performance. *European Journal of Business and Management* **4**, 2222–2839.
- Nik Bakhsh, N. 2019. Co-creation of Service Recovery and Post-Recovery Responses: The Impact of Cultural Values Orientations and Outcome Favorability. *Journal of service Science Research* **11**, 133–155.
- Park, J. & Ha, S. 2016. Co-creation of service recovery: Utilitarian and hedonic value and post-recovery responses. *Journal of Retailing and Consumer Services* **28**, 310–316.
- Patterson, P.G., Cowley, E. & Prasongsukarn, K. 2006. Service failure recovery: The moderating impact of individual-level cultural value orientation on perceptions of justice. *Journal of Research in Marketing* **23**, 263–277.
- Sajtos, L. & Chong, Y.S. 2018. Activating multiple roles of customer-firm relationships in service failures. *Journal of Service Theory and Practice* **2**, 250–270.
- Segarra-Moliner, J.R., Moliner-Tena, M.A. & Sanchez-Garcia, J. 2013. Relationship quality in business to business: a cross-cultural perspective from universities. *Marketing Intelligence & Planning* **31**, 196–215.
- Skarkova, L., Smeitkova, A., Satrudinov, D. & Vaculik, P. 2016. Influence of the packaging material on the quality parameters of tobacco during ageing. *Agronomy Research* **14**(S2), 1451–1459.
- Smith, A.K., Bolton, R.N. & Wagner, J. 1999. A model of customer satisfaction with service encounters involving failure and recovery. *Journal of Marketing Research* **36**, 356–373.
- Ulaga, W. & Eggert, A. 2006. Relationship Value and Relationship Quality: Broadening the Nomological Network of Business-to-Business Relationships. *European Journal of Marketing* **40**, 311–327.
- Vargo, S.L. & Lusch, R.F. 2004. Evolving to a New Dominant Logic for Marketing. *Journal of Marketing* **68**, 1–17.
- Winklhofer, H., Ennew, C. & Vieira, A.L. 2008. Relationship Quality: a literature review and research agenda. *Journal of Customer Behaviour* **7**, 269–291.
- Zhu, X. & Zolkiewski, J. 2015. Exploring service failure in a business-to-business context. *Journal of Service Marketing* **29**, 367–378.

## **Biological effectiveness of a new multifunctional biopesticide in the protection of organic potatoes from diseases**

I.I. Novikova<sup>1</sup>, V.B. Minin<sup>2,\*</sup>, J.A. Titova<sup>1</sup>, I.L. Krasnobaeva<sup>1</sup>, A.M. Zaharov<sup>2</sup>  
and A.N. Perekopsky<sup>2</sup>

<sup>1</sup>Federal State Budget Scientific Institution “All-Russian Research Institute of Plant Protection” (FSBSI VIZR), 3, Podbelskogo shosse, RU196608 Saint-Petersburg-Pushkin, Russia

<sup>2</sup>Institute for Engineering and Environmental Problems in Agricultural Production branch of the BFSBSI “Federal Scientific AgroEngineering Centre VIM (IEEP – branch of FSAC VIM), 3, Filtrovskoe shosse, p.o. Tiarlevos, RU196625 Saint-Petersburg, Russia

\*Correspondence: [minin.iamfe@mail.ru](mailto:minin.iamfe@mail.ru)

Received: January 29<sup>th</sup>, 2021; Accepted: June 22<sup>nd</sup>, 2021; Published: September 9<sup>th</sup>, 2021

**Abstract.** Crop disease control is of particular importance in organic crop production, as the use of chemical pesticides is prohibited there. A new multifunctional biofungicide Kartofin was selected and used to optimize the phytosanitary state of organic potatoes ecosystems. Previously of studies indicated the prospects of using the biofungicide to control numerous fungal and bacterial diseases during the potato growing season and storage of tubers. The crop rotation field experiment was carried out in 2017–2020 at the Experimental Station of the IEEP - BRANCH OF FSAC VIM near Saint-Petersburg (59°65 N and 30°38 E). The soil of experimental plots is sod-podzolic light loamy. In the potatoes (variety Udacha) field, a 2-factor field experiment was established which studied:

- the action of biofungicide Kartofin;
- the effect of the compost.

The experiment was established on the plots with the size 61.6 m<sup>2</sup> each. The experiment had four replications.

Three doses of the compost were used which corresponded to different levels of the potato productivity. Potatoes were treated with biofungicide at the time of planting and by foliar spray during the growing season. The combined use of compost at a dose of 4 t ha<sup>-1</sup> and biofungicide made it possible to achieve the yield of standard tubers of 27.3–28.2 t ha<sup>-1</sup> with their low incidence of fungal diseases. The biological effectiveness of the biofungicide Kartofin in reducing the prevalence and development of a complex of fungal diseases (alternariosis, late blight, stem form of rhizoctoniosis) on potato plants of the Udacha variety reached 82.2–89.9%.

**Key words:** biofungicide, biological control, organic cultivation, plant diseases, plant nutrition, potatoes.

## INTRODUCTION

In Russia, organic agriculture has a share of 0.2%, however, production and consumption of organic products are starting to develop actively. On January 1, 2020, Federal Law No. 280-FZ ‘On Organic Products and Amendments to Certain Legislative Acts of the Russian Federation’ entered into force. The new law will, for the first time, begin to regulate manufacturing, storage, transportation, labeling, and marketing of organic products. Potato is the third most important food crop, after rice and wheat, with a total production of more than 300 million metric tons, as established by the International Potato Center (2017) in Lima, Peru. The Russian Federation ranks third in the world in the production of potatoes, which is cultivated in all major regions of the country, including North-Western region.

Two major challenges need to be addressed for sustainable organic potato production: efficient controlling of the phytosanitary state of the agroecosystem and ensuring adequate mineral nutrition of potatoes. Both factors are limited by regulations that, on the one hand, prohibit the use of artificial fertilizers, especially nitrogen fertilizers, and, on the other hand, most synthetic pesticides. In this regard, the selection of effective and safe microbiological pesticides to reduce the population density of phytopathogenic species is of particular importance.

However, organic management focuses on managing the environment, creating healthy soil and choosing more resilient plant varieties, which allow plants to resist potential attacks from microorganisms. Due to the reduced or non-existing input of mineral fertilizers and pesticides, organic fields tend to enhance biodiversity compared to conventionally managed fields, thus positively contributing to this SDG (de Schaetzen, 2019). Organic farms generally have more plant diversity, greater faunal diversity (insects, soil fauna and microbes, birds) and often more habitat and landscape diversity (Reganold & Wachter, 2016). The main practices that contribute to disease control are long, balanced rotations, organic amendments and reduced tillage, all geared towards maintenance of the soil organic matter content and fertility (Van Bruggen et al., 2015; De Tulipa & De L.C., 2019).

We selected and used a new polyfunctional biofungicide Kartofin, SC (suspension concentrate) to optimize the phytosanitary state of agroecosystem when growing organic potatoes. The producer strain of *Bacillus subtilis*-I5-12/23 was selected as a result of extensive screening of antagonist microbial strains that are part of the State Collection of Microorganisms Pathogenic for Plants and their Pests of the All-Russian Research Institute of Plant Protection. On the basis of this strain, the biofungicide Kartofin, SC was developed. The collection was registered at the World Federation for Culture Collections, World Data Center for Microorganisms (WFCC WDCM, Japan) under No. 760 on January 28, 1998.

Preliminary, studies were carried out in a series of model, vegetation and field experiments with Kartofin, SC. The results of studies indicated the prospects of using the biofungicide Kartofin to control numerous fungal and bacterial diseases during the potato growing season and storage of tubers. The indicators of biological and economic efficiency (Guidelines..., 2009) were used to assess the effect of the biofungicide on reducing the development of potato infection with fungal and bacterial diseases. The biological effectiveness of biofungicide Kartofin in relation to the prevalence and development of diseases was 50–100%, the economic efficiency of the use of biofungicide increased by 18.4–22.5% (Novikova et al., 2019; Titova et al., 2019).

Previously, Swedish scientists and Estonian scientists conducted field experiments and underlined that soil fertility had a strong influence on the productivity and quality of organic potatoes. So, organic potatoes needed to be cultivated on healthy soils with sufficient humus content and compost must be used to ensure that they have sufficient mineral nutrition. Our preliminary studies indicated that fairly high yields of organic potatoes may be obtained under the conditions of the Leningrad region using compost produced on the basis of chicken manure in an aerobic biofermenter (Popov et al., 2018; Minin et al., 2020).

In organic farming, the construction of the healthiest plant, provided with sufficient nutrients and favorable microbiota, is of particular importance. This contributes to an increase in plant disease resistance and protection from phytopathogenic microorganisms. At the same time, a favorable microbiota promotes the supply of more nutrients to the plants, which, in turn, promotes more active plant growth.

The considered model of organic potato predicts its development, using the emerging weather characteristics, forming favorable soil conditions and regulating the composition of its microecosystems by introducing biological products based on microbes-antagonists of phytopathogens.

At this stage, we use statistical models, on the basis of which a simulation model will be developed in the future.

## MATERIALS AND METHODS

The field experiment was carried out in 2017–2020 at the Experimental Station of the Institute for Engineering and Environmental Problems in Agricultural Production (IEEP) - branch of FSAC VIM near Pavlovsk town, Saint-Petersburg (59°65 N and 30°38 E). The studies were carried out in the field organic crop rotation established in 2016. The crop rotation included the following crops: potato; red beat; barley with complementary seeding of clover and timothy; the 1<sup>st</sup> year perennial grass and legumes; the 2<sup>nd</sup> year perennial grasses; the 3<sup>rd</sup> year grass - after it's plowing in, the winter rye will be seeded for green manure. According to the Russian classification, the soil of experimental plots was sod-podzolic light loamy gleyic on residual carbonate moraine loam. It had a weak acidic reaction (pH = 6.5–6.6), high organic matter content (5.6%), and medium to high levels of available P and K.

In the field with potatoes (variety Udacha), a two-factor field experiment was established which studied the effect of the following factors:

- the action of biofungicide Kartofin, SC;
- the effect of the compost which provided the mineral nutrition of potatoes.

Experimental batches of biological fungicide Kartofin, SC based on *Bacillus subtilis* strain I-5 12/23 were developed for field trials. Producer strain is certified, deposited and maintained at the State Collection of Microorganisms Pathogenic for Plants and Their Pests at FSBSI VIZR (No. 760 on January 28, 1998 WFCC WDCM, Japan). Biological fungicide Kartofin, SC (titer not less than  $5 \times 10^{10}$  CFU mL<sup>-1</sup>) is intended to protect agricultural crops from fungal and bacterial diseases during vegetation and storage of crops. The active biologic's ingredients are cells (spores) and a complex of *B. subtilis* strain I-5 12/23 metabolites; preparative formulation is the suspension concentrate (SC).

The biological fungicide was developed in accordance with the approved in the FSBSI VIZR regulations, specifications and toxicological passport. The biofungicide's experimental batches were prepared by the submerged cultivation method in the Microbiocontrol Laboratory FSBSI VIZR. The titer of the producer strain was determined by the serial dilutions' method with inoculation of the 8<sup>th</sup> and 9<sup>th</sup> dilutions on Dried nutrient agar: pancreatic sprat hydrolysate - 15 g L<sup>-1</sup>, NaCl - 4.59 g L<sup>-1</sup>, microbiological agar - 20 g L<sup>-1</sup>, pH = 7.2 (Microgen Co. Ltd., Russia). The inoculum of the producer strain was preliminarily cultured in test tubes on the abovementioned oblique nutrient medium. The submerged cultivation was carried out in shaking flasks with 750 mL volume, containing 100 mL of nutrient medium: molasses - 15 g L<sup>-1</sup>, corn extract - 30 g L<sup>-1</sup>, pH = 7.8 (Research and Production Association 'ALTERNATIVE', Russia). Liquid phase inoculum of producer strain was grown at 27–28 °C for 3 days with aeration (180 rpm, New Brunswick™ Innova® 44 Shaker Incubator, Eppendorf, Germany). A sample was taken and microscopied to control the bacterial growth stage and the presence of foreign microbiota every day.

The fermentation process was stopped after 85–90 % spores producing in the culture liquid (CL). The CL was separated for 10 min at 3,000 rpm in the centrifuge OS-6MC (Dastan Inc., Kyrgyzstan) and then 0.2 % potassium sorbate was added to the spore suspension concentrate put into 1,000 mL wide-mouth bottles, PE-LD (VITLAB GmbH, Germany). The initial culture fluid titer was 5.2×10<sup>10</sup> CFU mL<sup>-1</sup>, the finished biologics Kartofin, SC titer was 8.2×10<sup>10</sup> CFU mL<sup>-1</sup>.

The studies were carried out with the compost produced in the Laboratory of organic waste bioconversion of IEEP - BRANCH OF FSAC VIM by the aerobic fermentation of the bedding poultry manure supplied by a poultry farm in the Leningrad Region (Briukhanov et al., 2017). It characterized by a high dry matter content (nearly 40%) and a high content of nitrogen and phosphorus (Table 1). Two compost doses were used; they were calculated by a sequentially doubling amount of nitrogen: 80 and 160 kg N ha<sup>-1</sup> providing medium and high levels of potato productivity. By weight, this corresponded to application of 4.3 t ha<sup>-1</sup> and 8.6 t ha<sup>-1</sup> of compost. The compost was applied before ridging, followed by embedding the fertilizer by disking.

The potato variety Udacha was cultivated. This potato variety is a new one, relatively resistant to late blight, perfectly adapts to various soils and weather conditions, it characterized by good taste and smoothness of the tuber surface (Shabanov, 2016). Potatoes were obtained from the seed farm (super elite and elite classes). Potatoes were treated with the biofungicide at the time of planting and by foliar spray during the growing season. For this purpose, a specially designed sprayer was installed on the planter and on the cultivator. Inter-row cultivation was carried out regularly, starting from the second week after planting, using an experimental specimen

**Table 1.** The averaged characteristics of the compost

Parameter	Designation	Units	Value
Moisture content	MC	%	62.2
H <sup>+</sup>	pH	-	8.5
N <sub>total</sub> content	N <sub>total</sub>	mg kg <sup>-1</sup>	4,970.0
NH <sub>4</sub> <sup>+</sup> content	NH <sub>4</sub> <sup>+</sup>	mg kg <sup>-1</sup>	2,770.0
NO <sub>3</sub> <sup>-</sup> content	NO <sub>3</sub> <sup>-</sup>	mg kg <sup>-1</sup>	890.0
K <sup>+</sup> content	K <sup>+</sup>	mg kg <sup>-1</sup>	2,890.0
P <sub>total</sub> content	P <sub>total</sub>	mg kg <sup>-1</sup>	2,690.0
Ash content		%	19.2



of a row-crop cultivator of an original design that provides deep loosening of inter rows. Weed vegetation was removed mechanically using small rotary harrow BRU-0.7 harrows mounted on the cultivator.

A plot size was  $5.6 \times 11 \text{ m} = 61.6 \text{ m}^2$ , with four replications in a complete randomized design. Potato planting in 2020 was carried out on May, 27, harvesting on September, 4.

All the results obtained in the experiment are placed in a database (Minin et al., 2020), which allows statistical processing of all research results using the Program STATISTICA 10. Mean comparison of data was made by using least significant difference (*LSD*) test at 5% error probability.

Observations of the growth rate of biomass (by the phases of plant development), phytosanitary conditions and soil properties were carried out regularly. Soil samples were taken from the arable horizon (0–25 cm) four times per season. Analytical studies were performed at the FSBSI VIZR Laboratory and the IEEP - BRANCH OF FSAC VIM Chemical Analytical Laboratory in accordance with the relevant GOSTs. Determination of nitrates and ammonium in soil was carried out using the ion metric method, GOST 26951-86.

## RESULTS AND DISCUSSION

The sum of active temperatures (above 10° C) during the growing season (May - August) in the four years under consideration (2017–2020), varied from 1,625.5 to 2153.6. The average yield of the total potato biomass by variants varied from 17.4 to 40.8 t ha<sup>-1</sup> at the same time.

The weather conditions presented in Table 2. It should be noted that if the sum of active temperatures characterizes the thermal and light regimes, then the hydrothermal coefficient (HTC) is a complex indicator reflecting both thermal and water regimes of the agroecosystem. The presented data indicate significant differences in the considered indicators between years.

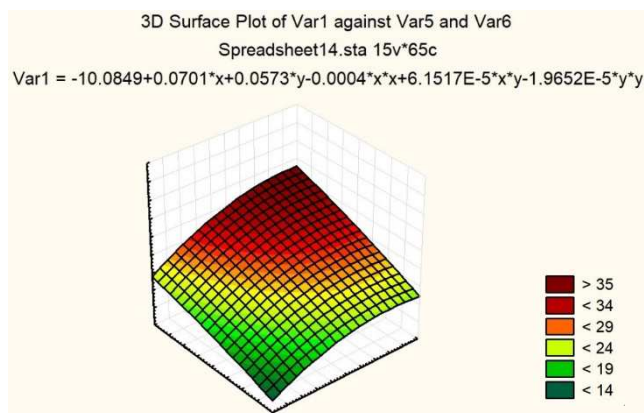
**Table 2.** The sum of active temperatures and the hydrothermal coefficient (HTC) during the growing seasons of 2017–2020

Year	The sum of active temperatures			Hydrothermal Coefficient (HTC)			
	May - June	May - August	June - August	May	June	July	August
2017	573	1,626	1,431	0.45	1.69	2.48	2.83
2018	912	2,154	1,719	0.64	1.02	2.85	2.02
2019	901	1,941	1,600	2.11	1.42	3.52	1.80
2020	778	1,899	1,697	0.59	2.25	3.41	3.80

The correlation matrix, combining the results for all years and all indicators, indicates that the biological yield of potatoes had a closer relationship with the studied factors than the yield of standard products. Therefore, further we give more dependences linking biological production with the studied factors. However, there is a close relationship between biological yields and standard yields (*Y*), approximated by the equation:

$$Y = -4,105 + 0.794 B1 + 0.003 B2 \quad R = 0.956$$

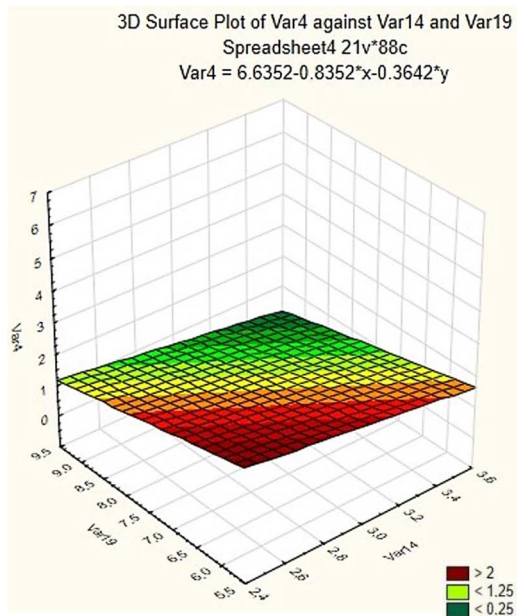
where B1 – total biological yield of potatoes; B2 – Sum of active temperature of May - August.



**Figure 1.** Dependence of the biological yield of potatoes (Var 1) on the compost dose (Var 5) and the sum of active temperatures in May - June (Var 6).  $R = 0.800$ .

We are interested in the relationship between yield of potatoes or proportion of diseased plants and the doses of compost and indicators of weather conditions. For this reason we use the software Program STATISTICA 10 and analysed our data with Multiple Regressions. We tried linear and quadratic dependencies and chosed those equations that had a higher correlation coefficient. Fig. 1 shows the dependence of the biological yield of potato tubers on the level of nitrogen applied with compost and the sum of active temperatures in May - June. Obviously, the presented quadratic function demonstrates non-linear relationships. The compost dose becomes more and more effective as the sum of active temperatures increases in May - June. In addition, it is important to note the great role of the temperature regime at the very beginning of potato development on its final yield. The Fig. 2 demonstrates the dependence of the share of potato tubers on the sum of active temperatures in May - June, at the very beginning of potato plant development, and moisture content in July.

Influence of the compost and the biofungicide Kartofin, SC on potato yield during the growing seasons of 2017–2020 presented in Table 3. The use of the compost in the studied doses or Kartofin, SC (separately) led to an increase in yield by 1.2–1.3 times compared to the control without the use of fertilizer and biofungicide (Table 3).



**Figure 2.** Dependence of the proportion of potatoes tubers damaged by diseases in the total yield (%) Var. 4 on the sum of active temperatures for May - June (Var. 7) and HTC for July (Var. 15) for 2017–2020.  $R = 0.629$ .

**Table 3.** Influence of the compost and the biofungicide Kartofin, SC on potato yield during the growing seasons of 2017–2020

Variants Compost (kg of N ha <sup>-1</sup> )	Biofungicide	Years of investigation				The average yield for 2018–2020 years
		2017	2018	2019	2020	
Total Biological Yield, t ha <sup>-1</sup>						
0	-	-	21.3	23.3	20.8	21.0
80	-	-	29.6	30.9	25.0	28.0
0	Kartofin, SC	17.5	27.7	34.6	23.1	28.5
80	Kartofin, SC	23.0	32.9	35.7	28.5	32.4
160	Kartofin, SC	20.7	33.7	43.0	34.2	37.0
<i>LSD</i> <sub>0,95</sub>		1.6	3.5	5.4	3.4	
Yield of Standard Tubers, t ha <sup>-1</sup>						
0	-	-	17.1	22.8	20.3	20.1
80	-	-	21.3	30.5	25.9	25.9
0	Kartofin, SC	14.0	24.2	29.5	22.5	25.4
80	Kartofin, SC	18.7	27.6	32.0	26.9	28.8
160	Kartofin, SC	17.3	25.8	42.2	31.8	33.3
<i>LSD</i> <sub>0,95</sub>		1.6	1.8	4.0	2.1	

The combined use of compost and Kartofin, SC provided an increase in the yield of the total mass of tubers and standard potato tubers by 1.5 times. It was the synergistic effect of these biological products, which persisted throughout the entire research period for organic potato cultivation during the growing seasons of 2017–2020 (Table 3). Such a steady trend of obtaining the organic potatoes' increased yields in four years is due to the phytosanitary situation improvement in planting potatoes when using the biofungicide Kartofin, SC as well as providing nutrition to potato plants through the use of organic fertilizers. An improvement in the habitus and development of plants, a decrease in the diseases' development of the aerial part during each growing season and, as a consequence, a decrease in the tubers damage by phytopathogens were observed annually. More detailed studies of the potato diseases controlling by the biofungicide during the growing season were carried out in 2020.

**Table 4.** The influence of the biofungicide Kartofin SC and the compost on the spread of fungal diseases on potatoes of the variety Udacha in the growing season 2020

Variants	Prevalence / development of fungal diseases				On tubers, %
	Development phase of aerial potato plants part, %				
	Bud- formation	Blooming	Closing the rows	Before potato herbage cutting	
Control 1 (without biofungicide)	2.3/0.6	29.4/14.2	22.6/11.4	48.1/33.1	100/49.1
Control 2 (without biofungicide) + Compost 80 kg of N ha <sup>-1</sup>	0	16.5/7.3	11.5/6.1	36.2/24.6	100/45.7
Kartofin, SC	0	3.9/1.6	4.1/2.1	20.6/11.2	92.3/44.6
Kartofin, SC + Compost 80 kg of N ha <sup>-1</sup>	0	3.1/1.1	3.2/1.7	30.2/18.6	97.9/38.0

*Note:* disease prevalence / disease development.

The use of the biofungicide Kartofin, SC had a significant effect on the phytosanitary state of the organic potatoes' agroecosystem by the 4th year of research – the growing season 2020 (Tables 3, 4).

The prevalence of fungal diseases on potato plants decreased by 2 times in comparison with the control both without compost and with its use in the studied doses (Table 4). The best effect of using biofungicide was revealed in a threefold decrease in the development of fungal diseases of potato plants (Table 4). A 1.3-fold persistent decrease in the development of fungal diseases on tubers was also observed (Table 4).

The biological effectiveness of the biofungicide Kartofin, SC and the compost, calculated for the 4<sup>th</sup> year of research, is presented in Table 5. The data indicates the high efficiency of the biofungicide in organic growing of potatoes: the prevalence and development of fungal diseases decreased by more than 3 times as in plants by the end of the growing season, and on tubers (Table 4). The efficiency of Kartofin, SC in reducing the prevalence and development of fungal diseases during the growing season and during the formation of tubers was more than 80%. The combination of compost and biofungicide reduced the prevalence and development of fungal diseases on 85–92%, due to the synergistic effect (Table 5).

**Table 5.** Biological efficiency of the biofungicide Kartofin, SC and the compost on Udacha variety potatoes in the growing season 2020

Variants	Biological effectiveness in reducing the prevalence / development of fungal diseases				
	Development phase of aerial potato plants part, %				On tubers, %
	Bud-formation	Blooming	Closing the rows	Before potato herbage cutting	
Compost 80 kg of N ha <sup>-1</sup> (without biofungicide)	100/100	43.8/48.8	49.3/46.1	24.4/25.6	0/6.8
Kartofin SC	100/100	86.8/88.7	82.2/81.2	57.1/66.1	7.7/8.9
Kartofin SC +	100/100	89.9/92.1	86.1/84.8	37.1/43.8	2.1/22.3
Compost 80 kg of N ha <sup>-1</sup>					

Note: disease prevalence / disease development.

Thus, the biological effectiveness of the biological product Kartofin, SC in reducing the prevalence of a complex of fungal diseases (alternariosis, late blight, stem form of rhizoctoniosis) on potato plants of the Udacha variety reached 82.2–89.9%. The development of fungal diseases on potatoes growing on the plots where the biofungicide Kartofin SC was applied was significantly (3–9 times) lower than in the control plots without biofungicide application, during the entire observation period - 1.6–11.2% and 14.2–33.1%, respectively. The biological effectiveness in reducing the development of a complex of fungal diseases was estimated in the range of 81.2–92.1%. A synergistic effect was observed with the combined use of the studied doses of compost and biofungicide Kartofin, SC, leading to a 2–3-fold increase in efficiency.

It was shown that the biofungicide Kartofin SC reduced the infection of tubers in comparison with the control by 5–11%, providing 9–22% efficiency of its application. The biological yield of tubers of the Udacha variety on the control plots without compost application was 20.8 t ha<sup>-1</sup>, with the application of compost - 25.1 t ha<sup>-1</sup>. In variants with

the use of a biofungicide and in combination with compost, this figure reached 23.1–25.8 t ha<sup>-1</sup>. Thus, the use of organic fertilizers and biofungicide provided an increase in the yield of tubers of the Udacha variety by a factor of 1.5 compared to the control without the application of compost and a biofungicide. The yield of standard tubers increased from 20.2 t ha<sup>-1</sup> in the control to 24.1 and 25.1 t ha<sup>-1</sup> with the addition of compost and biofungicide, respectively.

## CONCLUSIONS

1. As a result of the analysis of information for four years, a particular value of the sum of active temperatures in May - June was established to ensure a high yield of organic potatoes and reduce the incidence of tuber diseases.

2. The efficiency of the selected version of the technology for the production of organic potatoes has been confirmed. The combined use of compost at a dose of 4 t ha<sup>-1</sup> and the biofungicide Kartofin, SC made it possible to achieve the yield of standard tubers of 27.3–28.2 t ha<sup>-1</sup> with their low incidence of fungal diseases.

3. The results obtained make it possible to recommend the inclusion of the biofungicide Kartofin SC in the developed technology for the cultivation of organic potatoes. The biofungicide Kartofin, SC had a significant impact on the yield of potatoes of the Udacha variety and the phytosanitary state of the agrobiocenosis of organic potatoes, reducing the prevalence and development of a complex of fungal diseases on vegetative plants and tubers. The biological effectiveness in reducing the development of a complex of fungal diseases was estimated in the range of 81.2–92.1%. A synergistic effect was observed with the combined use of the studied doses of compost and biofungicide Kartofin, SC, leading to a 2–3-fold increase in efficiency.

ACKNOWLEDGEMENTS. This work was supported by the Russian-Finnish project 'Environmentally Friendly Smart Organic Agriculture' (EFSOA) in a frame of the South-East Finland - Russia CBC 2014–2020 Programme.



## REFERENCES

- de Schaetzen, S. 2019. Organic Agriculture and the Sustainable Development Goals: Part of the Solution. *www.nature&more.com*. 76 pp.
- Briukhanov, A., Subbotin, I., Uvarov, R. & Vasilev, E. 2017. Method of designing of manure utilization technology. *Agronomy research* **15**(3), 658–663.
- De, Tulipa & De, L.C. 2019. Disease Management in Organic Agriculture. *International Journal of Recent Scientific Research* **10**(07(B)), 33458–33461. doi: 10.24327/IJRSR
- Guidelines for registration tests of fungicides in agriculture*, 2009, St. Petersburg, 379 pp. (in Russian).
- Minin, V.B., Popov, V.D., Maksimov, D.A., Ustroev, A.A., Papushin, E. & Melnikov, S.P. 2020. Developing of Modern Cultivation Technology of Organic Potatoes. *Agronomy Research*. **18**(S2), 1359–1367.

- Novikova, I.I., Boikova, I.V., Pavlyushin, V.A., Zeiruk, V.N., Vasilyeva, S.V., 2019. Derevyagina M.K. Bacterial strain *Bacillus subtilis* B-94 VISR for protection of potatoes from diseases during vegetation and storage, increase of yield and improvement of quality of tubers. *Patent of the Russian Federation* No. 2729576 dated 06.12.2019.
- Popov, V.D., Minin, V.B., Maksimov, D.A. & Papushin, E.A. 2018. Justification of the intellectual system of organic production management in crop production. *Technologies and technical means of mechanized production of crop and livestock products: Theor. and scientific. - prakt. journal/IAEP*, **94**. St. Petersburg, 2018, 28–41. doi 10.24411/0131-5226-2018-10086 (in Russian).
- Reganold, J. P. & Wachter, J. M. (2016). Organic agriculture in the Twenty–first century. *Nature Plants* **2**(2), 15221. doi: 10.1038/nplants.2015.221.
- Shabanov, A.E., Zhevara, S.V., Anisimov, B.V., Kiselev, A.I., Dolgova, T.I., Malyuta, O.V. & Zebrin, S.N. 2016. *Parameters of potential yield of potato varieties of the selection center VNIKH*, (reference) / FSBIU VNIKH; M., 13 pp. (in Russian).
- Titova, J.A., Novikova, I.I., Boykova, I.V., Pavlyushin, V.A. & Krasnobaeva, I.L. 2019. Novel solid-phase multibiorecycled biologics based on *Bacillus subtilis* and *Trichoderma asperellum* as effective potato protectants against *Phytophthora* disease. *Sel'Sokhozyaistvennaya biologiya [Agricultural Biology]*, **54**(5), 1002–1013. doi: 10.15389/agrobiology.2019.5.1002 eng.
- Van Bruggen Ariena, HC, A Gamlielb Abraham, Maria R Finckh. 2015. Plant disease management in organic farming systems. Review. *wileyonlinelibrary.com*. doi 10.1002/ps.4145

## **Diagnosis of the functional state of transformed acid soils agroecosystems depending on long-term anthropogenic loads**

Y. Olifir<sup>\*</sup>, A. Habryel, T. Partyka, O. Havryshko and H. Konyk

Institute of Agriculture of Carpathian region NAAS, 5, Hrushevskoho Str., UA81115 Obroshyne, Pustomyty district, Lviv region, Ukraine

<sup>\*</sup>Correspondence: [olifir.yura@gmail.com](mailto:olifir.yura@gmail.com)

Received: March 6<sup>th</sup>, 2021; Accepted: June 11<sup>th</sup>, 2021; June 22<sup>nd</sup>, 2021

**Abstract.** The main priority of agro-industrial production has always been and remains to provide the global population and its yearly increments with food. The issue of soil fertility improvement is still the most important task of agricultural science. The assessment of the agroecological condition of Albic Stagnic Luvisol using carbon dioxide emission, redox potential, and biotic activity was carried out, based on modern methodological approaches, such as soil quality evaluation via ecologically-related biological parameters. Carbon dioxide emission, redox, and biological processes in long-term stationary experiment depend on the degree of soil acidity reduction. Soil acidification can be minimized through chemical melioration with the combined application of different doses of mineral fertilizers and manure. It was found that carbon dioxide emission is optimal in an organo-mineral fertilizing system with application of 10 t of manure per 1 ha and N<sub>65</sub>P<sub>68</sub>K<sub>68</sub> with lime dose (2.5 t ha<sup>-1</sup>) calculated according to pH buffering capacity. It is due to oxidative and moderately oxidative conditions created. This organo-mineral fertilizing system also increases the number of aerobic bacteria and overall biological activity. The mineral fertilization and the use of Albic Stagnic Luvisol without fertilizers are accompanied by increased mineralization, growth of reductive processes, and the number of moulds. Studies have shown that it is advisable to include CO<sub>2</sub> emission, redox potential and biological activity along with physicochemical and agrochemical soil properties to assess the influence of different anthropogenic loads on soil formation.

**Key words:** acidity, Albic Stagnic Luvisol, CO<sub>2</sub> emission, fertilizers, liming, redox potential, microbiological activity.

**Used abbreviations:** Eh: soil redox potential; rH<sub>2</sub>: Clark's index; CFU: colony-forming unit; n: norm; HA: humic acids; FA: fulvic acids; NAAS: National Academy of Agrarian Sciences of Ukraine.

### **INTRODUCTION**

Solving the problem of food security and providing the global population and its yearly increments with food has always been and remains the main priority of agro-industrial production (Parikh & James, 2012; Yemets, 2012; Calicioglu, 2019). So, the issue of soil fertility improvement is one of the most important tasks of agricultural

science (Havlin & Heiniger, 2020). Studies aimed at preserving and maintaining the stability of ecosystems and their components are especially relevant due to the current climate change and intense anthropogenic impact.

Precision agriculture is crucial to the formation of a profitable and high-quality harvest through continuous monitoring of the basic functions of soils, timely correction and implementation of individual components of agricultural technologies. The natural potential fertility of Albic Stagnic Luvisol (WRB, 2015) in Ukrainian Western Forest-Steppe is only 1.2–1.4 t ha<sup>-1</sup> of grain units due to high acidity and low nutrient content. Though its acidity is genetically inherited, an efficient system of fertilizers and agro-melioration can prevent its further acidification. Nowadays soil acidification on a global scale leads to deterioration of agro-ecological status and loss of fertility - the main function of soils (Tian & Niu, 2015; Goulding, 2016; Neina, 2019).

Diagnosis of fertility elements through soil testing and optimization of their condition is a key principle for the balanced use of acidic soils. Fertility elements are defined as elementary material carriers of soil regimes that are involved in the biological cycle and directly affect plant growth and development (Truskavetskyi et al., 2020).

It should be noted that in recent years the average global concentration of greenhouse gases in the atmosphere, including carbon dioxide, is increasing due to significant climate change (Green et al., 2019). Carbon dioxide flows from the soil into the atmosphere depend primarily on the processes that occur in the soil under the influence of various anthropogenic factors during land use, such as disturbance of soil aggregates (Ontl & Schulte, 2012). The imbalance of soil carbon cycles leads to the loss of both organic matter, essential available nutrients and additional entry of greenhouse gases into the atmosphere, which further intensifies the global warming effects (Popirnyi et al., 2020).

Therefore, a clear account of the C-CO<sub>2</sub> flow to the atmosphere is necessary for assessing peculiarities of carbon dioxide production by soils. It is also important to identify trends in soil properties changes (Trofymenko et al., 2019). The values of CO<sub>2</sub> emission together with soil ability to sequester it are an important component of sustainable land use in the context of climate change.

The quantitative characteristics of the processes occurring in the soil environment, their direction and their intensity are reflected in the redox potential. However, the absolute values of the redox potential do not always adequately represent redox conditions created in different agroecosystems, as the intensity of the redox potentials is significantly affected by the reaction of the environment. Soil redox potential (Eh) and pH are the main parameters of plant growth that determine soil fertility (Kanwar, 2015; Cottes et al., 2020). The relationship between them is reflected by Clark's index (rH<sub>2</sub>):

$$rH_2 = \frac{Eh}{30} + 2 pH \text{ (Mamontov et al., 2006).}$$

Redox potential is the most readily available indicator of the soil redox system. It covers the entire range in which the various inorganic redox systems operate (Yu & Rinklebe, 2013). The redox potential of aerobic soils, which are mostly cultivated, is given little attention. Although this important parameter cannot be ignored, as the transformation of plant residues, rate of organic substances accumulation and composition are closely related to Eh. The redox processes are also associated with the conversion of nitrogen compounds, phosphorus, sulphur, iron, manganese in soils (Kyrylchuk & Bonishko, 2011).



An important diagnostic indicator that objectively assesses the state of edaphic comfort is the biological activity of the soil (El-Ramady et al., 2014). The living part of the soil not only provides the mineralization and immobilization mechanism of organic matter but also performs several global regulatory functions in the formation of soil fertility. Therefore, due to the high lability, microorganisms are sensitive to transformations that occur in the soil during its agricultural use and can serve as environmental indicators of these changes (Symochko et al., 2017).

Redox potential and pH of the soil largely determine the types of metabolism that occur in the bacterial community in the early stages of development, and therefore are important parameters of biological activity and affect the development of microorganisms (Husson, 2013).

Such studies are especially relevant for Albic Stagnic Luvisol, which occupy large areas in Europe and Ukrainian Western Forest-Steppe zone in particular. They are characterized by the high acidity of the soil solution and low fertility. Due to climate change, the problem of environmentally friendly use of acidic soils has become much more acute. Systematic management of soil fertility makes it possible to normalize anthropogenic loads harmonizing soil productive functions with ecological ones (Truskavetskyi & Tsapko, 2016).

Obtaining objective information about the state and changes of the agroecosystems, their components under the influence of various agrogenic factors is possible only in stationary experiments. In this regard the results of the impact assessment of long-term agricultural loads with different doses and ratios of fertilizers, manure and lime in a long-term stationary experiment are noteworthy.

Our research aimed to evaluate the impact of long-term application of various fertilizing systems and periodic liming on the agro-ecological condition of the soil using informative diagnostic indicators of carbon dioxide emission, redox potential and biological activity for effective management of Albic Stagnic Luvisol fertility.

## MATERIALS AND METHODS

Research work was performed during IX crop rotation in the classical stationary experiment (49°47'54.3"N 23°52'26.9"E) of the Laboratory of Agricultural Chemistry (Institute of Agriculture of the Carpathian region NAAS), established in 1965 and registered as a long-term agricultural field experiment of NAAS (NAAS registration certificate No. 29).

The long-term experiment is placed on three fields, each has 18 variants in triplicate. The location of the variants is single-tiered, equential. The total plot area is 168 m<sup>2</sup>, accounting - 100 m<sup>2</sup>. Crop rotation is four-field with the following crops: corn for silage - spring barley with the sowing of meadow clover - meadow clover - winter wheat. Agricultural cultivation techniques, tillage and crop care are standard for the Ukrainian Western Forest-Steppe zone.

The agrochemical characteristics of the arable layer of Albic Stagnic Luvisol before the experiment start were as follows: humus content (according to Tyurin) 1.42%, pH<sub>KCl</sub> 4.2, hydrolytic acidity (according to Kappen) 4.5, exchangeable acidity (according to Sokolov) - 0.6 mg-eq 100 g<sup>-1</sup> of soil, the content of mobile aluminium 60.0, mobile phosphorus (according to Kirsanov) and exchangeable potassium (according to Maslova) - 36.0 and 50.0 mg kg<sup>-1</sup> of soil respectively.

After 50 years of soil use, these values in control variant without fertilizers have not undergone significant changes: humus content is 1.48%,  $\text{pH}_{\text{KCl}}$  4.3, hydrolytic acidity 4.5 mg-eq 100 g<sup>-1</sup> of soil, the content of mobile aluminium 60.7, mobile phosphorus and exchangeable potassium (according to Kirsanov) are 36.5 and 46.3 mg kg<sup>-1</sup> of soil respectively. Different fertilizer systems led to significantly opposite changes in soil properties. Optimal organo-mineral fertilizer system with liming led to lowering of hydrolytic acidity up to 2.28 mg-eq 100 g<sup>-1</sup>, mobile aluminium content - 4.20 mg kg<sup>-1</sup> and increasing humus content to 1.93%,  $\text{pH}_{\text{KCl}}$  5.38, mobile phosphorus and exchangeable potassium to 188.6 and 190.4 mg kg<sup>-1</sup> of soil respectively. Mineral fertilizer systems caused much lower humus content (1.59%),  $\text{pH}_{\text{KCl}}$  4.12, an increase of hydrolytic acidity to 4.69 mg-eq 100 g<sup>-1</sup>, mobile aluminium to 75.0, mobile phosphorus and exchangeable potassium to 167.5 and 128.8 mg kg<sup>-1</sup>, respectively.

Semi-overripe cattle manure with straw bedding, ammonium nitrate (34.5%), granular superphosphate (19.5%), potassium salt (40%), nitroammophos (NPK 16%) was used in the experiment. When using nitroammophos, NPK content was balanced with simple fertilizers. Manure (40–60 t ha<sup>-1</sup>) was applied before corn crops. Phosphorus-potassium fertilizers were applied in autumn, and nitrogen fertilizers - before pre-sowing cultivation. Liming according to the scheme was performed before the ninth crop rotation. Limestone flour (93.5% CaCO<sub>3</sub>) was used as limestone material. Starting from the VIII rotation the second mow of meadow clover was ploughed as an organic fertilizer in all variants of the experiment.

Carbon dioxide emission was studied in 2016–2018 in the phases of spring tillering (BBCH26), stem elongation (BBCH31-33), and full ripeness (BBCH89) during winter wheat vegetation. It ends the ninth crop rotation. CO<sub>2</sub> measurements were carried out in plots with different fertilizer system. The experimental factors were: liming, organic and mineral fertilizers. The variants included:

- control (without fertilizer, var. 1);
- organo-mineral fertilizing system (10 t of manure per ha of crop rotation area + N<sub>65</sub>P<sub>68</sub>K<sub>68</sub>) with periodic liming by 1.0 n of CaCO<sub>3</sub> (6.0 t of limestone flour per ha) according to hydrolytic acidity (var. 7);
- the same fertilizing system with an optimal dose of lime (2.5 t ha<sup>-1</sup>), calculated according to acid-base buffering capacity (var. 8);
- mineral fertilizing system (N<sub>105</sub>P<sub>101</sub>K<sub>101</sub>) with liming by 1.5 n of CaCO<sub>3</sub> (9.0 t ha<sup>-1</sup>) according to hydrolytic acidity (var. 17);
- the same fertilizing system with applying CaCO<sub>3</sub> (2.5 t ha<sup>-1</sup>) according to acid-base buffering capacity (var. 18);
- mineral fertilizing system (N<sub>65</sub>P<sub>68</sub>K<sub>68</sub>, var. 15).

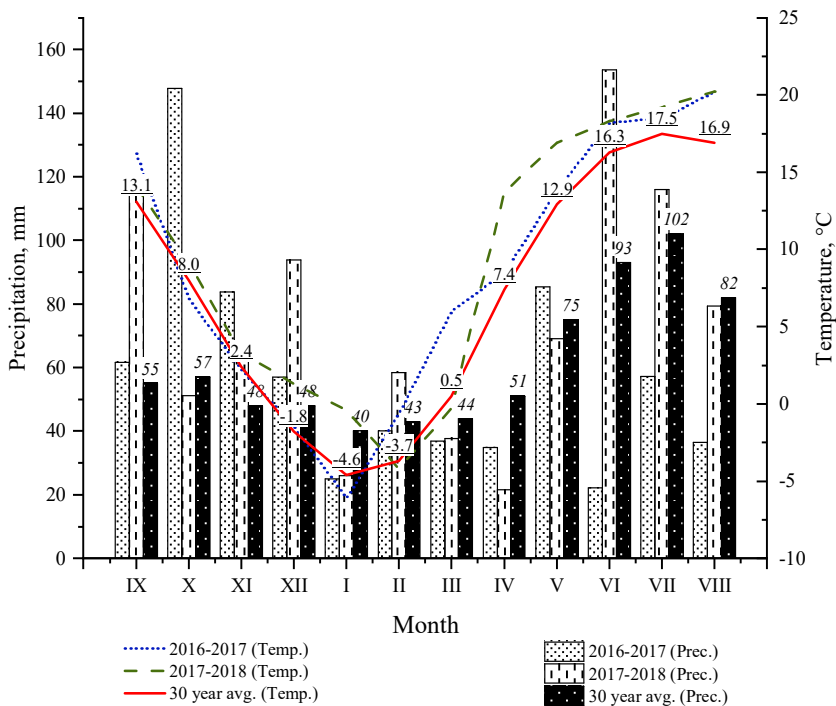
CO<sub>2</sub> measurements from soil surface were made in the field on a two-channel infrared gas analyser CO<sub>2</sub>-meter 'K-30 Probe' and related software (DAS 100) using standard procedures (Pumpanen et al., 2004). Measurements were performed 3–5 times a day followed by a determination of the average value.

The redox potential was measured with a pH-150MA millivoltmeter following DSTU ISO 11271:2004.

Soil samples from the arable layer of Albic Stagnic Luvisol (0–25 cm) were prepared by DSTU ISO 11464-2001 after winter wheat harvesting. Laboratory and analytical studies were performed in a certified agrochemical laboratory of the Institute

of ACR NAAS. The  $pH_{KCl}$  determination was performed by potentiometric method at 1:2.5 soil:KCl ratio using a pH meter ‘pH-301’ and glass electrodes (DSTU ISO 10390:2007). The population of microorganisms of the main ecological and trophic groups was enumerated by culturing selected soil samples (soil suspension) on special growth media (agar, Endo and Sabouraud). Viable plate count was conducted in 21 days depending on the growth rate and physiological characteristics of the group. Proteolytic and total biological activity of the soil was determined by application method according to the intensity of decomposition of the gelatine layer of X-ray film and linen cloth respectively. The films were buried for 30 days in the upper fertile layer of soil (0–25 cm) in triplicate. After digging out and drying, the degree of decomposition of the fabric and the gelatine layer was determined as a percentage.

Climatic conditions during the 2016–2018 years of research had their peculiarities. The average temperature was higher compared to the long-term average (7.1 °C). The deviation of the average monthly air temperature was + 1.4–2.2 °C in spring and + 1.9–2.8 °C in summer. The amount of precipitation in the 2016–2017 season was insufficient throughout the growing period (total precipitation: 688 mm). In April-May there was a decrease in rainfall by 11.7–4.2 mm. The subsequent period of intensive growth and crop formation was characterized by an even greater shortage in the summer months (June-August) - 13.6–34.5 mm. The second season was wet (887.5 mm), compared to the average long-term data (738 mm) (Fig. 1).



**Figure 1.** Agrometeorological parameters of the two growing seasons.

Statistical processing of the obtained research results was performed using OriginPro 2019b software (OriginLab Corporation, USA, 2019). Data were compared using the *Tukey test*. Differences between samples were considered statistically significant at  $P < 0.05$ . The data in the tables are presented as the arithmetic mean with standard deviation ( $x \pm SD$ ).

## RESULTS AND DISCUSSION

The intensity of CO<sub>2</sub> emission in the field of winter wheat was lowest in the control plots (var. 1) - 7.3–13.5 ppm min<sup>-1</sup> and 8.7–13.0 ppm min<sup>-1</sup> in the variant of the mineral fertilizing system (var. 15). Under the organo-mineral fertilizing system with liming with 1.0 n of CaCO<sub>3</sub> according to hydrolytic acidity (var. 7), it was 10.5–14.7 ppm min<sup>-1</sup>. It slightly exceeded the same fertilizing system with lime application calculated by acid-base buffering capacity (var. 8).

In summer emission of CO<sub>2</sub> increased in all variants and amounted to 20.5 ppm min<sup>-1</sup> in control and under mineral fertilization. In the variant of the organo-mineral fertilizing system with liming by 1.0 n of CaCO<sub>3</sub> according to hydrolytic acidity, it was 18.7 against 14.5 ppm min<sup>-1</sup> of the same fertilizing system with CaCO<sub>3</sub> dose calculated by the acid-base buffering capacity. Calculation of lime dose by pH buffering capacity optimizes the CO<sub>2</sub> flow during a period of intensive growth and development of plants. Instead, the application of high doses of lime calculated by hydrolytic acidity contributes to the increase in mineralization processes and unproductive loss of soil carbon (Tsapko et al., 2018).

According to Fuentes et al. (2006), the fast CO<sub>2</sub> release from the soil after liming is a result of two parallel processes: a chemical process, as a consequence of the CaCO<sub>3</sub> hydrolysis reaction in the soil; a biological, caused by increased microbial activity due to improved soil conditions (higher pH, better availability of organic substrates etc.). The effect of lime on CO<sub>2</sub> release is proportional to the liming rate.

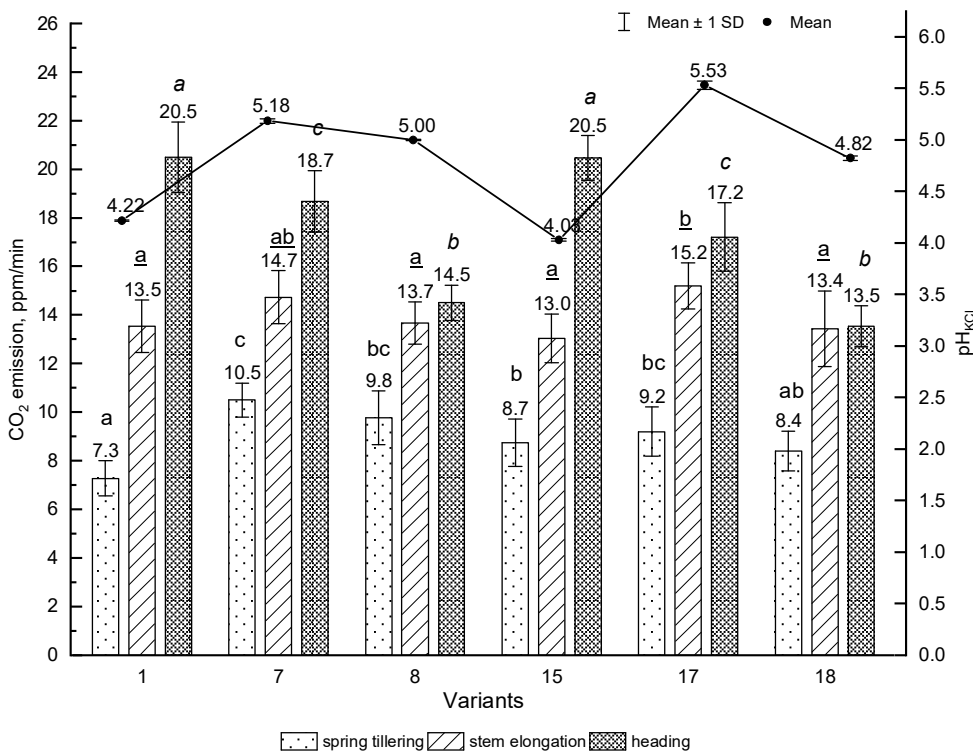
In a mineral fertilizing system with liming by 1.5 n of CaCO<sub>3</sub> according to hydrolytic acidity, the intensity of CO<sub>2</sub> release also exceeded the variant with the same fertilizing system on the background of lime application calculated by acid-base buffering capacity and was 17.2 and 13.5 ppm min<sup>-1</sup> respectively (Fig. 2).

Thus, the dynamics of CO<sub>2</sub> emission in the field of winter wheat during plant growth and development confirms that the introduction of high doses of lime calculated by hydrolytic acidity is accompanied not only by significant material costs but also environmental problems, increasing the concentration of carbon dioxide in agroecosystems.

In our previous studies conducted in the VII-VIII crop rotations on Albic Stagnic Luvisol, it was found that emission of carbon dioxide in the field of corn for silage after application of lime and fertilizers as well as its aftereffect under spring barley is the highest in organo-mineral and mineral fertilizing systems on the background of liming with the 1.0–1.5 norm of CaCO<sub>3</sub> by hydrolytic acidity. It significantly outweighs the same fertilizing system with the background of liming by an optimal dose of CaCO<sub>3</sub> calculated by pH buffering capacity (Habriel et al., 2016).

It is noteworthy that under the mineral fertilizing system in the field of winter wheat, the intensity of CO<sub>2</sub> emission is quite high and close to absolute control. At a low level of crop formation (1.97–2.58 t ha<sup>-1</sup>), this indicates additional losses of mobile

organic matter compounds at high acidity of the soil solution ( $\text{pH}_{\text{KCl}} = 4.03$  and  $4.22$  respectively). It was found in previous studies, that in these variants is a present accumulation of mobile 1 + 1 'a' fraction of fulvic acids, which are capable of rapid mineralization and migration in the soil profile (Snitynskyi et al., 2015). This dependence together with a decrease in  $\text{pH}_{\text{KCl}}$  indicates the negative consequences of this anthropogenic impact and leads to increased soil degradation.



**Figure 2.** CO<sub>2</sub> emission under winter wheat during the period of intensive growth and development, the end of ninth crop rotation ( $LSD_{05} \text{ CO}_2 = 0.52 \text{ ppm min}^{-1}$ ,  $n = 6$ ). Mean values labelled with the same letter are not significantly different from each other according to the results of comparison using the *Tukey test* ( $P < 0.05$ ); different lowercase letters indicate statistical significance between variants in the phase of spring tillering; underlined - in the phase of stem elongation; italic - in the heading phase.

Our studies have shown that during long-term ploughing (more than 50 years) of Albic Stagnic Luvisol on the variant without fertilizing (control), the redox potential in the profile varied from moderately oxidative 514 mV in arable and sub-arable soil horizons to weakly oxidative 494 mV in Ehg and 458 mV in Beg soil horizons. The  $\text{pH}_{\text{KCl}}$  in control underwent the following changes: 4.22; 4.18; 4.31; 4.13. Weak oxidative conditions (446 mV) at  $\text{pH}_{\text{KCl}}$  4.22–4.47 were observed in the illuvial and BCg (440 mV) horizons. In parent CBg horizon, Eh was at the level of 437 mV. Long-term crop rotation, ploughing of organic residues (stubble, 2nd mow of meadow clover) in control without fertilizers leads to the development of weakly oxidative redox processes in the genetic horizons of the soil (Table 1).

Under organo-mineral fertilizing system on the background of liming with a full dose of CaCO<sub>3</sub> by hydrolytic acidity, there was a more contrasting change in Eh compared to the control. The elevated value of the Eh potential 628 mV in the AEg(arable) horizon indicates the development of intense oxidative processes in it. In AEg(sub-arable) and Ehg horizons, Clark's index is 29.3 and 27.1. Conditions in these layers are characterized as moderately oxidative. Down from Beg horizon (depth 51 cm), Eh varied sharply from weakly oxidative (420 mV) to weakly reductive processes in the underlying Bg and BCg genetic horizons (388–370 mV respectively). The lowest values of redox potential (363 mV) and weakly reductive redox regime for this fertilizing system was observed in strongly illuviated and strongly gleyed BCG horizon with Clark's index of 20.2 and pH<sub>KCl</sub> of 4.05.

Prolonged application of only mineral fertilizers on Albic Stagnic Luvisol resulted in the redox potential decrease in all genetic horizons compared to the control without fertilizers (Table 1). Such changes are caused by unsatisfactory agrophysical soil properties, an increase in gley content, acidity, and mobile aluminium compounds, and a decrease in aeration and organic matter content (Tkachenko et al., 2017).

**Table 1.** Change of redox potential in the profile of Albic Stagnic Luvisol depending on different anthropogenic loads ( $\bar{x} \pm SD$ ,  $n = 6$ )

Genetic horizons	Horizon thickness (m)	pH <sub>KCl</sub>	Eh (mV)	rH <sub>2</sub>
Without fertilizers (control) (var. 1)				
AEg(arable)	0–0.18	4.22 ± 0.02 <sup>a</sup>	514 ± 7.1 <sup>a</sup>	25.6
AEg(sub-arable)	0.18–0.31	4.18 ± 0.01 <sup>ac</sup>	514 ± 7.2 <sup>a</sup>	25.5
Ehg	0.31–0.64	4.31 ± 0.01 <sup>b</sup>	494 ± 8.2 <sup>a</sup>	25.1
Beg	0.64–1.10	4.13 ± 0.01 <sup>c</sup>	458 ± 8.5 <sup>b</sup>	23.5
Bg	1.10–1.31	4.22 ± 0.03 <sup>a</sup>	446 ± 5.2 <sup>b</sup>	23.3
BCg	1.31–1.80	4.47 ± 0.02 <sup>e</sup>	440 ± 9.5 <sup>b</sup>	23.6
CBg	1.80–2.00	4.35 ± 0.03 <sup>b</sup>	437 ± 7.1 <sup>b</sup>	23.3
-	<i>LSD</i> <sub>05</sub>	0.15	-	-
N <sub>105</sub> P <sub>101</sub> K <sub>101</sub> + 10 t of manure per ha + CaCO <sub>3</sub> (1.0 by hydrolytic acidity) (var. 12)				
AEg(arable)	0–0.20	5.15 ± 0.01 <sup>a</sup>	628 ± 11.5 <sup>a</sup>	31.2
AEg(sub-arable)	0.20–0.33	5.10 ± 0.01 <sup>b</sup>	575 ± 11.2 <sup>b</sup>	29.3
Ehg	0.33–0.51	4.24 ± 0.02 <sup>c</sup>	560 ± 6.7 <sup>b</sup>	27.1
Beg	0.51–0.77	3.88 ± 0.01 <sup>d</sup>	420 ± 6.0 <sup>c</sup>	21.7
Bg	0.77–1.38	3.85 ± 0.01 <sup>d</sup>	388 ± 6.0 <sup>d</sup>	20.6
BCg	1.38–1.87	3.97 ± 0.01 <sup>e</sup>	370 ± 6.8 <sup>de</sup>	20.2
BCG	1.87–2.10	4.05 ± 0.02 <sup>f</sup>	363 ± 5.7 <sup>e</sup>	20.2
-	<i>LSD</i> <sub>05</sub>	0.74	-	-
N <sub>65</sub> P <sub>68</sub> K <sub>68</sub> (var. 15)				
AEg(arable)	0–0.22	4.03 ± 0.01 <sup>ad</sup>	426 ± 10.3 <sup>a</sup>	22.3
AEg(sub-arable)	0.22–0.35	3.98 ± 0.01 <sup>bd</sup>	416 ± 12.0 <sup>ba</sup>	21.8
Ehg	0.35–0.61	4.17 ± 0.01 <sup>c</sup>	398 ± 8.5 <sup>b</sup>	21.6
Beg	0.61–0.87	4.00 ± 0.01 <sup>d</sup>	368 ± 8.7 <sup>c</sup>	20.3
Bg	0.87–1.50	4.07 ± 0.01 <sup>a</sup>	323 ± 6.4 <sup>d</sup>	18.9
BCg	1.50–1.80	4.04 ± 0.01 <sup>a</sup>	318 ± 9.6 <sup>d</sup>	18.7
CBG	1.80–2.00	4.11 ± 0.02 <sup>e</sup>	311 ± 5.9 <sup>d</sup>	18.6
-	<i>LSD</i> <sub>05</sub>	0.09	-	-

Note: values that have at least one identical letter within a table row do not differ in the Tukey test ( $P < 0.05$ ).

Decreased redox potential leads to excessive accumulation of  $\text{Fe}^{2+}$ ,  $\text{Mn}^{2+}$  and  $\text{Al}^{3+}$  compounds, toxic to plants (Kyrylchuk & Bonishko, 2011). This contributes to even greater acidification of soils and adversely affect plant nutrition, which ultimately dramatically reduces crop yields and leads to soil degradation.

As a result, the inclusion of Albic Stagnic Luvisol in the system of agriculture while using only mineral fertilizers is accompanied by changes in the redox potential in the direction of reduction - i.e., strengthening of reductive processes.

At the same time, a decrease of Eh value in the lower soil horizons in the mineral fertilizing system and control variants also indicates an increase in reductive processes due to worsening of aeration consequently to soil waterlogging, which is due to disruption of soil air exchange with atmospheric air and significantly reduced oxygen diffusion rate.

Redox fluctuations influencing the microbial cenosis of the soil. In particular, fungi grow better than bacteria under moderate reduction conditions at  $\text{Eh} > +250$  mV, while bacteria grow better at  $\text{Eh} < 0$  (Seo & DeLaune, 2010). Similarly, each species of microorganism is adapted to a certain pH range (Lauber et al., 2009).

The reason for the low biological activity of control and in the case of long-term use of the only mineral fertilizing system is a small number of crop residues used by microflora as nutrient and energy material at high acidity of the soil solution ( $\text{pH}_{\text{KCl}} 4.20\text{--}4.05$ , hydrolytic acidity  $4.68\text{--}5.03$  cmol  $\text{kg}^{-1}$  of soil).

Studies have shown that the mineral fertilizing system with optimal norms of lime calculated by acid-base buffering capacity together with a decrease in  $\text{pH}_{\text{KCl}}$  to 4.56 and an increase in hydrolytic acidity to  $3.77$  cmol  $\text{kg}^{-1}$  of soil caused a decrease in total biological and protease activity to 22.70 and 4.15% respectively. Under this fertilizing system, but with  $\text{CaCO}_3$  application according to hydrolytic acidity ( $\text{pH}_{\text{KCl}} 5.65$ , hydrolytic acidity  $1.80$  cmol  $\text{kg}^{-1}$  of soil), total biological and protease activities were higher and amounted to 29.47 and 4.52% respectively. Therefore, there is a direct relationship between the value of acidity ( $\text{pH}_{\text{KCl}}$ ) and biological activity of the soil.

The number of microorganisms in soil depends on and liming. The largest number of aerobic bacteria in one gram of soil (microbial count) was found in the variant with a joint application of mineral, organic fertilizers and liming -  $3.4 \cdot 10^{10}$  CFU  $\text{g}^{-1}$ . The smallest amount  $2.8 \cdot 10^7$  CFU  $\text{g}^{-1}$  was in the control and the mineral fertilizing system. The application of manure and lime had a particularly favourable effect on the number of saprophytic bacteria, increasing their number by 2–4 times compared to the control and the variant with mineral fertilizing. This is primarily due to the much larger inflow of organic residues into the soil and the acidity neutralization of the soil solution.

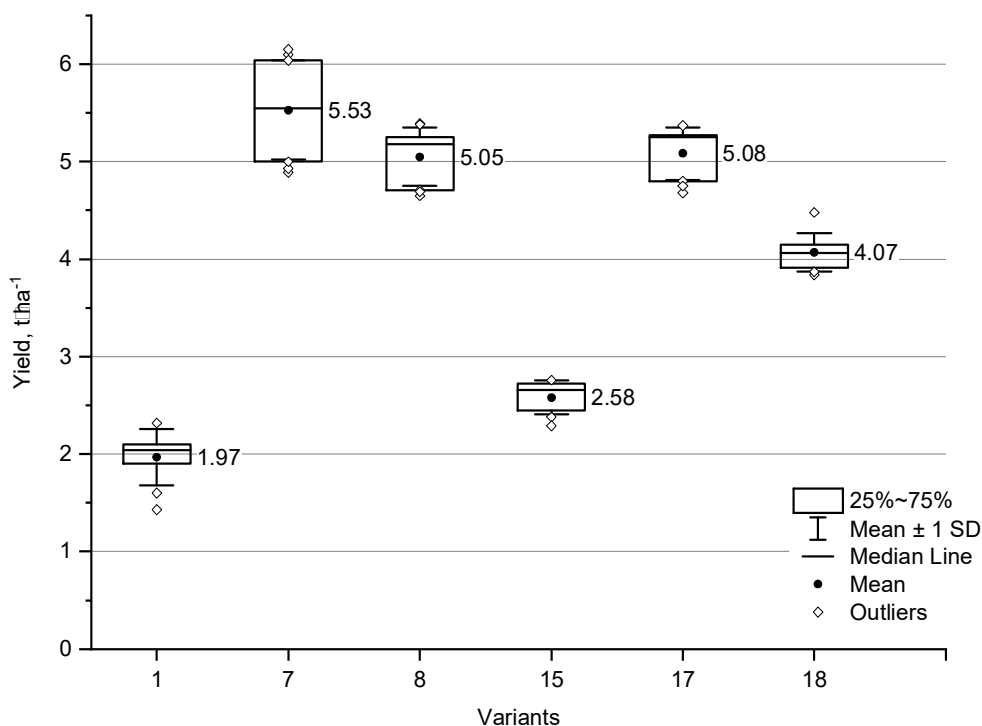
Unsatisfactory physicochemical properties of the soil in mineral fertilizing and control variants are due to the critically low  $\text{pH}_{\text{KCl}}$  value (4.05–4.22) for the growth and development of most crops, high content of mobile aluminium compounds ( $11.8\text{--}60.0$  mg  $\text{kg}^{-1}$ ), calcium deficiency ( $20\text{--}18$  mg  $\text{kg}^{-1}$ ), humate-fulvate type of humus ( $C_{\text{HA}} : C_{\text{FA}} = 0.64$ ). Under such unfavourable soil conditions, the growth and development of the plants' root system, its functional properties (both absorbable and excretory) are slowed down.

The largest number of moulds was observed in the control without fertilizers and only mineral fertilizers variants (17–18 thousand CFU  $\text{g}^{-1}$  of soil). In the variants of organo-mineral and mineral fertilizing with liming, the number of micromycetes decreased to 10–9 thousand CFU  $\text{g}^{-1}$  of soil.

Studies conducted in the long-term stationary experiment of the Institute of ACR showed that the content of the *Escherichia coli* bacteria group, which belong to potentially pathogenic bacteria and have high environmental plasticity, is significantly lower than the content of other microorganisms. It changes slightly in the experimental variants and their number to some extent depends on humidity and temperature (Snitynskyi et al., 2014).

Systematic fertilization and periodic liming improve the physicochemical, agrochemical and biological properties, primarily due to the reduction of soil acidity. So it is possible to obtain rather high and stable yields of crops in the conditions of Albic Stagnic Luvisol.

The highest grain yield of winter wheat ( $5.53 \pm 0.58 \text{ t ha}^{-1}$ ) was provided by the organo-mineral fertilizing system with periodic liming by one norm of lime. The increase is  $3.56 \text{ t ha}^{-1}$  compared to the control without fertilizers, where the value of winter wheat yield was  $1.97 \pm 0.29 \text{ t ha}^{-1}$ . The use of the same fertilizing system but with an application of an optimal lime dose calculated according to acid-base buffering capacity increased the yield of winter wheat to  $5.05 \pm 0.32 \text{ t ha}^{-1}$  (Fig. 3).



**Figure 3.** Influence of different fertilizing systems and periodic liming on the yield of winter wheat,  $\text{t ha}^{-1}$  ( $n = 9$ ).

Intensive mineral fertilizing with an application of only mineral fertilizers in crop rotation for more than 50 years provided a winter wheat yield of  $2.58 \pm 0.12 \text{ t ha}^{-1}$ , which is only 0.61 higher than the control variant. A sufficiently high winter wheat productivity ( $5.09 \pm 0.31 \text{ t ha}^{-1}$ ) was ensured by the joint application of 1.5 norms of mineral



fertilizers and 1.5 norms of CaCO<sub>3</sub> according to hydrolytic acidity. Liming with a dose of CaCO<sub>3</sub> calculated by acid-base buffering capacity formed a slightly lower yield of 4.08 ± 0.20 t ha<sup>-1</sup>.

The traditional acidic soils cultivation system of applying high doses of lime, calculated according to hydrolytic acidity does not provide progressive development of soil formation processes on an environmentally friendly basis due to significant leaching of calcium in groundwater, excessive mineralization and emission of carbon dioxide. In short-term crop rotation, it is expedient to apply lime fertilizers at a dose calculated by pH buffering capacity with repeated liming before each of the following rotations (shorter than 5-year interval) (Loide, 2010.). It will provide a gradual shift of acid-base balance and environmentally safe use of acidic soils.

## CONCLUSIONS

It is advisable to use carbon dioxide emission, redox potential and biotic activity along with agronomic characteristics as informative diagnostic indices of Albic Stagnic Luvisol to substantiate the optimal doses of fertilizers and lime, ensure balanced natural cycles of substances and high fertility level. They allow quantifying different levels of anthropogenic impact on the transformation of the agroecosystems.

An organo-mineral fertilizing system with liming by CaCO<sub>3</sub> dose based on pH buffering capacity optimizes carbon dioxide emission to the greatest extent by creating oxidative and moderately oxidative conditions, increasing the number of aerobic bacteria and overall biological activity. Mineral fertilizing system and the inclusion of Albic Stagnic Luvisol in agriculture without fertilizers provide a low level of crop productivity, which is accompanied by additional CO<sub>2</sub> losses due to mineralization of mobile humus compounds. Together with a decrease in pH<sub>KCl</sub>, it leads to a strengthening of reductive processes and soil degradation. Such conditions ensure a decrease in total biological and protease activity and an increase in the number of fungal microflorae.

Thus, in short crop rotations, it is advisable to apply lime fertilizers at a dose calculated by pH buffering capacity with repeated liming before each rotation. This will ensure a gradual shift in acid-base balance and environmentally safe use of acidic soils while obtaining high productivity.

## REFERENCES

- Calicioglu, O., Flammini, A., Bracco, S., Bellù L. & Sims, R. 2019. The Future Challenges of Food and Agriculture: An Integrated Analysis of Trends and Solutions. *Sustainability* **11**(1), 1–21. <https://doi.org/10.3390/su11010222>
- Cottes, J., Saquet, A., Palayret, L., Husson, O., Beghin, R., Allen, D., Scheiner, J., Cabanes, C. & Guirese, M. 2020. Effects of soil redox potential (Eh) and pH on growth of sunflower and wheat. *Archives of Agronomy and Soil Science* **66**(4), 473–487. <https://doi.org/10.1080/03650340.2019.1622096>
- El-Ramady, H.R., Alshaal, T., Amer, M.M., Domokos-szabolcsy, E., Elhawat, N., Joe, P. & Fári, M. 2014. Soil Quality and Plant Nutrition. *Sustainable Agriculture Reviews* **14**, 345–447. [https://doi.org/10.1007/978-3-319-06016-3\\_11](https://doi.org/10.1007/978-3-319-06016-3_11)
- Fuentes, J., Bezdicsek, D., Flury, M., Albrecht, S. & Smith, J. 2006. Microbial activity affected by lime in a long-term no-till soil. *Soil & Tillage Research* **88**, 123–131. <https://doi.org/10.1016/j.still.2005.05.001>

- Goulding, K.W.T. 2016. Soil acidification and the importance of liming agricultural soils with particular reference to the United Kingdom. *Soil Use and Management* **32**(3), 390–399. <https://doi.org/10.1111/sum.12270>
- Green, J.K., Seneviratne, S.I., Berg, A.M., Findell, K.L., Hagemann, S., Lawrence, D.M. & Gentile, P. 2019. Large influence of soil moisture on long-term terrestrial carbon uptake. *Nature* **565**, 476–479. <https://doi.org/10.1038/s41586-018-0848-x>
- Habriel, A.Y., Snitynskyi, V.V., Olifir, Y.N. & Hermanovych, O.M. 2016. Features of gas-regulating function of light-gray forest surface-covered soil under different systems of its use. *Stiinta Agricola* **1**, 13–17 (in Russian).
- Havlin, J. & Heiniger, R. 2020. Soil Fertility Management for Better Crop Production. *Agronomy* **10**(9), 1349. <https://doi.org/10.3390/agronomy10091349>
- Husson, O. 2013. Redox potential (Eh) and pH as drivers of soil/plant/microorganism systems: a transdisciplinary overview pointing to integrative opportunities for agronomy. *Plant and Soil* **362**, 389–417. <https://doi.org/10.1007/s11104-012-1429-7>
- IUSS Working Group WRB. 2015. World Reference Base for Soil Resources 2014, update 2015 International soil classification system for naming soils and creating legends for soil maps. *World Soil Resources Reports* **106**, FAO, Rome. <http://www.fao.org/3/i3794en/i3794en.pdf>
- Kanwar, L.S. 2015. Redox Potential and pH as Major Drivers of Fertility in Submerged Rice Soils: A Conceptual Framework for Management. *Communications in Soil Science and Plant Analysis* **46**(13), 1597–1606. <https://doi.org/10.1080/00103624.2015.1043451>
- Kyrylchuk, A.A. & Bonishko, O.S. 2011. *Soil chemistry. Fundamentals of theory and workshop*. Lviv: Ivan Franko Lviv National University. 354 pp. (in Ukrainian).
- Lauber, C.L., Hamady, M., Knight, R. & Fierer, N. 2009. Pyrosequencing-based assessment of soil pH as a predictor of soil bacterial community structure at the continental scale. *Applied and Environmental Microbiology* **75**, 5111–5120.
- Loide, V. 2010. Relieving the calcium deficiency of field soils by means of liming. *Agronomy Research* **8**, 415–420.
- Mamontov, V.G., Panov, N.P., Kaurichev, I.S. & Ignatiev, N.N. 2006. *General soil science*. Moscow: Koloss, 456 pp. (in Russian).
- Neina, D. 2019. The Role of Soil pH in Plant Nutrition and Soil Remediation. *Applied and Environmental Soil Science*. Article ID 5794869: 9. <https://doi.org/10.1155/2019/5794869>
- Ontl, T.A. & Schulte, L.A. 2012. Soil Carbon Storage. *Nature Education Knowledge* **3**(10):35
- Parikh, S.J. & James, B.R. 2012. Soil: The Foundation of Agriculture. *Nature Education Knowledge* **3**(10), 2.
- Popirnyi, M.A., Siabruk, O.P., Akimova, R.V. & Shevchenko, M.V. 2020. The newest integrative methods of research of stabilization of organic carbon at different tillage. *Agrochemistry and soil science* **90**, 13–28. <https://doi.org/10.31073/acss90-02> (in Ukrainian).
- Pumpanen, J., Kolari, P., Ilvesniemi, H., Minkkinen, K., Vesala, T., Niinistö, S., Lohila, A., Larmola, T., Morero, M., Pihlatie, M., Janssens, I., Yuste, J.C., Grünzweig, J.M., Reth, S., Subke, J.-A., Savage, K., Kutsch, W., Østreg, G., Ziegler, W., Anthoni, P., Lindroth, A. & Hari, P. 2004. Comparison of different chamber techniques for measuring soil CO<sub>2</sub> efflux. *Agricultural and Forest Meteorology* **123**, 159–176. <https://doi.org/10.1016/j.agrformet.2003.12.001>
- Seo, D.C. & DeLaune, R.D. 2010. Effect of redox conditions on bacterial and fungal biomass and carbon dioxide production in Louisiana coastal swamp forest sediment. *Science of the Total Environment* **408**, 3623–3631
- Snitynskyi, V.V., Habryiel, A.I., Hermanovych, O.M. & Olifir, Yu.M. 2014. Biological activity of light gray forest surface gleyed soil depending on the anthropogenic impact. *Agricultural microbiology* **19**, 47–52. (in Ukrainian).
- Snitynskyi, V.V., Habryiel, A.I., Olifir, Yu.M. & Hermanovych, O.M. 2015. Humus state and carbon dioxide emissions in agroecosystems. *Agroecological journal* **1**, 53–58 (in Ukrainian).

- Symochko, L.I., Dem'ianiuk, O.S. & Symochko, V.V. 2017. Bioindication and biotesting of soils – modern methodological approaches. *Scientific Bulletin of Uzhhorod University: Biology* **42**, 77–81 (in Ukrainian).
- Tian, D. & Niu, S. 2015. A global analysis of soil acidification caused by nitrogen addition. *Environmental Research Letters* **10**(2), 024019. <https://doi.org/10.1088/1748-9326/10/2/024019>
- Tkachenko, M.A., Havryshko, O.S., Olifir, Y.M. & Partyka, T.V. 2017. Anthropogenic impact on morphological features of the profile and physicochemical parameters of light gray forest surface-gleyed soil with a different use. *Collection of scientific works of the National Scientific Center "Institute of Agriculture of NAAS"* **4**, 15–28.
- Trofymenko, P., Trofymenko, N., Veremeienko, S. & Borysov, F. 2019. Methodology for determining the intensity of soil respiration and carbon emissions by agricultural landscapes of the Left Bank Polissya at the end of the growing season. *Bulletin of LNAU: Agronomy* **23**, 238–243. <https://doi.org/10.31734/agronomy2019.01.238> (in Ukrainian).
- Truskavetskyi, R., Zubkovska, V. & Khyzhniak, I. 2020. Innovative models of soil fertility management. *Bulletin of LNAU: Agronomy* **24**, 181–186. <https://doi.org/10.31734/agronomy2020.01.181> (In Ukrainian).
- Truskavetskyi, R.S. & Tsapko, Yu.L. 2016. *Fundamentals of soil fertility management*. Kharkiv: FOP Brovin O.V., 388 pp. (in Ukrainian).
- Tsapko, Yu.L., Desyatnik, K.A. & Ogorodnya, A.I. 2018. Acid soils amelioration – modern opinions and ways forward. *AgroChemistry and Soil Science* **87**, 11–15. <https://doi.org/10.31073/acss87-02> (In Ukrainian).
- Yemets', Yu.H. 2012. The competitiveness of agricultural products in the context of food security of Ukraine. *Scientific works of Poltava state Agricultural Academy: Economic sciences* **5**(3), 116–120 (in Ukrainian).
- Yu, K. & Rinklebe, J. 2013. Soil Redox Potential and pH Controllers. *Methods in Biogeochemistry of Wetlands* **10**, 107–116. <https://doi.org/10.2136/sssabookser10.c7>

## Theoretical research into operation of rotary potato harvester

J. Olt<sup>1,\*</sup>, V. Bulgakov<sup>2</sup>, V. Bonchik<sup>3</sup>, Z. Ruzhylo<sup>2</sup>, V. Volskiy<sup>4</sup>, V. Melnik<sup>5</sup>,  
Ye. Ihnatiev<sup>6</sup> and H. Kaletnik<sup>7</sup>

<sup>1</sup>Estonian University of Life Sciences, Institute of Technology, 56 Kreutzwaldi Str., EE 51006 Tartu, Estonia

<sup>2</sup>National University of Life and Environmental Sciences of Ukraine, 15 Heroyiv Oborony Str., UA 03041 Kyiv, Ukraine

<sup>3</sup>State Agrarian and Engineering University in Podilia, 13 Shevchenko Str., UA 32300 Kamenets-Podilsky, Ukraine

<sup>4</sup>National Scientific Centre, “Institute for Agricultural Engineering and Electrification”, 11 Vokzalna Str., Glevakcha 1, Vasylkiv District, UA 08631 Kyiv Region, Ukraine

<sup>5</sup>Kharkiv Petro Vasilenko National Technical University of Agriculture, 44 Alchevskih Str., UA 61002 Kharkiv, Ukraine

<sup>6</sup>Dmytro Motorny Tavria State Agrotechnological University, 18<sup>B</sup> Khmelnytsky Ave, UA 72310, Melitopol, Zaporozhye Region, Ukraine

<sup>7</sup>Vinnytsia National Agrarian University of Ukraine, 3 Soniacha Str., UA21008 Vinnytsia, Ukraine

\*Correspondence: [jyri.olt@emu.ee](mailto:jyri.olt@emu.ee)

Received: May 25<sup>th</sup>, 2021; Accepted: June 22<sup>nd</sup>, 2021; Published: June 28<sup>th</sup>, 2021

**Abstract.** The topic of the paper is the determination and justification of the rational design and kinematic parameters of clod breaking tools in rotary potato harvesters with the aim of improving their separating efficiency. A new mathematical model has been developed for the motion of a soil particle on the working surfaces of the cone-shaped and cylindrical vanes in the rotary tool of the new design developed by the authors. Differential equations have been generated for the motion of a soil clod as a material particle from the moment of its arrival to the surface of the vane until the moment of its departure from the said surface. As a result of the completed investigations, relations have been established between the time of contact and absolute displacement of the soil particle and the velocity of its departure from the rotor vane surface, on the one hand, and the kinematic and design parameters of the rotor, on the other hand. For example, when the machine translation velocity increases, the absolute displacement of the soil particle within the interval from the time zero to the moment of its departure from the vane surface increases from 0.59 m to 0.65 m, the velocity of soil particle departure from the vane surface - from 1.61 m s<sup>-1</sup> to 1.81 m s<sup>-1</sup>. The highest values of the absolute displacement of the soil particle and the velocity of its departure from the vane surface are achieved at a machine translation velocity of 2.0 m s<sup>-1</sup>. The time of the contact between the material particle and the vane surface decreases with the rise of the translation velocity. When the rotor rotation frequency varies within the range from 20 min<sup>-1</sup> to 100 min<sup>-1</sup>, the absolute velocity, with which the soil particle leaves the vane surface, rises to 4 m s<sup>-1</sup>. The duration of the contact between the material particle and

the vane reaches its maximum value of 0.33 s, when the rotor rotation frequency varies within the range of 30–40 min<sup>-1</sup>.

**Key words:** clod-crushing, harvesting machine, loamy soil, potato, soil separation, vertical rotor.

## INTRODUCTION

The separation of tubers from soil clods is a very important operation in the process of harvesting potatoes, especially in case of potato harvesters working on heavy loam soils (Peters, 1997; Bishop et al., 2012; Wei et al., 2017). In such soils, the soil clods are hard to break, which results in their arrival together with tubers onto the potato harvester separating tools, where their separation is rather complicated. That applies, first of all, to the soil clods of the size that is equal to or greater than the size of the tubers. In that case, the soil content in the potato heap arriving to the hopper exceeds 20%, which does not meet the agronomical standards. When operating on heavy loam soils, the potato heap cleanness rate does not exceed 55–74%, while the tuber damage rate varies within the range of 18–25% (Lü et al., 2015; Bulgakov et al., 2020; Ruzhylo et al., 2020).

In view of the above-said, the need arises to disintegrate the soil clods already at the stage of tuber lifting, i.e. prior to their arrival onto the cleaning tools. Meeting these conditions will facilitate raising the efficiency of use of combined units on heavy soils and reducing the potato tuber loss and damage rates (Bulgakov et al., 2019).

The fundamental basis for the research into the laws governing the process of soil clod disintegration in relation to the mechanical factors is outlined in the studies by the prominent scientists: Vasilenko (1996; 1998), Petrov (2004), Ruyschaert et al. (2006); Gao et al., 2011; Ichiki et al., 2013; Lü et al. (2015, 2017), Feng et al. (2017); Wang et al. (2017); Xin & Liang (2017); Bulgakov et al. (2018a, 2018b, 2018c, 2019), Nowak et al. (2019); Siberev et al. (2019); Wei et al. (2019a, 2019b), Issa et al. (2020); Ruzhylo et al., 2020.

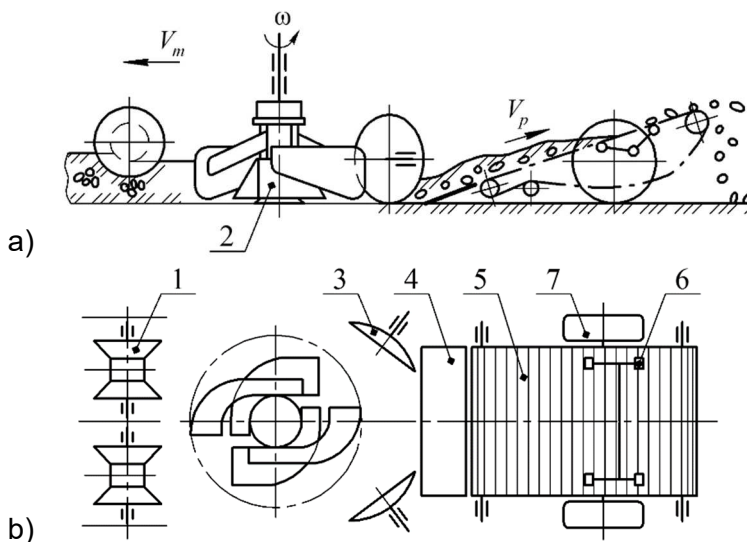
The studies have established that the efficiency of using the various methods of breaking soil clods depends on the mechanical strength of the said clods and the tuber damage rate. The strength of the clods, in its turn, depends on the physical and mechanical properties of the soil (Vasilenko, 1998; Petrov, 2004; Ruyschaert et al., 2006).

When analysing the interaction between the clod crushing tools and the tuber-bearing soil bed of the potato row, special attention has to be paid to the disintegration of clods under dynamic load conditions (Wei et al., 2017). In view of the above-said, similar research has been carried out with regard to the case of the collision between the tubers and clods, on the one hand, and the riddle chain surface, on the other hand. In this case, it has been suggested that dynamic clod breaking can be used at the initial stage of the work process, that is, in the zone of lifting the tuber-bearing soil slice and transferring it to the riddle chain, where the large amount of soil reliably protects the tubers from mechanical damage (Bulgakov et al., 1999).

The fundamental research into the motion of a material point on the surfaces of tools in agricultural machines is presented in the papers (Vasilenko, 1996 and 1998).

The authors have developed a new design of the rotary tool (Bulgakov et al., 2021), Ihnatiev et al., 2021; Olt et al., 2021) which provides for reducing the soil clods to sufficiently small sizes, at which they are easily separated from tubers on the potato harvester's web elevator.

The design and process schematic model of the tractor-hitched two-row potato harvester of the new design developed by the authors is presented in Fig. 1.



**Figure 1.** Design and process schematic model of new potato harvester: a – side view; b – top view: 1 – depth rollers; 2 – vertical rotor; 3 – spherical discs; 4 – lifting share; 5 – slat elevator; 6 – elevator belt vibrator; 7 – transport wheels (Bulgakov et al., 2021).

The work process with the use of the new potato harvester proceeds as follows. As the harvester travels in the potato field directly on the two potato rows, the depth rollers 1 press down the upper parts of the row beds, breaking them through a certain depth. The vertical rotor 2 with its upper and lower beaters rotating in the opposite directions with respect to each other and equipped with vanes travels along the centreline of the inter-row spacing between the potato rows under consideration at a pre-set depth. The travelling rotor establishes such conditions that the conically set vanes of the lower beater grasp the tuber-bearing soil beds of both the rows from below and dump them into the central part of the inter-row spacing. The tuber-bearing bed that has been completely disintegrated by the vanes of the upper beater is shifted to the centre of the inter-row spacing by the two spherical discs 3, which are set at a pre-set distance from the diameter of the rotor 2 and at an angle of attack with respect to the potato harvester motion direction. Because of the different directions of the rotary motion performed by the lower and upper beaters of the rotor, the potato heap is actively separated into different components. Also, when the tuber-bearing soil bed is shifted to the centre of the inter-row spacing by the spherical discs 3, potato tubers are extracted from the heap and cast on the surface of the inter-row spacing. After the tuber-bearing soil bed is disintegrated and partially deployed into separate components, a windrow is formed, which is picked up by the solid share 4 (the share does not dig in the soil, but only slides with its working edge on the soil surface) and fed onto the slat elevator 5. And this is the area, where the final separation of the impurities takes place, as they fall down through the openings between the slats of the elevator. In case of separating a damp potato heap, the working leg of the slat elevator 5 can be additionally put in oscillatory motion with the use of the vibrator 6, thus ensuring the high quality of cleaning potato tubers from impurities. The

frame of the machine is supported by the transport wheels 7. The machine is equipped with the devices for adjustment of the depth, at which the vertical rotor 2 runs in the soil, the rotation frequency of its lower and upper beaters as well as other adjustments. The potato tubers completely cleaned from impurities are either discharged to the area in the field, where the harvesting has been finished, or loaded to the hopper.

The tests and field experiment investigations carried out by the authors (Bulgakov et al., 2021) with the tractor-hitched potato harvester under consideration have yielded good results, which proves the achieved level of performance with regard to the quality and efficiency of potato harvesting. This achievement provides grounds for recommending the use of the described new principle of potato tuber harvesting in commercial potato harvesters.

The aim of the study was to determine and justify the rational design and kinematic parameters for the rotary tool in the potato harvester in order to improve its separating capacity, basing on the generation of a mathematical model for the motion performed by loosened soil on the vanes of the vertical rotor, the calculations with the use of the model and the analysis of the obtained results.

## MATERIALS AND METHODS

The authors have carried out theoretical investigations in order to substantiate the rational design and kinematic parameters of the discussed potato harvester.

As is known, the work process of many tools in potato harvesters, including the machine under consideration, implies the transfer of materials over their surfaces.

Therefore, in order to select the rational design parameters for the tools in the above-mentioned machines, it is necessary to determine the kinematic and dynamic parameters of the motion performed by the material on their surfaces. For that purpose, the differential equations of the motion performed by soil particles on the working surfaces of the vanes have to be generated (Kheiry et al., 2018).

When developing the mathematical model of the vertical rotor operation process, it is necessary to take into account that the motion of soil particles on the vane surfaces takes place in the continuous soil medium. For that reason, it is appropriate to assume that the soil particles move on the working surfaces of the vanes in constant contact, as distinct from the series-produced potato harvester tools, in which the tuber-bearing soil bed is disintegrated with the use of impact processes.

After the analysis of the scientific papers (Petrov, 2004; Blahovec & Židova, 2004; Hevko et al., 2016; Pshechenkov et al., 2018; Gulati & Singh, 2019) about the research into the motion of materials on the surfaces of tools in machines, it becomes obvious that the mathematical model of the vertical rotor operation process has to be generated basing on the following assumptions:

- interaction between the rotor vanes and the soil mass implies developing a complex rheological model, which takes into account the physical and mechanical properties of the material;
- in order to determine the possible displacements of the soil mass during the disintegration process (displacement of the tuber-bearing soil bed), it is necessary to regard its displacement as the displacement of a material particle;
- in view of the fact that the displaced soil interacts not only with the vane, but also with the main, undisplaced soil mass, some cases are possible, where the latter

interaction forces reduce the impact of the friction force, although, it still cannot be considered negligible.

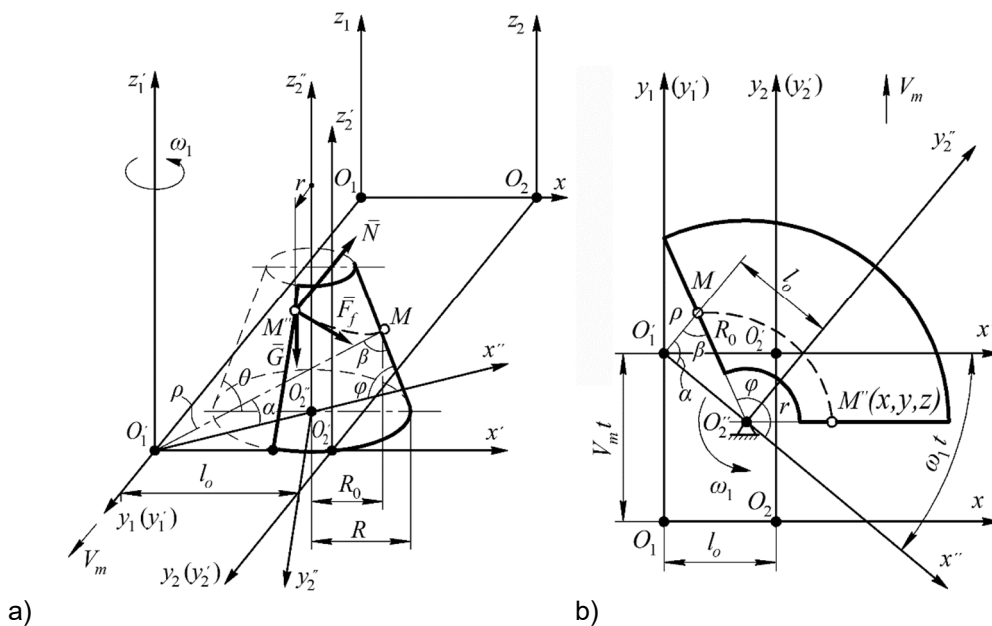
In order to investigate the process of the soil particle moving on the working surfaces of the vanes that are offset with respect to the vertical rotation axis, it is necessary to determine theoretically the conditions for the motion of the soil particle on the cone-shaped vane and the cylindrical vane, respectively, in constant contact with them. The following assumptions have been made in the process of generating the differential equations of motion:

- velocity of the soil particle at the moment of its arrival onto the surface of the vane is equal to zero;
- angular velocity of the vane is constant;
- soil particle moves along the vane.

### Theory and modelling

The next step is to generate the differential equations of motion for the soil particle moving over the working surfaces of the vanes, first for the lower beater, then for the upper one.

The generation of equations is started with the lower beater. A vane of the lower beater performs rotary motion in the horizontal plane counter-clockwise at a constant angular velocity and also performs uniform translational motion together with the potato harvester. The first step is to design the equivalent schematic model of the motion performed by the material point  $M$  (soil particle) on the surface of the cone-shaped vane under consideration (Fig. 2).



**Figure 2.** Equivalent schematic model of motion performed by material point  $M$  on cone-shaped surface of rotor's lower vane: a) position of vane in three-dimensional Cartesian coordinate system  $O_1x_1y_1z_1$ ; b) position of vane in two-dimensional Cartesian coordinate system  $O_1x_1y_1$ .



The following elements of the model are shown in the diagrams presented in Fig. 2:  $M$  – random material point (soil particle) moving along the vane;  $R_0$  – initial radius of the point  $M$ ;  $r$  – radius of the point  $M$  at the moment of its departure from the vane;  $\rho$  – polar radius of the point  $M$ ;  $\varphi$  – angular coordinate defining the position of the material point  $M$  on the surface of the vane at an arbitrary instant of time  $t$ ;  $\alpha$  – angle between the polar radius and the axis  $x''$ ;  $\beta$  – angle between the polar radius and the initial radius of the material point  $M$ .

The absolute coordinate system  $O_1x_1y_1z_1$  and the moving coordinate system  $O_2x_2y_2z_2$  with the rotation axis  $O_1z_1$  are selected in such a way that the moving coordinate system is rigidly bound with the vane and moves together with it relative to the absolute coordinate system in translation along the axis  $O_1y_1$ , rotating at the same time about the axis  $O_1z_1$ . Further, the system of coordinates  $O_2''x_2''y_2''z_2''$  is introduced for the rotation of the conical surface itself about the axis  $O_2''z_2''$  up to the moment, when the soil clod departs from the surface of the cone.

In view of the fact that the working surface of the vane is at an angle of  $\Theta$  to the horizon and is limited by the borders of the lower and upper bases of the cone, the soil particle can be placed on this surface at an arbitrary position and its motion path can be considered as the path of the motion performed by the material point  $M$  along the vane with the support of the horizontal plane (Vasilenko, 1996).

It is assumed that the coordinates of the moving material point  $M$  relative to the absolute coordinate system  $O_1x_1y_1z_1$  are equal to  $x$ ,  $y$  and  $z$ , i.e.  $M(x, y, z)$ .

In order to investigate the kinematics of the motion performed by the material point  $M$  along the working surface of the vane, it is necessary to generate the equation of the cone-shaped vane surface with reference to the absolute coordinate system  $O_1x_1y_1z_1$ . It is effectively a constraint equation of the following form:

$$f(x, y, z, t) = [x + l_0 \cdot \cos(\omega_1 t)]^2 + [y - V_m t + l_0 \cdot \sin(\omega_1 t)]^2 - (R \cdot \tan \Theta - z)^2 = 0, \quad (1)$$

where  $t$  – current time [s];  $l_0$  – distance between the axes  $y_1$  and  $y_2$ , [m];  $\omega_1$  – angular velocity of the lower beater [ $s^{-1}$ ];  $R$  – radius of the lower base of the cone [m];  $\Theta$  – angle between the cone's generator and its lower base [deg].

Further, the system of the parametric equations that describe the motion of the material point  $M$  on the working surface of the vane with reference to the absolute coordinate system  $O_1x_1y_1z_1$  has to be generated:

$$\left. \begin{aligned} x &= r \cdot \cos(\varphi + \omega_1 t) - l_0 \cdot \cos(\omega_1 t), \\ y &= V_m t + r \cdot \sin(\varphi + \omega_1 t) - l_0 \cdot \sin(\omega_1 t), \\ z &= \tan \Theta \cdot (R_0 - r). \end{aligned} \right\} \quad (2)$$

where  $r$  – radius of the circle at the height corresponding to the  $z$  coordinate of the material point  $M$  [m];  $\varphi$  – angular coordinate that defines the position of the material point  $M$  on the working surface of the vane at an arbitrary instant of time  $t$  during the rotation [deg].

For the purpose of generating the differential equation of the motion performed by the soil particle relative to the absolute coordinate system  $O_1x_1y_1z_1$  on the cone-shaped surface of the vane, Lagrange's dynamic equations of the first kind can be used (Vasilenko, 1996).

$$\left. \begin{aligned} m\ddot{x} &= \sum_{k=1}^n F_{kx} + \frac{\partial f}{\partial x} \lambda, \\ m\ddot{y} &= \sum_{k=1}^n F_{ky} + \frac{\partial f}{\partial y} \lambda, \\ m\ddot{z} &= \sum_{k=1}^n F_{kz} + \frac{\partial f}{\partial z} \lambda. \end{aligned} \right\} \quad (3)$$

where  $m$  – mass of the soil particle [kg];  $\ddot{x}$ ,  $\ddot{y}$  and  $\ddot{z}$  – projections of the soil particle acceleration on the respective coordinate axes [ $m \cdot s^{-2}$ ];  $\lambda$  – Lagrange's undetermined multiplier;  $\sum_{k=1}^n F_{kx}$ ,  $\sum_{k=1}^n F_{ky}$  and  $\sum_{k=1}^n F_{kz}$  – algebraic sum of the projections of the force acting on the soil particle [N].

Taking into account the equivalent schematic model (Fig. 2), the following system of differential equations is obtained:

$$\left. \begin{aligned} m\ddot{x} &= F_{fx} + \frac{\partial f}{\partial x} \lambda, \\ m\ddot{y} &= F_{fy} + \frac{\partial f}{\partial y} \lambda, \\ m\ddot{z} &= F_{fz} - mg + \frac{\partial f}{\partial z} \lambda. \end{aligned} \right\} \quad (4)$$

where  $F_{fx}$ ,  $F_{fy}$  and  $F_{fz}$  – projections of the friction forces  $\bar{F}_f$  on the coordinate axes  $O_1x$ ,  $O_1y_1$ ,  $O_1z_1$ , respectively;  $g$  – acceleration of gravity [ $m \cdot s^{-2}$ ].

The next step is to find the partial derivatives that are present in the system of Eqs (4). For that purpose, the parametric equation of the surface (1), i.e. the constraint equation, has to be differentiated with respect to the respective coordinates. The following is obtained:

$$\left. \begin{aligned} \frac{\partial f}{\partial x} &= 2[x + l_0 \cdot \cos(\omega_1 t)], \\ \frac{\partial f}{\partial y} &= 2[y - V_m t + l_0 \cdot \sin(\omega_1 t)], \\ \frac{\partial f}{\partial z} &= 2(R \cdot \tan \Theta - z). \end{aligned} \right\} \quad (5)$$

After substituting for  $x$ ,  $y$  and  $z$  in the obtained partial derivatives (5) their parametric Eqs (2), the following expressions for the partial derivatives are arrived at:

$$\left. \begin{aligned} \frac{\partial f}{\partial x} &= 2[r \cdot \cos(\varphi + \omega_1 t) - l_0 \cdot \cos(\omega_1 t) + l_0 \cdot \cos(\omega_1 t)] = 2r \cdot \cos(\varphi + \omega_1 t), \\ \frac{\partial f}{\partial y} &= 2[V_m t + r \cdot \sin(\varphi + \omega_1 t) - l_0 \cdot \sin(\omega_1 t) - V_m t + l_0 \cdot \sin(\omega_1 t)] = \\ &= 2r \cdot \sin(\varphi + \omega_1 t), \\ \frac{\partial f}{\partial z} &= 2(R - R_0 + r) \cdot \tan \Theta. \end{aligned} \right\} \quad (6)$$

By substituting the expressions (6) into the system of differential Eqs (3), the following is obtained:

$$\left. \begin{aligned} m\ddot{x} &= F_{f_x} + 2r \cdot \cos(\varphi + \omega_1 t) \cdot \lambda, \\ m\ddot{y} &= F_{f_y} + 2r \cdot \sin(\varphi + \omega_1 t) \cdot \lambda, \\ m\ddot{z} &= F_{f_z} - mg + 2(R - R_0 + r) \cdot \tan\Theta \cdot \lambda. \end{aligned} \right\} \quad (7)$$

At the same time, the force of friction  $\bar{F}_f$  is determined, as is known, in accordance with the Coulomb's law with the use of the following expression:

$$F_f = f \cdot N \quad (8)$$

where  $N$  – normal reaction of the constraint (in this case, the vane surface);  $f$  – coefficient of friction.

The friction force projections  $\bar{F}_{f_x}$ ,  $\bar{F}_{f_y}$ ,  $\bar{F}_{f_z}$  on the coordinate axes are determined in accordance with the following well-known expressions:

$$F_{f_x} = F_f \cdot \frac{\dot{x}}{\sqrt{\dot{x}^2 + \dot{y}^2 + \dot{z}^2}}, \quad (9)$$

$$F_{f_y} = F_f \cdot \frac{\dot{y}}{\sqrt{\dot{x}^2 + \dot{y}^2 + \dot{z}^2}}, \quad (10)$$

$$F_{f_z} = F_f \cdot \frac{\dot{z}}{\sqrt{\dot{x}^2 + \dot{y}^2 + \dot{z}^2}}. \quad (11)$$

Moreover, in accordance with Vasilenko (1998) the following expression holds true:

$$N = \Delta \cdot \lambda, \quad (12)$$

where  $\Delta$  – modulus of the gradient of the function defined by the constraint equation.

According to Vasilenko (1998):

$$\Delta = \sqrt{\left(\frac{\partial f}{\partial x}\right)^2 + \left(\frac{\partial f}{\partial y}\right)^2 + \left(\frac{\partial f}{\partial z}\right)^2} \quad (13)$$

On the basis of the above considerations, it becomes possible to write the expressions (9) – (11) in the following form:

$$F_{f_x} = f \cdot \Delta \cdot \lambda \cdot \frac{\dot{x}}{\sqrt{\dot{x}^2 + \dot{y}^2 + \dot{z}^2}}, \quad (14)$$

$$F_{f_y} = f \cdot \Delta \cdot \lambda \cdot \frac{\dot{y}}{\sqrt{\dot{x}^2 + \dot{y}^2 + \dot{z}^2}}, \quad (15)$$

$$F_{f_z} = f \cdot \Delta \cdot \lambda \cdot \frac{\dot{z}}{\sqrt{\dot{x}^2 + \dot{y}^2 + \dot{z}^2}}. \quad (16)$$

By substituting the obtained expressions (14) – (16) into the system of Eqs (7), the following system of differential equations is obtained:

$$\left. \begin{aligned} m\ddot{x} &= \lambda \cdot \left[ 2r \cdot \cos(\varphi + \omega_1 t) + f \cdot \Delta \cdot \frac{\dot{x}}{\sqrt{\dot{x}^2 + \dot{y}^2 + \dot{z}^2}} \right], \\ m\ddot{y} &= \lambda \cdot \left[ 2r \cdot \sin(\varphi + \omega_1 t) + f \cdot \Delta \cdot \frac{\dot{y}}{\sqrt{\dot{x}^2 + \dot{y}^2 + \dot{z}^2}} \right], \\ m\ddot{z} &= \lambda \cdot \left[ 2(R - R_0 + r) \cdot \tan \Theta + f \cdot \Delta \cdot \frac{\dot{z}}{\sqrt{\dot{x}^2 + \dot{y}^2 + \dot{z}^2}} \right] - mg. \end{aligned} \right\} \quad (17)$$

After that, Lagrange's multiplier is derived from the first equation in the system (17). Its value is as follows:

$$\lambda = \frac{m\ddot{x}}{2r \cdot \cos(\varphi + \omega_1 t) + f \cdot \Delta \cdot \frac{\dot{x}}{\sqrt{\dot{x}^2 + \dot{y}^2 + \dot{z}^2}}} \quad (18)$$

The obtained value of the multiplier  $\lambda$ , as per expression (18), is substituted into the second and third equations of the system (17), which results in the following:

$$\left. \begin{aligned} m\ddot{y} &= \frac{m\ddot{x}}{2r \cdot \cos(\varphi + \omega_1 t) + f \cdot \Delta \cdot \frac{\dot{x}}{\sqrt{\dot{x}^2 + \dot{y}^2 + \dot{z}^2}}} \times \\ &\times \left[ 2r \cdot \sin(\varphi + \omega_1 t) + f \cdot \Delta \cdot \frac{\dot{y}}{\sqrt{\dot{x}^2 + \dot{y}^2 + \dot{z}^2}} \right], \\ m\ddot{z} &= \frac{m\ddot{x}}{2r \cdot \cos(\varphi + \omega_1 t) + f \cdot \Delta \cdot \frac{\dot{x}}{\sqrt{\dot{x}^2 + \dot{y}^2 + \dot{z}^2}}} \times \\ &\times \left[ 2(R - R_0 + r) \cdot \tan \Theta + f \cdot \Delta \cdot \frac{\dot{z}}{\sqrt{\dot{x}^2 + \dot{y}^2 + \dot{z}^2}} \right] - mg. \end{aligned} \right\} \quad (19)$$

The system of differential Eqs (19) is just the desired system of differential equations describing the motion of the soil particle on the conical surface of the lower beater.

However, in order to solve the above system of differential equations, it is necessary to transform it into the parametric form. For that purpose, each component of the system of equations (19) has to be transformed into the parametric form.

As the system of equations (19) contains the second derivatives of the coordinates with time, that is:  $\ddot{x}$ ,  $\ddot{y}$ ,  $\ddot{z}$ , these derivatives have to be derived from the system of equations (2) by means of their twofold differentiation.

After the first differentiation of the above-mentioned equations, the following expressions are obtained for the first-order derivatives:

$$\left. \begin{aligned} \dot{x} &= \dot{r} \cdot \cos(\varphi + \omega_1 t) - r \cdot (\dot{\varphi} + \omega_1) \cdot \sin(\varphi + \omega_1 t) + l_0 \cdot \omega_1 \cdot \sin(\omega_1 t), \\ \dot{y} &= V_m + \dot{r} \cdot \sin(\varphi + \omega_1 t) + r \cdot (\dot{\varphi} + \omega_1) \cdot \cos(\varphi + \omega_1 t) + l_0 \cdot \omega_1 \cdot \cos(\omega_1 t), \\ \dot{z} &= \tan \Theta \cdot (-\dot{r}) = -\dot{r} \cdot \tan \Theta, \end{aligned} \right\} \quad (20)$$

where  $\dot{r}$  – projection of the velocity of the position vector  $\vec{r}$  on its direction;  $\dot{\varphi}$  – projection of the angular velocity on the perpendicular to the position vector  $\vec{r}$ .

After the second differentiation of the equations under consideration, the following expressions are obtained for the second derivatives:

$$\left. \begin{aligned} \ddot{x} &= \ddot{r} \cdot \cos(\varphi + \omega_1 t) - \dot{r} \cdot (\dot{\varphi} + \omega_1) \cdot \sin(\varphi + \omega_1 t) - \dot{r} \cdot (\dot{\varphi} + \omega_1) \cdot \sin(\varphi + \omega_1 t) - \\ &\quad - r \cdot \ddot{\varphi} \cdot \sin(\varphi + \omega_1 t) - r \cdot (\dot{\varphi} + \omega_1)^2 \cdot \cos(\varphi + \omega_1 t) + l_0 \cdot \omega_1^2 \cdot \cos(\omega_1 t), \\ \ddot{y} &= \ddot{r} \cdot \sin(\varphi + \omega_1 t) + \dot{r} \cdot (\dot{\varphi} + \omega_1) \cdot \cos(\varphi + \omega_1 t) + \dot{r} \cdot (\dot{\varphi} + \omega_1) \cdot \cos(\varphi + \omega_1 t) + \\ &\quad + r \cdot \ddot{\varphi} \cdot \cos(\varphi + \omega_1 t) - r \cdot (\dot{\varphi} + \omega_1)^2 \cdot \sin(\varphi + \omega_1 t) + l_0 \cdot \omega_1^2 \cdot \sin(\omega_1 t), \\ \ddot{z} &= -\ddot{r} \cdot \tan \Theta. \end{aligned} \right\} \quad (21)$$

Further, in accordance with (13), the gradient of the function defined by the constraint equation is determined by substituting the expressions (5) into (13). The result is:

$$\Delta = 2\sqrt{[x + l_0 \cdot \cos(\omega_1 t)]^2 + [y - V_m t + l_0 \cdot \sin(\omega_1 t)]^2 + (R \cdot \tan \Theta - z)^2}. \quad (22)$$

After substituting for  $x$ ,  $y$  and  $z$  in the expression (22) their expressions (2) and carrying out a number of transformations, the following is obtained:

$$\Delta = 2\sqrt{r^2 + (R - R_0 + r)^2 \cdot \tan^2 \Theta}. \quad (23)$$

Also, the expressions contained in (9), (10) and (11) have to be determined with the use of the expressions (20). First, the following designation is introduced:

$$\sqrt{\dot{x}^2 + \dot{y}^2 + \dot{z}^2} = A. \quad (24)$$

Then, taking into account (20), the following is obtained:

$$\begin{aligned} A &= \sqrt{[\dot{r} \cdot \cos(\varphi + \omega_1 t) - r \cdot (\dot{\varphi} + \omega_1) \cdot \sin(\varphi + \omega_1 t) + l_0 \cdot \omega_1 \cdot \sin(\omega_1 t)]^2 + \\ &\quad + [V_m + \dot{r} \cdot \sin(\varphi + \omega_1 t) + r \cdot (\dot{\varphi} + \omega_1) \cdot \cos(\varphi + \omega_1 t) + l_0 \cdot \omega_1 \cdot \cos(\omega_1 t)]^2 + \\ &\quad + (-\dot{r} \cdot \tan \Theta)^2}. \end{aligned} \quad (25)$$

Consequently:

$$\begin{aligned} \frac{\dot{x}}{\sqrt{\dot{x}^2 + \dot{y}^2 + \dot{z}^2}} &= \frac{\dot{x}}{A} = \\ &= \frac{\dot{r} \cdot \cos(\varphi + \omega_1 t) - r \cdot (\dot{\varphi} + \omega_1) \cdot \sin(\varphi + \omega_1 t) + l_0 \cdot \omega_1 \cdot \sin(\omega_1 t)}{A}, \end{aligned} \quad (26)$$

$$\begin{aligned} \frac{\dot{y}}{\sqrt{\dot{x}^2 + \dot{y}^2 + \dot{z}^2}} &= \frac{\dot{y}}{A} = \\ &= \frac{V_m + \dot{r} \cdot \sin(\varphi + \omega_1 t) + r \cdot (\dot{\varphi} + \omega_1) \cdot \cos(\varphi + \omega_1 t) + l_0 \cdot \omega_1 \cdot \cos(\omega_1 t)}{A}, \end{aligned} \quad (27)$$

$$\frac{\dot{z}}{\sqrt{\dot{x}^2 + \dot{y}^2 + \dot{z}^2}} = \frac{\dot{z}}{A} = -\frac{\dot{r} \cdot \tan \Theta}{A} \quad (28)$$

By substituting the expressions (21), (23), (26)–(28) into the respective expressions in the system of equations (19), the system of differential equations in the unknown  $r$  and  $\varphi$  is arrived at, which has to be solved by numerical methods on the PC.

In case of the upper beater vane, the motions to be given consideration are the clockwise rotary motion at a constant angular velocity of  $\omega_2$  in the horizontal plane as well as the uniform translation motion together with the potato harvester with reference

to the absolute coordinate system  $O_1xy_1$ . The diagram of the position of the soil particle  $M$  on the working surface of the cylindrical vane offset with respect to the vertical rotation axis  $O_1z_1$  (point  $O_1$ ) and the forces acting on it are presented in Fig. 3.

In the schematic model presented in Fig. 3, the following forces are shown:  $N$  – normal reaction of the constraint;  $F_f$  – force of friction. The designations are as follows:  $V$  – radial velocity of the particle;  $O_1xy_1$  – absolute (fixed) coordinate system;  $O_2xy_2$  – moving coordinate system that is rigidly bound with the vane and moves together with it with reference to the absolute coordinate system  $O_1xy_1$  in translation along the  $O_1y_1$  axis and simultaneously in rotation about the  $O_1z_1$  axis (point  $O_1$ ). The coordinate system  $O'_1x'y'_1$  moves together with the vane along the  $O_1y_1$  axis at the potato harvester's translation velocity  $V_m$  in such a way that its axis  $O'_1x'$  remains always parallel to the  $O_1x$  axis and it plays an ancillary part (for convenience in the representation of angles in Fig. 3 at an arbitrary instant of time  $t$ ); the coordinate system  $O''_2x''y''_2$  is introduced for the purpose of analysing the rotation of the cylindrical vane itself about the  $O''_2z''_2$  axis (point  $O''_2$ ).

The displacement of the soil particle on the working surface of the cylindrical vane is assumed to be the motion of the material point  $M$  relative to the fixed coordinate system  $O_1xy_1$ . In order to analyse the kinematics of the motion performed by the material point  $M$  on the working surface of the cylindrical vane, it is necessary to generate the respective vane surface equation, i.e. the constraint equation, which appears as follows:

$$f(x, y, t) = [x + l_0 \cos(\omega_2 t)]^2 + [y - V_m t + l_0 \sin(\omega_2 t)]^2 - R_0^2 = 0, \quad (29)$$

where  $\omega_2$  – angular velocity of the upper beater [ $s^{-1}$ ].

The parametric equations describing the motion of the material point  $M$  on the working surface of the vane relative to the fixed coordinate system  $O_1xy_1$  have the following form:

$$\left. \begin{aligned} x &= R_0 \cdot \left[ \cos(\varphi + \omega_2 t) - \frac{l_0}{R_0} \cdot \cos(\omega_2 t) \right], \\ y &= V_m t + R_0 \cdot \left[ \sin(\varphi + \omega_2 t) - \frac{l_0}{R_0} \cdot \sin(\omega_2 t) \right], \end{aligned} \right\} \quad (30)$$

where  $\varphi$  – angular coordinate of the material point  $M$ ;  $x, y$  – absolute coordinates of the material point  $M$  moving on the surface of the vane.

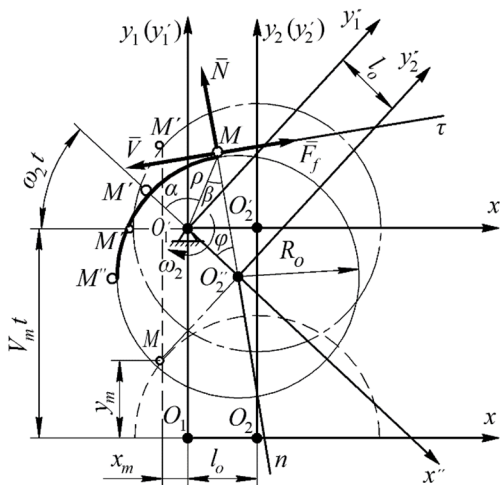


Figure 3. Schematic model of interaction between soil particle  $M$  and working surface of cylindrical vane in upper beater.

The derivative  $\dot{\varphi}$ , the same as the function  $\varphi$  itself, are to be determined with the use of the respective dynamic equations. For that purpose, the Lagrange's equations of the second kind can be used. The angular coordinate  $\varphi$  is taken as the generalised coordinate.

The Lagrange's equation of the second kind in the generalised coordinate  $\varphi$  appears as follows:

$$\frac{d}{dt} \frac{\partial T}{\partial \dot{\varphi}} - \frac{\partial T}{\partial \varphi} = Q_{\varphi} \quad (31)$$

where  $T$  – kinetic energy of the material point;  $\varphi$  – generalised coordinate;  $\dot{\varphi}$  – generalised velocity;  $Q_{\varphi}$  – generalised force corresponding to the generalised coordinate  $\varphi$ .

With the use of the expression (30), the kinetic energy  $T$  of the material point  $M$  can be expressed in terms of the generalised velocity. The result is as follows:

$$T = \frac{m \cdot (\dot{x}^2 + \dot{y}^2)}{2}. \quad (32)$$

The following expressions are obtained for the derivatives  $\dot{x}$ ,  $\dot{y}$ :

$$\left. \begin{aligned} \dot{x} &= R_0 \left[ -(\dot{\varphi} + \omega_2) \cdot \sin(\varphi + \omega_2 t) + \frac{l_0}{R_0} \cdot \omega_2 \cdot \sin(\omega_2 t) \right], \\ \dot{y} &= V_m + R_0 \left[ (\dot{\varphi} + \omega_2) \cdot \cos(\varphi + \omega_2 t) - \frac{l_0}{R_0} \cdot \omega_2 \cdot \cos(\omega_2 t) \right]. \end{aligned} \right\} \quad (33)$$

Taking into account the equation (31) and the expressions (32) and (33), the partial derivatives of the  $\dot{x}^2$  and  $\dot{y}^2$  expressions with respect to the generalised coordinate  $\varphi$  are obtained:

$$\left. \begin{aligned} \frac{\partial \dot{x}^2}{\partial \varphi} &= R_0^2 \left[ 2(\dot{\varphi} + \omega_2)^2 \cdot \sin(\varphi + \omega_2 t) \cdot \cos(\varphi + \omega_2 t) - \right. \\ &\quad \left. - 2 \cdot \frac{l_0}{R_0} \cdot \omega_2 \cdot (\dot{\varphi} + \omega_2) \cdot \sin(\omega_2 t) \cdot \cos(\varphi + \omega_2 t) \right], \\ \frac{\partial \dot{y}^2}{\partial \varphi} &= -2R_0^2 \cdot (\dot{\varphi} + \omega_2)^2 \cdot \cos(\varphi + \omega_2 t) \cdot \sin(\varphi + \omega_2 t) + \\ &\quad + 2R_0^2 \cdot \frac{l_0}{R_0} \cdot \omega_2 (\dot{\varphi} + \omega_2) \cdot \cos(\omega_2 t) \cdot \sin(\varphi + \omega_2 t) - \\ &\quad - 2V_m \cdot R_0 \cdot (\dot{\varphi} + \omega_2) \cdot \sin(\varphi + \omega_2 t). \end{aligned} \right\} \quad (34)$$

The partial derivatives of  $\dot{x}^2$  and  $\dot{y}^2$  with respect to the generalised velocity  $\dot{\varphi}$  appear as follows:

$$\left. \begin{aligned} \frac{\partial \dot{x}^2}{\partial \dot{\varphi}} &= R_0^2 \left[ 2(\dot{\varphi} + \omega_2) \cdot \sin^2(\varphi + \omega_2 t) - 2 \frac{l_0}{R_0} \cdot \omega_2 \cdot \sin(\omega_2 t) \cdot \sin(\varphi + \omega_2 t), \right] \\ \frac{\partial \dot{y}^2}{\partial \dot{\varphi}} &= 2R_0^2 \cdot (\dot{\varphi} + \omega_2) \cdot \cos^2(\varphi + \omega_2 t) - 2R_0^2 \cdot \frac{l_0}{R_0} \cdot \omega_2 \cdot \cos(\omega_2 t) \cdot \cos(\varphi + \omega_2 t) + \\ &\quad + 2V_m \cdot R_0 \cdot \cos(\varphi + \omega_2 t). \end{aligned} \right\} \quad (35)$$

Taking into account the Eq. (31) as well as the expressions (34) and (35), after a number of transformations the following expressions can be obtained:

$$\left. \begin{aligned} \frac{d}{dt} \left( \frac{\partial \dot{x}^2}{\partial \dot{\varphi}} \right) - \frac{\partial \dot{x}^2}{\partial \varphi} &= 2R_0^2 \cdot \ddot{\varphi} \cdot \sin^2(\varphi + \omega_2 t) + R_0^2 \cdot (\varphi + \omega_2)^2 \cdot \sin^2(\varphi + \omega_2 t) - \\ &- 2 \frac{l_0}{R_0} \cdot \omega_2^2 \cdot R_0^2 \cdot \cos(\omega_2 t) \cdot \sin(\varphi + \omega_2 t), \\ \frac{d}{dt} \left( \frac{\partial \dot{y}^2}{\partial \dot{\varphi}} \right) - \frac{\partial \dot{y}^2}{\partial \varphi} &= 2R_0^2 \cdot \ddot{\varphi} \cdot \cos^2(\varphi + \omega_2 t) - R_0^2 \cdot (\varphi + \omega_2)^2 \cdot \sin^2(\varphi + \omega_2 t) + \\ &+ 2 \frac{l_0}{R_0} \cdot \omega_2^2 \cdot R_0^2 \cdot \sin(\omega_2 t) \cdot \cos(\varphi + \omega_2 t). \end{aligned} \right\} \quad (36)$$

Finally, the left side of the Eq. (31) obtains the following form after substituting into it the expressions (36):

$$\begin{aligned} \frac{d}{dt} \left( \frac{\partial T}{\partial \dot{\varphi}} \right) - \frac{\partial T}{\partial \varphi} &= \frac{m}{2} \cdot \frac{d}{dt} \left( \frac{\partial \dot{x}^2}{\partial \dot{\varphi}} \right) + \frac{d}{dt} \left( \frac{\partial \dot{y}^2}{\partial \dot{\varphi}} \right) - \left( \frac{\partial \dot{x}^2}{\partial \varphi} + \frac{\partial \dot{y}^2}{\partial \varphi} \right) = \\ &= \frac{m}{2} \left\{ 2R_0^2 \cdot [\sin^2(\varphi + \omega_2 t) + \cos^2(\varphi + \omega_2 t)] \ddot{\varphi} + \right. \\ &+ 2R_0^2 \cdot \frac{l_0}{R_0} \cdot \omega_2^2 \cdot [\sin(\omega_2 t) \cdot \cos(\varphi + \omega_2 t) - \cos(\omega_2 t) \cdot \sin(\varphi + \omega_2 t)] \left. \right\} = \\ &= \frac{m}{2} \left\{ 2R_0^2 \cdot \ddot{\varphi} + 2R_0^2 \cdot \frac{l_0}{R_0} \cdot \omega_2^2 \cdot \left[ \sin(\omega_2 t) \cdot \left( \cos \varphi \cdot \cos(\omega_2 t) - \right. \right. \right. \\ &\left. \left. \left. - \sin \varphi \cdot \sin(\omega_2 t) \right) - \cos(\omega_2 t) \cdot \left( \sin \varphi \cdot \cos(\omega_2 t) + \cos \varphi \cdot \sin(\omega_2 t) \right) \right] \right\} = \\ &= \frac{m}{2} \left[ 2R_0^2 \cdot \ddot{\varphi} + 2R_0^2 \cdot \frac{l_0}{R_0} \cdot \omega_2^2 \cdot \left( -\sin^2(\omega_2 t) \cdot \sin \varphi - \cos^2(\omega_2 t) \cdot \sin \varphi \right) \right] = \\ &= \frac{m}{2} \left[ 2R_0^2 \cdot \ddot{\varphi} - 2R_0^2 \cdot \frac{l_0}{R_0} \cdot \omega_2^2 \cdot \sin \varphi \right]. \end{aligned} \quad (37)$$

In this case, the generalised force is the moment of friction  $M_{z_1}(\bar{F}_f)$  with respect to the axis  $O_1z_1$ , which is determined in accordance with the following expression:

$$M_{z_1}(\bar{F}_f) = F_f \cdot N \cdot R_0, \quad (38)$$

where  $N$  – normal reaction of the constraint surface;  $f$  – coefficient of friction;  $R_0$  – radius of the cylindrical vane.

In order to determine the force of friction, it is necessary to determine the normal reaction  $N$  of the cylindrical vane, which in the general case can be represented by the following expression:

$$N = m \cdot \frac{Df(x, y, t)}{|\text{grad } f|}, \quad (39)$$

where  $m$  – mass of the soil particle [kg];  $D$  – differential operator (Vasilenko, 1998).

In the expression (39), the numerator and the denominator have to be determined. The following expressions have been obtained for them:



$$\begin{aligned}
Df(x, y, t) &= 2 \left\{ \left[ \dot{x} - \omega_2 \cdot l_0 \cdot \sin(\omega_2 t) \right]^2 + \right. \\
&+ \left[ \dot{y} - V_m + \omega_2 \cdot l_0 \cdot \cos(\omega_2 t) \right]^2 + \\
&+ \left[ x + l_0 \cdot \cos(\omega_2 t) \right] \cdot \left[ -l_0 \cdot \omega_2^2 \cdot \cos(\omega_2 t) \right] - \\
&- l_0 \cdot \omega_2^2 \cdot \sin(\omega_2 t) \cdot \left[ y - V_m t + l_0 \cdot \sin(\omega_2 t) \right] \left. \right\} = \\
&= 2R_0 \left[ R_0 \cdot (\dot{\varphi} + \omega_2)^2 - l_0 \cdot \omega_2^2 \cdot \cos \varphi \right],
\end{aligned} \tag{40}$$

and:

$$\begin{aligned}
|\text{grad } f| &= \sqrt{\left( \frac{df}{dx} \right)^2 + \left( \frac{df}{dy} \right)^2} = \\
&= \sqrt{4 \left[ x + l_0 \cdot \cos(\omega_2 t) \right]^2 + 4 \left[ y - V_m t + l_0 \cdot \sin(\omega_2 t) \right]^2} = 2R_0.
\end{aligned} \tag{41}$$

After substituting the expressions (40) and (41) into the expression (39), the following expression is obtained for the normal reaction  $N$ :

$$N = m \left[ l_0 \cdot \omega_2^2 \cdot \cos \varphi - R_0 \cdot (\dot{\varphi} + \omega_2)^2 \right]. \tag{42}$$

Taking into account the expressions (31), (37) and (42), the following differential equation is obtained for describing the motion of a soil particle on the cylindrical surface of the upper beater vane offset with respect to the vertical rotation axis with due account for the friction forces:

$$R_0^2 \left( \ddot{\varphi} - \frac{l_0}{R_0} \cdot \omega_2^2 \cdot \sin \varphi \right) = f_f \left[ R_0 (\dot{\varphi} + \omega_2)^2 - l_0 \cdot \omega_2^2 \cdot \cos \varphi \right] R_0 \tag{43}$$

or

$$\ddot{\varphi} = \frac{l_0}{R_0} \cdot \omega_2^2 \cdot \sin \varphi + f_f \left[ (\dot{\varphi} + \omega_2)^2 - \frac{l_0}{R_0} \cdot \omega_2^2 \cdot \cos \varphi \right]. \tag{44}$$

The initial conditions for solving the differential Eq. (44) are as follows:  
at  $t = 0$ :

$$\begin{aligned}
\varphi_0 &= 0, \\
\dot{\varphi}_0 &= \frac{V_m}{R_0} - \omega_2 \left( 1 - \frac{l_0}{R_0} \right).
\end{aligned} \tag{45}$$

The condition of the soil particle motion in constant contact with the working surface of the cylinder-shaped vane is represented by the following in equation:

$$\frac{N}{m \cdot R_0} = \omega_2^2 \cdot \frac{l_0}{R_0} \cdot \cos \varphi - (\dot{\varphi} + \omega_2)^2 \geq 0. \tag{46}$$

After substituting the numerical data into the above relations, it is possible to obtain their solutions and analyse the effect that the design and kinematic parameters of the rotor vanes have on the process of breaking the tuber-bearing soil bed.

## RESULTS

Further, the calculations carried out in the Mathcad environment with regard to the cylindrical vane are described.

The kinematic parameters of the motion performed by the soil particle on the working surface of the cylindrical vane have the following numerical values:

$$R_0 = 0.5 \text{ m};$$

$$l_0 = 0.3 \text{ m}; n = 50 \text{ min}^{-1};$$

$$V_m = 1.38 \text{ m s}^{-1}; \omega_2 = 5.23 \text{ s}^{-1}.$$

The initial conditions defined by the Eqs (30) and (33) at the moment of time  $t = 0$  appear as follows:

$$x(0) = R - l_0,$$

$$x'(0) = 0,$$

$$y(0) = 0,$$

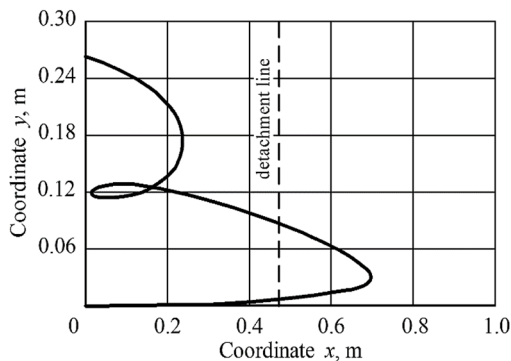
$$y'(0) = 0,$$

With the use of the parametric Eqs (30), the trajectory of the motion performed by the material point in the coordinate system  $O_1x_1y_1$  has been plotted, as is shown in Fig. 4.

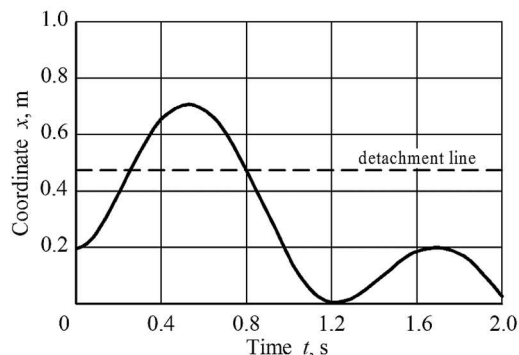
It is necessary to plot graphs also for the variation of the abscissa  $x(t)$  of the material point  $M$  (Fig. 5) and its ordinate  $y(t)$  (Fig. 6) with the time  $t$ .

As is seen in the graph presented in Fig. 4, the departure of the material point  $M$  from the vane surface starts at the abscissa  $x = 0.47 \text{ m}$  and the ordinate  $y = 0.075 \text{ m}$ .

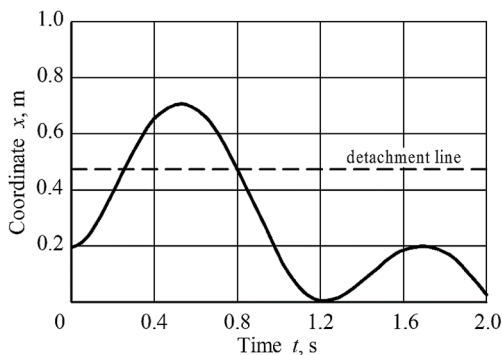
With the use of the earlier obtained expression (33), graphs can be plotted for the relations between the velocity modulus of the material point  $M$  and its velocity projections on the fixed coordinate axes  $O_1xy_1$ , on the one hand, and the time of its motion on the working surface of the vane, on the other hand (Fig. 7).



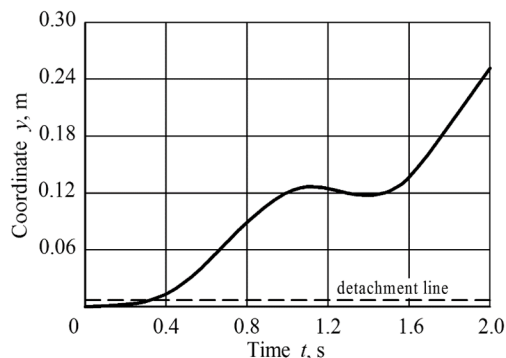
**Figure 4.** Motion path of material point  $M$  on cylindrical surface of vane in coordinate system  $O_1xy_1$ .



**Figure 5.** Relation between abscissa  $x$  of material point  $M$  and time  $t$ .



**Figure 5.** Relation between abscissa  $x$  of material point  $M$  and time  $t$ .



**Figure 6.** Relation between ordinate  $y$  of material point  $M$  and time  $t$ .

The modulus of the speed  $V$  of the material point in the fixed coordinate system  $O_1xy_1$  is determined with the use of the following expression:

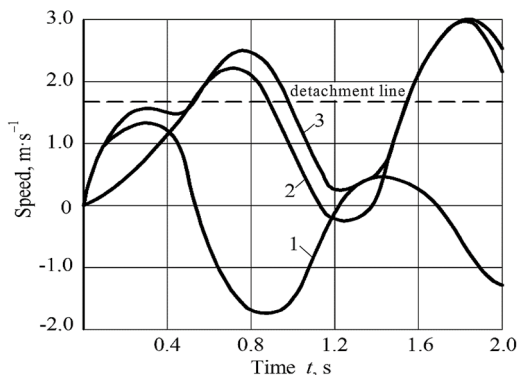
$$V = \sqrt{(V_x)^2 + (V_y)^2} \quad (47)$$

As is obvious from the graphs presented in Fig. 7, the modulus of the speed  $V$  of the material point  $M$  shows rather unstable behaviour in terms of the interaction with the vane surface as a function of the motion time.

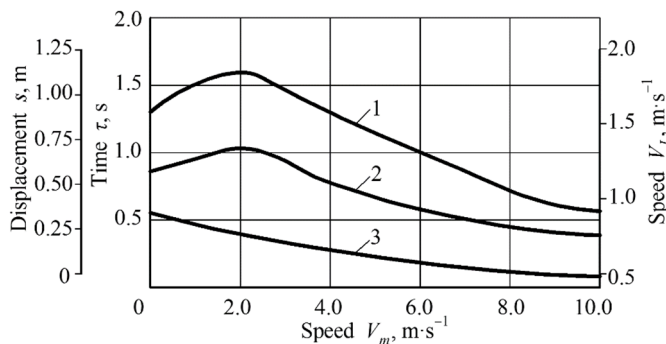
In order to determine the kinematic parameters of the vertical rotor's cylindrical vane, it is necessary to analyse theoretically the effect of the translation speed  $V_m$  of the motion performed by the potato harvester and the rotor rotation frequency  $n_p$  on the duration of stay of the material point on the vane surface, its absolute displacement  $s$  and the absolute speed  $V_L$  of its departure from the vane surface.

On the basis of the obtained analytical relations, after substituting the numerical values with the use of the PC, the following relation graphs have been plotted (Figs 8 and 9).

After analysing the graphs presented in Fig. 8, it becomes obvious that the absolute displacement and speed of the material point  $M$  from the zero point of the time  $t$  to the moment of its departure from the vane surface increase from 0.59 m, 1.61 m s<sup>-1</sup>, respectively, to 0.65 m, 1.81 m s<sup>-1</sup>. The greatest values of the absolute displacement and velocity of the material point  $M$  equal to 0.67 m and 1.94 m s<sup>-1</sup>, respectively, are reached at the translation speed of the potato harvester equal to 2.0 m s<sup>-1</sup>. The duration of stay of the material point  $M$  on the vane surface decreases with the increase of the translation velocity.

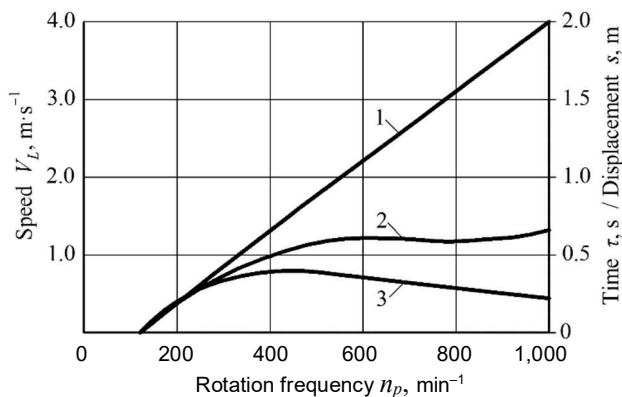


**Figure 7.** Relations between modulus of speed  $V$  of material point  $M$  (3) as well as speed projections  $V_x$  (1),  $V_y$  (2) on fixed coordinate axes  $O_1xy_1$  and time  $t$ .



**Figure 8.** Relations between duration of stay  $\tau$  (3), absolute displacement  $s$  (2), speed  $V_L$  of departure of material point  $M$  from vane surface (1) and machine translation speed  $V_m$ .

The analysis of the relation graph presented in Fig. 9 proves that, in case of the rotor rotation frequency equal to  $20 \text{ min}^{-1}$ , the material point  $M$  does not interact with the vane surface and is in the standstill condition ( $V = 0$ ) with reference to the fixed axes  $O_1x_1y_1$ , while the initial absolute coordinates are  $x(0) = R_0 - l_0 = 0.2 \text{ m}$ ,  $y(0) = 0$ .



**Figure 9.** Relations between duration of stay  $\tau$  (3), absolute displacement  $s$  (2), speed  $V_L$  of departure of material point  $M$  from vane surface (1) and rotor rotation frequency  $n_p$ .

The absolute speed of the departure of the material point  $M$  from the vane surface rises to  $4 \text{ m s}^{-1}$ , when the rotor rotation frequency  $n_p$  increases in the range from  $20 \text{ min}^{-1}$  to  $100 \text{ min}^{-1}$ .

When the rotor rotation frequency  $n_p$  is within the range of  $30\text{--}40 \text{ min}^{-1}$ , the duration of the contact between the material point  $M$  and the vane reaches its maximum value equal to  $0.33 \text{ s}$ , which indicates the effective capture and transportation of parts of the potato tuber bearing soil bed by the rotor.

## CONCLUSIONS

1. The new design of a rotary tool for the potato harvester, which has a vertical axis of rotation and travels in the inter-row spacing between two adjacent potato rows, has been proposed.

2. The mathematical model of the motion of a soil particle on the working surfaces of the vanes in the rotary tool of the new design has been developed.

3. The relations have been established between the duration of stay, absolute displacement and velocity of departure from the rotor vane surface of the soil particle, on the one hand, and the rotor's kinematic and design parameters, on the other hand. For example, when the machine's translational motion velocity increases, the absolute displacement of the soil particle in the period from the zero instant of time to the moment, when the particle departs from the vane surface, rises from  $0.59 \text{ m}$  to  $0.65 \text{ m}$ , the velocity of the particle departure from the vane surface - from  $1.61 \text{ m s}^{-1}$  to  $1.81 \text{ m s}^{-1}$ . The absolute displacement and velocity of the soil particle reach their highest levels of  $0.67 \text{ m}$  and  $1.94 \text{ m s}^{-1}$ , respectively, at the translation velocity of the machine equal to  $2.0 \text{ m s}^{-1}$ . The time of the material particle staying on the vane surface decreases with the increase of the translation velocity.

4. The absolute speed of the departure of the material point from the vane surface increases to  $4 \text{ m s}^{-1}$ , as the rotor rotation frequency varies in the range from  $20 \text{ min}^{-1}$  to  $100 \text{ min}^{-1}$ .
5. The duration of the contact between the material particle and the vane reaches its maximum value equal to 0.33 s, when the rotor rotation frequency is within the range of  $30\text{--}40 \text{ min}^{-1}$ .

## REFERENCES

- Bishop, C., Rees, D., Cheema, M.U.A., Harper, G. & Stroud, G. 2012. *Potatoes*. Crop Post-Harvest: Science and Technology: Perishables. Book Chapter, pp. 179–189.
- Blahovec, J. & Židova, J. 2004. Potato bruise spot sensitivity dependence on regimes of cultivation. *Research in Agricultural Engineering* **50**(3), 89–95. doi: 10.17221/4932.RAE.
- Bulgakov, V., Bonchik, V., Holovach, I., Fedosiy, I., Volskiy, V., Melnik, V., Ihnatiev, Ye., Olt, J. 2021. Justification of parameters for novel rotary potato harvesting machine. *Agronomy Research* **19**(S2), 984–1007. doi: 10.15159/AR.21.079
- Bulgakov, V.M., Gevko, R.B., Glado, Y.B., Pavh, I.I. 1999. Theoretical justification of process of conveying and separating roots with drag conveyors. In: *Proc. National University of Agriculture*, 15–18.
- Bulgakov V., Holovach I., Ruzhylo Z., Fedosiy I., Ihnatiev Ye., Olt J. 2020. Theory of oscillations performed by tools in spiral potato separator. *Agronomy Research* **18**(1), 38–52. doi: 10.15159/AR.20.058
- Bulgakov, V., Nikolaenko, S., Adamchuk, V., Ruzhylo, Z. & Olt, J. 2018a. Theory of retaining potato bodies during operation of spiral separator. *Agronomy Research* **16**(1), 41–51. doi: 10.15159/AR.18.036
- Bulgakov, V., Nikolaenko, S., Adamchuk, V., Ruzhylo, Z. & Olt, J. 2018b. Theory of impact interaction between potato bodies and rebounding conveyor. *Agronomy Research* **16**(1), 52–64. doi: 10.15159/AR.18.037
- Bulgakov, V., Nikolaenko, S., Adamchuk, V., Ruzhylo, Z. & Olt, J. 2018c. Mathematical model of cleaning potatoes on surface of spiral separator. *Agronomy Research* **16**(4), 1590–1606. doi: 10.15159/AR.18.173
- Bulgakov, V., Pascuzzi, S., Nikolaenko, S., Santoro, F., Anifantis, A.S. & Olt, J. 2019. Theoretical study on sieving of potato heap elements in spiral separator. *Agronomy Research* **17**(1), 33–48. doi: 10.15159/AR.19.073
- Feng, B., Sun, W., Shi, L., Sun, B., Zhang, T. & Wu, J. 2017. Determination of restitution coefficient of potato tubers collision in harvest and analysis of its influence factors. *Nongye Gongcheng Xuebao/Transactions of the Chinese society of agricultural engineering* **33**(13), 50–57.
- Gao, G., Zhang, D. & Liu, J. 2011. Design of a new soil-tuber separation device on potato harvesters. *CCTA 2010: Computer and Computing Technologies in Agriculture*, IV, 604–612. doi: 10.1007/978-3-642-18354-6\_71
- Gulati, S. & Singh, M. 2019. Design and development of two row tractor operated potato combine harvester. *Potato Journal* **46**(1), 81–85.
- Hevko, R.B., Tkachenko, I.G., Synii, S.V. & Flonts, I.V. 2016. Development of design and investigation of operation process of small-scale root crop and potato harvesters. *INMATEH-Agricultural Engineering* **49**(2), 53–60.
- Ichiki, H., Nguyen Van, N. & Yoshinaga, K. 2013. Stone-clod separation and its application to potato in Hokkaido. *Engineering in Agriculture Environment and Food* **6**(2), 77–85.
- Ihnatiev, Ye., Bulgakov, V., Bonchik, V., Ruzhylo, Z., Zaryshnyak, A., Volskiy, V., Melnik, V. & Olt, J. 2021. Experimental research into operation of potato harvester with rotary tool. *Agraarteadus / Journal of Agricultural Science* **32**(1), 41–48. doi: 10.15159/jas.21.15

- Issa, I.I.M., Zhang, Z., El-Kolaly, W., Yang, X. & Wang, H. 2020. Design, ansys analysis and performance evaluation of potato digger harvester. *International Agricultural Engineering Journal* **29**(1), 60–73.
- Kheiry, A.N.O., Elssir, A., Rahma, A.E., Mohamed, M.A., Omer, E.A., Gong, H.J. & Liwei, Y. 2018. Effect of operation variables of potato digger with double chain conveyors on crop handling and machine performance. *Int. J. of Environmental & Agricultural Research* **4**(6), 87–101.
- Lü, J.Q., Sun, H., Dui, H., Peng, M.M. & Yu, J.Y. 2017. Design and experiment on conveyor separation device of potato digger under heavy soil condition. *Transactions of the CSAM* **48**(11), 146–155 (in Chinese).
- Lü, J.Q., Tian, Z.E., Yang, Y., Shang, Q.Q. & Wu, J.E. 2015. Design and experimental analysis of 4U2A type double-row potato digger. *Transactions of the CSAE* **31**(6), 17–24 (in Chinese).
- Nowak, J., Bulgakov, V., Holovach, I., Olt, J., Arak, M., Ruzhylo, Z. & Nesvidomin, A. 2019. Oscillation theory of the free ends of the spiral separator for a potato heap. In: X International Scientific Symposium FMPMSA 2019: *Farm Machinery and Process Management in Sustainable Agriculture* 157–162. doi: 10.24326/fmpmsa.2019.1.
- Olt, J., Adamchuk, V., Kornushyn, V., Melnik, V., Kaletnik, H., Ihnatiev, Ye. & Ilves, R. 2021. Research into the parameters of a potato harvester's potato heap distributor, and the justification of those parameters. *Agraarteadus / Journal of Agricultural Science* **32**(1), 92–99. doi: 10.15159/jas.21.19
- Pshechenkov, K.A., Maltsev, S.V. & Smirnov, A.V. 2018. Technology of potatoes combine harvesting on loamy soils in the Central region of Russia. *Potato and Vegetables* **4**, 19–21 (in Russian).
- Peters, R. 1997. Damage of potato tubers: A Review. *Potato Research* **39**(Spec. Issue), 479–484.
- Petrov, G. 2004. *Potato harvesting machines*. Mashinostroenije / Mechanical Engineering, Moskow, Russia, 320 pp. (in Russian).
- Ruysschaert, G., Poesen, J., Verstraeten, G. & Govers, G. 2006. Soil losses due to mechanized potato harvesting. *Soil & Tillage Research* **86**(1), 52–72. doi: 10.1016/j.still.2005.02.016.
- Ruzhylo, Z., Bulgakov, B., Adamchuk, V., Bondarchuk, A., Ihnatiev, Y., Krutyakova, V., Olt, J. 2020. Experimental research into impact of kinematic and design parameters of a spiral potato separator on quality of plant residues and soil separation. *Agraarteadus / Journal of Agricultural Science* **31**(2), 202–207. doi: 10.15159/jas.20.26.
- Siberev, A., Aksenov, A., Dorokhov, A. & Ponomarev, A. 2019. Comparative study of the force action of harvester work tools on potato tubers. *Research in Agricultural Engineering* **65**(3), 85–90. doi: 10.17221/96/2018-RAE
- Vasilenko, P.M. 1996. *Introduction to agricultural mechanics*. Kiev, Ukraine, Ed. NAU, 252 pp.
- Vasilenko, P.M. 1998. *Fundamentals of analytical methods in agricultural mechanics*. Kiev, Ukraine, Ed. NAU, 28 pp.
- Wang, X., Sun, J., Xu, Y., Li, X. & Cheng, P. 2017. Design and experiment of potato cleaning and sorting machine. *Nongye Jixie Xuebao/Transactions of the Chinese Society for Agricultural Machinery* **48**(10), 316–322 and 279.
- Wei, Z., Li, X. & Sun, C. 2017. Analysis of potato mechanical damage in harvesting and cleaning and sorting storage. *Journal of Agricultural Science and Technology* **19**(8), 63–70. doi: 10.6041/j.issn.1000-1298.2019.01.014
- Wei, Z., Li, H., Sun, C., Li, X., Su, G. & Liu, W. 2019a. Design and Experiment of Potato Combined Harvester Based on Multi-stage Separation Technology. *Nongye Jixie Xuebao/Transactions of the Chinese Society for Agricultural Machinery* **50**(1), 129–140. doi: 10.6041/j.jssn.1000-1298.2019.01.014
- Wei, Z., Li, H., Sun, C., Su, G., Liu, W. & Li, Z. 2019b. Experiments and analysis of a conveying device for soil separation and clod-crushing for a potato harvester. *Applied Engineering in Agriculture* **35**(6), 987–996. doi: 10.13031/aea.13283
- Xin, L. & Liang, J. 2017. Design of potato harvester. *Journal of Mechanical Engineering Research and Developments* **40**(2), 380–384.

## Woodworking wastewater biomass effective separation and its recovery

S. Vitolina<sup>1,\*</sup>, G. Shulga<sup>1</sup>, B. Neiberte<sup>1</sup> and S. Reihmane<sup>2</sup>

<sup>1</sup>Latvian State Institute of Wood Chemistry, 27 Dzerbenes Street, LV–1006 Riga, Latvia

<sup>2</sup>Riga Technical University, Faculty of Material Science and Applied Chemistry, 3/7 Paula Valdena Street, LV–1048 Riga, Latvia

\*Correspondence: [sanita.vitolina@gmail.com](mailto:sanita.vitolina@gmail.com)

Received: February 13<sup>th</sup>, 2021; Accepted: May 2<sup>nd</sup>, 2021; Published: August 18<sup>th</sup>, 2021

**Abstract.** The aim of the study was to develop a new Al-based hybrid coagulant that was effective in removing wood biomass from the wastewater formed in water basins of plywood plants during hydrothermal treatment of birch wood. The organic-inorganic coagulant was prepared by interaction of high molecular polyethyleneimine (PEI) with the inorganic polyaluminium chloride-based composite coagulant (KHPAC) in aqueous medium. Owing to the hybrid nature, the developed coagulant could simultaneously perform both the coagulation and flocculation function. The influence of a hybrid coagulant composition, its dosage, pH and a temperature on the efficiency of wastewater biomass separation was investigated. The best coagulation-flocculation efficiency was achieved with the hybrid coagulant having a mass ratio of PEI/KHPAC equal to 0.3–0.5 and at the optimal dosage of 70–80 mg L<sup>-1</sup>, reaching 97% yield of the total wood biomass and 60% yield of the lignin recovery. The efficient dosage of PEI and KHPAC in hybrid coagulant was about 1.4–1.8 and 1.7–2.2 times lower than if these coagulants/flocculants were used alone. As a result of the coagulation-flocculation process, wood biomass sludge is formed, which is a sufficiently large source of renewable organic matter, with the potential to obtain value-added products. The components of the biomass sludge were found to have surface activity and binder properties, as well as cation exchange capacity. Based on these properties, its ability to structure dusty soil particles with the formation of mechanically resistant soil aggregates was studied.

**Key words:** al-based hybrid coagulant, coagulation/flocculation, soil structuring, woodworking wastewater.

### INTRODUCTION

The production of veneer in Latvia and many countries of East Europe is accomplished by the hydrothermal treatment of hardwood in special open water basins for 16–18 h at a temperature of 40–60 °C. The formed wastewater contains very high concentrations of water-soluble wood extractives, hemicelluloses and lignin compounds. Lignin and its derivatives can form highly toxic compounds and are responsible for the high chemical oxygen demand (COD) (Ali & Sreekrishnan, 2001). Therefore, the effluent from the wood hydrothermal treatment basins needs to be treated before being

discharged. A part of the wood processing enterprises does not have centralized wastewater treatment plants, and the applied technologies provide only the wastewater dilution and discharge to sewerage networks. However, in order to gain maximum benefit according to Circular Bioeconomy, the production process should be planned as effectively as possible, striving for the development of environmentally friendly technologies, the residues of which are raw materials for another technology. It can be considered as the recovery of sustainable resources, reducing the impact on the environment, waste generation and management. It is a large enough source of renewable organic substances with the potential to obtain value added products on the basis of wood wastewater biomass. Wastewater treatment by-products are basically eliminated by the combustion method for energy production (Spinosa et al., 2011). As sludge contains a variety of nutrients for plants, so it is widely used in agriculture (39% of sewage sludge produced in the European Union) as fertilizer to improve growing conditions (Lazdina et al., 2011; Kumar et al., 2017; Zapałowska et al., 2020). The use of wastewater sludge in the production of sorbents (Lin et al., 2014; Brovkina et al., 2020) and construction materials (Sales et al., 2011; Soucy et al., 2014) is also studied.

Since the wood hydrothermal treatment wastewater biomass sludge contains large quantities of hemicellulose and lignin compounds, having surface activity and binder properties as well as cation exchange capacity, this biomass can have the potential use in soil structuring and dust road control. Worldwide, for unpaved road dust control, calcium and magnesium chlorides as well as synthetic polymer binders are widely used. However, they are relatively expensive, have the low weather resistance, and some of them are not environmentally friendly (Addo et al., 2004). At the same time, dust suppressors based on a wood polymer such as lignin are eco-sound and widely used (Dustex, Earthbind 100, Nodust, Road Loc), especially in North America.

The most applied methods for removal of various suspended and colloidal pollutants from wastewater are coagulation and flocculation. High charges cations, such as  $\text{Fe}^{3+}$  or  $\text{Al}^{3+}$ , are some of the most effective reagents for destabilizing the colloids. Therefore, polyvalent inorganic salts such as  $\text{AlCl}_3$ ,  $\text{Al}_2(\text{SO}_4)_3$ ,  $\text{FeCl}_3$ ,  $\text{Fe}_2(\text{SO}_4)_3$  are widely used as coagulants (Ahmad et al., 2008). Different cationic and anionic polyelectrolytes are widely used as flocculants in wastewater treatment (Gregory & Barany, 2011). Currently, the research in the field of coagulation-flocculation process is focused on the development of more effective and less expensive hybrid composite materials, which are constituted of both inorganic and organic compounds, in view of their better performance compared to that of conventional inorganic-based coagulants, and their lower cost compared to organic-based flocculants (Lee et al., 2011). The hybrid composite materials are reported to be more efficient compared to conventional inorganic coagulants due to the synergism effect of two components in one composite material (Yang et al., 2004; Lee et al., 2012). Furthermore, the application of the inorganic-organic composite materials in the wastewater treatment required only one-unit operation in comparison with the bioperational system: at first, coagulation, then, flocculation (Lee et al., 2011).

The aim of this study was to develop a new Al-based hybrid coagulant that is effective in removing biomass from the wastewater of wood hydrothermal treatment, formed during veneer production, and to study the efficiency of its composition, dosage, pH and a temperature on wastewater biomass separation and purification quality of the treated wastewater. The possibility of the separated biomass sludge to structure dusty soil was investigated.



## MATERIALS AND METHODS

### Model system

Taking into account the fact that the composition of the birch wood pre-treatment wastewater obtained in veneer production is inconstant, for the investigation of the coagulation/flocculation process, a model system of the wastewater with unambiguous and stable characteristics was chosen (Vitolina et al., 2014). The model wastewater (MW) was obtained by a hydrothermal treatment of birch sawdust performed with 0.01M NaOH at a hydromodulus of 1/50 (a mass ratio of the oven dry sawdust to water) and a temperature of 90 °C for 4 h. After the treatment, the obtained model solution was separated from the sawdust treated through a filtration. The main parameters of the MW are listed in the Table 1.

**Table 1.** Parameters of model wastewater

pH	Biomass content, mg L <sup>-1</sup>	Density, g cm <sup>-3</sup>	COD, mgO L <sup>-1</sup>	PI, mgO L <sup>-1</sup>	Color, mg LPt <sup>-1</sup>
9.0–9.1	1,400 ± 67	0.998	1,285 ± 30	320 ± 10	746 ± 19

The defined elemental composition of the dried biomass was the following: 37.75% C; 4.78% H; 56.69% O; 0.30% N; 0.14% S, 0.34% of inorganic matter. The obtained results of the biomass fractionation showed that the content of the lignin and hemicelluloses fractions in the solid biomass corresponded to 13.5% and 75.2%, respectively, but other water-soluble products of the wood matrix destruction were 11.3%. The main component of water-soluble hemicelluloses in the wastewater was xylan (Shulga et al., 2012). The zeta potential value of the hydrolysate close to - 30 mV testified the high stability and the enhanced content of charged functional groups in the biomass. With decreasing pH to 2.0, the Z potential value of the hydrolysate fell to - 10 mV, reflecting the decrease in the ionisation degree of the hydroxyl and carboxyl groups in the water-soluble lignin and hemicelluloses fragments.

### Coagulants/flocculants

To select the most appropriate cationic polyelectrolyte for development of a new inorganic-organic coagulant, the efficiency of various commercial cationic polyelectrolytes as flocculants for wood biomass separation from the model wastewater was investigated. Three different cationic polyelectrolytes including polyethyleneimine (PEI), polydiallyldimethylammonium chloride (PDADMAC) and chitosan with different molecular weights were examined for estimation of the efficiency of biomass removal (Table 2). All polyelectrolytes were purchased from Sigma-Aldrich.

**Table 2.** The polyelectrolytes used

Polyelectrolytes	Molecular weight (g mol <sup>-1</sup> )
PDADMAC <sub>LMW</sub>	100,000–200,000
PDADMAC <sub>MMW</sub>	200,000–350,000
PDADMAC <sub>HMW</sub>	400,000–500,000
Chitosan <sub>LMW</sub>	200,000
Chitosan <sub>MMW</sub>	350,000
Chitosan <sub>HMW</sub>	500,000
PEI <sub>LMW</sub>	1,300
PEI <sub>HMW</sub>	750,000

A polyelectrolyte which showed the best biomass flocculation efficiency was selected as an organic component of the new hybrid coagulant. As an inorganic component, the previously developed Al-based inorganic composite coagulant

(KHPAC) based on polyaluminium chloride (PAC) and aluminium chloride (AlCl<sub>3</sub>) (Shulga et al., 2014) was used. Polyaluminium chloride (Polypacs-30) (30% Al<sub>2</sub>O<sub>3</sub>, 80–85% basicity) was purchased from the Industrial Holding AMK-Group (Russia). A composition of the hybrid coagulant was represented as the mass ratio of a cationic polyelectrolyte to KHPAC that varies in the range of 0.15–1.0. All the used reagents were of analytical grade.

### Coagulation/flocculation experiment

The coagulation process was carried out in a jar by mixing the equal volumes of the MW and a coagulant/flocculant solutions and stirring the obtained suspension with a magnetic stirring bar at 200 rpm for 1 min, followed by slow mixing at 40 rpm for 2 min. A coagulant/flocculant dosage was added to the MW solution in the range of 10–140 mg L<sup>-1</sup>. The Experiments were conducted at pH values ranging from 3 to 10 by addition of HCl or NaOH and in the temperature range of 13–60 °C using a thermostat. The flocs formed were allowed to settle for 120 min. After sedimentation and filtration MW samples were taken for analysis. Each experiment was carried out three times. The results are presented as mean values. The effectiveness of the coagulant/flocculant was measured based on the removal of total wastewater biomass and one of the wood components - lignin that contributes to color pollution in wastewater and removing lignin-containing substances is comparatively difficult. The residual concentration of the biomass and water-soluble lignin and lignin substances was defined by measuring the obtained filtrate's optical density at 490 and 280 nm using the previously obtained correlation curves for the biomass and lignin. Color and chemical oxygen demand (COD) was measured according to the ISO 7887:1994 and ISO 6060:1989, respectively. The coagulation/flocculation efficiency was determined, comparing the initial parameters of the model solution with the parameters obtained for the filtrate after coagulation/flocculation, using the following formula (Eq. 1):

$$\text{removal (\%)} = \left( \frac{C_i - C_f}{C_i} \right) \cdot 100, \quad (1)$$

where  $C_i$  and  $C_f$  are initial and final concentrations of wood biomass, water-soluble lignin and lignin substances, chemical oxygen demand and color. Sludge volume index (SVI) was calculated by dividing the settleability (settled sludge volume after 30 minutes) by the suspended solids concentration. The zeta potential and particle size measurements were obtained by using Malvern Zetasizer Nano Series model SZ machine.

### Soil structuring experiment

Soil structuring experiments were conducted using a dusty sand/clay model soil with a clay fraction content varied from 0–70%. Clay for this study was taken from Lielaucis quarternary clay deposit (Latvia), but sand was taken from Baltic Sea coast. The average chemical composition and the average particle size distribution of the used clay and sand soil are given in Table 3 and Table 4, respectively.

**Table 3.** Average chemical composition of clay (%)

SiO <sub>2</sub>	Al <sub>2</sub> O <sub>3</sub>	Fe <sub>2</sub> O <sub>3</sub>	TiO <sub>2</sub>	CaO	MgO	CO <sub>2</sub>	K <sub>2</sub> O	Na <sub>2</sub> O	SO <sub>3</sub>
45.47	12.27	5.34	0.67	11.60	4.87	11.22	4.04	0.52	< 0.1

**Table 4.** Average particle size distribution of sand and clay (%)

Sample	> 0.25 mm	0.25–0.05 mm	0.05–0.01 mm	< 0.01 mm
Sand	3.1	93.7	0.3	3.0
Clay	2.3	9.6	26.3	63.4

In the work, the model soil particles less than 0.25 mm were used. The soil aggregates (> 0.25 mm) were obtained by manual mixing the soil with 1.0–5.0 g dL<sup>-1</sup> biomass water suspensions during 3 minutes. The used wood biomass had a gel form with content of a dry matter about 10% and was obtained by centrifugation of the precipitated biomass sludge at 6,000 rpm during 20 min without its followed drying. The water suspensions with the defined biomass concentration were prepared by intensive mixing the biomass gel with water at 100 rpm for 10 min using a mechanical mixer. The content of the biomass in the soil samples varied from 0.2% to 0.8% on their dry matter. The fractional composition of the dried structured soil was determined by dry sieving, using a set of sieves (AS200 Retsch). Each experiment was carried out three times. The results are presented as mean values.

## RESULTS AND DISCUSSION

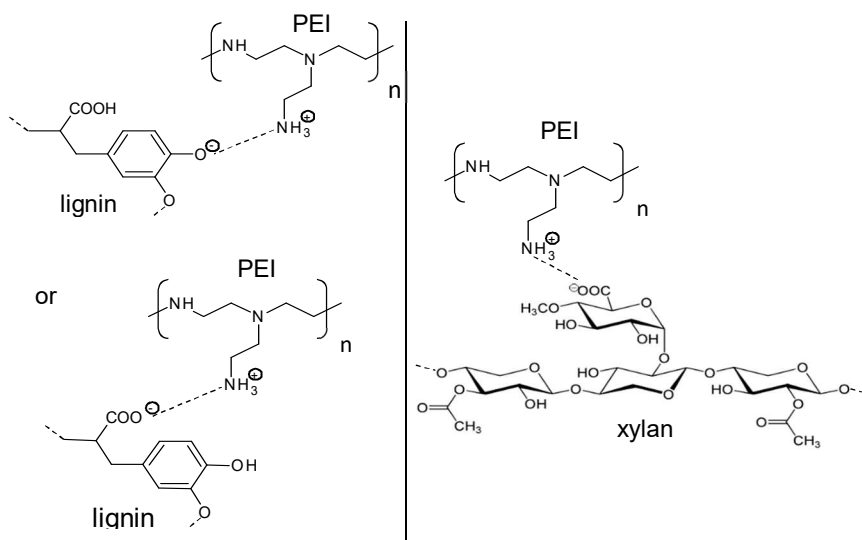
### Biomass removal by coagulation-flocculation

Using the cationic polyelectrolytes (Table 2) with different molecular weight, the efficiency of biomass removal from the birch wood hydrothermal treatment model wastewater was studied to select the most efficient cationic polymer for the development of a new hybrid composite coagulant. It is known that water-soluble low-molecular weight lignins and hemicelluloses interact with cationic polyelectrolytes in aqueous medium mainly via the electrostatic mechanism (Ström & Stenius, 1981; Shulga et al., 2002; Mocchiutti et al., 2016). As a result of the electrostatic interaction between the cationic polyelectrolytes and the biomass components, polyelectrolyte complexes (PEC) (Li & Pelton, 1992; Shulga et al., 2009) are formed (Fig. 1). The formation of insoluble PEC occurs at the stoichiometric mass ratio of the interacted components. If the applied dosage of the cationic polyelectrolyte is less or greater than the effective dosage, corresponded the stoichiometric mass ratio of the polyelectrolyte and hemicelluloses/lignin, wastewater biomass does not flocculate due to the formation of water-soluble non-stoichiometric PEC particles.

The results of the flocculation experiments with PDADMAC showed that the optimal pH range for the efficient biomass removal was pH 7–8 with an optimal dosage of 50 mg L<sup>-1</sup>, at which the total biomass and lignin removal reached 1,288 mg L<sup>-1</sup> or 92% and 171 mg L<sup>-1</sup> or 55%, respectively. It was determined that the molecular weight of PDADMAC practically did not affect its efficiency. The biomass removal efficiency of PDADMAC with a molecular weight of 200,000–350,000 g mol<sup>-1</sup> was only 1.5% better than that for PDADMAC<sub>LMW</sub> and PDADMAC<sub>HMW</sub>.

Compared to PDADMAC, chitosan is a more pH-sensitive polymer and works effectively only in acidic conditions due to the presence of amino groups. It is known that 96–97% of its amino groups are protonated at pH 5, while only 7–10% of amino groups are protonated at pH 7.5 (Van Haute et al., 2015). The protonation also results in a change in the structure of the chitosan molecule from a compact in weak alkaline medium to elongated conformation as a result of the electrostatic repulsion between the

polymeric chains. It was found that the optimal conditions for the formation of stable biomass flocs in the case of chitosan were the following: the pH values varied from 4 to 5 at the optimal dosage of 35 mg L<sup>-1</sup>. The total biomass yield was of 1,285 mg L<sup>-1</sup> or 92%, but lignin recovery was closed to 126 mg L<sup>-1</sup> or 41%. In the case of chitosan, a molecular weight effect on flocculation efficiency is observed. At the same optimal dosage and pH, chitosan with medium and low molecular weight shows on average 3% better biomass removal efficiency and 11–13% increase in lignin removal compared to high molecular weight chitosan samples.



**Figure 1.** Simplified possible electrostatic interaction pathway between PEI and the main biomass components (lignin and xylan) in the formation polyelectrolyte complexes.

PEI like chitosan is a pH-sensitive polymer which acts as a proton sponge in acidic conditions. The pH medium also affects the PEI structure that has an impact on the interaction with the wastewater biomass components. At basic medium PEI molecules are weakly protonated and have a highly coiled structure, while at acidic conditions the molecules chains are highly protonated and elongated (Choudhury & Roy, 2013). Our results showed that the optimal conditions for PEI with low molecular weight for the flocculation of the model wastewater were the following: the dosage of 14–20 mg L<sup>-1</sup> and pH 4–5. To achieve the best biomass and lignin removal efficiency with the high-molecular weight PEI a larger dosage was required. The defined optimal PEI<sub>HMW</sub> dosage was 25–35 mg L<sup>-1</sup> at pH 6. At the defined optimal conditions PEI<sub>HMW</sub> shows 4% higher biomass and 11% better lignin removal efficiency than PEI<sub>LMW</sub>.

Table 5 shows that the total biomass removal efficiency does not differ significantly for all the polyelectrolytes and achieves 91–93%. At the same time, there are significant differences in the lignin extraction efficiency. Chitosan is the worst flocculant for water-soluble lignin and lignin-containing substances. Its efficiency is by 16–18% lower than for PDADMAC and PEI and directly correlates with the MW color reduction. An important coagulation/flocculation parameter is pH. Using PEI, as compared to PDADMAC, in the flocculation process it is not necessary to use alkali to ensure the

desired pH; also pH fits in the permissible pH value range for wastewater prior to its discharge to the sewerage network or for reuse. The optimal pH values of the biomass flocculation with PEI lied within the optimal pH range of coagulation with Al-based coagulants (Brovkina et al., 2020), which was important for the development of a new hybrid composite coagulant.

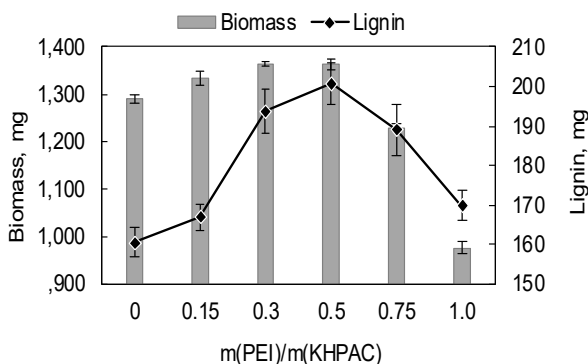
Based on the comparison of obtained results (Table 5), high molecular weight PEI, which showed the best flocculation ability among the studied polyelectrolytes, was selected as an organic component of the new hybrid composite coagulant. The polyaluminium-based composite coagulant - KHPAC, shown higher coagulation ability than other Al-based salts (Brovkina et al., 2020), was chosen as an inorganic component of the composite. The composite coagulant PEI-KHPAC in the polymer colloidal complex form is formed due to the donor-acceptor interaction between the uncharged nitrogen atoms in imine groups and aluminium ions. Taking into account the hydration shell around the aluminium ions, the complex is stabilized with hydrogen bonds (Vitolina, 2018). Owing to the hybrid nature, comprising an organic flocculant and an inorganic coagulant, the obtained hybrid coagulant should simultaneously perform both coagulation and flocculation function. This could increase the biomass removal efficiency and simultaneously reduce the optimal dosage relative to PEI and KHPAC, if they act separately.

The coagulation-flocculation process with the developed hybrid coagulant can be described as the adsorption of hemicelluloses and lignin fragments on the PEI-KHPAC particle surface as a result of the neutralization of biomass surface polar groups (–OH and –COOH) and PEI-KHPAC positively charged surface amino groups, followed by the aggregation of biomass coagulated particles, owing to the ‘bridge formation’ mechanism. The bridging mechanism can be explained by the presence of loops and tail in the PEI chains, included in the formation of the PEI-KHPAC, and, when another biomass molecule (with free absorption centers) comes across these ‘defects’, binding takes place and the biomass flocs are formed.

The treatment effect of the model wastewater with PEI-KHPAC, prepared with the different mass ratio of PEI to KHPAC, at pH 6 is shown in Fig. 2. The obtained results show that PEI-KHPAC is characterised by the highest efficiency when the ratio of PEI

**Table 5.** Efficiency of the investigated cationic polymers at optimal parameters

Parameters	PDADM AC	Chitosan	PEI
Molecular weight	medium	medium	high
Optimal dosage, mg L <sup>-1</sup>	50	35	35
Optimal pH	8	5	6
Biomass, mg	1,288	1,285	1,309
Lignin, mg	171	126	175
Color removal, %	88.6	85.2	91.4
COD removal, %	39.2	41.9	44.0

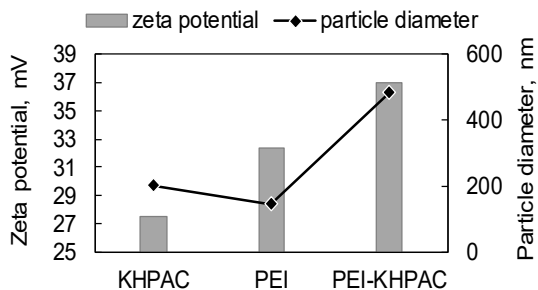


**Figure 2.** Total biomass and lignin removal efficiency as a function of composite mass ratio of PEI/KHPAC; pH 6, dosage-100 mg L<sup>-1</sup>, 20 °C.

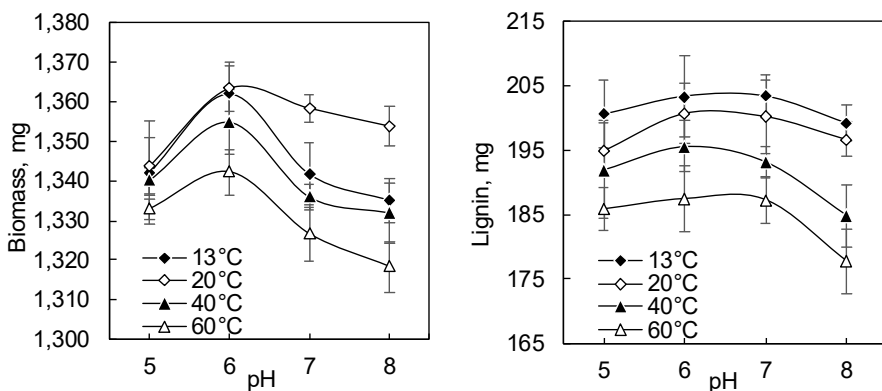
to KHPAC changes in the range of 0.3–0.5. Herewith, the removal rates of the biomass and lignin reached 1,364 mg L<sup>-1</sup> and 194–201 mg L<sup>-1</sup>, respectively.

Fig. 3 shows average particle diameter and zeta potentials for the nanoparticles of PEI-KHPAC and its components - PEI and KHPAC in water solutions. Compared with the case of KHPAC and PEI, the nanoparticles of PEI-KHPAC are characterized by a higher zeta potential and a greater average particle diameter, which indicates the formation of new coagulant particles as a result of the interaction of PEI and polyvalent aluminium ions.

The pH of wastewater is one of the important factors affecting the coagulation-flocculation efficiency. The coagulation-flocculation performance of PEI-KHPAC was studied in the pH range of 5–8. Fig. 4 shows that the amount of the separated biomass increases by increasing the pH from 5 to 6 and further decreases in neutral and alkaline media. PEI-KHPAC demonstrates the best efficiency of the lignin extraction at pH 6–7. Based on the obtained results, it was concluded that pH 6 is the optimal medium for the treatment of MW with PEI-KHPAC.



**Figure 3.** Zeta potential and average particle diameter of PEI-KHPAC and its components; composite mass ratio 0.5.



**Figure 4.** Total biomass and lignin removal efficiency with PEI-KHPAC as a function pH and temperature; composite mass ratio 0.5, dosage-100 mg L<sup>-1</sup>.

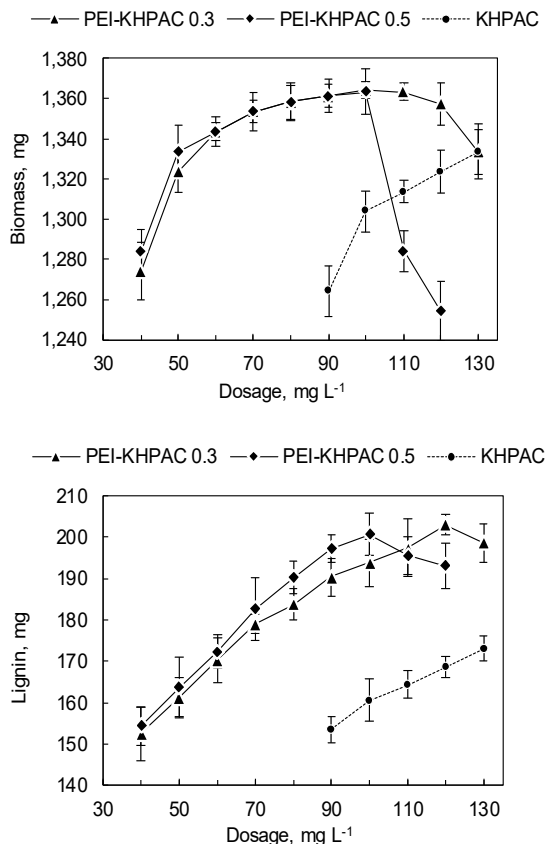
Since the coagulation-flocculation process is sensitive to temperature changes (Sahu & Chaudhari, 2013), the comparative efficiency of PEI-KHPAC in the temperature range of 13–60 °C was investigated. According to Fig. 4, the drop of temperature below 20 °C practically does not affect the biomass yield values at pH 6, but, with increasing pH more than 6, the efficiency of the treatment with PEI-KHPAC sufficiently decreases. The growth of the temperature up to 40 and 60 °C worsens the efficiency of the coagulation-flocculation process that can be explained by the dependence of dissociation degrees of the hemicelluloses/lignin components of the wood biomass on a temperature. It is seen (Fig. 4) that the best yield of lignin is at 13 °C, which

is consistent with the fact that at lower temperatures the ionisation of the phenolic hydroxyl groups is favourable (Norgren & Lindström, 2000).

The efficiency of the biomass and lignin removal with PEI-KHPAC, having various mass ratio of PEI to KHPAC equal to 0.3 and 0.5, respectively, in comparison with KHPAC was studied at pH 6 by varying the coagulants dosage (Fig. 5).

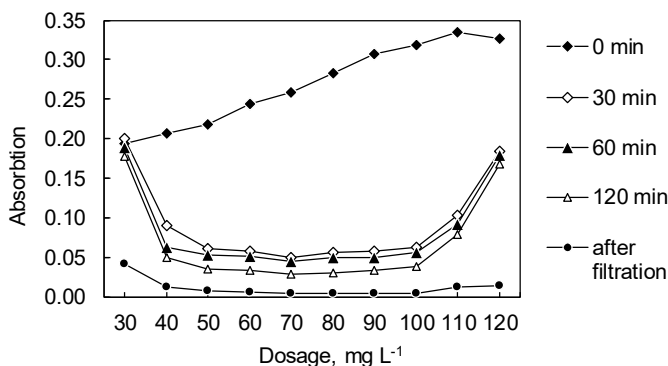
It is shown that the hybrid coagulant is characterised by a higher yield both the biomass and lignin than the inorganic coagulant at the same dosages. A similar trend of the dependence of the biomass and lignin yield on the applied dosage is observed for both compositions of PEI-KHPAC, namely, the biomass and lignin removal increases to a maximum value and then decreases with the dosage growing. This is consistent with the fact that a certain dosage of the coagulant PEI-KHPAC is needed to provide the stoichiometric mass ratio of the coagulant to the hemicelluloses/ lignin components in the model wastewater. According to Fig. 5, with increasing PEI-KHPAC dosage from 40 to 70 mg L<sup>-1</sup>, the biomass yield increases, reaching 1,353–1,358 mg L<sup>-1</sup> or 97%. The effect of further increasing the dosage on the removed biomass quantity is not pronounced, and already at a dosage > 100 mg L<sup>-1</sup> the coagulant efficiency decreases. In the case of lignin, the removal efficiency increases linearly with the coagulant dosage and achieves the maximal value at 100 mg L<sup>-1</sup> for PEI-KHPAC composition of 0.5 and 120 mg L<sup>-1</sup> for the composition of 0.3, reaching a 201–203 mg L<sup>-1</sup> lignin yield or 65%.

Fig. 6 shows the changes in the MW absorption over time as a function of PEI-KHPAC dosage. The initial MW absorption increases with the increase of PEI-KHPAC dosage, reaching a maximal value at a dosage of 110 mg L<sup>-1</sup>. As follows from the Fig. 6, the sedimentation process of the formed flocs is practically realized within 30 minutes at PEI-KHPAC dosage range of 40–100 mg L<sup>-1</sup> and is accompanied by the formation of the dense sludge at the bottom of the cylinders (Fig. 6, a). The obtained filtrates of the treated model wastewater were visually transparent in colour at the optimal applied dosages. The performed analysis of the sizes of the formed flocs showed that, after 30 min of the coagulation-flocculation process, their diameter varied

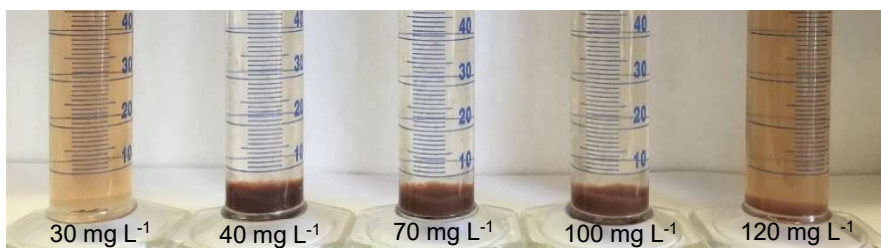


**Figure 5.** Total biomass and lignin removal efficiency of the coagulants as a function of dosage; pH 6, 20 °C.

in the range of 1,114–1,242 nm. At the same time, the sizes of the flocs formed with PEI and KHPAC applied separately were significantly lower, i.e. 664–842 nm and 331–499 nm, respectively.

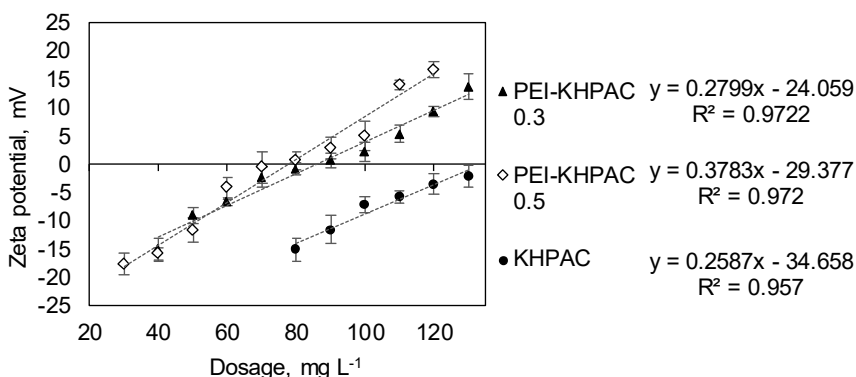


**Figure 6.** MW absorption (490 nm) changes during coagulation-flocculation process as a function of time and PEI-KHPAC dosage; composite mass ratio - 0.5, pH 6, 20 °C.



**Figure 6a.** Settlement of flocs during the coagulation-flocculation process after 30 min using PEI-KHPAC with various applied dosages; composite mass ratio 0.5, pH 6.

The zeta potential profiles for the MW after coagulation with PEI-KHPAC and KHPAC as the function of a dosage at pH 6 are presented in Fig. 7.



**Figure 7.** Zeta potential profiles for the MW at pH 6 after coagulation with PEI-KHPAC and KHPAC as a function of coagulant dosage.



According to Pefferkorm (2006), if the charge neutralization is the only path for coagulation, the zeta potential should be in excellent correlation with the coagulant dosage, and the optimal efficiency is achieved when zeta potential is close to zero. It can be seen that the zeta potential changes correlate very well with the applied coagulants dosages. There is a linear correlation ( $R > 0.97$ ) between the filtrate zeta potential and the applied dosages of PEI-KHPAC with a mass ratio of 0.3 and 0.5. This indicates that the formation of the flocs mostly occurs according to the charge neutralization mechanism, because the maximal yield of the wood biomass is reached when the zeta potential of the treated MW is close to zero. It can be seen (Fig. 7) that, for the both compositions of PEI-KHPAC, the negative values of a zeta potential for the filtrates, formed after the MW treatment, exceed zero at the applied dosages more than 70–80 mg L<sup>-1</sup>. With the further increasing the dosage of the coagulant, the zeta potential of the filtrates increases, but the biomass removal efficiency no longer grows significantly, which can point to the composite coagulant dosage excess. In turn, for KHPAC, in the range of 30–130 mg L<sup>-1</sup> of the applied dosage, the filtrate zeta potential still remains negative, which indicates that the complete neutralization of biomass particles has not yet occurred.

Table 6 shows a comparison of the optimal parameters (dosage, pH) and efficiency (biomass and lignin yield, the color of treated MW, COD, etc.) of the coagulation-flocculation process at 20 °C using the KHPAC and the hybrid coagulant PEI-KHPAC with two compositions.

**Table 6.** Efficiency of coagulants at optimal parameters

Parameters	KHPAC	PEI-KHPAC <sub>0.3</sub>	PEI-KHPAC <sub>0.5</sub>
Optimal	100	80	70
Optimal pH	6	6	6
Biomass, mg	1,304	1358	1,353
Lignin, mg	161	184	183
Color removal, %	85.4	89.8	89.3
COD removal, %	46.7	49.7	47.8
Aluminium	0.063	0.032	0.025
SVI, mL g <sup>-1</sup>	107	74	74

In accordance with the data in Table 6, the yield of the biomass and lignin using the hybrid coagulant at the optimal dosage is higher by 4.1% and 14.3% compared with KHPAC, who's the optimal dosage is by 25–43% higher than that in the case of the hybrid coagulant. It is known that residual aluminium concentration in wastewater is a very important parameter from health perspectives and should be carefully considered, when an aluminium coagulant is applied in the water treatment. Since the aluminium salt content in the hybrid coagulant is 1.7–2.2 times lower than in KHPAC, the concentration of residual aluminium in the filtrate is essentially decreased. The performed study showed that the concentration of residual aluminium ions in the filtrates of the MW treated with the hybrid coagulant was 2–2.5 times lower than that in the filtrates after the treatment with KHPAC. Higher rates of the biomass and lignin yield when treating the MW with the hybrid coagulant lead to the increase in such important indicators of wastewater treatment as color removal and COD removal in comparison with those for the inorganic coagulant. The developed coagulant PEI-KHPAC is characterized also by a good sedimentation kinetic, which is confirmed by the sludge volume index (SVI) values. For PEI-KHPAC, this index is lower than 100 mL g<sup>-1</sup>, which is an important parameter from the technological point of view. It is known that when adding aluminium salt coagulant, a pH value of the treated wastewater decreases, and its decrease depends on the initial pH value of the wastewater. In this study, we have found that by adding the

optimal KHPAC dosage to the MW, a pH value of the MW decreases from pH 9 to pH 4. In order to achieve the optimal coagulation pH 6, it was necessary to add sodium hydroxide to the MW. In turn, by using the optimal dosages of PEI-KHPAC, the pH values of MW varied in the range of 6.0–6.5, which already was the optimal value for the coagulation/flocculation process. Such a manner, it is not necessary to add alkali to achieve the required pH that is a substantial advantage from the reagent-saving, cost and technology viewpoint.

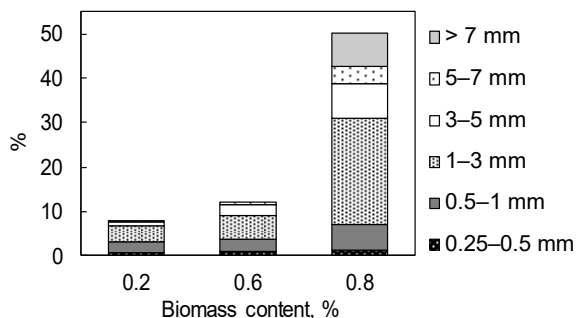
### Use of biomass sludge in soil structuring

Since the surface of the precipitated biomass contains both completely hydrophobic regions, which are formed as a result of the interaction of the biomass components with the PEI-KHPAC hybrid coagulant, and free functional groups (carboxyl-, hydroxyl-, amino-), which are located in the coagulate segments (e.g., tails, loops), the separated biomass particles have to exhibit binding properties. Taking into account a possible application of the separated biomass, its ability to structure dusty soil particles with the formation mechanically resistant soil aggregates was studied. It was supposed that the wastewater biomass can adsorb on the sandy soil particles due to physicochemical interactions, including Van der Waals forces and hydrogen bonds between Si-OH groups of the soil and the biomass particles' carboxyl-, hydroxyl- and amino groups, locating in the biomass coagulate segments. With the increase of the clay particles content in the model soil composition, besides hydrogen bonds and Van der Waals forces, the contribution of the hydrophobic interaction between the biomass and the soil particles should increase.

The precipitated biomass was used after the centrifugation in a wet state (a moisture content is 93%), without its drying. The biomass suspensions with a defined concentration were obtained by diluting the biomass with water and actively mixing them with the mechanical mixer during for 10 min. As dusty soil samples, a sandy soil and a model sand/clay soil with the clay content from 30% to 70% and the soil particles < 0.25 mm were used.

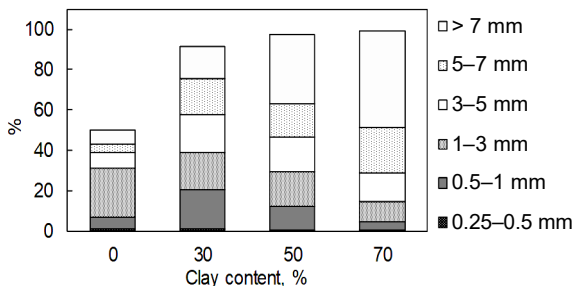
An important parameter that shows effectiveness of the application of the structure forming agent is a fractional composition of the treated soil. The fractional composition of the sandy soil treated with the biomass suspensions as a function of the content of biomass is given in Fig. 8.

It can be seen that, with increasing the content of the biomass, the amount of the soil aggregates in the fractional composition increases from 10% to 50%. The growth of the amount of the soil aggregates is also accompanied by their sizes enhancement. It can be seen that the main fraction (more than 50%) in the aggregated sandy soil part is a medium-sized one with a diameter of 1–3 mm, which essentially grows with increasing the biomass content from 0.2% to 0.8%.

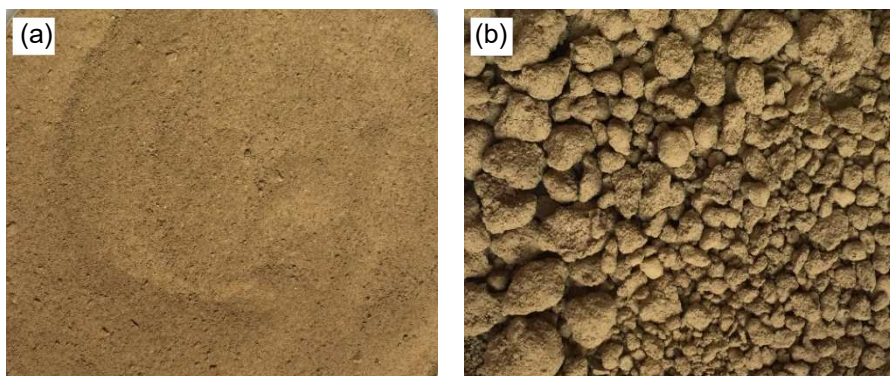


**Figure 8.** Fractional composition of the treated sandy soil as a function of the content of biomass sludge.

The structuring the model sand/clay soil shows that, with increasing the clay content in the soil, the soil aggregate amount remarkably increases and shifts to a higher content of the large soil species (Fig. 9). Using the model soil with 70% clay content, the amount of the aggregates achieves 98% of the soil mass at the 0.8% biomass content (Fig. 10) and that is 48% higher than the total aggregate mass in the treated sandy soil at the same biomass content. Compared with the treated sandy soil, where the amount of the large soil aggregates (> 3 mm) represents 38% of all aggregates formed, this amount in the model sand/clay soil grows to 57–85% with increasing the content of the clay from 30% to 70%.



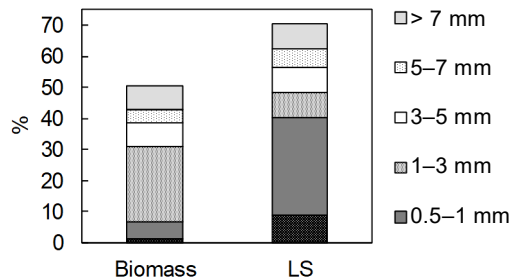
**Figure 9.** Fractional composition of the treated sand soil as a function of the clay content in the soil, biomass concentration 0.8%.



**Figure 10.** Model soil before (a) and after (b) structuring with precipitated wastewater biomass, clay content 70%, biomass concentration 0.8%.

For the comparative assessment of the wastewater biomass capacity to structure soil, softwood lignosulphonates (LS), a wood chemical processing by-product, which is widely used as a dust suppressor for control unpaved road (Addo et al., 2004), were selected. LS were characterised by the following empirical formula of the phenylpropane chain:  $C_9H_{6.89}O_{2.57}(OCH_3)_{0.71}(SO_3)_{0.35}(OHph)_{0.68}(CO)_{0.36}$ . The average weight molecular mass of LS calculated from its viscosimetric data in 0.1 M NaCl was equal to 28,000 g mol<sup>-1</sup>. According to Fig. 11, when treating the soil with the biomass suspension, the total soil aggregate content is equal to 50% of the soil mass, while using the LS, the amount of the aggregates is higher and accounts for 70% of the soil mass. However, the comparison of the fractional compositions of the both treated soil samples shows that

the separated biomass is capable of forming aggregates of a larger diameter than LS at the same content in the soil. Aggregated part of the soil samples structured with LS are primarily composed of the fraction with a diameter of 0.5–1 mm representing 32% of total soil mass, but the samples structured with the separated biomass contain mainly the fraction with the larger size aggregates with a diameter of 1–3 mm, which is 24% of total soil mass. A higher content of large soil aggregates formed by the separated wood biomass could positively effect on the wind erosion resistance of dusty soils.



**Figure 11.** Fractional composition of the sand soil treated with the separated biomass and lignosulphonate, biomass concentration 0.8%.

## CONCLUSIONS

This study successfully proved the effectiveness of the developed hybrid coagulant, formed as a result of the interaction between high molecular PEI and the polyaluminium-based composite coagulant (KHPAC), in separation of the wood biomass from the model solution, simulating wastewater of a woodworking enterprise. It is concluded that the properties of the new coagulant and its coagulation-flocculation efficiency may vary, changing its composition in a narrow range. Using the model wastewater, it was found that the best coagulation-flocculation efficiency is observed for the hybrid coagulant with a mass ratio (PEI/KHPAC) of 0.3–0.5 at the optimal dosage of 70–80 mg L<sup>-1</sup> and pH 6. At these parameters, the yield of the total wood biomass and lignin reaches 97% and 60%, respectively, color and COD removal close to 90% and 50%, respectively. The efficient dosage of PEI and KHPAC in hybrid coagulant is about 1.4–1.8 and 1.7–2.2 times lower than if coagulants/flocculants are used alone, but the content of the residual aluminium ions in the model wastewater filtrate is 2–2.5 times lower than that for the KHPAC coagulant.

The results of soil structuring experiments show that the separated wastewater biomass is capable of structuring dusty soil and to form soil aggregates. With increasing the clay content in the soil composition, the total aggregates' content in the soil essentially grows, wherein the amount of fine aggregates fraction decreases and the amount of the coarse aggregates fraction enhances.

## REFERENCES

- Addo J.Q., Sanders T.G., Chenard M. 2004. Road dust suppression: effect on maintenance stability, safety and the environment, phases 1–3, MPC Report No. 04–156.
- Ahmad A.L., Wong S.S., Teng T.T. 2008. Improvement of alum and PACl coagulation by polyacrylamides (PAMs) for the treatment of pulp and paper mill wastewater, *Chemical Engineering Journal* **137**, 510–517
- Ali M., Sreekrishnan T.R. 2001. Aquatic toxicity from pulp and paper mill effluents: a review, *Advances in Environmental Research* **5**, 175–196.

- Brovkina J., Shulga G., Ozolins J., Neiberte B., Verovkins A., Lakevics V. 2020. The advanced application of the wood-originated wastewater sludge, *Agronomy Research* **18**(S1), 729–741.
- Choudhury C.K., Roy S. 2013. Structural and dynamical properties of polyethylenimine in explicit water at different protonation states: A molecular dynamics study, *Soft matter* **9**(7), 2269–2281.
- Gregory J., Barany S. 2011. Adsorption and flocculation by polymers and polymer mixtures, *Advances in Colloid and Interface Science* **169**, 1–12.
- Kumar V., Chopra A.K., Kumar A. 2017. A review on sewage sludge (Biosolids) a resource for sustainable agriculture, *Archives of Agriculture and Environmental Science* **2**(4), 340–347.
- Lazdina D., Bardule A., Lazdins A., Stola J. 2011. Use of waste water sludge and wood ash as fertiliser for Salix cultivation in acid peat soils, *Agronomy Research* **9** (1–2), 305–314.
- Lee K.E., Morad N., Teng T.T., Poh B.T. 2011. An application study of inorganic-organic composite polymer in flocculating reactive dye wastewater under different conditions, *Proc. International Conference on Biology, Environment and Chemistry IPCBEE*, Singapore, vol. 24, 139–143.
- Lee K.E., Morad N., Teng T.T., Poh B.T. 2012. Development, characterization and the application of hybrid materials in coagulation/flocculation of wastewater: a review, *Chemical Engineering Journal* **203**, 370–386.
- Li P., Pelton R. 1992. Wood pulp washing I. Complex formation between kraft lignin and cationic polymers, *Colloid. Surface* **64**(3–4), 217–222.
- Lin L., Xu X., Papelis C., Cath T.Y., Xu P. 2014. Sorption of metals and metalloids from reverse osmosis concentrate on drinking water treatment solids, *Separation and Purification Technology* **134**, 37–45.
- Mocchiutti P., Schnell C. N., Rossi D. G., Peresin M. S., Zanuttini M. A., Galván M. V. 2016. Cationic and anionic polyelectrolyte complexes of xylan and chitosan. Interaction with lignocellulosic surfaces, *Carbohydrate Polymers* **150**, 89–98.
- Norgren M., Lindström B. 2000. Dissociation of phenolic groups in kraft lignin at elevated temperatures, *Holzforschung*, **54**, 519–527.
- Pefferkorn E. 2006. Clay and oxide destabilization induced by mixed alum/macromolecular flocculation aids, *Advances in Colloid and Interface Science* **120**, 33–45.
- Sahu O.P., Chaudhari P.K. 2013. Review on Chemical treatment of industrial waste water, *Journal of Applied Sciences and Environmental Management* **17**(2), 241–257.
- Sales A., De Souza F.R., Almeida F.R. 2011. Mechanical properties of concrete produced with a composite of water treatment sludge and sawdust, *Construction and Building Materials* **25**(6), 2793–2798.
- Shulga G., Kalyuzhnaya R., Zezin A., Kabanov V. 2002. Effect of the molecular mass of lignosulphonate on the interaction with polymeric cation in dilute aqueous solutions and the properties of products formed, *Cellulose Chemistry and Technology* **36**(4), 225–241.
- Shulga G., Shakels V., Aniskevicha O., Zakharova J., Skudra S. 2009. Interfacial properties of polyelectrolyte complexes incorporating kraft lignin, *Holzforschung* **63**(6), 711–714.
- Shulga G., Vitolina S., Brovkina J., Neiberte B., Puke M., Vedernikovs N., Turks M., Rjabovs V. 2012. *Characterization of biomass from the wood hydrolyzate and its isolation with organic and inorganic polycation*, Proc. of the 12th European Workshop on Lignocellulosics and Pulp, EWLP-2012. Espoo, Finland, August 27–30, 2012, 512–515.
- Shulga G., Brovkina J., Neiberte B., Ozolins J., Neilands R. 2014. A method for wastewater treating from lignin and hemicellulose substances at wood processing plants. Latvian Patent, No. 14789 B. (in Latvian)

- Soucy J., Koubaa A., Migneault S., Riedl B. 2014. The potential of paper mill sludge for wood-plastic composites, *Industrial Crops and Products* **54**, 248–256.
- Spinosa L., Ayol A., Baudez J.C., Canziani R., Jenicek P., Leonard A., Rulkens W., Xu G., van Dijk L. 2011. Sustainable and innovative solutions for sewage sludge management. *Water* **3**, 702–717.
- Ström G., Stenius P. 1981. Formation of complexes, colloids and precipitates in aqueous mixtures of lignin sulphonate and some cationic polymers, *Colloid Surface* **2**(4), 357–371.
- Van Haute S., Uyttendaele M., Sampers I. 2015. Coagulation of turbidity and organic matter from leafy-vegetable wash-water using chitosan to improve water disinfectant stability, *LWT - Food Science and Technology* **64**, 337–343.
- Vitolina S., Shulga G., Neiberte B., Livcha S., Verovkins A., Puke M., Reihmane S. 2014. The efficiency of biomass removal from model woodworking wastewater with polyethylenimine. *Selected papers of 9th International Conference Environmental Engineering (9th ICEE)*, Vilnius, Lithuania. doi: 10.3846/enviro.2014.067
- Vitolina S. 2018. *Efficient separation of biomass from veneer production hydrothermal treatment wastewater, its characterization and application possibility*, PhD Thesis, Riga Technical University, Riga, Latvia.
- Yang W.Y., Qian J.W., Shen Z.Q. 2004. A novel flocculant of Al(OH)<sub>3</sub>-polyacrylamide ionic hybrid, *Journal of Colloid and Interface Science* **273**, 400–405.
- Zapałowska A., Puchalski Cz., Stankowski S., Gibczyńska M. 2020. Fertilisation with ash from wood and with sewage sludge versus contents of macro-and microelements in the soil following cultivation of *Helianthus tuberosus* L. *Agronomy Research* **18**(2), 650–661.

## Suitability of various onion (*allium cepa*) varieties for drying and long-term storage

O. Zavadzka<sup>1</sup>, I. Bobos<sup>1</sup>, I. Fedosiy<sup>1</sup>, H. Podpriatov<sup>1</sup>, O. Komar<sup>1</sup>, B. Mazur<sup>1</sup> and J. Olt<sup>2,\*</sup>

<sup>1</sup>National University of Life and Environmental Sciences of Ukraine, 15 Heroyiv Oborony Str., UA 03041 Kyiv, Ukraine

<sup>2</sup>Estonian University of Life Sciences, Institute of Technology, 56 Kreutzwaldi Str., EE 51006 Tartu, Estonia

\*Correspondence: [jyri.olt@emu.ee](mailto:jyri.olt@emu.ee)

Received: April 15<sup>th</sup>, 2021; Accepted: July 21<sup>st</sup>, 2021; Published: July 22<sup>nd</sup>, 2021

**Abstract.** In the paper, the results are presented obtained in the research into the fresh bulbs and the dried products of 9 onion varieties cultivated in the conditions of the Ukrainian Forest Steppe area with regard to their economical biology, biochemical, marketability and organoleptic indices. The varieties that are most suitable for convection drying and long-term storage have been identified. It has been established that the marketability of both the fresh bulbs and dried products depends on the masses of the bulbs. The Bronze d’Amposta and Harmony varieties deliver the greatest amount of marketable output (94.0 and 93.2%) featuring marketable bulbs with masses of 67.4 g and 70.4 g, respectively ( $r = 0.82$ ). As the bulb mass increases, the amount of non-standard ( $r = -0.81$ ) and small ( $r = -0.76$ ) particles in the dried product decreases substantially. It has been found that the content of solid matter and sugars in fresh bulbs has effect on the yield and quality of the dried and reconstituted products. The Harmony and Skvirskaya varieties, the bulbs of which during the vegetation season build up 12.9% and 13.8% of solid matter, respectively, are distinguished by the highest dry product yield - 17.1 and 16.8%, respectively. Correlation has been established between the contents of solid matter and sugars in fresh bulbs ( $r = +0.58$ ). During the tasting of reconstituted onion products, the highest scores were awarded to the samples produced from the Skvirskaya and Harmony varieties - 7.0 points each on the 9-point scale, as their bulbs had accumulated over 7.0% of sugars (total). Judging by the aggregate of the researched indices, the Harmony and Skvirskaya varieties of onions are the most suitable for convection drying. It has been established that the preservation of onions in the conditions of stationary buried storage without artificial cooling depends on the duration of storage and the specific varietal features. Within the five months of the test storage, the preservation of bulbs of all the varieties was high and varied within the range of 80–93%. Longer storage is expedient only in case of the Harmony, Skvirskaya and Gospodinya, for which the bulb preservation rates for a seven month storage period has been shown to be equal to 90.2, 88.4 and 87.2%, respectively. It has been proved that the quantity of healthy bulbs depends to a significant extent on the solid matter content in the bulbs ( $r = 0.93$ ).

**Key words:** bulb, drying, marketability, onion, quality, solid matter, storage, variety.

## INTRODUCTION

Onions are a high yield and highly profitable vegetable crop, a widely used and valuable article of food that is consumed fresh, long-term stored and processed (Sych et al., 2010; Bobos & Zavadska, 2016). Onion bulbs are a source of biologically valuable agents, mineral salts and minor nutrient elements (calcium, potassium, magnesium, phosphorus and iron) that are indispensable for the human body (Block, 1985; Griffiths et al., 2002). The phytoncides concentrated in large quantities in the basal plate possess antibacterial, antifungal and other therapeutic properties. For that reason, onions have been used in medicine since the times of Hippocrates and their curative properties are acknowledged throughout the world (Sych et al., 2010). They are applied as a helminthicide, a remedy against scorbute, for strengthening the immunity and protecting from oncological diseases (Challier et al., 1998; Griffiths et al., 2002).

The content of main biochemical components in the bulbs varies depending on the variety, type of soil, applied fertilisers and weather conditions (Bolotskihh, 2001; Forney et al., 2010). Overall, fresh bulbs contain 12–16% of solid matter, 6–10% of sugars (fructose, saccharose, maltose, inulin), 1.6–2.5% of proteins, 0.8–1.3% of fibres (Block, 1985; Zavadska & Hrabovenko, 2016). Bulbs have greater nutritional value comparing with green leaves (Sych et al., 2010). Pungent varieties generally contain more solid matter, sugars and essential oils than sweet ones (Skaletska et al., 2014a). Because of that, they are more suitable for long-term storage and processing.

The issues of storage and processing have always been and will remain topical for any commodity producer of onions. Indeed, the production of this crop follows a seasonal pattern, the main harvesting output is obtained in the summer-autumn period and it is not fully consumed by the population. The almost whole harvested crop has to be stored for a certain period of time or processed. Due to the absence of dedicated stationary storage facilities and the inability to process the required amounts of raw stock, each year about 25–30% of the harvested crop is lost (Davydenko et al., 2020; Zavadska et al., 2020).

Storing vegetables is a multifaceted problem contingent on many factors. The onions' storage potential depends mostly on the variety, the climatic conditions during the vegetation, the dosing and timing of fertilizer treatment, watering, growth-regulating chemical dressing, the time of harvesting and the storage conditions (Suojala, 2001; Adamicki, 2005; Forney et al., 2010; Petropoulos et al., 2017; Irkov et al., 2018). The term of onion storage is contingent on the state of true dormancy. The ability of bulbs to remain in the state of dormancy has developed in the process of their evolution as the adaptation to adverse environment conditions (Ilić et al., 2009; Downes et al., 2010). The duration of this period is the characteristic feature of a specific variety – it is longer for late varieties and shorter for early ones (Sych et al., 2010; Bobos & Zavadska, 2016). On the one hand, the bulb dormancy duration depends on the amount of stored nutrients in the bulb, therefore, the greater their reserve is, the longer the period of storage can be, but that is not always the case (Skaletska et al., 2014a).

The germination of bulbs is prevented, first of all, by the application of cold. In case of onions, a temperature of  $0 \pm 1$  °C significantly extends the period of dormancy (Ilić et al., 2009; Petropoulos et al., 2017). Higher temperatures in the storage promote a rise in the respiration intensity of the bulbs and the increased loss of the mass and solid



matter. At lower storage temperatures (below minus 3 °C) the risk of freezing the bulbs with their subsequent rapid damage arises (Sych et al., 2010).

The relative air humidity in facilities for storing onions of any designated purpose may not exceed 70–75%. During their storage, bulbs are more sensitive to an increase in the relative air humidity in the storage facility, than to an increase in the temperature. When the outer scales are wetted, the bulb comes out of the state of dormancy, starts sprouting and is in danger of rapid damage by diseases and complete loss of quality (Ilić et al., 2009).

Among the existing various ways of processing harvested vegetable crops, drying is the most widely used and economically sound method (Khan et al., 2016; Asiah et al., 2017). Dried onion is a nutritional ingredient of great commercial value that is popular throughout the world and is an indispensable component in all vegetable dry mixes added to starters, garnishes, sauces etc. It imparts to the prepared meals characteristic smell and taste and also enriches them with biologically valuable agents (Abdou et al., 2018; Edith et al., 2018).

Onion bulbs as the subject of drying are marked by a high water content, while the solid matter content in them is relatively low (Skaletska et al., 2014a). The bulk of the water is present in the free movable state and only about 5% of it is combined with cell colloids and reliably retained (Pavlović et al., 2011). That makes relatively easy to lightly dry the raw stock to a moisture content of 12–14% and complicates the removal of the remaining moisture (Dev et al., 2006; Arslan & Özcan, 2010; Asiah et al., 2017; Abdou et al., 2018; Bulgakov et al., 2020).

The quality of dried onion depends to a significant extent on the method of drying and the quality of feed stock, first of all, the varietal features and biochemical agents content (Dev et al., 2006; Abdou et al., 2018; Seifu et al., 2018). In the assessment of any fresh vegetable stock with respect to its suitability for drying, it is important to take into account the contents of solid matter, biologically valuable agents and sugars, as they have effect on the yield and quality of the dried product (Mota et al., 2010; Zavadska, 2020). In order to achieve high quality in the mechanical processing of bulbs, the following properties are essential: shape of the bulb, firmness, integrity of the skin and the strength of its bond with the fruit body. The thinner and tenderer the covering layer is, the easier the bulb is peeled. The presence of greened bulbs is not allowed, because in that case the dried product will have an atypical greenish colour (Zavadska & Hrabovenko, 2016). All the above-mentioned properties depend to a significant extent on the varietal features.

Thus, in accordance with the results of the research carried out in different countries, the suitability of onions for long-term storage and the possibility to obtain high quality dried products depends to a considerable extent on the varietal features. Every year, new varieties of onions come to the market, but their suitability for storage and processing is not fully investigated. The issue of storing onion bulbs in buried stationary storage facilities without artificial refrigeration, where the temperature conditions can vary has not been researched to a sufficient extent. The results obtained in the research can be used by scientists and manufacturers engaged in the cultivation, storage and processing of *Allium cepa* (Breu, 1996).

The aim of the paper was to investigate the marketability, biometric, biochemical, organoleptic and production indices of the quality of fresh bulbs and dried products of

various *Allium cepa* varieties in order to identify those that are most suitable for long-term storage and convection drying.

## MATERIALS AND METHODS

The research was carried out in the period of 2012–2016 in the National University of Life and Environmental Sciences of Ukraine (NULES) following the single-factor experiment technique (Bondarenko & Yakovenko, 2001). Onions of the varieties under investigation were grown in the experimental collection field of the NULES without watering.

The total area of the recorded plots was equal to 144 m<sup>2</sup>, one plot - 6 m<sup>2</sup>. The research was carried out with three replicates. The seeds were sown following the 20 +50 cm pattern, the density was arranged to be at 600,000 plants per hectare. All the varieties including the reference one were sown simultaneously in the first ten-day period of April (05.04.2017, 07.04.2018, 06.04.2019). In the crop rotation system, onions were cultivated after cucumbers.

The location of the experimental plot was in the Forest Steppe zone. The climate of the zone was moderately continental, with warm summer and not cold winter. The soil in the plot was dark gray, medium podzolized, light loam. The thickness of the humus horizon was equal to 24–28 cm. The experimental plot featured a low humus content - 1.5–2.2%, a medium hydrolyzable nitrogen content - 26–38 mg kg<sup>-1</sup>, the labile phosphorus content was equal to 43–61 mg kg<sup>-1</sup> and potassium content was equal to 28–34 mg kg<sup>-1</sup> (Bobos et al., 2019; Zavadska, 2020). Overall, the soil and climate conditions in the experimental vegetable field were favourable for cultivating bulbous vegetable crops. According to the results of the analysis of the weather conditions during the growth seasons in the years of research (2017–2019), there was extremely great diversity in the moisture supply and temperature distribution within the vegetation periods. Rain spell were followed by prolonged droughts, which sometimes resulted in the marked decline in the moisture content of the soil and that, in its turn, affected the quality of the bulbs. The vegetation periods of 2017 and 2019 were dominated by rainless weather. The monthly average air temperatures were 1.5–2.0 °C higher than the respective long-term ones, while the amount of precipitation from April to September was lower than the long-term norm by 240–300 mm. The most favourable weather for plants occurred during their vegetation in 2019.

After the completion of prospecting experiments, nine varieties and hybrids of onions suitable for cultivation in the Forest Steppe region were included in the programme of research. The thoroughly researched and widely cultivated Skvirskaya variety (Fig. 1) was chosen as the reference variety. The programme of research is presented in Table 1.



**Figure 1.** Bulbs of Skvirskaya reference variety. Ukrainian breeding, mid-season, semi-pungent, multi-purpose variety, vegetation period of 100–110 days, average bulb mass of 50–94 g.

Apart from the traditional onion cultivars of white and yellow colours, it was decided to include in the research design also the Bronze d'Amposta variety of Dutch origin with reddish-bronze coloured bulbs (Fig. 2).

After harvesting the ripe onions, one most characteristic replication of each variety was subjected to the comprehensive analysis of unmarketable bulbs. These were classified into fractions and separately weighed, then the percentage of the total mass of the harvest was calculated and the marketability was determined.

Fresh bulbs were appraised by the set of biometric indices. The average mass of the marketable bulb was determined using the average sample with a mass of 10 kg taken from all replications. The number of bulbs in the sample was counted and the average mass was calculated to an accuracy of 1 g. The bulbs typical for the variety under consideration were used to measure the diameter in the largest cross-section as well as their length. The bulb's shape index was determined as the ratio of its length to its diameter. The biometric indices of bulbs were appraised by the measure of stability, using for that purpose the Lewis's stability factor [ $S.F. = X_{max} \cdot (X_{min})^{-1}$ ]. Its value varies from 1.0 up. The closer the factor is to 1.0, the more stable the index under investigation is.

4 kg of bulbs of each variety were sampled for drying with three replicates. They were weighed, classified, washed by hand, peeled removing the dry scales and basal plate with rootlet remnants, then the amount of waste was determined. After peeling, the bulbs were again washed in running water, cut by hand into cubes dimensioned  $1.0 \pm 0.2 \times 1.0 \pm 0.2$  cm. The cut product was uniformly distributed over the trays of the Sadochok 2-M drying cabinet at a rate of  $2 \text{ kg m}^{-2}$  and loaded into the process chamber of the drying cabinet (Fig. 3). The drying apparatus employed in the experiments was a chamber-type dryer operating on the batch loading principle. Prior to loading a batch, the drying chamber was heated in advance to a temperature of  $50 \text{ }^\circ\text{C}$ . All the trays were loaded into the dryer simultaneously. In order to ensure uniform drying-up, the raw stock was stirred several times in the course of drying.

The shredded product was dried at a temperature of  $60 \text{ }^\circ\text{C}$  until its moisture content reached 10–12%. The earlier research has proved that such a temperature is optimal for drying onion, it ensures the preservation of the organoleptic properties and biologically valuable agents (Seifu et al., 2018).

After the drying was complete, the product was cooled down, samples were taken for biochemical and technological analysis and packed in airtight polythene bags. The dried product was stored in darkness at a temperature of  $12\text{--}16 \text{ }^\circ\text{C}$  and a relative air humidity of 65–70%.



**Figure 2.** Bulbs of Bronze d'Amposta Dutch-origin variety (Antaria Ltd). Mid-season, multi-purpose variety, average bulb mass - 140–150 g, diameter - 8–10 cm, potential yield - over  $60 \text{ t ha}^{-1}$ .



**Figure 3.** General appearance of chamber-type convection dryer with onion test samples in the process of drying. Power supply of drier: 220 V, 50 Hz, power rating - 1,250 W. Fresh onion batch load is 18 kg, at one tray load of 2 kg. Maximum temperature in process chamber -  $65 \pm 5$  °C. Control of drying conditions is semi-automatic.

The research into the suitability of onion bulbs for long-term storage was carried out in the period of 2017–2019. Standard bulbs were used in the experiments. They were placed in capron mesh bags in order to make 5 kg samples with 4 replications. The bulbs were stored in a stationary buried storage facility at a temperature of  $0...+2$  °C within the main interval (October to February), the relative air humidity was maintained at a level of 70–75%. Checking was carried out in 2.5 months and at the end of storage (in 7 months).

The biochemical, organoleptic and laboratory testing and analysis of the fresh bulbs and dried products was carried out at the facilities of the research-and-study laboratory under the Department of Storage, Processing and Standardization of Crop Products, NUBiP, in accordance with the standard practices (Skaletska et al., 2014a, 2014b).

For the purpose of determining the biochemical indices, for each variety an average sample of shredded product with a mass of 2 kg was taken, 100 g of fresh product were sampled with 3 replicates and then immediately the required tests were performed. The solid matter content was determined in accordance with DSTU ISO 751 with the use of thermal gravimetric analysis by drying the sample in the drying cabinet at a temperature of  $100\text{--}105$  °C until the mass became constant. 30 g of shredded fresh bulbs were picked from the prepared laboratory sample and placed into the previously dried, weighed and enumerated weighing cups, then weighed to an accuracy of 0.01 g. After that, the weighing cups were opened, placed into the drying cabinet and dried, first, at a temperature of  $50\text{--}60$  °C (4–5 h), then 4–6 h at  $100\text{--}105$  °C. After the drying, the weighing cups were closed with caps, cooled down in the exsiccator and weighed. Then they were opened again and the drying continued for another 1.5–2.0 h, after which the weighing was repeated. The procedure was repeated until a constant mass was reached (the difference between two consequent weighing results did not exceed 0.02 g).

The soluble solid matter content was determined with the use of a refractometer in accordance with the provisions of DSTU ISO 2173. 10–20 g of shredded mass were picked from the laboratory sample,  $1\text{--}2$  cm<sup>3</sup> of onion juice were filtered from the mass, then 2–3 drops of the juice were placed on the prism of the refractometer. 4–5 readings

were taken, then the mean refractive index was calculated with a correction for the temperature. The Bertrand's method was used for determining the content of sugars (total), while the content of vitamin C was determined with the use of 2,6-dichlorophenolindophenol solution (of blue colour) reduced to the colourless compound by extracts from plants containing ascorbic acid (Skaletska et al., 2014b).

The tasting assessment of the dry and reconstituted products of onions was carried out by the panel of at least 7 experts using the 9-point scale. Part of the combined sample of the dry product was placed on a white piece of paper, then the appearance, shape of particles and product colour were determined under diffused bright daylight illumination. In the assessment of the colour, its density, uniformity and correspondence to the initial stock colour were taken into account. When determining the body, the elasticity, firmness, fragility and flowability were taken note of. In the evaluation of the flavour and taste, their purity and intensity are assessed as well as the absence of extraneous odours and tastes.

The dried onion was determined as follows: a batch weighing 2.5 g was placed into a 100 mL beaker and poured over with 50 mL of distilled water (with a temperature of 20 °C). The batch had swollen for one hour. 50 mL of distilled water with the same temperature were filtered through a funnel with a paper filter, in 20 and 40 minutes after that, the funnel with the damp filter was weighed.

In one hour, the content of the beaker was filtered through the weighed funnel with the filter, it had been left for 30 minutes to drain the water, then the funnel with the swollen batch was weighed. The weight of the swollen batch was determined as the difference between the weights of the funnel with the filter and the batch. The swelling grade was calculated as the ratio between the mass of the dried batch taken for analysis (2.5 g) and the mass of the swollen batch after 60 min of soaking.

The research results were processed with the use of mathematical methods, the least significant difference (LSD), the correlation and regression relations were determined following the standard practices.

The biometrical indices of the bulbs were estimated by their stability factor with the use of the Lewis stability factor ( $S.F. = X_{max}/X_{min}$ ). The latter's value varies from 1.0 and higher: the closer the factor is to 1.0, the more stable the index under investigation is.

The mathematical analysis of the data was carried out following the standard methods of the variance analysis (Bondarenko & Yakovenko, 2001) with the use of the Agrostat computer programme for the statistical analysis of data. The correlation between the quality indices under research and the regression coefficients were calculated with the use of the Microsoft Excel programme.

## RESULTS AND DISCUSSION

The onion varieties under investigation significantly differed as regards their biometrical and commodity indices (Table 1).

The bulb masses varied within the range of 54.20–70.45 g. The heaviest bulbs were produced by the Harmony variety - 70.4 g, which was by 3.6 g greater than in case of the reference cultivar, the lightest ones were produced by Gospodinya (54.5 g) and Mavka (54.2 g). The earlier research has proved that the uniformity of the bulbs with regard to their masses has an effect on the amount of waste generated during their mechanical cleaning. Another known fact is that bulbs with more equal masses are better

preserved in storage. As is seen from the research results, the Bronze d'Amposta and Skvirskaya (reference) varieties have the most uniform bulbs with regard to their masses. The Lewis stability factor (S.F.) of these cultivars is the closest to 1.0.

**Table 1.** Biometrical indices and marketability of bulbs for different varieties, average for 2012–2014

Name of variety, hybrid	Mass of commodity bulb		Diameter (mm)	Shape index	Marketability (%)
	g	S.F.			
Skvirskaya (reference)	66.8	1.08	53 ± 2	0.9	93.4
Arenal F <sub>1</sub>	63.6	1.16	50 ± 3	1.1	89.3
Bronze d'Amposta	67.4	1.04	55 ± 2	1.0	94.5
Buran	58.6	1.17	48 ± 4	1.0	90.4
Harmony	70.4	1.10	53 ± 2	1.3	95.2
Gospodinya	54.5	1.22	45 ± 3	1.1	88.4
Grandina	65.4	1.11	53 ± 3	1.1	92.0
Mavka	54.2	1.20	48 ± 4	1.2	89.5
Sherpa F <sub>1</sub>	56.7	1.28	44 ± 4	0.9	87.4
<i>LSD</i>	3.4				2.8

The diameter of the bulbs is another important standardized quality index. In accordance with the effective standard, the first commercial grade accepts bulbs with a diameter of at least 50 mm. The bulbs of the Skvirskaya (reference), Bronze d'Amposta, Harmony, Grandina varieties and the hybrids Arenal F<sub>1</sub>, Sherpa F<sub>1</sub> met the requirements of the effective standard with respect to this index and, therefore, were classified as the first commercial grade bulbs in accordance with the results of the marketability appraisal.

The next index represents the shape of the bulbs. Among the examined varieties, the Harmony cultivar had the longest bulbs, their shape index was equal to 1.3. The bulbs of the Skvirskaya (reference) and Sherpa varieties had a flattened and rounded shape (shape index - 0.9).

The marketability of the bulbs in the variety range under investigation was rather high varying within the range of 87.4–95.2%. The greatest shares of commodity specimen were delivered by the Harmony and Bronze d'Amposta varieties - 95.2 and 94.5%, respectively. The lowest commodity ratio was obtained for the bulbs of the Sherpa F<sub>1</sub> hybrid - 87.4%, which was 6% lower as compared to the reference variety. The correlation analysis carried out by the authors resulted in establishing the essential direct relation between the mass of the bulb and its marketability -  $r = 0.82 \pm 0.6$ . The regression analysis showed that an increase of 1 g in the mass of the bulb improved their commodity ratio by 0.77%.

As has been proved by the data in the literature and the authors' own research, the contents of the main biochemical components, especially solid matter and sugars, are the most important factors that determine the output and quality of dried product. Among the researched varieties, the greatest amount of solid matter was accumulated in the bulbs of the Harmony and Skvirskaya (reference) varieties - 12.9% and 13.8%, respectively, the lowest - in the bulbs of the Bronze d'Amposta variety - 9.5% (by 4.3% (substantial difference) lower than in the reference case). In all other cases under consideration no significant difference was found with regard to this index (Table 2).

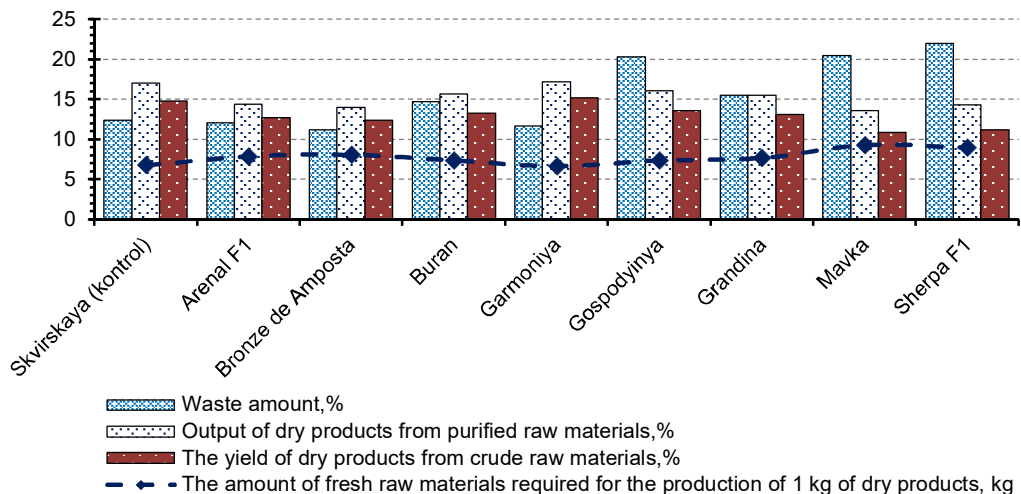
**Table 2.** Contents of main biochemical components in fresh bulbs of different onion varieties, average for 2012–2014

Name of variety, hybrid	Content in bulbs (%)			Vitamin C (mg %)
	Solid matter	Acids	Sugars, total	
Skvirskaya (reference)	13.8 ± 1.2	0.32 ± 0.04	7.8 ± 0.4	6.2 ± 1.0
Arenal F <sub>1</sub>	11.6 ± 0.9	0.42 ± 0.05	6.3 ± 0.3	4.0 ± 0.4
Bronze d'Amposta	9.5 ± 0.4	0.46 ± 0.04	6.4 ± 0.3	4.5 ± 0.8
Buran	11.4 ± 0.7	0.34 ± 0.03	7.3 ± 0.4	4.4 ± 0.7
Harmony	12.9 ± 1.1	0.35 ± 0.02	7.3 ± 0.3	6.5 ± 0.6
Gospodinya	12.3 ± 0.8	0.37 ± 0.04	6.2 ± 0.2	5.7 ± 1.1
Grandina	12.1 ± 1.0	0.38 ± 0.03	7.3 ± 0.3	5.1 ± 0.6
Mavka	11.4 ± 0.7	0.45 ± 0.05	5.3 ± 0.2	4.7 ± 0.5
Sherpa F <sub>1</sub>	10.7 ± 0.8	0.23 ± 0.02	5.7 ± 0.3	3.3 ± 0.6

The greatest amounts of sugars (total) were found in the bulbs of the Skvirskaya (reference), Harmony and Buran varieties - 7.8 and equally 7.3% each, respectively. It has been established that there is an average direct correlation between the solid matter content and the sugar content in the bulbs -  $r = + 0.58 \pm 0.02$ .

The highest contents of titratable acids were found in the bulbs of the Bronze d'Amposta and Mavka varieties - 0.46 and 0.4%, respectively, the lowest - in the bulbs of the Sherpa F<sub>1</sub> hybrid - 0.23%. The bulbs of other varieties did not show any significant difference in this component. The greatest amounts of vitamin C were contained in the fresh bulbs of the Skvirskaya (reference) and Harmony varieties - over 6 mg %.

The quantity of waste generated in the process of mechanically cleaning the bulbs and preparing them for drying depended on the variety (Fig. 4). The smallest amount of waste was generated in the process of preparing the raw material for drying by the bulbs of the Bronze d'Amposta variety - 11.2%, which was 1.2% less than in case of the reference variety (non-significant difference). Little waste was generated also by the bulbs of the Harmony variety - 11.7%, which was 0.7% less than in case of the reference variety.

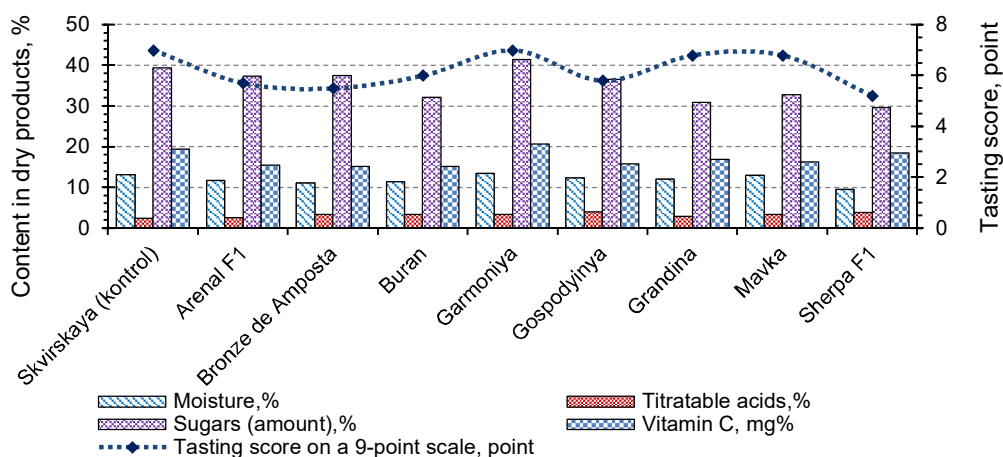


**Figure 4.** Amount of waste and yield of dried products for different varieties of onions, average for 2012–2014.

As regards the yield of finished commodity from cleaned raw material, the Harmony and Skvirskaya (reference) varieties stood out - 17.2 and 17.0%, respectively. The research results proved that the solid matter content in the initial stock and the generated waste amount had the greatest effect on this index. In view of that, the smallest amount of the fresh product was needed to obtain 1 kg of the dried product in case of the bulbs of the Harmony and Skvirskaya (reference) varieties - 6.7 and 6.8 kg, respectively.

For the consumers of dried products, the important factors are the content of biochemical components, the biological and nutritional value as well as the organoleptic indicators (Fig. 5).

The greatest solid matter content was found in the dried product made from the bulbs of the Sherpa F<sub>1</sub> hybrid, - in excess of 90 %. The highest sugar content was in the dried products of the Harmony and Bronze d'Amposta varieties - 41.4 and 40.5%, respectively, which was 2.7 and 2.1% more than in case of the reference variety.



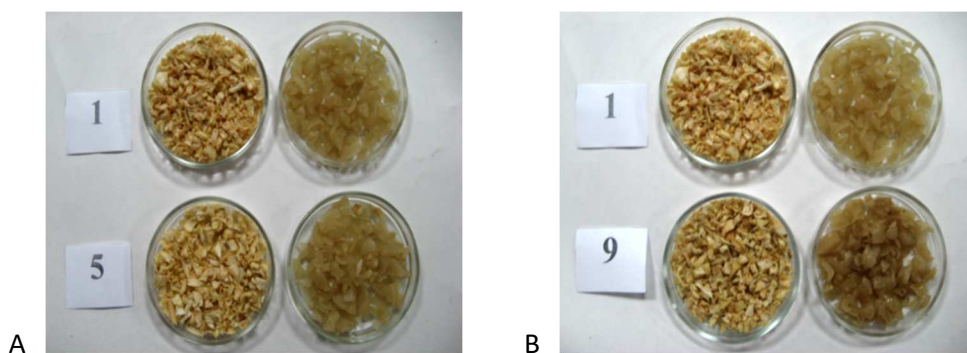
**Figure 5.** Tasting score and content of main biochemical elements in dried products of different varieties of onions, average for 2012–2014.

As was obvious from the obtained data, the moisture content depended on the sugar content. The correlation analysis carried out by the authors resulted in establishing the direct relation between the two indices -  $r = + 0.62 \pm 0.12$ .

The dried products contained considerable amounts of vitamin C - 15.1 to 20.7 mg %. The dried product of the Harmony variety exhibited a high biological value - 20.7 mg % of vitamin C, which was 1.4 mg % more than in case of the reference variety. Also, almost all the mineral salts and minor nutrient elements were preserved in the drying process (Sasongko et al., 2020).

As a result of tasting the reconstituted product, the highest scores were awarded to the samples produced from onions of the Skvirskaya (reference) and Harmony varieties - 7.0 points each on the 9-point scale, the lowest - the Sherpa F<sub>1</sub> hybrid (5.2 points). In the reconstituted product of the Sherpa hybrid, the particles had a soft texture and a relatively dark colour (Fig. 6). Sufficiently high scores were awarded to the dried and reconstituted products of the Mavka and Grandina varieties - 6.8 points.





**Figure 6.** Samples of dried and reconstituted onion products, 2013 harvest.

A: 1 – Skvirskaya (reference); 9 – Sherpa F<sub>1</sub> hybrid; tasting score awarded to samples of reconstituted Sherpa hybrid product- 5.2 points on 9-point scale because of dark colour and soft texture of particles. B: 1 – Skvirskaya (reference); 5 – Harmony variety; tasting score awarded to samples of these varieties - 7.0 points on 9-point scale. Dried and reconstituted particles had minimum change of colour as compared to initial stock, elastic texture, distinctive intense flavour.

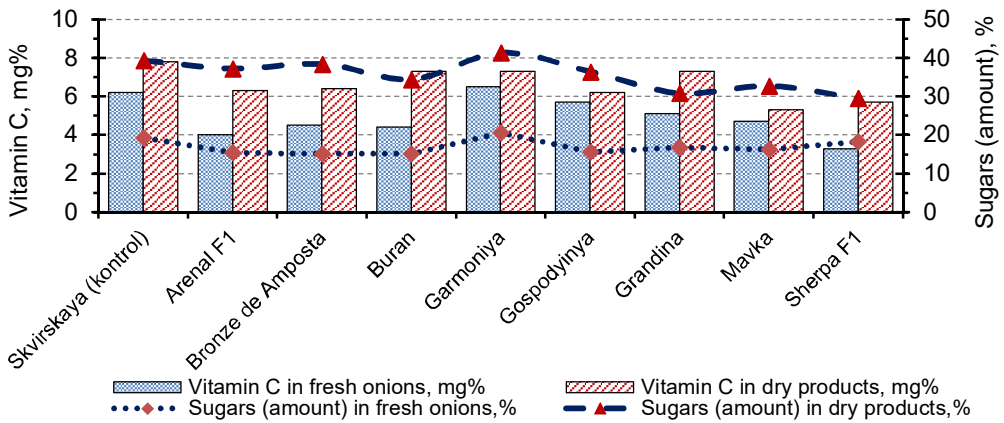
A rather low score was awarded by the tasting panel to the samples of reconstituted product of the Bronze d’Amposta variety - 5.5 points on the 9-point scale, which was 1.5 points lower as compared to the reference variety (Fig. 7). It ought to be noted that the dried product of this variety achieved a rather high score in the tasting procedure (6.4 on the 9-point scale), met the requirements of the effective standard, had an elastic texture, distinctive flavour and taste.

Dried onion contains a considerably greater amount of nutritious and biologically valuable components in comparison to the initial stock (Fig. 8).

For example, in the researched raw material the content of vitamin C varied within the range of 3.3–6.5 mg %, while in the dried products - 15.1–20.7 mg % (three-fold rise). However, after reassessment, it had been established that considerable loss of vitamin C took place during the preparation of the raw material to drying and in the process of drying itself. The extent of this loss depended on the varietal features. The lowest loss of ascorbic acid happened in the products of the Mavka, Gospodinya and Grandina varieties - within the range of 45–50% of the initial content in the raw material. Higher loss of vitamin C content, comparing to the reference variety, took place in the process of drying the raw material of the Harmony variety (4.5% more) and the greatest loss rate was in case of the Sherpa F<sub>1</sub> hybrid (13.4% more). In the latter case, the loss of ascorbic acid exceeded 60%.

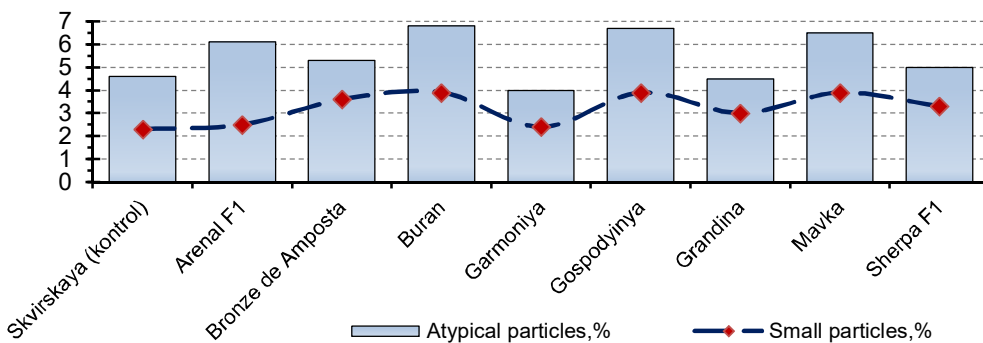


**Figure 7.** Samples of dried and reconstituted products of Skvirskaya (reference) (1) and Bronze d’Amposta (3) varieties, 2013 harvest: tasting score of dried product samples of Bronze d’Amposta variety - 6.8 points on 9-point scale, reconstituted product - 5.5 points. Reconstituted product had non-uniform darkish colour, soft texture.



**Figure 8.** Contents of vitamin C (mg %) and sugars (total, %) in fresh bulbs and dried products of different varieties of onions, average for 2012–2014.

A similar concentration in dried onion was observed for sugars - their content varied within the range of 30–40%, while in the initial stock the figures were 5.3–7.8%. However, unlike vitamin C, the content of sugars in some cases even increased during the drying process in comparison to the initial stock. For example, in the dried product of the Bronze d'Amposta variety their content increased by 1.2% as compared to the initial stock. Obviously, in the process of drying, transformation of polysaccharides into monosaccharides and disaccharides took place and that resulted in the increase of the total sugars.



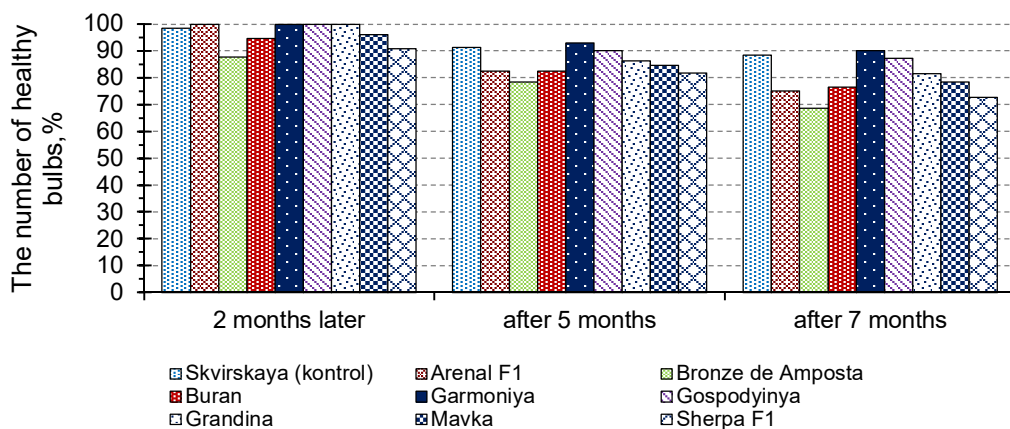
**Figure 9.** Contents of atypical and small particles (%) in dried products of different varieties of onions, average for 2012–2014.

When assessing the quality of any product, another issue of importance is its compliance with the specifications of the effective standard, in particular, the presence of atypical and small particles (Fig. 9). In the research, the atypical particles included those burned during the drying or having black spots and/or a colour unusual for the variety, also the remnants of dry scales and basal plates. Their content depended on the variety and varied within the range of 4.0 to 6.7%. The greatest amounts of such particles were registered in the dried product samples of the Gospodinya and Mavka varieties - 6.7 and 6.5%, respectively.

The results of investigations had proved that there was an essential inverse correlation between the commodity bulb mass and the amount of atypical ( $r = -0.81$ ) and small ( $r = -0.76$ ) particles in the finished commodity. That is, when the bulb mass grew, the amount of non-standard (atypical and small) particles in the dried product considerably decreased. Accordingly, the lowest quantities of such particles were present in the dried product samples of the varieties with greater commodity bulb masses - Harmony, Skvirskaya (reference), Grandina, Bronze d'Amposta.

Thus, by the results of the appraisal of dried onion products with respect to their commodity indices, the Harmony, Skvirskaya (reference) and Grandina varieties stood out with their samples containing 4.0–4.6% of atypical and 2.3–3.0% of small particles.

The scope of investigations included also the research into the suitability of bulbs of different onion varieties for long-term storage. The amount of healthy bulbs at different stages of storage to a significant extent depended on the varietal features and duration of storage (Fig. 10).



**Figure 10.** Amount of healthy onion bulbs during long-term storage in case of different varieties and hybrids, average for 2014–2016.

Throughout the first two months (until the end of October) of the storage in the conditions of a stationary buried storage facility without artificial cooling, the integrity of the bulbs of the Arenal F<sub>1</sub> hybrid and the Harmony, Gospodyinya and Grandina varieties was 100%. The bulbs of the Bronze d'Amposta variety started germinating already at this stage (8.5% of sprouted bulbs). After five months of storage (by the end of January) the bulbs of the Sherpa F<sub>1</sub> hybrid had also started germinating - circa 18% of them were sprouted within this storage interval. The greatest amount of healthy bulbs after five months of storage (by the end of January) was registered in the samples of the Harmony and Skvirskaya (reference) varieties - 93.0 and 91.2%, respectively.

In seven months after the start of storage, the bulb integrity rates of the varieties under investigation varied within the range of 68.7 to 90.2%.

The highest suitability for long-term storage was shown by the bulbs of the Harmony, Skvirskaya (reference) and Gospodyinya varieties - their integrity was at levels of 90.2, 88.4 and 87.2%, respectively. The most substantial losses were observed in the last month of the storage period (March), which can be explained by the temperature

fluctuations in the storage facility at that time. At the end of the storage period, the samples of the Bronze d'Amposta, Sherpa, Arenal varieties featured a significant share of sprouted, soft bulbs. In the absence of storage facilities with artificial cooling systems, it is advisable to complete the sale of onion bulbs within 5 months after their harvesting, thus ensuring their high marketability and minimum losses. It has been established that there is an essential correlation between the content of solid matter and the amount of healthy bulbs preserved in the process of storage ( $r = 0.93$ ), which is supported by the data in the own studies and from other authors. The completed calculations on the regression relationship have proved that an increase of 1.0% in the solid matter content results in the amount of healthy bulbs improving by 0.83%.

## CONCLUSIONS

As regards the aggregate of the quality indices determined for the fresh and dried onion products, the Harmony and Skvirskaya (reference) varieties are the most suitable ones for convection drying. The fresh bulbs and dried raw material of these varieties feature well-balanced contents of main biochemical components and high organoleptic indicators, deliver a great output of dried products (in excess of 17%). In order to produce 1 kg of dried products, it is necessary to input 6.7 kg of fresh raw material of the Harmony variety and 6.8 kg - of the Skvirskaya variety. The dried onion contain significant amounts of vitamin C - 15.1 to 20.7 mg %. The dried products of the Harmony variety have a high biological value - 20.7 mg % of vitamin C.

The bulbs of the Harmony, Skvirskaya and Gospodinya varieties are the most suitable for long-term storage in the conditions of a stationary buried storage facility without artificial cooling - the share of healthy bulbs after seven months of storage is 90.2, 88.4 and 87.2%, respectively. The share of healthy bulbs essentially depends on the solid matter content in them ( $r = 0.93$ ). In the absence of storage facilities with artificial cooling systems, it is advisable to complete the sale of onion bulbs within 5 months after their harvesting, which will ensure their high marketability and the minimum loss of quality.

## REFERENCES

- Adamicki, F. 2005. Effects of pre-harvest treatments and storage conditions on quality and shelf-life of onions. *Acta Horticulturae* **688**, 229–238. doi: 10.17660/ActaHortic.2005.688.31
- Abdou Bouba Armand, Scher, J., Aboubakar, Goudoum Augustin, Roger, P., Montet, D. & Moses, M.C. 2018. Effect of three drying methods on the physicochemical composition of three varieties of onion (*Allium cepa* L). *Journal of Food Science and Nutrition* **1**(2), pp. 17–24. doi: 10.35841/food-science.1.2.17-24
- Arslan, D. & Özcan, M.M. 2010. Study the effect of sun, oven and microwave drying on quality of onion slices. *LWT – Food Science and Technology* **43**(7), 1121–1127. doi: 10.1016/j.lwt.2010.02.019
- Asiah, N., Djaeni, M. & Hii, C.L. 2017. Moisture Transport Mechanism and Drying Kinetic of Fresh Harvested Red Onion Bulbs under Dehumidified Air. *International Journal of Food Engineering* **13**(9), No. 20160401. doi: 10.1515/ijfe-2016-0401
- Block, E. 1985. The chemistry of garlic and onions. *Scientific American* **252**(3), 114–119. doi: 10.1038/scientificamerican0385-114

- Bobos, I.M. & Zavadzka, O.B. 2016. *Improved technology for onions*. A Monograph, Kiev: CP Komprint, 248 pp. (in Ukrainian).
- Bobos, I., Fedosy, I., Zavadzka, O., Tonha, O. & Olt, J. 2019. Optimization of plant densities of dolichos (*Dolichos lablab l. var. lignosus*) bean in the right-bank of forest-steppe of Ukraine. *Agronomy Research* **17**(6), 2195–2202. <https://doi.org/10.15159/AR.19.223>
- Bolotskihh, A.S. 2001. *Ukrinian vegetables*. Kharkiv: Orbita, 1088 pp. (in Ukrainian),
- Bondarenko, G.L. & Yakovenko, K.I. 2001. Methods of experimenting in vegetable farming and melon growing. Kharkiv: Osnova, 369 pp. (in Ukrainian)
- Breu, W. 1996. *Allium cepa L. (Onion) Part 1: Chemistry and analysis*. *Phytomedicine* **3**(3), 293–306. doi: 10.1016/S0944-7113(96)80069-9
- Bulgakov, V., Holovach, I., Kiurchev, S., Pascuzzi, S., Arak, M., Santoro, F., Anifantis, A.S. & Olt, J. 2020. The theory of vibrational wave movement in drying grain mixture. *Agronomy Research* **18**(2), 360–375. doi: 10.15159/AR.20.051
- Challier, B., Perarnau, J.-M. & Viel, J.-F. 1998. Garlic, onion and cereal fibre as protective factors for breast cancer: A French case-control study. *European Journal of Epidemiology* **14**(8), 737–747. doi: 10.1023/A:1007512825851
- Davydenko, A., Podpriatov, H., Gunko, S., Voitsekhivskiy, V., Zavadzka, O., Bober, A. 2020. The qualitative parameters of potato tubers in dependence on variety and duration of storage. *Slovak Journal of Food Sciences* **14**, 1097–1104. <https://doi.org/10.5219/1392>
- Dev, R., Subanna, V.C., Ahlawat, O.P., Gupta, P. & Huddar, A.G. 2006. Effect of pretreatments on the quality characteristics of dehydrated onion rings during storage. *Journal of Food Science and Technology* **43**(6), 571–574.
- Downes, K., Choje, G.A. & Terry, L.A. 2010. Postharvest application of ethylene and 1-methylcyclopropene either before or after curing affects onion (*Allium cepa L.*) bulb quality during long term cold storage. *Postharvest Biology and Technology* **55**(1), 36–44. doi: 10.1016/j.postharvbio.2009.08.003.
- Edith, D.M.J., Dimitry, M.Y., Richard, N.M., Armand, A.B., Léopold, T.N. & Nicolas, N.Y. 2018. Effect of drying treatment on nutritional, functional and sensory properties of three varieties of onion powders. *Journal of Food Measurement and Characterization* **12**(4), 2905–2915. doi: 10.1007/s11694-018-9906-1
- Forney, C.F., Jordan, M.A., Campbell-Palmer, L., Fillmore, S., McRae, K. & Best, K. 2010. Sulfur fertilization affects onion quality and flavor chemistry during storage. *Acta Horticulturae* **877**(14), 163–168. doi: 10.17660/ActaHortic.2010.877.14.
- Griffiths, G., Trueman, L., Crowther, T., Thomas, B. & Smith, B. 2002. Onions - A global benefit to health. *Phytotherapy Research* **16**(7), 603–615. doi: 10.1002/ptr.1222
- Ilić, Z., Milenković, L., Djurovka, M. & Trajković, R. 2009. The effect of long-term storage on quality attributes and storage potential of different onion cultivars. *Acta Horticulturae* **830**(92), 635–642. doi: 10.17660/ActaHortic.2009.830.92
- Irkov, I.I., Selivanov, V.G. & Romanovskiy, N.V. 2018. Parameter optimization for onion harvesting machine with swath emplacement. *Potato and vegetables* **4**, 16–17. UDK 635.1:631.358. (in Russian).
- Khan, M.K.I., Ansar, M., Nazir, A. & Maan, A.A. 2016. Sustainable dehydration of onion slices through novel microwave hydro-diffusion gravity technique. *Innovative Food Science and Emerging Technologies* **33**, 327–332. doi: 10.1016/j.ifset.2015.12.010
- Mota, C.L., Luciano, C., Dias, A., Barroca, M.J. & Guiné, R.P.F. 2010. Convective drying of onion: Kinetics and nutritional evaluation. *Food and Bioprocess Processing* **88**(2–3), 115–123. doi: 10.1016/j.fbp.2009.09.004
- Pavlović, N., Cvikić, D., Zdravković, J., Mijatović, M. & Brdar-Jokanović, M. 2011. Mode of inheritance of dry matter content in onion (*Allium cepa L.*). *Genetika* **43**(1), 19–27. doi: 10.2298/GENSR1101019P

- Petropoulos, S.A., Ntatsi, G. & Ferreira, I.C.F.R. 2017. Long-term storage of onion and the factors that affect its quality: A critical review. *Food Reviews International* **33**(1), 62–83. doi: 10.1080/87559129.2015.1137312
- Sasongko, S.B., Hadiyanto, H., Djaeni, M., Perdanianti, A.M. & Utari, F.D. 2020. Effects of drying temperature and relative humidity on the quality of dried onion slice. *Heliyon* **6**(7), e04338. doi: 10.1016/j.heliyon. 2020.e04338
- Seifu, M., Tola, Y.B., Mohammed, A. & Astatkie, T. 2018. Effect of variety and drying temperature on physicochemical quality, functional property, and sensory acceptability of dried onion powder. *Food Science and Nutrition* **6**(6), 1641–1649. doi: 10.1002/fsn3.707
- Skaletska, L.F., Podpriatov, G.I. & Zavadzka, O.B. 2014a. *Storage and processing technology: methods for the effective use of farm and garden crops: A Monograph*. Kiev: Centre of Information Technologies, 202 pp. (in Ukrainian).
- Skaletska, L.F., Podpriatov, G.I. & Zavadzka, O.B. 2014b. *Scientific research methods for storing and processing plant crops*. Kiev: CP KOMPRINT, 416 pp. (in Ukrainian).
- Suojala, T. 2001. Effect of harvest time on storage loss and sprouting in onion. *Agricultural and Food Science* **10**(4), 323–333. doi: 10.23986/afsci.5704
- Sych, Z.D., Fedosyi, I.A. & Podpriatov, H.I. 2010. *Postharvest Technology of Vegetable Crops*. Kiev, 439 pp. (in Ukrainian).
- Zavadzka, O., Bobos, I., Fedosiy, I., Podpriatov, G. & Olt, J. 2020. Studying the storage and processing quality of the carrot taproots (*Daucus carota*) of various hybrids. *Agronomy Research* **18**(3), 2271–2284. <https://doi.org/10.15159/ar.20.199>
- Zavadzka, O. & Hrabovenko, V. 2016. The quality of fresh and dried onions (*Allium Cepa*) different varieties. *Scientific World Journal, Agriculture* **16**(11), 73–79.

## INSTRUCTIONS TO AUTHORS

Papers must be in English (British spelling). English will be revised by a proofreader, but authors are strongly urged to have their manuscripts reviewed linguistically prior to submission. Contributions should be sent electronically. Papers are considered by referees before acceptance. The manuscript should follow the instructions below.

**Structure:** Title, Authors (initials & surname; an asterisk indicates the corresponding author), Authors' affiliation with postal address (each on a separate line) and e-mail of the corresponding author, Abstract (up to 250 words), Key words (not repeating words in the title), Introduction, Materials and methods, Results and discussion, Conclusions, Acknowledgements (optional), References.

### Layout, page size and font

- Use preferably the latest version of **Microsoft Word**, doc., docx. format.
- Set page size to **ISO B5 (17.6×25 cm)**, all **margins at 2 cm**. All text, tables, and figures must fit within the text margins.
- Use single line spacing and **justify the text**. Do not use page numbering. Use **indent 0.8 cm** (do not use tab or spaces instead).
- Use font Times New Roman, point size for the title of article **14 (Bold)**, author's names 12, core text 11; Abstract, Key words, Acknowledgements, References, tables, and figure captions 10.
- Use *italics* for Latin biological names, mathematical variables and statistical terms.
- Use single ('...') instead of double quotation marks ("...").

### Tables

- All tables must be referred to in the text (Table 1; Tables 1, 3; Tables 2–3).
- Use font Times New Roman, regular, 10 pt. Insert tables by Word's 'Insert' menu.
- Do not use vertical lines as dividers; only horizontal lines (1/2 pt) are allowed. Primary column and row headings should start with an initial capital.

### Figures

- All figures must be referred to in the text (Fig. 1; Fig. 1 A; Figs 1, 3; Figs 1–3). Use only black and white or greyscale for figures. Avoid 3D charts, background shading, gridlines and excessive symbols. Use font **Arial, 10 pt** within the figures. Make sure that thickness of the lines is greater than 0.3 pt.
- Do not put caption in the frame of the figure.
- The preferred graphic format is Excel object; for diagrams and charts EPS; for half-tones please use TIFF. MS Office files are also acceptable. Please include these files in your submission.
- Check and double-check spelling in figures and graphs. Proof-readers may not be able to change mistakes in a different program.

### References

- **Within the text**

In case of two authors, use '&', if more than two authors, provide first author 'et al.':  
Smith & Jones (1996); (Smith & Jones, 1996);

Brown et al. (1997); (Brown et al., 1997)

When referring to more than one publication, arrange them by following keys: 1. year of publication (ascending), 2. alphabetical order for the same year of publication:

(Smith & Jones, 1996; Brown et al., 1997; Adams, 1998; Smith, 1998)

- **For whole books**

Name(s) and initials of the author(s). Year of publication. *Title of the book (in italics)*. Publisher, place of publication, number of pages.

Shiyatov, S.G. 1986. *Dendrochronology of the upper timberline in the Urals*. Nauka, Moscow, 350 pp. (in Russian).

- **For articles in a journal**

Name(s) and initials of the author(s). Year of publication. Title of the article. *Abbreviated journal title (in italic)* volume (in bold), page numbers.

Titles of papers published in languages other than English, should be replaced by an English translation, with an explanatory note at the end, e.g., (in Russian, English abstr.).

Karube, I. & Tamiya, M.Y. 1987. Biosensors for environmental control. *Pure Appl. Chem.* **59**, 545–554.

Frey, R. 1958. Zur Kenntnis der Diptera brachycera p.p. der Kapverdischen Inseln. *Commentat.Biol.* **18**(4), 1–61.

Danielyan, S.G. & Nabaldiyan, K.M. 1971. The causal agents of meloids in bees. *Veterinariya* **8**, 64–65 (in Russian).

- **For articles in collections:**

Name(s) and initials of the author(s). Year of publication. Title of the article. Name(s) and initials of the editor(s) (preceded by In:) *Title of the collection (in italics)*, publisher, place of publication, page numbers.

Yurtsev, B.A., Tolmachev, A.I. & Rebristaya, O.V. 1978. The floristic delimitation and subdivisions of the Arctic. In: Yurtsev, B. A. (ed.) *The Arctic Floristic Region*. Nauka, Leningrad, pp. 9–104 (in Russian).

- **For conference proceedings:**

Name(s) and initials of the author(s). Year of publication. Name(s) and initials of the editor(s) (preceded by In:) *Proceedings name (in italics)*, publisher, place of publishing, page numbers.

Ritchie, M.E. & Olf, H. 1999. Herbivore diversity and plant dynamics: compensatory and additive effects. In: Olf, H., Brown, V.K. & Drent R.H. (eds) *Herbivores between plants and predators. Proc. Int. Conf. The 38<sup>th</sup> Symposium of the British Ecological Society*, Blackwell Science, Oxford, UK, pp. 175–204.

### **Please note**

- Use ‘.’ (not ‘,’) for decimal point: 0.6 ± 0.2; Use ‘,’ for thousands – 1,230.4;
- Use ‘-’ (not ‘-’) and without space: pp. 27–36, 1998–2000, 4–6 min, 3–5 kg
- With spaces: 5 h, 5 kg, 5 m, 5 °C, C : D = 0.6 ± 0.2;  $p < 0.001$
- Without space: 55°, 5% (not 55 °, 5 %)
- Use ‘kg ha<sup>-1</sup>’ (not ‘kg/ha’);
- Use degree sign ‘°’: 5 °C (not 5 °C).